THE ROLE OF NEUROINFLAMMATION IN CHRONIC PAIN DEVELOPMENT AND MAINTENANCE

EDITED BY: Francesco De Logu, Serena Boccella, Francesca Guida and Gabriela Trevisan

PUBLISHED IN: Frontiers in Pharmacology

frontiers Research Topics

frontiers

ISSN 1664-8714
ISBN 978-2-88974-321-6
DOI 10.3389/978-2-88974-321-6

About Frontiers

Frontiers is more than just an open-access publisher of scholarly articles: it is a pioneering approach to the world of academia, radically improving the way scholarly research is managed. The grand vision of Frontiers is a world where all people have an equal opportunity to seek, share and generate knowledge. Frontiers provides immediate and permanent online open access to all its publications, but this alone is not enough to realize our grand goals.

Frontiers Journal Series

The Frontiers Journal Series is a multi-tier and interdisciplinary set of open-access, online journals, promising a paradigm shift from the current review, selection and dissemination processes in academic publishing. All Frontiers journals are driven by researchers for researchers; therefore, they constitute a service to the scholarly community. At the same time, the Frontiers Journal Series operates on a revolutionary invention, the tiered publishing system, initially addressing specific communities of scholars, and gradually climbing up to broader public understanding, thus serving the interests of the lay society, too.

Dedication to Quality

Each Frontiers article is a landmark of the highest quality, thanks to genuinely collaborative interactions between authors and review editors, who include some of the world's best academicians. Research must be certified by peers before entering a stream of knowledge that may eventually reach the public - and shape society; therefore, Frontiers only applies the most rigorous and unbiased reviews.
Frontiers revolutionizes research publishing by freely delivering the most outstanding research, evaluated with no bias from both the academic and social point of view. By applying the most advanced information technologies, Frontiers is catapulting scholarly publishing into a new generation.

What are Frontiers Research Topics?

Frontiers Research Topics are very popular trademarks of the Frontiers Journals Series: they are collections of at least ten articles, all centered on a particular subject. With their unique mix of varied contributions from Original Research to Review Articles, Frontiers Research Topics unify the most influential researchers, the latest key findings and historical advances in a hot research area! Find out more on how to host your own Frontiers Research Topic or contribute to one as an author by contacting the Frontiers Editorial Office: frontiersin.org/about/contact

THE ROLE OF NEUROINFLAMMATION IN CHRONIC PAIN DEVELOPMENT AND MAINTENANCE

Topic Editors:
Francesco De Logu, University of Florence, Italy
Serena Boccella, University of Campania Luigi Vanvitelli, Italy
Francesca Guida, University of Campania Luigi Vanvitelli, Italy
Gabriela Trevisan, Federal University of Santa Maria, Brazil

Citation: De Logu, F., Boccella, S., Guida, F., Trevisan, G., eds. (2022). The Role of Neuroinflammation in Chronic Pain Development and Maintenance. Lausanne: Frontiers Media SA. doi: 10.3389/978-2-88974-321-6

Table of Contents

frontiers in Pharmacology

EDITORIAL
published: 23 December 2021
doi: 10.3389/fphar.2021.821534

Editorial: The Role of Neuroinflammation in Chronic Pain Development and Maintenance

Francesco De Logu[1]*, *Serena Boccella*[2]* and *Francesca Guida*[2]

[1]Department of Health Sciences, Clinical Pharmacology and Oncology Section, University of Florence, Florence, Italy, [2]University of Campania Luigi Vanvitelli, Napoli, Italy

Keywords: pain, inflammation, chronic pain, nervous system, inflammatory cell

Editorial on the Research Topic

The Role of Neuroinflammation in Chronic Pain Development and Maintenance

Inflammation is originated by tissue injury and triggers several biochemical reactions that sensitize the nervous system for pain perception. Chronic inflammation induces adaptive changes that can cause altered pain signal processes. Indeed, inflammatory mediators provokes structural and functional changes in the peripheral or central sensory circuits, resulting in pain like behaviors, such as hyperalgesia, allodynia, and spontaneous pain. Accumulating evidence suggests that central sensitization is driven by neuroinflammatory processes mediated by activation/proliferation of resident microglia and glial cells with the consequent release of inflammatory mediators; furthermore, several recent studies are relating the role of non-neuronal cells of the peripheral nervous system with the modulation of neuroinflammation involved in the development and maintenance of chronic pain.

Currently treatments for chronic pain are quite unsatisfying. Therefore, there is a need for research aimed at discovering novel biological targets for new pharmacological approaches. Recently the authors collectively participated in the study of neuropathic pain and the role of HCAR2 expressed by Schwann cells in a sciatic nerve ligation model. (Boccella et al.).

In this Research Topic, different signaling implicated in neuroinflammation and chronic pain and possible therapeutic approaches have been described:

➢ Borbèly et al. investigate the role of tachykinin hemokinin-1 (HK-1) in arthritis by using different mouse models mimicking pathophysiology of rheumatoid arthritis in humans and integrative methodology (functional, *in vivo* optical imaging, cell cultures) with special emphasis on pain. They provide the first evidence that HK-1 mediates several arthritic inflammatory mechanisms and pain by direct activation of primary sensory neurons not via its classical NK1 receptor.
➢ Li et al., summarize the current knowledge of the role of microglia during sepsis by showing the contribute of these cells in long-term sensorial and cognitive deficits. The Authors appropriately illustrate the activation of microglia in the Central nervous system by describing specific neurotransmissions and molecular pathways which may promote the cognitive damage and chronic pain during sepsis.
➢ Pacini et al. test the effects of the natural antioxidant thioctic acid which is clinically used as racemic mixture. The Authors report preclinical and clinical evidences suggesting positive properties of thioctic acid in the treatment of low back pain with a more relevant efficacy of (+)-thioctic acid as compared to (+/−)-thioctic acid on pain, on time of onset of therapeutic effects.
➢ De Caro et al., show the anti-inflammatory and analgesic properties of Perampanel, the selective non-competitive AMPA receptor antagonist in acute (tail flick and hot plate tests) and chronic pain

OPEN ACCESS

Edited and reviewed by:
Paola Patrignani,
University of Studies G. d'Annunzio Chieti and Pescara, Italy

Correspondence:
Francesco De Logu
francesco.delogu@unifi.it
Serena Boccella
boccellaserena@gmail.com

Specialty section:
This article was submitted to Inflammation Pharmacology, a section of the journal Frontiers in Pharmacology

Received: *24 November 2021*
Accepted: *02 December 2021*
Published: *23 December 2021*

Citation:
De Logu F, Boccella S and Guida F (2021) Editorial: The Role of Neuroinflammation in Chronic Pain Development and Maintenance. Front. Pharmacol. 12:821534. doi: 10.3389/fphar.2021.821534

(Chronic constriction injury). They also suggest the involvement of the cannabinergic system (i.e., activation of cannabinoid type 1 receptor, CBR1) in Perampanel actions.

➢ Scuteri et al., provide a systematic review and meta-analysis assessing the efficacy of essential oils in pain. They describe the literature search conducted on databases relevant for medical scientific literature, i.e., PubMed/MEDLINE, Scopus, and Web of Science following the PRISMA (Preferred Reporting Items for Systematic reviews and Meta-Analyses) criteria. Among a total number of 30 studies included, three investigated neuropathic pain conditions.

➢ Borges et al., review recent clinical and preclinical studies investigating the epidermal growth factor receptor (EGFR) signaling pathway in chronic pain states. EGFR inhibitors are known for their use as cancer therapeutics however recent evidence suggested their clinical use for treating chronic pain. Here, the Authors provide an overview of EGFR signaling, highlighting possible mechanisms by which EGFR and its ligands may influence pain hypersensitivity and modulate inflammatory mediators of pain.

➢ Brik et al., investigate the behavioral and biochemical changes after intra-articular injection of sodium monoiodoacetate (MIA). This model mimics the degenerative changes observed in osteoarthritic patients. The Authors have characterized grading changes after injection of 1, 2 or 3 mg of MIA over a 28-day period. They report significant dose- and time-dependent changes in both gene expression and protein secretion levels of inflammatory factors.

➢ Mazzitelli et al., provide a direct evidence for the modulation of pain-like behaviors and spinal neuronal activity by basolateral amygdala-central nucleus (BLA–CeA) signaling and central nucleus-corticotropin releasing factor (CeA–CRF) neurons on under normal conditions and in an arthritis pain model.

➢ Ma et al., reveal the (fat-mass and obesity-associated protein) FTO-triggered epigenetic mechanism of matrix metallopeptidase 24 (MMP24) upregulation in the spinal cord after spinal nerve ligation (SNL). They show that blocking the SNL-induced increase of MMP24 in the spinal cord mitigate pain hypersensitivity both in the development and maintenance phase without altering the basal/acute responses or locomotor functions. The Authors suggest that MMP24 may be an endogenous initiator of neuropathic pain and could be a potential target for this disorder's prevention and treatment.

➢ Bruno et al., indicate that β-adrenergic receptors (β-ARs), mainly β2-and β3-ARs, contribute to tumor proliferation and progression and cancer-associated pain in a mouse model of cancer pain generated by the para-tibial injection of K7M2 osteosarcoma cells. This study highlights the ability of β-ARs antagonists in modulating both tumor growth and the neuroinflammation, showing a new therapeutic targets for cancer therapy and associated pain.

AUTHOR CONTRIBUTIONS

FL, SB, and FG wrote and revised the editorial.

Conflict of Interest: The authors declare that the research was conducted in the absence of any commercial or financial relationships that could be construed as a potential conflict of interest.

Publisher's Note: All claims expressed in this article are solely those of the authors and do not necessarily represent those of their affiliated organizations, or those of the publisher, the editors and the reviewers. Any product that may be evaluated in this article, or claim that may be made by its manufacturer, is not guaranteed or endorsed by the publisher.

frontiers in Pharmacology

REVIEW
published: 27 November 2020
doi: 10.3389/fphar.2020.600421

Microglia: A Potential Therapeutic Target for Sepsis-Associated Encephalopathy and Sepsis-Associated Chronic Pain

Yi Li†, Lu Yin†, Zhongmin Fan†, Binxiao Su, Yu Chen, Yan Ma, Ya Zhong, Wugang Hou, Zongping Fang and Xijing Zhang**

Department of Anaesthesiology and Perioperative Medicine, Xijing Hospital, The Fourth Military Medical University, Xi'an, China

Neurological dysfunction, one of the severe manifestations of sepsis in patients, is closely related to increased mortality and long-term complications in intensive care units, including sepsis-associated encephalopathy (SAE) and chronic pain. The underlying mechanisms of these sepsis-induced neurological dysfunctions are elusive. However, it has been well established that microglia, the dominant resident immune cell in the central nervous system, play essential roles in the initiation and development of SAE and chronic pain. Microglia can be activated by inflammatory mediators, adjacent cells and neurotransmitters in the acute phase of sepsis and then induce neuronal dysfunction in the brain. With the spotlight focused on the relationship between microglia and sepsis, a deeper understanding of microglia in SAE and chronic pain can be achieved. More importantly, clarifying the mechanisms of sepsis-associated signaling pathways in microglia would shed new light on treatment strategies for SAE and chronic pain.

Keywords: sepsis, sepsis-associated encephalopathy, chronic pain, microglia, neuroinflammation

OPEN ACCESS

Edited by:
Serena Boccella, University of Campania Luigi Vanvitelli, Italy

Reviewed by:
Ellen Niederberger, University Hospital Frankfurt, Germany
Germany Livio Luongo, University of Campania Luigi Vanvitelli, Italy

****Correspondence:***
Xijing Zhang
zhangxj918@163.com
Zongping Fang
zongping03@163.com

†These authors have contributed equally to this work

Specialty section:
This article was submitted to Inflammation Pharmacology, a section of the journal Frontiers in Pharmacology

Received: *30 August 2020*
Accepted: *23 October 2020*
Published: *27 November 2020*

Citation:
Li Y, Yin L, Fan Z, Su B, Chen Y, Ma Y, Zhong Y, Hou W, Fang Z and Zhang X (2020) Microglia: A Potential Therapeutic Target for Sepsis-Associated Encephalopathy and Sepsis-Associated Chronic Pain. Front. Pharmacol. 11:600421. doi: 10.3389/fphar.2020.600421

INTRODUCTION

Sepsis is a primary fatal syndrome in intensive care units (ICUs) that is characterized by an imbalance in the pro- and anti-inflammatory systems after infection (van der Poll et al., 2017). Sepsis is commonly accompanied by multiorgan dysfunctions and causes severe disturbances in the nervous system, such as sepsis-associated encephalopathy (SAE) and chronic pain (Shankar-Hari and Rubenfeld, 2016). SAE is defined as diffuse cerebral dysfunction during sepsis, while sepsis-associated chronic pain is partly a reflection of central sensitization with synaptic plasticity and increased neuronal responsiveness (Helbing et al., 2018; Ji et al., 2018). Both of these conditions can lead to long-lasting decrements in health-related quality of life for patients. To be specific, it has been demonstrated that SAE can cause long-term neurological deficits, including cognitive deficits (10–20%) and anxiety and stress disorders (10–30%) (Iwashyna et al., 2010; Battle et al., 2013; Helbing et al., 2018). Moreover, 31–70% of sepsis survivors claim to suffer from pain 6 months after discharge from the hospital (Carpenter et al., 2019). Given that there is still a lack of specific treatment options proposed for SAE and sepsis-associated chronic pain, understanding the mechanisms of the pathological alterations in the brain is essential for developing effective treatments to avoid the potentially devasting effects of sepsis.

Microglia, the resident immune cells in the brain, modulate multiple brain functions via cytokines and their interactions with neurons and nonneuronal cells (Greenhalgh et al., 2020). Cytokines

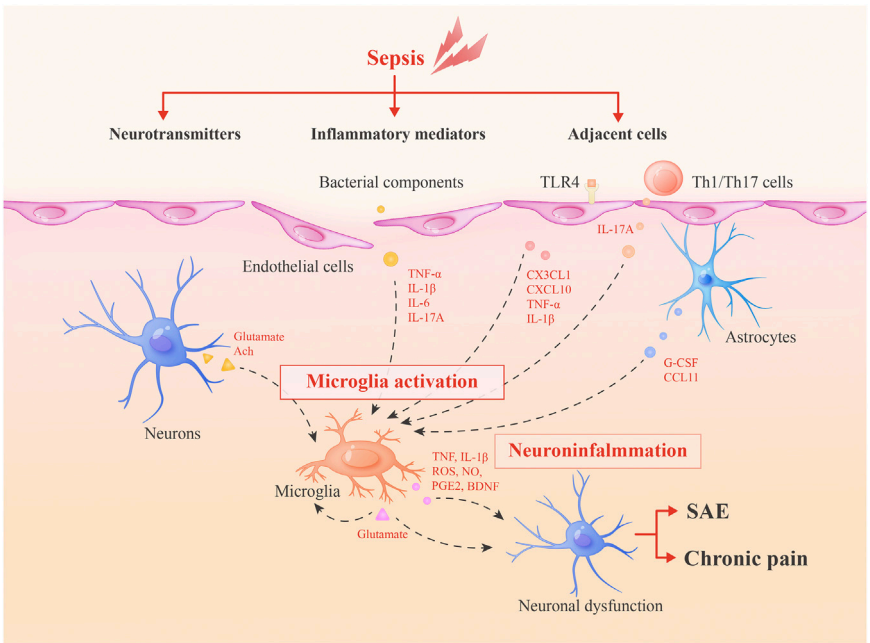

FIGURE 1 | Roles of microglia in SAE and sepsis-associated chronic pain. During sepsis, microglia can be activated by inflammatory mediators, adjacent cells and neurotransmitters. Then, activated microglia integrate neuroinflammation and cause neuronal dysfunctions via secreted inflammatory mediators or glutamate to lead to SAE and chronic pain. Glutamate may form a positive feedback mechanism in microglia activation.

protect the immune system against adverse stimuli and maintain homeostasis, but cytokine dysregulation can induce neurotoxicity, as has been verified in patients with neurodegenerative disorders (van Gool et al., 2010). The relationship between systemic infection and microglial activation in the brain was confirmed in septic patients more than a decade ago (Lemstra et al., 2007). Microglial activation in the brain was further demonstrated in an animal model of sepsis induced by lipopolysaccharide (LPS) and caecal ligation and puncture (Szollosi et al., 2018). SAE and sepsis-associated chronic pain are thought to be the consequences of inflammation in the brain (Michels et al., 2015a; Baumbach et al., 2016). Moreover, microglial activation contributes to neuroinflammation during sepsis; thus, it is believed that microglial activation plays an essential role in SAE and sepsis-associated chronic pain (Sharshar et al., 2014). The correlation between activated microglia and neurological deficits in sepsis has been reported in a few studies; however, the underlying mechanisms need to be further explored.

In this review, we summarize the current knowledge of the activation of microglia during sepsis and roles of these cells in long-term cognitive deficits and chronic pain, to shed new light on the development of novel therapeutics for SAE and sepsis-associated chronic pain (**Figure 1**).

Activation of Microglia in the Central Nervous System During Sepsis

Under physiological conditions, microglia are in a resting state, characterized by branched morphology and surveillance of the microenvironment to maintain homeostasis; when these cells encounter pathological insults, this resting phenotype will switch to an activated amoeboid form and exert destructive or neuroprotective effects (Hoogland et al., 2015). Microglial activation in the brain has been observed in both LPS-treated murine models and patients who died from sepsis, suggesting that microglia are relevant to systemic inflammation and pathology in the central nervous system (CNS) (Fukushima et al., 2015; Westhoff et al., 2019). Peripheral inflammation induces the immune response in the CNS via several pathways, which might contribute to the considerable roles of microglia in sepsis.

1. Inflammatory Mediators

Bacterial components stimulate microglia via pattern recognition receptors such as Toll-like receptors (TLR-2, TLR-4, and TLR-9) and nucleotide-binding oligomerization domain-2 (NOD2) (Ye et al., 2019). In addition, it has been verified that cytokines (particularly tumour necrosis factor α (TNF-α), interleukin 1β (IL-1β), and interleukin 6 (IL-6)), which are generated peripherally during sepsis, transmit signals through the impaired blood-brain barrier (BBB) and activate microglia to modulate neuronal function (van Gool et al., 2010). The IL-17A/IL-17R signaling pathway has also been reported to play an important role in stimulating microglia. The IL-17A/IL-17R signaling pathway facilitates microglial secretion of inflammatory factors, including IL-1β and IL-23, which exacerbate the secretion of IL-17A from immune cells and create a vicious cycle of sustained, amplified inflammation in the brain (Ye et al., 2019).

2. Adjacent Cells

Adjacent cells have modulatory effects on microglia. Astrocytic end-feet express multiple cytokine receptors and attach to vascular endothelial cells or leptomeningeal cells in the peripheral blood vessels, allowing astrocytes to initially respond to systemic inflammation (Shimada and Hasegawa-Ishii, 2017). Then, inflammatory signals are conveyed and activate microglia through astrocyte-generated cytokines, such as granulocyte-colony stimulating factor (G-CSF) and CCL11(Shimada and Hasegawa-Ishii, 2017). G-CSF acts as a microglial growth factor, and CCL11 can promote the microglial migration to inflamed foci and facilitate microglial production of reactive oxygen species (ROS), ultimately resulting in excitotoxic neuronal death (Shimada and Hasegawa-Ishii, 2017). Simultaneously, in cultured cells, astrocytes produce anti-inflammatory substances, including transforming growth factor (TGF) and prostaglandin E2 (PGE2), which downregulate microglial activity and restrict neuroinflammation (Michels et al., 2017). However, whether this anti-inflammatory effect exists *in vivo* of murine models of sepsis has not been fully studied.

Endothelial cells also play important roles in modulating microglial functions. Wang, H. et al. showed that endothelial cell activation can result in increased leukocyte adhesion, which is responsible for elevated CX3CL1 expression on endothelial cells, activating and guiding microglia toward the inflamed brain during sepsis (Wang et al., 2015). Furthermore, TLR-4 on endothelial cells is also an important inducer of microglial activation by regulating the secreting of CXCL10, TNF-α and IL-1β(Chen and Trapp, 2016). In the experimental autoimmune encephalomyelitis (EAE) mouse model, it was demonstrated that peripheral Th1/Th17 cells were initially recruited to the brain and produced massive amounts of IL-17A, inducing the activation of resident microglia and prolonging the inflammatory response (Murphy et al., 2010). Since the IL-17A/IL-17R pathway is a vital component in microglia-mediated neuroinflammation in sepsis, it is possible that Th1/Th17 cells play a similar role in this context.

3. Neurotransmitters

Microglia express receptors of various neurotransmitters, including glutamate, acetylcholine (Ach), and so on, which cooperate with each other to maintain normal neuronal functions (Wolf et al., 2017). During sepsis, imbalanced expressions of these neurotransmitters exert negative effects on microglia and alter the equilibrium in the brain. In BV2 cells (a murine microglial cell line), LPS increases the Ca^{2+} concentration and upregulates CaMKII phosphorylation, thus inducing ERK1/2 and NF-κB phosphorylation, which stimulate microglial activation and the expression of pro-inflammatory cytokines and enzymes (Wu et al., 2018). These processes are regulated by overexpressed glutamate during sepsis and the inhibition of glutamate receptors (N-methyl-D-aspartate (NMDA) receptors) could attenuate those effects (Wu et al., 2018). On the contrary, Ach and nicotine can reduce LPS-induced TNF-α release from microglia through the activation of α-nAChR, which was reported to deliver an anti-inflammatory signal. However, the downregulation of cholinergic neurons during sepsis eliminates this effect (Dal-Pizzol et al., 2014).

MICROGLIA IN SEPSIS-ASSOCIATED ENCEPHALOPATHY

The Mechanisms of Sepsis-Associated Encephalopathy

SAE is a common but severe complication of sepsis. During SAE, the brain exhibits acute and long-lasting pathological alterations in mouse models and human patients. Cerebrovascular impairment and neuroinflammation are defined as the two main triggering mechanisms of SAE. On the one hand, impaired cerebrovascular-related changes in cerebral perfusion were observed in patients with severe sepsis or septic shock, which have been demonstrated to facilitate SAE (Schramm et al., 2012). On the other hand, brain cytokines and chemokines are generated within a few hours of sepsis onset in murine models, which lead to increased permeability of the BBB, causing immune cells, inflammatory factors and other substances in the periphery to enter the brain and induce disturbances (Comim et al., 2011). Cerebral endothelial activation is also a pathophysiological condition in the progression of SAE and has been reported to induce robust inflammation, abnormal BBB permeability, and even facilitate coagulation by the release of pro-inflammatory cytokines and nitric oxide (NO) (Sharshar et al., 2010; Heming et al., 2017).

Many other mechanisms are also likely to participate in the pathogenesis of SAE. Neuronal necrosis and apoptosis are thought to directly induce neuronal loss in the brain following LPS-induced SAE (Deng et al., 2013). And, it is possible that mitochondrial dysfunction and increased levels of reactive oxygen/nitrogen species can promote neuronal death (Heming et al., 2017). Astrocytes can be activated and exert effects during SAE via astrogliosis (Deng et al., 2013). In addition, activated microglia in this situation release inflammatory mediators to consequently impair the BBB and suppress neuronal activity (Deng et al., 2013). Complement cascade is also a phenomenon caused by overactive inflammation during sepsis, leading to deleterious effects in SAE (Jacob et al., 2007). Furthermore, changes in neurotransmission, such as glutamate-related neuronal excitotoxicity, facilitate neuronal apoptosis under the septic condition (Heming et al., 2017). The dopaminergic, β-adrenergic, cholinergic, and GABA receptor systems are all impaired during sepsis, which might result from NO produced by endothelial cells or elevated levels of circulating amino acids (Heming et al., 2017).

Activated Microglia in SAE and Cognitive Dysfunction

Cognitive dysfunction is a common but severe consequence of SAE. Delirium is a typical symptom in the acute phase of SAE that occurs in 50% of patients (Mazeraud et al., 2020). Even after

effective treatment, a large number of individuals who survive sepsis also develop long-term cognitive deficits and seem to have a higher risk of suffering from dementia (Widmann and Heneka, 2014). The correlation between those long-term brain dysfunctions and delirium in the acute phase of SAE has been reported (MacLullich et al., 2009), and the shared mechanisms underlying these two phenomena are receiving much more attention. Activated microglia have recently been proposed to play a role in accelerating SAE and have a close relationship with cognitive changes. Consistently, inhibition of microglia by an intracerebroventricular (ICV) injection of minocycline decreased acute brain oxidative damage, inflammation, and long-term cognitive impairment in sepsis survivors (Michels et al., 2015b). Thus, exploring the roles of microglia in SAE and long-term cognitive impairment will deepen our understanding of pathology of SAE and probably offer a potential therapeutic target for those patients.

Activated microglia lead to neuronal dysfunctions and memory impairment via releasing large amounts of pro-inflammatory mediators and inducing the expression of multiple enzymes during sepsis (Wu et al., 2018). For example, working memory, as well as hippocampal-dependent memory, has a negative correlation with the level of IL-1β, which can be released by activated microglia in SAE (Tang et al., 2018). In addition, Nox2 (a member of the NADPH oxidase family), GRK2 (G protein-coupled receptor kinase 2) and NO-producing enzymes (such as inducible nitric oxide synthase) in microglia regulate oxidative and nitrosative stress during inflammation, contributing to the amplification of pro-inflammatory mediators production, as well as long-term brain deficits after sepsis (Hernandes et al., 2014; Widmann and Heneka, 2014; Kawakami et al., 2018). Neurotransmitters can also be regulated by activated microglia. A moderate level of glutamate is released by neurons, astrocytes, and homeostatic microglia. However, toxic amounts of glutamate are produced by activated microglia through a mechanism that involves connexin channels and the cystine/glutamate antiporter system (Bozza et al., 2013; Michels et al., 2017). As glutamate has a regulatory effect on microglia, it seems that glutamate forms a positive feedback mechanism in microglia activation.

It is important to note that elderly individuals with neurodegenerative diseases have increased levels of innate inflammation in the brain and are vulnerable to delirium (van Gool et al., 2010). In animal sepsis models, neurobehavioural impairments are highly distinct in those with certain pre-existing conditions (Lemstra et al., 2007). Microglia are known to play crucial roles in mediating inflammatory processes associated with various neurodegenerative diseases (Tang et al., 2018). In these contexts, once microglia are activated or primed, this status is believed to be sustained for a long time (Lemstra et al., 2007). Thus, during sepsis, it is well accepted that when activated/primed microglia encounter a subsequent exogenous stimulus, these cells are inclined to exert an exaggerated response and produce enormous levels of cytokines, facilitating brain disturbances and exacerbating SAE (Lemstra et al., 2007).

MICROGLIA IN SEPSIS-ASSOCIATED CHRONIC PAIN

The Mechanisms of Chronic Pain

Pain is a key defense system that enables the host to detect and avoid harmful stimuli. A complex and properly functioning neural circuit is necessary for the perception of pain. Briefly, noxious stimuli excite the peripheral ends of primary afferent sensory neurons, through which excitatory information is conveyed to the nociceptive projection neurons in the spinal dorsal horn and further up to those in the brainstem and higher brain regions, processing the sensory and affective components of pain (Inoue and Tsuda, 2018). Although acute pain is considered to exert a protective effect on the host, once the pain persists for more than 3 months and develops into chronic and recurrent pain, it becomes a disease condition (Milligan and Watkins, 2009). There are several types of chronic pain, including neuropathic pain, inflammatory pain, cancer-associated pain and drug-induced pain after chemotherapy and chronic opioid exposure. All of these types of pain are characterized by spontaneous pain, as well as evoked pain in response to noxious (hyperalgesia) or non-noxious (allodynia) stimuli (Ji et al., 2018).

Abnormal excitability in the CNS and the activation of glial cells, including astrocytes, microglia, oligodendrocytes in the CNS and satellite glial cells, Schwann cells in the peripheral nervous system, are believed to be the two basic pathogeneses contributing to chronic pain (Ji et al., 2013). Persistent peripheral inflammation leads to the increased release of neurotransmitters from the primary afferent central terminals to the spinal cord and brain, producing a state of neuronal hyperactivity and hyperexcitability (Ji et al., 2018). Besides, synaptic plasticity, LTP and disinhibition of inhibitory signaling can all contribute to pain hypersensitivity (Kyranou and Puntillo, 2012; Ji et al., 2018). Glia activation is another driver of chronic pain. These cells are regulated by several neuromodulators such as ATP, CSF, chemokines, neuropeptides and facilitate neuroinflammation and chronic pain via glia-produced factors indispensably (Ji et al., 2018). Notably, more and more researchers are proposing that neuroinflammation is highly effective in modulating pain sensitivity and is recognized to be associated with the persistence and chronification of human pain conditions (Ji et al., 2018). For example, TNF, IL-1β, and IL-6 rapidly modulate the function of neurotransmitter receptors to result in enhanced excitatory synaptic transmission and suppressed inhibitory synaptic transmission in the spinal pain circuit (Kawasaki et al., 2008). What's more, neuroinflammation is also participating in inducing and sustaining spinal cord LTP in chronic pain (Ji et al., 2018).

Activated Microglia in Sepsis-Associated Chronic Pain

Chronic pain is a frequently reported consequence of critical care illnesses, with 31–70% of septic patients claiming pain 6 months after discharge from the hospital (Carpenter et al., 2019). The most likely cause of this pain can be inflammation, and microglia are believed to contribute to this pathology. Microglia activation

was observed in animal model of inflammatory pain as long ago as 1999 (Chen et al., 2018). And, functional imaging reveals glia activation in patients with chronic pain (Loggia et al., 2015).

Increasing evidence suggests that microglia drive central sensitization via microglial mediators, mainly TNF and IL-1β(Chen et al., 2018). For example, TNF induces spontaneous excitatory postsynaptic current by modulating the activities of TRPV1, AMPAR and NMDAR in spinal neurons (Chen et al., 2018). In addition, the cytokines PGE2 and brain-derived neurotrophic factor (BDNF) released by microglia can modulate inhibitory synaptic transmission via pre-, post- and extra-synaptic mechanisms. Disinhibition and LTP in the CNS also have tight correlations with activated microglia, as it has been suggested that TNF and IL-1β secreted by microglia are individual factors to induce LTP in spinal dorsal horn neurons (Ji et al., 2013; Chen et al., 2018). Intriguingly, microglia signaling is sex-dependent and spinal microglia play little or no role in regulating neuropathic pain in female rodents. This may result from the distinct expression levels of testosterone in male and female rodents and T cells appear to replace the role of microglia in neuropathic pain in female rodents (Sorge et al., 2015). Furthermore, spinal microglia priming also increases vulnerability to pain enhancement in mice via augmented microglia production of pro-inflammatory products (Hains et al., 2010).

Bacterial infections can induce pain in rodents. For example, the bacterium *staphylococcus aureus* causes pain not only in a direct manner through activating nociceptors, but also in an indirect manner via the intermediating effects of immune cells and secreted inflammatory substances (Chiu et al., 2013). What's more, LPS has been demonstrated to produce pain hypersensitivity by sensitizing TRPV1 in nociceptors (Diogenes et al., 2011). Although an increasing number of studies are focusing on the roles of microglia in chronic pain as described above, it is worth noting that most studies are conducted after nerve injury, not bacterial infections in murine models. This can partly attribute to the absence of models mimicking and criteria evaluating the chronic pain after bacterial infections, particularly sepsis. For instance, after subcutaneous injection of bacteria in the mouse hid-paw, the infection-induced mechanical hypersensitivity seems to begin declining in 6 h and disappear in 72 h (Chiu et al., 2013). And it has been reported that shoulder pain is the most frequently reported chronic pain of ICU survivors, which is difficult to evaluate in murine models (Battle et al., 2013). The states and functions of microglia are distinct in different circumstances, such as in neuropathic pain and inflammatory pain (Milligan and Watkins, 2009). Therefore, there is still a long way to go in understanding the exact roles of microglia in sepsis and sepsis-associated chronic pain.

TREATMENT

Treatment of SAE

In recent years, our understanding of the pathophysiology of sepsis has improved. However, there is still no targeted treatment for sepsis or its complications: SAE and chronic pain. Strategies for SAE treatment are still based on the management of sepsis and the clinical manifestations of SAE, including seizure, delirium and coma (Mazeraud et al., 2020). The use of sedation is a controversial issue. Dexmedetomidine, an alpha agonist agent, has shown beneficial effects in patients with septic shock (Mazeraud et al., 2020). However, in a recent larger study, no significant advantage was observed for critically ill patients in the dexmedetomidine group (Shehabi et al., 2019). Moreover, benzodiazepines and opioids should be avoided since they are independent risk factors for the development of acute SAE in the ICU. Neuroprotective agents have also been considered options for SAE treatment. For example, impaired cholinergic neurotransmission has an important role in the development of delirium in SAE. However, rivastigmine, an inhibitor of acetylcholinesterase and butyrylcholinesterase, caused higher mortality and longer median duration of delirium than the placebo in critically ill patients (van Eijk et al., 2010). So, it is necessary to seek for new therapeutic strategies of SAE. For example, during SAE, synaptic activity is significantly reduced. Since GABA-A receptors participate in most neuronal inhibitory synapses, GABA-A may become a new target for the prevention and treatment of delirium (Molnar et al., 2018).

Treatment of Chronic Pain

There is limited knowledge about sepsis-induced chronic pain. Experimental and clinical data show that there is a close relationship between inflammation and pain perception. As the most serious systemic inflammation, sepsis may induce not only acute changes in nociception but also long-lasting alterations in the CNS, increasing the risk of chronic pain conditions associated with ICU stays (Baumbach et al., 2016). For the treatment of pain, the first step includes non-opioid analgesics such as paracetamol and non-steroidal anti-inflammatory drugs (NSAIDs), which reduce inflammation and pain by reducing the effects of the cyclooxygenases COX-1 and COX-2 and reduce the production of inflammatory mediators. In the second step of pain treatment, the weak opioids codeine and dihydrocodeine are added. Opioids mimic the effects of natural pain by reducing the chemicals (endorphins) that activate opioid receptors in the CNS, thereby reducing the transmission of noxious signals. The third step requires strong opioids, which are more effective than weak opioids but also have more serious side effects (Hylands-White et al., 2017). Other treatment approaches for chronic pain management includes: adjuvant drugs, dealing with cognitive, emotional and behavioural disorders in chronic pain conditions, psychological and social approaches (Hylands-White et al., 2017). Besides, with advances in our understanding of mechanisms of chronic pain, cell-based therapy is now an option for treating chronic pain, such as stem cell therapy and so on (Chakravarthy et al., 2017).

Microglia as the Therapeutic Target of SAE and Sepsis-Associated Chronic Pain

Microglial activation facilitates brain damage during sepsis; thus, the modulation of microglial activation seems to be a relevant approach for treating SAE and chronic pain. For example, recombinant IL-17A can enhance neuroinflammation and

microglial activation in caecal ligation and puncture mice. As expected, neutralizing antibodies against IL-17A or IL-17R can reduce CNS inflammation and microglial activation, thereby reducing cognitive dysfunction (Ye et al., 2019). Plus, several plant-derived substances, such as resveratrol, sophoraflavanone G (SG), attractylone, and β-elemene, have also been shown to inhibit microglial-mediated neuroinflammation and improve memory performance in mice with SAE (Guo et al., 2016; Sui et al., 2016; Pan et al., 2019; Tian et al., 2019).

In addition, studies of the roles of microglia in chronic pain have provided several new therapeutic approaches. And many efforts to inhibit microglial activation significantly reduced chronic pain. The strategies targeting on microglia can be roughly divided into three aspects. First, treatments targeting specific receptors necessary for microglial activation, such as TLR4, which has been reported to be a trigger of microglial activation (Bruno et al., 2018), the p38 MAPK pathways, and P2X4R. Second, treatments suppressing the release of microglial mediators, such as pro-inflammatory factors. Third, treatment targeting the mediators released by microglial. For example, low-dose naltrexone was shown to inhibit microglia activation similar to TLR4 inhibitor, and be an effective treatment for chronic pain in a pilot clinical trial (Younger and Mackey, 2009; Wang et al., 2016).

However, there are still many difficulties regarding robust and consistent laboratory results and clinical trials. One of the reasons is likely that microglia can also exert protective effects in the CNS. While cerebral synaptic activity is decreased in SAE, activated microglia insert their processes into the synaptic cleft to displace the axosomatic inhibitory synapses of neurons and thus increase neuronal excitatory activity, which results in the activation of synaptic NMDA receptors to exert anti-apoptotic and neuroprotective effect (Chen and Trapp, 2016). What's more, complex interactions of microglia and other cells *in vivo*, polyphyletic effects of microglia-targeted drugs, differences between human and murine microglia, and distinct roles of microglia between female and male all can contribute to the disappointing clinical results. Thus, Ru-Rong Ji et al. proposed that the best strategy is to restore microglia normal function by pro-resolution approaches, such as pharmacological approaches, including CB2 (cannabinoid type 2) agonists, cell therapies and neuromodulation (Ji et al., 2016).

The endocannabinoid system (ECS) and its endogenous ligands play an important role on modulating the activation of microglia. The ECS mainly includes cannabinoid receptor type 1 (CB1R) and type 2 (CB2R), their small, lipid ligands (eCBs), and enzymes acting on synthesizing and degrading eCBs (Lutz et al., 2015). CB1R is mainly expressed in neurons, while CB2R is enriched in microglia (Stella, 2009). In neuroinflammatory and neurodegenerative disease conditions, CB2R is upregulated significantly in microglia, promoting phenotype alternation and anti-proinflammatory signaling in microglia (Tanaka et al., 2020). And some researchers have revealed that several molecules focusing on modulating CBR, such as endogenous fatty acid amide palmitoylethanolamide (PEA), can increase phagocytosis and migratory activity of microglia (Guida et al., 2017). Yet, further study is needed in designing microglial-targeted drugs that are effective in sepsis-associated chronic pain and in humans.

CONCLUSION

SAE and chronic pain are frequent but severe complications of the dysregulated host response in sepsis. Numerous mechanisms have been implicated in the development of these conditions, among which activated microglia play a significant role. However, no specific treatments or standardized management suggestions are available in the current medical guidelines for sepsis and the associated complications. Therefore, the modulation of microglial activity, although still in the preclinical phase, may be an interesting therapeutic strategy.

AUTHOR CONTRIBUTIONS

All authors listed have made a substantial, direct, and intellectual contribution to the work and approved it for publication.

FUNDING

This study was supported by National Nature Science Foundation Grant No. 81870961, the National Natural Science Shaanxi Province Natural Science Basic Research Programme-Key Projects (No. 2018JZ8004), and the Shaanxi Province Key Research and Development Programme (No. 2020ZDXM-SF-002) to XZ; the National Nature Science Foundation Grant No. 81801308 to ZF.

REFERENCES

Battle, C. E., Lovett, S., and Hutchings, H. (2013). Chronic pain in survivors of critical illness: a retrospective analysis of incidence and risk factors. *Crit. Care* 17(3), R101. doi:10.1186/cc12746

Baumbach, P., Gotz, T., Gunther, A., Weiss, T., and Meissner, W. (2016). Prevalence and characteristics of chronic intensive care-related pain: The role of severe sepsis and septic shock. *Crit. Care Med.* 44(6), 1129–1137. doi:10.1097/CCM.0000000000001635

Bozza, F. A., D'Avila, J. C., Ritter, C., Sonneville, R., Sharshar, T., and Dal-Pizzol, F. (2013). Bioenergetics, mitochondrial Dysfunction, and oxidative stress in the pathophysiology of septic encephalopathy. *Shock* 39, 10–16.

Bruno, K., Woller, S. A., Miller, Y. I., Yaksh, T. L., Wallace, M., Beaton, G., et al. (2018). Targeting toll-like receptor-4 (TLR4)-an emerging therapeutic target for persistent pain states. *Pain* 159(10), 1908–1915. doi:10.1097/j.pain.0000000000001306

Carpenter, K. C., Hakenjos, J. M., Fry, C. D., and Nemzek, J. A. (2019). The influence of pain and analgesia in rodent models of sepsis. *Comp. Med.* 69(6), 546–554. doi:10.30802/AALAS-CM-19-000004

Chakravarthy, K., Chen, Y., He, C., and Christo, P. J. (2017). Stem cell Therapy for chronic pain management: review of uses, advances, and adverse effects. *Pain Physician* 20(4), 293–305.

Chen, G., Zhang, Y. Q., Qadri, Y. J., Serhan, C. N., and Ji, R. R. (2018). Microglia in pain: detrimental and protective roles in pathogenesis and resolution of pain. *Neuron* 100(6), 1292–1311. doi:10.1016/j.neuron.2018.11.009

Chen, Z., and Trapp, B. D. (2016). Microglia and neuroprotection. *J. Neurochem.* 136(Suppl. 1), 10–17. doi:10.1111/jnc.13062

Chiu, I. M., Heesters, B. A., Ghasemlou, N., Von Hehn, C. A., Zhao, F., Tran, J., et al. (2013). Bacteria activate sensory neurons that modulate pain and inflammation. *Nature* 501(7465), 52–57. doi:10.1038/nature12479

Comim, C. M., Vilela, M. C., Constantino, L. S., Petronilho, F., Vuolo, F., Lacerda-Queiroz, N., et al. (2011). Traffic of leukocytes and cytokine up-regulation in the central nervous system in sepsis. *Intensive Care Med.* 37(4), 711–718. doi:10.1007/s00134-011-2151-2

Dal-Pizzol, F., Tomasi, C. D., and Ritter, C. (2014). Septic encephalopathy: does inflammation drive the brain crazy? *Br. J. Psychiatr.* 36(3), 251–258. doi:10.1590/1516-4446-2013-1233

Deng, Y. Y., Fang, M., Zhu, G. F., Zhou, Y., and Zeng, H. K. (2013). Role of microglia in the pathogenesis of sepsis-associated encephalopathy. *CNS Neurol. Disord. rug Targets* 12(6), 720–725. doi:10.2174/18715273113126660178

Diogenes, A., Ferraz, C. C., Akopian, A. N., Henry, M. A., and Hargreaves, K. M. (2011). LPS sensitizes TRPV1 via activation of TLR4 in trigeminal sensory neurons. *J. Dent. Res.* 90(6), 759–764. doi:10.1177/0022034511400225

Fukushima, S., Furube, E., Itoh, M., Nakashima, T., and Miyata, S. (2015). Robust increase of microglia proliferation in the fornix of hippocampal axonal pathway after a single LPS stimulation. *J. Neuroimmunol.* 285, 31–40. doi:10.1016/j.jneuroim.2015.05.014

Greenhalgh, A. D., David, S., and Bennett, F. C. (2020). Immune cell regulation of glia during CNS injury and disease. *Nat. Rev. Neurosci.* 21(3), 139–152. doi:10.1038/s41583-020-0263-9

Guida, F., Luongo, L., Boccella, S., Giordano, M. E., Romano, R., Bellini, G., et al. (2017). Palmitoylethanolamide induces microglia changes associated with increased migration and phagocytic activity: involvement of the CB2 receptor. *Sci. Rep.* 7(1). doi:10.1038/s41598-017-00342-1

Guo, C., Yang, L., Wan, C. X., Xia, Y. Z., Zhang, C., Chen, M. H., et al. (2016). Anti-neuroinflammatory effect of Sophoraflavanone G from Sophora alopecuroides in LPS-activated BV2 microglia by MAPK, JAK/STAT and Nrf2/HO-1 signaling pathways. *Phytomedicine* 23(13), 1629–1637. doi:10.1016/j.phymed.2016.10.007

Hains, L. E., Loram, L. C., Weiseler, J. L., Frank, M. G., Bloss, E. B., Sholar, P., et al. (2010). Pain intensity and duration can be enhanced by prior challenge: initial evidence suggestive of a role of microglial priming. *J. Pain* 11(10), 1004–1014. doi:10.1016/j.jpain.2010.01.271

Helbing, D.-L., Böhm, L., and Witte, O. W. (2018). Sepsis-associated encephalopathy. *Can. Med. Assoc. J.* 190(36), E1083. doi:10.1503/cmaj.180454

Heming, N., Mazeraud, A., Verdonk, F., Bozza, F. A., Chretien, F., and Sharshar, T. (2017). Neuroanatomy of sepsis-associated encephalopathy. *Crit. Care* 21(1), 65. doi:10.1186/s13054-017-1643-z

Hernandes, M. S., D'Avila, J. C., Trevelin, S. C., Reis, P. A., Kinjo, E. R., Lopes, L. R., et al. (2014). The role of Nox2-derived ROS in the development of cognitive impairment after sepsis. *J. Neuroinflam.* 11, 36. doi:10.1186/1742-2094-11-36

Hoogland, I. C., Houbolt, C., van Westerloo, D. J., van Gool, W. A., and van de Beek, D. (2015). Systemic inflammation and microglial activation: systematic review of animal experiments. *J. Neuroinflammation* 12, 114. doi:10.1186/s12974-015-0332-6

Hylands-White, N., Duarte, R. V., and Raphael, J. H. (2017). An overview of treatment approaches for chronic pain management. *Rheumatol. Int.* 37(1), 29–42. doi:10.1007/s00296-016-3481-8

Inoue, K., and Tsuda, M. (2018). Microglia in neuropathic pain: cellular and molecular mechanisms and therapeutic potential. *Nat. Rev. Neurosci.* 19(3), 138–152. doi:10.1038/nrn.2018.2

Iwashyna, T. J., Ely, E. W., Smith, D. M., and Langa, K. M. (2010). Long-term cognitive impairment and functional disability among survivors of severe sepsis. *J. Am. Med. Assoc.* 304(16), 1787–1794. doi:10.1001/jama.2010.1553

Jacob, A., Hensley, L. K., Safratowich, B. D., Quigg, R. J., and Alexander, J. J. (2007). The role of the complement cascade in endotoxin-induced septic encephalopathy. *Lab. Invest.* 87(12), 1186–1194. doi:10.1038/labinvest.3700686

Ji, R. R., Berta, T., and Nedergaard, M. (2013). Glia and pain: is chronic pain a gliopathy? *Pain* 154 (Suppl. 1), S10–S28. doi:10.1016/j.pain.2013.06.022

Ji, R. R., Chamessian, A., and Zhang, Y. Q. (2016). Pain regulation by non-neuronal cells and inflammation. *Science* 354(6312), 572–577. doi:10.1126/science.aaf8924

Ji, R. R., Nackley, A., Huh, Y., Terrando, N., and Maixner, W. (2018). Neuroinflammation and central sensitization in chronic and widespread pain. *Anesthesiology* 129(2), 343–366. doi:10.1097/ALN.0000000000002130

Kawakami, M., Hattori, M., Ohashi, W., Fujimori, T., Hattori, K., Takebe, M., et al. (2018). Role of G protein-coupled receptor kinase 2 in oxidative and nitrosative stress-related neurohistopathological changes in a mouse model of sepsis-associated encephalopathy. *J. Neurochem.* 145(6), 474–488. doi:10.1111/jnc.14329

Kawasaki, Y., Zhang, L., Cheng, J. K., and Ji, R. R. (2008). Cytokine mechanisms of central sensitization: distinct and overlapping role of interleukin-1beta, interleukin-6, and tumor necrosis factor-alpha in regulating synaptic and neuronal activity in the superficial spinal cord. *J. Neurosci.* 28(20), 5189–5194. doi:10.1523/JNEUROSCI.3338-07.2008

Kyranou, M., and Puntillo, K. (2012). The transition from acute to chronic pain: might intensive care unit patients be at risk? *Ann. Intensive Care* 2(1), 36. doi:10.1186/2110-5820-2-36

Lemstra, A. W., Groenint Woud, J. C., Hoozemans, J. J., van Haastert, E. S., Rozemuller, A. J., Eikelenboom, P., et al. (2007). Microglia activation in sepsis: a case-control study. *J. Neuroinflam.* 4, 4. doi:10.1186/1742-2094-4-4

Loggia, M. L., Chonde, D. B., Akeju, O., Arabasz, G., Catana, C., Edwards, R. R., et al. (2015). Evidence for brain glial activation in chronic pain patients. *Brain* 138(Pt 3), 604–615. doi:10.1093/brain/awu377

Lutz, B., Marsicano, G., Maldonado, R., and Hillard, C. J. (2015). The endocannabinoid system in guarding against fear, anxiety and stress. *Nat. Rev. Neurosci.* 16(12), 705–718. doi:10.1038/nrn4036

MacLullich, A. M., Beaglehole, A., Hall, R. J., and Meagher, D. J. (2009). Delirium and long-term cognitive impairment. *Int. Rev. Psychiatr.* 21(1), 30–42. doi:10.1080/09540260802675031

Michels, M., Sonai, B., and Dal-Pizzol, F. (2017). Polarization of microglia and its role in bacterial sepsis. *J. Neuroimmunol.* 303, 90–98. doi:10.1016/j.jneuroim.2016.12.015

Michels, M., Steckert, A. V., Quevedo, J., Barichello, T., and Dal-Pizzol, F. (2015a). Mechanisms of long-term cognitive dysfunction of sepsis: from blood-borne leukocytes to glial cells. *Intens. Care Med. Exp.* 3(1), 30. doi:10.1186/s40635-015-0066-x

Michels, M., Vieira, A. S., Vuolo, F., Zapelini, H. G., Mendonca, B., Mina, F., et al. (2015b). The role of microglia activation in the development of sepsis-induced long-term cognitive impairment. *Brain Behav. Immun.* 43, 54–59. doi:10.1016/j.bbi.2014.07.002

Milligan, E. D., and Watkins, L. R. (2009). Pathological and protective roles of glia in chronic pain. *Nat. Rev. Neurosci.* 10(1), 23–36. doi:10.1038/nrn2533

Molnar, L., Fulesdi, B., Nemeth, N., and Molnar, C. (2018). Sepsis-associated encephalopathy: a review of literature. *Neurol. India* 66(2), 352–361. doi:10.4103/0028-3886.227299

Murphy, A. C., Lalor, S. J., Lynch, M. A., and Mills, K. H. (2010). Infiltration of Th1 and Th17 cells and activation of microglia in the CNS during the course of experimental autoimmune encephalomyelitis. *Brain Behav. Immun.* 24(4), 641–651. doi:10.1016/j.bbi.2010.01.014

Pan, C., Si, Y., Meng, Q., Jing, L., Chen, L., Zhang, Y., et al. (2019). Suppression of the RAC1/MLK3/p38 signaling pathway by beta-elemene alleviates sepsis-associated encephalopathy in mice. *Front. Neurosci.* 13, 358. doi:10.3389/fnins.2019.00358

Schramm, P., Klein, K. U., Falkenberg, L., Berres, M., Closhen, D., Werhahn, K. J., et al. (2012). Impaired cerebrovascular autoregulation in patients with severe sepsis and sepsis-associated delirium. *Crit. Care* 16(5), R181. doi:10.1186/cc11665

Shankar-Hari, M., and Rubenfeld, G. D. (2016). Understanding long-Term outcomes following sepsis: implications and challenges. *Curr. Infect. Dis. Rep.* 18(11), 37. doi:10.1007/s11908-016-0544-7

Sharshar, T., Bozza, F., and Chrétien, F. (2014). Neuropathological processes in sepsis. *Lancet Neurol.* 13(6), 534–536. doi:10.1016/s1474-4422(14)70064-x

Sharshar, T., Polito, A., Checinski, A., and Stevens, R. D. (2010). Septic-associated encephalopathy—everything starts at a microlevel. *Crit. Care* 14(5), 199. doi:10.1186/cc9254

Shehabi, Y., Howe, B. D., Bellomo, R., Arabi, Y. M., Bailey, M., Bass, F. E., et al. (2019). Early sedation with dexmedetomidine in critically ill patients. *N. Engl. J. Med.* 380(26), 2506–2517. doi:10.1056/NEJMoa1904710

Shimada, A., and Hasegawa-Ishii, S. (2017). Histological architecture underlying brain-immune cell–cell interactions and the cerebral response to systemic inflammation. *Front. Immunol.* 8, 17. doi:10.3389/fimmu.2017.00017

Sorge, R. E., Mapplebeck, J. C., Rosen, S., Beggs, S., Taves, S., Alexander, J. K., et al. (2015). Different immune cells mediate mechanical pain hypersensitivity in male and female mice. *Nat. Neurosci.* 18(8), 1081–1083. doi:10.1038/nn.4053

Stella, N. (2009). Endocannabinoid signaling in microglial cells. *Neuropharmacology* 56, 244–253. doi:10.1016/j.neuropharm.2008.07.037

Sui, D. M., Xie, Q., Yi, W. J., Gupta, S., Yu, X. Y., Li, J. B., et al. (2016). Resveratrol protects against sepsis-associated encephalopathy and inhibits the NLRP3/IL-1beta Axis in microglia. *Mediat. Inflamm.* 2016, 1045657. doi:10.1155/2016/1045657

Szollosi, D., Hegedus, N., Veres, D. S., Futo, I., Horvath, I., Kovacs, N., et al. (2018). Evaluation of brain nuclear medicine imaging tracers in a murine model of sepsis-associated encephalopathy. *Mol. Imag. Biol.* 20(6), 952–962. doi:10.1007/s11307-018-1201-3

Tanaka, M., Sackett, S., and Zhang, Y. (2020). Endocannabinoid modulation of microglial phenotypes in neuropathology. *Front. Neurol.* 11, 112–154. doi:10.3389/fneur.2020.00087

Tang, H., Ji, M., Zong, M., Jia, M., Luo, D., Zhou, Z., et al. (2018). Individual differences in the brain are associated with resilience versus susceptibility to lipopolysaccharide-induced memory impairment. *Neurosci. Lett.* 662, 361–367. doi:10.1016/j.neulet.2017.10.064

Tian, M., Qingzhen, L., Zhiyang, Y., Chunlong, C., Jiao, D., Zhang, L., et al. (2019). Attractylone attenuates sepsis-associated encephalopathy and cognitive dysfunction by inhibiting microglial activation and neuroinflammation. *J. Cell. Biochem.* 4, 12–27. doi:10.1002/jcb.27983

van der Poll, T., van de Veerdonk, F. L., Scicluna, B. P., and Netea, M. G. (2017). The immunopathology of sepsis and potential therapeutic targets. *Nat. Rev. Immunol.* 17(7), 407–420. doi:10.1038/nri.2017.36

van Eijk, M. M. J., Roes, K. C. B., Honing, M. L. H., Kuiper, M. A., Karakus, A., van der Jagt, M., et al. (2010). Effect of rivastigmine as an adjunct to usual care with haloperidol on duration of delirium and mortality in critically ill patients: a multicentre, double-blind, placebo-controlled randomised trial. *Lancet* 376(9755), 1829–1837. doi:10.1016/s0140-6736(10)61855-7

van Gool, W. A., van de Beek, D., and Eikelenboom, P. (2010). Systemic infection and delirium: when cytokines and acetylcholine collide. *Lancet* 375(9716), 773–775. doi:10.1016/S0140-6736(09)61158-2

Wang, H., Hong, L. J., Huang, J. Y., Jiang, Q., Tao, R. R., Tan, C., et al. (2015). P2RX7 sensitizes Mac-1/ICAM-1-dependent leukocyte-endothelial adhesion and promotes neurovascular injury during septic encephalopathy. *Cell Res.* 25(6), 674–690. doi:10.1038/cr.2015.61

Wang, X., Zhang, Y., Peng, Y., Hutchinson, M. R., Rice, K. C., Yin, H., et al. (2016). Pharmacological characterization of the opioid inactive isomers (+)-naltrexone and (+)-naloxone as antagonists of toll-like receptor 4. *Br. J. Pharmacol.* 173(5), 856–869. doi:10.1111/bph.13394

Westhoff, D., Engelen-Lee, J. Y., Hoogland, I. C. M., Aronica, E. M. A., van Westerloo, D. J., van de Beek, D., et al. (2019). Systemic infection and microglia activation: a prospective postmortem study in sepsis patients. *Immun. Ageing* 16, 18. doi:10.1186/s12979-019-0158-7

Widmann, C. N., and Heneka, M. T. (2014). Long-term cerebral consequences of sepsis. *Lancet Neurol.* 13(6), 630–636. doi:10.1016/s1474-4422(14)70017-1

Wolf, S. A., Boddeke, H. W. G. M., and Kettenmann, H. (2017). Microglia in physiology and disease. *Annu. Rev. Physiol.* 79(1), 619–643. doi:10.1146/annurev-physiol-022516-034406

Wu, Q., Zhao, Y., Chen, X., Zhu, M., and Miao, C. (2018). Propofol attenuates BV2 microglia inflammation via NMDA receptor inhibition. *Can. J. Physiol. Pharmacol.* 96(3), 241–248. doi:10.1139/cjpp-2017-0243

Ye, B., Tao, T., Zhao, A., Wen, L., He, X., Liu, Y., et al. (2019). Blockade of IL-17a/IL-17R pathway protected mice from sepsis-associated encephalopathy by inhibition of microglia activation. *Mediat. Inflamm.* 2019, 8461725. doi:10.1155/2019/8461725

Younger, J., and Mackey, S. (2009). Fibromyalgia symptoms are reduced by low-dose naltrexone: a pilot study. *Pain Med.* 10(4), 663–672. doi:10.1111/j.1526-4637.2009.00613.x

Conflict of Interest: The authors declare that the research was conducted in the absence of any commercial or financial relationships that could be construed as a potential conflict of interest.

frontiers in Pharmacology

ORIGINAL RESEARCH
published: 13 January 2021
doi: 10.3389/fphar.2020.594479

Hemokinin-1 as a Mediator of *Arthritis*-Related Pain via Direct Activation of Primary Sensory Neurons

Éva Borbély[1,2†], Ágnes Hunyady[1,2†], Krisztina Pohóczky[1,2,3], Maja Payrits[1,2], Bálint Botz[1,4], Attila Mócsai[5], Alexandra Berger[6], Éva Szőke[1,2†] and Zsuzsanna Helyes[1,2,7†]*

[1]*János Szentágothai Research Centre and Centre for Neuroscience, University of Pécs, Pécs, Hungary,* [2]*Department of Pharmacology and Pharmacotherapy, Medical School, University of Pécs, Pécs, Hungary,* [3]*Department of Pharmacology, Faculty of Pharmacy, University of Pécs, Pécs, Hungary,* [4]*Department of Medical Imaging, Medical School, University of Pécs, Pécs, Hungary,* [5]*Department of Physiology, Semmelweis University, Budapest, Hungary,* [6]*Princess Margaret Cancer Centre, University Health Network, Toronto, ON, Canada,* [7]*PharmInVivo Ltd., Pécs, Hungary*

The tachykinin hemokinin-1 (HK-1) is involved in immune cell development and inflammation, but little is known about its function in pain. It acts through the NK1 tachykinin receptor, but several effects are mediated by a yet unidentified target. Therefore, we investigated the role and mechanism of action of HK-1 in arthritis models of distinct mechanisms with special emphasis on pain. Arthritis was induced by i.p. K/BxN serum (passive transfer of inflammatory cytokines, autoantibodies), intra-articular mast cell tryptase or Complete Freund's Adjuvant (CFA, active immunization) in wild type, HK-1- and NK1-deficient mice. Mechanical- and heat hyperalgesia determined by dynamic plantar esthesiometry and increasing temperature hot plate, respectively, swelling measured by plethysmometry or micrometry were significantly reduced in HK-1-deleted, but not NK1-deficient mice in all models. K/BxN serum-induced histopathological changes (day 14) were also decreased, but early myeloperoxidase activity detected by luminescent *in vivo* imaging increased in HK-1-deleted mice similarly to the CFA model. However, vasodilation and plasma protein extravasation determined by laser Speckle and fluorescent imaging, respectively, were not altered by HK-1 deficiency in any models. HK-1 induced Ca^{2+}-influx in primary sensory neurons, which was also seen in NK1-deficient cells and after pertussis toxin-pretreatment, but not in extracellular Ca^{2+}-free medium. These are the first results showing that HK-1 mediates arthritic pain and cellular, but not vascular inflammatory mechanisms, independently of NK1 activation. HK-1 activates primary sensory neurons presumably via Ca^{2+} channel-linked receptor. Identifying its target opens new directions to understand joint pain leading to novel therapeutic opportunities.

Keywords: experimental arthritis, arthritic pain, primary sensory neuron, neuroinflammation, tachykinin, *in vivo* optical imaging

OPEN ACCESS

Edited by:
Francesco De Logu,
University of Florence, Italy

Reviewed by:
Marco Sisignano,
Institut für Klinische Pharmakologie Universitätsklinikum Frankfurt, Germany
Raquel Tonello,
New York University, United States

****Correspondence:***
Agnes Hunyady
agnes.hunyady@gmail.com

†These authors have contributed equally to this work

Specialty section:
This article was submitted to Inflammation Pharmacology, a section of the journal Frontiers in Pharmacology

Received: *13 August 2020*
Accepted: *09 December 2020*
Published: *13 January 2021*

Citation:
Borbély É, Hunyady Á, Pohóczky K, Payrits M, Botz B, Mócsai A, Berger A, Szőke É and Helyes Z (2021) Hemokinin-1 as a Mediator of Arthritis-Related Pain via Direct Activation of Primary Sensory Neurons. Front. Pharmacol. 11:594479. doi: 10.3389/fphar.2020.594479

INTRODUCTION

Rheumatoid arthritis (RA) is the most common autoimmune disorder of the joints characterized by chronic inflammation and severe pain. Although the inflammation can be effectively controlled by nonsteroidal anti-inflammatory drugs (NSAIDs), steroids, disease-modifying antirheumatic drugs (DMARDs) and biologic agents (Sparks, 2019), pain is often resistant to these drugs

(McWilliams and Walsh, 2019). Persistent pain has resulted in an increased use of opioids among RA patients (Day and Curtis, 2019), though opioids are not effective in all cases (Chancay et al., 2019) suggesting more complex pain pathomechanisms in RA and making pain management an unmet medical need.

The joints are densely innervated by capsaicin-sensitive peptidergic sensory nerves (Donaldson et al., 1995) expressing, among others, the transient receptor potential vanilloid 1 (TRPV1) and ankyrin 1 (TRPA1) ion channels activated by a broad range of inflammatory mediators (Pinho-Ribeiro et al., 2017). These nerves play an important role in complex neuro-vascular-immune interactions resulting in chronic pain (Sun and Dai, 2018). Recently, intensive investigations have been initiated to reveal sensitization processes at molecular (Sommer and Kress, 2004) and histological levels alike (Ebbinghaus et al., 2019) that convert inflammatory to neuropathic pain and contribute to persistent arthritic pain. Exploration of its pathophysiological processes is hindered by the fact that no single animal model can mimic every aspect of RA, conclusions drawn using different models might not necessarily apply to the human disease (Krock et al., 2018). Studying the role of endogenous molecules of the sensory-vascular-immune interactions is essential to identify key mediators and potential novel drug targets.

Tachykinins are a family of neuropeptides that have been shown to play important roles in immune mechanisms, inflammatory vascular changes and pain (Onaga, 2014). Their best-known member, substance *p* (SP) acts mainly through the tachykinin neurokinin-1 receptor (NK1R), but can also bind to the other two tachykinin receptors, NK2R and NK3R, with much lower affinities. NK1R plays a key role in the wind-up mechanism in the spinal dorsal horn (Herrero et al., 2000), which is a crucial element in central sensitization leading to chronic pain. SP through NK1R also sensitizes the peripheral terminals of nociceptors (Nakamura-Craig and Smith, 1989). NK1R antagonists were developed as analgesic drug candidates, but despite promising preclinical results, they did not prove to be effective in human pain conditions. Therefore, tachykinins fell outside the focus of pain research until the discovery of hemokinin-1 (HK-1) in 2000 (Zhang et al., 2000) beginning a new era in this field. HK-1, encoded by the preprotachykinin-4 gene (*Tac4*), was first isolated from bone marrow B-cells (Zhang et al., 2000), and plays a role in T-lymphopoesis as well (Zhang and Paige, 2003). HK-1 consists of 11 amino acids, it has a close structural resemblance to SP, with seven matching aminoacids. HK-1 has the highest affinity to the NK1R similarly to SP (Morteau et al., 2001), but it has been proven that HK-1 can exert effects through other, so far unidentified target(s) (Borbély and Helyes, 2017). Our research group was the first to describe the mediator role of HK-1 in the chronic adjuvant-induced mouse model of inflammation and related nociception (Borbély et al., 2013). Recently, we proved that HK-1 is involved not only in inflammatory, but also nerve ligation-induced neuropathic pain, which develops independently of inflammation with prominent central sensitization mechanisms (Hunyady et al., 2019). The present work focused on investigating the involvement of HK-1 in arthritis models of distinct mechanisms with special emphasis on pain, nociceptive sensory neurons and the molecular mechanism of action.

MATERIALS AND METHODS

Animals and Ethics

Experiments were performed on inbred 12–18-week-old (25–30 g) male *Tac4* gene-deficient (*Tac4*$^{-/-}$) knockout (KO) and NK1 receptor-deleted (*Tacr1*$^{-/-}$) mice and their C57BL/6J wild type controls (WT) purchased from Charles-River Ltd. (Hungary). The original *Tacr1*$^{-/-}$ breeding pairs (De Felipe et al., 1998) were obtained from the University of Liverpool, United Kingdom, The *Tac4*$^{-/-}$ strain was donated by A. Berger (Berger et al., 2010). Both KO strains were generated on C57BL/6J background and backcrossed to homozygosity for over five generations. The mutated allele's germline transmission and excision of the selection cassette were verified by PCR analysis. The experimenters were blinded from the genotype and treatments in all cases. Animals were bred and kept in the conventional Laboratory Animal House of the Department of Pharmacology and Pharmacotherapy, University of Pécs at 24–25°C, 12 h light/dark cycles on wood shaving bedding in a standard polycarbonate cage with two to six mice per cage and provided with standard rodent diet and water ad libitum.

All experiments were carried out according to the European Communities Council Directive of 2010/63/EU, Consideration Decree of Scientific Procedures of Animal Experiments (243/1988) and Ethical Codex of Animal Experiments and to the NIH guidelines (Guide for the Care and Use of Laboratory Animals, NIH Publication 86–23). The project was approved by the Ethics Committee on Animal Research of the University of Pécs and license was provided (BA 02/2000–2/2012).

Serum Transfer Arthritis

K/BxN arthritogenic and BxN non-arthritogenic sera were harvested as described earlier (Jakus et al., 2010). Arthritis was induced by intraperitoneally (i.p.) injecting 150–150 µL of the arthritogenic serum on the 0 and 3 day of the experiment. The control groups received the same amount of non-arthritogenic serum. The mechanonociceptive threshold, heat threshold and cold tolerance were measured (methods described below). Paw edema was quantified using plethysmometry (Ugo Basile 7140), bodyweight was monitored after the first serum administration as a parameter of general well-being. Weight loss was given as the percentage of lost weight compared to pretreatment control values. Arthritis severity was scored using a semiquantitative visual scale where 0–0.5 was no change and 10 was maximal inflammation (Jakus et al., 2010). Swelling and redness of all four feet were considered for the score. To assess joint function mice were placed on a horizontal grid, the grid was turned upside-down and the latency to fall was measured. The grasping ability needed in this test correlates with the joint function. *In vivo* imaging was performed with IVIS Lumina II (PerkinElmer; 60 s acquisition, F/Stop = 1, Binning = 8) before treatment and 2 and 6 days after to quantify plasma extravasation and

myeloperoxidase (MPO) activity, as described below. We chose these time points to collect data from the acute phase on day 2 when the vascular inflammatory components are predominant, and from the chronic phase on day 6, when the cellular inflammatory mechanisms are more remarkable (Horváth et al., 2016). On the 14th day after serum administration tibiotarsal joints were removed for histological staining with Safranin stain. Fibroblast proliferation, leukocyte invasion and thickness of synovium were evaluated with 0–3 score depending on severity, the maximum possible score being 9.

Mast Cell Tryptase (MCT)-Induced Acute Knee Monoarthritis

MCT can be found in abundance in synovial fluid contributing to the inflammation in different types of arthritis (RA, osteoarthritis, spondyloarthritis) by activating the protease-activated receptor 2 (PAR2) on the sensory nerves and inflammatory cells. To investigate acute inflammatory synovial microcirculatory changes, 1 h after guanethidine (12 mg/kg i. p., Sigma) pretreatment, MCT (Merck Millipore) was applied topically to the synovial membrane of the knee joint (12 μg/ml, 20 μL), after removing the skin under ketamine- and xylazine-induced (100 mg/kg and 10 mg/kg i. p, respectively) anesthesia. Contralateral knee joint was treated with 0.9% saline. Blood flow was continuously monitored by laser Speckle imaging for 40 min after the treatment, and the differences compared to the baseline values of the respective area were calculated. To measure acute inflammatory hyperalgesia and edema, MCT was injected intra-articularly (20 μL, 12 μg/ml) into the right knee joint. The paw mechanonociceptive threshold and knee diameter were measured at 2, 4, and 6 h post-injection.

Complete Freund's Adjuvant (CFA)-Induced Subacute Knee Monoarthritis

CFA is heat-killed *Mycobacterium tuberculosis* suspended in paraffin oil (1 mg/ml; Sigma-Aldrich) which is taken up by macrophages, activate their reactive oxygen species, cytokine and enzyme generation within a few hours causing localized arthritis of the injected joint without severe systemic symptoms.

CFA (20 μL) was injected into the right mouse knee joint under ketamin-xylazine anesthesia as described above. Contralateral knee joint was treated with 20 μL 0.9% saline. Paw mechanonociceptive threshold and antero-posterior knee diameter were measured 2, 6, and 24 h after CFA administration, changes were expressed as percentage of change compared to the pre-injection values. MPO activity was measured 24 h after treatment.

Measurement of the Mechanonociceptive and Heat Thresholds

The mechanonociceptive threshold was measured with the dynamic plantar esthesiometer (DPE; Ugo Basile 37000) before (to determine baseline nociceptive threshold) and after treatment. The post-treatment values are shown as the percentage of threshold-decrease of the individual mouse compared to its baseline thresholds. Heat threshold was determined as the temperature where the animal showed nocifensive behavior (shaking, licking, lifting of the hind paw) on increasing temperature hot plate (IITC Life Sciences), the cut-off value was set at 53 °C. Cold hyperalgesia was given as the latency to paw-withdrawal from 0°C water.

In vivo Optical Imaging

Mice were anesthetized with ketamine-xylazine anesthesia for *in vivo* imaging with IVIS Lumina II (PerkinElmer; 120s acquisition, F/stop = 1, Binning = 8) instrument and Living Image® software (PerkinElmer). Luminol sodium salt (5-amino-2,3-dihydro-1,4-phthalazine-dione; 150 mg/kg) injection was given i. p. in sterile PBS solution for MPO imaging. MPO from neutrophil granulocytes produces reactive oxygen species which interact with luminol and result in luminescent signals which we measured 10 min after administration. Luminescence was expressed as total radiance (total photon flux/s) in identical Regions of Interests (ROIs) around the joints.

Inflammatory vascular leakage was evaluated by fluorescence imaging with the Fluorescent Molecular Tomography (FMT) 2000 system (PerkinElmer Ltd.) using the 680 nm laser of the equipment. A micellar formulation of the fluorescent IR-676 dye (Spectrum-Info) dissolved in a 5 w/v% aqueous solution of Kolliphor HS 15 (polyethylene-glycol-15-hydroxystearate; Sigma-Aldrich) was given i. v. in a 0.5 mg/kg dose under ketamine-xylazine anesthesia. The measurement was carried out 20 min afterward dye administration with fluorescence expressed as the calculated amount of fluorophore (pmol) (Botz et al., 2015) in identical Regions of Interests (ROIs) around the ankle joints.

Tissue Preparation and Protocol for qPCR

L3-L5 lumbar spinal cord and the respective dorsal root ganglia (DRG; total of six DRGs pooled per mouse) were obtained from WT mice 6 days after treatment when behavioral results showed the greatest difference between WT and *Tac4*$^{-/-}$ animals. Mice were divided into three groups: K/BxN treated arthritic (n = 8), BxN serum treated control (n = 5) and intact control (n = 7). Spinal cord samples of *Tac4*$^{-/-}$ mice served as negative (n = 3), while inguinal lymph nodes from WT mice served as positive controls (n = 2).

Tissue samples were harvested after cervical dislocation and placed immediately into 500 μL TRI reagent (Molecular Research Center, Inc.), snap-frozen on dry ice, then stored on -80°C until processing.

Tissue samples were thawed out on ice and homogenized in TRI reagent. After homegenization, total RNA was extracted using Direct-zol RNA MicroPrep (Zymo Research) according to the manufacturer's instructions (Aczél et al., 2020). The quantity of the extracted RNA was examined using Nanodrop ND-1000 Spectrophotometer V3.5 (Nano-Drop Technologies, Inc.). RNA samples were treated with dnase I in order to remove contamining genomic DNA, and 500 ng of RNA was reverse transcribed into cDNA using High Capacity cDNA

Reverse Transcription Kit (Thermo Fisher Scientific). SensiFAST™ Probe Lo-ROX Kit (Meridiane Bioscience, Memphis, United States) was used according to the manual in the QuantStudio five Real-Time PCR System (Thermo Fisher Scientific). Transcripts of the reference gene *glucuronidase beta* (*Gusb*, Kecskés et al., 2020) and the target gene *Tac4* were evaluated using FAM-conjugated specific probes (Mm01197698_m1, and Mm00474083_m1 respectively, Thermo Fisher Scientific). The gene expression was calculated using ΔΔCt method (Pfaffl, 2001).

Primary Cultures of Trigeminal Ganglion (TG) Neurons

TG cultures were prepared from neonatal NMRI mice. Ganglia were excised in ice-cold phosphate-buffered saline (PBS), incubated in PBS containing collagenase Type XI (1 mg/ml) and then in PBS with deoxyribonuclease I (1,000 units/ml) for 8 min. Cells were plated on poly-D-lysin-coated glass coverslips in a medium containing Dulbecco's-Modified Eagle Medium-low glucose (D-MEM), 5% horse serum, 5% newborn calf serum, 5% fetal bovine serum, 0.1% penicillin-streptomycin, 200 ng/ml nerve growth factor (NGF). Cells were maintained at 37°C in a humidified atmosphere with 5% CO2 (Szoke et al., 2010).

Ratiometric Technique of Intracellular Free Calcium Concentration ([Ca^{2+}]i) Measurement with the Fluorescent Indicator Fura-2 AM.

One-two-day-old neurons were incubated for 30 min at 37°C with 1 μM of fluorescent Ca^{2+} indicator dye, fura-2-AM. Cells were washed with extracellular solution (ECS). Calcium transients were detected with microfluorimetry as described elsewhere (Szoke et al., 2010). Fluorescent imaging was performed with an Olympus LUMPLAN FI/x20 0.5 W water immersion objective and a digital camera (CCD, SensiCam PCO) and a Monochromator (Polychrome II., Till Photonics) (generated light: 340 and 380 nm, emitted light: 510 nm). Axon Imaging Workbench 2.1 (AIW, Axon Instruments) software was used, R = F340/F380 was monitored, data were subsequently processed by the Origin software version 7.0 (Originlab Corp.). Ratiometric response peak magnitude was measured. Capsaicin (330 nM), AITC (100 μM), HK-1 (500 nM, 1 μM) and SP (500 nM, 1 μM) were administered during the experiments. CP99994, AMG 9810 and HC 030031 were administered in 10 μM concentration.

Drugs and Chemicals

AITC (Sigma) was dissolved in dimethyl sulfoxide (DMSO) (Sigma) to obtain 10 mM stock solution. Further dilutions were made with ECS solution to reach final concentrations of 100 μM. Capsaicin (Sigma) was dissolved in DMSO to obtain a 10 mM stock solution. Further dilutions were made with ECS or Hank's solution to reach final concentrations of 330 or 100 nM, respectively. Penicillin-streptomycin was purchased from Gibco. D-MEM-low glucose, collagenase type XI, deoxyribonuclease I, horse serum, newborn calf serum, fetal bovine serum, poly-D-lysine, glycine, NGF, pertussis toxin (PTX), SP, HK-1 were purchased from Sigma. CP99994, AMG 9810 and HC 030031 were purchased from Tocris.

Statistical Analysis

The treatments were not randomized within cages to prevent control animals from harming the arthritic animals. Results are expressed as the means ± SEM of n = 6–10 mice per group in case of *in vivo* functional tests. Data obtained in these experiments were analyzed with repeated measures two-way ANOVA followed by Bonferroni's post-test with GraphPad Prism 5 software. In all cases $p < 0.05$ was accepted as statistically significant.

RESULTS

HK-1 Mediates Mechanical Hyperalgesia, Paw Edema and Decrease in Heat Threshold in Chronic Immune Arthritis

Compared to pre-treatment control values, a significant decrease in pain threshold developed in WT mice by the 5th day of the experiment (-33.5 ± 4.1%). This spontaneously resolved by the end of the 3rd week. *Tac4*$^{-/-}$ mice showed significantly milder decrease in the pain threshold (-19.4 ± 3.8% on day 5) throughout the entire experiment (**Figure 1A**). The decrease in heat threshold began in WT mice at the 4th day (47.6 ± 1.3°C) and was significantly less severe in *Tac4*$^{-/-}$ mice (50.6 ± 0.8°C) (**Figure 1B**).

Paw edema developed by the 3rd day of the experiment (43.8 ± 7.2% in WT), and spontaneously resolved by 2 weeks after serum administration with significantly milder edema seen in *Tac4*$^{-/-}$ mice (**Figure 1C**). Decrease in cold tolerance, body weight and time spent on grid occurred in the experiment, but gene deletion resulted in no difference (**Figures 1D–F**). Change in mechanonociceptive threshold, arthritis score, paw volume, cold tolerance, body weight and time spent on grid in NK1R deficient mice showed no difference compared to WT mice (**Supplementary Figure S1**).

HK-1 Decreases MPO-Activity in K/BxN Serum-Transfer Arthritis

Tac4$^{-/-}$ mice showed a marked increase in MPO-activity 2 days after serum administration (6,16 × 105 ± 6,83 × 104 p/s), whereas in WT mice it became significant on the 4th day (409,917 ± 56729) (**Figure 2A**). An increase in plasma extravasation was detectable in both groups on the 2nd and 6th day, but no effect of the gene-deletion could be observed (**Figure 2B**). Representative pictures of MPO-activity can be seen on **Figure 2C**.

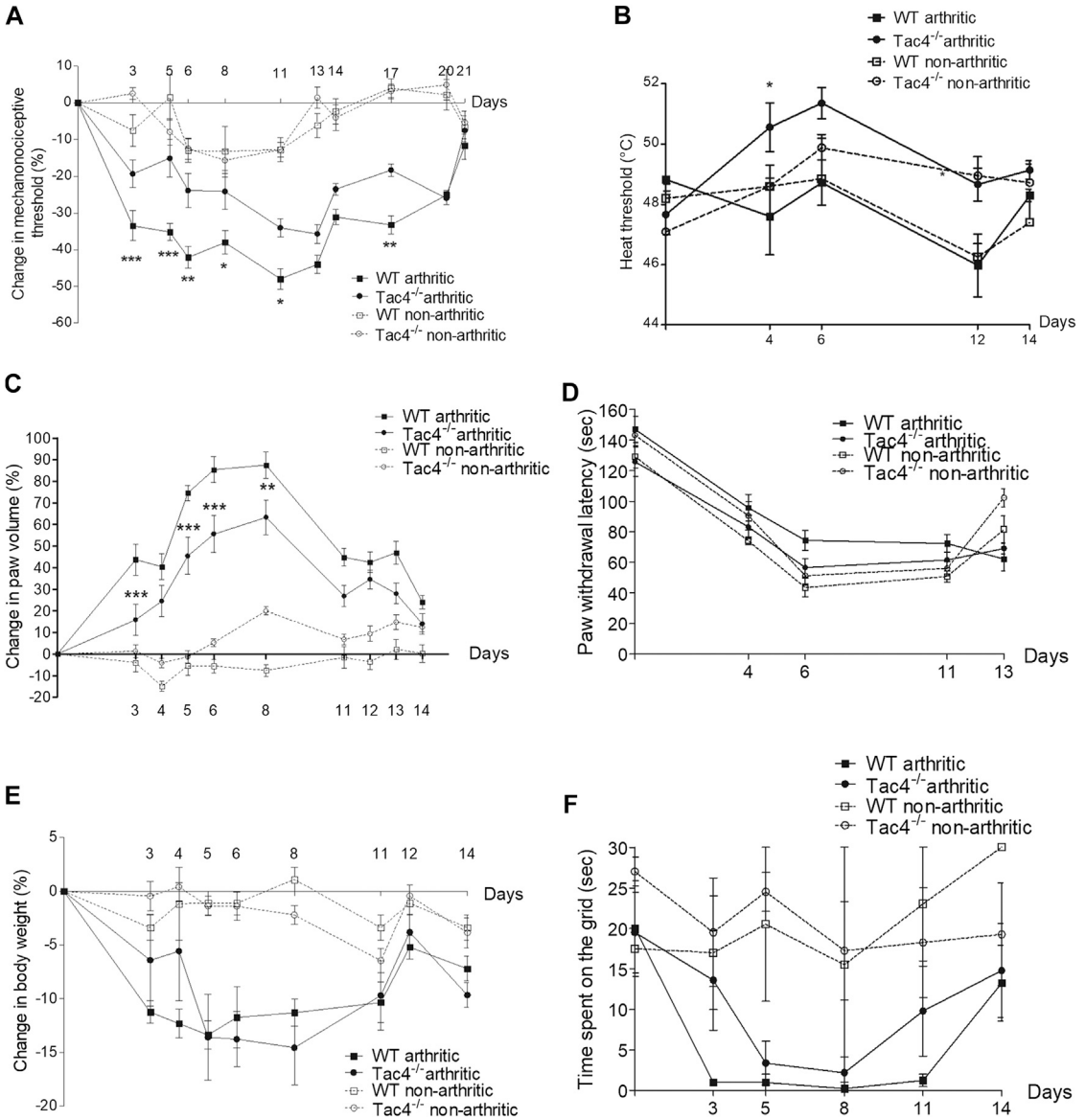

FIGURE 1 | Change in mechanonociceptive threshold **(A)**, heat threshold **(B)**, paw volume **(C)**, cold tolerance **(D)**, body weight **(E)** and time spent on grid **(F)** in K/BxN serum-induced arthritis of wild type (WT) and hemokinin-1-deficient (*Tac4*$^{-/-}$) mice in comparison with BxN serum-treated non-arthritic groups (n = 4–10 per group; $^{*}p < 0.05$, $^{**}p < 0.01$, $^{***}p < 0.001$ vs. arthritic WT, repeated measures two-way ANOVA + Bonferroni's post test).

HK-1 Increases Histopathological Arthritis Severity

On the 14th day of the experiment WT mice had a severity score of 4.0 ± 0.5 out of a maximum of nine points, while *Tac4*$^{-/-}$ mice had a significantly lower score of 2.5 ± 0.5 (**Figure 3**).

Tac4 mRNA Expression in DRG and Spinal Cord

Tac4 mRNA showed a stable expression in the DRG throughout the experiment, with a slight, non-significant decrease on day 6 (**Supplementary Figure S3**). In dorsal spinal cord samples, *Tac4* specific signals were not detectable. The specificity of the reaction was proved by using inguinal lymph nodes as positive control. RNA samples of *Tac4*$^{-/-}$ mice served as negative controls, in which samples we did not observe any amplification products with the applied probes.

HK-1 Mediates Mechanical Hyperalgesia and Knee Edema in MCT-Induced Acute Monoarthritis

Mechanical hyperalgesia developed in WT mice 2 days after MCT administration (-11.8 ± 4.0%), while knee edema developed on the 4th day (13.3 ± 1.6). Both parameters were significantly less

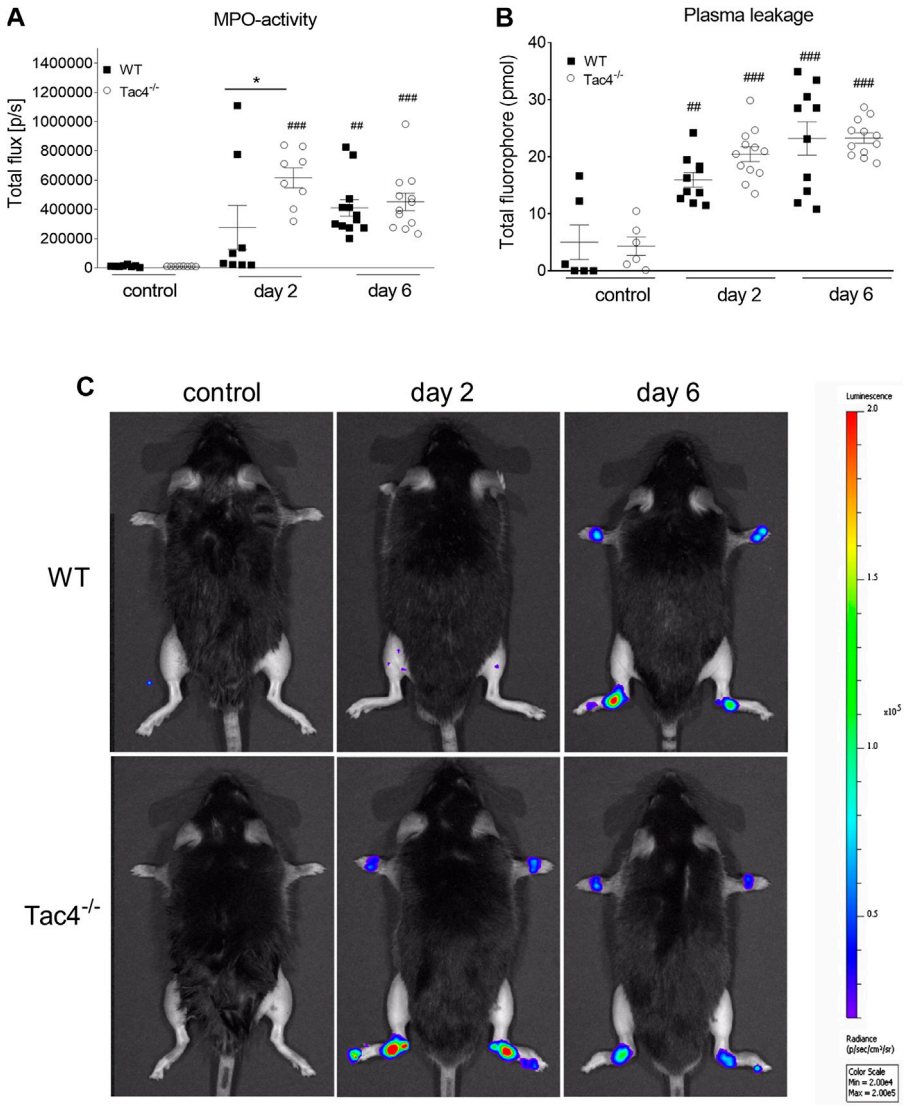

FIGURE 2 | Quantitative evaluation of MPO-activity **(A)** and IR-676 dye extravasation **(B)** in K/BxN arthritogenic serum-treated wild type (WT) and hemokinin-1-deficient (*Tac4*$^{-/-}$) mice. Representative images of MPO-activity **(C)**. Box plots demonstrate medians with the upper and lower quartiles and all individual data points; *n* = 6–12 per group; **p* < 0.05 vs. WT, ##*p* < 0.01, ###*p* < 0.001 vs. control (one-way ANOVA + Bonferroni's post test).

severe in *Tac4*$^{-/-}$ mice. Increase in blood flow was detectable in the first 40 min after treatment but showed no significant difference between the groups (**Figure 4**).

HK-1 Mediates Mechanical Hyperalgesia and Knee Edema, but Decreases MPO Activity in CFA-Induced Subacute Knee Inflammation

Mechanical hyperalgesia and knee edema were detectable 2, 6 and 24 h after the CFA administration. *Tac4*$^{-/-}$ mice had a significantly milder mechanical hyperalgesia at every time point and less severe knee edema at 24 h. *Tac4*$^{-/-}$ mice showed a significant increase in MPO-activity (457,125 ± 94397) (**Figure 5**). Changes in mechanonociceptive threshold and knee volume did not show significant difference to WT mice in NK1R deficient mice (**Supplementary Figure S2**).

HK-1 Directly Activates Primary Nociceptive Sensory Neurons

First, the effects of HK-1 and SP were investigated. Both peptides in 500 nM (**Figures 6A–E**) and SP in 1 μM concentration (data not shown) had no effect on Ca^{2+}-influx, but 1 μM HK-1 caused remarkable Ca^{2+}-influx (R = 0.67 ± 0.07) in 26.39 ± 4.5% of the neurons (19 out of 72). In the next step, we investigated the mechanism of HK-1 action and the characteristics of the Ca^{2+}-signal. The NK1 receptor antagonist CP99994 did not influence the HK-1 response, 20.93 ± 3.8% of the cells (9 out of 43) responded with Ca^{2+}-influx (R = 0.62 ± 0.08). This was

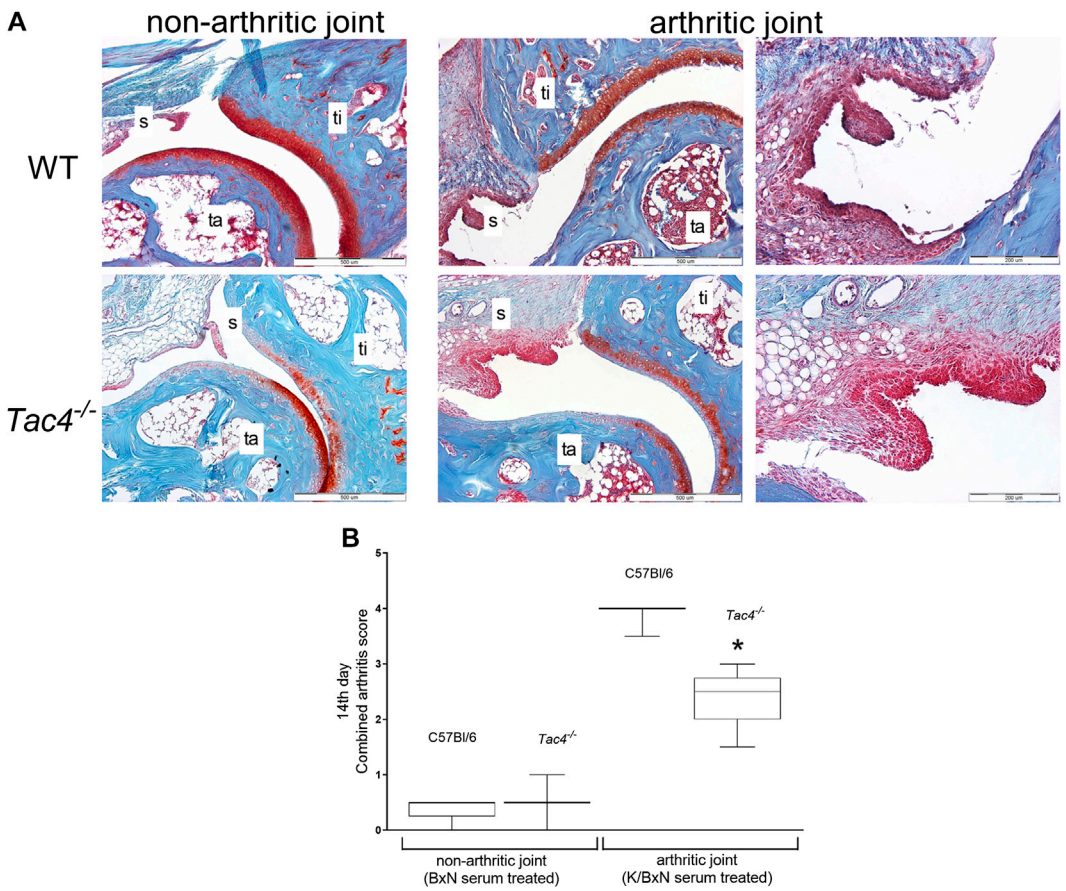

FIGURE 3 | Representative histopathological pictures of safranin O-stained tibiotarsal joint showing ×100 and ×200 magnifications with 500 and 200 μm scale bars, respectively. ti = tibia, ta = tarsus, s = synovium **(A)**. Semiquantitative histopathological score of K/BxN serum treated wild type (WT) and hemokinin-deficient (*Tac4*$^{-/-}$) arthritic mice in comparison with non-arthritic controls. Box plots demonstrate the medians with upper and lower quartiles of n = three to five per group (*p < 0.05 vs. WT, Mann-Whitney test) **(B)**.

similar in neurons of NK1R gene-deleted mice (21.4 ± 3.5%, nine out of 42 responsive cells, R = 0.49 ± 0.04). The G-protein-coupled receptor (GPCR) blocker PTX influenced neither the ratio of the responding neurons (24.49 ± 3.6%; 12 out of 49) nor the extent of the response (R = 0.74 ± 0.03) to HK-1. In order to investigate potential HK-1-induced Ca^{2+}-release from intracellular stores as a consequence of PTX-insensitive GPCR mechanism, we did measurements using Ca^{2+} free ECS. No Ca^{2+}-signal was detected in this condition indicating that HK-1 evokes Ca^{2+}-influx from the extracellular space. The response to HK-1 was detected in the presence of the TRPV1 antagonist AMG8910, 22.7 ± 4% of the cells (5 out of 22) responded with Ca^{2+}-influx (R = 0.7 ± 0.28) and the TRPA1 antagonist HC 030031, 19.2 ± 4.7% of the cells (5 out of 26) responded with Ca^{2+}-influx (R = 0.32 ± 0.26).

In the next experiment four or five repeated treatments of capsaicin on the same cultured sensory neurons were performed, and the effect of 500 nM HK-1 and SP was investigated on capsaicin-evoked Ca^{2+}-influx. The first application of 330 nM capsaicin induced transient Ca^{2+}-accumulation which gradually decreased in response to the second capsaicin stimulus due to TRPV1 (transient receptor potential cation channel subfamily V member 1) desensitization. Meanwhile, both HK-1 and SP administered in separate cultures after the second capsaicin stimulus diminished the desensitization as shown by the third and fourth capsaicin-evoked responses (**Figures 6F–I**).

DISCUSSION

Here we provide the first evidence for an important role of HK-1 in pain transmission using different arthritis models. This is likely to be mediated by direct activation of primary sensory neurons via NK1R-independent, PTX-insensitive, but extracellular Ca^{2+}-dependent mechanism. Besides its key importance in pain development, HK-1 has a complex regulatory function in joint inflammatory processes: it mediates edema formation and histopathological alterations including inflammatory cell accumulation, but inhibits early neutrophil/macrophage-dependent MPO-activity increase in the chronic model.

K/BxN induced arthritis is a widely accepted chronic passive transfer disease model (Malcangio, 2020), MCT is an important

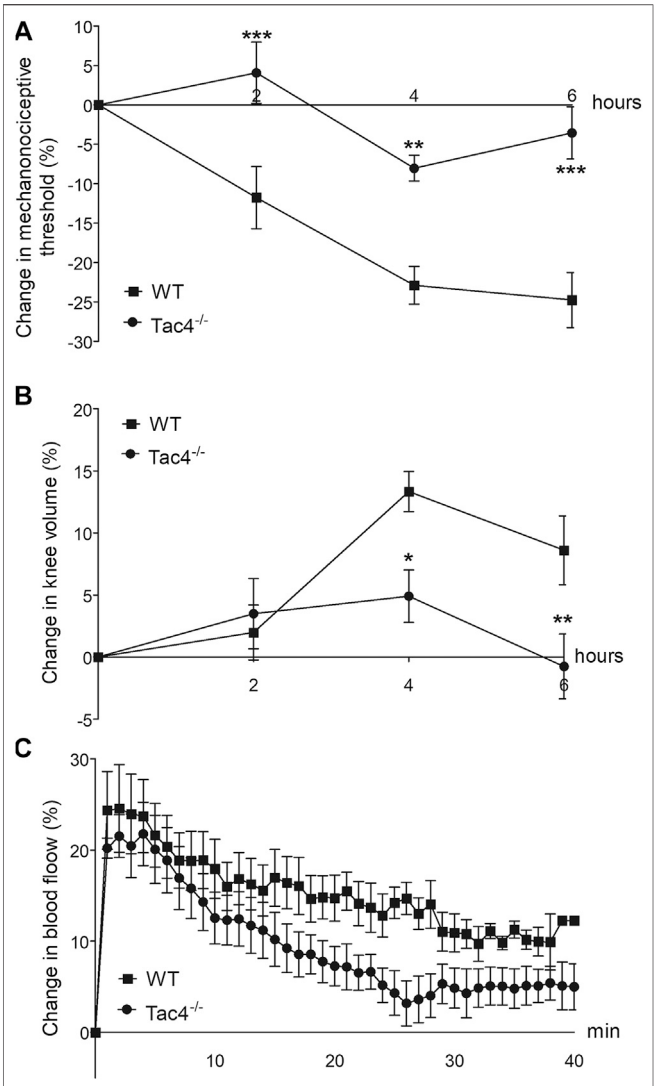

FIGURE 4 | Changes in mechanonociceptive threshold **(A)**, knee diameter **(B)** and blood flow **(C)** in mast cell tryptase-induced acute arthritis of wild type (WT) and hemokinin-1-deficient (*Tac4*$^{-/-}$) mice. Data points demonstrate the means ± SEM of n = 5–10 per group; $^{*}p < 0.05$, $^{**}p < 0.01$, $^{***}p < 0.001$ vs. WT (repeated measures two-way ANOVA + Bonferroni's post test).

local mediator of inflammation (Kobayashi and Okunishi, 2002), mediating its effects through sensory neurons (Borbély et al., 2016), and acute CFA (Billiau and Matthys, 2001) induced arthritis is initiated by macrophages. Using these three methods we could obtain a more detailed picture on how HK-1 influences the development of joint inflammation and related pain.

The deficiency of HK-1, but not the NK1R resulted in significantly decreased swelling in the acute models and also in the early phase of the chronic experiment. Plasma leakage was not altered by HK-1 on days 2 and 6, but only venular fenestration and dye extravasation at the timepoints of the examination can be detected with the applied *in vivo* fluorescent imaging technique (Botz et al., 2015). This is one component of the edema formation, but it does not exclusively explain paw swelling differences at the respective observation timepoints mainly due to different kinetics of the different components of the vascular changes (vasodilation and leakage). We found no difference in edema formation in the chronic adjuvant-induced active immunization-based model in HK-1 or NK1R deficient mice (Borbély et al., 2013), therefore, the edemogenic action of HK-1 seems to develop in a much earlier phase of the inflammatory process. The arteriolar vasodilation and microcirculation-increase was not affected either by HK-1-deletion in the MCT-model, which suggests that HK-1 is not a predominant regulator of the vascular (Borbély et al., 2013) functions.

Cellular inflammatory response in the chronic arthritis model, as shown by the histopathological arthritis score, was significantly reduced in HK-1-deficient mice. These results are supported by the well-established immunoregulatory role of HK-1. B-cells play an important role in RA, restricting their function has been shown to ameliorate autoimmune arthritis (Tóth et al., 2019), and HK-1 plays a critical role in the development of these cells (Zhang et al., 2000). It also influences monocyte/macrophage development (Berger et al., 2007) and neutrophils *in vitro* (Klassert et al., 2008), which play a role in arthritis development (Smith and Haynes, 2002). We found that despite reduced functional and morphological inflammatory alterations, MPO increase related to neutrophil and macrophage activation occurred earlier (on day 2) in the absence of HK-1. This virtual contradiction can be explained by data showing that although MPO is generally known as a mediator of tissue damage and inflammation, it has been shown to prevent inflammation as well (Arnhold and Flemmig, 2010). The elevation of MPO especially in the early phase of the inflammatory cascade is considered to be protective, though the mechanism is not well understood. MPO products have been suggested to downregulate innate immunity, facilitate the switch to adaptive immunity and inhibit T-cell reponses (Prokopowicz et al., 2012). We have seen similar relation between elevated MPO and decreased inflammatory parameters in a previous study (Horváth et al., 2016). Since HK-1 and MPO are both produced by neutrophils, they might have direct interactions, but these have not yet been studied. There is limited evidence about the involvement of HK-1 in pain which, in agreement with our present results, found it to be pro-nociceptive. Intracerebroventricular administration of low dose (1–10 pmol) HK-1 caused nocifensive behavior, while high dose (≥0.1 nmol) caused analgesia, all of which could be counteracted by an NK1R antagonist, as well as opioid antagonists (Fu et al., 2005). Other studies have shown that lumbar intrathecal administration of 0.1 nmol HK-1 caused pain reaction in mice which could be inhibited by an NMDA receptor antagonist (Watanabe et al., 2016), but not an NK1R antagonist (Watanabe et al., 2010). These results suggest that high doses of HK-1 might have non-specific actions resulting in divergent outcomes. Our earlier paper provided evidence that HK-1 has an important role in neuropathic pain and microglia activation (Hunyady et al., 2019). Other studies found that HK-1 mRNA expression increases in the dorsal spinal cord of neuropathic rats which could be blocked by inhibiting microglia activation and

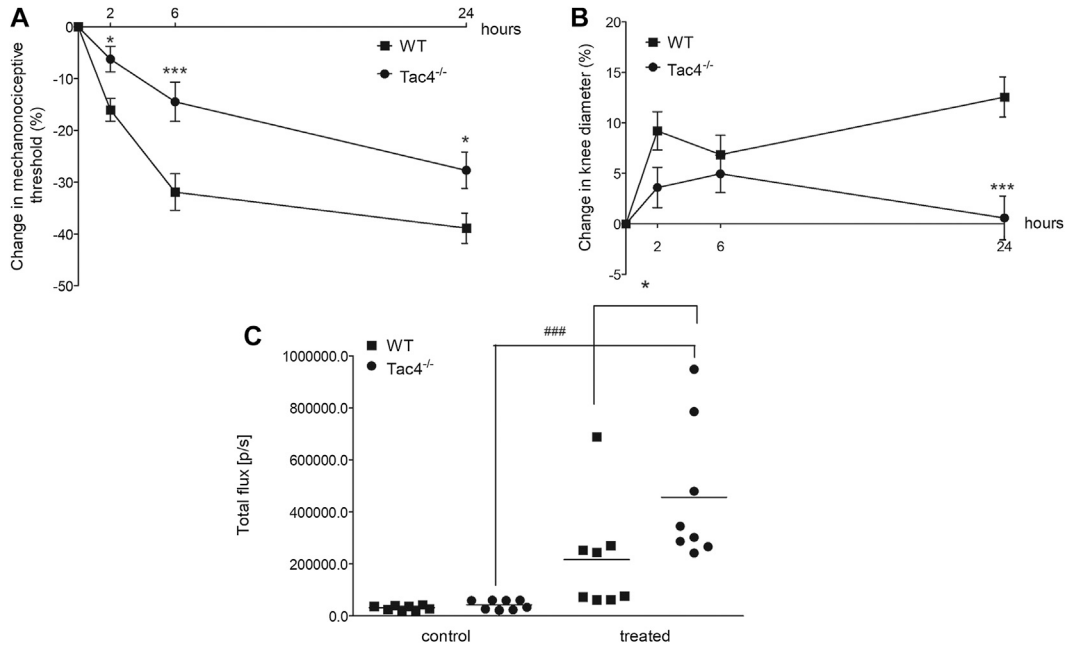

FIGURE 5 | Changes in mechanonociceptive threshold **(A)**, AP knee diameter **(B)**, and MPO-activity **(C)** in CFA-induced acute arthritis of WT and HK-1-deficient (*Tac4*$^{-/-}$) mice. Data points demonstrate the means ± SEM **(A)**, **(B)** or medians with upper and lower quartiles of n = 8–15 per group; *$p < 0.05$, **$p < 0.01$, ***$p < 0.001$ vs. WT, ###$p < 0.001$ vs. control (repeated measures two-way ANOVA + Bonferroni's post test; for MPO activity: one-way ANOVA + Bonferroni's post test).

alleviating pain (Matsumura et al., 2008). Our current results show that HK-1 mediates both the early inflammatory pain, and the late neuropathic-type pain in arthritis observed during the 3rd week of the K/BxN experiment (Christianson et al., 2010), while other studies showed the activation of spinal microglia in experimental arthritis (Agalave et al., 2014). Earlier findings showed significantly decreased HK-1 mRNA in the DRG in the collagen antibody induced arthritis (CAIA) mouse model (Makino et al., 2012), which is in agreement with the tendency we demonstrated in the present paper, although the decrease was not statistically significant due to individual variations. Joint inflammation was alleviated by NK1R antagonists in the CAIA model, while the pain could only be inhibited by indomethacin. In agreement with these findings we have also showed that the NK1 receptor does not play a role in arthritic pain, however, we conclude that HK-1 might be an important mediator in an NK1R-independent manner by directly activating primary sensory neurons.

Despite little information about HK-1 in pain and arthritis, the best-known member of the tachykinin family, SP, and the NK1R have been thoroughly investigated in these conditions (Zieglgänsberger, 2019). It is well established that SP via NK1R activation is involved in pain, which initiated considerable pharmacological research in this field. Despite the proof-of-concept of SP as a pain mediator, unfortunately, NK1R-antagonists have failed as analgesics in clinical trials (Botz et al., 2017), suggesting a yet unknown mechanism that can circumvent NK1R-targeted approaches. SP mediates chondrocyte differentiation in cell cultures (Millward-Sadler et al., 2003) and vasodilation in arthritic mice (Keeble et al., 2005) through the NK1 receptor. SP-like immunoreactivity was shown to increase in the primary sensory neurons of dorsal root ganglia (DRG) of arthritic mice (Willcockson et al., 2010), but the number of sensory nerve fibers of the arthritic joint capsule, that are the main sources of SP, decreased (Buma et al., 2000). Since SP and HK-1 cannot be differentiated by immunological methods, it is possible that these immunohistochemistry data referred (at least partially) to HK-1 expression.

In order to explore the direct effect and mechanism of action of HK-1, we did further studies on cultured primary sensory neurons. HK-1, but not SP, induced Ca^{2+}-influx into these neurons. HK-1-induced direct Ca^{2+}-influx could be seen during PTX administration and also in sensory neurons derived from *NK1R*$^{-/-}$ animals. The main finding of our experiments was that the Ca^{2+}-influx was coming from the extracellular space in an NK1R-independent manner since the signal disappeared in Ca^{2+}-free extracellular solution. It suggests an ion channel-coupled receptorial mechanism, but not TRPV1- or TRPA1-mediated mechanism, since the TRPV1 receptor antagonist AMG9810 and the TRPA1 receptor antagonist HC 030031 did not influence the HK-1-induced Ca^{2+} influx response. Furthermore, even lower concentrations of both HK-1 (similarly to SP) diminished desensitization of the TRPV1 receptor that upon repeated capsaicin administration could also contribute to the peripheral pain generating and maintaining effect of HK-1. The neuronal activating potential of HK-1 is supported by earlier data showing the ability of HK-1 to evoke direct post-synaptic activation of cholinergic hippocampal neurons in a tetrodotoxin-resistant manner. However, unlike sensory neurons, this response was not inhibited in Ca^{2+}-fee media and was similar to the effect of SP (Morozova et al., 2008).

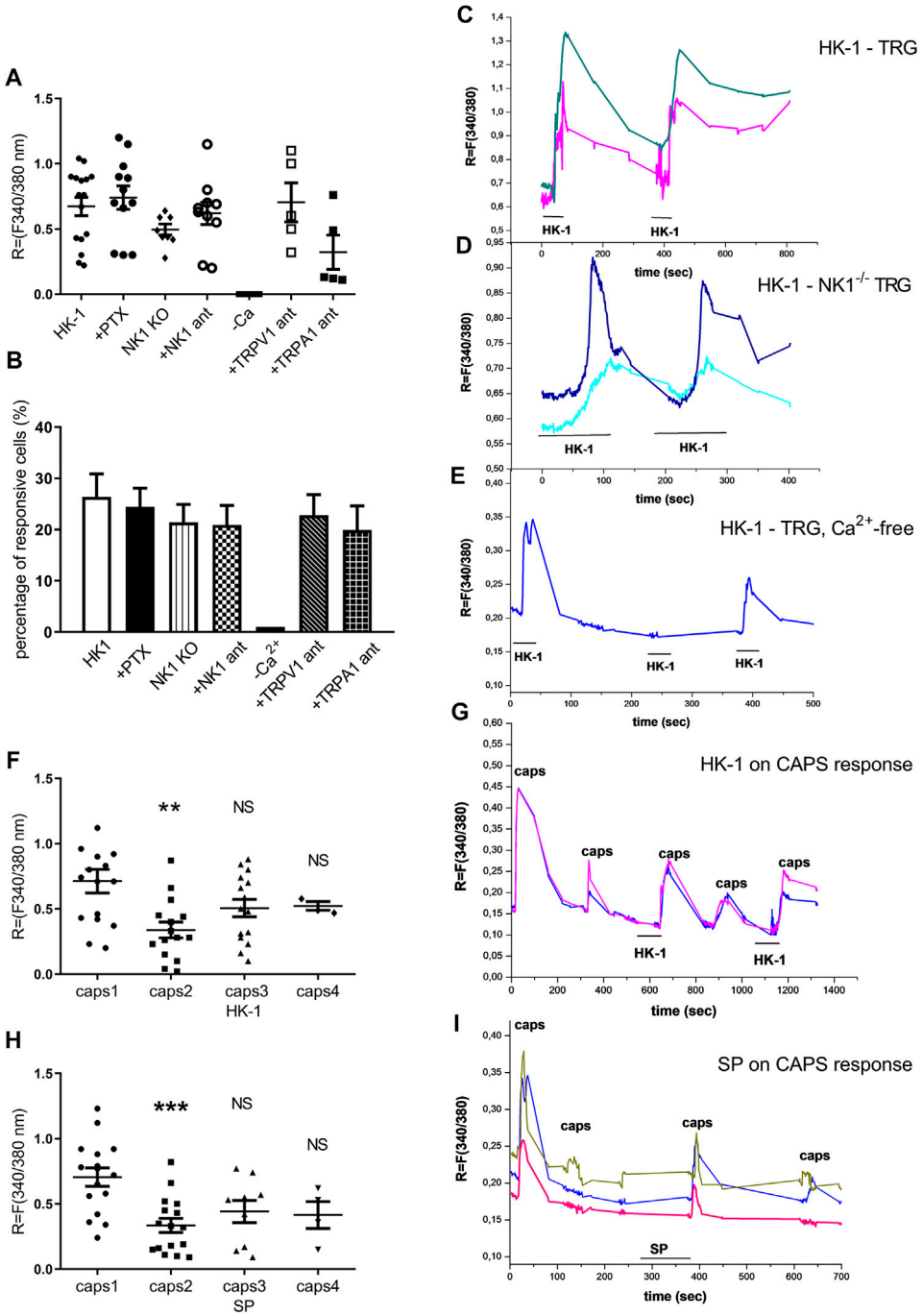

FIGURE 6 | Effect of HK-1 and SP in cultured primary sensory neurons. Change in the fluorescence ratio (R = F340/F380) in HK-1-sensitive cells (●) is presented. ●: HK-1 and PTX co-administration, ◆: fluorescence signal in neurons from *NK1R*$^{-/-}$ animals, ○: HK-1 and CP99994 NK1 receptor antagonist administration, □: HK-1 and AMG9810 TRPV1 receptor antagonist, ■: HK-1 and HC 030031 TRPA1 receptor antagonist. No signal was detected in Ca^{2+}-free extracellular solution. N = 19–49 cells/group **(A)**. The percentage of responsive cells to HK-1, HK-1+PTX, HK-1 in Ca^{2+}-free condition, HK-1+NK1 receptor antagonist CP99994 and HK-1 in TG from *NK1R*$^{-/-}$ animals, HK-1 + TRPV1 receptor antagonist AMG9810 and HK-1 + TRPA1 receptor antagonist HC 030031 is presented. Ca^{2+}-responses are presented in % of total number of examined neurons. N = 19–49 cells per group **(B)**. Original Ca^{2+}-imaging registrations after HK-1 administration. Increases of R = 340/380 fluorescence in fura-2 loaded cultured TG neurons **(C)**. Original Ca^{2+}-imaging registrations after HK-1 administration in TG neurons from NK1 gene deficient mice **(D)**. Original Ca^{2+}-imaging registrations after HK-1 administration in Ca^{2+}-free solution **(E)**. Effect of HK-1 on capsaicin-induced Ca^{2+}-influx. Increases of R = 340/380 fluorescence in fura-2 loaded neurons are presented, $^{**}p < 0.01$, NS (vs. caps1, one-way ANOVA with Bonferroni's multiple comparison post hoc test, n = 16) **(F)**. Effect of HK-1 on capsaicin-induced Ca^{2+}-influx. Original Ca^{2+}-imaging registrations after capsaicin and HK-1 administration **(G)**. Effect of SP on capsaicin-induced Ca^{2+}-influx. Increases of R = 340/380 fluorescence in fura-2 loaded neurons are presented, $^{***}p < 0.001$, NS (vs. caps1, one-way ANOVA with Bonferroni's multiple comparison post hoc test, n = 17) **(H)**. Effect of SP on capsaicin-induced Ca^{2+}-influx. Original Ca^{2+}-imaging registrations after capsaicin and SP administration **(I)**.

Some limitations of the present study are that we only performed our experiments on male mice to avoid the influencing factors of the estrus cycle and that we could detect HK-1 neither qualitatively by immunohistochemistry nor quantitatively by immune assays due to the lack of antibodies able to differentiate it from SP.

In conclusion, we provide the first evidence using three different mouse models mimicking distinct mechanisms of rheumatoid arthritis and integrative methodology (functional, *in vivo* optical imaging, cell cultures) that HK-1 mediates several arthritic inflammatory mechanisms and pain by direct activation of primary sensory neurons not via its classical NK1 receptor. The main translational value is that we modeled the late neuropathic component of arthritic pain related to neuropathic mechanisms without inflammatory symptoms and describe the involvement of HK-1 in this process. These findings add to the growing evidence that HK-1 has another, so far unidentified target initiating further research in this direction.

DATA AVAILABILITY STATEMENT

The original contributions presented in the study are included in the article/**Supplementary Material**, further inquiries can be directed to the corresponding author.

ETHICS STATEMENT

The animal study was reviewed and approved by Ethics Committee on Animal Research of the University of Pécs.

AUTHOR CONTRIBUTIONS

All authors were involved in drafting the article or revising it critically for important intellectual content, and all authors approved the final version to be published. ZH and AH had full access to all the data in the study and take responsibility for the integrity of the data and the accuracy of the data analysis. ÉB and AH, and also ÉS and ZH contributed equally to this work, respectively.

FUNDING

This work was supported by EFOP-3.6.2-16-2017-00008 "The role of the neuroinflammation in neurodegeneration: from molecules to clinics", 2017-1.2.1-NKP-2017-00002 (NAP-2; Chronic Pain Research Group), EFOP-3.6.1.-16-2016-0004 and GINOP 2.3.2-15-2016-00050 "PEPSYS". ÉB 2019 and ÉS 2017 were supported by the János Bolyai Research Scholarship of the Hungarian Academy of Sciences. KP was supported by GYTK-KA-2020-01, University of Pécs Faculty of Pharmacy and the New National Excellence Program of the Ministry for Innovation and Technologies from the source of the National Research, Development and Innovation Fund ÚNKP-20-4-II-PTE-465. BB 2019 was supported by the János Bolyai Research Scholarship of The Hungarian Academy of Sciences and the ÚNKP-20-5-PTE-540 New National Excellence Program of the Ministry for Innovation and Technology. The University of Pécs is acknowledged for a support from the 17886-4/23018/FEKUTSTRAT excellence grant. AM was supported by the "Élvonal" program from the Hungarian National Agency for Research, Development and Innovation (KKP 129954).

ACKNOWLEDGMENTS

We would like to thank Tamás Kiss, Anikó Perkecz, László Kereskai and Katinka Békefi for their assistance in the experiments, Ágnes Kemény for preparing the histology images for publication, Kata Bölcskei for revising the manuscript as well as Alexandra Berger, Christopher J. Paige and John P. Quinn for providing the original breeding pairs of the KO mice. The *in vivo* imaging studies were performed in the Small Animal *In Vivo* Imaging Core Facility of the Szentágothai Research Center (University of Pécs, Hungary).

SUPPLEMENTARY MATERIAL

The Supplementary Material for this article can be found online at: https://www.frontiersin.org/articles/10.3389/fphar.2020.594479/full#supplementary-material.

REFERENCES

Aczél, T., Kecskés, A., Kun, J., Szenthe, K., Bánáti, F., Szathmary, S., et al. (2020). Hemokinin-1 gene expression is upregulated in trigeminal ganglia in an inflammatory orofacial pain model: potential role in peripheral sensitization. *Int. J. Mol. Sci.* 21 (8), 2938. doi:10.3390/ijms21082938

Agalave, N. M., Larsson, M., Abdelmoaty, S., Su, J., Baharpoor, A., Lundbäck, P., et al. (2014). Spinal HMGB1 induces TLR4-mediated long-lasting hypersensitivity and glial activation and regulates pain-like behavior in experimental arthritis. *Pain* 155, 1802–1813. doi:10.1016/j.pain.2014.06.007

Arnhold, J., and Flemmig, J. (2010). Human myeloperoxidase in innate and acquired immunity. *Arch. Biochem. Biophys.* 500, 92–106. doi:10.1016/j.abb.2010.04.008

Berger, A., Benveniste, P., Corfe, S. A., Tran, A. H., Barbara, M., Wakeham, A., et al. (2010). Targeted deletion of the tachykinin 4 gene ($TAC4^{-/-}$) influences the early stages of B lymphocyte development. *Blood* 116, 3792–3801. doi:10.1182/blood-2010-06-291062

Berger, A., Tran, A. H., and Paige, C. J. (2007). Co-regulated decrease of Neurokinin-1 receptor and Hemokinin-1 gene expression in monocytes and macrophages after activation with pro-inflammatory cytokines. *J. Neuroimmunol.* 187, 83–93. doi:10.1016/j.jneuroim.2007.04.019

Billiau, A., and Matthys, P. (2001). Modes of action of Freund's adjuvants in experimental models of autoimmune diseases. *J. Leukoc. Biol.* 70, 849–860. doi:10.1189/jlb.70.6.849

Borbély, E., Hajna, Z., Sándor, K., Kereskai, L., Tóth, I., Pintér, E., et al. (2013). Role of tachykinin 1 and 4 gene-derived neuropeptides and the neurokinin 1 receptor in adjuvant-induced chronic arthritis of the mouse. *PloS One* 8, e61684. doi:10.1371/journal.pone.0061684

Borbély, É., and Helyes, Z. (2017). Role of hemokinin-1 in health and disease. *Neuropeptides* 64, 9–17. doi:10.1016/j.npep.2016.12.003

Borbély, É., Sándor, K., Markovics, A., Kemény, Á., Pintér, E., Szolcsányi, J., et al. (2016). Role of capsaicin-sensitive nerves and tachykinins in mast cell tryptase-

induced inflammation of murine knees. *Inflamm. Res.* 65, 725–736. doi:10.1007/s00011-016-0954-x

Botz, B., Bölcskei, K., and Helyes, Z. (2017). Challenges to develop novel anti-inflammatory and analgesic drugs. *Wiley Interdiscip. Rev. Nanomed. Nanobiotechnol.* 9, e1427. doi:10.1002/wnan.1427

Botz, B., Bölcskei, K., Kemény, Á., Sándor, Z., Tékus, V., Sétáló, G., et al. (2015). Hydrophobic cyanine dye-doped micelles for optical *in vivo* imaging of plasma leakage and vascular disruption. *J. Biomed. Optic.* 20, 016022. doi:10.1117/1.JBO.20.1.016022

Buma, P., Elmans, L., Berg, W. B. V. D., and Schrama, L. H. (2000). Neurovascular plasticity in the knee joint of an arthritic mouse model. *Anat. Rec.* 260, 51–61. doi:10.1002/1097-0185(20000901)260:1<51::AID-AR60>3.0.CO;2-9

Chancay, M. G., Guendsechadze, S. N., and Blanco, I. (2019). Types of pain and their psychosocial impact in women with rheumatoid arthritis. *Womens Midlife Health.* 5, 3. doi:10.1186/s40695-019-0047-4

Christianson, C. A., Corr, M., Firestein, G. S., Mobargha, A., Yaksh, T. L., and Svensson, C. I. (2010). Characterization of the acute and persistent pain state present in K/BxN serum transfer arthritis. *Pain* 151, 394–403. doi:10.1016/j.pain.2010.07.030

Day, A. L., and Curtis, J. R. (2019). Opioid use in rheumatoid arthritis: trends, efficacy, safety, and best practices. *Curr. Opin. Rheumatol.* 31, 264–270. doi:10.1097/BOR.0000000000000602

De Felipe, C., Herrero, J. F., O'Brien, J. A., Palmer, J. A., Doyle, C. A., Smith, A. J., et al. (1998). Altered nociception, analgesia and aggression in mice lacking the receptor for substance P. *Nature* 392, 394–397. doi:10.1038/32904

Donaldson, L. F., McQueen, D. S., and Seckl, J. R. (1995). Neuropeptide gene expression and capsaicin-sensitive primary afferents: maintenance and spread of adjuvant arthritis in the rat. *J. Physiol.* 486, 473–482. doi:10.1113/jphysiol.1995.sp020826

Ebbinghaus, M., Müller, S., Banchet, G. S. von., Eitner, A., Wank, I., Hess, A., et al. (2019). Contribution of inflammation and bone destruction to pain in arthritis: a study in murine glucose-6-phosphate isomerase–induced arthritis. *Arth. Rheum.* 71, 2016–2026. doi:10.1002/art.41051

Fu, C.-Y., Kong, Z.-Q., Wang, K.-R., Yang, Q., Zhai, K., Chen, Q., et al. (2005). Effects and mechanisms of supraspinal administration of rat/mouse hemokinin-1, a mammalian tachykinin peptide, on nociception in mice. *Brain Res.* 1056, 51–58. doi:10.1016/j.brainres.2005.07.020

Herrero, J. F., Laird, J. M., and López-García, J. A. (2000). Wind-up of spinal cord neurones and pain sensation: much ado about something? *Prog. Neurobiol.* 61, 169–203. doi:10.1016/s0301-0082(99)00051-9

Horváth, Á., Tékus, V., Boros, M., Pozsgai, G., Botz, B., Borbély, É., et al. (2016). Transient receptor potential ankyrin 1 (TRPA1) receptor is involved in chronic arthritis: *in vivo* study using TRPA1-deficient mice. *Arthritis Res. Ther.* 18, 6. doi:10.1186/s13075-015-0904-y

Hunyady, Á., Hajna, Z., Gubányi, T., Scheich, B., Kemény, Á., Gaszner, B., et al. (2019). Hemokinin-1 is an important mediator of pain in mouse models of neuropathic and inflammatory mechanisms. *Brain Res. Bull.* 147, 165–173. doi:10.1016/j.brainresbull.2019.01.015

Jakus, Z., Simon, E., Balázs, B., and Mócsai, A. (2010). Genetic deficiency of Syk protects mice from autoantibody-induced arthritis. *Arthritis Rheum.* 62, 1899–1910. doi:10.1002/art.27438

Keeble, J., Blades, M., Pitzalis, C., Castro da Rocha, F. A., and Brain, S. D. (2005). The role of substance P in microvascular responses in murine joint inflammation. *Br. J. Pharmacol.* 144, 1059–1066. doi:10.1038/sj.bjp.0706131

Kecskés, A., Pohóczky, K., Kecskés, M., Varga, Z. V., Kormos, V., Szöke, É., et al. (2020). Characterization of neurons epressing the novel analgesic drug target somatostatin receptor 4 in mouse and human brains. *Int. J. Mol. Sci.* 21 (20), 7788. doi:10.3390/ijms21207788

Klassert, T. E., Pinto, F., Hernández, M., Candenas, M. L., Hernández, M. C., Abreu, J., et al. (2008). Differential expression of neurokinin B and hemokinin-1 in human immune cells. *J. Neuroimmunol.* 196, 27–34. doi:10.1016/j.jneuroim.2008.02.010

Kobayashi, Y., and Okunishi, H. (2002). Mast cells as a target of rheumatoid arthritis treatment. *Jpn. J. Pharmacol.* 90, 7–11. doi:10.1254/jjp.90.7

Krock, E., Jurczak, A., and Svensson, C. I. (2018). Pain pathogenesis in rheumatoid arthritis-what have we learned from animal models?. *Pain* 159 (Suppl. 1), S98–S109. doi:10.1097/j.pain.0000000000001333

Makino, A., Sakai, A., Ito, H., and Suzuki, H. (2012). Involvement of tachykinins and NK1 receptor in the joint inflammation with collagen type II-specific monoclonal antibody-induced arthritis in mice. *J. Nippon Med. Sch.* 79, 129–138. doi:10.1272/jnms.79.129

Malcangio, M. (2020). Translational value of preclinical models for rheumatoid arthritis pain 161, 1399–1400. *Pain* doi:10.1097/j.pain.0000000000001851

Matsumura, T., Sakai, A., Nagano, M., Sawada, M., Suzuki, H., Umino, M., et al. (2008). Increase in hemokinin-1 mRNA in the spinal cord during the early phase of a neuropathic pain state. *Br. J. Pharmacol.* 155, 767–774. doi:10.1038/bjp.2008.301

McWilliams, D. F., and Walsh, D. A. (2019). Pain mechanisms in rheumatoid arthritis. Available at: https://www.clinexprheumatol.org/abstract.asp?a=12176 (Accessed December 3, 2019).

Millward-Sadler, S. J., Mackenzie, A., Wright, M. O., Lee, H.-S., Elliot, K., Gerrard, L., et al. (2003). Tachykinin expression in cartilage and function in human articular chondrocyte mechanotransduction. *Arthritis Rheum.* 48, 146–156. doi:10.1002/art.10711

Morozova, E., Wu, M., Dumalska, I., and Alreja, M. (2008). Neurokinins robustly activate the majority of septohippocampal cholinergic neurons. *Eur. J. Neurosci.* 27, 114–122. doi:10.1111/j.1460-9568.2007.05993.x

Morteau, O., Lu, B., Gerard, C., and Gerard, N. P. (2001). Hemokinin 1 is a full agonist at the substance P receptor. *Nat. Immunol.* 2, 1088. doi:10.1038/ni1201-1088

Nakamura-Craig, M., and Smith, T. W. (1989). Substance P and peripheral inflammatory hyperalgesia. *Pain* 38, 91–98. doi:10.1016/0304-3959(89)90078-x

Onaga, T. (2014). Tachykinin: recent developments and novel roles in health and disease. *Biomol. Concepts* 5, 225–243. doi:10.1515/bmc-2014-0008

Pfaffl, M. W. (2001). A new mathematical model for relative quantification in real-time RT-PCR. *Nucleic Acids Res.* 2001, 29. doi:10.1093/nar/29.9.e45

Pinho-Ribeiro, F. A., Verri, W. A., Jr, and Chiu, I. M. (2017). Nociceptor sensory neuron-immune interactions in pain and inflammation. *Trends Immunol. Jan.* 38 (1), 5–19. doi:10.1016/j.it.2016.10.001

Prokopowicz, Z., Marcinkiewicz, J., Katz, D. R., and Chain, B. M. (2012). Neutrophil myeloperoxidase: soldier and statesman. *Arch. Immunol. Ther. Exp.* 60 (1), 43–54. doi:10.1007/s00005-011-0156-8

Smith, J. B., and Haynes, M. K. (2002). Rheumatoid arthritis—a molecular understanding. *Ann. Intern. Med.* 136, 908. doi:10.7326/0003-4819-136-12-200206180-00012

Sommer, C., and Kress, M. (2004). Recent findings on how proinflammatory cytokines cause pain: peripheral mechanisms in inflammatory and neuropathic hyperalgesia. *Neurosci. Lett.* 361, 184–187. doi:10.1016/j.neulet.2003.12.007

Sparks, J. A. (2019). Rheumatoid arthritis. *Ann. Intern. Med.* 170, ITC1–ITC16. doi:10.7326/AITC201901010

Sun, W.-H., and Dai, S.-P. (2018). Tackling pain associated with rheumatoid arthritis: proton-sensing receptors. *Adv. Exp. Med. Biol.* 1099, 49–64. doi:10.1007/978-981-13-1756-9_5

Szoke, E., Börzsei, R., Tóth, D. M., Lengl, O., Helyes, Z., Sándor, Z., et al. (2010). Effect of lipid raft disruption on TRPV1 receptor activation of trigeminal sensory neurons and transfected cell line. *Eur. J. Pharmacol.* 628, 67–74. doi:10.1016/j.ejphar.2009.11.052

Tóth, D. M., Ocskó, T., Balog, A., Markovics, A., Mikecz, K., Kovács, L., et al. (2019). Amelioration of autoimmune arthritis in mice treated with the DNA methyltransferase inhibitor 5′-azacytidine. *Arthritis Rheum.* 71, 1265–1275. doi:10.1002/art.40877

Watanabe, C., Mizoguchi, H., Bagetta, G., and Sakurada, S. (2016). Involvement of spinal glutamate in nociceptive behavior induced by intrathecal administration of hemokinin-1 in mice. *Neurosci. Lett.* 617, 236–239. doi:10.1016/j.neulet.2016.02.027

Watanabe, C., Mizoguchi, H., Yonezawa, A., and Sakurada, S. (2010). Characterization of intrathecally administered hemokinin-1-induced nociceptive behaviors in mice. *Peptides* 31, 1613–1616. doi:10.1016/j.peptides.2010.04.025

Willcockson, H. H., Chen, Y., Han, J. E., and Valtschanoff, J. G. (2010). Effect of genetic deletion of the vanilloid receptor TRPV1 on the expression of Substance P in sensory neurons of mice with adjuvant-induced arthritis. *Neuropeptides* 44, 293–297. doi:10.1016/j.npep.2010.02.003

Zhang, Y., Lu, L., Furlonger, C., Wu, G. E., and Paige, C. J. (2000). Hemokinin is a hematopoietic-specific tachykinin that regulates B lymphopoiesis. *Nat. Immunol.* 1, 392–397. doi: doi:10.1038/80826

Zhang, Y., and Paige, C. J. (2003). T-cell developmental blockage by tachykinin antagonists and the role of hemokinin 1 in T lymphopoiesis. *Blood* 102, 2165–2172. doi:10.1182/blood-2002-11-3572

Zieglgänsberger, W. (2019). Substance P and pain chronicity. *Cell Tissue Res*. 375, 227–241. doi:10.1007/s00441-018-2922-y

Conflict of Interest: Zsuzsanna Helyes is the strategic director and shareholder of PharmInVivo Ltd. (Pécs, Hungary) and shareholder of Algonist Biotechnologies Gmbh, (Wien, Austria). Eva Szoke is also a shareholder of Algonist Biotechnologies Gmbh, (Wien, Austria), but there is no conflict of interest with the present work. These companies were not involved in the study design, funding, collection, analysis, interpretation of data, the writing of this article or the decision to submit it for publication. The remaining authors declare that the research was conducted in the absence of any commercial or financial relationships that could be construed as a potential conflict of interest.

GLOSSARY

AITC allyl isothiocyanate

CAIA collagen antibody induced arthritis

CFA complete Freund's adjuvant

DMARD disease-modifying antirheumatic drugs

D-MEM Dulbecco's-Modified Eagle Medium-low glucose

DMSO dimethyl sulfoxide

DPE dynamic plantar esthesiometer

DRG dorsal root ganglion

ECS extracellular solution

GPCR G-protein-coupled receptor

HK-1 hemokinin-1

i.p. intraperitoneal

i.v. intravenous

KO knockout

MCT mast cell tryptase

MPO Myeloperoxidase

NGF nerve growth factor

NK1R tachykinin neurokinin-1 receptor

NK2R tachykinin neurokinin-2 receptor

NK3R tachykinin neurokinin-3 receptor

NMDA N-metil-d-aspartic acid

NSAID nonsteroidal anti-inflammatory drugs

PAR2 protease-activated receptor two

PBS phosphate-buffered saline

PCR Polymerase chain reaction

PTX pertussis toxin

RA rheumatoid arthritis

ROI region of interest

SP substance P

Tac4 preprotachykinin-4 gene

Tacr1 tachykinin receptor one gene, encodes NK1R

TG trigeminal ganglion

TRPA1 transient receptor potential cation channel subfamily A member one

TRPV1 transient receptor potential cation channel subfamily V member one

WT wild type

frontiers in Pharmacology

ORIGINAL RESEARCH
published: 01 February 2021
doi: 10.3389/fphar.2020.620221

Analgesic and Anti-Inflammatory Effects of Perampanel in Acute and Chronic Pain Models in Mice: Interaction With the Cannabinergic System

Carmen De Caro[1†], Claudia Cristiano[2†], Carmen Avagliano[2], Mariarosaria Cuozzo[2], Giovanna La Rana[2], Gabriella Aviello[2], Giovambattista De Sarro[1], Antonio Calignano[2], Emilio Russo[1] and Roberto Russo[2‡]*

[1]Department of Health Sciences, School of Medicine, University of Catanzaro, Catanzaro, Italy, [2]Department of Pharmacy, University of Naples Federico II, Naples, Italy

Pain conditions, such as neuropathic pain (NP) and persistent inflammatory pain are therapeutically difficult to manage. Previous studies have shown the involvement of glutamate receptor in pain modulation and in particular same of these showed the key role of the AMPA ionotropic glutamate receptor subtype. Antiseizure medications (ASMs) are often used to treat this symptom, however the effect of perampanel (PER), an ASM acting as selective, non-competitive inhibitor of the AMPA receptor on the management of pain has not well been investigated yet. Here we tested the potential analgesic and anti-inflammatory effects of PER, in acute and chronic pain models. PER was given orally either in acute (5 mg/kg) or repeated administration (3 mg/kg/d for 4 days). Pain response was assessed using models of nociceptive sensitivity, visceral and inflammatory pain, and mechanical allodynia and hyperalgesia induced by chronic constriction injury to the sciatic nerve. PER significantly reduced pain perception in all behavioral tests as well as CCI-induced mechanical allodynia and hyperalgesia in acute regimen (5 mg/kg). This effect was also observed after repeated treatment using the dose of 3 mg/kg/d. The antinociceptive, antiallodynic and antihyperalgesic effects of PER were attenuated when the CB_1 antagonist AM251 (1 mg/kg/i.p.) was administered before PER treatment, suggesting the involvement of the cannabinergic system. Moreover, *Ex vivo* analyses showed that PER significantly increased CB_1 receptor expression and reduced inflammatory cytokines (i.e. TNFα, IL-1β, and IL-6) in the spinal cord. In conclusion, these results extend our knowledge on PER antinociceptive and antiallodynic effects and support the involvement of cannabinergic system on its mode of action.

Keywords: perampanel, AMPA receptor, pain, inflammation, CB1 receptor

OPEN ACCESS

Edited by:
Francesca Guida, University of Campania Luigi Vanvitelli, Italy

Reviewed by:
Danilo De Gregorio, McGill University, Canada
Fulvio D'Acquisto, University of Roehampton London, United Kingdom

***Correspondence:**
Russo Roberto
roberto.russo@unina.it

[†]These authors have contributed equally to this work
[‡]ORCID: Russo Roberto orcid.org/0000-0001-5950-1617

Specialty section:
This article was submitted to Inflammation Pharmacology, a section of the journal Frontiers in Pharmacology

Received: *22 October 2020*
Accepted: *30 November 2020*
Published: *01 February 2021*

Citation:
De Caro C, Cristiano C, Avagliano C, Cuozzo M, La Rana G, Aviello G, De Sarro G, Calignano A, Russo E and Russo R (2021) Analgesic and Anti-Inflammatory Effects of Perampanel in Acute and Chronic Pain Models in Mice: Interaction With the Cannabinergic System. Front. Pharmacol. 11:620221. doi: 10.3389/fphar.2020.620221

INTRODUCTION

Neuropathic pain (NP) is a chronic pain condition characterized by different symptoms, including abnormal increase of sensitivity to innocuous stimuli (allodynia), and/or exacerbated sensitivity to noxious stimuli (hyperalgesia) (Jensen and Finnerup, 2014). NP is usually caused by one or multiple injuries at the central and/or peripheral nervous system as a result of a cascade of neurobiological processes. There are many medications available for pain sufferers, ranging from over-the-counter products to prescription medications including analgesics, antidepressants and antiseizure medications. Recently, antiseizure medications (ASMs) have shown to play an important role in the management of pain and especially in chronic NP (Sidhu and Sadhotra, 2016) and their use – also in combination with opioid analgesics - has been approved by the Food and Drug Administration (Chaparro et al., 2012). Antiepileptic drugs (AEDs) exert their antiseizure as well as analgesic effects by blocking sodium channels, increasing GABA-mediated inhibition, binding on specific subtype of calcium channels, and reducing glutamate release or blocking its ionotropic receptors (Bialer, 2012; Sidhu and Sadhotra, 2016; Tomić et al., 2018).

Alpha-amino-3-hydroxyl-5-methyl-4-isoxazole-propionate (AMPA) receptors mediate fast excitatory transmission and have a critical role in synaptic plasticity in the spinal cord (Latremoliere and Woolf, 2009). They are tetramers consisting of dimers of four different subunits, GluA1-4, all of which are expressed in the dorsal horn (DH) (Polgár et al., 2008). Activation of AMPA receptor triggers intracellular cation influx resulting in membrane depolarization, which in turn leads to N-methyl-D-aspartate (NMDA) activation, an increased influx of Ca^{2+} in the intracellular space (Hanada et al., 2011). High levels of intracellular Ca^{2+} activate signal transduction pathways responsible for the hyper-excitability of post-synaptic neurons (Douyard et al., 2007), thus AMPA receptor activation may be critical in the initiation of pathophysiological changes resulting in pain development.

It has been reported that upregulation of AMPA receptors in DH neurons causes central sensitization for a long period of time (Gwak et al., 2007). Moreover, peripheral inflammatory pain induces upregulation of Ca^{2+} permeable AMPA receptors at both synapses and the extra synaptic membranes of DH interneurons (Chizh et al., 2000; Adedoyin et al., 2010) the latter being linked to persistent pain. Some studies claimed a prominent role of AMPA receptor modulation in (Davidson et al., 1997; McRoberts et al., 2001). For instance, several studies imply a prominent role of AMPA receptors in the initiation of NP, as well as in different neurodegenerative conditions (Adedoyin et al., 2010) (Gwak et al., 2007). Although the analgesic effect of AMPA antagonists is supported by emerging preclinical evidence (Khan et al., 2019), their use needs to be further tested and their clinical potential remain to be investigated.

PER [2-(2-oxo-1-phenyl-5-pyridin-2-yl-1,2-dihydro- pyridin-3-yl) benzonitrile hydrate 4:3] is the first selective non-competitive AMPA receptor antagonist approved for the treatment of epilepsy (Hanada et al., 2011). It exerts a broad spectrum of antiseizure activity in preclinical models of either partial or generalized seizures (Hanada et al., 2011; Russo et al., 2012; Russmann et al., 2016; Citraro et al., 2017) and in patients with epilepsy (Di Bonaventura et al., 2017; Leo et al., 2018; Potschka and Trinka, 2019). To date, a few studies in rats have shown the effects of PER in attenuating pain in chronic constriction injury-induced (CCI) models of NP and the partial involvement of the opioid system on its mode of action (Khangura et al., 2017; Hara et al., 2020). In this study, we aimed at exploring the analgesic effects of both single and repeated PER administration in specific rodent models of acute and chronic pain and studied the potential involvement of the cannabinergic system in its modulation of neuroinflammation at spinal cord level.

MATERIALS AND METHODS

Animals

Male CD1 mice (25–30 g) were purchased from Charles River Italy (Lecco, Italy) and housed in cages in a room kept at 22 ± 1°C with a 12:12 h light/dark cycle. The animals were acclimated to their environment for 1 week and had ad libitum access to standard rodent diet. Procedures involving animals and their care were conducted in conformity with international and national law and policies (EU Directive 2010/63/EU for animal experiments) and approved by the Institutional Committee on the Ethics of Animal Experiments (CSV) of the University of Naples "Federico II" and by the Ministero della Salute under protocol no.996/2016-PR. At the end of all procedures, animals were euthanized by CO_2 overdose. As suggested by the animal welfare protocol, all efforts were made to minimize animal suffering and to use only the number of animals necessary to produce reliable scientific data.

Drugs and Chemicals

PER (EISAI S.r.l., Milan, Italy) was dissolved in 10% PEG, 5% Tween 80 and 85% water and administered by gavage either at 5 mg/kg (0.3 mL/mouse) dose for the oral single acute treatment or at 3 mg/kg (0.3 mL/mouse) dose for repeated treatments (4 consecutive days, at 9–10 am). AM251 (Sigma-Aldrich, Italy) was dissolved in DMSO and injected intraperitoneally (i.p.) 1 h before PER administration at the dose of 1 mg/kg. Formalin (5% in saline), λ-carrageenan (1% in saline) and all other products used were purchased from Tocris or Sigma-Aldrich (Italy).

Acute Pain Models

Tail Flick and Hot Plate tests

Each mouse was tested 1, 3, and 5 h after the administration of the acute dose of 5 mg/kg or after the last dose of 3 mg/kg/d repeated treatment, in both tail flick and hot plate tests. In the first test, tail-flick was evoked by a source of radiant heat, which was focused on the dorsal surface of the tail (de Novellis et al., 2012). The cut-off imposed was 15 s to prevent tissue damage. In the second test, mice were placed on a 55.5 ± 0.5°C hot plate apparatus to measure the latency (s) of either first hind paw pain response or jumping off the plate. The cut-off imposed was 60s to avoid tissue damage. Control mice received vehicle only.

Acetic Acid Evoked Writhing

Mice were placed separately into cages and allowed to acclimate for at least 10 min and then visceral pain was induced by i.p., injection (0.5 mL/mouse) of 0.6% acetic acid. In both acute and repeated drug administration, tests started 1 h after PER treatment (after the fourth dose in case of the repeated protocol). Control mice received vehicle only. The measurement of nociception severity was determined by the number of abdominal constrictions known as writhing. The number of writhing episodes was recorded over a period of 25 min (Russo et al., 2016).

Formalin-Evoked Hind-Paw Licking

Mice received injections of formalin (5% v/v in saline; 20 µl/paw), into the plantar surface of the right hind paw using a 27-gauge needle fitted to a microsyringe. Paw licking was monitored immediately after formalin administration by an observer blind to the experimental treatments during two epochs: 0–15 min (early phase) and 15–45 min (late phase) (Sasso et al., 2012). PER effect was evaluated after single and repeated administrations; formalin test was performed 1 h after the last treatment.

Paw Edema

Paw edema was induced by a sub-plantar injection of 50 µl of sterile saline containing 1% λ –carrageenan into the right hind paw. Paw volumes were measured by a plethysmometer apparatus (Ugo Basile, Milan, Italy) at different time intervals: before injection (0) and 1, 3, 5, 24, 48, and 72 h after administration of carrageenan. PER was administered orally at the single dose of 5 mg/kg 30 min before carrageenan injection. The increase of paw volume was evaluated as the difference between the paw volume measured at each time point and the basal paw volume measured immediately before carrageenan injection (D'Agostino et al., 2007).

Neuropathic Pain model

Chronic Constriction Injury

The sciatic nerve of mice was surgically ligated, as previously described (Russo et al., 2016). Briefly, mice (n = 6 each group) were first anesthetized with i.p., injection of xylazine (10 mg/kg) and ketamine (100 mg/kg), and then a small incision in the middle left thigh (2 cm in length) was performed to expose the sciatic nerve. The nerve was loosely ligated at two distinct sites (spaced at a 2-mm interval) around the entire diameter of the nerve using silk sutures (7–0). In sham-operated animals, the nerve was exposed but not ligated. Four days after surgery, mice were treated orally with PER using the dose of 5 mg/kg for acute treatment and 3 mg/kg for repeated administrations, as described above. On day 7 after surgery, mechanical allodynia and hyperalgesia were measured.

Mechanical Hyperalgesia

Paw withdrawal threshold (g) to mechanical stimuli was measured using the Randall–Selitto analgesimeter for mice (Ugo Basile, Varese, Italy). Latencies of paw withdrawal to a calibrated pressure were assessed on both ligated and contralateral paws on day before ligation, and again on day 7 following sciatic nerve ligation (CCI), therefore each paw was tested twice per session. Cut-off force was set at 100 g.

Mechanical Allodynia

To assess for changes in sensation or in the development of mechanical allodynia, sensitivity to tactile stimulation was measured using the Dynamic Plantar Aesthesiometer (DPA, Ugo Basile, Italy), which is an automated version of the von Frey hair assessment (Mannelli et al., 2013). Mice were placed in Plexiglas boxes (30 × 30 × 25 cm) with a mesh metal floor covered by a plastic dome that enabled the animal to walk freely, but not to jump. When a trial is initiated, the device raises the filament to touch the foot and progressively increases force until the animal withdraws its foot, or until it reaches a maximum of 5 g of force (cut-off). The DPA automatically records the force at which the foot is withdrawn. Mice were acclimated for 15 min to the environment. Each paw was tested twice per session and the test was performed on day before ligation, and again on day 7 following CCI. The means of the paws' withdrawal was expressed in grams.

Western Blot Analysis on Spinal Cord

Mice treated with acute (5 mg/kg) or repeated (3 mg/kg) PER doses were euthanized and the spinal cord was removed via dissection for the following determinations. Tissues were homogenized in lysis buffer (50 mM Tris–HCl, pH 7.4; 1 mM EDTA; 100 mM NaCl; 20 mM NaF; 3 mM Na_3VO_4; 1 mM PMSF with 1% (v/v) Nonidet P-40; and protease inhibitor cocktail). After 45 min, lysates were centrifuged at 12,000 rpm for 20 min at 4°C and the supernatant was stored at −80°C until use. Protein concentrations were estimated using bovine serum albumin as a standard in a Bradford reagent assay. Proteins were separated on SDS-PAGE, transferred to nitrocellulose membranes, and incubated with the primary anti-CB_1 antibody (cat no P0369, Sigma Aldrich). The signal was visualized with the ECL system (Pierce) by Image Quant (GE Healtcare, Milan, Italy). Protein bands were densitometrically quantified using Quantity One software (Bio-Rad Laboratories). Membranes were incubated with anti-β-actin (dilution 1:15000; Sigma–Aldrich; Milan Italy) for normalization.

Real-Time Polymerase Chain Reaction Analysis

Total RNA was extracted from the spinal cord using Trizol (Ambion). Two micrograms of total RNA were used in first-strand cDNA synthesis (Promega, Madison, WI) according to the manufacturer's instructions. PCRs were performed with a Bio-Rad CFX96 Connect Realtime PCR System instrument and software (Bio-Rad Laboratories). The PCR conditions were 15 min at 95°C followed by 40 cycles of two-step PCR denaturation at 94°C for 15 s, annealing extension at 55°C for 30 s and extension at 72°C for 30 s. Each sample contained 500 ng cDNA in 2X QuantiTech SYBRGreen PCR Master Mix and gene-specific primers for *Tnfa*, *Il1b*, and *Il6* were purchased from Qiagen (Hilden, Germany). The relative expression of mRNA was

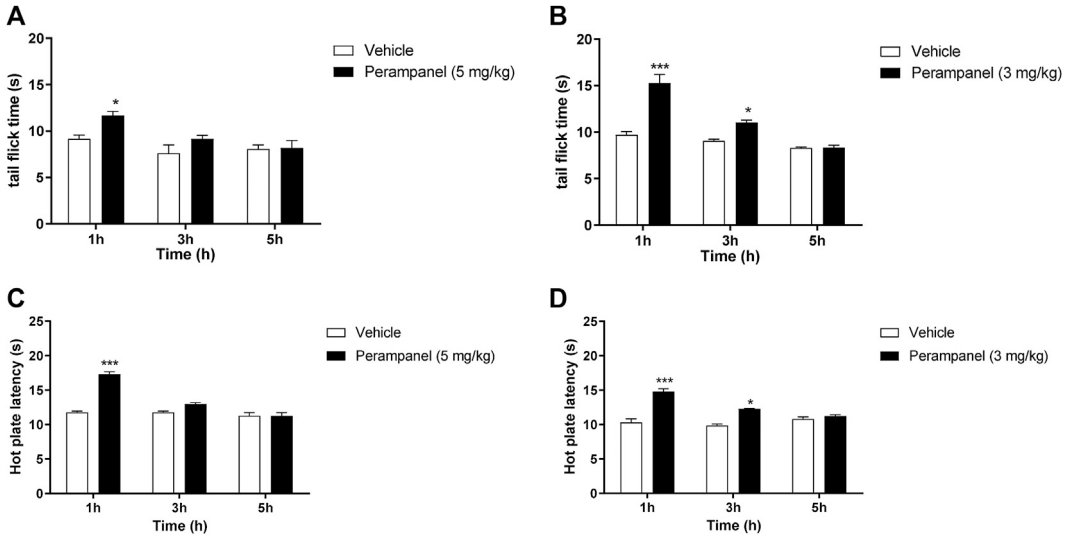

FIGURE 1 | Analgesic effect of PER on tail flick and hot plate tests. Mice were tested 1, 3, and 5 h following acute or repeated oral PER administration. Effect of **(A)** acute PER (5 mg/kg) and **(B)** repeated PER (3 mg/kg/d) for 4 consecutive days administration in the tail flick test. Effect of **(C)** acute PER (5 mg/kg) and **(D)** repeated PER (3 mg/kg/d) for 4 consecutive days in the hot plate test. Data are shown as means ± S.E.M, n = 6–7/group; $^{*}p < 0.05$, $^{***}p < 0.001$ vs. Vehicle, followed by two-way ANOVA Bonferroni's post-hoc test.

normalized to *Gapdh* as housekeeping gene, and the data were analyzed according to the 2–ΔΔCT method.

Statistical Analysis

The results were expressed as mean ± S.E.M. Data were analyzed using t test, one- or two-ways ANOVA (as appropriated) followed by Tukey's or Bonferroni's post hoc comparison test. The P-values $^{*}p < 0.05$, $^{**}p < 0.01$, and $^{***}p < 0.001$ vs. Vehicle group; $^{+}p < 0.05$, $^{++}p < 0.01$ vs. CCI-PER; $^{\#}p < 0.5$, $^{\#\#}p < 0.01$, $^{\#\#\#}p < 0.001$, and $^{\#\#\#\#}p < 0.0001$ vs. Vehicle sham group were considered statistically significant.

RESULTS

Analgesic Effect of PER on Tail Flick and Hot Plate Latency

Nociception was firstly evaluated by tail-flick and the hot-plate tests (**Figure 1**). The tail flick latency, expressed in seconds, was measured at 1, 3, and 5 h after PER administration (Panels A and B). Acute oral administration of PER (5 mg/kg) produced significant changes in tail flick latency only 1 h following administration ($^{*}p < 0.05$ vs vehicle; $F_{(2,\ 30)} = 17{,}02$ for factor time; $F_{(1,\ 30)} = 10{,}13$ for factor treatment; $F_{(2,\ 30)} = 0{,}8148$ for time X treatment interaction, followed by two-way ANOVA Bonferroni's post-hoc test)

Figure 1A No effect was observed at 3 and 5 h after the injection. Repeated daily oral administration, using a lower dose of PER (3 mg/kg) for 4 consecutive days, produced a marked and significant increase in the latency of the nociceptive reaction, with a maximal effect 1 h after oral administration ($^{***}p < 0.001$ vs. vehicle; **Figure 1B**). This effect remained significant up to 3 h after the last PER administration ($^{*}p < 0.05$ vs. vehicle; $F_{(2,\ 30)} = 15{,}79$ for factor time; $F_{(1,\ 30)} = 16{,}79$ for factor treatment; $F_{(2,30)} = 4{,}440$ for time X treatment interaction, followed by two-way ANOVA Bonferroni's post-hoc test; **Figure 1B**).

To confirm these results, we measured heat nociception also using the hot plate test at the same time points. Similarly, single oral administration of PER at the dose of 5 mg/kg significantly attenuated hypersensitivity in response to thermal stimulus during the first hour ($^{***}p < 0.001$ vs vehicle; $F_{(2,\ 36)} = 25{,}65$ for factor time; $F_{(1,\ 36)} = 15{,}28$ for factor treatment; $F_{(2,\ 36)} = 5{,}555$ for time X treatment interaction, followed by two-way ANOVA Bonferroni's post-hoc test; **Figure 1C**), while repeated administrations of PER at the dose of 3 mg/kg significantly reduced hypersensitivity up to 3 h after the last PER administration ($^{***}p < 0.001$ and $^{*}p < 0.5$ vs. vehicle; $F_{(2,\ 36)} = 18{,}11$ for factor time; $F_{(1,\ 36)} = 20{,}43$ for factor treatment; $F_{(2,\ 36)} = 3{,}658$ for time X treatment interaction, followed by two-way ANOVA Bonferroni's post-hoc test; **Figure 1D**).

Analgesic Effect of PER on Visceral Pain

PER efficacy in reducing the nocifensive behavior was studied using the acetic acid-induced writhing test, where i.p., injection of 0.6% acetic acid normally determines approx. 40 writhing episodes (**Figures 2A,B**). Acute oral administration of PER (5 mg/kg) induced a significant reduction of nocifensive behavior ($^{*}p < 0.05$ vs. vehicle; t = 3,029 Unpaired t test, two-tailed; **Figure 2A**). Similarly, repeated oral administration of PER showed significant reduction of writhing episodes compared to controls ($^{**}p < 0.001$ vs. vehicle; t = 4,269 Unpaired t test, two-tailed; **Figure 2B**).

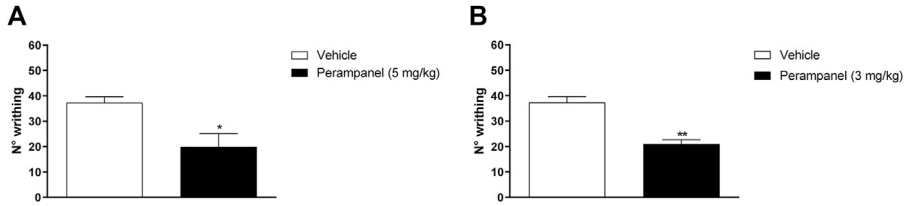

FIGURE 2 | Effect of PER in a model of visceral pain. Mice were tested following the intraperitoneal 0.6% acetic acid injection. **(A)** Number of writhing after a single administration of vehicle or PER (5 mg/kg); **(B)** number of writhing after repeated oral PER (3 mg/kg/d) for 4 consecutive days administration. Data are shown as means ± S.E.M, n = 6–7/group; *$p < 0.05$, **$p < 0.01$ PER vs. Vehicle, unpaired t test, two-tailed.

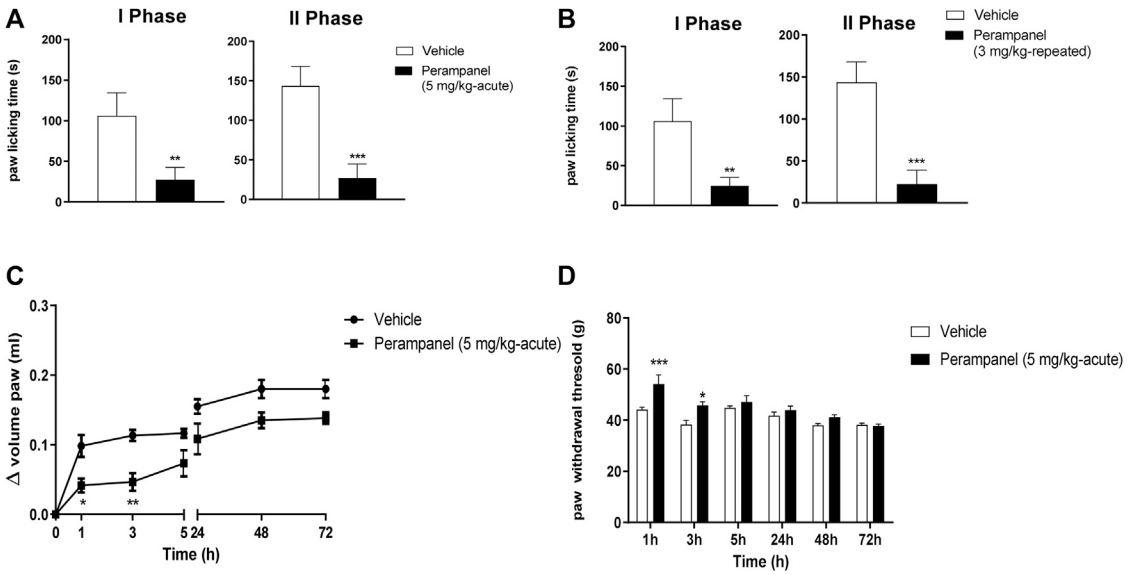

FIGURE 3 | Effect of PER in formalin **(A,B)** and carrageenan **(C,D)** animal models. In A and B mice were tested following formalin (5%) intraplanar administration; **(A)** time spent in paw licking after a single vehicle or PER (5 mg/kg) administration, **(B)** time spent in paw licking after repeated oral vehicle or PER (3 mg/kg/d) for 4 consecutive days administration. **C** and **D**, mice were tested following carrageenan (1%) intraplanar injection. Paw oedema **(C)** and paw withdrawal latency **(D)** were evaluated following oral acute vehicle or PER (5 mg/kg) administration. Data are shown as means ± S.E.M, n = 6–7/group; *$p < 0.05$, **$p < 0.01$, ***$p < 0.001$ PER vs. Vehicle, followed unpaired t test, two-tailed or two-way ANOVA Bonferroni's post-hoc test.

Anti-Inflammatory Effect of PER

The anti-inflammatory effects of PER were tested using the formalin test (**Figure 3**). Intraplantar administration of formalin induced a marked pain behavior, characterized by two phases, an intense early sensorial phase (0–15 min after injection), and a second inflammatory phase (15–45 min after injection). Single oral administration of PER (5 mg/kg) given 1 h before the test, produced an effect in both phases (**$p < 0.001$; ***$p < 0.0001$ vs. vehicle; t = 5.976 Unpaired t test, two-tailed phase I; t = 9.394 Unpaired t test, two-tailed phase II, **Figure 3A**). A similar effect on both phases was observed also after repeated administrations of PER (3 mg/kg) up to 4 days (**$p < 0.001$; ***$p < 0.0001$ vs. vehicle; t = 6.582 Unpaired t test, two-tailed phase I; t = 9.987 Unpaired t test, two-tailed phase II; **Figure 3B**).

Considering the effect of PER in the second phase of formalin test, known as inflammatory phase, we tested this drug in the carrageenan-induced paw edema model of inflammatory pain (**Figures 3C,D**). Following carrageenan injection, paw edema develops in two phases: an acute phase in the first 5 h and a second phase peaking at 72 h (28). The acute treatment with PER (5 mg/kg) 30 min before carrageenan administration reduced paw edema in a time-dependent manner. During the first phase (0–5 h), PER inhibited edema formation for 3 h after carrageenan injection (*$p < 0.05$; **$p < 0.01$; $F_{(6, 70)}$ = 42,00 for factor time; $F_{(1, 70)}$ = 42,34 for factor treatment; $F_{(6, 0)}$ = 1,435 for time X treatment interaction, followed two-way ANOVA Bonferroni's post-hoc test; **Figure 3C**), while in the second phase, PER treatment did to affect edema formation. The same mice were also subjected to the Randall-Selitto test (**Figure 3D**). Results showed an increased in paw withdrawal latency of PER group in the first 24 h compared to control group (*$p < 0.05$; ***$p < 0.001$; $F_{(5, 60)}$ = 12,97 for factor time; $F_{(1,60)}$ = 19,71 for factor treatment; $F_{(5,60)}$ = 2,828 for time X treatment interaction, followed two-way ANOVA Bonferroni's post-hoc test; **Figure 3D**), while no effect was observed at 48 and 72 h.

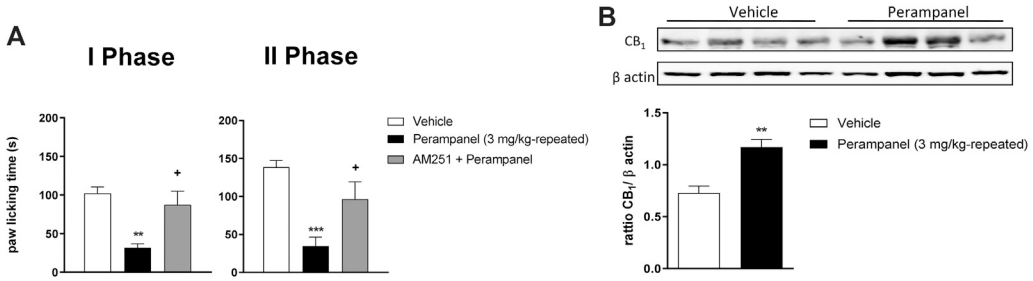

FIGURE 4 | CB1 involvement in PER-induced analgesia in formalin test. **(A)** Time spent in paw licking after a repeated (4 consecutive days) oral vehicle, PER (3 mg/kg) administration. The CB1 antagonist, AM251 (1 mg/kg/ip) was administrated one hour before the last administration. **(B)** CB1 Protein expression in the spinal cord of mice treated with vehicle or PER (3 mg/kg). Data are shown as means ± S.E.M, n = 6–7/group; $^{*}p < 0.05$, $^{**}p < 0.01$, $^{***}p < 0.001$ vs. Vehicle. $^{+}p < 0.05$ vs. PER followed two-way ANOVA Bonferroni's post-hoc test or unpaired t test, two-tailed.

Involvement of Cannabinergic System on PER's Anti-Inflammatory Activity

The contribution of CB_1 receptors in PER effects was investigated using the CB1 antagonist AM251 (1 mg/kg/ip), injected one hour before the last PER administration in the repeated scheme of 3 mg/kg. Results clearly showed that AM251 was able to reverse the effect of PER in both phases of formalin test ($^{+}p < 0.05$ vs. Perampanel; $F_{(2, 15)} = 10{,}14$ for treatment phase I; $F_{(2, 15)} = 11{,}11$ for treatment phase II, followed one-way ANOVA Bonferroni's post-hoc test; **Figure 4A**). At this experimental time point, CB_1 protein expression of PER treated mice in the spinal cord was also determined. As reported in **Figure 4B** western blot analysis, PER treatment induced a significant increase in expression of CB_1 receptor compared to vehicle group $^{**}p < 0.001$ vs. vehicle; t = 4,354, Unpaired t test, two-tailed).

Perampanel Effect in CCI-Induced Neuropathic Pain

To examine whether PER was able to reduce allodynia and hyperalgesia associated with NP, we induced peripheral neuropathy in mice by ligation of sciatic nerve. Four days after ligature, we started the acute (5 mg/kg; **Figures 5A,C**) and repeated (3 mg/kg; **Figures 5B,D**) treatment with PER given orally. At day 7 we tested pain threshold after thermal and mechanical noxious stimuli. It was observed a significant increase in paw withdrawal threshold of vehicle-treated mice compared to sham mice in response to von-Frey test, suggesting the development of mechanical allodynia and the cute PER administration (5 mg/kg) significantly reduced the number of ipsilateral paw withdrawals. Acute PER administration (5 mg/kg) significantly reduced the number of ipsilateral paw withdrawals at 1 h post treatment ($^{\#}p < 0.05$; $^{\#\#}p < 0.01$ vs. Sham; $^{**}p < 0.01$ vs CCI-vehicle; $F_{(1{,}931,\ 28{,}96)} = 1{,}145$ for factor time; $F_{(2,\ 15)} = 29{,}32$ for factor treatment; $F_{(4,\ 30)} = 3{,}532$ for time X treatment interaction, followed by two-way ANOVA Tukey's post-hoc test; **Figure 5A**).

Similarly, increased paw withdrawal latency was also observed in Randall-Selitto test, indicating the development of mechanical hyperalgesia until 3 h post treatment ($^{\#\#\#}p < 0.001$, $^{\#\#\#\#}p < 0.0001$ vs. Sham;$^{*}p < 0.05$; $^{***}p < 0.001$ vs. CCI-vehicle; $F_{(1{,}783,\ 26{,}75)} = 4{,}673$ for factor time; $F_{(2,\ 15)} = 111{,}8$ for factor treatment; $F_{(4,\ 30)} = 14{,}93$ for time X treatment interaction, followed by two-way ANOVA Tukey's post-hoc test; **Figure 5C**).

On the other hand, repeated oral PER administration (3 mg/kg) significantly induced a significant antiallodynic ($^{\#}p < 0.05$; $^{\#\#}p < 0.01$ vs. Sham;$^{*}p < 0.05$; $^{**}p < 0.01$ vs CCI-vehicle; $F_{(1{,}900,\ 28{,}49)} = 0{,}5204$ for factor time; $F_{(2,\ 15)} = 17{,}63$ for factor treatment; $F_{(4,\ 30)} = 1{,}103$ for time X treatment interaction, followed by two-way ANOVA Tukey's post-hoc test; **Figure 5B**) and anti-hyperalgesic effect ($^{\#\#\#}p < 0.001$, $^{\#\#\#\#}p < 0.0001$ vs. Sham; $^{*}p < 0.05$; $^{***}p < 0.001$ vs. CCI-vehicle; $F_{(1{,}447,\ 21{,}70)} = 4{,}170$ for factor time; $F_{(2,\ 15)} = 121{,}7$ for factor treatment; $F_{(4,\ 30)} = 3{,}440$ for time X treatment interaction, followed by two-way ANOVA Tukey's post-hoc test; **Figure 5D**) at all experimental times (1, 3, and 5 h post treatment).

Involvement of Cannabinergic System on Anti-Neuropathic PER Activity

Western blot analysis showed that mice with CCI expressed reduced levels of CB1 receptor protein in the spinal cord, while the repeated treatment with PER (3 mg/kg) restored CB1 receptor expression in the spinal cord ($^{*}p < 0.05$ vs. CCI-vehicle; $F_{(2,\ 6)} = 8{,}158$ followed by one-way ANOVA Tukey's post-hoc test; **Figure 6A**). These data suggested a potential involvement of the cannabinergic system in the mechanism of action of PER, therefore a specific CB1 antagonist, AM251 (1 mg/kg, ip) was used for the in vivo tests. AM251 was administered 30 min before last PER (3 mg/kg) administration in CCI mice; mice treated with AM251 showed a significant decreased PER effect in both mechanical allodynia and hyperalgesia ($^{\#}p < 0.05$; $^{\#\#}p < 0.01$ vs. Sham;$^{*}p < 0.05$; $^{**}p < 0.01$ vs. CCI-vehicle; $^{+}p < 0.05$ vs. CCI-PER; $F_{(1{,}809,\ 45{,}21)} = 0{,}8809$ for factor time; $F_{(4,\ 25)} = 30{,}90$ for factor treatment; $F_{(8,\ 50)} = 0{,}4047$ for time X treatment interaction, followed by two-way ANOVA Tukey's post-hoc test; **Figure 6B**; ($^{\#\#}p < 0.01$, $^{\#\#\#}p < 0.001$, $^{\#\#\#\#}p < 0.0001$ vs. Sham; $^{*}p < 0.05$; $^{***}p < 0.001$ vs. CCI-vehicle $^{+}p < 0.05$ $^{++}p < 0.01$ vs. CCI-PER; $F_{(1{,}977,\ 49{,}41)} = 3{,}560$ for factor time; $F_{(4,\ 25)} = 94{,}49$

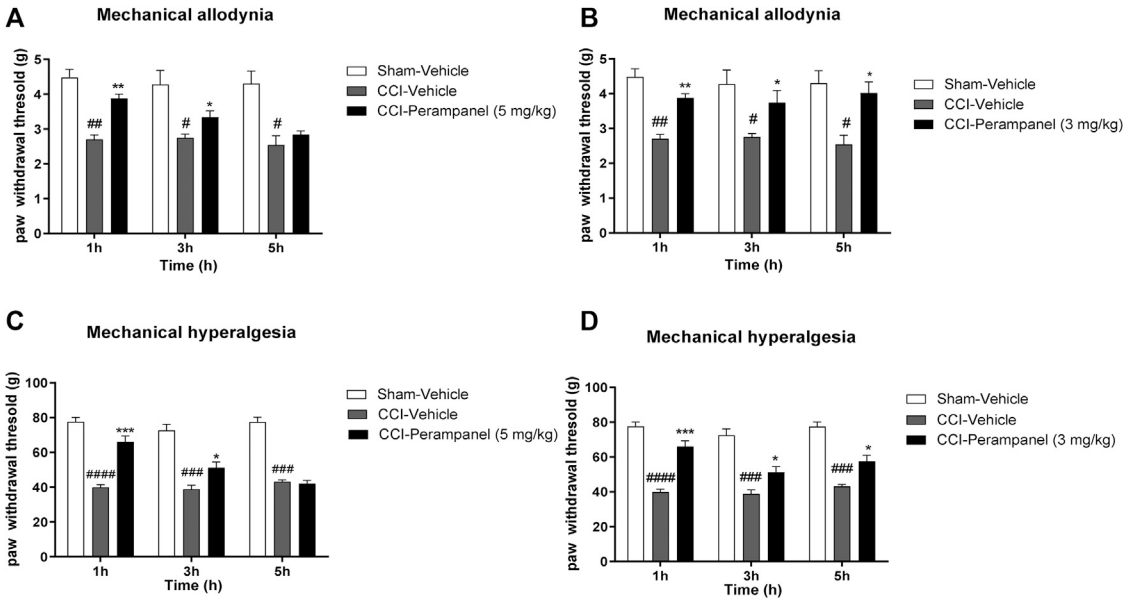

FIGURE 5 | PER effect in CCI-induced neuropathic pain. Time course effect of vehicle or PER after single **(A**,**C)** and repeated for 4 days **(C**,**D)** oral administration. Antiallodynic PER effect after **(A)** acute (5 mg/kg) and **(B)** repeated (3 mg/kg) administration in Von Frey test, on day 7 following sciatic nerve ligation. Antihyperalgesic PER effect after **(C)** acute (5 mg/kg) and **(D)** repeated (3 mg/kg) administration in Randall-Selitto test, on day 7 following sciatic nerve ligation. Sham group represent not ligated animals. Data are shown as means ± S.E.M, n = 6–7/group; *$p < 0.05$, **$p < 0.01$, ***$p < 0.001$ vs. Vehicle. #$p < 0.05$, ##$p < 0.01$, ###$p < 0.001$ vs. Sham-Vehicle, followed by two-way ANOVA Tukey's post-hoc test.

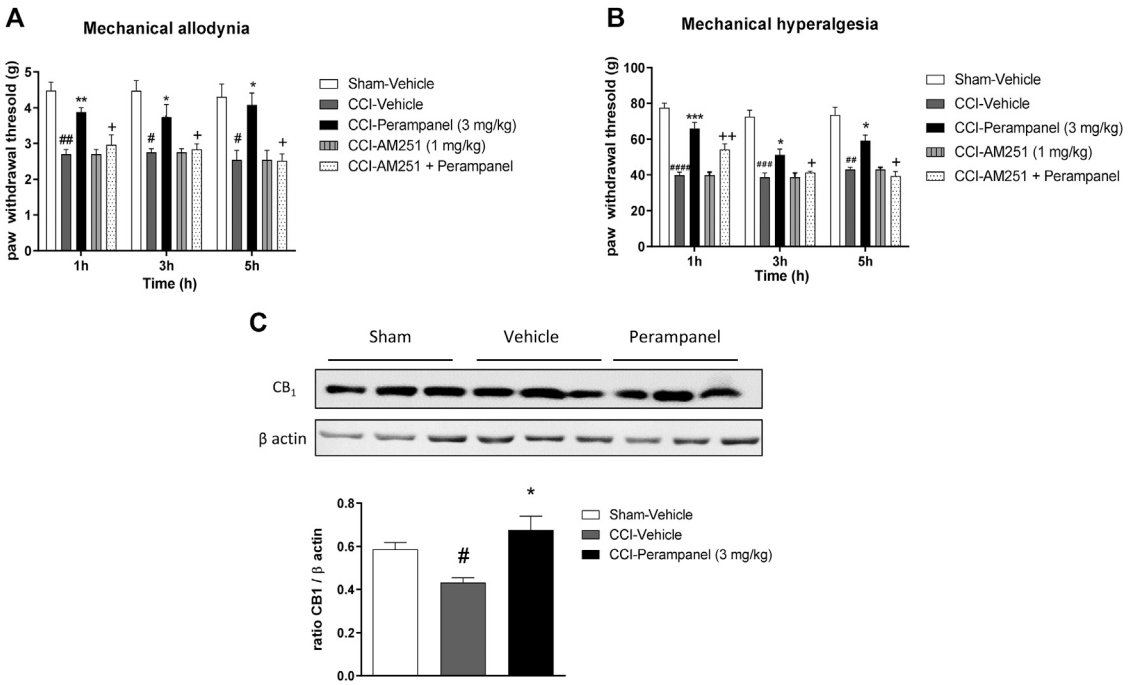

FIGURE 6 | CB1 involvement in PER-induced neuropathic pain reduction. **(A)** CB1 protein expression in the spinal cord of Sham- and CCI-mice treated with vehicle and PER (3 mg/kg). **(B)** Antiallodynic and **(C)** Antihyperalgesic PER effect at 1, 3, and 5 h post treatment with or without CB1 antagonist, AM251, (1 mg/kg/ip). The antagonist was administrated one hour before the last administration. Data are shown as means ± S.E.M, n = 6–7/group; *$p < 0.05$, **$p < 0.01$, ***$p < 0.001$ vs Vehicle. #$p < 0.05$, ##$p < 0.01$, ###$p < 0.001$ vs. Sham-Vehicle. +$p < 0.05$ vs. PER, followed by two-way ANOVA Tukey's post-hoc test.

for factor treatment; $F_{(8,\ 50)}$ = 2,173 for time X treatment interaction, followed by two-way ANOVA Tukey's post-hoc test; **Figure 6C**).

Evaluation of Pro-Inflammatory Cytokines in CCI-Mice Spinal Cord

Since inflammation has been associated with the pathogenesis and progression of chronic pain, we finally investigated the possible modulation of cytokines involved in the inflammatory process in CCI-mice treated with vehicle and PER at spinal cord level. On day 7 after surgery, CCI vehicle-group showed a significant increased expression of pro-inflammatory cytokines (TNFα, IL-1β, and IL-6) in spinal cord ($^{\#}p < 0.05$; $^{\#\#\#}p < 0.0001$ vs. sham-Vehicle; **Figures 7A–C**). Significant reduction of all these cytokines were observed in CCI PER treated mice ($^{*}p < 0.05$ vs. CCI-vehicle; **Figure 7A–C**) (TNFα, $F_{(2,17)}$ = 14.21; IL-1β, $F_{(2,17)}$ = 15.23; IL-6, $F_{(2,17)}$ = 6.815; followed by one-way ANOVA Tukey's post-hoc test).

DISCUSSION

Pain is a complex debilitating and frustrating pathology that may interfere with sleep, work, and activities, eventually leading to reduced quality of life. At same way also pain management is difficult and can lead to harmful effects if not properly administered and monitored. Numerous types of receptors involved in various signaling pathways are activated in pain perception. They can be considered targets for the modulation of pain and studied to discover novel analgesic molecules. For instance, antagonists of TRPV1, TRPM8, ASICs, AMPA, NMDA, mGlu, NK1, and CGRP receptors have shown to be effective in several animal models of pain (Khan et al., 2019); similarly, the activation of specific pathways, such as opioidergic, serotoninergic and cannabinergic systems has shown analgesic properties by modulating the central and peripheral perception of painful stimuli (Scherrer et al., 2009; Palit et al., 2011; De Gregorio et al., 2019).

In the present, study we evaluated the anti-nociceptive effects of PER, a highly selective non-competitive AMPA receptors antagonist, in several mouse models of acute and chronic pain and for the first time, we assessed a possible correlation between the glutamatergic and the cannabinergic system. PER is currently used in clinics as a broad spectrum ASM but it has shown efficacy also in some models of other neurological disorders such as multiple sclerosis, Parkinson disease and migraine (Akamatsu et al., 2016; Lattanzi et al., 2018; Tringali et al., 2018). Different studies have suggested that in cultured rat cortical neurons, PER inhibits the AMPA-induced increase in intracellular Ca^{2+}, while in contrast to its effect on AMPA receptors, PER caused little or no inhibition of NMDA-induced Ca^{2+} responses, indicating a selectivity for AMPA receptors versus NMDA receptors (Hanada et al., 2011). It is well known that AMPA receptors regulate excitatory neurotransmission in pain pathways (Woolf and Salter, 2000). In fact, glutamate release in the spinal dorsal horn after nerve injury and peripheral inflammation is an important contributor to pathological pain (through AMPA receptors) inducing a postsynaptic depolarization that is able to remove the Mg^{2+} block from the NMDA receptor (Ruscheweyh et al., 2011). Moreover, studies in hippocampal slices have also demonstrated that PER selectively blocks AMPA receptor-mediated synaptic transmission and neuronal excitation that are the established causes for the development of NP (Ceolin et al., 2012). It was also shown that spinal AMPA receptors contribute to the central sensitization associated with acute pain. In fact, treatment with different doses of morphine showed hypersensitivity to mechanical stimulation but intrathecal administration of a Ca^{2+} permeable selective AMPA receptor blocker disrupted morphine-induced mechanical sensitivity with an increased GluA4 expression and phosphorylation in homogenates of dorsal horn (Cabañero et al., 2013). Moreover, Tao has also shown that inflammation-induced changes in AMPA receptor subunits (i.e., GluA1 membrane insertion and GluA2 internalization) at postsynaptic membranes of dorsal horn neurons are involved in central sensitization in persistent inflammatory pain (Tao, 2010).

Based on this background, we started to investigate the analgesic effect of PER in the tail flick and hot plate tests in order to evaluate spinal nociceptive reflex and supra-spinally responses, after acute or repeated administrations. We used repeated regimen to understand if a poor-active dose (3 mg/kg) in our experimental condition could to be more efficacy and prolonged in the time, despite its short half-life (1.6 h). In both tests PER showed a significant antinociceptive activity following both acute and chronic regimen. Moreover,

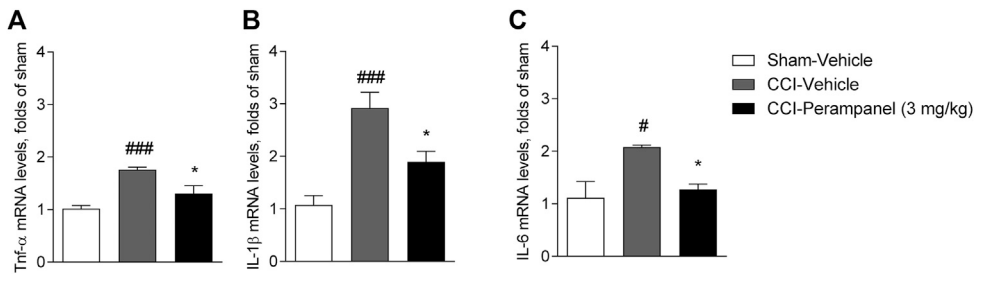

FIGURE 7 | Expression of pro-inflammatory cytokines in spinal cord on day 7 after sciatic nerve ligation. **(A)** mRNA level of TNFα. **(B)** mRNA level of IL-1β. **(C)** mRNA level of IL-6. Data are shown as means ± S.E.M, n = 6–7/group using ordinary one-way ANOVA; $^{*}p < 0.05$, vs. Vehicle. $\#p < 0.05$, $\#\#\#p < 0.001$ vs. Sham-Vehicle followed by one-way ANOVA Tukey's post-hoc test.

animals treated for 4 days showed a more prolonged in time activity but did not correlate to a greater effectiveness between the two posological regimens. Our results confirm that AMPA receptors represent an important target to modulate pain sensation. Then, we better characterized PER effects using acute and chronic animal pain models such as, chemical-induced visceral pain using writhing test, the paw licking test and paw edema to assess somatic pain with inflammatory and neurogenic component, and in pathologic conditions due to neuropathic pain. This approach allowed us to analyze the efficacy of PER oral administration on pain perception and also its capability to modulate inflammation. Previous authors have shown that selective, noncompetitive AMPA receptor antagonists, such as SYM 2206, CFM-2, and GYKI 52466, produced antinociceptive effects in the spinal cord of mice with neuropathic and inflammatory pain (Garry et al., 2003). In agreement with these data, results showed that single (5 mg/kg) and repeated (3 mg/kg/d for 4 days) PER administration significantly attenuated writhing episodes, reduced paw edema and formalin-induced pain. In this last experiment, PER reduced the response in both the early phase in which Aδ and C-fibers are triggered, and the late phase characterized by sensitization of nociceptive spinal neurons (Coderre et al., 1993). This specific effect of PER seems to go beyond the modulation of the AMPA channel, suggesting that probably other systems are involved in its mode of action. A link between the glutamatergic and the cannabinergic systems has been previously demonstrated. The endocannabinoids anandamide (AEA) and 2-arachidonoylglycerol (2-AG) are synthesized "*on demand*" from membrane lipids in response to cellular signals such as activation of the postsynaptic glutamate receptors, moreover, cannabinoid agonists inhibit glutamate release in many synapses in the central nervous system, including the prefrontal cortex (Melis et al., 2004), hippocampus and cerebellum (Misner and Sullivan, 1999), striatum (Huang et al., 2001; Robbe et al., 2001), and spinal cord (Morisset and Urban, 2001). Moreover, Palazzo and coworkers showed that endogenous glutamate could tonically modulate nociception through mGlu and NMDA receptors in the periaqueductal grey (PAG) matter and the stimulation of these receptors seems to be required for cannabinoid-induced analgesia (Palazzo et al., 2001).

In our study, we considered the correlation between AMPA modulation and cannabinergic activity by assessing CB_1 receptor expression in the spinal cord of mice with CCI and we studied the in vivo efficacy of PER using the CB_1 receptor antagonist AM251. Results clearly showed that PER effects were cannabinergic system-dependent, in fact AM251 was able to reduce PER activity and western blot analysis showed a significantly increased expression of this receptor in comparison with non-treated animals. It is known that pathological conditions, such as nerve injury and/or peripheral inflammation, are an important contributor to long-term potentiation (LTP) of glutamatergic transmission (Ruscheweyh et al., 2011). Glutamate release via activation of presynaptic AMPA receptors initiates the postsynaptic depolarization necessary to remove the Mg^{2+} block from the NMDA receptor channel, which can sequentially induce Ca^{2+} influx, LTP, and hyperalgesia. In the current study, oral PER administration attenuated mechanical and cold hyperalgesia in CCI mice, in agreement with other authors (Murai et al., 2016; Khangura et al., 2017; Hara et al., 2020). Moreover, CB_1 antagonist AM251, reverted these effects, underlining once again a strong correlation between PER effect and the cannabinergic activity. Finally, an increasing amount of studies suggest that neuroinflammation and pro-inflammatory cytokines are important factors in the development and maintenance of NP (Sweitzer et al., 2001; Zhang and An, 2007). In our study PER reduced proinflammatory cytokine levels suggesting a reduction of the inflammatory state at spinal cord level.

In conclusion, our evidences support the potential use of PER as an analgesic. By means of specific mouse models of pain, we further extend our knowledge on its mechanism of action indicating a clear involvement of the cannabinergic system as well as an anti-inflammatory action. Therefore, while PER mechanism should be further studied also in order to understand the link between AMPA receptors and cannabinergic systems, its potential clinical use on pain therapy should start to be considered.

DATA AVAILABILITY STATEMENT

The original contributions presented in the study are included in the article/Supplementary Material, further inquiries can be directed to the corresponding author.

ETHICS STATEMENT

The animal study was reviewed and approved by The Institutional Committee on the Ethics of Animal Experiments (CSV) of the University of Naples "Federico II" and by the Ministero della Salute under protocol no.996/2016-PR.

AUTHOR CONTRIBUTIONS

DC, CC, CA, and MC Methodology in vivo, LG data curation, DC, CC, and RR writing—original draft preparation, AG and RE review and editing, AC and DG supervision.

FUNDING

This work was partly supported by: 1) the Italian Ministry of Health. Grant No. GR-2013-02355028; 2) Italian Ministry of University and Research (MIUR) Prot. 2017B9NCSX.

ACKNOWLEDGMENTS

We thank Giovanni Esposito and Angelo Russo for animal care and assistance.

REFERENCES

Adedoyin, M. O., Vicini, S., and Neale, J. H. (2010). Endogenous N-acetylaspartylglutamate (NAAG) inhibits synaptic plasticity/transmission in the amygdala in a mouse inflammatory pain model. *Mol. Pain*. 6, 60. doi:10.1186/1744-8069-6-60

Akamatsu, M., Yamashita, T., Hirose, N., Teramoto, S., and Kwak, S. (2016). The AMPA receptor antagonist perampanel robustly rescues amyotrophic lateral sclerosis (ALS) pathology in sporadic ALS model mice. *Sci. Rep*. 6, 28649. doi:10.1038/srep28649

Bialer, M. (2012). Why are antiepileptic drugs used for nonepileptic conditions? *Epilepsia* 53 (Suppl. 7), 26–33. doi:10.1111/j.1528-1167.2012.03712.x

Cabañero, D., Baker, A., Zhou, S., Hargett, G. L., Irie, T., Xia, Y., et al. (2013). Pain after discontinuation of Morphine treatment is associated with synaptic increase of GluA4-containing AMPAR in the Dorsal Horn of the Spinal Cord. *Neuropsychopharmacology*. 38, 1472–1484. doi:10.1038/NPP.2013.46

Morón, L., Bortolotto, Z. A., Bannister, N., Collingridge, G. L., Lodge, D., and Volianskis, A. (2012). A novel anti-epileptic agent, perampanel, selectively inhibits AMPA receptor-mediated synaptic transmission in the hippocampus. *Neurochem. Int*. 61, 517–522. doi:10.1016/J.NEUINT.2012.02.035

Chaparro, L. E., Wiffen, P. J., Moore, R. A., and Gilron, I. (2012). Combination pharmacotherapy for the treatment of neuropathic pain in adults. *Cochrane Database Syst. Rev*. 2012, CD008943. doi:10.1002/14651858.CD008943.pub2

Chizh, B. A., Schlütz, H., Scheede, M., and Englberger, W. (2000). The N-methyl-D-aspartate antagonistic and opioid components of d-methadone antinociception in the rat spinal cord. *Neurosci. Lett*. 296, 117–120. doi:10.1016/s0304-3940(00)01638-4

Citraro, R., Leo, A., Franco, V., Marchiselli, R., Perucca, E., De Sarro, G., and Russo, E. (2017). Perampanel effects in the WAG/Rij rat model of epileptogenesis, absence epilepsy, and comorbid depressive-like behavior. *Epilepsia* 58, 231–238. doi:10.1111/epi.13629

Russo, T. J., Fundytus, M. E., McKenna, J. E., Dalal, S., and Melzack, R. (1993). The formalin test: a validation of the weighted-scores method of behavioural pain rating. *Pain*. 54, 43–50. doi:10.1016/0304-3959(93)90098-A

D'Agostino, G., La Rana, G., Russo, R., Sasso, O., Iacono, A., Esposito, E., et al. (2007). Acute intracerebroventricular administration of palmitoylethanolamide, an endogenous peroxisome proliferator-activated receptor-alpha agonist, modulates carrageenan-induced paw edema in mice. *J. Pharmacol. Exp. Ther*. 322, 1137–1143. doi:10.1124/jpet.107.123265

Calignano, E. M., Coggeshall, R. E., and Carlton, S. M. (1997). Peripheral NMDA and non-NMDA glutamate receptors contribute to nociceptive behaviors in the rat formalin test. *Neuroreport*. 8, 941–946. doi:10.1097/00001756-199703030-00025

De Gregorio, D., McLaughlin, R. J., Posa, L., Ochoa-Sanchez, R., Enns, J., Lopez-Canul, M., et al. (2019). Cannabidiol modulates serotonergic transmission and reverses both allodynia and anxiety-like behavior in a model of neuropathic pain. *Pain* 160, 136–150. doi:10.1097/j.pain.0000000000001386

Gobbi, V., Luongo, L., Guida, F., Cristino, L., Palazzo, E., Russo, R., et al. (2012). Effects of intra-ventrolateral periaqueductal grey palmitoylethanolamide on thermoceptive threshold and rostral ventromedial medulla cell activity. *Eur. J. Pharmacol*. 676, 41–50. doi:10.1016/j.ejphar.2011.11.034

Maione, C., Labate, A., Maschio, M., Meletti, S., and Russo, E. (2017). AMPA receptors and perampanel behind selected epilepsies: current evidence and future perspectives. *Expert Opin. Pharmacother*. 18, 1751–1764. doi:10.1080/14656566.2017.1392509

Douyard, J., Shen, L., Huganir, R. L., and Rubio, M. E. (2007). Differential neuronal and glial expression of GluR1 AMPA receptor subunit and the scaffolding proteins SAP97 and 4.1N during rat cerebellar development. *J. Comp. Neurol*. 502, 141–156. doi:10.1002/cne.21294

Garry, E. M., Moss, A., Delaney, A., O'Neill, F., Blakemore, J., Bowen, J., et al. (2003). Neuropathic sensitization of behavioral reflexes and Spinal NMDA receptor/CaM kinase II interactions are disrupted in PSD-95 mutant mice. *Curr. Biol*. 13, 321–328. doi:10.1016/S0960-9822(03)00084-8

Gwak, Y. S., Kang, J., Leem, J. W., and Hulsebosch, C. E. (2007). Spinal AMPA receptor inhibition attenuates mechanical allodynia and neuronal hyperexcitability following spinal cord injury in rats. *J. Neurosci. Res*. 85, 2352–2359. doi:10.1002/jnr.21379

Hanada, T., Hashizume, Y., Tokuhara, N., Takenaka, O., Kohmura, N., Ogasawara, A., et al. (2011). Perampanel: a novel, orally active, noncompetitive AMPA-receptor antagonist that reduces seizure activity in rodent models of epilepsy. *Epilepsia*. 52, 1331–1340. doi:10.1111/j.1528-1167.2011.03109.x

Hara, K., Haranishi, Y., and Terada, T. (2020). Intrathecally administered perampanel alleviates neuropathic and inflammatory pain in rats. *Eur. J. Pharmacol*. 872, 172949. doi:10.1016/j.ejphar.2020.172949

Huang, C. C., Lo, S. W., and Hsu, K. S. (2001). Presynaptic mechanisms underlying cannabinoid inhibition of excitatory synaptic transmission in rat striatal neurons. *J. Physiol. (Lond)*. 532, 731–748. doi:10.1111/j.1469-7793.2001.0731e.x

Jensen, T. S., and Finnerup, N. B. (2014). Allodynia and hyperalgesia in neuropathic pain: clinical manifestations and mechanisms. *Lancet Neurol*. 13, 924–935. doi:10.1016/S1474-4422(14)70102-4

Khan, A., Khan, S., and Kim, Y. S. (2019). Insight into pain modulation: nociceptors sensitization and therapeutic targets. *Curr. Drug Targets* 20, 775–788. doi:10.2174/1389450120666190131114244

Khangura, R. K., Bali, A., Kaur, G., Singh, N., and Jaggi, A. S. (2017). Neuropathic pain attenuating effects of perampanel in an experimental model of chronic constriction injury in rats. *Biomed. Pharmacother*. 94, 557–563. doi:10.1016/j.biopha.2017.07.137

Latremoliere, A., and Woolf, C. J. (2009). Central sensitization: a generator of pain hypersensitivity by central neural plasticity. *J. Pain*. 10, 895–926. doi:10.1016/j.jpain.2009.06.012

Lattanzi, S., Brigo, F., Trinka, E., Zaccara, G., Cagnetti, C., Del Giovane, C., et al. (2018). Efficacy and safety of cannabidiol in epilepsy: A systematic review and meta-analysis. *Drugs* 78, 1791–1804. doi:10.1007/s40265-018-0992-5

Silvestrini, A., Giovannini, G., Russo, E., and Meletti, S. (2018). The role of AMPA receptors and their antagonists in status epilepticus. *Epilepsia*. 59, 1098–1108. doi:10.1111/epi.14082

Mannelli, L. D. C., D'Agostino, G., Pacini, A., Russo, R., Zanardelli, M., Ghelardini, C., et al. (2013). Palmitoylethanolamide is a disease-modifying agent in peripheral neuropathy: pain relief and neuroprotection share a PPAR-Alpha-mediated mechanism. *Mediators Inflamm*. 2013, 328797. doi:10.1155/2013/328797.2013

McRoberts, J. A., Coutinho, S. V., Marvizón, J. C., Grady, E. F., Tognetto, M., Sengupta, J. N., et al. (2001). Role of peripheral N-methyl-D-aspartate (NMDA) receptors in visceral nociception in rats. *Gastroenterology* 120, 1737–1748. doi:10.1053/gast.2001.24848

Mayer, M., Perra, S., Muntoni, A. L., Pillolla, G., Lutz, B., Marsicano, G., et al. (2004). Prefrontal cortex stimulation induces 2-arachidonoyl-glycerol-mediated suppression of excitation in dopamine neurons. *J. Neurosci*. 24, 10707–10715. doi:10.1523/JNEUROSCI.3502-04.2004

Pistis, D. L., and Sullivan, J. M. (1999). Mechanism of cannabinoid effects on long-term potentiation and depression in hippocampal CA1 neurons. *J. Neurosci*. 19, 6795–6805. doi:10.1523/JNEUROSCI.19-16-06795.1999

Morisset, V., and Urban, L. (2001). Cannabinoid-induced presynaptic inhibition of glutamatergic EPSCs in substantia gelatinosa neurons of the rat spinal cord. *J. Neurophysiol*. 86, 40–48. doi:10.1152/jn.2001.86.1.40

Murai, N., Sekizawa, T., Gotoh, T., Watabiki, T., Takahashi, M., Kakimoto, S., et al. (2016). Spontaneous and evoked pain-associated behaviors in a rat model of neuropathic pain respond differently to drugs with different mechanisms of action. *Pharmacol. Biochem. Behav*. 141, 10–17. doi:10.1016/J.PBB.2015.11.008

Nagakura, E., Marabese, I., de Novellis, V., Oliva, P., Rossi, F., Berrino, L., et al. (2001). Metabotropic and NMDA glutamate receptors participate in the cannabinoid-induced antinociception. *Neuropharmacology* 40, 319–326. doi:10.1016/s0028-3908(00)00160-x

Maione, S., Sheaff, R. J., France, C. R., McGlone, S. T., Potter, W. T., Harkness, A. R., et al. (2011). Serotonin transporter gene (5-HTTLPR) polymorphisms are associated with emotional modulation of pain but not emotional modulation of spinal nociception. *Biol. Psychol*. 86, 360–369. doi:10.1016/j.biopsycho.2011.01.008

Rhudy, E., Watanabe, M., Hartmann, B., Grant, S. G., and Todd, A. J. (2008). Expression of AMPA receptor subunits at synapses in laminae I-III of the rodent spinal dorsal horn. *Mol. Pain*. 4, 5. doi:10.1186/1744-8069-4-5

Potschka, H., and Trinka, E. (2019). Perampanel: does it have broad-spectrum potential?. *Epilepsia*. 60, 22–36. doi:10.1111/epi.14456

Robbe, D., Alonso, G., Duchamp, F., Bockaert, J., and Manzoni, O. J. (2001). Localization and mechanisms of action of cannabinoid receptors at the glutamatergic synapses of the mouse nucleus accumbens. *J. Neurosci.* 21, 109–116. doi:10.1523/JNEUROSCI.21-01-00109.2001

Ruscheweyh, R., Wilder-Smith, O., Drdla, R., Liu, X. G., and Sandkühler, J. (2011). Long-term potentiation in spinal nociceptive pathways as a novel target for pain therapy. *Mol. Pain.* 7, 20. doi:10.1186/1744-8069-7-20

Russmann, V., Salvamoser, J. D., Rettenbeck, M. L., Komori, T., and Potschka, H. (2016). Synergism of perampanel and zonisamide in the rat amygdala kindling model of temporal lobe epilepsy. *Epilepsia.* 57, 638–647. doi:10.1111/epi.13328

Russo, E., Gitto, R., Citraro, R., Chimirri, A., and De Sarro, G. (2012). New AMPA antagonists in epilepsy. *Exp. Opin. Investig. Drugs.* 21, 1371–1389. doi:10.1517/13543784.2012.705277

Russo, R., De Caro, C., Avagliano, C., Cristiano, C., La Rana, G., Mattace Raso, G., et al. (2016). Sodium butyrate and its synthetic amide derivative modulate nociceptive behaviors in mice. *Pharmacol. Res.* 103, 279–291. doi:10.1016/j.phrs.2015.11.026

Calignano, O., Russo, R., Vitiello, S., Raso, G. M., D'Agostino, G., Iacono, A., et al. (2012). Implication of allopregnanolone in the antinociceptive effect of N-palmitoylethanolamide in acute or persistent pain. *Pain.* 153, 33–41. doi:10.1016/j.pain.2011.08.010

Calignano, G., Imamachi, N., Cao, Y. Q., Contet, C., Mennicken, F., O'Donnell, D., et al. (2009). Dissociation of the opioid receptor mechanisms that control mechanical and heat pain. *Cell.* 137, 1148–1159. doi:10.1016/j.cell.2009.04.019

Basbaum, H. S., and Sadhotra, A. (2016). Current status of the new antiepileptic drugs in chronic pain. *Front. Pharmacol.* 7, 276. doi:10.3389/FPHAR.2016.00276

Sweitzer, S., Martin, D., and DeLeo, J. A. (2001). Intrathecal interleukin-1 receptor antagonist in combination with soluble tumor necrosis factor receptor exhibits an anti-allodynic action in a rat model of neuropathic pain. *Neuroscience.* 103, 529–539. doi:10.1016/s0306-4522(00)00574-1

Tao, Y.-X. (2010). Dorsal horn alpha-amino-3-hydroxy-5-methyl-4-isoxazolepropionic acid receptor trafficking in inflammatory pain. *Anesthesiology* 112, 1259–1265. doi:10.1097/ALN.0B013E3181D3E1ED

Tomić, M., Pecikoza, U., Micov, A., Vučković, S., and Stepanović-Petrović, R. (2018). Antiepileptic drugs as analgesics/adjuvants in inflammatory pain: current preclinical evidence. *Pharmacol. Ther.* 192, 42–64. doi:10.1016/j.pharmthera.2018.06.002

Tringali, G., Currò, D., and Navarra, P. (2018). Perampanel inhibits calcitonin gene-related peptide release from rat brainstem in vitro. *J. Headache Pain* 19, 107. doi:10.1186/s10194-018-0940-5

Woolf, C. J., and Salter, M. W. (2000). Neuronal plasticity: Increasing the gain in pain. *Science* 288, 1765–1769. doi:10.1126/science.288.5472.1765

Zhang, J. M., and An, J. (2007). Cytokines, inflammation, and pain. *Int. Anesthesiol. Clin.* 45, 27–37. doi:10.1097/AIA.0b013e318034194e

Conflict of Interest: RE has received speaker fees or fundings and has participated in advisory boards for Eisai, Pfizer, GW Pharmaceuticals, UCB pharma, Arvelle Therapeutics.

The remaining authors declare that the research was conducted in the absence of any commercial or financial relationships that could be construed as a potential conflict of interest.

frontiers in Pharmacology

ORIGINAL RESEARCH
published: 24 February 2021
doi: 10.3389/fphar.2021.607572

Comparative Assessment of the Activity of Racemic and Dextrorotatory Forms of Thioctic (Alpha-Lipoic) Acid in Low Back Pain: Preclinical Results and Clinical Evidences From an Open Randomized Trial

Alessandra Pacini[1†], Daniele Tomassoni[2†], Elena Trallori[3], Laura Micheli[3], Francesco Amenta[4†], Carla Ghelardini[3], Lorenzo Di Cesare Mannelli[3†] and Enea Traini[4†]*

[1]Department of Experimental and Clinical Medicine, Anatomy and Histology Section, University of Florence, Florence, Italy, [2]School of Biosciences and Veterinary Medicine, University of Camerino, Camerino, Italy, [3]Department of Neuroscience, Psychology, Drug Research and Child Health (NEUROFARBA)-Pharmacology and Toxicology Section, University of Florence, Florence, Italy, [4]Section of Human Anatomy, School of Pharmacy, University of Camerino, Camerino, Italy

OPEN ACCESS

Edited by:
Francesca Guida, University of Campania Luigi Vanvitelli, Italy

Reviewed by:
Stefano Comai, University of Padua, Italy
Carmela Belardo, Second University of Naples, Italy

***Correspondence:**
Lorenzo Di Cesare Mannelli
lorenzo.mannelli@unifi.it

[†]These authors have contributed equally to this work

Specialty section:
This article was submitted to Inflammation Pharmacology, a section of the journal Frontiers in Pharmacology

Received: *17 September 2020*
Accepted: *15 January 2021*
Published: *24 February 2021*

Citation:
Pacini A, Tomassoni D, Trallori E, Micheli L, Amenta F, Ghelardini C, Di Cesare Mannelli L and Traini E (2021) Comparative Assessment of the Activity of Racemic and Dextrorotatory Forms of Thioctic (Alpha-Lipoic) Acid in Low Back Pain: Preclinical Results and Clinical Evidences From an Open Randomized Trial. Front. Pharmacol. 12:607572. doi: 10.3389/fphar.2021.607572

Peripheral neuropathies, characterized by altered nociceptive and muscular functions, are related to oxidative stress. Thioctic acid is a natural antioxidant existing as two optical isomers, but most clinically used as racemic mixture. The present study investigated the central nervous system's changes which followed loose-ligation-derived compression of sciatic nerve, the putative neuroprotective role of thioctic acid and the pain-alleviating effect on low-back pain suffering patients. Loose ligation of the right sciatic nerve was performed in spontaneously hypertensive rats (SHR), a model of increased oxidative stress, and in normotensive Wistar-Kyoto rats (WKY). Animals with sciatic nerve ligation were left untreated or were treated intraperitoneally for 15 days with 250 $\mu mol \cdot kg^{-1} \cdot die^{-1}$ of (+/–)-thioctic acid; 125 $\mu mol \cdot kg^{-1} \cdot die^{-1}$ of (+/–)-thioctic acid; 125 $\mu mol \cdot kg^{-1} \cdot die^{-1}$ of (+)-thioctic acid lysine salt; 125 $\mu mol \cdot kg^{-1} \cdot die^{-1}$ of (–)-thioctic acid; 300 $\mu mol \cdot kg^{-1} \cdot die^{-1}$ pregabalin. Control SHR and WKY rats received the same amounts of vehicle. The clinical trial NESTIORADE (Sensory-Motor Neuropathies of the Sciatic Nerve: Comparative evaluation of the effect of racemic and dextro-rotatory forms of thioctic acid) examined 100 patients (49 males and 51 females aged 53 ± 11 years) dividing them into two equal-numbered groups, each treated daily for 60 days with 600 mg of (+/–)-thioctic acid or (+)-thioctic acid, respectively. The trial was registered prior to patient enrollment at EudraCT website (OSSC Number: 2011-000964-81). In the preclinical study, (+)-thioctic acid was more active than (+/–)- or (–)-enantiomers in relieving pain and protecting peripheral nerve as well as in reducing oxidative stress and astrogliosis in the spinal cord. Main findings of NESTIORADE clinical trial showed a greater influence on painful symptomatology, a quicker recovery and a better impact on quality of life of (+)-thioctic acid vs. (+/–)-thioctic acid. These data may have a pharmacological and

pharmacoeconomical relevance and suggest that thioctic acid, above all (+)-enantiomer, could be considered for treatment of low-back pain involving neuropathy.

Keywords: neuropathic pain, thioctic acid, antioxidant, food supplement, neuroprotection

INTRODUCTION

Neuropathic pain is a form of chronic pain caused by lesions to central or peripheral nervous system, which may be consequent to mechanical damage or diseases. It is characterized by altered nociceptive threshold and pain response, resulting in allodynia and hyperalgesia (Riego et al., 2018). The lumbosacral syndrome is a frequent neuropathic pathology described by a strong low back pain which may come from damage or irritation of sciatic nerve roots (Delitto et al., 2012). Treatment of its symptoms is still debated: the comparative evaluation of efficacy and tolerability of different drug categories (anti-inflammatory drugs, corticosteroids, antidepressants, anticonvulsants, muscle relaxants and opioids), concludes that most of the analyzed studies are poor quality and the data insufficient to provide guidance in the long-term treatment of the disease (Pinto et al., 2012; Schnitzer et al., 2004).

The excessive and unbalanced presence of reactive oxygen and nitrogen species causes oxidative stress, which alters the structure of the biomolecules and consequently induces neuronal damage (Adibhatla and Hatcher, 2010), inflammatory events and negative loop of excitotoxicity of afferent nociceptors, thus contributing to pain chronicization. Antioxidant agents, like thioctic (alpha-lipoic) acid, proved a therapeutic potential against neuropathy (Shay et al., 2009; Oyenihi et al., 2015).

Thioctic acid is a natural substance, synthetized *de novo* in mammalian mitochondria and existing as two optical isomers (+)-, endogenously produced and biologically active, and (−)-enantiomers. Racemic (+/−)-thioctic acid is sold worldwide as a registered drug or in nutraceutical market as dietary supplement and was reported to be a valid pharmacological agent in treating oxidative stress related diseases (Packer et al., 1995; Vasdev et al., 2000; Gomes and Negrato, 2014). Clinical studies showed that treatments with the racemic compound were able to reduce neuropathic low back pain (Memeo and Loiero, 2008; Ranieri et al., 2009). Even if the racemic mixture is the most widely used because of its stability, recent studies developed salt derivatives of (+)-thioctic acid with enough stability for a therapeutic use on its own (Ranieri et al., 2009; Amenta et al., 2010). Comparative studies revealed that (+)-thioctic acid displays a more pronounced activity than the racemic (+/−)-thioctic acid in several preclinical paradigms (Amenta et al., 2010; Lokhandwala, 2010). In the present study, we aimed to investigate if the (+)-thioctic acid is more active than its racemic congener on painful symptoms of sensory-motor neuropathies of the sciatic nerve in both a preclinical and clinical setting. The strain of spontaneously hypertensive rats (SHR), genetically harbouring hypertension and oxidative stress, was chosen and underwent to the loose ligation of the sciatic nerve (Tayebati et al., 2012). Pain relieving as well as neuroprotective and antioxidant effects of thioctic acid forms were compared to those of the reference drug pregabalin, a currently in-use anticonvulsant for treating chronic pain (Gilron et al., 2015; Xu et al., 2016). Based on the evidence from preclinical study, a clinical trial, named NESTIORADE (Sensory motor neuropathy of the sciatic nerve: Comparative assessment of the effectiveness of racemic and dextrorotatory forms of thioctic acid), was designed and conducted.

MATERIAL AND METHODS

Preclinical Study

Animals

Twenty-week-old male SHR (n = 42) and age-matched WKY (n = 42) rats were used. The animals were kept at 23 ± 1 °C with a 12 h light/dark cycle, light at 7 a.m. and fed with standard laboratory diet and tap water *ad libitum*. 24 h before the test, the animals were placed in the experimental room for acclimatization. All animal manipulations were carried out according to the Directive 2010/63/EU of the European Parliament and of the European Union council (September 22, 2010, amended by Regulation (EU) 2019/1010) on the protection of animals used for scientific purposes and to the ethical guidelines of the University of Florence, consistent with the Guide for the Care and Use of Laboratory Animals of the US National Institutes of Health (NIH Publication No. 85-23, revised 1996; University of Florence assurance number: A5278-01). Formal approval to conduct the experiments described was obtained from the Italian Ministry of Health and from the Animal Subjects Review Board of the University of Florence. Experiments involving animals were reported according to ARRIVE guidelines. All efforts were made to minimize animal suffering and to reduce the number of animals used.

Peripheral Mononeuropathy Rat Model

Neuropathy was induced in rats anaesthetized with 400 mg/kg chloral hydrate intraperitoneally (i.p.) Chronic Constriction Injury (CCI), according to the procedure described by (Bennett and Xie, 1988). Under aseptic conditions, the right common sciatic nerve was exposed at the level of the middle thigh by blunt dissection and four chromic cat gut ligatures (4-0, Ethicon, Norderstedt, Germany) were tied loosely around the nerve with about 1 mm spacing. After that hemostasis was confirmed, incision was closed in layers. After a period of recovery from surgery, animals were housed one per cage with free access to water and standard laboratory chow. Control animals were sham operated.

TABLE 1 | Primary antibodies used in immunohistochemistry.

Primary antibody	Company Cat. No.	Dilution IHC
Anti-neurofilament 200kDa, clone RT-97 (NF)	Monoclonal antibody, Merck-Millipore (Cat. No. MAB5262)	1:500
Anti-myelin basic protein (MBP)	Monoclonal antibody, Merck-Millipore (Cat. No. NE1019)	1:500
Anti-glial fibrillary acidic protein (GFAP)	Monoclonal antibody, Merck-Millipore USA (Cat. No. MAB3402)	1:500
Anti-8-OHdG	Monoclonal antibody clone 2E2, Trevigen (Cat. No. 4354-MC-050)	1:250
Anti-mouse biotinylated	Polyclonal antibody, Merck-Millipore (Cat. No. AP124B)	1:200
Anti-mouse	Alexa fluor 488®, CellSignaling technology (Cat. No. #4408S)	1:100

Animal Treatment

Thioctic acid, as (+/−)-compound, lysine salt (+)-enantiomer and (−)-enantiomer, was pursued from Sintactica (Milan, Italy). Compounds were solubilized in NaOH-supplemented physiologic solution and buffered to 7.4 pH by adding HCl. Different racemic and thioctic acid salt compounds were solubilized in saline and injected intraperitoneally (i.p.). Rats were treated for 15 days with intraperitoneal injection of 250 $\mu mol \cdot kg^{-1} \cdot die^{-1}$ (+/−)-thioctic acid (n = 6); 125 $\mu mol \cdot kg^{-1} \cdot die^{-1}$ (+/−)-thioctic acid (n = 6); 125 $\mu mol \cdot kg^{-1} \cdot die^{-1}$ (+)-thioctic acid lysine salt (n = 6); 125 $\mu mol \cdot kg^{-1} \cdot die^{-1}$ (−)-thioctic acid (n = 6); 300 $\mu mol \cdot kg^{-1} \cdot die^{-1}$ pregabalin (n = 6). Control CCI and SHAM (operated without ligating sciatic nerve) SHR and WKY rats (n = 6 each) received the same amounts of vehicle. To note, 250 $\mu mol \cdot kg^{-1} \cdot die^{-1}$ thioctic acid lysine salt (+)-enantiomer (about 90 mg/kg) can be converted in the human dosage of 569 mg (considering 70 kg body weight) accordingly to Reagan-Shaw et al. (2008) and Nair and Jacob (2016) using the equation [(rat dose mg kg^{-1}/12.3) x 70].

Paw Pressure Test

One hour after the last drug administration, the nociceptive threshold was determined with an analgesimeter (Ugo Basile, Varese, Italy) (Leighton et al., 1988). A constantly increasing pressure was applied by a mechanical device to a small area of the dorsal surface of the paw, using a blunt conical probe. Mechanical pressure was increased until vocalization or a withdrawal reflex occurred while rats were lightly restrained. Vocalization or withdrawal reflex thresholds were expressed in grams. Rats scoring below 40 g or over 75 g during the test before drug administration (25%) were discarded. An arbitrary cut-off value of 250 g was adopted. The paw pressure test was repeated in a second session at 24 h after the first experiments.

Tissue Processing

One hour after completion of the paw pressure test, animals were sacrificed by cervical dislocation. The right sciatic nerve, was exposed, excised and the portion containing the ligature was removed. Contralateral nerves were also dissected out and a portion equivalent to that of ligated nerve was removed.

Paraffin Embedding and Staining

After animal sacrifice, sciatic nerves were fixed *in situ* with 4% formalin in phosphate buffered saline (pH 7.4). Following gradual dehydration in ethanol, nerve samples were embedded in paraffin (Diapath, Milan, Italy). Transverse 10 µm sections were cut on a microtome (Leica, RM 2145), and mounted on polylysine coated slides.

Sciatic Nerve Analysis: Histochemistry and Immunohistochemistry

Consecutive paraffin sections (10 µm thick) were stained alternatively with Mallory's trichrome staining, to investigate morphology of different nerve components and occurrence of oedema and inflammatory infiltrates, or processed for immunohistochemistry techniques. Oedema and infiltrate were graded by an arbitrary scale starting from 1, mild infiltrate and oedema up to 10, severe infiltrate and widespread oedema. Sections were processed for 200 kDa neurofilament protein (NF) immunoreactivity, for Myelin Basic protein (MBP) or Glial fibrillary acidic protein (GFAP) immunohistochemistry using a mouse monoclonal antibody, as detailed in **Table 1**. Briefly, after deparaffinization and rehydration, sections were incubated in H_2O_2 3% for 20 min, and in a blocking solution of bovine serum albumin (BSA) in phosphate buffer saline (PBS) 0.1 M pH 7.4 for 1 h at room temperature. Incubation with primary antibodies was performed over night at 4 °C at condition detailed in **Table 1**. After three washes in PBS, sections were incubated in a goat antimouse-biotinylated secondary antibody. The product of the immune reaction was revealed using a biotin–streptavidin immunostaining kit (Vectastain ABC Kit Elite, Vector, Cat. No. PK 6100) and 3.3′-diamino benzidine (DAB) as a chromogen (DAB peroxidase substrate, Vector Cat. No 4100). After washing, sections were then dehydrated in ethanol, mounted in mounting medium and observed under a light microscope. Control sections were processed in the same way but using a non-immune mouse IgG instead of the primary antibody. These sections did not develop specific immunostaining (data not shown). Sections processed for immunohistochemistry were viewed under a light microscope connected to the screen of IAS 2000 image analyzer. The intensity of axonal NF immunostaining and the intensity of MBP immunostaining developed in myelin sheaths were assessed microdensitometrically with an image analysis system, calibrated to take as "zero" the background developed in sections incubated with a non-immune serum and "100" as the conventional value of maximum intensity of staining.

Spinal Cord Analysis: Malondialdehyde (MDA) Levels and DNA Oxidation Status

In portions of spinal cord, oxidative stress indicators were evaluated: malondialdehyde (MDA) levels via thiobarbituric acid reactive substances (TBARS) kit (Cayman, Chemical Company, Ann Arbor, MI, United States Cat. No. 10009055); DNA oxidation by 8-OHdG immunohistochemistry. Paraffin sections of spinal cord were processed for 8-OHdG immunohistochemistry, using monoclonal antibodies as detailed **Table 1**. After deparaffinization and rehydratation, sections were incubated in a blocking solution of bovine serum albumin (BSA) in phosphate buffer saline (PBS) 0.1 M pH 7.4 for 1 h at room temperature. Incubation with primary antibodywas performed over night at 4°Cat condition detailed in **Table 1**. After three washes in PBS, sections were incubated in a biotinylated secondary antibody solution (**Table 1**).

Protein Oxidation Status: Western Blot Analysis of Carbonylated Proteins

Samples of spinal cord, taken from six rats for each group, were homogenized in lysis buffer, as previously described (Tayebati et al., 2017). We assessed protein carbonylation by treating equal amounts of protein according to protocol of OxyBlot Protein detection kit (Millipore, USA, Cat. No. S7150). The kit provides a system to perform the immunoblot detection of carbonyl groups introduced into proteins by oxidative reactions. As a consequence, carbonyl groups are introduced into the side chains of all proteins independently of the molecular weight. The samples were separated by 8% SDS polyacrylamide gel, transferred onto nitrocellulose and blotted with the specific antibodies of the kit that recognize all the oxidized protein with different molecular weight. Band intensities were measured by densitometry with IAS 2000 image analyzer (Biosystem, Rome, Italy).

Clinical Study

NESTIORADE is a comparative open trial, approved by the Ethic Committee of "Azienda Ospedaliera Universitaria Maggiore della Carità, Novara" and "Aziende Sanitarie Locali" of Novara, Biella, Vercelli and Verbano Cusio Ossola (NEST 2009) and written informed consent was obtained from all subjects participating in the trial. The trial was registered prior to patient enrollment at https://eudract.ema.europa.eu (OSSC Number: 2011-000964-81; principal investigator: Prof. Francesco Pipino; date of registration: February 28, 2011). The study recruited 100 patients (49 males and 51 females, with a mean age of 53 ± 11 years) who met criteria for inclusion and agreed to participate at the trial. The number of participants were chosen to ensure a minimum statistical power of 90% and alpha of 5%, considering variance and effect of primary outcomes. Patients were divided by block randomization using a random generation number into two different groups of 50 subjects each and were assigned to a 600 mg/day treatment with (+/−)-thioctic acid (Group 1), or to a 600 mg/day treatment with (+)-thioctic acid (Group 2). Treatments lasted 60 days. Study was not controlled by placebo due to a request of the ethic committee, that did not allow to keep patients without therapy during pain condition. (+/−)-thioctic acid therapy was considered safe, effective and a good reference thanks to publications that highlighted the efficacy and safety of its use in similar pathologies (Memeo and Loiero, 2008; Ranieri et al., 2009).

Inclusion criteria were:

- Radiculopathy of the lower limbs,
- Diagnosis confirmed by CT or MRI,
- Unilateral or bilateral presentation,
- First event,
- Onset of symptomatology not exceeding 40 days.

Exclusion criteria were:

- Cognitive deficits or psychiatric disorders,
- Specific indication for surgical treatment of symptomatology,
- Poor compliance toward inclusion in the study,
- Concomitant neoplastic pathology,
- Chemotherapy or immunosuppressive treatment ongoing,
- Under treatment with thioridazine hydrochloride.

The evaluation of time loss/disappearance of symptoms was performed by using multidimensional scales designed for neuropathic pain (Xiong et al., 2015) listed below:

(1) Neuropathy Symptoms and Change (NSC) (Dyck et al., 2002);
(2) Neuropathy Impairment Score (NIS) (Dyck et al., 2002);
(3) Neuropathic Total Symptom Score-6 (NTSS-6) (Bastyr et al., 2005).

To better assess the impact of the compared treatments on life quality of patients, the following parameters were evaluated:

(1) Consumption of analgesics during the whole treatment period;
(2) Quality of sleep.

This manuscript adheres to the applicable CONSORT guidelines. (**Figure 1**).

Statistical Analysis

All data of different parameters were expressed as mean ± S.D. (n = 6), calculated from single animal data. The significance of differences between groups of treatment was analyzed by analysis of variance (ANOVA) followed by the Newman-Keuls test, while for the analysis of the differences within the group over time, Student' t-test for paired data were performed. For analyzing the different treatment over time a two way ANOVA for repeated measure was used. X-squared (X^2) test was performed to evaluate differences in qualitative data. Data were collected by researchers blind to the treatments.

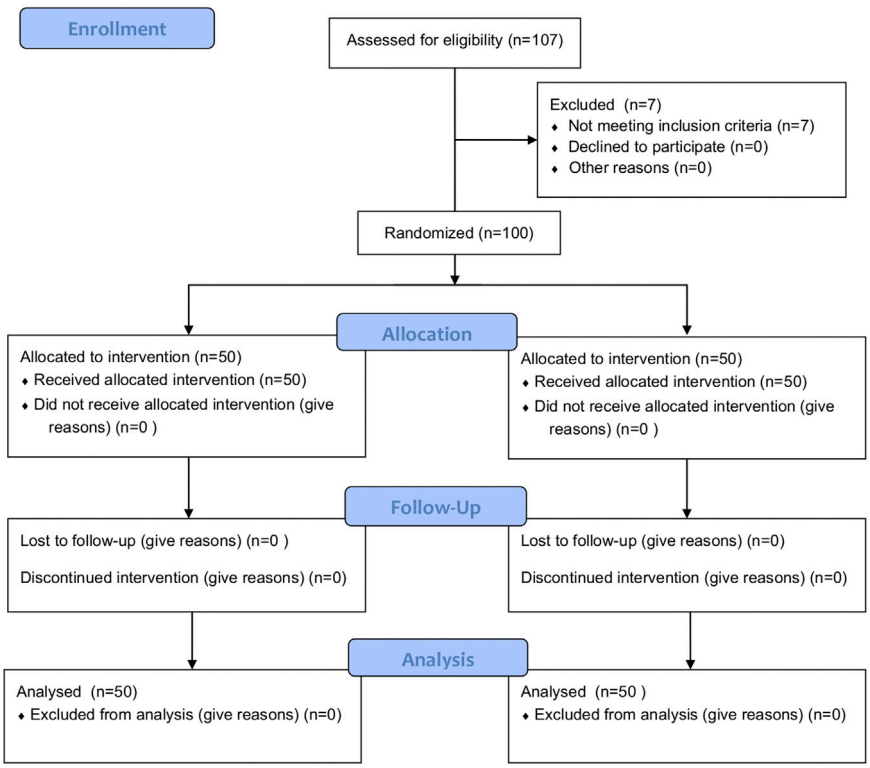

FIGURE 1 | CONSORT flow diagram of the clinical study NESTIORADE (Sensory motor neuropathy of the sciatic nerve: Comparative assessment of the effectiveness of racemic and dextrorotatory forms of thioctic acid).

RESULTS

Preclinical Results

Paw Pressure Test

CCI SHR and CCI WKY rats were treated intraperitoneally (i.p.) for 15 days with (+/−)-thioctic acid (125–250 μmol·kg^{-1}·die^{-1}) (+)-thioctic acid (125 μmol·kg^{-1}·die^{-1}), (−)-thioctic acid (125 μmol·kg^{-1}·die^{-1}) or pregabalin (300 μmol·kg^{-1}·die^{-1}), starting on the day of the surgery. Likewise, control SHAM and CCI animals were treated i. p. with vehicle (data not shown). At the end of the treatment, mechanical hypersensitivity was evaluated in all the experimental groups of both strains, WKY (**Figure 2A**) and SHR (**Figure 2B**), via paw pressure test on ipsilateral and contralateral paw (1 h after the last treatment). Vehicle-treated CCI animals presented an altered response to the noxious stimulus on the ipsilateral paw, tolerating a bit more than half of control weight; there was no significant difference in pain response between the strains in all the experimental conditions. No difference were reported between the left paw of vehicle-treated CCI and SHAM group. A beneficial effect was observed with repeated (+/−)-thioctic acid 250 μmol·kg^{-1}·die^{-1} treatment (p = 0.0005), since it increased pain threshold of the ipsilateral paw of CCI animals; treatment with the half dose of (+)-thioctic acid produced the same positive effects (p = 0.0004). Half dose of racemic mixture induced a lower but however significant (p = 0.0008) improvement in pain sensitization. The analgesic activity of both compounds was comparable to the outcomes of pregabalin administrations; conversely, repeated treatment with (−)-enantiomeric isoform of thioctic acid was not active. Similar results were obtained repeating measurements 24 h after the last administration of thioctic acid forms (data not shown).

Morphological Analysis: Sciatic Nerve

After the behavioral tests, animals were sacrificed, both sciatic nerves and spinal cord tissue were explanted. Sciatic nerve sample tissues were stained and processed: Mallory's trichrome staining

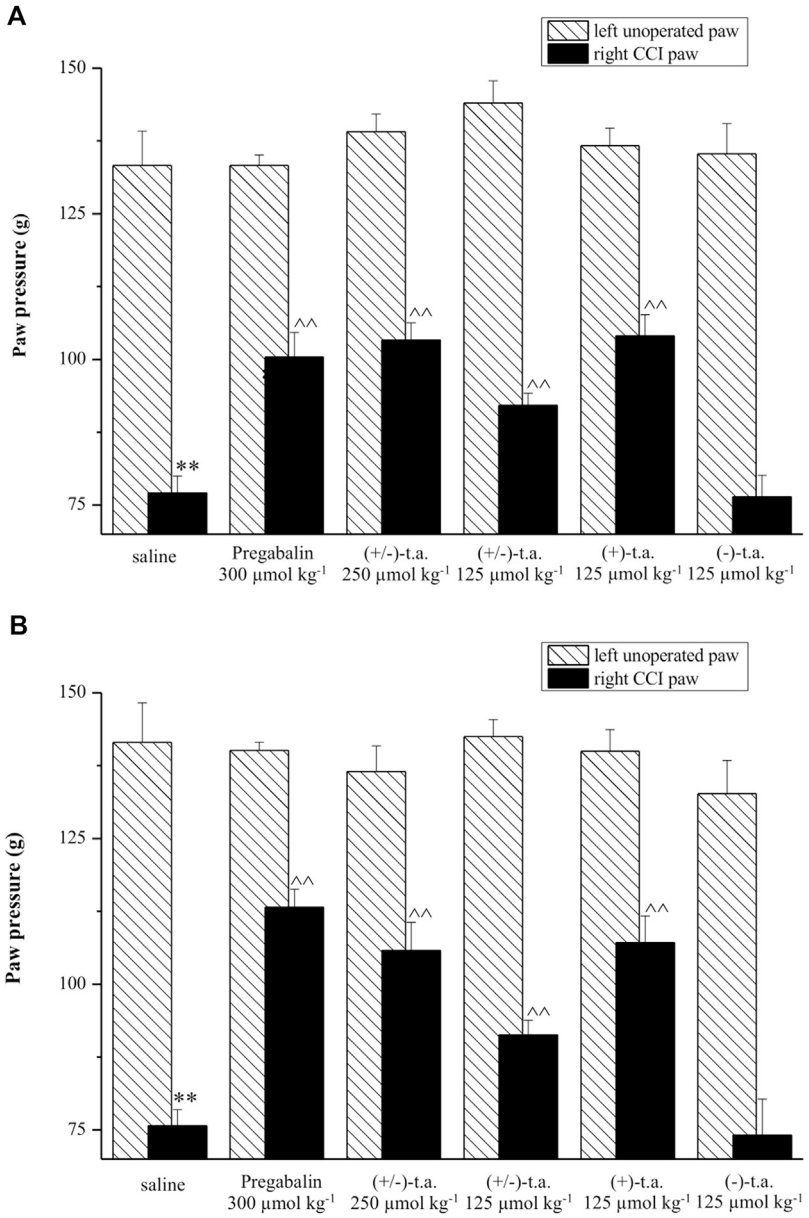

FIGURE 2 | Paw pressure test. Paw pressure test on operated (CCI) and unoperated paws of WKY **(A)** and SHR **(B)** following treatment with 300 μmol·kg^{-1}·die^{-1}pregabalin, 250 and 125 μmol·kg^{-1}·die^{-1} (+/–)-thioctic acid (t.a.), 125 μmol·kg^{-1}·die^{-1} (+)- and (–)-thioctic acid or with vehicle (saline). Each experimental group is $n = 6$; data are expressed as mean ± SEM, in grams. $^{**}p < 0.01$ vs the left unoperated paw value, $^{\wedge}p < 0.01$ vs CCI + saline solution.

(**Supplementary Figure S1**); immunohistochemistry for neurofilament (NF, **Figure 3**) and myelin basic protein (MBP, **Figure 4**).

Mallory's trichrome staining on CCI right sciatic nerve highlighted a massive degeneration of myelinated and non-myelinated axons distal to the ligation site both in WKY (data not shown) and SHR rats (**Supplementary Figure S1**), induced by constriction injury. In CCI SHR sciatic nerve, Mallory's trichrome staining of distal-to-ligation right sciatic nerve showed: a typical Wallerian degeneration with less compact oedematous axons and accumulation of inflammatory cells, absence or damage of myelin sheaths and a scarcely identifiable myelin-axon border (**Supplementary Figure S1A**). These changes were partly inhibited only by the treatment with (+/–)-thioctic acid 250 μmol·kg^{-1}·die^{-1} (**Supplementary Figure S1C**) and (+)-thioctic acid (**Supplementary Figure S1D**). Administrations of (+/–)-thioctic acid 125 μmol·kg^{-1}·die^{-1} (**Supplementary Figure S1B**) and (–)-thioctic acid (**Supplementary Figure S1E**) left the morphology of damaged nerve unaltered. Pregabalin injections (**Supplementary Figure S1F**), restored the morphology of the nerve countering the reduction of axon and myelin thickness in nerve fibers of the lesioned nerve.

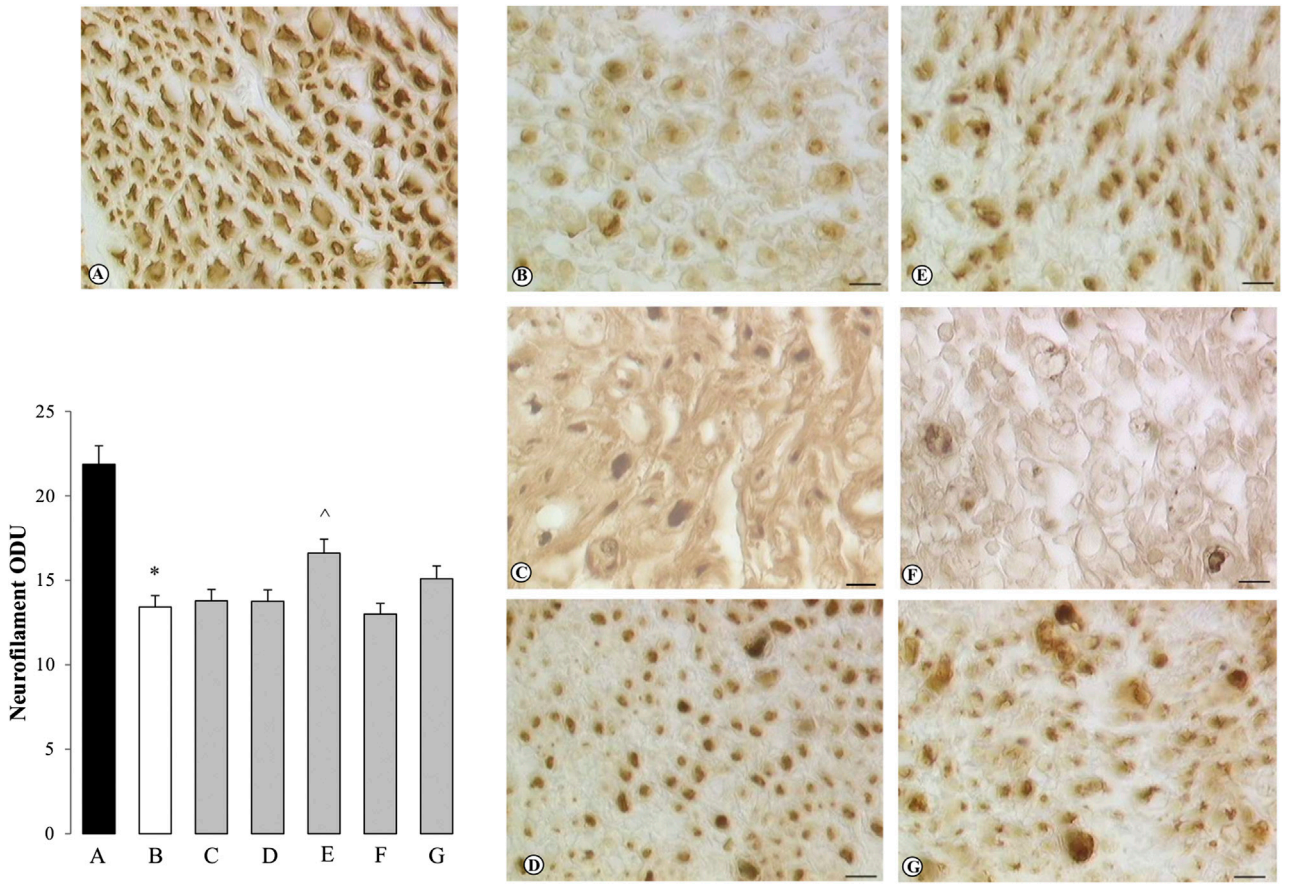

FIGURE 3 | Sections of sciatic nerve processed for neurofilament immunohistochemistry. Treatments are indicated as follows: **(A)** SHAM SHR + saline solution; **(B)** CCI SHR + saline solution; **(C)** CCI SHR + (+/–)-thioctic acid 125 μmol·kg^{-1}·die^{-1}; **(D)** CCI SHR + (+/–)- thioctic acid 250 μmol·kg^{-1}·die^{-1}; **(E)** CCI SHR + (+)- thioctic acid 125 μmol·kg^{-1}·die^{-1}; **(F)** CCI SHR + (–)-thioctic acid 125 μmol·kg^{-1}·die^{-1}; **(G)** CCI SHR + pregabalin 300 μmol·kg^{-1}·die^{-1}. Left-bottom graph represents a densitometric analysis of the expression of neurofilament. Each experimental group is $n = 6$; data, expressed as Optical Density Unit (ODU), are the mean ± SEM. Calibration bar: 10 μm *$p < 0.05$ vs SHAM SHR, ^$p < 0.05$ vs CCI SHR + saline solution.

Sections of sciatic nerve explanted from SHAM SHR were processed for NF immunohistochemistry: they developed a dark brown axonal staining, with a particularly intense immunoreaction in the external part of axons (**Figure 3A**). Reduced NF immunoreactivity was observed in the distal to ligation sciatic nerve from control (untreated) CCI SHR rats (**Figure 3B**) as also demonstrated by quantitative analysis, expressed as Optical Density Unity (ODU) in the left-bottom graph, that showed a significantly ($p = 0.0006$) decrease of quantitative immunoreaction (**Figure 3**, graph column B). Only the treatment with (+)-thioctic acid augmented axonal NF immunoreactivity in the distal part of the sciatic nerve in a significant way ($p = 0.0025$) (**Figure 3**, panel and graph column E). MBP immunostaining showed a physiological pattern of myelin organization in the SHAM operated rats, with dark brown immunoreactivity in the myelin sheaths (**Figure 4A**). As showed by quantitative analysis (**Figure 4**, left-bottom graph), a remarkable reduction ($p = 0.0005$) of MBP immunoreactivity was evident in the distal part of the ligated nerve (panel and graph column B). Treatment with racemic thioctic acid 250 μmol·kg^{-1}·die^{-1} (panel and graph column D) and (+)-thioctic acid (panel and graph column E) significantly raised MBP immunoreactivity ($p = 0.0003$) in the distal part of ligated nerve, while the other compounds produced no improvements.

Morphological and Biochemical Analysis: Spinal Cord

In the spinal cord we investigated oxidative stress signals: the levels of malondialdehyde (MDA) (**Supplementary Figure S2**), protein carbonylation and 8-hydroxy-2′-deoxyguanosine (8-OHdG) (**Figure 5**: i-ii and iii-iv, respectively).

SHAM non-hypertensive and hypertensive rats had similar MDA levels, while a statistically significant raise ($p = 0.034$) was observed in the neuropathic SHR group (**Supplementary Figure S2**, column C) in comparison to control SHAM SHR (Supplementary **Supplementary Figure S2**, column B); all treatments were unsuccessful at recovery.

Densitometry analysis (**Figure 5ii**) on blotted carbonylated protein (**Figure 5i**), showed that SHAM-operated WKY and SHR (A, B bands/columns) displayed the same low level protein

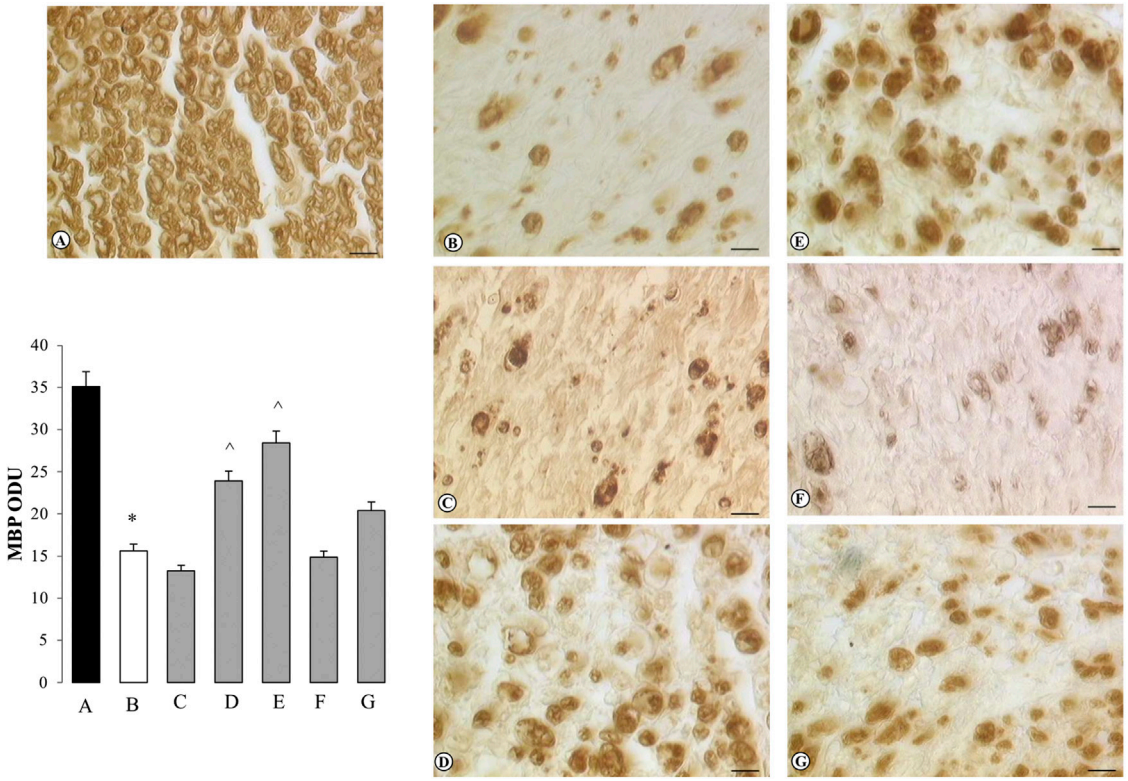

FIGURE 4 | Sections of sciatic nerve processed for myelin basic protein (MBP) immunohistochemistry. Treatments are indicated as follows: **(A)** SHAM SHR + saline solution; **(B)** CCI SHR + saline solution; **(C)** CCI SHR + (+/−)-thioctic acid 125 μmol·kg^{-1}·die^{-1}; **(D)** CCI SHR +(+/−)-thioctic acid 250 μmol·kg^{-1}·die^{-1}; **(E)** CCI SHR + (+)-thioctic acid 125 μmol·kg^{-1}·die^{-1}; **(F)** CCI SHR + (−)-thioctic acid 125 μmol·kg^{-1}·die^{-1}; **(G)** CCI SHR + pregabalin 300 μmol·kg^{-1}·die^{-1}. Left-bottom graph represents a densitometric analysis of the expression of myelin basic protein. Each experimental group is $n = 6$; data, expressed as Optical Density Unit (ODU), are the mean ± SEM. Calibration bar: 10 μm $^{*}p < 0.05$ vs SHAM SHR, $^{\wedge}p < 0.05$ vs CCI SHR + saline solution.

oxidation, while CCI-induced neuropathy resulted in higher carbonylated protein values in spinal tissue of CCI SHR animals (C band/column). (+/−)-thioctic acid 250 μmol·kg^{-1}·die^{-1} lowered carbonylated proteins to control values (D band/column), the same result was gained by dextrorotatory enantiomer administrations (F band/column) and both treatments resembled pregabalin effects (H band/column). Conversely, the treatment with (+/−)-thioctic acid 125 μmol·kg^{-1}·die^{-1}and with (−)-thioctic acid (E, G bands/columns) lead to a very slight non-significant reduction of protein oxidation. Expression of 8-OHdG in dorsal horns of spinal cord was investigated through immunohistochemistry and related densitometric analisys (**Figure 5iii,iv**). CCI SHR rats (panel/column C-bis) spinal cord displayed more pronounced levels ($p = 0.028$) of 8-OHdG as compared to SHAM WKY and SHR rodents' spinal cord (panel/column A and B, respectively), markedly in the cell body neurons of dorsal horns. Treatments with almost all forms of thioctic acid induced an antioxidant effect (panel/column D, E, F), only (−)-thioctic acid (panel/column G) injections produced no amelioration, similarly to pregabalin (panel/column H).

In addition, we evaluated the neuroprotective effects of thioctic acid from *ex-vivo* analysis on the spinal cord (**Figures 6i–6ii**). Dorsal horn sections were probed with GFAP antibody (**Figure 6i**): the number of GFAP-positive cells was comparable between SHAM SHR and WKY rats (panels A and B), therefore we moved on the analysis of SHR animals. Sciatic nerve ligation induced an activation of astrocytes with high production of GFAP and ramified branches (panel C), while treating with (+/−)-thioctic acid 250 μmol·kg^{-1}·die^{-1} restored the physiological state (panel D). Injections with (+)-thioctic acid (panel F) reproduced the same result of double-concentrated racemic compound (panel D); conversely, an opposite effect was obtained by the treatment with 125 μmol·kg^{-1}·die^{-1} racemic compound and (−)-enantiomer (panel E and G, respectively). A pattern of activated astrocytes was also observed in the spinal cord of pregabalin treated rats (panel H). These observations were confirmed by the analysis of mean area (μm^2) of GFAP-immunopositive astrocytes, from both dorsal and ventral horns (**Figure 6ii**). No significant differences between the two regions were noticeable in each experimental group. In the dorsal horn, sham WKY and SHR rats presented the same quantity of immunoreactive tissue while CCI SHR animals had 30% more GFAP-positive tissue. Treatments with (+/−)-thioctic acid 250 μmol·kg^{-1}·die^{-1} ($p = 0.005$ *vs.* CCI) and (+)-enantiomer 125 μmol·kg^{-1}·die^{-1} ($p = 0.032$ *vs.* CCI) reduced the area almost to non-neuropathic values, while glial activation was confirmed in groups treated with 125 μmol·kg^{-1}·die^{-1} racemic

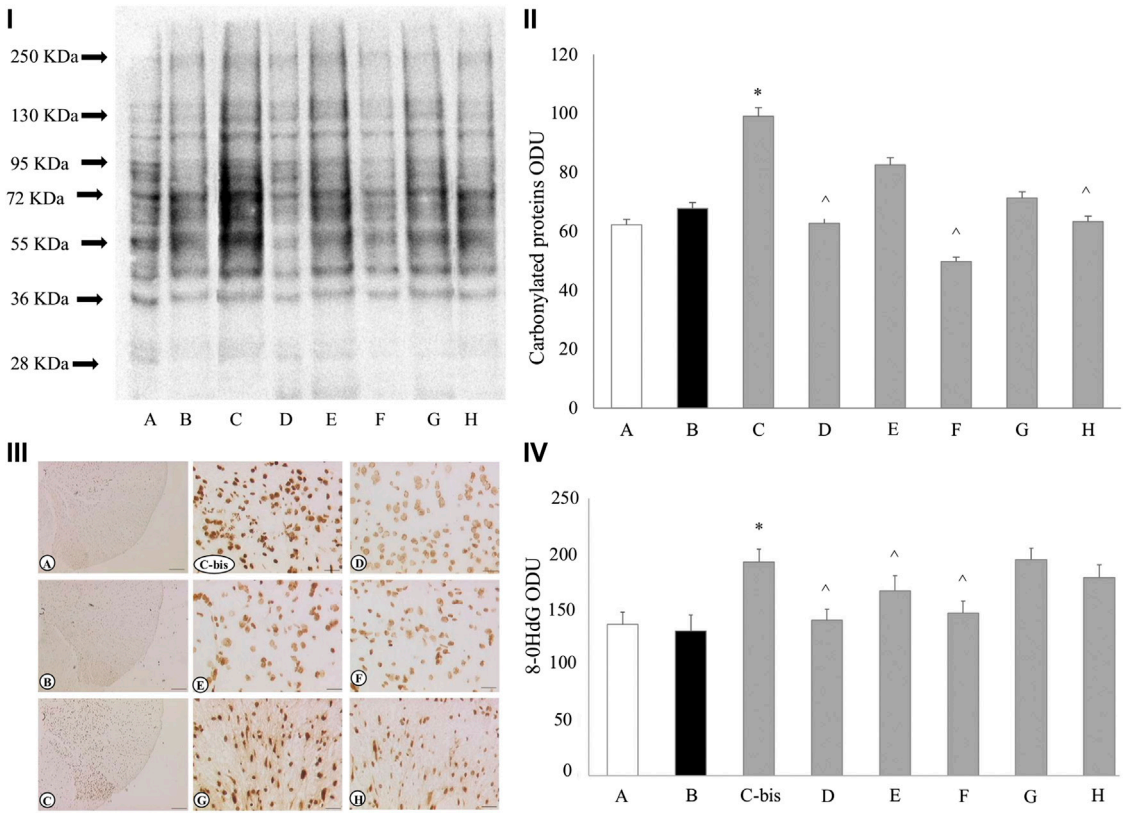

FIGURE 5 | Oxidative stress status in the spinal cord (lumbar region L5). Carboxylated proteins blotting of the spinal cord (i) and its densitometric analysis (ii). Sections of dorsal horns of spinal cord (lumbar region L5) processed for immunohistochemistry of 8-OHdG (iii) and densitometric analysis (iv). Calibration bar of iii): A-C 200 μm; Cbis-H: 25 μm; densitometric analysis was performed on 25 μm calibration bar-images. In all panels, treatments are indicated as follows: **(A)** SHAM WKY + saline solution; **(B)** SHAM SHR + saline solution; C, Cbis) CCI SHR + saline solution; **(D)** CCI SHR + (+/–)-thioctic acid 250 μmol·kg^{-1}·die^{-1}; **(E)** CCI SHR + (+/–)-thioctic acid 125 μmol·kg^{-1}·die^{-1}; **(F)** CCI SHR + (+)-thioctic acid 125 μmol·kg^{-1}·die^{-1}; **(G)** CCI SHR + (–)-thioctic acid 125 μmol·kg^{-1}·die^{-1}; **(H)** CCISHR + Pregabalin 300 μmol·kg^{-1}·die^{-1}. Data are expressed as mean ± SEM. *p < 0.05 vs SHAM SHR + saline solution; ^p < 0.05 vs CCI SHR + saline solution.

thioctic acid, (−)-enantiomer and pregabalin. In the ventral horn the pattern is the same.

Clinical Results

Neuropathy Symptoms and Change (NSC) Parameter

Initial (baseline) values for the NSC scale averaged 17.2 ± 5.1 in Group 1 patients (+/−)-thioctic acid and 17.6 ± 5.3 in Group 2 patients (+)-thioctic acid. After 60 days of treatment, these values decreased to 13.0 ± 5.4 in group 1 patients and 11.3 ± 4.8 in group 2 patients (**Table 2**). This reduction was statistically significant vs. baseline for both treatments (respectively p = 0.0000 and p = 0.0000 for the two groups at the two-sided Student's t test for paired data). The average reduction for this scale was of 4.12 ± 3.13 points for patients of Group 1 and 6.26 ± 4.30 points for patients of Group 2 (**Table 2**) (p = 0.0003, ANOVA). (**Supplementary Figure S3A**). Values of the NSC scale were also used to assess the percentage change compared to the starting value. Percentage changes resulted to be of 24.7 ± 17.3% in Group 1 patients and 34.4 ± 19.1% in Group 2 patients (**Table 2**) (p = 0.009, ANOVA). To analyze the different treatment over time a two way ANOVA for repeated measure was performed: data showed significative results for the model (p = 0.0000) and for the time (p = 0.0000) and treatment (p = 0.048) parameters.

Neuropathic Injury Score Parameter

Initial (baseline) average values for the NIS scale were 4.30 ± 3.08 in Group 1 patients and 4.28 ± 4.22 in Group 2 patients. After 60 days of therapy, values decreased to 2.64 ± 2.99 in Group 1 patients and 1.94 ± 3.80 in Group 2 patients (**Table 2**). This reduction was statistically significant *vs.* baseline for both treatments (p = 0.0000 for both groups at two sided Student's t test for paired data). The average reduction in the scale was of 1.66 ± 1.81 points in Group 1 patients and 2.34 ± 2.56 points for Group 2 patients (**Table 2**). This reduction did not reach statistical significance at the ANOVA (p = 0.308). (**Supplementary Figure S3B**). Values of NIS were also evaluated in terms of percent reduction compared to the starting value: the decrease, which averaged 40.2 ± 43.3% in Group 1 patients and 53.9 ± 44.4% in Group 2 patients (**Table 2**), was not statistically significant (p = 0.121). Results of the two way

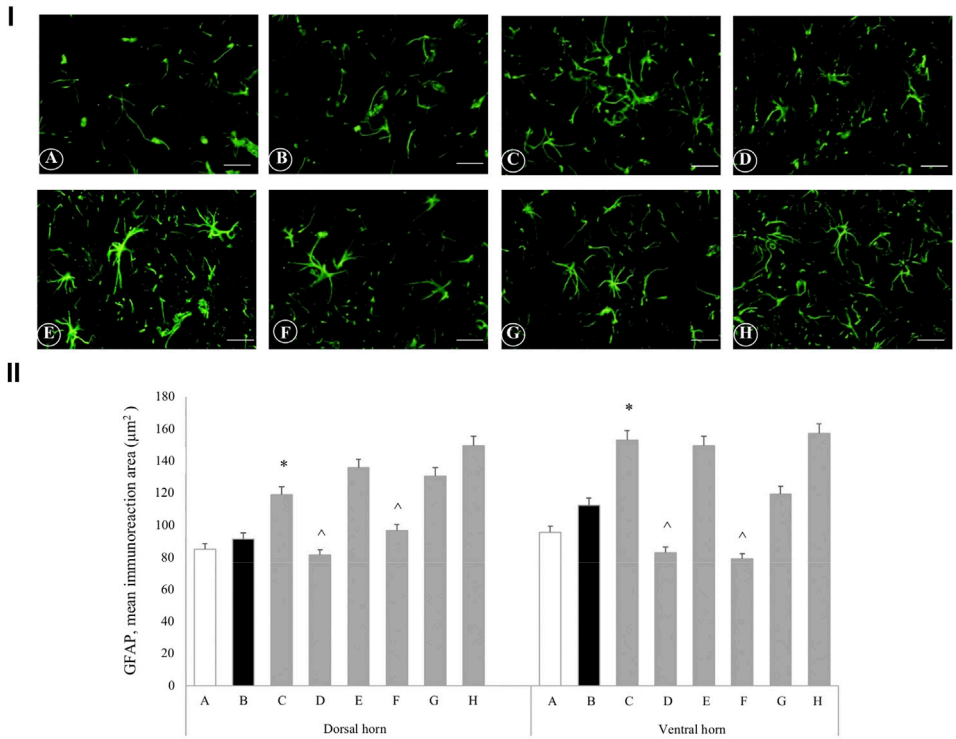

FIGURE 6 | Astrocytes activation: GFAP immunohistochemistry in spinal cord. Sections of dorsal horn of spinal cord (images A-H, i) processed for the immunohistochemistry of glial fibrillary acid protein (GFAP) and densitometric analysis (ii) of the mean immunoreaction area in both dorsal and ventral horns. In all panels, treatments are indicated as follows: **(A)** SHAM WKY + saline solution; **(B)** SHAM SHR + saline solution; **(C)** CCI SHR + saline solution; **(D)** CCI SHR + (+/–)-thioctic acid 250 μmol·kg^{-1}·die^{-1}; **(E)** CCI SHR + (+/–)-thioctic acid 125 μmol·kg^{-1}·die^{-1}; **(F)** CCI SHR + (+)-thioctic acid 125 μmol·kg^{-1}·die^{-1}; **(G)** CCI SHR + (–)-thioctic acid 125 μmol·kg^{-1}·die^{-1}; **(H)** CCI SHR + Pregabalin 300 μmol·kg^{-1}·die^{-1}. Calibration bar: 25 μm. Data are expressed as mean ± SEM; *p < 0.05 vs SHAM SHR + saline solution; ^p < 0.05 vs CCI SHR + saline solution.

ANOVA for repeated measure showed significative results for the model (p = 0.0000) and for the time (p = 0.0000) but not significative for treatment (p = 0.474) parameter.

Neuropathy Total Symptom Score-6 (NTSS-6) Parameter

Initial (baseline) average values for the NTSS-6 scale were 4.01 ± 2.56 in Group 1 patients and 3.86 ± 2.95 in Group 2 patients. After 60 days of treatment these values decreased to 2.65 ± 2.36 in Group 1 patients and 1.98 ± 2.47 in Group 2 patients (**Table 2**). This reduction was statistically significant vs. baseline for both treatments (p = 0.0000 for both groups at two sided Student's t test for paired data). The average reduction in the scale was of 1.35 ± 1.95 points for Group 1 patients and 1.88 ± 1.96 points for Group 2 patients (**Table 2**). This decrease was not significant at the ANOVA analysis (p = 0.165). (**Supplementary Figure S3C**). Data were also evaluated as percent reduction compared to the baseline: this analysis resulted in the 36.2 ± 39.7% in the Group 1 patients and in the 53.7 ± 40.2% in the Group 2 patients (**Table 2**) (p = 0.031, ANOVA). Results of the two way ANOVA for repeated measure showed significative results for the model (p = 0.0000) and for the time (p = 0.0000) but not significative for treatment (p = 0.264) parameter.

Quality of Life

Both treatment with thioctic acid were safe, no patients withdrawn from study; of the 107 patients considered, 7 did not meet the inclusion criteria (first manifestation, presentation before 40 days). Of the patients only one experienced side effects after about a month of treatment, with loss of taste and a sense of bitterness in the mouth. The manifestation was considered a "possible" side effect, but did not lead to discontinuation of therapy and ended before the last visit of the study. Considered quality of life criteria included the response rate to therapy, the half-lives of pain, changes in sleep quality and changes in painkillers assumption. As to NSC parameter, the response rate to therapy was 84% in Group 1 patients (+/–)-thioctic acid and 94% in Group 2 patients (+)-thioctic acid. As to NIS parameter, the response was positive in 60% of patients of Group 1 and in 66% patients of Group 2. For NTSS-6 scale, a positive response to therapy was observed in 64% patients of Group 1 and in 78% patients of Group 2 (**Table 3**).

Half-life of pain, representing the time during which the parameters were considered, reached half of the initial value: for NSC it was 125 days in Group 1 patients and 84 days in Group 2 patients with a 32% reduction for (+)-thioctic acid as compared to (+/–)-thioctic acid. The half-life parameter for NIS was 78 days

TABLE 2 | Neuropathy Symptoms and Change scale (NSC), Neuropathy Impairment Score (NIS) and Neuropathy Total Symptom Score-6 (NTSS-6) in Group 1 patients [(+/–)-thioctic acid)] and in Group 2 patients [(+)-thioctic acid] at baseline (T0) and after 60 days of treatment (Tlast).Data are means ± S.D. Response rate and pain half-life data represent the percentage of patients with reduction of pain score respect to baseline after treatment (response ratio) and the days for pain half-life.

Neuropathy symptoms and change scale (NSC), neuropathy impairment score (NIS) and neuropathy total symptom Score-6 (NTSS-6)			
Pain scales		**Group 2 (+)-thioctic acid**	**Group 1 (+/–)-thioctic acid**
NCS	T0	17.6 ± 5.3	17.2 ± 5.1
	Tlast	11.3 ± 4.8*#	13.0 ± 5.4*
Reduction from baseline		6.26 ± 4.30#	4.12 ± 3.13
Percentage reduction		34.4 ± 19.1#	24.7 ± 17.3
Response rate		94°	84
Pain half-life		84	125
NIS	T0	4.28 ± 4.22	4.30 ± 3.08
	Tlast	1.94 ± 3.80*	2.64 ± 2.99*
Reduction from baseline		2.34 ± 2.56	1.66 ± 1.81
Percentage reduction		53.9 ± 44.4	40.2 ± 43.3
Response rate		66	60
Pain half-life		55	78
NTSS-6	T0	3.86 ± 2.95	4.01 ± 2.56
	Tlast	1.98 ± 2.47*	2.65 ± 2.36*
Reduction from baseline		1.88 ± 1.96	1.35 ± 1.95
Percentage reduction		53.7 ± 40.2#	36.2 ± 39.7
Response rate		78°	64
Pain half-life		62	89

$p < 0.05$ vs T0 evaluated by Student's t-test for paired data; #$p < 0.05$ vs Group 1 patients evaluated by ANOVA Test; °$p < 0.05$ vs. Group 1 patients, X^2 test.

TABLE 3 | Sleep quality and pain killer intake variations in Group 1 [(+/–)-thioctic acid)] and in Group 2 [(+)-thioctic acid]. Data shown represent the absolute number and the percentage of patients.

Sleep quality and pain killer intake variations			
Quality of life **Quality of sleep**	**Group 2 (+)-thioctic acid**	**Group 1 (+/–)-thioctic acid**	**Significance at the X squared test**
Improved	33 (66%)	24 (48%)	p = 0,00,097
Unchanged	17 (34%)	25 (50%)	
Worsened	0 (0%)	1 (2%)	
Painkiller intake			
Increased	1 (2%)	1 (2%)	p = 0,01,593
Unchanged	13 (26%)	20 (40%)	
Reduced	36 (72%)	29 (58%)	

in Group 1 patients and 55 days in Group 2 patients, with a 29% reduction for (+)-thioctic acid as compared to (+/–)-thioctic acid. Assessment of half-lives for the scale NTSS-6 resulted in 86 days in Group 1 patients and 62 days in Group 2 patients, with a reduction of 29% in favor of (+)-thioctic acid (**Table 3**).

Assessment of sleep quality showed in Group 1 patients a 48% of sleep improvement, a 50% of lack of difference and a 2% of worsening. In Group 2 patients, a 66% of sleep improvement, a 34% of no differences and no cases of worsening were reported (**Table 3**).

Analysis of the need to add painkiller to the antioxidant-based therapy revealed in Group 1 patients a reduction of analgesics intake in 58% of individuals, no changes in 40% of them and an increase in 2% of subjects. In Group 2, 72% of patients reduced the use of painkillers, which remained unchanged in 26% of cases. In 2% of examined patients, analgesic medication was increased (**Table 3**).

Gender Influence Evaluation

The stratification of data by gender showed that the groups were mostly homogeneous in the distribution with regard to both sex and age (Group 1: 24 female, mean age 53.0 ± 10.0; 26 male, mean age 53.5 ± 12.5; Group 2: 27 female, mean age 54.6 ± 11.4; 23 male, mean age 52.7 ± 11.4)

The analysis performed by two-way ANOVA for repeated data considering the variables of sex and treatment showed at the end of the study that none of the three pain parameters considered were influenced by the sex of the participants. (NSC: overall value $p = 0.006$, treatment $p = 0.005$, gender $p = 0.172$; NIS: overall value

$p = 0.403$, treatment $p = 0.335$, gender $p = 0.377$; NTSS-6: overall value $p = 0.379$, treatment $p = 0.171$, gender $p = 0.876$).

DISCUSSION

Low back pain is becoming one of the most common diseases in industrialized countries, due to inappropriate postural attitudes and sedentary lifestyles: more than 70% of individuals are estimated to suffer of low back pain at least one time in their life (Baron et al., 2016); it is the fifth reason for medical consultation in the United States (U.S.) and about a quarter of U.S. adults experienced low back pain for at least one whole day over a period of three months (Deyo et al., 2006). The guidelines of the European Federation of Neurological Societies (EFNS) and of the International Association for the Study of Pain (IASP) have been considering the use of different classes of drugs, such as analgesics, antidepressants and anticonvulsants, for the treatment of neuropathic pain (Dworkin et al., 2007; Attal et al., 2010).

A proper treatment of low back pain should not only control pain, but also maintain/restore nerve function. Oxidative stress reduces neuronal function and local blood flow, limiting the arrival of nutrients to nerve cells (Mitsui et al., 1999; Memeo and Loiero, 2008). Antioxidant products, therefore, could contribute to control symptoms and act on the pathogenesis as well (Ranieri et al., 2009). Thioctic acid is a natural fatty acid endogenously produced by mammalian cells and chemically existing as two optical isomers. It is an essential component of some mitochondrial enzyme complexes, important in the glucose metabolism (de Arriba et al., 2003) and able to actively counter various forms of oxidative stress (Tibullo et al., 2017). The dextrorotatory enantiomer is better recognized by enzymes (Streeper et al., 1997) and maximum plasma concentration (Cmax) is approximately 40–50% higher with (+)-thioctic acid than with (+/−)-thioctic acid at the same dose (Carlson et al., 2007).

Preclinical experiments on CCI-SHR showed that following a 15-days cure with thioctic acid (racemic form, dextrorotary and levorotary enantiomers), neuropathic hypertensive rats ameliorated their altered algesic sensitivity and oxidative stress levels. Moreover, the treatment with (+)-enantiomer was as effective as with double-concentrated racemic (+/−)-thioctic acid and the nociceptive threshold closely reached that obtained by administrating pregabalin; on the contrary, the levorotatory enantiomer alone was as ineffective as injecting the saline solution. All these data suggested a prominently active role of the dextrorotatory enantiomer in the racemic mixture. Accordingly, previous studies on chemotherapy-induced neuropathy described similar results: thioctic acid acutely dosed to vincristine-treated rats reversed allodynia symptoms; chronic injections of 15, 30, and 60 mg/kg of (+/−)-thioctic acid on neuropathic rodents, which were given paclitaxel, significantly reduced mechanical and cold allodynia (Kahng et al., 2015; Sun et al., 2019). As previously reported (Tomassoni et al., 2013), SHR rats showed higher values of systolic blood pressure as compared to WKY rats. CCI did not induce an increase of blood pressure values, nor different formulations of racemic and enantiomer thioctic acid affected blood pressure values in SHR. These results demonstrated that the analgesic and neuroprotective effects of thioctic acid was not mediated by a decrease of systolic blood pressure (Tomassoni et al., 2013).

Microanatomical analysis of this study revealed changes after loose ligation of the sciatic nerve: either axonal components of the nerve and myelin sheaths were affected, involving myelinated and unmyelinated nerve fibers. These findings support and extend previous studies reporting the degeneration of axonal components and myelin sheaths, with decrease of NF and MBP in the portion of nerve which is distal to the ligation (Di Cesare Mannelli et al., 2009; Tomassoni et al., 2018).

Thioctic acid, above all the (+)-enantiomer form, exerted a protective activity on the peripheral nerve portion affected by ligation, not shared by pregabalin. We would suppose that amelioration of hyperalgesia after treatment may partly depend on the effects that thioctic acid induced on sciatic nerve morphology, due to the antioxidant ability to scavenge and inactivate free radicals. Its supplementation as natural antioxidant has already demonstrated multiple beneficial effects (Tibullo et al., 2017) and (+)-thioctic acid showed the most pronounced activity.

Studies about the mechanisms of neuropathic pain following injury of peripheral nerves demonstrated that nerve damage was related to altered neuronal plasticity and aberrant function of glial cells in the lumbar spinal cord (Cirillo et al., 2015; De Luca et al., 2016). These neuroglial plastic changes induce both neuronal/astrocytic activation and alteration of neuroglial interactions, determining maladaptive synaptic plasticity in the spinal somatosensory system, which seems to be directly responsible for the neuronal hyperexcitability and the enhanced synaptic transmission that sustain neuropathic pain (Gwak and Hulsebosch, 2009; Wang et al., 2009).

As previously demonstrated (Cirillo et al., 2011, Cirillo et al., 2012; Colangelo et al., 2012), our evidence confirms that in the lumbar spinal cord CCI is associated with reactive gliosis, characterized by hypertrophy of astrocytes and their activation, and with an increase of oxidative stress phenomena in the somatosensory neurons of the dorsal horn. Here, the beneficial effects of thioctic acid were related to its antioxidant properties, like the ability to restore the intrinsic antioxidant systems, supporting their production or cell accessibility (Shay et al., 2009; Goraca et al., 2011; Salehi et al., 2019). The compound, in particular its dextrorotatory enantiomer, lowered the oxidation status of proteins and the expression of 8-OHdG in the somatosensory neurons of the dorsal horn: it might be, in a positive loop, linked to effects on astrocytes cells, since treatments with dextrorotatory enantiomer and double-concentrated racemic formulation reduced size of astrocytes and GFAP expression.

These data from spinal cord could explain the protection of (+)-thioctic acid on the brain. In a previous study we indicated, after mono-lateral CCI of sciatic nerve, augmented GFAP expression mainly in the gray matter of sensory cortex and decreased NF expression as a consequence of nerve damage; we also showed that treatment with antioxidants, but not with pregabalin, prevented to some extent astrogliosis and neuronal

damage in cerebral cortex, similarly to the present findings in spinal cord (Tomassoni et al., 2013).

Encouraged by the findings of the preclinical study, which pointed out a more prominent activity of (+)-thioctic acid as compared to the other tested forms of thioctic acid, resembling or even exceeding the efficacy of pregabalin, a clinical study was set up (using a dosage comparable to the preclinical evaluation, Reagan-Shaw et al. (2008) and Nair and Jacob (2016). The results of the clinical study confirmed the efficacy of the antioxidant thioctic acid in the treatment of the peripheral neuropathy without differences in male and female (Memeo and Loiero, 2008; Ranieri et al., 2009; Agathos et al., 2018; Mrakic-Sposta et al., 2018; Salehi et al., 2019; Passiatore et al., 2020) being also characterized by good safety profile which makes it suitable for prolonged treatment even in the chronic phase of this disease (Ametov et al., 2003; Ziegler et al., 2006). Anyway, it should be carefully prescribed and monitored since the possibility of side effects as recently emerged in a preclinical toxicologic study (Lucarini et al., 2020). The results of clinical study show a greater effectiveness of (+)-thioctic acid compared to (+/−)-thioctic acid in terms of major impact on pain symptoms, rapidity of therapeutic effects onset and, more generally, better quality of life, as confirmed by the response rate to therapy. Our results are consistent with the effects observed in the same period of time (60 days) in other studies (Mrakic-Sposta et al., 2018; Passiatore et al., 2020), even if with minor side effects with respect to those observed in patients treated with a dose higher than 600 mg/day (Mrakic-Sposta et al., 2018). The advantage in using (+)-thioctic acid, as compared to the racemic form, may be related to an increased bioavailability of this enantiomer, that boosts its antioxidant activity (Maglione et al., 2015) as well as to higher biological activity. Preclinical and clinical evidences suggest positive properties of thioctic acid in the treatment of low back pain with a more relevant efficacy of (+)-thioctic acid compared to (+/−)-thioctic acid on pain, on time of onset of therapeutic effects and on quality of life of patients suffering from the symptoms under study. These observations are worthy of further analysis, but they make it a good candidate for treatment of low back pain.

The raw data supporting the conclusion of this article will be made available by the authors, without undue reservation.

ETHICS STATEMENT

The studies involving human participants were reviewed and approved by "Azienda Ospedaliera Universitaria Maggiore della Carità" (Novara) and "Aziende Sanitarie Locali" of Novara, Biella, Vercelli, and Verbano Cusio Ossola. The patients/participants provided their written informed consent to participate in this study.

The animal study was reviewed and approved by the Italian Ministry of Health and the Animal Subjects Review Board of the University of Florence.

AUTHOR CONTRIBUTIONS

LM and LDCM planned and performed *in vivo* experiments, AP and DT performed molecular and *ex vivo* analysis; ET planned and followed the clinical trial; ET analyzed data, performed statistical analysis and drafted the manuscript; CG and FA revised data and drafted the manuscript. All authors have read and agreed to the published version of the manuscript.

FUNDING

This research was funded by University of Florence, University of Camerino and by Ministry of Education, University and Research of Italy (MIUR).

ACKNOWLEDGMENTS

The authors acknowledge Professor Francesco Pipino in Surgery Department, Orthopedic and Trauma Unit, Monza Hospital (Monza, Italy) when he actively and proficiently collaborated to the study, and thank Giuseppe Buzzi, Michele Poma, Fabio Francese, working at Santa Rita Clinic (Vercelli, Italy), who planned and followed the clinical trial.

SUPPLEMENTARY MATERIAL

The Supplementary Material for this article can be found online at: https://www.frontiersin.org/articles/10.3389/fphar.2021.607572/full#supplementary-material.

REFERENCES

Adibhatla, R. M., and Hatcher, J. F. (2010). Lipid oxidation and peroxidation in CNS health and disease: from molecular mechanisms to therapeutic opportunities. *Antioxid. Redox Signaling* 12 (1), 125–169. doi:10.1089/ars.2009.2668

Agathos, E., Tentolouris, A., Eleftheriadou, I., Katsaouni, P., Nemtzas, I., Petrou, A., et al. (2018). Effect of α-lipoic acid on symptoms and quality of life in patients with painful diabetic neuropathy. *J. Int. Med. Res.* 46 (5), 1779–1790. doi:10.1177/0300060518756540

Amenta, F., Di Cesare Mannelli, L., Mancini, M., Rapisarda, G., Tayebati, S. K., Tomassoni, D., et al. (2010). "Metabolismo e farmacocinetica dell'acido tioctico nell'uomo," in *R(+) Dalla Ricerca di Base alle Applicazioni Cliniche dell'Enantiomero Naturale di un Antiossidante Multifunzionale*. Editor F. Amenta, V. Costigliola, and M. F. Lokhandwala (Pisa, Italy: Pacini Editore), 23–33.

Ametov, A. S., Barinov, A., Dyck, P. J., Hermann, R., Kozlova, N., Litchy, W. J., et al. (2003). The sensory symptoms of diabetic polyneuropathy are improved with alpha-lipoic acid: the sydney trial. *Diabetes Care* 26 (3), 770–776. doi:10.2337/diacare.26.3.770

Attal, N., Cruccu, G., Baron, R., Haanpää, M., Hansson, P., Jensen, T. S., et al. (2010). EFNS guidelines on the pharmacological treatment of neuropathic pain: 2010 revision. *Eur. J. Neurol.* 17 (9), 1113-e88. doi:10.1111/j.1468-1331.2010.02999.x

Baron, R., Binder, A., Attal, N., Casale, R., Dickenson, A. H., and Treede, R. D. (2016). Neuropathic low back pain in clinical practice. *Eur. J. Pain* 20 (6), 861–873. doi:10.1002/ejp.838

Bastyr, E. J., III, Price, K. L., and Bril, V. (2005). Development and validity testing of the neuropathy total symptom score-6: questionnaire for the study of sensory symptoms of diabetic peripheral neuropathy. *Clin. Ther.* 27 (8), 1278–1294. doi:10.1016/j.clinthera.2005.08.002

Bennett, G. J., and Xie, Y. K. (1988). A peripheral mononeuropathy in rat that produces disorders of pain sensation like those seen in man. *Pain* 33 (1), 87–107. doi:10.1016/0304-3959(88)90209-6

Carlson, D. A., Smith, A. R., Fischer, S. J., Young, K. L., and Packer, L. (2007). The plasma pharmacokinetics of R-(+)-lipoic acid administered as sodium R-(+)-lipoate to healthy human subjects. *Altern. Med. Rev. J. Clin. Ther.* 12 (4), 343–351.

Cirillo, G., Bianco, M. R., Colangelo, A. M., Cavaliere, C., Daniele, de. L., Zaccaro, L., et al. (2011). Reactive astrocytosis-induced perturbation of synaptic homeostasis is restored by nerve growth factor. *Neurobiol. Dis.* 41 (3), 630–639. doi:10.1016/j.nbd.2010.11.012

Cirillo, G., Colangelo, A. M., Berbenni, M., Ippolito, V. M., De Luca, C., Verdesca, F., et al. (2015). Purinergic modulation of spinal neuroglial maladaptive plasticity following peripheral nerve injury. *Mol. Neurobiol.* 52 (3), 1440–1457. doi:10.1007/s12035-014-8943-y

Cirillo, G., Colangelo, A. M., Bianco, M. R., Cavaliere, C., Zaccaro, L., Sarmientos, P., et al. (2012). BB14, a Nerve Growth Factor (NGF)-like peptide shown to be effective in reducing reactive astrogliosis and restoring synaptic homeostasis in a rat model of peripheral nerve injury. *Biotechnol. Adv.* 30 (1), 223–232. doi:10.1016/j.biotechadv.2011.05.008

Colangelo, A. M., Cirillo, G., Lavitrano, M. L., Alberghina, L., and Papa, M. (2012). Targeting reactive astrogliosis by novel biotechnological strategies. *Biotechnol. Adv.* 30 (1), 261–271. doi:10.1016/j.biotechadv.2011.06.016

de Arriba, S. G., Loske, C., Meiners, I., Fleischer, G., Lobisch, M., Wessel, K., et al. (2003). Advanced glycation endproducts induce changes in glucose consumption, lactate production, and ATP levels in SH-SY5Y neuroblastoma cells by a redox-sensitive mechanism. *J. Cereb. Blood Flow Metab.* 23 (11), 1307–1313. doi:10.1097/01.wcb.0000090622.86921.0e

De Luca, C., Savarese, L., Colangelo, A. M., Bianco, M. R., Cirillo, G., Alberghina, L., et al. (2016). Astrocytes and microglia-mediated immune response in maladaptive plasticity is differently modulated by NGF in the ventral horn of the spinal cord following peripheral nerve injury. *Cell. Mol. Neurobiol.* 36 (1), 37–46. doi:10.1007/s10571-015-0218-2

Delitto, A., George, S. Z., Van Dillen, L., Whitman, J. M., Sowa, G., Shekelle, P., et al. (2012). Low back pain. *J. Orthop. Sports Phys. Ther.* 42, A1–A57. doi:10.2519/jospt.2012.42.4.A110.2519/jospt.2012.0301

Deyo, R. A., Mirza, S. K., and Martin, B. I. (2006). Back pain prevalence and visit rates: estimates from U.S. national surveys, 2002. *Spine* 31 (23), 2724–2727. doi:10.1097/01.brs.0000244618.06877.cd

Di Cesare Mannelli, L., Ghelardini, C., Calvani, M., Nicolai, R., Mosconi, L., Toscano, A., et al. (2009). Neuroprotective effects of acetyl-L-carnitine on neuropathic pain and apoptosis: a role for the nicotinic receptor. *J. Neurosci. Res.* 87 (1), 200–207. doi:10.1002/jnr.21815

Dworkin, R. H., O'Connor, A. B., Backonja, M., Farrar, J. T., Finnerup, N. B., Jensen, T. S., et al. (2007). Pharmacologic management of neuropathic pain: evidence-based recommendations. *Pain* 132 (3), 237–251. doi:10.1016/j.pain.2007.08.033

Dyck, P. J., Turner, D. W., Davies, J. L., O'Brien, P. C., Dyck, P. J. B., Rask, C. A., et al. (2002). Electronic case-report forms of symptoms and impairments of peripheral neuropathy. *Can. J. Neurol. Sci./J. Can. des Sci. Neurol.* 29 (3), 258–266. doi:10.1017/S0317167100002043

Gilron, I., Baron, R., and Jensen, T. (2015). Neuropathic pain: principles of diagnosis and treatment. *Mayo Clin. Proc.* 90 (4), 532–545. doi:10.1016/j.mayocp.2015.01.018

Gomes, M. B., and Negrato, C. A. (2014). Alpha-lipoic acid as a pleiotropic compound with potential therapeutic use in diabetes and other chronic diseases. *Diabetol. Metab. Syndr.* 6, 80. doi:10.1186/1758-5996-6-80

Gorąca, A., Huk-Kolega, H., Piechota, A., Kleniewska, P., Ciejka, E., and Skibska, B. (2011). Lipoic acid - biological activity and therapeutic potential. *Pharmacol. Rep.* 63 (4), 849–858. doi:10.1016/s1734-1140(11)70600-4

Gwak, Y. S., and Hulsebosch, C. E. (2009). Remote astrocytic and microglial activation modulates neuronal hyperexcitability and below-level neuropathic pain after spinal injury in rat. *Neuroscience* 161 (3), 895–903. doi:10.1016/j.neuroscience.2009.03.055

Kahng, J., Kim, T. K., Chung, E. Y., Kim, Y. S., and Moon, J. Y. (2015). The effect of thioctic acid on allodynia in a rat vincristine-induced neuropathy model. *J. Int. Med. Res.* 43 (3), 350–355. doi:10.1177/0300060515569287

Leighton, G. E., Rodriguez, R. E., Hill, R. G., and Hughes, J. (1988). kappa-Opioid agonists produce antinociception after i.v. and i.c.v. but not intrathecal administration in the rat. *Br. J. Pharmacol.* 93 (3), 553–560. doi:10.1111/j.1476-5381.1988.tb10310.x

Lokhandwala, M. F. (2010). "Acido tioctico : farmacologia ed applicazioni terapeutiche di un antiossidante particolare," in *R(+) Dalla Ricerca di Base alle Applicazioni Cliniche dell'Enantiomero Naturale di un Antiossidante Multifunzionale*. Editor F. Amenta, V. Costigliola, and M. F. Lokhandwala (Pisa, Italy: Pacini Editore S.p.A), 7–15.

Lucarini, E., TralloriTomassoni, E. D., Amenta ì, F., Ghelardini, C., Pacini, A., and Di Cesare Mannelli, L. (2020). Toxicological profile of the pain-relieving antioxidant compound thioctic acid in its racemic and enantiomeric forms. *Antioxidants* 9 (8), 749. doi:10.3390/antiox9080749

Maglione, E., Marrese, C., Migliaro, E., Marcuccio, F., Panico, C., Salvati, C., et al. (2015). Increasing bioavailability of (R)-alpha-lipoic acid to boost antioxidant activity in the treatment of neuropathic pain. *Acta Biomed.* 86 (3), 226–233.

Memeo, A., and Loiero, M. (2008). Thioctic acid and acetyl-L-carnitine in the treatment of sciatic pain caused by a herniated disc: a randomized, double-blind, comparative study. *Clin. Drug Invest.* 28 (8), 495–500. doi:10.2165/00044011-200828080-00004

Mitsui, Y., Schmelzer, J. D., Zollman, P. J., Mitsui, M., Tritschler, H. J., and Low, P. A. (1999). Alpha-lipoic acid provides neuroprotection from ischemia-reperfusion injury of peripheral nerve. *J. Neurol. Sci.* 163 (1), 11–16. doi:10.1016/s0022-510x(99)00017-9

Mrakic-Sposta, S., Vezzoli, A., Maderna, L., Gregorini, F., Montorsi, M., Moretti, S., et al. (2018). R(+)-Thioctic acid effects on oxidative stress and peripheral neuropathy in type II diabetic patients: preliminary results by electron paramagnetic resonance and electroneurography. *Oxid. Med. Cell. Longev.* 2018, 1767265. doi:10.1155/2018/1767265

Nair, A. B., and Jacob, S. (2016). A simple practice guide for dose conversion between animals and human. *J. Basic Clin. Pharm.* 7 (2), 27–31. doi:10.4103/0976-0105.177703

Oyenihi, A. B., Ayeleso, A. O., Mukwevho, E., and Masola, B. (2015). Antioxidant strategies in the management of diabetic neuropathy. *BioMed. Res. Int.* 2015, 515042. doi:10.1155/2015/515042

Packer, L., Witt, E. H., and Tritschler, H. J. (1995). alpha-Lipoic acid as a biological antioxidant. *Free Radic. Biol. Med.* 19 (2), 227–250. doi:10.1016/0891-5849(95)00017-r

Passiatore, M., Perna, A., De-Vitis, R., and Taccardo, G. (2020). The use of alfa-lipoic acid-R (ALA-R) in patients with mild-moderate carpal tunnel syndrome: a randomised controlled open label prospective study. *Malaysian Orthop. J.* 14 (1), 1–6. doi:10.5704/MOJ.2003.001

Pinto, R. Z., Maher, C. G., Ferreira, M. L., Ferreira, P. H., Hancock, M., Oliveira, V. C., et al. (2012). Drugs for relief of pain in patients with sciatica: systematic review and meta-analysis. *BMJ* 344, e497. doi:10.1136/bmj.e497

Ranieri, M., Sciuscio, M., Cortese, A. M., Santamato, A., Di Teo, L., Ianieri, G., et al. (2009). The use of alpha-lipoic acid (ALA), gamma linolenic acid (GLA) and rehabilitation in the treatment of back pain: effect on health-related quality of life. *Int. J. Immunopathol. Pharmacol.* 22 (Suppl 3), 45–50. doi:10.1177/03946320090220s309

Reagan-Shaw, S., Nihal, M., and Ahmad, N. (2008). Dose translation from animal to human studies revisited. *Faseb. J.* 22 (3), 659–661. doi:10.1096/fj.07-9574LSF

Riego, G., Redondo, A., Leánez, S., and Pol, O. (2018). Mechanism implicated in the anti-allodynic and anti-hyperalgesic effects induced by the activation of heme oxygenase 1/carbon monoxide signaling pathway in the central nervous system of mice with neuropathic pain. *Biochem. Pharmacol.* 148, 52–63. doi:10.1016/j.bcp.2017.12.007

Salehi, B., Berkay Yilmaz, Y., Antika, G., Boyunegmez Tumer, T., Fawzi Mahomoodally, M., Lobine, D., et al. (2019). Insights on the use of alpha-lipoic acid for therapeutic purposes. *Biomolecules* 9. doi:10.3390/biom9080356

Schnitzer, T. J., Ferraro, A., Hunsche, E., and Kong, S. X. (2004). A comprehensive review of clinical trials on the efficacy and safety of drugs for the treatment of low back pain. *J. Pain Symptom Manage.* 28 (1), 72–95. doi:10.1016/j.jpainsymman.2003.10.015

Shay, K. P., Moreau, R. F., Smith, E. J., Smith, A. R., and Hagen, T. M. (2009). Alpha-lipoic acid as a dietary supplement: molecular mechanisms and therapeutic potential. *Biochim. Biophys. Acta* 1790 (10), 1149–1160. doi:10.1016/j.bbagen.2009.07.026

Streeper, R. S., Henriksen, E. J., Jacob, S., Hokama, J. Y., Fogt, D. L., and Tritschler, H. J. (1997). Differential effects of lipoic acid stereoisomers on glucose metabolism in insulin-resistant skeletal muscle. *Am. J. Physiol. Endocrinol. Metab.* 273 (1), E185–E191. doi:10.1152/ajpendo.1997.273.1.E185

Sun, H., Guo, X., Wang, Z., Wang, P., Zhang, Z., Dong, J., et al. (2019). Alphalipoic acid prevents oxidative stress and peripheral neuropathy in nab-paclitaxel-treated rats through the Nrf2 signalling pathway. *Oxid. Med. Cell. Longev.* 2019, 1–11. doi:10.1155/2019/3142732

Tayebati, S. K., Martinelli, I., Moruzzi, M., Amenta, F., and Tomassoni, D. (2017). Choline and choline alphoscerate do not modulate inflammatory processes in the rat brain, *Nutrients*, 9 (10), 1084. doi:10.3390/nu9101084

Tayebati, S. K., Tomassoni, D., and Amenta, F. (2012). Spontaneously hypertensive rat as a model of vascular brain disorder: microanatomy, neurochemistry and behavior. *J. Neurol. Sci.* 322 (1-2), 241–249. doi:10.1016/j.jns.2012.05.047

Tibullo, D., Li Volti, G., Giallongo, C., Grasso, S., Tomassoni, D., Anfuso, C. D., et al. (2017). Biochemical and clinical relevance of alpha lipoic acid: antioxidant and anti-inflammatory activity, molecular pathways and therapeutic potential. *Inflamm. Res.* 66 (11), 947–959. doi:10.1007/s00011-017-1079-6

Tomassoni, D., Amenta, F., Di Cesare Mannelli, L., Ghelardini, C., Nwankwo, I. E., Pacini, A., et al. (2013). Neuroprotective activity of thioctic acid in central nervous system lesions consequent to peripheral nerve injury. *BioMed. Res. Int.* 2013, 1–14. doi:10.1155/2013/985093

Tomassoni, D., Di Cesare Mannelli, L., Bramanti, V., Ghelardini, C., Amenta, F., and Pacini, A. (2018). Treatment with acetyl-L-carnitine exerts a neuroprotective effect in the sciatic nerve following loose ligation: a functional and microanatomical study. *Neural Regener. Res.* 13 (4), 692–698. doi:10.4103/1673-5374.230297

Vasdev, S., Ford, C. A., Parai, S., Longerich, L., and Gadag, V. (2000). Dietary α-lipoic acid supplementation lowers blood pressure in spontaneously hypertensive rats. *J. Hypertens.* 18 (5), 567–573. doi:10.1097/00004872-200018050-00009

Wang, W., Wang, W., Mei, X., Huang, J., Wei, Y., Wang, Y., et al. (2009). Crosstalk between spinal astrocytes and neurons in nerve injury-induced neuropathic pain. *PLoS One* 4 (9), e6973. doi:10.1371/journal.pone.0006973

Xiong, Q., Lu, B., Ye, H., Wu, X., Zhang, T., and Li, Y. (2015). The diagnostic value of neuropathy symptom and change score, neuropathy impairment score and Michigan neuropathy screening instrument for diabetic peripheral neuropathy. *Eur. Neurol.* 74 (5-6), 323–327. doi:10.1159/000441449

Xu, L., Zhang, Y., and Huang, Y. (2016). Advances in the treatment of neuropathic pain. *Adv. Exp. Med. Biol.* 904, 117–129. doi:10.1007/978-94-017-7537-3_9

Ziegler, D., Ametov, A., Barinov, A., Dyck, P. J., Gurieva, I., Low, P. A., et al. (2006). Oral treatment with alpha-lipoic acid improves symptomatic diabetic polyneuropathy: the SYDNEY 2 trial. *Diabetes Care* 29 (11), 2365–2370. doi:10.2337/dc06-1216

Conflict of Interest: The authors declare that the research was conducted in the absence of any commercial or financial relationships that could be construed as a potential conflict of interest.

frontiers in Pharmacology

SYSTEMATIC REVIEW
published: 01 March 2021
doi: 10.3389/fphar.2021.640128

Efficacy of Essential Oils in Pain: A Systematic Review and Meta-Analysis of Preclinical Evidence

Damiana Scuteri[1,2], Kengo Hamamura[3], Tsukasa Sakurada[4], Chizuko Watanabe[5], Shinobu Sakurada[5], Luigi Antonio Morrone[6], Laura Rombolà[6], Paolo Tonin[2], Giacinto Bagetta[1]* and Maria Tiziana Corasaniti[7,8]*

[1]Pharmacotechnology Documentation and Transfer Unit, Section of Preclinical and Translational Pharmacology, Department of Pharmacy, Health and Nutritional Sciences, University of Calabria, Rende, Italy, [2]Regional Center for Serious Brain Injuries, S. Anna Institute, Crotone, Italy, [3]Laboratory of Chemical Pharmacology, Faculty of Pharmaceutical Sciences, Daiichi University of Pharmacy, Fukuoka, Japan, [4]Center for Supporting Pharmaceutical Education, Faculty of Pharmaceutical Sciences, Daiichi University of Pharmacy, Fukuoka, Japan, [5]Department of Physiology and Anatomy, Faculty of Pharmaceutical Sciences, Tohoku Medical and Pharmaceutical University, Sendai, Japan, [6]Section of Preclinical and Translational Pharmacology, Department of Pharmacy, Health and Nutritional Sciences, University of Calabria, Rende, Italy, [7]Department of Health Sciences, University "Magna Graecia" of Catanzaro, Catanzaro, Italy, [8]School of Hospital Pharmacy, University "Magna Graecia" of Catanzaro, Catanzaro, Italy

OPEN ACCESS

Edited by:
Francesca Guida, University of Campania Luigi Vanvitelli, Italy

Reviewed by:
Franca Marino, University of Insubria, Italy
Agnieszka Barbara Najda, University of Life Sciences of Lublin, Poland

***Correspondence:**
Giacinto Bagetta
giacinto.bagetta@unical.it
Laura Rombolà
laura.rombola@unical.it

Specialty section:
This article was submitted to Inflammation Pharmacology, a section of the journal Frontiers in Pharmacology

Received: *10 December 2020*
Accepted: *18 January 2021*
Published: *01 March 2021*

Citation:
Scuteri D, Hamamura K, Sakurada T, Watanabe C, Sakurada S, Morrone LA, Rombolà L, Tonin P, Bagetta G and Corasaniti MT (2021) Efficacy of Essential Oils in Pain: A Systematic Review and Meta-Analysis of Preclinical Evidence. Front. Pharmacol. 12:640128. doi: 10.3389/fphar.2021.640128

Background: The demand for essential oils (EOs) has been steadily growing over the years. This is mirrored by a substantial increase in research concerned with EOs also in the field of inflammatory and neuropathic pain. The purpose of this present systematic review and meta-analysis is to investigate the preclinical evidence in favor of the working hypothesis of the analgesic properties of EOs, elucidating whether there is a consistent rational basis for translation into clinical settings.

Methods: A literature search has been conducted on databases relevant for medical scientific literature, i.e., PubMed/MEDLINE, Scopus, and Web of Science from database inception until November 2, 2020, following the PRISMA (Preferred Reporting Items for Systematic reviews and Meta-Analyses) criteria for systematic reviews and meta-analyses.

Results: The search was conducted in order to answer the following PICOS (participants/population, interventions, comparisons, outcomes, and study design) question: are EOs efficacious in reducing acute nociceptive pain and/or neuropathic pain in mice experimental models? The search retrieved 2,491 records, leaving 954 studies to screen after the removal of duplicates. The title and abstract of all 954 studies were screened, which left 127 records to evaluate in full text. Of these, 30 articles were eligible for inclusion.

Conclusion: Most studies (27) assessed the analgesic properties of EOs on acute nociceptive pain models, e.g. the acetic acid writhings test, the formalin test, and the hot plate test. Unfortunately, efficacy in neuropathic pain models, which are a more suitable model for human conditions of chronic pain, had fewer results (only three studies). Moreover, some methodologies raised concerns in terms of the risk of bias. Therefore, EOs with proven efficacy in both types of pain were corroborated by methodologically consistent studies, like the EO of bergamot, which should be studied in clinical trials to enhance the translational impact of preclinical modeling on clinical pain research.

Keywords: essential oils, pain models, inflammatory pain, neuropathic pain, chronic pain, systematic review, meta-analysis

1 INTRODUCTION

1.1 Rationale

Essential oils (EOs) containing components in exact proportion contributing synergically to the whole plant effect, have been used in traditional medicine for centuries since *The Divine Farmer's Materia Medica*, the first text of Chinese Traditional Medicine, representing a form of combinatorial medicine (Li and Weng, 2017). The search for natural and green products is constantly increasing the use of essential oils and the demand for these products from developing countries. There has been a remarkable increase in the import of EOs by the European market from 2011–2018 (Eurostat) and it is estimated that the demand for essential oils in the global market will grow by 7.5% from 2020 to 2027 (GVR, 2020). These data are mirrored by the steady increase of research on EOs that pave the way for the development of these products.

Identifying the year 1880 as this field emerged (Wood and Reichut, 1880), we found a remarkable increase in publications concerned with EOs up to 2020 (**Figures 1A,B**) (see also (Scuteri et al., 2017a)). EOs have shown several beneficial properties, many of which concern the treatment of neurologic diseases, mood disturbances, and pain. Modulation of the γ-aminobutyric acid (GABA) neurotransmission and blockade of neuronal voltage-gated sodium channels (Na + channels) as well as activity on serotonergic neurotransmission are proposed as mechanisms involved in the action of EOs endowed with anxiolytic and anti-nociceptive properties like bergamot essential oil (BEO) (Rombolà et al., 2017; Scuteri et al., 2018a; Scuteri et al., 2019a; Scuteri et al., 2019b; Rombolà et al., 2019; Rombola et al., 2020), lavender essential oil (LEO) (Lopez et al., 2017), and melissa (lemon balm) (Abuhamdah et al., 2008; Awad et al., 2009). The cholinergic system is targeted by extracts of plants as sage (Perry et al., 2000; Savelev et al., 2003; Savelev et al., 2004), ginkgo (Stein et al., 2015; Zhang et al., 2018), and lemon balm (Dastmalchi et al., 2009; Guginski et al., 2009), showing therapeutic potential for diseases like dementia. The gathered evidence shows the potential benefits of EOs in the treatment of pain in fragile patients for whom several drugs can be more harmful, e.g. in aging or chronic neurologic diseases such as dementia (Achterberg et al., 2020). Pain is associated with mood disturbances (Evans, 1987; Husebo et al., 2011) influenced by aging (Hamm and Knisely, 1985; Scuteri et al., 2020a) and neuropathology (Scherder et al., 2003) and its treatment represents a field of strong inappropriateness in patients suffering from Alzheimer's disease. (Scuteri et al., 2017b; Scuteri et al., 2018b; Achterberg et al., 2020; Scuteri et al., 2020f). Therefore, aromatherapy represents a fundamental tool for the safer handling of pain.

Despite a large amount of continuously growing research on EOs, a real translation of aromatherapy into clinical settings and the treatment of pain has not occurred. Research efforts have aimed to discover the mechanisms at the root of the analgesic activity of EOs, often focusing on the single components commonly present in different plant oils e.g., linalool, limonene, pinene, eugenol, and cinnamal. For instance, linalool, limonene, and pinene contribute to the anxiolytic and antidepressant properties of some EOs (see (Lizarraga-Valderrama, 2020)). In particular, some natural components of plants have been suggested as possible candidates for an analgesic action in neuropathic pain (Quintans et al., 2014). However, the strongest effect of EOs is due to the whole phytocomplex made up of various plant components that need to be present in a precise ratio to exert the so called *entourage* effect (Ribeiro, 2018). Definite combination of the constituents of EOs is necessary, but further studies are needed to highlight the exact active composition for each EO. The EOs of the species Citrus contain volatile components (85–99%), most abundantly terpenoids, and a non-volatile fraction including coumarins i.e. bergapten inducing phototoxicity (Zaynoun et al., 1977). Thus, the EO of bergamot has been deprived of bergapten (Bagetta et al., 2010), but is still endowed

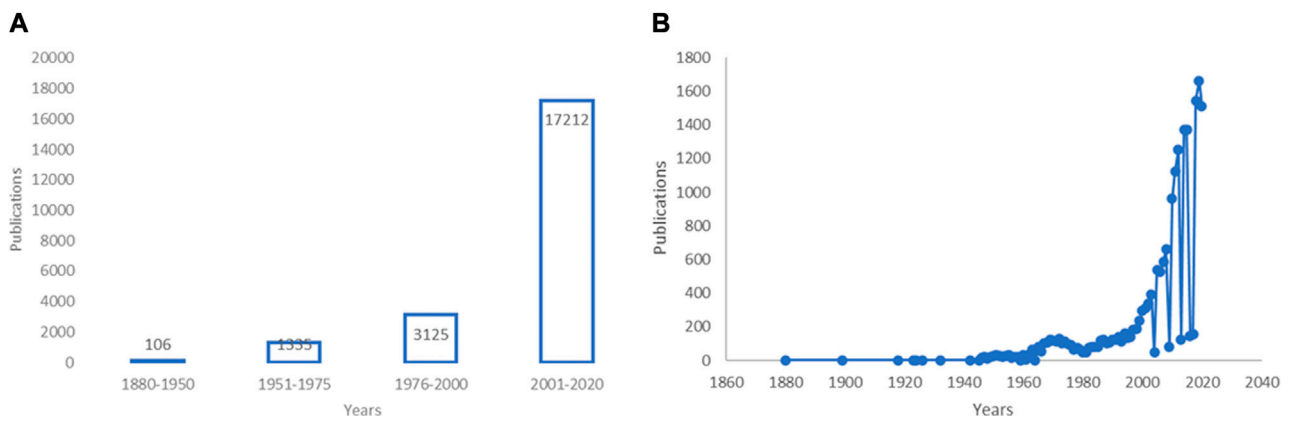

FIGURE 1 | Research in the field of essential oils (EOs) over the years.**(A,B)** Increase of research in the field of essential oils (EOs). **(A)** A PubMed advanced search using the key word "essential oils" combined with the dates of publication from 1880 to present through the Boolean operator AND has retrieved an increase from 106 to 17,212 (date of last search November 19, 2020) of results. The first interval "1880–1950" is wider because no great amount of research in this field has been detected up until the 1950s. **(B)** Data are presented per year of publication based on search query "essential oils" (date of last search November 25, 2020). Modified from (Scuteri et al., 2017a).

with its characteristics. The EO of bergamot can modulate the synaptic level of glutamate and this occurs when it is used as a bergapten-free fraction (Morrone et al., 2007). Hence, a mixture of monoterpene hydrocarbons within the volatile fraction may be responsible for bergamot analgesic activity since glutamate is significantly involved in the pain descending pathway due to metabotropic glutamate receptors mGluR7 and mGluR8 (Boccella et al., 2020). The novel phytocannabinoid cannabidihexol, with the terpenophenolic core of cannabidiol and Δ9-tetrahydrocannabinol, has proven to significantly reduce the late phase of the formalin test at low doses in C57BL/6J mice (Linciano et al., 2020). Cannabidiol oil has been demonstrated to reduce traumatic brain injury-induced allodynia (Belardo et al., 2019). Certain EOs have been proven to have enhanced efficacy if combined: e.g., peppermint and caraway oil are significantly effective on post-inflammatory visceral hyperalgesia only when used in combination (Adam et al., 2006). Likewise, the route of administration and the time of exposure can influence the effects of EOs (Scuteri et al., 2018a; Koyama and Heinbockel, 2020). Moreover, some EOs are efficacious in a preclinical setting (Sarmento-Neto et al., 2015), but often only in a definite model of pain, usually acute e.g. the acetic acid-induced writhings, that does not find a significant counterpart in clinic. Furthermore, EOs are often administered as *gavage* or for inhalation not always allowing an exact determination of the dose.

Clinical trials in aromatherapy are few, small and methodologically limited, hence it is not always possible to draw rigorous conclusions, particularly in dementia. As recently demonstrated in a Cochrane systematic review by Ball et al. (2020), the design, reporting and consistency of outcome measurement have been identified as the weakest points and need to be improved in the future. Thus, despite accumulating preclinical and clinical evidence for EOs (Scuteri et al., 2020d) and nutraceuticals (Scuteri et al., 2020e) in lots of forms and supplements, which have been studied in several neurodegenerative conditions, a sound rationale for their clinical use, especially in treating chronic pain (Lakhan et al., 2016), has not yet emerged.

2 METHODS

2.1 Objectives

The present systematic review and meta-analysis aimed to verify the working hypothesis that EOs have analgesic properties by investigating preclinical evidence in favor of the latter, to understand whether there is a consistent rational basis for clinical translation. For this purpose, the objective was to assess the efficacy of EOs in preclinical models of both nociceptive and neuropathic pain through the PRISMA (Preferred Reporting Items for Systematic reviews and Meta-Analyses) (Liberati et al., 2009; Moher et al., 2009) criteria for systematic reviews and meta-analyses. The systematic review and meta-analysis focuses on the following PICOS (participants/population, interventions, comparisons, outcomes, and study design) question: are EOs efficacious in reducing acute nociceptive pain and/or neuropathic pain in mice experimental models? In particular, this work aimed at evaluating:

- analgesic effectiveness (outcome);
- of EOs with a known composition (interventions), and not single components or extracts, administered intraperitoneally (i.p.) or subcutaneously (s.c.) to allow determination of the exact dose and reproducibility;
- in male mice subjected to nociceptive or neuropathic pain models (participants/population);
- with respect to providing a vehicle or other treatments (comparators);
- in studies designed according to legislation to minimize the suffering of animals (study design).

To the best of our knowledge, this is the first meta-analysis of preclinical studies on the analgesic effects of EOs interventions in models of both nociceptive and neuropathic pain.

2.2 Protocol

The search strategy and extraction of data to answer to PICOS question followed the PRISMA (Liberati et al., 2009; Moher et al., 2009) criteria. Due to the nature of preclinical animal intervention systematic review and meta-analysis, the latter aims at investigating the consistency of the body of evidence for clinical translation without an outcome of clear human relevance. For this reason, it has not been registered in the International prospective register of systematic reviews PROSPERO. However, statistically analyzing basic research independent studies testing the same hypothesis with comparable parameters can: determine its consistency allowing to study that phenomenon in a larger sample surmounting the issues concerned with small sample sizes; correct confounders; improve reproducibility (Editorial, 2016). Thus, a systematic review and meta-analysis is fundamental to establish a real possible clinical translation of a preclinically studied effect since it can highlight whether it has been consistently proven with the most reliable human disease modelled approach. Two independent researchers ran the search in agreement with the previously established protocol and inclusion and exclusion criteria, including double-checking the retrieved results, and any conflicts found by them were resolved by a third author.

2.3 Eligibility Criteria

2.3.1 Inclusion Criteria

The analysis included studies assessing the antinociceptive effect of EOs, administered i. p. or s. c. to allow determination of the exact dose and reproducibility, with a known percentage of components on male mice subjected to nociceptive or neuropathic pain models. Compliance with animal welfare regulations was an inclusion criterion of the utmost importance. The studies included needed to be designed according to legislation to minimize animal suffering. Either acute nociceptive or neuropathic pain models are included. Independently of the model used, the outcome of the study had to be antinociception for eligibility.

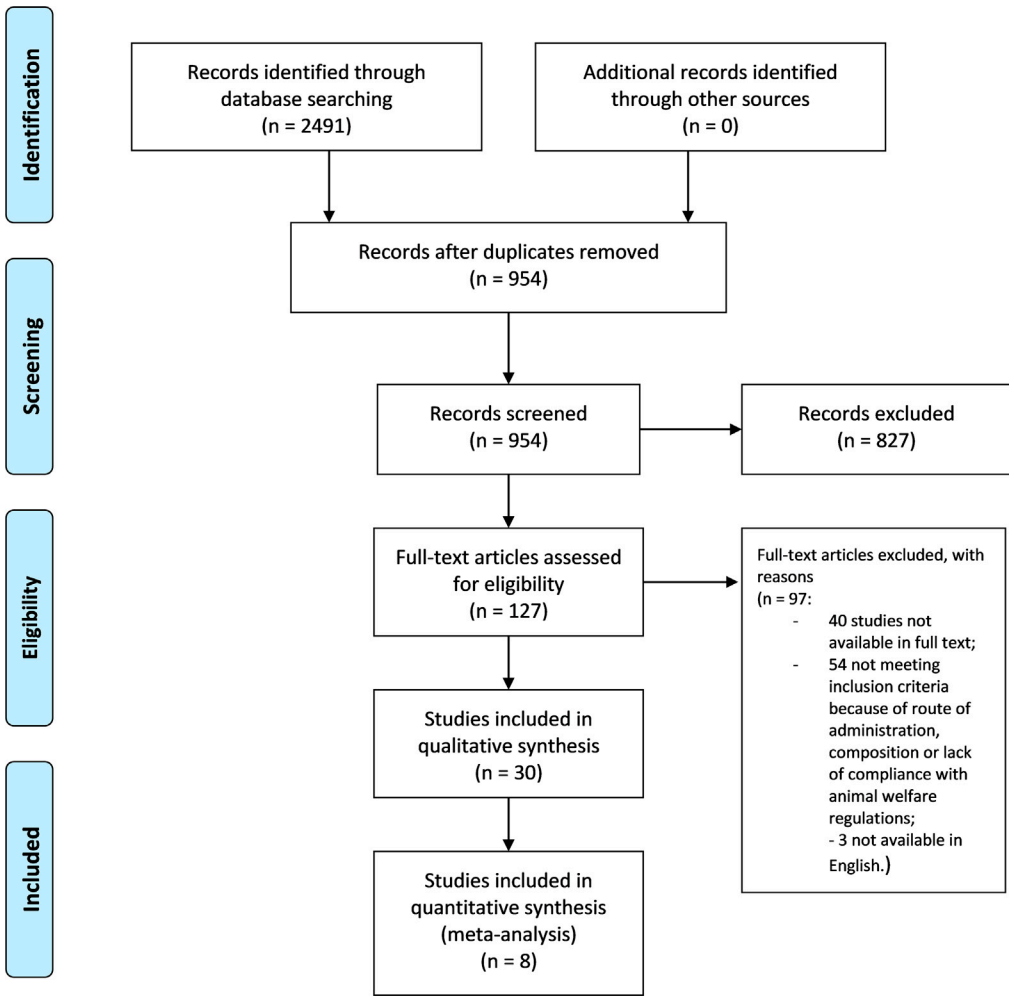

FIGURE 2 | Literature search and screening of retrieved records. PRISMA flow diagram (Moher et al., 2009) of the selection process of the studies eligible for qualitative and quantitative synthesis.

2.3.2 Exclusion Criteria

Studies on species different from mice or any strains and female gender were not eligible. The use of different species and genders would not allow comparison and the number of papers examining pain in non-rodent species is very small. Papers in which extracts or single plant components are used were excluded. Studies that did not consider ethics were excluded. Narrative or systematic reviews and meta-analysis, *in vitro* studies, abstracts and congress communications, proceedings, editorials, book chapters, and studies not published in English and not available in full text were not eligible.

2.4 Information Sources

A literature search was performed on PubMed/MEDLINE, Scopus, and Web of Science. Embase could not be searched as it was not freely/institutionally available. No restriction of publication date was applied and databases were searched for records matching the search strings used from their inception. The date of the last search was November 2, 2020. After the elimination of duplicate records, the first screening evaluated the title and abstract, and then the full text was assessed to define inclusion in qualitative and/or in quantitative synthesis.

2.5 Search Strategy

The following search terms and modifications were used as key words in combination: *essential oils, pain, animal pain models, antinociceptive activity, allodynia, Von Frey ('s test), hyperalgesia, Hargreaves ('test), hot plate, capsaicin test, formalin test, tail flick test, acetone test, complete Freund's adjuvant, streptozocin, chemotherapy(-induced), oxaliplatin, cisplatin, paclitaxel, docetaxel, vincristine, vinblastine, eribulin, bortezomib, thalidomide, neuropathy, mice.*

2.6 Data Collection Process

The eligibility of the studies was assessed independently by two authors to minimize the risk of excluding relevant records. The references list of the articles was examined to extend and refine the search. A complete consensus was reached and no relevant

conflicts were raised. The selection process is illustrated in the PRISMA flow diagram (**Figure 2**).

2.7 Synthesis, Risk of Bias, and Statistical Analysis

A systematic and narrative synthesis of the results, according to the Cochrane Consumers and Communication Review Group guidelines (Ryan, 2019 http://cccrg.cochrane.org, March 13, 2019 (accessed DATE).) was carried out. The risk of bias (internal validity) and the quality of the studies was assessed by two independent researchers through tools specific to preclinical animal studies like the Systematic Review Center for Laboratory Animal Experimentation (SYRCLE's) risk of bias (RoB) tool (Hooijmans et al., 2014) and the Collaborative Approach to Meta-Analysis and Review of Animal Data from Experimental Studies (CAMARADES) checklist for study quality (Macleod et al., 2004). Any discrepancies were resolved through consensus or with the help of a third author.

Meta-analyses were conducted using Cochrane Review Manager 5.3 (RevMan5.3; Copenhagen: The Nordic Cochrane Center, The Cochrane Collaboration). A minimum of five articles per outcome measure was required according to the systematic review protocol for animal intervention studies by SYRCLE. When the tests included in articles were multiple and performed at different times and doses, only the most significant time point for pain development and progression in the specific model was considered for meta-analysis and only data related to the most efficacious dose were included. Studies expressing the analgesic outcome in a comparable way were included in the meta-analysis. Data available and comparable, but not expressed with the same measure of effect size as proportional reduction of outcome in treated animals relative to untreated controls were converted in mean and standard deviation to allow statistical comparison. Data not available and not extractable from graphs using digital ruler software, e.g., PlotDigitizer 2.6.9, were excluded from quantitative analysis. The Higgins I^2 value was calculated to assess the heterogeneity of studies (Higgins and Thompson, 2002). Differences were presented as risk ratios (RR) including 95% confidence intervals (CI), using a random effect model (DerSimonian and Kacker, 2007) to manage the eventual heterogeneity of the studies and to assess intra- and inter-study variation. Publication bias was assessed through Egger's linear regression test to measure funnel plot asymmetry, adjusted through the "trim and fill" method (Egger et al., 1997; Duval and Tweedie, 2000; Sterne and Egger, 2001).

3 RESULTS

3.1 Selection Process and Data Collection

The search retrieved 2,491 results from databases and there were no results from additional searches. The records were screened for duplicates, leaving 954 studies. Title and abstract screening led to an initial exclusion of narrative or systematic reviews and meta-analysis, *in vitro* studies, abstracts and congress communications, proceedings, editorials, book chapters. This left 127 records in full text. Among these, two had to be excluded because the text was in Chinese (Li et al., 1991; Chen et al., 2011) and one was excluded because it was written in Spanish (Do Nascimento Silva et al., 2018). After full text screening, 30 studies were included in qualitative analysis: 40 studies were not available in full text and 54 were excluded because they did not meet inclusion criteria because of species used, route of administration, composition, or lack of compliance with animal welfare regulations. For instance, the study by Ali et al. (2012) in which the EO of Nepeta pogonosperma Jamzad et Assadi was proven to have significant efficacy at different doses in the tail-flick and formalin test in Wistar rats was therefore not eligible. Among the records included in qualitative analysis, eight were included in quantitative synthesis, reporting comparable outcomes and the exact number of animals used. The process of literature search and screening was illustrated in the PRISMA flow diagram (Moher et al., 2009) in **Figure 2**.

3.2 Qualitative Synthesis

The data obtained from the 46 studies included in the qualitative analysis were grouped according to Cochrane Consumers and Communication Review Group guidelines (Ryan, 2019 http://cccrg.cochrane.org, March 13, 2019 (accessed DATE).). These groups were based on the experimental pain model used in 1) EOs showing analgesia in nociceptive models, and 2) EOs with analgesic properties in neuropathic pain. The majority (27/30) of the studies used an acute nociceptive model. Studies providing a range and not an exact number of animals per group were not considered eligible for quantitative analysis. Studies expressing the analgesic outcome in a not comparable manner to the majority were excluded from the meta-analysis. The main characteristics of the studies with reference to the PICOS question are reported in **Tables 1**, **2**.

3.2.1 Essential Oils Endowed With Efficacy in Acute Nociceptive Models

Based on the obtained results, several EOs showed analgesic activity in acute nociceptive tests like the acetic acid writhings test, hot-plate test, and the formalin test, with the latter very useful since it includes features of both peripheral and central pain. In the study by Anaya-Eugenio et al. (2016) the EO of artemisia ludoviciana Nutt (Asteraceae) exerted dose-dependent antinociceptive activity in the hot-plate and the formalin test. It was less potent than the reference drug morphine and antagonism studies have revealed that it was inhibited by the non-selective opioid receptor antagonist naloxone. Inula britannica L (Asteraceae) has shown analgesia in the acetic acid writhings test, in the formalin test, in the tail-flick, and the glutamate test (Zarei et al., 2018). This effect is reversed by naloxone and potentiated by L-arginine, therefore all the studies performed with negative and positive controls highlighted the involvement of the opioid system and NO pathway (Zarei et al., 2018).

The EO of Myrcia pubiflora DC., Myrtaceae (Andrade et al., 2012) has demonstrated analgesic efficacy in the acetic acid

writhings test and the formalin test, but not in the hot plate test. From the same family, the EO of Eugenia candolleana DC (Myrtaceae) reduced the number of writhings and licking behavior in the second phase of the formalin test in a dose-dependent manner (only at the dose of 100 mg/kg in the first phase, but not the nociceptive reaction in the hot-plate test (Guimaraes et al., 2009)).

Clove bud oil (Eugenia caryophyllata, Myrtaceae) significantly reduced formalin-induced pain behavior but affected tail-flick response in a variable way (Halder et al., 2012). The study by Bae et al. (2020) considered basil for its i. p. administration and demonstrated analgesic properties linked to action on δ- and μ-opioid pathways. Moreover, it provides orofacial antinociception at high doses (Venâncio et al., 2011). Aristolochia trilobata L. demonstrated strong analgesia in the formalin test and was comparable to morphine in the acetic acid test (Quintans et al., 2017).

The EO of Croton conduplicatus Kunth (Euphorbiaceae) has shown efficacy (de Oliveira Júnior et al., 2017; de Oliveira et al., 2018): in the acetic acid test; on the formalin-induced nociceptive behavior at all the doses and in both phases, with effect antagonized by naloxone; on nociception in term of latency time at the highest dose (50 (deOliveira et al., 2018) and 100 (de Oliveira Júnior et al., 2017) mg/kg) in the hot-plate test. In particular, the mechanism of action of this EO has been proposed to be influenced by ATP-sensitive K+ channels, opioid and cholinergic systems (de Oliveira Júnior et al., 2017; de Oliveira et al., 2018).

Croton cordiifolius Baill (Euphorbiaceae) also had effective results in acetic acid, formalin, and glutamate but not the capsaicin test. This antinociceptive effect was independent on naloxone (Nogueira et al., 2015). Croton adamantinus Müll. Arg. showed a strongly effective comparison with morphine in reducing licking and was more efficacious than indomethacin in decreasing abdominal contortions (Ximenes et al., 2013). Of the study by Hajhashemi et al. (2009) only the experiments using the EO i. p. and on mice could be included in the analysis, showing the effectiveness of Heracleum persicum to be almost comparable to indomethacin in the reduction of the number of writhings.

In the study by Jahandar et al. (2018) only the experiments performed on mice were considered. Pycnocycla bashagardiana (Apiaceae) has not proven analgesic but anti-inflammatory properties. In another study by Ulku Karabay–Yavasoglu et al. (2006) only experiments with the formalin test in mice were considered. The EO of Satureja thymbra L (Lamiaceae) was demonstrated to have antinociceptive efficacy in both the early and late (also at a lower dose) phases of the formalin test (Ulku Karabay–Yavasoglu et al., 2006).

In the study by Katsuyama et al. (2015) the EO of bergamot (Citrus bergamia Risso) demonstrated significant dose-dependent analgesia in both phases of the formalin test, only when administered in the ipsilateral hindpaw and antagonized by naloxone hydrochloride and methiodide (not able to cross the blood brain barrier), suggesting the involvement of peripheral opioid mechanisms. This was earlier observed in the capsaicin test in which it also enhanced morphine analgesia (Sakurada et al., 2011).

Neroli (Citrus aurantium L.) significantly increases reaction time (at 40 mg/kg) in the hot-plate test and significantly decreased the number of writhings in the study by Khodabakhsh et al. (2015), with the latter effect potentiated by L-nitro arginine methyl ester (L-NAME). In the study by Khalid et al. (2011) the EO of Zingiber zerumbet (L.) Smith, dose-dependent and comparable to acetylsalicylic acid, inhibited the nociceptive response to capsaicin, acetic acid, glutamate, and phorbol 12-myristate 13-acetate (PMA). *Eucalyptus* EO has significantly reduced licking time in the second phase of the formalin test in the study by Lee et al. (2019), and this effect was mediated by the opioid system. It also reduced the number of writhings in a dose-dependent manner but did not display activity on thermal hyperalgesia (Lee et al., 2019). In the study by Lima et al. (2012) the EO of Chrysopogon zizanioides L (Roberty, Poaceae) produced antinociception similar to morphine in the acetic acid test, and this effect was partially reversed by naloxone. Moreover, it reduced the licking time in the second phase of the formalin test, but it did not demonstrate any effects in the Hargreaves' test.

A common trait is the presence of antiinflammatory analgesia devoid of thermal anti-hyperalgesic effect. The EO of Zhumeria majdae Rech. F. and Wendelbo (Lamiaceae) has displayed dose-related antinociceptive properties in the acetic acid and in the hot-plate test (Miraghazadeh et al., 2015). Chamaecyparis obtuse has also shown analgesia in the writhings and in the formalin, but not in the hot-plate test (Park et al., 2015). Furthermore, in the study by Mishra et al. (2010) *Senecio* rufinervis D.C. (Asteraceae) produced significant and dose-dependent inhibition of writhes and thermal hyperalgesia. In the study by Sharif et al. (2020) Tanacetum balsamita (Compositae) presented an anti-hyperalgesic effect. The antinociceptive properties exerted by Xylopia laevigata (Annonaceae) in the acetic acid and in the formalin test have not proven dependency on opioid pathways (Queiroz et al., 2014). The antinociceptive effect of Bunium persicum (Boiss.) is reversed by naloxone and attenuated by chlorpheniramine and cimetidine (Zendehdel et al., 2015), thus confirming the complex neuromodulation and the involvement of histamine in nociception (Hayashi et al., 2020). The main features of the studies on EOs analgesia in nociceptive models are summarized in **Table 1**.

3.2.2 Essential Oils Endowed With Efficacy in Neuropathic Models

Studies assessing the analgesic properties of EOs in neuropathic pain models are fundamental because these painful conditions are the most appropriate to model chronic neuropathic pain in humans. In the study by Komatsu et al. (2018) the EO of bergamot (Citrus bergamia Risso) was demonstrated to reduce partial sciatic nerve ligation (PSNL)-induced mechanical allodynia on the seventh post-operative day, in which it peaks (Kusunose et al., 2010). In the study by Kuwahata et al. (2013) the EO of bergamot increased mechanical thresholds dose-dependently and significantly at a dose of 20 μg/paw (Kuwahata et al., 2013). Moreover, this anti-allodynic effect is stronger than that of comparable doses of

TABLE 1 | Main characteristics of the studies included showing the efficacy of EOs in nociceptive models.

Study	EO [most representative components]	Route of administration	Control	Mice strain	Pain model	Analgesic outcome and sample size	Design
Anaya-Eugenio et al. (2016)	Artemisia ludoviciana [7)-camphor (21%), γ-terpineol (18%), borneol (18%),terpine-4-ol (3.5%),1,8-cineole (3.4%),lavanderlactone (3.4%), isoborneol (2.4%),camphen-6-ol (2.3%), *trans*-sabinylacet-ate (2.2%),andbornylacetate (2.2%]	i.p	Saline	ICR mice	1) Hot-plate test and 2) formalin test	1) Dose-dependent antinociceptive action (n = 8); 2) effectiveness in the first phase at the highest dose and in dose-dependent manner in the second phase (n = 8)	Use of increasing logarithmic dose (1, 10, 17.7, 31.6, and 100 mg/kg) according to allometric scaling. Use of a References drug: morphine sulfate. Antagonism studies with naloxone, atropine sulfate, L-nitro arginine methyl ester (L-NAME), or glibenclamide. No sample power calculation, randomization or blinding, or conflict of interest statement
Andrade et al. (2012)	Myrcia pubiflora DC., myrtaceae [caryophyllene oxide (22.2%), mustakone (11.3%), 1,8-cineole (5.4%), and tricyclene (5.3%)]	i.p	Vehicle (saline + Tween – 80 0.2%)	Swiss mice	1) Acetic acid-induced writhing test, 2) formalin test and 3) hot plate test	All the doses (25, 50, and 100 mg/kg) were active in acetic acid (n = 8) and formalin test (n = 8) and no dose in hot plate test (n = 8)	Random housing. Experiments performed between 9am and 4pm. Use of References drug morphine. No conflict of interest statement
Bae et al. (2020)	Ocimum basilicum L. (basil, lamiaceae) [linalool (56.6%), eugenol (18.1%), 1,8-cineole (6.93%), γ-cadinene (6.43%), and β-pinene (1.84%)]	i.p	Control (0.9% saline); vehicle (almond oil)	C57BL/6 mice	1) Acetic acid-induced writhing test, 2) formalin test and 3) hargreaves' test (n = 9)	EO (45 mg/kg) is effective in 1) acetic acid test (n = 8–10) and in 2) the second phase (n = 7–12), but only at a much higher dose (180 mg/kg) in 3) the hargreaves' test (n = 9)	Positive and negative control drugs have been used: morphine, indomethacin, naloxone, 5′-guanidinonaltrindole, naltrindole, L-NAME; L-arginine, and glibenclamide-hippuric acid. Mice have been randomly divided into groups. No conflict of interest statement
Quintans et al. (2017)	Aristolochia trilobata L. [6-methyl-5-hepten-2-ylacetate (SA) (21.49 ± 0.43%), germacrene D (15.07 ± 0.23%), bicyclogermacrene (8.84 ± 0.45%), linalool (6.85 ± 0.42%), (E)-caryophyllene (5.58 ± 0.12%), (E)-β-ocimene (5.56 ± 0.067%) and *p*-cymene (4.68 ± 0.10%)]	i.p	Vehicle (saline +0.2% tween	Swiss mice	1) Acetic acid test and 2) formalin test	1) EO (25, 50 and 100 mg/kg) has exerted analgesia comparable to morphine and sulcatyl acetate (n = 8); 2) EO (25, 50 and 100 mg/kg) has resulted active in the second phase and only at the highest dose in the first phase (n = 8)	Mice have been randomly assigned to groups. Experiments have been carried out from 08:00 a.m. to 04:00 p.m. (during light period) and in a blind manner. Morphine, acetylsalicylic acid and sulcatyl acetatehave been used as positive controls. No conflict of interest statement
de Oliveira Júnior et al. (2017)	Croton conduplicatus kunth [(E)-caryophyllene (13.72%), and caryophyllene oxide (13.15%) and monoterpene camphor (8.25%)]	i.p	Vehicle (0.9% saline +10 μL of tween 80, 10 ml/kg)	Swiss mice	1) Acetic acid-induced writhing test, 2) formalin test and 3) hot plate test	EO has resulted active at all doses in acetic acid (n = 6) and formalin test (n = 6) and at dose of 50 mg/kg in the hot-plate test (n = 6)	All the studies have been carried out by the same observers. Morphine and indomethacin as positive control. Antagonism studies (glibenclamide, naloxone and atropine). Random housing. Declaration of no conflict of interest
de Oliveira et al. (2018)	Croton conduplicatus kunth [monoterpenes 1,8-cineole (21.42%) and *p*-cymene (12.41%) and sesquiterpenes spathulenol (15.47%) and caryophyllene oxide (12.15%)]	i.p	Vehicle	Swiss mice	1) Acetic acid-induced writhing test, 2) formalin test and 3) hot plate test	EO (25, 50 and 100 mg/kg) has resulted active in acetic acid (n = 6) and formalin test (n = 6) and no dose in hot plate test (n = 6)	All the studies have been carried out by the same observers. Morphine and indomethacin as positive control. Antagonism studies (naloxone, atropine and flumazenil). Random housing. Declaration of no conflict of interest

(Continued on following page)

TABLE 1 | (*Continued*) Main characteristics of the studies included showing the efficacy of EOs in nociceptive models.

Study	EO [most representative components]	Route of administration	Control	Mice strain	Pain model	Analgesic outcome and sample size	Design
Guimaraes et al. (2009)	Eugenia candolleana DC. (myrtaceae) [β-elemene (35.87 ± 0.13%), **δ**-elemene (8.28 ± 0.02%), β-caryophyllene (8.15 ± 0.08%). viridiflorene (6.96 ± 0.05%) (Neves et al., 2017); leaves in serra da guia, poço Redondo-SE, Brazil (GPS: 9.58o47.05:S 37.52o24.11: W Guimaraes et al. (2009)]	i.p	Vehicle (saline +1 drop of Tween-80 0.2%)	Swiss mice	1) acetic acid-induced writhing test, 2) formalin test and 3) hot plate test	EO (25, 50, and 100 mg/kg) dose-dependently inhibits acetic acid (n = 10) and formalin-induced (n = 10), but not hot-plate (n = 10) behaviors	Experiments carried out between 09:00 h and 16: 00 h. References drug was acetylsalicylic acid. Random housing. No conflict of interest statement
Hajhashemi et al. (2009)	Heracleum persicum [hexyl butyrate (56.5%), octyl acetate (16.5%), hexyl 2-methylbutanoate (5.2%), hexyl isobutyrate (3.4%) and n-octyl 2-methylbutyrate (1.5%)]	i.p	Vehicle (1% solution of tween	Swiss mice	Acetic acid-induced writhing test	EO (50–100 mg/kg) has reduced writhings of 66 and 73% respectively (n = 6), in comparison with the 80% reduction of indomethacin	Indomethacin has been used as positive control. No conflict of interest statement
Halder at al. (2012)	Eugenia caryophyllata (clove oil; myrtaceae) [eugeno (87.34%), eugenyl acetate (5.18%), and beta-caryophyllene (2.01%)]	i.p	0.9% saline	Swiss mice	1) Formalin test and 2) tail-flick test	1) EO (0.1 ml/kg) has reduced licking/biting time in the first and (0.025, 0.05, and 0.1 ml/kg) in the second phase (n = 6); 2) effect of clove oil (0.1 ml/kg) (n = 6) at 30 min of reduced tail-flick latency resulted reverted by naloxone. Though not significantly, the dose 0.025 ml/kg of clove oil, at 30 and 60 min have increased the mean tail-flick latency	Experiments performed at daytime between 09:30 and 15:30. Morphine and acetylsalicylic acid have been used as References drugs. Naloxone has been used in the tail-flick test. No conflict of interest statement
Khalid et al. (2011)	Zingiber zerumbet (L.) smith [zerumbone (36.12%), humulene (10.03%), humulene oxide I (4.08%), humulene oxide II (2.14%), caryophyllene oxide II (1.66%) and caryophyllene oxide I (1.43%), camphene (14.29%), borneol (4.78%), camphor (4.18%), eucalyptol (3.85%), α-pinene (3.71%), γ-terpinene (2.00%), β-phellandrene (1.63%), 1-terpen4-ol (1.44%), β-myrcene (1.22%) and linalool (1.06%), as previously described Sulaiman et al. (2010)]	i.p	Vehicle	ICR mice	Capsaicin, acetic acid, glutamate and phorbol 12-myristate 13-acetate (PMA)-induced nociception	EO (50, 100, 200, 300 mg/kg) has exerted significant dose-dependent inhibition of: abdominal writhings (n = 10); capsaicin-induced neurogenic nociception (n = 10) similar to that of acetylsalicylic acid and of capsazepine; glutamate-induced nociception (n = 10) and of PMA-induced nociception (n = 10), comparable to acetylsalicylic acid	Blinded, randomized and controlled design. Acetylsalicylic acid and capsazepine have been used as References drug. Antagonism studies with L-arginine, N^{ω}-nitro-L-arginine, methylene blue and glibenclamide. No conflict of interest statement
Jahandar et al. (2018)	Pycnocycla bashagardiana (apiaceae) [myristicin (76.1%), E. β. Ocimene (4.1%), Z. β. Ocimene (3.8%) and β-eudesmol (2.9%)]	i.p	Vehicle	NMRI mice	1) Formalin test and 2) hot-plate test	1) EO (100, 200, and 400 mg/kg) has not shown antinociceptive activity in the formalin test (n = 6–8); 2) EO (50, 100, 200, and 400 mg/kg) has not shown antinociceptive activity in the hot-plate test	Morphine had been used as References drug. Declaration of no conflict of interest

(Continued on following page)

TABLE 1 | (*Continued*) Main characteristics of the studies included showing the efficacy of EOs in nociceptive models.

Study	EO [most representative components]	Route of administration	Control	Mice strain	Pain model	Analgesic outcome and sample size	Design
Katsuyama et al. (2015)	Bergamot (citrus bergamia risso) [0.38% D-limonene, 70.26% linalyl acetate, 18.95% linalool, 0.62% γ-terpinene, and 0.03% β-pinene]	s.c	Jojoba wax and none	ddY mice	Formalin test	Significant dose-dependent inhibition of both phases by EO (2.5, 5, 10 **μ**g) ($n = 10$)	All behavioral experiments have been carried out during the light period between 10:00 and 16:00. The animals have been tested in randomized order. Antagonism studies with naloxone hydrochloride and naloxone methiodide. No conflict of interest statement
Khodabakhsh et al. (2015)	Neroli (citrus aurantium L.) [linalool (28.5%), linalyl acetate (19.6%), nerolidol (9.1%), and E,E-farnesol (9.1%)]	i.p	Vehicle (sweet almond oil)	Wistar mice	1)acetic acid and 2) hot-plate test	1) Neroli (10 and 20 mg/kg) has significantly decreased the number of writhings ($n = 8$) and 2) has significantly increased latency time at dose of 40 mg/kg ($n = 8$)	Mice have been used only once and experiments have been conducted between 10.00 a.m. and 13 p.m. with normal room light. Diclofenac has been used as References drug and L-NAME as enhancer. No References to randomization of mice but only for the experimental part concerned with rats. No conflict of interest statement.
Lee et al. (2019)	Eucalyptus [(aromarant co. Ltd., rottingen, Germany); 1,8-cineole (61.46%), limonene (13.68%), **ρ**-cymene (8.55%), γ-terpinene (5.87%), α-pinene (4.95%), and α-phellandrene (1.09%) Jun et al. (2013)]	i.p	Control 0.9% saline and vehicle (almond oil)	C57BL/6 mice	1) Formalin test, 2) acetic acid test and 3) hargreaves' test	1) EO (11.5, 22.5, 45 mg/kg) has significantly reduced licking time in the second phase (n = 7–12); 2) dose-dependent reduction of the number of writhes (n = 8–10); 3) no significant effect ($n = 10$)	Antagonism studies with the k-opioid antagonist 5′-guanidinonaltrindole, the **δ**-opioid antagonist naltrindole and the **μ**-opioid antagonist naloxone (also + morphine). Indomethacin has been used as References drug for acetic acid test. Declaration of no conflict of interest
Lima et al. (2012)	Chrysopogon zizanioides L. (roberty, poaceae) [khusimol (19.57%), E-isovalencenol (13.24%), α-vetivone (5.25%), vetiselinenol (5.08%), α-cadinol (5.01%), α-vetivone (4.87%) and hydroxy-valencene (4.64%)]	i.p	Vehicle (distilled water with one drop of tween 80 0.2%)	Swiss mice	1) Formalin test, 2) acetic acid test and 3) hot-plate test	1) EO (50, and 100 mg/kg) has been effective in the second phase (n = 10); 2) EO (50, and 100 mg/kg) has produced antinociception similar to morphine ($n = 10$); 3) EO (25, 50, and 100 mg/kg) has not shown efficacy ($n = 10$)	Morphine and acetylsalicylic acid have been used as References drugs and naloxone for antagonism study. Random housing. No conflict of interest statement
Ximenes et al. (2013)	Croton adamantinus müll. Arg. [Methyl-eugenol (14.81%), 1,8-cineole (13.74%), bicyclogermacrene (8.06%) and β-caryophyllene (5.80%)]	i.p	Vehicle (cremophor 0.5%, 0.1 ml/10 g)	Swiss mice	1) Formalin test and 2) acetic acid test	1) EO (50 and 150 mg/kg) is effective in both phases, and in a comparable way to morphine in the second phase; 2) EO (50 and 150 mg/kg) is more effective than indomethacin. Unreported number of animals	For the acetic acid test, the observation has been conducted by a blind observer. Morphine and indomethacin have been used as References drugs. No conflict of interest statement

(Continued on following page)

TABLE 1 | (*Continued*) Main characteristics of the studies included showing the efficacy of EOs in nociceptive models.

Study	EO [most representative components]	Route of administration	Control	Mice strain	Pain model	Analgesic outcome and sample size	Design
Miraghazadeh et al. (2015)	Zhumeria majdae rech. F. and wendelbo (lamiaceae) [linalool (63.4%) and camphor (27.5%)]	i.p	Vehicle (sweet almond oil)	NMRI mice	1) Acetic acid test; 2) hot-plate test	1) EO (5, 10, 20, 40 mg/kg) has produced dose-dependent analgesia (n = 5); 2) EO (5, 20, 40 mg/kg) has significantly prolonged latency time in dose-related manner (n = 5)	Experiments have been conducted between 10.00 a.m. and 13.00 p.m. and mice used only once. Diclofenac has been used as References drug. No conflict of interest statement
Mishra et al. (2010)	*Senecio* rufinervis D.C. (Asteraceae) [germacrene D (40.19%), β-pinene (12.23%), β-caryophyllene (6.21%) and β-longipinene (4.15%)]	i.p	Vehicle (2% v/v tween 80)	Wistar albino mice	1) Acetic acid test; 2) hot-plate test	EO (25, 50, 75 mg/kg) has produced significant and dose-dependent inhibition of writhes and also of thermal hyperalgesia at the doses of 50 and 75 mg/kg (n = 6)	Pentazocine has been used as positive control. No conflict of interest statement
Nogueira et al. (2015)	Croton cordiifolius baill. (Euphorbiaceae) [1,8-cineol (25.09%), α-phellandrene (15.43%), β-cymene (8.02%), spathulenol (6.68%) and β-caryophyllene (6.58%)]	i.p	Vehicle (polyethoxylated castor oil - cremophor)	Swiss mice	1) Acetic acid test; 2) formalin test; 3) capsaicin test; 4) glutamate test	EO (50 and 100 mg/kg) has proven analgesia in all tests (n = 8) apart from capsaicin, comparable to indomethacin in its highest dose (acetic acid test) and higher than morphine (formalin test; in the second phase only at the highest dose). In gluatamate test only the highest dose has been effective. This effect id independent on naloxone	Indomethacin and morphine have been used as positive control and naloxone as antagonist. Declaration of no conflict of interest
Park et al. (2015)	Chamaecyparis obtuse [(mg/L): Isoprene 293, α-pinene 8,754, camphene 3,294, β-pinene 2,940, δ-3-carene 42, myrcene 36,440, α-phellandrene 697, α-terpinene 10,262, D-limonene 50,135, γ-terpinene 23,361, cymene 2,862, terpinolene 10,137, linalool 1824, camphor 250, bornyl acetate 74,903, α-humulene 1,628, terpineol 4,788, cedrol 7,230]	i.p	Control (distilled water containing 0.5% DMSO instead of treatments)	C57BL/6J mice	1) Formalin test, 2) acetic acid test, 3) hot-plate test and	EO (5 and 10 mg/kg) is effective in 1) formalin test (only at the lowest dose in the first phase) (n = 7–8) and in the 2) acetic acid test (n = 7–8), not in the hot-plate test (n = 10)	Acetylsalicylic acid has been used as positive control. No conflict of interest statement
Queiroz et al. (2014)	Xylopia laevigata (annonaceae) [γ-muurolene (17.78%), δ-cadinene (12.23%), bicyclogermacrene (7.77%), α-copaene (7.17%), germacrene D (6.54%), (E)-caryophyllene (5.87%), γ-cadinene (4.72%), aromadendrene (4.66%), and γ-amorphene (4.39%)]	i.p	Vehicle (saline +2 drops of tween 80 0.2%)	Swiss albino mice	1) Acetic acid test; 2) formalin test	EO (12.5, 25, 50 mg/kg) has significantly reduced the 1) acetic acid-induced writhings-induced nociception (n = 8) and the 2) two phases of the formalin test (n = 8)	Mice have been used only once. Morphine has been used as References drug. Naloxone has been used as antagonist. Declaration of no conflict of interest

(Continued on following page)

TABLE 1 | (*Continued*) Main characteristics of the studies included showing the efficacy of EOs in nociceptive models.

Study	EO [most representative components]	Route of administration	Control	Mice strain	Pain model	Analgesic outcome and sample size	Design
Sakurada et al. (2011)	Bergamot (citrus bergamia risso) [0.38% D-limonene, 70.26% linalyl acetate, 18.95% linalool, 0.62% γ-terpinene and 0.03% β-pinene]	s.c	Saline, jojoba wax and none	ddy mice	Capsaicin test	Dose-dependent inhibiton of nociceptive response by the EO (2.5, 5, 10, 20 μg/paw) significant only at the highest doses of 10 and 20 μg/paw (n = 10)	Mice have been tested in randomized order and behavioral experiments have been performed during the light period between 10:00 and 17:00h. Lidocaine hydrochloride monohydrate and morphine hydrochloride have been used as References drugs. Naloxone hydrochloride and methiodide have been used as antagonists. No conflict of interest statement
Sharif et al. (2020)	Tanacetum balsamita (compositae) [carvone (39.8%) and α-thujone (11.9%).].	i.p	Vehicle (sweet almond oil)	NMRI mice	Hot-plate test	EO produced anti-nociception only at the dose of 100, mg/kg) (n = 6–8)	Experiments have been conducted between 10.00 a.m. and 13.00 p.m. and mice used only once. Morphine has been used as positive control. No conflict of interest statement
Ulku Karabay–Yavasoglu et al. (2006)	Satureja thymbra L. (lamiaceae) [γ-terpinene (40.99%), carvacrol (17.50%), thymol (13.19%), and P-cymene (12.73%), β-caryophyllene (3.15%), α-thujene (1.98%), and thymylmethylether (1.94%)]	i.p	Vehicle (2% tween 20)	Albino mice	Formalin test	Analgesic effect in the early (50 and 100 mg/kg) and in the late (25, 50, and 100 mg/kg) phases of the formalin test (n = 10)	Animals were used only once and humanly sacrificed at the end of the test. Morphine has been used as References drug and naloxone as antagonist. No conflict of interest statement
Venâncio et al. (2011)	Ocimum basilicum L. (lamiaceae) [linalool (76.13%), geraniol (11.16%), 1,8-cineol (6.66%)]	i.p	Vehicle (saline + tween 80 0.2%)	Swiss mice	Orofacial formalin, glutamate and capsaicin-induced nociception	EO (50, 100, 200 mg/kg) is effective in all the doses at the highest doses (n = 8)	Mice have been used once in the study. Nociception tests have been conducted by the same observer. Morphine hydrochloride and lidocaine have been used as References drugs. No conflict of interest statement
Zarei et al. (2018)	Inula britannica L. (asteraceae) [viridiflorol (7.17%–8.20%) and himachalol (3.45%–8.71%) followed by 6,10,14-trimethyl-2-pentadecanone (5.43%–2.95%), 13-tetradecanolide (3.93%–4.87%) and 3-methyl-4-propyl-2,5-furandione (4.06%–0.29%) Todorova et al. (2017)]. Flowers of inula britannica collected from the slopes of mount alvand, hamadan (34°47′59.99″N, 48°30′59.99″E	i.p	Control (saline)	Swiss albino mice	1) tail-flick test; 2) acetic acid test; 3) formalin test and 4) glutamate-test	EO (25, 50, and 100 mg/kg) (n = 5) for all tests. 1) the highest dose has resulted effective; 2) the doses of 50 and 100 mg/kg have been effective; 3) the highest dose is comparable to morphine; 4) only the highest dose is significantly active	Experiments have been carried out between 8 a.m. and 12 p.m. Morphine, naloxone, L-Arginine, methylene blue, glibenclamide, naltrindole, nor-binaltorphimine and naloxonazine have been used as positive and negative controls. Declaration of no conflict of interest

(Continued on following page)

TABLE 1 | (*Continued*) Main characteristics of the studies included showing the efficacy of EOs in nociceptive models.

Study	EO [most representative components]	Route of administration	Control	Mice strain	Pain model	Analgesic outcome and sample size	Design
Zendehdel et al. (2015)	Bunium persicum (boiss.) [germacrene-d (22.1–24.1%) and E-caryophyllene (26.6–38%) Sofi et al. (2009)]. Samples of the plant identified at the division of pharmacognosy, faculty of pharmacy, tehran university of medical sciences, Iran	i.p	Control (Tween-80 (0.5%)	Albino NMRI mice	Acetic acid test	EO (0.001, 0.01, 0.05, 0.1, 0.5 and 1%; 10 ml/kg) (n = 7). The EO 0.01% has significantly reduced contortions (90.7% vs 38.13% of indomethacin) and this effect has been inhibited by naloxone and reduced by chlorpheniramine and cimetidine	Experiments have been conducted during the light phase (10:00–17:00 h). Antagonism studies have been performed using naloxone, the serotonergic receptor antagonist cyproheptadine, the histamine H1-receptor antagonist chlorpheniramineand the histamine H2-receptor antagonist cimetidine. Indomethacin has been used as References drug. No conflict of interest statement

Studies characteristics in response to PICOS (participants/population, interventions, comparisons, outcomes, and study design) question for records including acute nociceptive pain models; n = *number of animals. The order of references in the table follows that in the text.*

morphine, of which the EO of bergamot enhances the activity (Kuwahata et al., 2013), and it was reversed by naloxone methiodide, peripherally μ-opioid receptor preferring antagonist, β-funaltrexamine hydrochloride, selective μ-opioid receptor antagonist, and β-endorphin antiserum, but not by the non-selective δ-opioid receptor antagonist naltrindole and by the selective κ-opioid receptor antagonist nor-binaltorphimine. Importantly, the study by Hamamura et al. (2020) in which the EO of bergamot was administered s. c. with an osmotic pump to allow a continuous delivery devoid of smell during PSNL, demonstrated that the anti-allodynic effect of this EO is systemic and does not depend on olfactory stimulation. In this study (Hamamura et al., 2020) the increase of planar activity during the light period induced by PSNL, with the maximum effect at the seventh post-operative day and like allodynia, was shown to be abolished by continuously administered EO. This effect is antagonized by naloxone hydrochloride. Observation lasting 14 days with a theoretical duration of the osmotic pump of one week can mimic administration during chronic pain. The main features of the studies on EOs anti-allodyinic properties are summarized in **Table 2**.

3.3 Risk of Bias Assessment

The studies included in the qualitative analysis were assessed for methodological quality according to the SYRCLE's RoB tool (Hooijmans et al., 2014) and the CAMARADES checklist (Macleod et al., 2004; Hooijmans et al., 2014; Suokas et al., 2014), based on the Cochrane RoB (Sterne et al., 2019). These items comprise all the possible forms of bias. 1) Selection bias–sequence generation (allocation sequence able to produce comparable groups). 2) Selection bias–baseline characteristics (comparable and not adjusted for confounders in the analysis). 3) Selection bias–allocation concealment (during the enrollment). 4) Performance bias–random housing and randomization during the study. 5) Performance bias–blinding of investigators during the study. 6) Detection bias–random outcome assessment. 7) Detection bias–blinding of outcome assessors. 8) Attrition bias (animals eventually excluded from outcome assessment). 9) Reporting bias–reports free of selective outcome reporting. Finally, 10) other sources of bias: lack of evidence of induced pain using the selected behavioral outcome measure before EO administration and examination (i.e., sham procedure), clear description of methods with number of animals used, attention to circadian regulation for behavioral studies, use of the same observer for behavioral tests, use of control and positive and negative control drugs, sample size calculation, statement of conflict of interest, statement of compliance with animal welfare regulations and attention to ethics.

In terms of the two items regarding selection bias, no study reported the method of allocation and, even though they conducted baseline measures, none of the studies describe how experimental groups were composed to ensure homogeneity and consistency. Only the study by *Lima* and collaborators (Lima et al., 2012) in which mice with baseline latencies of more than 10 s, and studies by de Oliveira Júnior and colleagues (de Oliveira Júnior et al., 2017; de Oliveira et al., 2018) of more than 20 s, at the hot-plate were excluded from the experiments.

As reported in **Table 1**, five studies (Guimaraes et al., 2009; Andrade et al., 2012; Lima et al., 2012; de Oliveira Júnior et al., 2017; de Oliveira et al., 2018) adopted random housing of mice. The paper by Khodabakhsh et al. reported no randomization of mice but only of rats, which are not included in this systematic review and meta-analysis (Khodabakhsh et al., 2015). Mice were tested in a randomized order in studies by Sakurada and collaborators and Katsuyama et al., 2015 (Sakurada et al., 2011; Katsuyama et al., 2015). In the study by Bae et al. (2020) mice were randomly assigned to groups. The study by Khalid et al. (2011) used a blind, randomized design. Mice were randomly assigned to groups and experiments were performed in a blind manner in the study by Quintans and coworkers (Quintans et al., 2017).

TABLE 2 | Main characteristics of the studies included showing efficacy of EOs in neuropathic models.

Study	EO	Route of administration	Control	Mice strain	Pain model	Analgesic outcome and sample size	Design
Hamamura et al. (2020)	Bergamot (citrus bergamia risso) [D-limonene (39.60%), linalyl acetate (31.09%), and linalool (9.55%)]	s.c., with the aid of an osmotic pump	Jojoba wax	ddY mice	Partial sciatic nerve ligation	Reduction of the induced increase of planar activity during the light period at the 7th post-operative day (control *n* = 6; EO n = 9)	Acclimatization to the lighting conditions for 1 week. After basal measures before surgery, the mice have been observed for 14 days. Antagonism study with naloxone hydrochloride. Declaration of no conflict of interest. Sham procedure
Komatsu et al. (2018)	Bergamot (citrus bergamia risso) [0.38% D-limonene, 70.26% linalyl acetate, 18.95% linalool, 0.62% γ-terpinene, and 0.03% of β-pinene]	s.c	Jojoba wax and saline	ddY mice	Partial sciatic nerve ligation	On post-operative day 7, the EO of bergamot (5.0, 10.0, and 20.0 μg/paw) has attenuated dose-dependently mechanical allodynia, significantly at the dose of 20.0 μg/paw (*n* = 10)	Antagonism studies with naloxone methiodide (μ-opioid receptor preferring antagonist), β-funaltrexamine hydrochloride (selective μ-opioid receptor antagonist), β-endorphin antiserum, naltrindole (non-selective δ-opioid receptor antagonist) and nor-binaltorphimine (selective κ-opioid receptor antagonist). Behavioral tests have been performed between 10:00 and 16:00 h and for 2 days before the start of the experiment for acclimatation of the mice to the testing procedures. Sham procedure. No conflict of interest statement
Kuwahata et al. (2013)	Bergamot (citrus bergamia risso) [0.38% of D-limonene, 70.26% of linalyl acetate, 18.95% of linalool, 0.62% of γ-terpinene, and 0.03% of β-pinene]	s.c	Jojoba wax + saline	ddY mice	Partial sciatic nerve ligation	Dose-dependent reduction (5, 10, 20 μg) of tactile allodynia 7 days after surgery (*n* = 10)	Behavioral experiments have been carried out from 10:00 a.m. to 6:00 p.m. and mice have been used only once. Morphine hydrochloride has been used as References drug. Sham procedure. No conflict of interest statement

Studies characteristics relative to PICOS (participants/population, interventions, comparisons, outcomes, and study design) question for retrieved records about neuropathic pain models; n = number of animals. The order of references in the table follows that in the text.

Moreover, in the study by Ximenes et al. (2013), the observation was conducted by a blind observer, but the number of animals used for behavioral testing was not reported, only for histological assays. Otherwise, the number of animals per group was reported, but studies that provided a range and not an exact number were not considered eligible for quantitative analysis. Attrition and reporting biases cannot be assessed from the full text of the included studies. Importantly, sham procedure and the certainty of exact execution of the pain model is present only in studies on allodynia, i.e., the studies by Hamamura et al. (2020), Komatsu et al. (2018a), and Kuwahata et al. (2013).

Attention to the circadian rhythm in behavioral testing was reported by the following studies: (Andrade et al., 2012; Quintans et al., 2017; Guimaraes et al., 2009; Halder et al., 2012; Katsuyama et al., 2015; Khodabakhsh et al., 2015; Miraghazadeh et al., 2015; Sakurada et al., 2011; Sharif et al., 2020; Zarei et al., 2018; Zendehdel et al., 2015; Komatsu et al., 2018b; Kuwahata et al., 2013). All the studies used control and positive and negative modulators. Importantly, multiple controls were used in the following studies (Katsuyama et al., 2015; Komatsu et al., 2018b; Kuwahata et al., 2013; Sakurada et al., 2011). Behavioral testing was conducted by the same observers in the following studies (de Oliveira Júnior et al., 2017; de Oliveira et al., 2018; Venâncio et al., 2011). Sample size calculation was not reported and the conflict of interest statement is present only in eight studies (Queiroz et al., 2014; Nogueira et al., 2015; de Oliveira Júnior et al., 2017; de Oliveira et al., 2018; Jahandar et al., 2018; Zarei et al., 2018; Lee et al., 2019; Hamamura et al., 2020). This could be due to the lack of requirement of these aspects in journals in the last few years. A statement of compliance with animal welfare regulations is reported in all the studies since it is an inclusion criterion. Moreover, six studies (Ulku Karabay–Yavasoglu et al., 2006; Venâncio et al., 2011; Queiroz et al., 2014; Khodabakhsh et al., 2015; Miraghazadeh et al., 2015; Sharif et al., 2020) also stated that they used each mouse only once, thus proving particular attention to animal welfare. Importantly, only the study by Hamamura et al. (2020) reported acclimatization to lighting conditions for one week and that an observation period of 14 days can model examination during chronic pain.

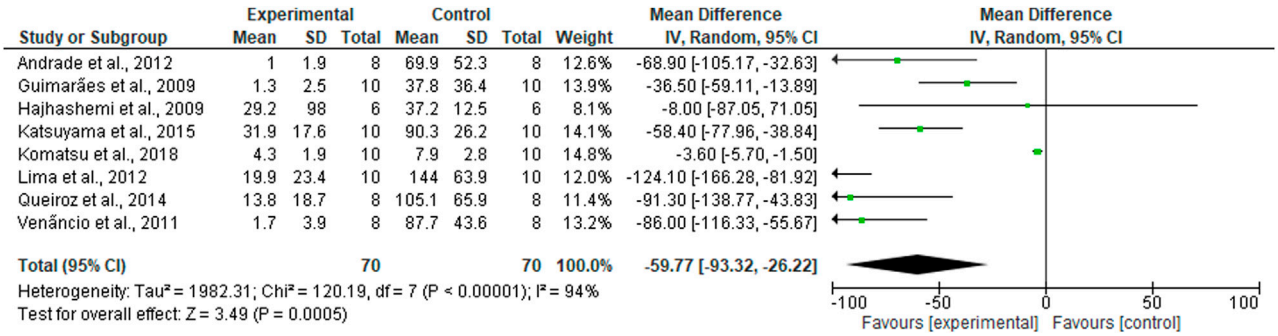

FIGURE 3 | Forest plot for EOs-induced analgesia. The results of the meta-analysis favor the efficacy of the EOs, but they are affected by high heterogeneity (Mean difference MD −59.77; 95% CI (−93.32) - (−26.22); I^2 = 94%; p < 0.00001).

3.4 Meta-Analysis

This meta-analysis comprises eight studies for a total of 140 mice. The studies were considered comparable when the analgesic outcome was expressed as mean ± standard error of the mean (SEM) since these measures could be converted for meta-analysis in mean and standard deviation (SD). Moreover, only studies reporting the exact number of animals per group were included in quantitative analysis. Studies investigating the same pain model were considered. The formalin test pain model was chosen since it provides a biphasic nociceptive response. Due to the sensitization processes occurring during the second phase, the study on mechanical allodynia expressed has been included (Komatsu et al., 2018b). The results of the forest plot favor the analgesic efficacy of EO (Mean difference MD −59.77; 95% CI (−93.32) - (−26.22); I^2 = 94%; p < 0.00001; **Figure 3**), but need to be carefully examined because of the extremely high heterogeneity, which is also confirmed by the asymmetry of the funnel plot analysis standing for high risk of publication bias, small studies and high differences in study precision.

4 DISCUSSION

Interest in the use of EOs and aromatherapy has been continuously growing during the last few decades in parallel with preclinical research. However, in spite of all this effort of preclinical research, it is necessary to establish whether there is a strong rationale for the clinical use of EOs. This issue is even more controversial in the field of pain relief since the use of aromatherapy could reduce the dose of painkillers endowed with serious side effects, particularly in under studied areas of neuropathic pain, like opioids (Morrone et al., 2017; Scuteri et al., 2020b). Alternative pain treatments could increase time in treatment before the loss of efficacy. This is relevant to fragile populations, e.g., patients suffering from dementia, who are often undertreated compared to cognitively intact counterparts, more so during the Sars-CoV2 pandemic (Scuteri et al., 2020c).

This systematic review and meta-analysis assesses the efficacy of EOs in preclinical models of acute inflammatory nociception and neuropathic pain to understand if there is a rational basis for clinical translation. Several EOs from multiple families were found to be efficacious, in particular, croton and bergamot EOs have been extensively studied. It is noteworthy that 27 out of the 30 studies included in the qualitative analysis were only performed on acute pain models like writhings and the hot plate test. These tests are very useful since they are easy to conduct and provide fast results, but they do not resemble clinical pain conditions. Taking this into account, the quantitative analysis only includes studies on formalin test, which is more similar to clinical conditions due to its biphasic nature, and the only study on mechanical allodynia that could compare to the other seven included.

All these studies included in this review have a different experimental design and most of them present serious concerns in terms of selection, performance, and detection biases. Most studies do not adhere to the guidelines for Animal Research: Reporting *In Vivo* Experiments (ARRIVE), which are fundamental for accurate *in vivo* preclinical research (Rice et al., 2013). Another methodological aspect responsible for bias in the meta-analysis is that control groups were often used in more than one experiment, and studies including multiple comparisons can introduce errors. Thus, this systematic review and meta-analysis points to the importance of appropriate *in vivo* modeling to enhance the translational impact of pain research. Future research is necessary to improve the methodological quality and homogeneity of studies.

The results of the meta-analysis highlighted the efficacy of EOs in preclinical pain, but these data are downgraded due to the high heterogeneity of the studies. In particular, the analyzed EOs present the analgesic efficacy required by the recommendations of the Initiative on Methods, Measurement, and Pain Assessment in Clinical Trials (IMMPACT) (Turk et al., 2003), according to which a decrease in pain is defined as clinically meaningful if it accounts for a 30% to 36% reduction. However, this is referred to chronic pain and this systematic review and meta-analysis have found that only the EO of bergamot had proven efficacy both in nociceptive and in neuropathic pain models. Moreover, it was also studied for 14 days, an experimental setting suitable for modeling chronic pain (Hamamura et al., 2020).

Another important issue is that the consolidated data come from hypothesis-generating completely original preclinical studies and that they are then confirmed by hypothesis-driven studies (Mikolajewicz and Komarova, 2019). In this case, the EO of bergamot was confirmed to have strong analgesic properties in some of the most used and reliable models of inflammatory pain, i.e., formalin and capsaicin test in different experiments, sharing with most EO mechanisms involving opioid neurotransmission, and also in the PSNL. To the best of our knowledge, this is the first meta-analysis of preclinical studies on the analgesic effects of EOs and its working hypothesis was verified for bergamot EO, which could represent an important pharmacological tool for pain management in clinical settings. Along with clinical translations, more efforts are required to standardize *in vivo* preclinical studies in the field of pain research to allow for consistent research able to elucidate the mechanisms responsible for the analgesic properties of EOs.

DATA AVAILABILITY STATEMENT

The original contributions presented in the study are included in the article.

AUTHOR CONTRIBUTIONS

DS, GB, TS, SS, and MTC. conceived the study. All Authors participated in preparation and read and approved the final manuscript.

FUNDING

DS is a post-doc recipient of a research grant salary as part of the research project (Tutor: GB) "Pharmacoepidemiology of drugs used in the treatment of neuropsychiatric symptoms and pain in people aged (over 65) with dementia" funded by Calabria Region (POR Calabria FESR-FSE 2014/2020—Linea B) Azione 10.5.12.

REFERENCES

Abuhamdah, S., Huang, L., Elliott, M. S., Howes, M. J., Ballard, C., Holmes, C., et al. (2008). Pharmacological profile of an essential oil derived from Melissa officinalis with anti-agitation properties: focus on ligand-gated channels. *J. Pharm. Pharmacol.* 60 (3), 377–384. doi:10.1211/jpp.60.3.0014

Achterberg, W., Lautenbacher, S., Husebo, B., Erdal, A., and Herr, K. (2020). Pain in dementia. *Pain Rep.* 5, e803. doi:10.1097/PR9.0000000000000803

Adam, B., Liebregts, T., Best, J., Bechmann, L., Lackner, C., Neumann, J., et al. (2006). A combination of peppermint oil and caraway oil attenuates the post-inflammatory visceral hyperalgesia in a rat model. *Scand. J. Gastroenterol.* 41 (2), 155–160. doi:10.1080/00365520500206442

Ali, T., Javan, M., Sonboli, A., and Semnanian, S. (2012). Evaluation of the antinociceptive and anti-inflammatory effects of essential oil of Nepeta pogonosperma Jamzad et Assadi in rats. *Daru* 20, 48. doi:10.1186/2008-2231-20-48

Anaya-Eugenio, G. D., Rivero-Cruz, I., Bye, R., Linares, E., and Mata, R. (2016). Antinociceptive activity of the essential oil from *Artemisia* ludoviciana. *J. Ethnopharmacol* 179, 403–411. doi:10.1016/j.jep.2016.01.008

Andrade, G. S., Guimaraes, A. G., Santana, M. T., Siqueira, R. S., Passos, L. O., Machado, S. M. F., et al. (2012). Phytochemical screening, antinociceptive and anti-inflammatory effects of the essential oil of Myrcia pubiflora in mice. *Revista Brasileira De Farmacognosia* 22 (1), 181–188. doi:10.1590/s0102-695x2011005000205

Awad, R., Muhammad, A., Durst, T., Trudeau, V. L., and Arnason, J. T. (2009). Bioassay-guided fractionation of lemon balm (Melissa officinalis L.) using an *in vitro* measure of GABA transaminase activity. *Phytother Res.* 23 (8), 1075–1081. doi:10.1002/ptr.2712

Bae, A. H., Kim, G., Seol, G. H., Lee, S. B., Lee, J. M., Chang, W., et al. (2020). Delta- and mu-opioid pathways are involved in the analgesic effect of Ocimum basilicum L in mice. *J. Ethnopharmacol* 250, 112471. doi:10.1016/j.jep.2019.112471

Bagetta, G., Morrone, L. A., Rombolà, L., Amantea, D., Russo, R., Berliocchi, L., et al. (2010). Neuropharmacology of the essential oil of bergamot. *Fitoterapia* 81 (6), 453–461. doi:10.1016/j.fitote.2010.01.013

Ball, E. L., Owen-Booth, B., Gray, A., Shenkin, S. D., Hewitt, J., and McCleery, J. (2020). Aromatherapy for dementia. *Cochrane Database Syst. Rev.* 8, CD003150. doi:10.1002/14651858.CD003150.pub3

Belardo, C., Iannotta, M., Boccella, S., Rubino, R. C., Ricciardi, F., Infantino, R., et al. (2019). Oral cannabidiol prevents allodynia and neurological dysfunctions in a mouse model of mild traumatic brain injury. *Front. Pharmacol.* 10, 352. doi:10.3389/fphar.2019.00352

Boccella, S., Marabese, I., Guida, F., Luongo, L., Maione, S., and Palazzo, E. (2020). The modulation of pain by metabotropic glutamate receptors 7 and 8 in the dorsal striatum. *Curr. Neuropharmacol.* 18 (1), 34–50. doi:10.2174/1570159X17666190618121859

Chen, Y., Zhao, Y. Y., Wang, X. Y., Liu, J. T., Huang, L. Q., and Peng, C. S. (2011). [GC-MS analysis and analgesic activity of essential oil from fresh rhizoma of *Cyperus* rotundus]. *Zhong Yao Cai* 34 (8), 1225–1229.

Dastmalchi, K., Ollilainen, V., Lackman, P., Boije af Gennäs, G., Dorman, H. J., Järvinen, P. P., et al. (2009). Acetylcholinesterase inhibitory guided fractionation of Melissa officinalis L. *Bioorg. Med. Chem.* 17 (2), 867–871. doi:10.1016/j.bmc.2008.11.034

de Oliveira Júnior, R. G., Ferraz, C. A. A., Silva, J. C., de Oliveira, A. P., Diniz, T. C., E Silva, M. G., et al. (2017). Antinociceptive effect of the essential oil from *Croton* conduplicatus Kunth (euphorbiaceae). *Molecules* 22 (6), 900. doi:10.3390/molecules22060900

de Oliveira, R. G., Ferraz, C. A. A., Silva, J. C., Teles, R. B. D., Silva, M. G., Diniz, T. C., et al. (2018). Neuropharmacological effects of essential oil from the leaves of *Croton* conduplicatus Kunth and possible mechanisms of action involved. *J. Ethnopharmacology* 221, 65–76. doi:10.1016/j.jep.2018.04.009

DerSimonian, R., and Kacker, R. (2007). Random-effects model for meta-analysis of clinical trials: an update. *Contemp. Clin. Trials* 28 (2), 105–114. doi:10.1016/j.cct.2006.04.004

Do Nascimento Silva, A., Bomfim, H. F., Magalhães, A. O., Da Rocha, M. L., and Lucchese, A. M. (2018). Chemical composition and antinociceptive activity of essential oil from myrcia rostrata dc. (myrtaceae) in animal models. *Quimica Nova* 41 (9), 982–988. doi:10.21577/0100-4042.20170274

Duval, S., and Tweedie, R. (2000). Trim and fill: a simple funnel-plot-based method of testing and adjusting for publication bias in meta-analysis. *Biometrics* 56 (2), 455–463. doi:10.1111/j.0006-341x.2000.00455.x

Editorial. (2016). Meta-analysis in basic biology. *Nat. Methods* 13 (12), 959. doi:10.1038/nmeth.4102

Egger, M., Davey Smith, G., Schneider, M., and Minder, C. (1997). Bias in meta-analysis detected by a simple, graphical test. *BMJ* 315 (7109), 629–634. doi:10.1136/bmj.315.7109.629

Evans, L. K. (1987). Sundown syndrome in institutionalized elderly. *J. Am. Geriatr. Soc.* 35 (2), 101–108. doi:10.1111/j.1532-5415.1987.tb01337.x

Guginski, G., Luiz, A. P., Silva, M. D., Massaro, M., Martins, D. F., Chaves, J., et al. (2009). Mechanisms involved in the antinociception caused by ethanolic extract obtained from the leaves of Melissa officinalis (lemon balm) in mice. *Pharmacol. Biochem. Behav.* 93 (1), 10–16. doi:10.1016/j.pbb.2009.03.014

Guimaraes, A. G., Melo, M. S., Bonfim, R. R., Passos, L. O., Machado, S. M. F., Ribeiro, A. D., et al. (2009). Antinociceptive and anti-inflammatory effects of the essential oil of Eugenia candolleana DC., Myrtaceae, on mice. *Revista*

Brasileira De Farmacognosia 19 (4), 883–887. doi:10.1590/s0102-695x2009000600016

GVR (2020). Report No.: 978-1-68038-549-6. 1-153. Essential oils market size, share & trends analysis report by application (food & beverages, spa & relaxation), by product (orange, peppermint), by sales channel, and segment forecasts, 2020–2027.

Hajhashemi, V., Sajjadi, S. E., and Heshmati, M. (2009). Anti-inflammatory and analgesic properties of Heracleum persicum essential oil and hydroalcoholic extract in animal models. *J. Ethnopharmacol* 124 (3), 475–480. doi:10.1016/j.jep.2009.05.012

Halder, S., Mehta, A. K., Mediratta, P. K., and Sharma, K. K. (2012). Acute effect of essential oil of Eugenia caryophyllata on cognition and pain in mice. *Naunyn Schmiedebergs Arch. Pharmacol.* 385 (6), 587–593. doi:10.1007/s00210-012-0742-2

Hamamura, K., Katsuyama, S., Komatsu, T., Scuteri, D., Bagetta, G., Aritake, K., et al. (2020). Behavioral effects of continuously administered bergamot essential oil on mice with partial sciatic nerve ligation. *Front. Pharmacol.* 11, 1310. doi:10.3389/fphar.2020.01310

Hamm, R. J., and Knisely, J. S. (1985). Environmentally induced analgesia: an age-related decline in an endogenous opioid system. *J. Gerontol.* 40 (3), 268–274. doi:10.1093/geronj/40.3.268

Hayashi, T., Watanabe, C., Katsuyama, S., Agatsuma, Y., Scuteri, D., Bagetta, G., et al. (2020). Contribution of histamine to nociceptive behaviors induced by intrathecally administered cholecystokinin-8. *Front. Pharmacol.* 11, 590918. doi:10.3389/fphar.2020.590918

Higgins, J. P., and Thompson, S. G. (2002). Quantifying heterogeneity in a meta-analysis. *Stat. Med.* 21 (11), 1539–1558. doi:10.1002/sim.1186

Hooijmans, C. R., Rovers, M. M., de Vries, R. B., Leenaars, M., Ritskes-Hoitinga, M., and Langendam, M. W. (2014). SYRCLE's risk of bias tool for animal studies. *BMC Med. Res. Methodol.* 14 (1), 43. doi:10.1186/1471-2288-14-43

Husebo, B. S., Ballard, C., Sandvik, R., Nilsen, O. B., and Aarsland, D. (2011). Efficacy of treating pain to reduce behavioural disturbances in residents of nursing homes with dementia: cluster randomised clinical trial. *BMJ* 343, d4065. doi:10.1136/bmj.d4065

Jahandar, F., Asgarpanah, J., Najafizadeh, P., and Mousavi, Z. (2018). Anti-inflammatory activity and chemical composition of Pycnocycla bashagardiana fruit's essential oil in animal models. *Iran J. Basic Med. Sci.* 21 (2), 188–193. doi:10.22038/ijbms.2017.20860.5426

Jun, Y. S., Kang, P., Min, S. S., Lee, J. M., Kim, H. K., and Seol, G. H. (2013). Effect of eucalyptus oil inhalation on pain and inflammatory responses after total knee replacement: a randomized clinical trial. *Evid. Based Complement. Alternat Med.* 2013, 502727. doi:10.1155/2013/502727

Katsuyama, S., Otowa, A., Kamio, S., Sato, K., Yagi, T., Kishikawa, Y., et al. (2015). Effect of plantar subcutaneous administration of bergamot essential oil and linalool on formalin-induced nociceptive behavior in mice. *Biomed. Res.* 36 (1), 47–54. doi:10.2220/biomedres.36.47

Khalid, M. H., Akhtar, M. N., Mohamad, A. S., Perimal, E. K., Akira, A., Israf, D. A., et al. (2011). Antinociceptive effect of the essential oil of Zingiber zerumbet in mice: possible mechanisms. *J. Ethnopharmacol* 137 (1), 345–351. doi:10.1016/j.jep.2011.05.043

Khodabakhsh, P., Shafaroodi, H., and Asgarpanah, J. (2015). Analgesic and anti-inflammatory activities of Citrus aurantium L. blossoms essential oil (neroli): involvement of the nitric oxide/cyclic-guanosine monophosphate pathway. *J. Nat. Med.* 69 (3), 324–331. doi:10.1007/s11418-015-0896-6

Komatsu, T., Katsuyama, S., Uezono, Y., Sakurada, C., Tsuzuki, M., Hamamura, K., et al. (2018a). Possible involvement of the peripheral Mu-opioid system in antinociception induced by bergamot essential oil to allodynia after peripheral nerve injury. *Neurosci. Lett.* 686, 127–132. doi:10.1016/j.neulet.2018.08.053

Komatsu, T., Katsuyama, S., Uezono, Y., Sakurada, C., Tsuzuki, M., Hamamura, K., et al. (2018b). Possible involvement of the peripheral Mu-opioid system in antinociception induced by bergamot essential oil to allodynia after peripheral nerve injury. *Neurosci. Lett.* 686, 127–132. doi:10.1016/j.neulet.2018.08.053

Koyama, S., and Heinbockel, T. (2020). The effects of essential oils and terpenes in relation to their routes of intake and application. *Int. J. Mol. Sci.* 21 (5), 1558. doi:10.3390/ijms21051558

Kusunose, N., Koyanagi, S., Hamamura, K., Matsunaga, N., Yoshida, M., Uchida, T., et al. (2010). Molecular basis for the dosing time-dependency of anti-allodynic effects of gabapentin in a mouse model of neuropathic pain. *Mol. Pain* 6, 83. doi:10.1186/1744-8069-6-83

Kuwahata, H., Komatsu, T., Katsuyama, S., Corasaniti, M. T., Bagetta, G., Sakurada, S., et al. (2013). Peripherally injected linalool and bergamot essential oil attenuate mechanical allodynia via inhibiting spinal ERK phosphorylation. *Pharmacol. Biochem. Behav.* 103 (4), 735–741. doi:10.1016/j.pbb.2012.11.003

Lakhan, S. E., Sheafer, H., and Tepper, D. (2016). The effectiveness of aromatherapy in reducing pain: a systematic review and meta-analysis. *Pain Res. Treat.* 2016, 8158693. doi:10.1155/2016/8158693

Lee, G., Park, J., Kim, M. S., Seol, G. H., and Min, S. S. (2019). Analgesic effects of eucalyptus essential oil in mice. *Korean J. Pain* 32 (2), 79–86. doi:10.3344/kjp.2019.32.2.79

Li, F. S., and Weng, J. K. (2017). Demystifying traditional herbal medicine with modern approach. *Nat. Plants* 3 (8), 17109. doi:10.1038/nplants.2017.109

Li, W., Chen, Y., Wang, X., and Qu, S. (1991). [Pharmacological studies on the volatile oil isolated from the leaves of Pinus pumila (Pall.) Regel]. *Zhongguo Zhong Yao Za Zhi* 16 (3), 172–192.

Liberati, A., Altman, D. G., Tetzlaff, J., Mulrow, C., Gøtzsche, P. C., Ioannidis, J. P., et al. (2009). The PRISMA statement for reporting systematic reviews and meta-analyses of studies that evaluate health care interventions: explanation and elaboration. *PLos Med.* 6, e1000100. doi:10.1371/journal.pmed.1000100

Lima, G. M., Quintans-Júnior, L. J., Thomazzi, S. M., Almeida, E. M. S. A., Melo, M. S., Serafini, M. R., et al. (2012). Phytochemical screening, antinociceptive and anti-inflammatory activities of Chrysopogon zizanioides essential oil. *Braz. J. Pharmacognosy* 22 (2), 443–450. doi:10.1590/S0102-695X2012005000002

Linciano, P., Citti, C., Russo, F., Tolomeo, F., Laganà, A., Capriotti, A. L., et al. (2020). Identification of a new cannabidiol n-hexyl homolog in a medicinal cannabis variety with an antinociceptive activity in mice: cannabidihexol. *Sci. Rep.* 10 (1), 22019. doi:10.1038/s41598-020-79042-2

Lizarraga-Valderrama, L. R. (2020). Effects of essential oils on central nervous system: focus on mental health. *Phytother Res.* [Epub ahead of print]. doi:10.1002/ptr.6854

López, V., Nielsen, B., Solas, M., Ramírez, M. J., and Jäger, A. K. (2017). Exploring pharmacological mechanisms of lavender (lavandula angustifolia) essential oil on central nervous system targets. *Front. Pharmacol.* 8, 280. doi:10.3389/fphar.2017.00280

Macleod, M. R., O'Collins, T., Howells, D. W., and Donnan, G. A. (2004). Pooling of animal experimental data reveals influence of study design and publication bias. *Stroke* 35 (5), 1203–1208. doi:10.1161/01.STR.0000125719.25853.20

Mikolajewicz, N., and Komarova, S. V. (2019). Meta-analytic methodology for basic research: a practical guide. *Front. Physiol.* 10, 203. doi:10.3389/fphys.2019.00203

Miraghazadeh, S. G., Shafaroodi, H., and Asgarpanah, J. (2015). Analgesic and antiinflammatory activities of the essential oil of the unique plant Zhumeria majdae. *Nat. Prod. Commun.* 10 (4), 669–672. doi:10.1590/s2175-97902019000217011

Mishra, D., Bisht, G., Mazumdar, P. M., and Sah, S. P. (2010). Chemical composition and analgesic activity of *Senecio* rufinervis essential oil. *Pharm. Biol.* 48 (11), 1297–1301. doi:10.3109/13880209.2010.491083

Moher, D., Liberati, A., Tetzlaff, J., Altman, D. G., and Group, P. (2009). Preferred reporting items for systematic reviews and meta-analyses: the PRISMA statement. *PLos Med.* 6, e1000097. doi:10.1371/journal.pmed.1000097

Morrone, L. A., Rombolà, L., Pelle, C., Corasaniti, M. T., Zappettini, S., Paudice, P., et al. (2007). The essential oil of bergamot enhances the levels of amino acid neurotransmitters in the hippocampus of rat: implication of monoterpene hydrocarbons. *Pharmacol. Res.* 55 (4), 255–262. doi:10.1016/j.phrs.2006.11.010

Morrone, L. A., Scuteri, D., Rombolà, L., Mizoguchi, H., and Bagetta, G. (2017). Opioids resistance in chronic pain management. *Curr. Neuropharmacol* 15 (3), 444–456. doi:10.2174/1570159X14666161101092822

Neves, I. A., Rezende, S. R. F., Kirk, J. M., Pontes, E. G., de Carvalho, M., and Gamble, A. (2017). Composition and larvicidal activity of essential oil of Eugenia candolleana DC. (MYRTACEAE) against *Aedes aegypti*. *Rev. Virtual Quim.* 9 (6), 2305–2315. doi:10.21577/1984-6835.20170138

Nogueira, Lde. M., Da Silva, M. R., Dos Santos, S. M., De Albuquerque, J. F., Ferraz, I. C., de Albuquerque, T. T., et al. (2015). Antinociceptive effect of the essential oil obtained from the leaves of croton cordiifolius baill. (Euphorbiaceae) in mice. *Evid. Based Complement. Alternat Med.* 2015, 620865. doi:10.1155/2015/620865

Park, Y., Jung, S. M., Yoo, S. A., Kim, W. U., Cho, C. S., Park, B. J., et al. (2015). Antinociceptive and anti-inflammatory effects of essential oil extracted from Chamaecyparis obtusa in mice. *Int. Immunopharmacol* 29 (2), 320–325. doi:10.1016/j.intimp.2015.10.034

Perry, N. S., Houghton, P. J., Theobald, A., Jenner, P., and Perry, E. K. (2000). *In-vitro* inhibition of human erythrocyte acetylcholinesterase by salvia lavandulaefolia essential oil and constituent terpenes. *J. Pharm. Pharmacol.* 52 (7), 895–902. doi:10.1211/0022357001774598

Queiroz, J. C., Antoniolli, A. R., Quintans-Júnior, L. J., Brito, R. G., Barreto, R. S., Costa, E. V., et al. (2014). Evaluation of the anti-inflammatory and antinociceptive effects of the essential oil from leaves of xylopia laevigata in experimental models. *Sci. World J.* 2014, 816450. doi:10.1155/2014/816450

Quintans, J. S., Alves, R. D., Santos, D. A., Serafini, M. R., Alves, P. B., Costa, E. V., et al. (2017). Antinociceptive effect of Aristolochia trilobata stem essential oil and 6-methyl-5-hepten-2yl acetate, its main compound, in rodents. *Z. Naturforsch C J. Biosci.* 72 (3-4), 93–97. doi:10.1515/znc-2016-0053

Quintans, J. S., Antoniolli, A. R., Almeida, J. R., Santana-Filho, V. J., and Quintans-Júnior, L. J. (2014). Natural products evaluated in neuropathic pain models - a systematic review. *Basic Clin. Pharmacol. Toxicol.* 114 (6), 442–450. doi:10.1111/bcpt.12178

Ribeiro, S. (2018). "Whole organisms or pure compounds? Entourage effect versus drug specificity," in *Plant medicines, healing and psychedelic science*. Editors B. Labate and C. Cavnar (Cham: Springer).

Rice, A. S. C., Morland, R., Huang, W., Currie, G. L., Sena, E. S., and Macleod, M. R. (2013). Transparency in the reporting of *in vivo* pre-clinical pain research: the relevance and implications of the ARRIVE (Animal Research: reporting in Vivo Experiments) guidelines. *Scand. J. Pain* 4 (2), 58–62. doi:10.1016/j.sjpain.2013.02.002

Rombolà, L., Tridico, L., Scuteri, D., Sakurada, T., Sakurada, S., Mizoguchi, H., et al. (2017). Bergamot essential oil attenuates anxiety-like behaviour in rats. *Molecules* 22 (4), 614. doi:10.3390/molecules22040614

Rombolà, L., Scuteri, D., Adornetto, A., Straface, M., Sakurada, T., Sakurada, S., et al. (2019). Anxiolytic-like effects of bergamot essential oil are insensitive to flumazenil in rats. *Evid. Based Complement. Alternat Med.* 2019**,** 2156873. doi:10.1155/2019/2156873

Rombolà, L., Scuteri, D., Watanabe, C., Sakurada, S., Hamamura, K., Sakurada, T., et al. (2020). Role of 5-HT1A receptor in the anxiolytic-relaxant effects of bergamot essential oil in rodent. *Int. J. Mol. Sci.* 21 (7), 2597. doi:10.3390/ijms21072597

Ryan, R. (2019). Cochrane Consumers and Communication Review Group: data synthesis and analysis. Available at: http://cccrg.cochrane.org (Accessed March 13, 2019).

Sakurada, T., Mizoguchi, H., Kuwahata, H., Katsuyama, S., Komatsu, T., Morrone, L. A., et al. (2011). Intraplantar injection of bergamot essential oil induces peripheral antinociception mediated by opioid mechanism. *Pharmacol. Biochem. Behav.* 97 (3), 436–443. doi:10.1016/j.pbb.2010.09.020

Sarmento-Neto, J. F., do Nascimento, L. G., Felipe, C. F., and de Sousa, D. P. (2015). Analgesic potential of essential oils. *Molecules* 21 (1), E20. doi:10.3390/molecules21010020

Savelev, S., Okello, E., Perry, N. S., Wilkins, R. M., and Perry, E. K. (2003). Synergistic and antagonistic interactions of anticholinesterase terpenoids in Salvia lavandulaefolia essential oil. *Pharmacol. Biochem. Behav.* 75 (3), 661–668. doi:10.1016/s0091-3057(03)00125-4

Savelev, S. U., Okello, E. J., and Perry, E. K. (2004). Butyryl- and acetylcholinesterase inhibitory activities in essential oils of Salvia species and their constituents. *Phytother Res.* 18 (4), 315–324. doi:10.1002/ptr.1451

Scherder, E. J., Sergeant, J. A., and Swaab, D. F. (2003). Pain processing in dementia and its relation to neuropathology. *Lancet Neurol.* 2 (11), 677–686. doi:10.1016/s1474-4422(03)00556-8

Scuteri, D., Morrone, L. A., Rombolà, L., Avato, P. R., Bilia, A. R., Corasaniti, M. T., et al. (2017a). Aromatherapy and aromatic plants for the treatment of behavioural and psychological symptoms of dementia in patients with alzheimer's disease: clinical evidence and possible mechanisms. *Evid. Based Complement. Alternat Med.* 2017, 9416305. doi:10.1155/2017/9416305

Scuteri, D., Piro, B., Morrone, L. A., Corasaniti, M. T., Vulnera, M., and Bagetta, G. (2017b). The need for better access to pain treatment: learning from drug consumption trends in the USA. *Funct. Neurol.* 22 (4), 229–230. doi:10.11138/fneur/2017.32.4.229

Scuteri, D., Crudo, M., Rombolà, L., Watanabe, C., Mizoguchi, H., Sakurada, S., et al. (2018a). Antinociceptive effect of inhalation of the essential oil of bergamot in mice. *Fitoterapia* 129, 20–24. doi:10.1016/j.fitote.2018.06.007

Scuteri, D., Garreffa, M. R., Esposito, S., Bagetta, G., Naturale, M. D., and Corasaniti, M. T. (2018b). Evidence for accuracy of pain assessment and painkillers utilization in neuropsychiatric symptoms of dementia in Calabria region, Italy. *Neural Regen. Res.* 13 (9), 1619–1621. doi:10.4103/1673-5374.237125

Scuteri, D., Rombolà, L., Morrone, L. A., Bagetta, G., Sakurada, S., Sakurada, T., et al. (2019a). Neuropharmacology of the neuropsychiatric symptoms of dementia and role of pain: essential oil of bergamot as a novel therapeutic approach. *Int. J. Mol. Sci.* 20 (13), 3327. doi:10.3390/ijms20133327

Scuteri, D., Rombolá, L., Tridico, L., Mizoguchi, H., Watanabe, C., Sakurada, T., et al. (2019b). Neuropharmacological properties of the essential oil of bergamot for the clinical management of pain-related BPSDs. *Curr. Med. Chem.* 26 (20), 3764–3774. doi:10.2174/0929867325666180307115546

Scuteri, D., Berliocchi, L., Rombolà, L., Morrone, L. A., Tonin, P., Bagetta, G., et al. (2020a). Effects of aging on formalin-induced pain behavior and analgesic activity of gabapentin in C57BL/6 mice. *Front. Pharmacol.* 11, 663. doi:10.3389/fphar.2020.00663

Scuteri, D., Mantovani, E., Tamburin, S., Sandrini, G., Corasaniti, M. T., Bagetta, G., et al. (2020b). Opioids in post-stroke pain: a systematic review and meta-analysis. *Front. Pharmacol.* [Epub ahead of print]. doi:10.3389/fphar.2020.587050

Scuteri, D., Matamala-Gomez, M., Bottiroli, S., Corasaniti, M. T., De Icco, R., Bagetta, G., et al. (2020c). Pain assessment and treatment in dementia at the time of coronavirus disease COVID-19. *Front. Neurol.* 11, 890. doi:10.3389/fneur.2020.00890

Scuteri, D., Rombolà, L., Morrone, L. A., Monteleone, D., Corasaniti, M. T., Sakurada, T., et al. (2020d). "Exploitation of aromatherapy in dementia-impact on pain and neuropsychiatric symptoms," in *The neuroscience of dementia: diagnosis and management in dementia*. Editors V. R. Preedy and C. R. Martin (San Diego: Academic Press), 713–726.

Scuteri, D., Rombolà, L., Watanabe, C., Sakurada, S., Corasaniti, M. T., Bagetta, G., et al. (2020e). Impact of nutraceuticals on glaucoma: a systematic review. *Prog. Brain Res.* 257, 141–154. doi:10.1016/bs.pbr.2020.07.014

Scuteri, D., Vulnera, M., Piro, B., Bossio, R. B., Morrone, L. A., Sandrini, G., et al. (2020f). Pattern of treatment of behavioural and psychological symptoms of dementia and pain: evidence on pharmacoutilization from a large real-world sample and from a centre for cognitive disturbances and dementia. *Eur. J. Clin. Pharmacol.* [Epub ahead of print]. doi:10.1007/s00228-020-02995-w

Sharif, M., Najafizadeh, P., Asgarpanah, J., and Mousavi, Z. (2020). *In vivo* analgesic and anti-inflammatory effects of the essential oil from Tanacetum balsamita L. *Braz. J. Pharm. Sci.* 56, e18357. doi:10.1590/s2175-97902019000418357

Sofi, P. A., Zeerak, N. A., and Singh, P. (2009). Kala zeera (Bunium persicum Bioss.): a Kashmirian high value crop. *Turkish J. Biol.* 33, 249–258. doi:10.3906/biy-0803-18

Stein, C., Hopfeld, J., Lau, H., and Klein, J. (2015). Effects of ginkgo biloba extract EGb 761, donepezil and their combination on central cholinergic function in aged rats. *J. Pharm. Pharm. Sci.* 18 (4), 634–646. doi:10.18433/j3wc8v

Sterne, J. A., and Egger, M. (2001). Funnel plots for detecting bias in meta-analysis: guidelines on choice of axis. *J. Clin. Epidemiol.* 54 (10), 1046–1055. doi:10.1016/s0895-4356(01)00377-8

Sterne, J. A. C., Savović, J., Page, M. J., Elbers, R. G., Blencowe, N. S., Boutron, I., et al. (2019). RoB 2: a revised tool for assessing risk of bias in randomised trials. *BMJ* 366, l4898. doi:10.1136/bmj.l4898

Sulaiman, M. R., Tengku Mohamad, T. A., Shaik Mossadeq, W. M., Moin, S., Yusof, M., Mokhtar, A. F., et al. (2010). Antinociceptive activity of the essential oil of Zingiber zerumbet. *Planta Med.* 76 (2), 107–112. doi:10.1055/s-0029-1185950

Suokas, A. K., Sagar, D. R., Mapp, P. I., Chapman, V., and Walsh, D. A. (2014). Design, study quality and evidence of analgesic efficacy in studies of drugs in models of OA pain: a systematic review and a meta-analysis. *Osteoarthr Cartil* 22 (9), 1207–1223. doi:10.1016/j.joca.2014.06.015

Todorova, M., Trendafilova, A., Ivanova, V., Danova, K., and Dimitrov, D. (2017). Essential oil composition of Inula britannica L. from Bulgaria. *Nat. Prod. Res.* 31 (14), 1693–1696. doi:10.1080/14786419.2017.1285295

Turk, D. C., Dworkin, R. H., Allen, R. R., Bellamy, N., Brandenburg, N., Carr, D. B., et al. (2003). Core outcome domains for chronic pain clinical trials: IMMPACT recommendations. *Pain* 106 (3), 337–345. doi:10.1016/j.pain.2003.08.001

Ulku Karabay-Yavasoglu, N., Baykan, S., Ozturk, B., Apaydin, S., and Tuglular, I. (2006). Evaluation of the antinociceptive and anti-inflammatory activities of Satureja thymbra. L. Essential oil. *Pharm. Biol.* 44 (8), 585–591. doi:10.1080/13880200600896827

Venâncio, A. M., Marchioro, M., Estavam, C. S., Melo, M. S., Santana, M. T., Onofre, A. S. C., et al. (2011). Ocimum basilicum leaf essential oil and (-)-linalool reduce orofacial nociception in rodents: a behavioral and electrophysiological approach. *Braz. J. Pharmacognosy* 21 (6), 1043–1051. doi:10.1590/S0102-695X2011005000147

Wood, H. C., and Reichut, E. T. (1880). Note on the action upon the circulation of certain volatile oils. *J. Physiol.* 2, 446. doi:10.1113/jphysiol.1880.sp000073

Ximenes, R. M., De Morais Nogueira, L., Cassundé, N. M., Jorge, R. J., Dos Santos, S. M., Magalhães, L. P., et al. (2013). Antinociceptive and wound healing activities of *Croton* adamantinus Müll. Arg. essential oil. *J. Nat. Med.* 67 (4), 758–764. doi:10.1007/s11418-012-0740-1

Zarei, M., Mohammadi, S., and Komaki, A. (2018). Antinociceptive activity of Inula britannica L. and patuletin: in vivo and possible mechanisms studies. *J. Ethnopharmacol* 219, 351–358. doi:10.1016/j.jep.2018.03.021

Zaynoun, S. T., Johnson, B. E., and Frain-Bell, W. (1977). A study of oil of bergamot and its importance as a phototoxic agent. I. Characterization and quantification of the photoactive component. *Br. J. Dermatol.* 96 (5), 475–482. doi:10.1111/j.1365-2133.1977.tb07149.x

Zendehdel, M., Torabi, Z., and Hassanpour, S. (2015). Antinociceptive mechanisms of Bunium persicum essential oil in the mouse writhing test: role of opioidergic and histaminergic systems. *Veterinarni Medicina* 60 (2), 63–70. doi:10.17221/7988-VETMED

Zhang, L., Li, D., Cao, F., Xiao, W., Zhao, L., Ding, G., et al. (2018). Identification of human acetylcholinesterase inhibitors from the constituents of EGb761 by modeling docking and molecular dynamics simulations. *Comb. Chem. High Throughput Screen.* 21 (1), 41–49. doi:10.2174/1386207320666171123201910

Conflict of Interest: The authors declare that the research was conducted in the absence of any commercial or financial relationships that could be construed as a potential conflict of interest.

frontiers in Pharmacology

ORIGINAL RESEARCH
published: 28 April 2021
doi: 10.3389/fphar.2021.643605

Sodium Monoiodoacetate Dose-Dependent Changes in Matrix Metalloproteinases and Inflammatory Components as Prognostic Factors for the Progression of Osteoarthritis

*Marta Bryk‡, Jakub Chwastek‡, Jakub Mlost, Magdalena Kostrzewa† and Katarzyna Starowicz**

Department of Neurochemistry, Maj Institute of Pharmacology, Polish Academy of Sciences, Cracow, Poland

OPEN ACCESS

Edited by:
Serena Boccella, University of Campania Luigi Vanvitelli, Italy

Reviewed by:
Cristina Tecchio, University of Verona, Italy
Claudia Cristiano, University of Naples Federico II, Italy

***Correspondence:**
Katarzyna Starowicz
starow@if-pan.krakow.pl

†Magdalena Kostrzewa, Endocannabinoid Research Group, Institute of Biomolecular Chemistry, National Research Council of Italy, Napoli, Italy
‡These authors have contributed equally to this work

Specialty section:
This article was submitted to Inflammation Pharmacology, a section of the journal Frontiers in Pharmacology

Received: *18 December 2020*
Accepted: *01 March 2021*
Published: *28 April 2021*

Citation:
Bryk M, Chwastek J, Mlost J, Kostrzewa M and Starowicz K (2021) Sodium Monoiodoacetate Dose-Dependent Changes in Matrix Metalloproteinases and Inflammatory Components as Prognostic Factors for the Progression of Osteoarthritis. Front. Pharmacol. 12:643605. doi: 10.3389/fphar.2021.643605

Osteoarthritis (OA) is a degenerative joint disease that primarily affects people over 65 years old. During OA progression irreversible cartilage, synovial membrane and subchondral bone degradation is observed, which results in the development of difficult-to-treat chronic pain. One of the most important factors in OA progression is joint inflammation. Both proinflammatory and anti-inflammatory factors, as well as extracellular matrix degradation enzymes (matrix metalloproteinases (MMPs), play an important role in disease development. One of the most widely used animal OA models involves an intra-articular injection of sodium monoiodoacetate (MIA) directly into the joint capsule, which results in glycolysis inhibition in chondrocytes and cartilage degeneration. This model mimics the degenerative changes observed in OA patients. However, the dose of MIA varies in the literature, ranging from 0.5 to 4.8 mg. The aim of our study was to characterize grading changes after injection of 1, 2 or 3 mg of MIA at the behavioral and molecular levels over a 28-day period. In the behavioral studies, MIA injection at all doses resulted in a gradual increase in tactile allodynia and resulted in abnormal weight bearing during free walking sequences. At several days post-OA induction, cartilage, synovial membrane and synovial fluid samples were collected, and qPCR and Western blot analyses were performed. We observed significant dose- and time-dependent changes in both gene expression and protein secretion levels. Inflammatory factors (CCL2, CXCL1, IL-1β, COMP) increased at the beginning of the experiment, indicating a transient inflammatory state connected to the MIA injection and, in more severe OA, also in the advanced stages of the disease. Overall, the results in the 1 mg MIA group were not consistently clear, indicating that the lowest tested dose may not be sufficient to induce long-lasting OA-like changes at the molecular level. In the 2 mg MIA group, significant alterations in the measured factors were observed. In the 3 mg MIA group, MMP-2, MMP-3, MMP-9, and MMP-13 levels showed very strong upregulation, which may cause overly strong reactions in animals. Therefore, a dose of 2 mg appears optimal, as it induces significant but not excessive OA-like changes in a rat model.

Keywords: osteoarthritis, chronic pain, matrix metalloproteinases, cartilage, synovial membrane, synovial fluid, inflammation, pain

INTRODUCTION

Knee osteoarthritis (OA) is one of the leading causes of global chronic disability. A disease that affects joint tissues, including cartilage, subchondral bone, ligaments, and muscles, OA manifests with chronic pain, joint stiffness/tenderness, loss of flexibility, and cracking sounds while moving. In the United States in 2016, 14 million people suffered from symptomatic knee OA. More than half of all patients were <65 years old (Deshpande et al., 2016). Risk factors favoring disease development include age, obesity, joint injuries, abnormal joint loading (e.g., excessive sports), gender (women are more likely to develop foot, hip and knee OA than men) and genetic factors (Vina and Kent Kwoh, 2018). Recently, the Osteoarthritis Research Society International (OARSI) revised the OA definition, adding an inflammatory component as a crucial factor contributing to disease development. An important process reported in OA progression is synovitis, during which a number of inflammatory changes occur in the synovial membrane. This contributes to local inflammation, which leads to further cartilage degeneration and inflammatory factor influx (Mathiessen and Conaghan, 2017).

Several of the most important factors are cytokines, both proinflammatory, e.g., interleukin 1 β (IL-1β), tumor necrosis factor α (TNFα), IL-6, IL-15, IL-17, and IL-18, and anti-inflammatory, such as IL-4, IL-10, and IL-13 (Wojdasiewicz et al., 2014). Importantly, a low-grade inflammatory state is present in OA from the very early stages, long before external symptoms can be detected by patients (Scanzello, 2017), and contributes to pain sensitization. Knee synovitis can also be used as an OA diagnostic tool (Berlinberg et al., 2019). Moreover, inflammation involves activation of enzymes involved in articular extracellular matrix (ECM) degradation – the matrix metalloproteinases (MMPs), e.g., MMP-2, MMP-3, MMP-9, MMP-13. These enzymes are members of a large family of zinc-dependent proteolytic enzymes. They are involved in shaping collagen, proteoglycan aggrecan, and non-collagen matrix components in joint degradation (Mehana et al., 2019). MMPs belong to one of three groups. MMP-2 and MMP-9 are gelatinases that digest denatured collagens and gelatins. MMP-2 (but not MMP-9) digests type I, II, and III collagens. MMP-2 in humans is important for osteogenesis, as mutations in human MMP-2 result in an autosomal recessive form of multicentric osteolysis (Martignetti et al., 2001). Both MMP-2 and MMP-9 are involved in inflammatory processes (Hannocks et al., 2019). MMP-3, also called Stromelysin 1, is responsible for digesting ECM components and activates a number of proMMPs (e.g., proMMP-1). MMP-13 is a collagenase that cleaves interstitial collagens type I, II, and III at a specific site three-quarters of the way from the N-terminus and digests both ECM and non-ECM components (Visse and Nagase, 2003).

Unfortunately, current OA therapeutics are limited to reducing pain and relieving bothersome symptoms only. A greater understanding of the mechanisms underlying the disease is necessary for creating more effective therapies. An important strategy for OA investigation is the creation of more representative animal models. Among several animal OA models, the sodium monoiodoacetate (MIA) intra-articular (i.a.) injection model is widely used for pain research and efficacy evaluation of therapeutic interventions (Lampropoulou-Adamidou et al., 2014). This chemical model mimics changes observed in patients very well. Malek et al. described changes in knee sensitivity and knee morphometric analysis in response to 3 mg of MIA i.a. injection up to 28 days post-injection (Malek et al., 2015). Knee changes 28 days post-MIA injection were irreversible and closely reflected changes in severe, advanced OA stages in human patients. In turn, Pajak et al. demonstrated biphasic pain progression in both behavioral and biochemical tests. An initial pain threshold lowering was associated with an inflammatory reaction caused by i.a. injection. Nevertheless, after 14 days, a stable, lasting reduction in pain threshold was observed (Pajak et al., 2017). The dose of MIA used to induce OA in rats varies in the literature from 0.5 to 4.8 mg; however, 1 or 3 mg is the most commonly used dose (Havelin et al., 2016; Allen et al., 2017; Haywood et al., 2018; Lee et al., 2018; Lockwood et al., 2019; Que et al., 2019; Piao et al., 2020). This could result in either peripheral mechanisms of joint damage in OA development and/or centrally mediated mechanisms, both of which may be important for future disease-modifying drug design. Therefore, the aim of our study was to assess the complete characteristics of grading MIA-induced OA (1, 2 or 3 mg of MIA i.a.) in a rat model at both the behavioral and molecular levels over a 28-day period. The role of inflammatory components and ECM MMPs in a rat joint model with progressive OA severity was investigated. Differences elicited by selected MIA doses were noted; our research allowed us to identify the smallest dose needed to effectively induce OA in a rat model. Overall, the obtained data allow for detailed description of changes occurring in joint tissues (synovial membrane, cartilage and synovial fluid) during disease progression, which provides a superior understanding of OA pathology and mechanisms.

MATERIALS AND METHODS

Animals

In all experiments, male Wistar rats initially weighing 225–250 g were used (Charles River, Hamburg, Germany). Animals were housed 5 per cage in a 12/12 h light/dark cycle with food and water *ad libitum*. Behavioral experiments were performed between 9:00 and 12:00 am. Experiments were approved by the Local Bioethics Committee of the Maj Institute of Pharmacology (Cracow, Poland), approval numbers: 938/2012, 125/2018. Separate sets of animals were used for behavioral and biochemical studies. Depending on the experimental group, on days 2, 7, 21 or 28 of the experiment, animals were sacrificed, and joint tissue samples (cartilage, synovial membrane, synovial fluid) were collected. Healthy animals (examined via biochemical analysis) were sacrificed on various days (1 or 2 animals in each experimental day) to minimize the differences associated with the duration of the experiment. No differences in biochemical analysis were observed in the healthy group. In behavioral tests, animals were tested prior to MIA injection (day 0); to apply the 3R principle of animal testing, we

determined that no healthy group was necessary. Moreover, according to the 3R principle and based on our previous behavioral research were 1 mg (Mlost et al., 2018b; Mugnaini et al., 2020; Mlost et al., 2021) or 3 mg of MIA (Malek et al., 2015; Pajak et al., 2017; Mlost et al., 2018a; Bryk et al., 2020) were successfully used, we decided to examine only 1 and 3 mg MIA doses in behavioral tests to minimize the number of animals exposed to painful procedures.

Induction of OA

Animals were briefly anesthetized with 5% isoflurane (Aerrane, Baxter, United States) in 100% oxygen (3.5 L/min). The rear right knee skin surface was shaved and swabbed with 75% ethanol. Joint damage was induced by a single i.a. injection of 1, 2 or 3 mg of MIA (Sigma-Aldrich, Saint Louis, United States) dissolved in 50 µl of 0.9% physiological saline via a 30 G × 1/2" needle. All surgical procedures were performed under sterile conditions. After OA induction, animals were moved back into their home cages and observed until full recovery from anesthesia. Healthy animals did not undergo any injection. After i.a. injection, rats were maintained under the same conditions as the preoperative period. Changes in kinetic weight bearing (evaluated in the kinetic weight bearing test; KWB) and mechanical withdrawal thresholds (evaluated in von Frey's test) were recorded prior to i.a. injection (day 0) and 2, 7, 14, 21 and 28 days post-injection. Experimental groups consisted of n = 5–8 animals (for KWB test), n = 8 animals (for Von Frey test) and n = 5–6 animals for biochemical studies. In rare cases, individual samples had to be excluded from the analysis due to abnormalities during isolation or sample contamination, and groups were indicated by an appropriate n number.

Von Frey Test

For the assessment of mechanical allodynia, calibrated von Frey monofilaments (Bioseb, France) were used. Rats were placed in Plexiglas cages with a wire net floor 5 min before the experiment. Von Frey filaments were applied to the mid plantar surface of the ipsilateral hind paw according to the up and down method (Chaplan et al., 1994; Deuis et al., 2017). Each filament was applied three times for an approximately 2–3 s period or until a withdrawal response was evoked. After response, the paw was retested with monofilaments in descending order until no response occurred, at which point monofilaments were again applied in ascending order until the response could once again be evoked. The monofilament that evoked the final reflex was noted as the paw withdrawal latency. The strength of the von Frey monofilament bending forces was as follows: 0.4; 0.6; 1.0; 1.4; 2; 4; 6; 8; 10; 15 and 26 g as a cut-off for response.

Kinetic Weight Bearing

To characterize pain behavior in the MIA model, KWB, a novel instrument developed by Bioseb (France), was used. Sensors placed on the ground measure the weight borne by each individual paw during the walking sequence of a freely moving animal, while a built-in camera detects the center of gravity of the animal. Data collection was terminated when 5 validated runs were obtained, or after 6 min of acquisition. If the animal did not run during this time window, the measurement was repeated at the end of the session. Those who failed to make at least one validated run during the second session were excluded from the analysis (one animal in 3 mg of MIA group in day 7 and 28). Rats were trained to move through the test corridor (50 × 130 cm) for a week before the actual experiment. Measurements were made directly before MIA administration and 2, 7, 21 and 28 days post-MIA treatment. All recorded data were validated by an observer blinded to the study. The final results include information about the mean peak force and surface area applied by each rear paw. The presented results discuss only the most relevant parameters in the context of OA research: peak force (centinewton, cN) – the mean of the maximum forces of each rear paw and peak surface (cm^2) – the mean of the maximum surface of each rear paw.

RNA and Protein Isolation

Cartilage from the medial femoral condyle and synovial membrane fragments were collected with surgical scissors. After tissue collection, each sample was placed in RNA-later solution (Invitrogen, United States) and stored at −80°C. RNA and protein from the synovial membrane were isolated using TRIzol Reagent (Invitrogen, United States) according to the manufacturer's protocol. Extraction of high-quality RNA from cartilage was performed according to a protocol published by Le Bleu et al. (2017). Synovial fluid was collected by rinsing the joint capsule with 50 µl of physiological saline and aspiring the fluid with a syringe with a 25 G × 5/8" needle. Then, synovial fluid was immediately placed on ice and frozen at −80 °C. Equal volumes of samples were lyzed with 2% SDS and centrifuged at 12,000 × g. The supernatant was collected for immunoblotting.

Total RNA levels were measured with a Nanodrop spectrophotometer (ND-1000, Nanodrop; Labtech International, United Kingdom). Each sample was equalized to a concentration of 1 µg/µl and reverse transcribed to cDNA using an NG dART RT kit (EURx, Poland) according to the manufacturer's protocol. qPCR reactions were carried out using iTaq Universal Probes Supermix (Bio-Rad, United States) and TaqMan Assays (Thermo Fisher, Applied Biosystems, United States) in a Thermal Cycler CFX96 (Bio-Rad, United States). Cycle threshold values were calculated automatically via CFX Manager software. RNA abundance was calculated as ddCT $2^{-(\text{threshold cycle})}$ and *B2m* normalized. The TaqMan assay protocols used in the study are presented in the **Supplementary Material**.

Western Blot

The protein levels in the cartilage and synovial samples were estimated via BCA kit (Thermo-Fischer, United States), and equal amounts of proteins were denatured in 4 × Laemmli sample buffer (Bio-Rad, United States) and denatured at 96°C for 6 min. Equal volumes of synovial fluid samples were lyzed with 2% SDS and denatured with Laemmli buffer, such as cartilage and synovial samples. An equal amount of protein from the various experimental groups was separated on Criterion TGX 4–20% precast gels (Bio-Rad, United States) and transferred onto a PVDF membrane (Roche, Switzerland). After blocking with blocking reagent from the BM Chemiluminescence Western Blotting Kit (Roche, Switzerland), membranes were incubated

overnight with primary antibodies (detailed information in the **Supplementary Material**) using a SignalBoost Immunoreaction Enhancer Kit (Merc, Germany). The amount of β-actin was measured on the same membrane on which the other proteins were measured by mild stripping (using a protocol published by Abcam). In control samples of synovial fluid concentration of proteins was very low, so this tissue was normalized to volume and detection of reference proteins was not possible.

Statistical Analysis

Statistical analysis was performed using Statistica 13 (SatSoft Software, Tulsa, Oklahoma, Unitd States), and graphs were generated using Prism 8 (GraphPad Software La Jolla, California, United tates). Data are presented as the mean ± SEM; whiskers on the boxplot graphs show the minimum and maximum values. The results of the von Frey test were evaluated by two-way analysis of variance (ANOVA), followed by Tukey's HSD post-hoc test. The results from the KWB test were evaluated by one-way ANOVA on day 0 or two-way ANOVA on the following experimental days, followed by Tukey's HSD post-hoc test. The qPCR and Western blot results were evaluated by one-way ANOVA followed by Dunnett's post-hoc test, treating healthy animals as the control group. In behavioral tests, each group consisted of eight animals (von Frey test) or 5 animals (KWB test). In biochemical analyses, the experimental group sizes consisted of 3-6 samples per group (qPCR) or 4-5 samples per group (Western blot). Values of $p < 0.05$ (denoted * or #), $p < 0.01$ (denoted ** or ##), and $p < 0.001$ (denoted *** or ###) were considered to be statistically significant.

RESULTS

A significant difference in pain threshold was observed in both MIA doses, using the von Frey and KWB tests. Differences in tactile allodynia, as well as in paw pressure and surfaces applied to the ground between the rear right and rear left paws on subsequent experimental days were observed. Significant signs of pain were noticed from the 2nd day post-MIA treatment and persisted until the day 28. In biochemical analyses, statistically significant dose- and time-dependent changes in MMP and inflammation-related gene expression (qPCR) and protein production (Western blot technique) were observed. The results will be explained in details in the following sections.

Development of OA-Related Allodynia

MIA injection at both investigated doses (1 and 3 mg MIA i.a.) resulted in the development of mechanical allodynia in the ipsilateral hind paw (rear right) on day 2 ($p < 0.05$ for 1 mg of MIA and $p < 0.001$ for 3 mg of MIA; **Figure 1**), a phenomenon not observed on day 0. On day 2 a significant difference between tested doses was also observed ($p < 0.05$; **Figure 1**), which was not observed in the following days. OA rats showed a significant gradual reduction in withdrawal threshold that progressed with time in both experimental groups. The lowest mechanical withdrawal latency was observed at day 28. From day 7 on, the effect was similar in both groups (1 and 3 mg of MIA; $p < 0.001$; **Figure 1**). These results indicate that animals in whom OA symptoms were induced with both MIA doses, developed an OA-associated allodynia.

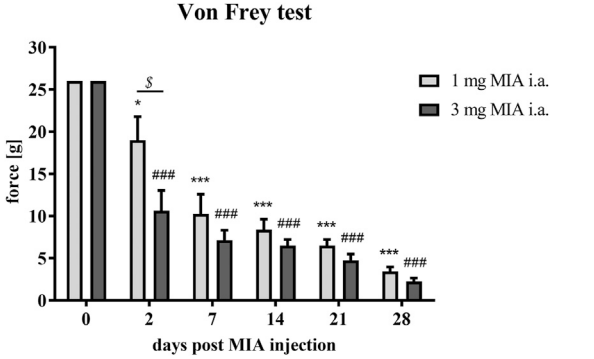

FIGURE 1 | Mechanical allodynia measured by quantifying tactile sensitivity during OA developme with MIA grading. Pain sensitivity was measured with von Frey filaments in the ipsilateral paw (rear right) prior to MIA injection and 2, 7, 14, 21, and 28 days post-MIA treatment (1 or 3 mg intra-articular injection; i. a.; n = 8 animals per group). Two-way ANOVA and Tukey's HSD post-hoc testing was performed. * denotes $p < 0.05$; *** denotes $p < 0.001$ in each day vs. day 0 in the 1 mg group; ### denotes $p < 0.001$ in each day vs. day 0 in the 3 mg group, $ denotes $p < 0.05$ 1 mg vs. the 3 mg group.

Paw Weight Bearing Differences During Free Walk

Rats were evaluated for paw force and surface distribution during a free walking sequence. A significant difference in both paw force (**Figures 2A–F**) and surface (**Figures 3A–F**) applied to the ground during free walking was observed for both MIA doses used to induce OA. Differences were observed in both experimental groups (1 or 3 mg MIA i.a.) on almost all experimental days (except days 7 and 14 in the peak surface analysis of the 1 mg MIA group); however, a stronger effect was elicited by 3 mg of MIA. Therefore it can be concluded that both MIA doses induced weight bearing differences in MIA-treated rats.

Inflammation During OA Progression

In the present study, cartilage oligomeric matrix protein (COMP) levels were measured in joint tissues isolated from osteoarthritic animals. In cartilage samples, a U-shaped pattern of protein production was observed following injection, with an initial decrease (significant only on day 7 in the 3 mg MIA group; $p < 0.05$; **Figure 4C**) and subsequent return to baseline (in the 2 and 3 mg MIA groups) or an increase (in the 1 mg MIA group; $0.01 > p > 0.001$; **Figures 4A–C**). In synovial membranes, in contrast, an initial increase (day 2) was solely observed in all experimental groups (MIA 1 mg; $0.01 > p > 0.001$; MIA 2 mg; $p < 0.05$; MIA 3 mg; $p < 0.001$; **Figures 4D–F**). In synovial fluid samples, an increase in COMP levels was detected in the latter stages of OA – exclusively on day 28 post-MIA treatment – in all groups (MIA 1 mg; $0.01 > p > 0.001$; MIA 2 mg; $p < 0.05$; MIA

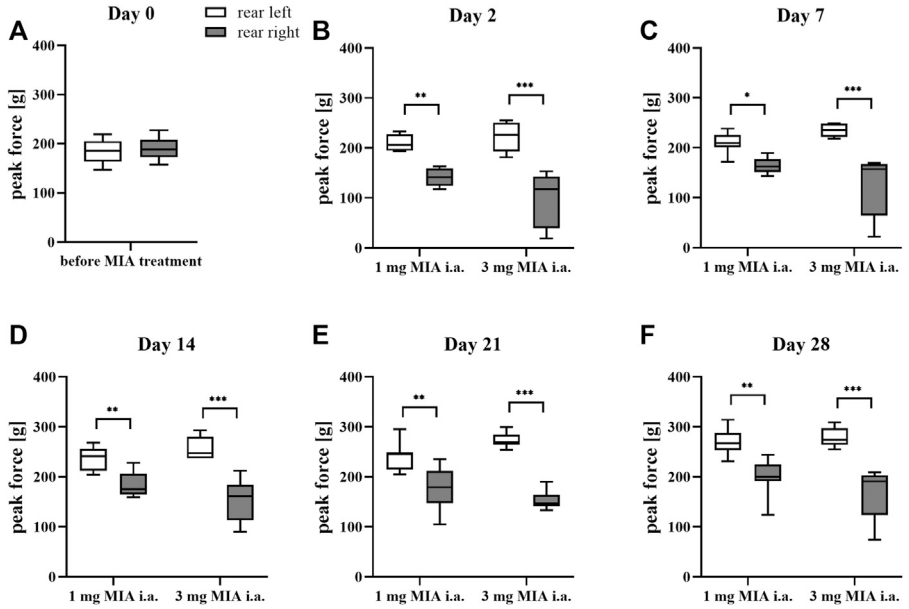

FIGURE 2 | Gait analysis in OA rats recorded with KWB by measuring the distribution of paw force applied to the ground during a free walk (for 1 and 3 mg of MIA i.a. groups) during a free walk. Measurements taken prior to the MIA injection (day 0; **A**) and 2, 7, 14, 21, and 28 days **(B–F)** post-MIA treatment (n = 5–8 animals per group). One-way ANOVA on day 0 or two-way ANOVA on the following experimental days and Tukey's HSD post-hoc tests were performed. * denotes $p < 0.05$; ** denotes $p < 0.01$; *** denotes $p < 0.001$.

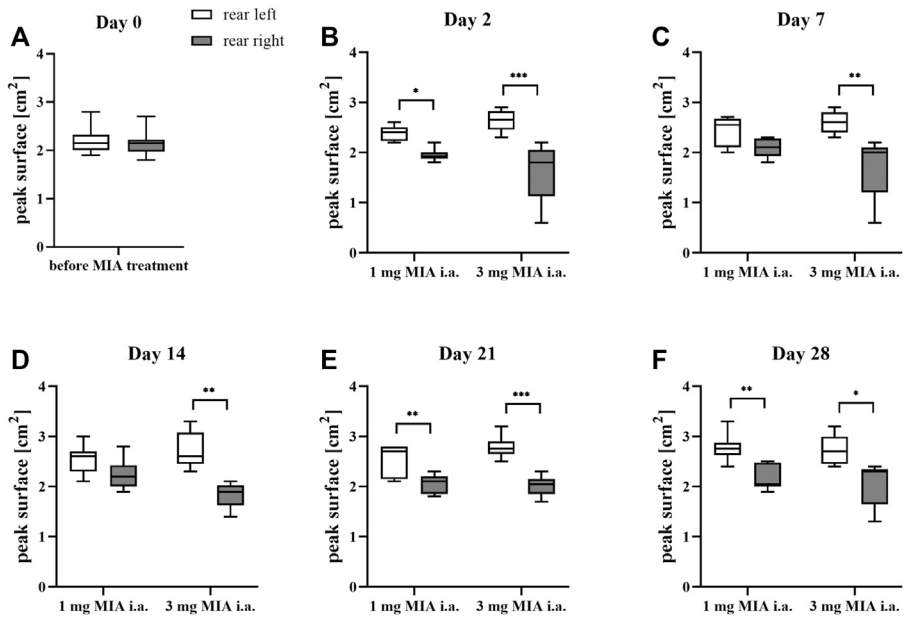

FIGURE 3 | Gait analysis in OA rats recorded with KWB by measuring the distribution of paw surfaces applied to the ground during free walks (for 1 and 3 mg of MIA i.a. groups) during a free walk. Measurements taken prior to the MIA injection (day 0; **A**) and 2, 7, 14, 21, and 28 days **(B–F)** post MIA treatment (n = 5–8 animals per group). One-way ANOVA on day 0 or two-way ANOVA on the following experimental days and Tukey's HSD post hoc test were performed. * denotes $p < 0.05$; ** denotes $p < 0.01$; *** denotes $p < 0.001$.

3 mg; $p < 0.001$; **Figures 4G–I**). The levels of various inflammation-related factors were measured only in the synovial fluid. Chemokine (C-C motif) ligand 2 (CCL2) levels showed an initial increase (day 2 at all MIA doses; $0.01 > p > 0.001$; **Figures 5A–C**). In the 1 mg MIA group, the CCL2 level returned to baseline, whereas in the 2 mg MIA group, it remained

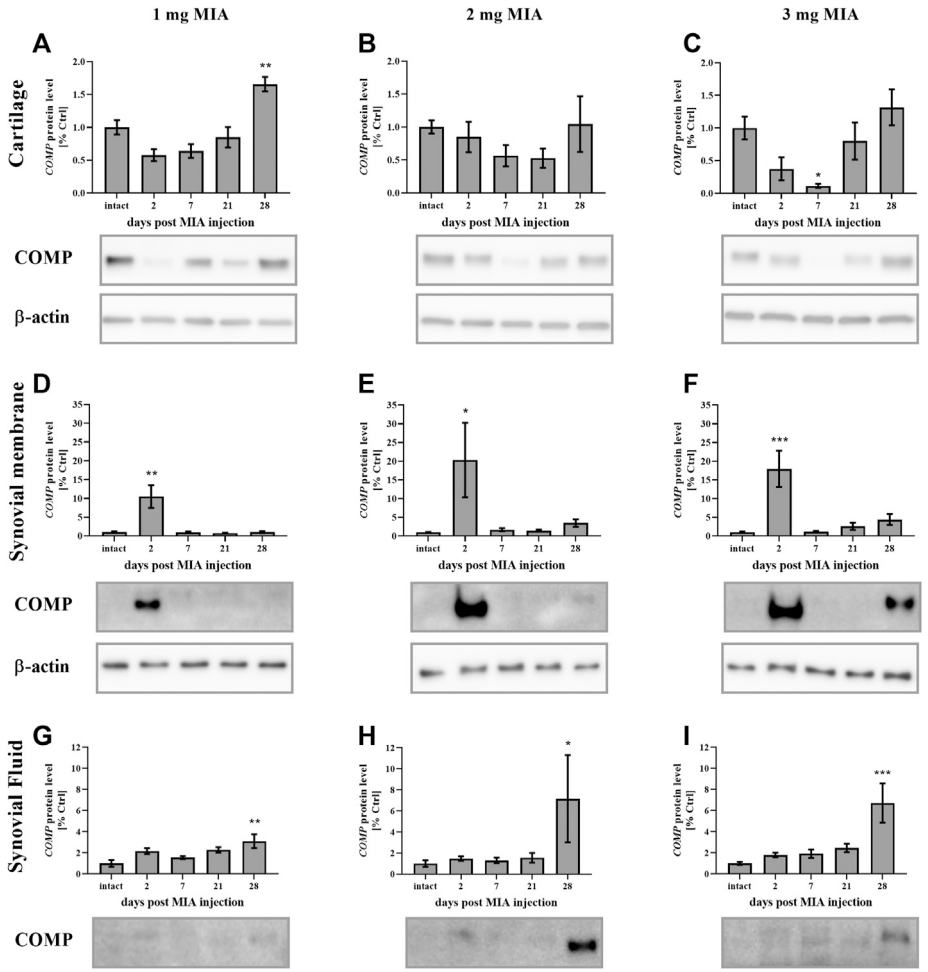

FIGURE 4 | Changes in COMP protein levels in cartilage **(A–C)**, synovial membrane **(D–F)** and synovial fluid **(G–I)** samples from osteoarthritic rats as measured by Western blot assay. Tissues were collected 2, 7, 21 or 28 days after OA induction. Results are presented as mean group fold change ± SEM in comparison to the control group (healthy animals), n = 4–5 samples per group. Data were analyzed with one-way ANOVA followed by Dunnett's post-hoc test. * denotes $p < 0.05$; ** denotes $p < 0.01$; *** denotes $p < 0.001$ vs. intact animals.

elevated throughout the experiment ($0.01 < p < 0.001$; **Figures 5A,B**). In the 3 mg MIA group, the CCL2 level was increased throughout the entire experimental period; however, these differences reached statistical significance only on day 2 ($0.01 > p > 0.001$; **Figure 5C**). A similar pattern was observed for chemokine (C-X-C motif) ligand 1 (CXCL1). The protein level was increased in synovial fluid by the 2nd day post-OA induction in all groups (MIA 1 mg; $p < 0.001$; MIA 2 mg; $p < 0.05$; MIA 3 mg; $0.01 > p < 0.001$; **Figures 5D–F**). In the 1 mg MIA group, this increase returned to baseline, whereas in the 2 and 3 mg MIA groups, it remained significantly upregulated on day 28 post-MIA treatment (MIA 2 mg; $p < 0.05$; MIA 3 mg; $0.01 > p > 0.001$; **Figures 5D–F**). The IL-1β levels in the synovial fluid in the 1 mg MIA group were increased on days 2 ($p < 0.001$), 7 ($p < 0.05$) and 28 ($p < 0.05$) post-MIA treatment (**Figure 5G**). In the 2 mg MIA group, this expression level was increased only on day 28 post-MIA treatment ($0.01 > p > 0.001$; **Figure 5H**). At the highest MIA dose (3 mg), IL-1β levels were increased on days 2 ($p < 0.05$) and 28 ($p < 0.001$) post-OA induction (**Figure 5I**). The above results show a dose-dependent inflammation in joint tissues isolated from osteoarthritic animals. The strongest effect was observed in the group in which OA was induced with MIA at a dose of 3 mg, however, a comparable effect was triggered by 2 mg of MIA.

Matrix Metalloproteinase Expression Changes During OA Progression

Changes in MMP Gene Expression During OA Development

MMP gene expression was measured in synovial membrane and cartilage tissues of osteoarthritic rats. *Mmp-2* gene expression significantly increased in the later stages of OA. In the synovial membrane samples, an increase was observed 7 days post-MIA injection (at all MIA doses; MIA 1 mg; $0.01 > p > 0.001$; MIA 2 mg; $p < 0.001$; MIA 3 mg; $p < 0.001$; **Table 1**), 21 days post-MIA

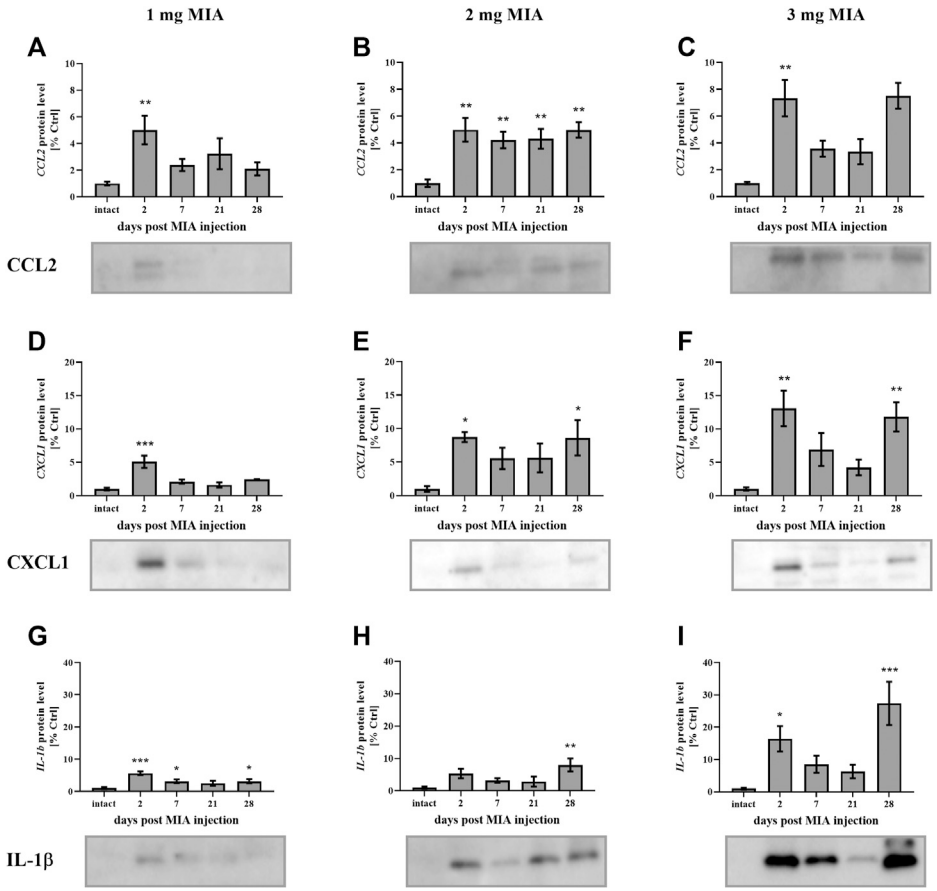

FIGURE 5 | Changes in the protein levels of the inflammation-related factors CCL2 **(A–C)**, CXCL1 **(D–F)**, and IL-1β **(G–I)** in the synovial fluid of osteoarthritic rats, as measured by Western blot assay. Tissues were collected 2, 7, 21 or 28 days after OA induction. The results are presented as the mean group fold change ± SEM in comparison to the control group (healthy animals), n = 5–6 samples per group. Data were analyzed with one-way ANOVA followed by Dunnett's post hoc test. * denotes $p < 0.05$; ** denotes $p < 0.01$; *** denotes $p < 0.001$ vs. intact animals.

injection (2 and 3 mg MIA groups; $0.01 < p < 0.001$ and $p < 0.001$ respectively) and 28 days post-MIA injection (1 and 3 mg MIA groups $0.01 < p < 0.001$ and $p < 0.001$ respectively). In the 2 mg MIA group, the *Mmp-2* expression level remained elevated on day 28 (similar to the 1 mg MIA group); however, these differences did not reach statistical significance. Similar results were observed in cartilage samples—an increase in *Mmp-2* abundance was observed starting at day 7 (in the 2 mg MIA group; $p < 0.05$) or day 21 (in the 1 and 3 mg MIA groups; $0.01 > p > 0.001$ and $p < 0.001$ respectively) that persisted until the end of the experiment (MIA 1 mg; $p < 0.05$; MIA 2 mg; $0.01 > p > 0.001$; MIA 3 mg; $p < 0.001$). The *Mmp-3* expression level in the 1 mg MIA group was elevated in the initial stages of OA (days 2 and 7; $0.01 > p > 0.001$; in the synovial membranes or day 2 in cartilage; $p < 0.05$). In the synovial membranes of the 2 mg MIA group, an increase in *Mmp-3* gene expression was observed starting at the beginning of the experiment; however, significance was reached only on day 21 ($p < 0.05$). In the cartilage samples, significant upregulation was observed on days 7 ($p < 0.05$) and 28 ($p < 0.001$) post-MIA treatment. In the synovial membranes samples of the 3 mg MIA group, *Mmp-3* expression was elevated throughout the entire experimental period (day 2; 7; 21; $0.01 > p > 0.001$; day 28 $p < 0.001$); in cartilage, it was elevated only in the later stages (days 21 and 28; $0.01 > p > 0.001$ and $p < 0.001$ respectively). The *Mmp-9* expression level in the synovial membranes was upregulated in the 1 mg MIA group, with a significant increase on days 2 ($p < 0.05$), 7 ($p < 0.001$) and 28 ($p < 0.001$) post-MIA treatment. In the 2 mg MIA group, the *Mmp-9* level increased; however, group variances were too substantial to reach statistical significance. In the 3 mg MIA group, *Mmp-9* expression also increased throughout the entire experimental period, with a significant elevation observed on experimental days 7 ($p < 0.001$) and 21 ($0.01 > p > 0.001$). In the cartilage samples, a significant increase in *Mmp-9* levels was observed at the advanced OA stages (on day 21in the 1 mg MIA group; $0.01 > p > 0.001$, on day 28 in the 2 mg MIA group; $p < 0.05$; and on days 7 and 21 in the 3 mg MIA group; $p < 0.05$). Nevertheless, a trend toward increasing expression was observed throughout the entire experiment, particularly in the synovial membrane samples. For *Mmp-13* gene expression, in the 1 mg MIA group, an elevation was observed only at the beginning of the experiment (day 2) in both tissue types (Synovial membrane; $p < 0.001$; Cartilage;

TABLE 1 | Transcript abundance levels of selected genes in synovial membrane and cartilage samples from osteoarthritic rats.

Tissue	Gene	MIA [mg]	Days post-MIA injection				
			Ctrl	2	7	21	28
Synovial membrane	*Mmp-2*	1	1.1 ± 0.2	1.7 ± 0.4	**2,9** ± 0,5**	1.7 ± 0.1	**2,6** ± 0,1**
		2		.9 ± 0.1	**6,4*** ± 0,8**	**4,1** ± 1,0**	2.5 ± 0.9
		3		1.1 ± 0.1	**7,2*** ± 0,5**	**3,5*** ± 0,3**	**4,4*** ± 0,3**
	Mmp-3	1	1.0 ± 0.1	**6,4** ± 2,1**	**9,8** ± 2,0**	2.3 ± 0.2	2.5 ± 0.6
		2		7.0 ± 1.1	5.9 ± 1.0	**10,7* ± 5,3**	2.9 ± 0.4
		3		**7,3** ± 1,6**	**6,7** ± 1,2**	**7,4** ± 0,9**	**14,0*** ± 1,9**
	Mmp-9	1	1,1 ± 0,2	**9,6* ± 1,6**	**30,7*** ± 1,8**	4,6 ± 2,1	**35,8*** ± 4,9**
		2		27.9 ± 4.4	26.5 ± 6.0	40.4 ± 15,4	36.9 ± 33.4
		3		28.6 ± 4.6	**94,5*** ± 18,3**	**75,1** ± 25,8**	20.6 ± 1.8
	Mmp-13	1	1,5 ± 0,7	**179,2*** ± 55,6**	53,2 ± 11,9	3,1 ± 1,3	3,2 ± 0,9
		2		163.8 ± 67.9	42.1 ± 5.2	137.1 ± 103.4	12.0 ± 5.4
		3		53.3 ± 17.2	**65,0* ± 9,5**	**80,5* ± 28,8**	**67,8* ± 24,3**
Cartilage	*Mmp-2*	1	1.1 ± 0.3	2.3 ± 0.7	1.8 ± 0.7	**4,6** ± 1,1**	**3,9* ± 0,8**
		2		1.1 ± 0.3	**2,7* ± 0,8**	**3,3** ± 0,5**	**3,5** ± 0,5**
		3		1.3 ± 0.2	1.1 ± 0.4	**8,1*** ± 0,8**	**4,3*** ± 0,7**
	Mmp-3	1	1.1 ± 0.2	**4,4* ± 1,3**	2.8 ± 0.4	2.2 ± 0.9	1.7 ± 0.6
		2		2.2 ± 0.7	**3,5* ± 0,8**	2.3 ± 0.7	**5,2*** ± 1,0**
		3		2.3 ± 0.8	2.2 ± 0.3	**4,2** ± 1,0**	**5,5*** ± 0,8**
	Mmp-9	1	1.0 ± 0.1	0.9 ± 0.1	1.1 ± 0.1	**1,9** ± 0,3**	1.3 ± 0.2
		2		1.1 ± 0.1	1.5 ± 0.2	1.6 ± 0.2	**2,6* ± 0,9**
		3		1.1 ± 0.1	**1,8* ± 0,2**	**1,8* ± 0,3**	1.6 ± 0.2
	Mmp-13	1	1.2 ± 0.3	**2,7* ± 0,5**	0.9 ± 0.2	1.1 ± 0.3	1.8 ± 0.7
		2		1.1 ± 0.3	0.8 ± 0.2	1.2 ± 0.2	1.3 ± 0.5
		3		1.4 ± 0.3	0.6 ± 0.3	**2,7** ± 0,4**	1.1 ± 0.3

The results were assessed by quantitative PCR (qPCR). Total RNA samples were collected 2, 7, 21 or 28 days after OA induction. The results are presented as the mean group fold change ± SEM in comparison to the control group (healthy animals), n = 3–6 samples per group. Data were analyzed with one-way ANOVA followed by Dunnett's post-hoc test.
** denotes $p < 0.05$.*
*** denotes $p < 0.01$.*
**** denotes $p < 0.001$ vs. intact animals (Ctrl).*
Statistically significant values are shown in bold.

$p < 0.05$). In the 2 mg MIA group, no results reached statistical significance. In the 3 mg MIA group, in the synovial membrane, an increase was observed throughout nearly the entire experiment (days 7, 21 and 28; $p < 0.05$); in cartilage, elevated expression of Mmp-13 was observed solely on day 21 post-MIA treatment ($0.01 > p > 0.001$). The results of this gene expression analysis are shown in **Table 1**. *Comp* expression in cartilage showed a decrease in the initial phases of OA in the 1 mg MIA group (day 2 and 7; $0.01 > p > 0.001$) and a subsequent increase in the 2 ($p < 0.05$) and 3 mg ($0.01 > p > 0.001$) MIA groups on day 21 (**see Supplementary Table S1**). In summary, the qPCR test showed a dose- and time-dependent changes in mRNA levels of *Mmps*.

MMP Protein Levels During OA Development

MMP-2 protein secretion was elevated in advanced OA stages in all experimental groups. In cartilage samples, a significant increase was observed solely on day 28 of the experiment at all MIA doses (MIA 1 mg; $p < 0.05$; MIA 2 mg; $0.01 > p > 0.001$; MIA 3 mg; $p < 0.001$; **Figures 6A–C**). In synovial membrane samples, MMP-2 protein levels were increased starting on day 7 (1 and 2 mg MIA groups; $p < 0.001$ and $p < 0.05$) or day 21 (3 mg MIA group; $p < 0.001$) and remained elevated until the end of the experiment (**Figures 6D–F**). In the synovial fluid of OA rats, MMP-2 was increased at the later stages of the disease, on day 28 (1 mg MIA group; $0.01 > p > 0.001$) or days 21 and 28 (2 and 3 mg MIA groups; $p < 0.001$; **Figures 6G–I**).

MMP-3 protein levels, in cartilage samples in the 1 mg MIA group, showed an early increase (on day 2 post-MIA treatment; $p < 0.05$;**Figure 7A**). A similar trend was observed in the 2 mg MIA group; however, these results did not reach statistical significance. In the 2 and 3 mg MIA groups, a significant increase in MMP-3 levels was observed in the later OA stages (days 28; $0.01 > p > 0.001$; or days 21;$p < 0.05$; and 28; $p < 0.001$; respectively; **Figures 7B,C**). In the synovial membrane samples, the lowest MIA dose did not significantly alter MMP-3 protein production (**Figure 7D**). In the 2 mg MIA group, an increase was observed only on day 21 ($p < 0.05$), whereas in the 3 mg MIA group, a significant increase was observed on days 21 and 28 post-MIA injection ($p < 0.05$ and $0.01 > p > 0.001$; **Figures 7E,F**).

In the synovial fluid samples, an increase in MMP-3 protein levels was detected in the early stages of OA. The lowest dose of MIA (1 mg) resulted in an early release of MMP-3 into the synovial fluid; a significant elevation was observed on days 2, 7 and 28, with a peak on day 2 ($p < 0.001$ and $0.01 > p > 0.001$; $p < 0.05$ respectively; **Figure 7G**). In the 2 mg MIA group, a trend toward increased expression was observed from the beginning of the experiment; however, only the results on day 28 reached statistical significance ($p < 0.05$; **Figure 7H**). Similar results were observed in the 3 mg MIA

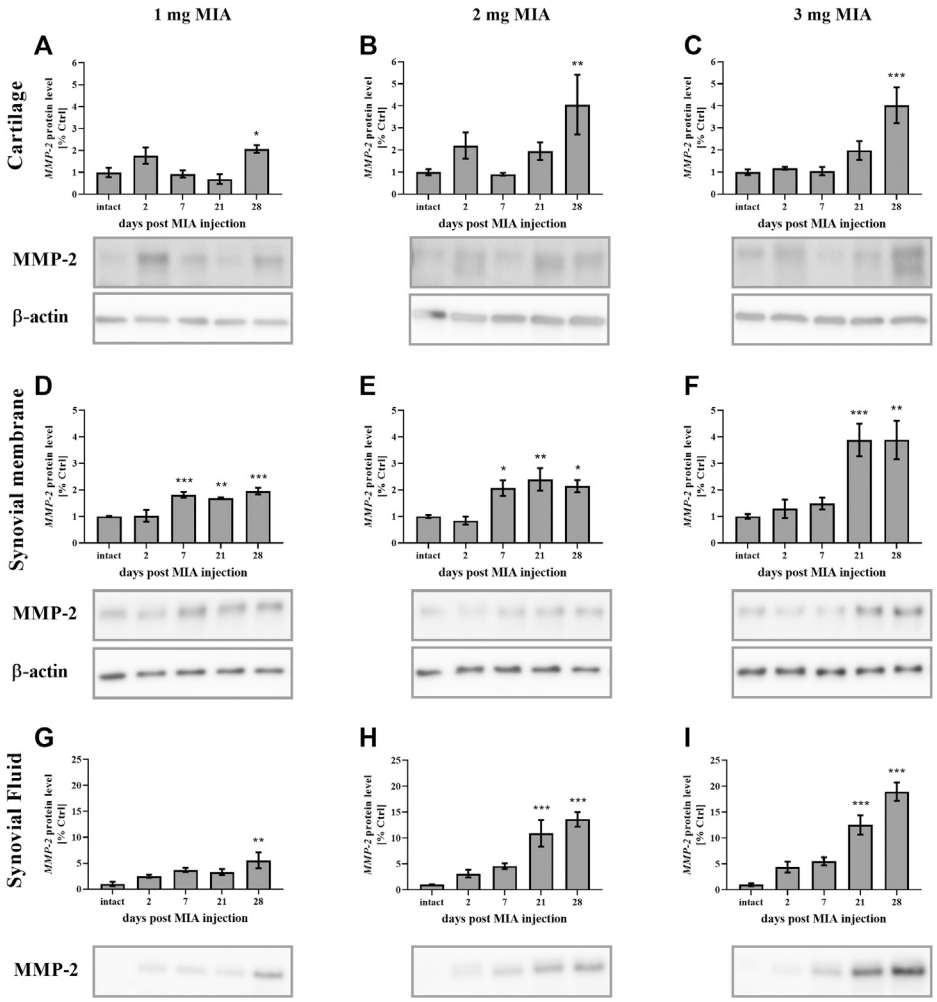

FIGURE 6 | Changes in MMP-2 protein levels in cartilage **(A–C)**, synovial membrane **(D–F)** and synovial fluid **(G–I)** samples of osteoarthritic rats as measured by Western blot assay. Tissues were collected 2, 7, 21 or 28 days after OA induction. The results are presented as the mean group fold change ± SEM in comparison to the control group (healthy animals), n = 4–5 samples per group. Data were analyzed with one-way ANOVA followed by Dunnett's post-hoc test. * denotes $p < 0.05$; ** denotes $p < 0.01$; *** denotes $p < 0.001$ vs. intact animals.

group, with a significant increase in MMP-3 levels on days 7 and 28 ($p < 0.05$; **Figure 7I**).

MMP-9 protein levels in cartilage samples at low MIA doses (1 and 2 mg MIA groups) showed no significant changes (**Figures 8A,B**). However, in the 3 mg MIA group, MMP-9 protein levels increased significantly on day 28 ($p < 0.05$; **Figure 8C**). In synovial membrane samples, in all tested MIA doses, MMP-9 levels increased exclusively in the early OA stages (day 2 post MIA treatment; MIA 1 mg; $0.01 > p > 0.001$; MIA 2 mg; $p < 0.05$; MIA 3 mg; $p < 0.001$), subsequently returning to baseline in the following experimental days (**Figures 8D–F**). Similar observations were noted for the synovial fluid samples – an early (day 2) increase in MMP-9 protein levels was detected at all MIA doses (MIA 1 mg; $0.01 > p > 0.001$; MIA 2 mg; $0.01 > p > 0.001$; MIA 3 mg; $p < 0.05$), followed by a return nearly to baseline and a final increase on the last experimental day (a significant increase was observed only in the 3 mg MIA group ($0.01 > p > 0.001$). However, a trend toward increased expression was also observed in the 2 mg MIA group; **Figures 8G–I**).

Regarding MMP-13, lower MIA doses (1 and 2 mg) were associated with an early increase (day 2) in MMP-13 production in cartilage ($p < 0.05$; both groups). However, in the 2 mg MIA group, an increase was also observed in the later OA stages (day 28; $p < 0.05$, with a trend toward increased expression on day 21; **Figures 9A,B**). In the 3 mg MIA group, there was a robust increase in MMP-13 levels on day 28 ($p < 0.001$; **Figure 9C**). In the synovial membrane, ambiguous results were obtained, with a significant increase identified only on day 2 in the 1 mg MIA group ($p < 0.05$; **Figures 9D–F**). In the synovial fluid samples, an increase in Mmp-13 levels was observed for almost the entire experimental period. In the 1 and 3 mg MIA groups, a significant increase was detected on days 2, 7 and 28 post-MIA treatment, whereas in the 2 mg MIA group, Mmp-13 levels significantly increased on days 2, 21 and 28 (**Figures 9G–I**).

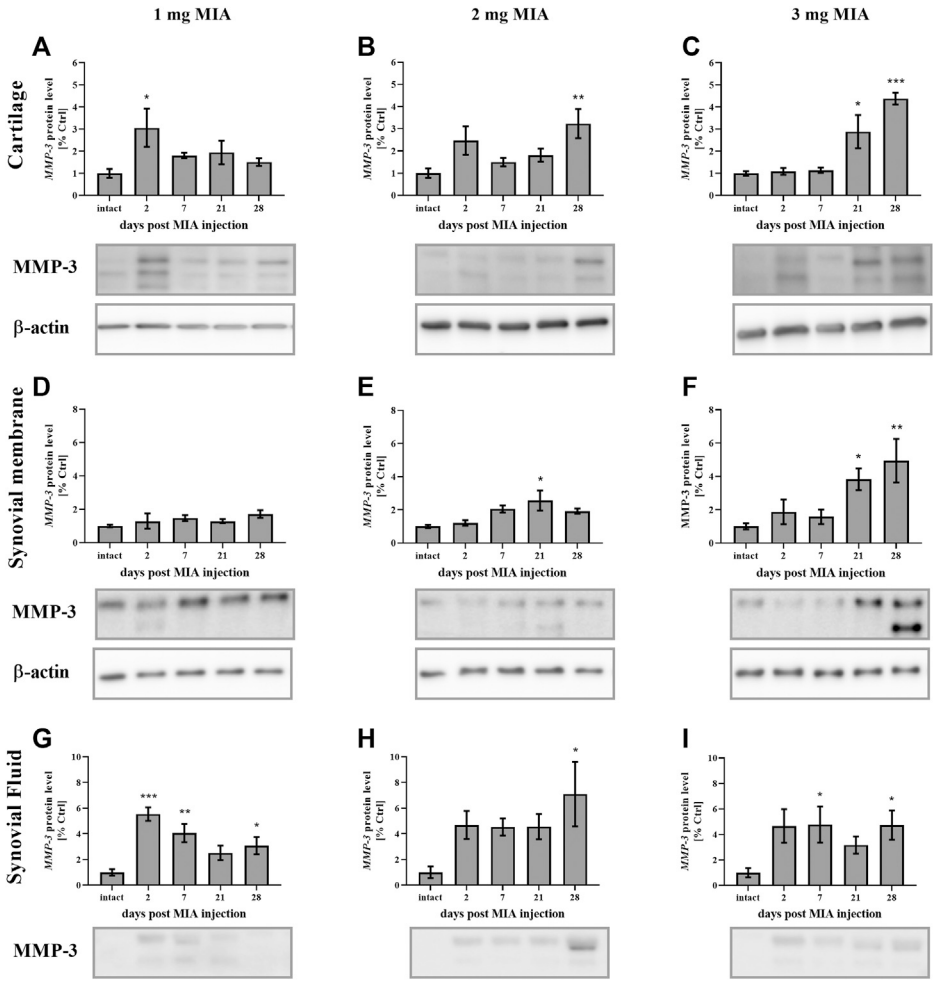

FIGURE 7 | Changes in MMP-3 protein levels in cartilage **(A–C)**, synovial membrane **(D–F)** and synovial fluid **(G–I)** samples of osteoarthritic rats as measured by Western blot assay. Tissues were collected 2, 7, 21 or 28 days after OA induction. The results are presented as the mean group fold change ± SEM in comparison to the control group (healthy animals), n = 4–5 samples per group. Data were analyzed with one-way ANOVA followed by Dunnett's post-hoc test. * denotes $p < 0.05$; ** denotes $p < 0.01$; *** denotes $p < 0.001$ vs. intact animals.

In summary, protein levels for investigated MMPs changed significantly in a dose- and time-dependent manner. All MIA doses significantly changed protein concentration in the synovial fluid, whereas in cartilage and synovial membrane significant changes were observed mostly in 2 and 3 mg of MIA groups.

DISCUSSION

In the current study, behavioral and biochemical OA-related changes were investigated. The molecular alterations in MMP and inflammation-related factor expression were measured during 28 days of OA progression across three MIA dose groups: 1, 2 or 3 mg of MIA i.a. In the behavioral study, both investigated MIA doses (1 and 3 mg) caused significant allodynia and disturbed weight bearing patterns starting on the second day of the experiment. Although a stronger effect was observed in the 3 mg MIA group, both doses were sufficient to trigger OA-like pain behavior in rats. Furthermore, at the molecular level, significant differences between the investigated doses were observed.

OA progression is associated with an inflammatory state (Goldring and Otero, 2011). OA-related knee pain correlates with joint synovitis, subarticular bone attrition, bone marrow lesions and meniscal tears (Torres et al., 2006; Baker et al., 2010). Moreover, synovitis and effusion are associated with cartilage degeneration and loss in human patients (Roemer et al., 2011). There are several pathways that reportedly play an important role in synovitis progression. Activated macrophages promote catabolic mediator production and Toll-like receptor (TLR) and NFκB pathway activation, which leads to proinflammatory chemokine and cytokine production (e.g., IL-1β, IL-2, IL-6, IL-8, IL-15, TNFα, CCL2, CCL5, CCL19) (Scanzello and Goldring,

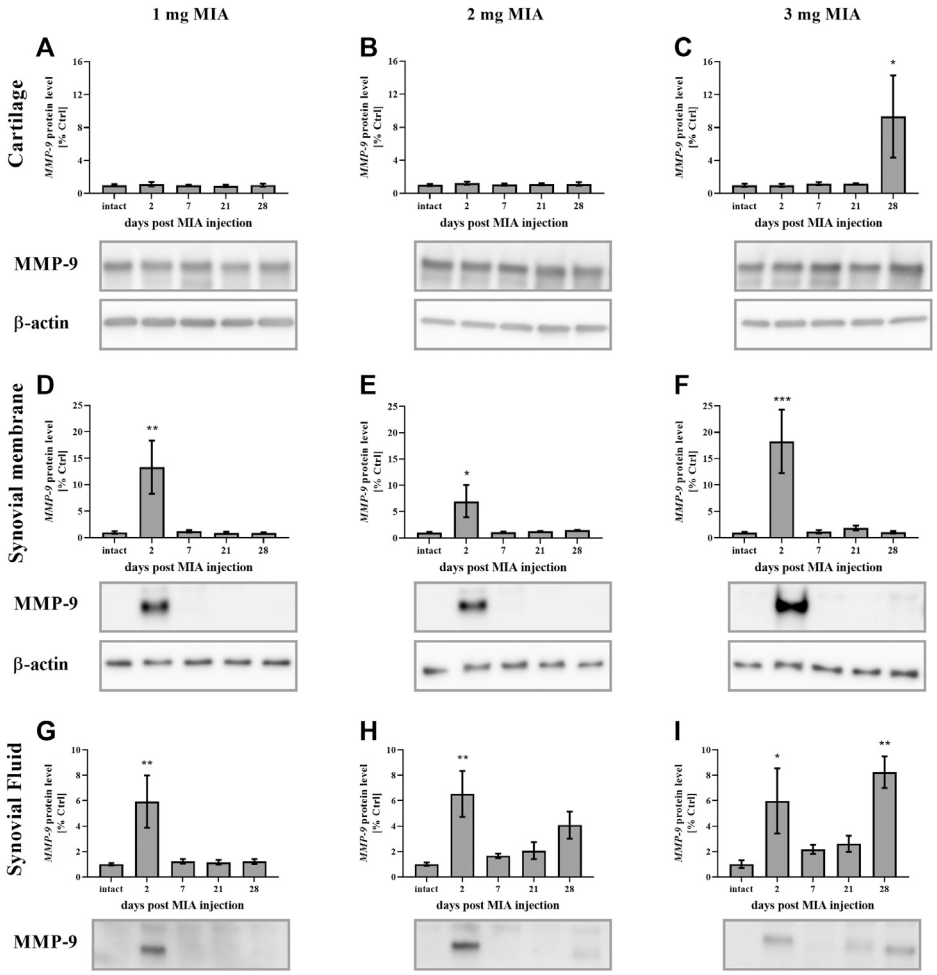

FIGURE 8 | Changes in MMP-9 protein levels in cartilage **(A–C)**, synovial membrane **(D–F)** and synovial fluid **(G–I)** samples of osteoarthritic rats as measured by Western blot assay. Tissues were collected 2, 7, 21 or 28 days after OA induction. The results are presented as the mean group fold change ± SEM in comparison to the control group (healthy animals), n = 4–5 samples per group. Data were analyzed with one-way ANOVA followed by Dunnett's post-hoc test. * denotes $p < 0.05$; ** denotes $p < 0.01$; *** denotes $p < 0.001$ vs. intact animals.

2012). Malek et al. previously observed an early increase in pain-related behavior in MIA-treated rats associated with transient inflammation triggered by i.a. MIA injection (Malek et al., 2015). Here, we observed an early peak (on day 2 post-MIA injection) in the gene expression of inflammation-related factors (*Ccl2, Cxcl-1, and Il-6*) in synovial membrane samples across all MIA doses (see **Supplementary Table S1**) and in protein levels in synovial fluid (CCL2, CXCL1, and IL-1β).

One of the most promising molecular markers of OA is COMP, which regulates and stabilizes the collagen network in cartilaginous tissue (Živanović et al., 2011). Upregulation of this protein in OA patient serum has been correlated with disease progression (Jung et al., 2006). In this study, the COMP levels in the synovial membrane were elevated in the early OA stages across all MIA doses; however, on day 28, upregulation was observed only in the 2 and 3 mg MIA groups (3- and 4-fold vs. the control group). In the synovial fluid, COMP levels were increased at the end of the experimental period (day 28 in all MIA doses).

In addition to inflammation-related factors, four MMPs were further investigated in this study. MMPs and their regulators (tissue inhibitors of metalloproteinases; TIMPs) are considered biological markers of OA (DeGroot et al., 2002; Rousseau and Garnero, 2012). Here, the levels of MMP-2, -3, -9, and -13 were determined. The gelatinases MMP-2 and MMP-9 are important factors in the pathogenesis of several diseases, including cancer, liver fibrosis, cardiovascular diseases and rheumatoid arthritis (Kurzepa et al., 2014; Radenkovic et al., 2014; Zhou et al., 2014; Radosinska et al., 2017). They are also reportedly involved in inflammation and inflammatory cell migration (Cui et al., 2017; Hannocks et al., 2019; Kim et al., 2012). Gelatinases also play an important role in the inflammatory response during the course of OA. In synoviocyte and anterior cruciate ligament fibroblast cell cultures, TNFα stimulation increases MMP-2 and MMP-3 levels

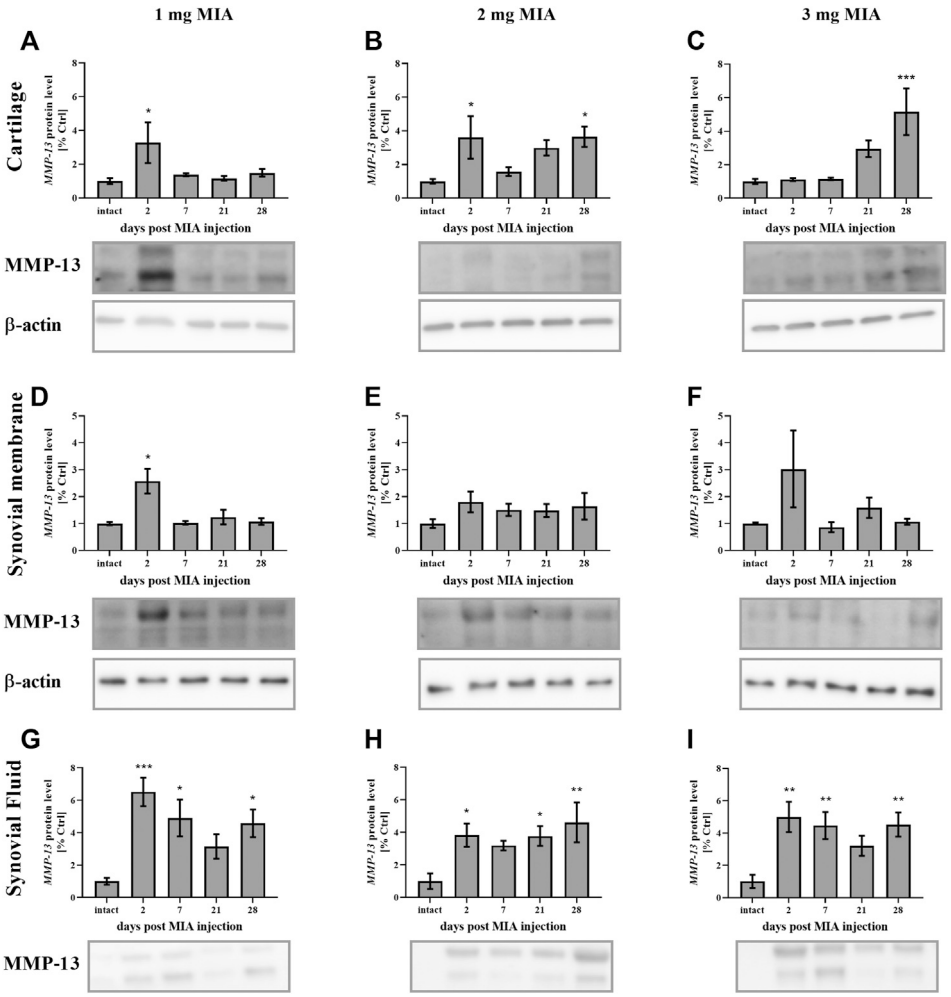

FIGURE 9 | Changes in MMP-13 protein levels in cartilage **(A–C)**, synovial membrane **(D–F)** and synovial fluid **(G–I)** samples of osteoarthritic rats as measured by Western blot assay. Tissues were collected 2, 7, 21 or 28 days after OA induction. The results are presented as the mean group fold change ± SEM in comparison to the control group (healthy animals), n = 4–5 samples per group. Data were analyzed with one-way ANOVA followed by Dunnett's post-hoc test. * denotes $p < 0.05$; ** denotes $p < 0.01$; *** denotes $p < 0.001$ vs. intact animals.

(Wang et al., 2019). In rheumatoid arthritis (RA) synovial fibroblasts, MMP-2 and MMP-9 contribute to cell survival, proliferation and migration. MMP-9 has been shown to stimulate RA synovial fibroblast-mediated inflammation, whereas MMP-2 exhibited the opposite effect (Xue et al., 2014). Moreover, MMP-9 expression and activation are reportedly increased in septic native knee arthritis patients in comparison to aseptic knee arthritis patients (Fotopoulos et al., 2012). In cartilage and synovial fluid of OA patients, gelatinase protein levels are increased (Alunno et al., 2017; Duerr et al., 2004; Kim et al., 2011; Lipari and Gerbino, 2013); however, there may be differences between Asian and Caucasian patients (Zeng et al., 2015). In the present study, the gelatinase MMP-2 showed a gradual dose- and time-dependent increase in both gene expression and protein production. A significant increase was observed in the advanced phases of the disease at all MIA doses (from day 7 in qPCR and from day 21 in Western blot). This indicates a role for MMP-2 in joint tissue degeneration and inflammation in the later stages of OA in a rat model. As described above, early inflammation connected to MIA i.a. injection may explain the early increase in MMP-9 protein secretion by synoviocytes into the synovial fluid observed in almost all experimental groups in the current study. A similar increase at the end of the experiment, observed in the 3 mg MIA dose group, may indicate the role of MMP-9 in ECM degradation in the advanced stages of the disease in the highest MIA dose group, in which the OA lesions are the most severe. Lower MIA doses (1 and 2 mg) may not be sufficient to trigger such an effect in a 4-week period. However, it remains possible that lower MIA doses could trigger such an effect if the experimental period were longer. Further experiments are needed to clarify this effect, although most studies report an experimental period of no longer than 4 weeks. Regarding the gene expression levels of *Mmp-9*, we

observed that synovial membrane samples provided a more substantial response than cartilage samples. The synovial membrane is a more secretory tissue compared to cartilage and is responsible for synovial fluid production, joint lubrication and maintaining homeostasis of the joint (Orr et al., 2017). In turn, cartilage does not play a primary secretory role in the joint and in fact degenerates over the course of the disease, further reducing its reactivity (Bryk et al., 2020).

MMP-3 (stromelysin 1) is also an important factor in osteoarthritis pathogenesis. In human synovial membrane cell culture and TNF-α-stimulated human cartilage experiments, MMP-3 levels are reportedly elevated (Sun et al., 2014). Additionally, in RA patients, MMP-3 serum levels are upregulated (Mahmoud et al., 2005) and can be reduced following anti-inflammatory (anti-TNFα) treatment (Sun et al., 2014). In OA patients, an elevated level of MMP-3 was also shown (Li et al., 2012). Moreover, the serum level of MMP-3 was higher in patients with OA changes in two or more locations (hands, hips, knees, spine, feet) than in people with only one location (knee joints) affected (Georgiev et al., 2018). In a reversible osteoarthritis rabbit model, MMP-3 and COMP levels were elevated in serum and synovial fluid samples from OA animals, which was correlated with OA severity (Chu et al., 2015). MMP-3 levels are also correlated with leptin concentrations in the synovial fluid of OA patients (Koskinen et al., 2011). In our study, at a low MIA dose (1 mg), MMP-3 gene expression and protein production increased in the initial stages of the experiment. At higher MIA doses (2 and 3 mg), we observed either late or constant upregulation of MMP-3 at both the gene and protein levels. This result may indicate an important role for MMP-3 in advanced OA (in the later experimental days at higher MIA doses). At the low MIA dose (1 mg), MMP-3 might be involved in the early inflammatory state; however, the OA grade in this group was lower than that in the 2 or 3 mg MIA groups; therefore, the contribution of MMP-3 to OA development may not be significant.

The final investigated matrix metalloproteinase, collagenase MMP-13, is an enzyme that plays a pivotal role in OA progression (Neuhold et al., 2001). Its knockout in mice results in deceleration of OA progression (Wang et al., 2013) and reduction of arthritis-evoked inflammation and cartilage erosion (Singh et al., 2013). In experimental equine OA, MMP-13 was elevated in synovial fluid samples (Ma et al., 2017). MMP-13 inhibition reduces cartilage erosion in animal models of RA (Jüngel et al., 2010) and blocks type II collagen degradation in bovine explants and human OA cartilage (Piecha et al., 2010). Moreover, in the synovial fluid of OA and RA patients, the level of MMP-13 is reportedly increased (Andereya et al., 2006; Kim et al., 2011; Özler et al., 2016). Li et al. demonstrated that in human OA cartilage, MMP-13 is elevated and suppresses cell proliferation (Li et al., 2019). MMP-13 also promotes cartilage degeneration via histone deacetylase (HDAC), and HDAC7 inhibition diminishes MMP-13 expression in chondrocytes (Higashiyama et al., 2010). MMP-13 inhibition may therefore also show therapeutic potential for OA treatment (Li et al., 2011). In the current study, MMP-13 protein levels in synovial fluid were elevated throughout the entire experimental period in all groups. In joint tissues, an early increase was observed at a lower MIA dose, whereas 3 mg MIA treatment resulted in MMP-13 elevation in cartilage samples in the later OA stages. *Mmp-13* gene expression was more elevated in synovial membrane samples than in cartilage, with a similar pattern of changes (an early increase at lower MIA doses and a prolonged increase at the highest dose). As noted above, the synovial membrane plays the primary secretory role in the joint and is responsible for synovial fluid production. This may explain the more significant effects observed in the synovial membrane than cartilage in *Mmp-13* gene expression, as well as its protein abundance in synovial fluid. Our results suggest that MMP-13 plays an important role in OA development, since its protein level (functionally more important than gene expression changes) was elevated across all groups. In the 3 mg MIA group, MMP-13 levels were also increased in cartilage at the later stages of OA, indicating that the highest MIA dose causes severe OA-like lesions in a rat model.

It should be noted that OA triggers not only local changes but also broader changes in the nervous system (Murphy et al., 2012; Clauw and Hassett, 2017). Thakur et al. investigated the influence of 1 or 2 mg MIA treatment on changes in dorsal root ganglion cells in OA animals, demonstrating that ATF-3 (a sensitive marker of peripheral neuron stress/injury) signaling was increased in 2 mg MIA-treated animals than in a 1 mg MIA treatment group. 2 mg MIA injection also reduced intraepidermal nerve fiber density in plantar hind paw skin and produced spinal cord dorsal and ventral horn microgliosis, which was not observed in a 1 mg MIA group (Thakur et al., 2012). These data are consistent with our results and suggest that 2 mg MIA, in addition to cartilage degeneration, evokes significant biochemical changes not only locally in the joint but also in the nervous system, although 1 mg MIA is not sufficient to trigger such changes.

CONCLUSION

In conclusion, at the behavioral level, both 1 and 3 mg MIA treatment triggered similar effects. However, at the biochemical level, 2 and 3 mg MIA treatment showed comparable effects, while 1 mg appeared insufficient to trigger substantive OA-like changes at the molecular level in a rat OA model. In turn, 3 mg MIA treatment provided the most severe response with respect to both inflammatory factor and MMP release. Although many global investigators use an MIA animal model to study the therapeutic potential of various compounds, the MIA-induced OA model in rats has not previously been fully described in the literature. Our results indicate that 2 mg MIA may represent the "gold standard" treatment, as the lowest possible dose that effectively triggers OA but does not induce overly high inflammation. Our study fills in critical missing information regarding OA development and progression in a rat model.

DATA AVAILABILITY STATEMENT

The raw data supporting the conclusions of this article will be made available by the authors, without undue reservation.

ETHICS STATEMENT

The animal study was reviewed and approved by the Local Bioethics Committee of the Maj Institute of Pharmacology (Cracow, Poland) (approval numbers: 938/2012 and 125/2018).

AUTHOR CONTRIBUTIONS

Conceptualization, KS, MB, JC, and JM; methodology, MB, JC, JM, and MK; formal analysis, JC, MB, and MK; investigation, MB, JC, MK, and JM; writing—original draft preparation, MB; writing—review and editing, JC, KS, MB, and MK; visualization, MB and MK; supervision, KS; project administration, KS; funding acquisition, KS. All authors have read and agreed to the published version of the manuscript.

FUNDING

This work was supported by National Science Center, Poland by grant SONATABIS/NCN/2012/07/E/NZ7/01269, OPUS7 UMO-2014/13/B/NZ7/02311 and IF PAN statutory funds.

SUPPLEMENTARY MATERIAL

The Supplementary Material for this article can be found online at: https://www.frontiersin.org/articles/10.3389/fphar.2021.643605/full#supplementary-material

REFERENCES

Allen, J., Imbert, I., Havelin, J., Henderson, T., Stevenson, G., Liaw, L., et al. (2017). Effects of treadmill exercise on advanced osteoarthritis pain in rats. *Arthritis Rheumatol.* 69 (7), 1407–1417. doi:10.1002/art.40101

Alunno, A., Falcinelli, E., Luccioli, F., Petito, E., Bartoloni, E., Momi, S., et al. (2017). Platelets contribute to the accumulation of matrix metalloproteinase type 2 in synovial fluid in osteoarthritis. *Thromb. Haemost.* 117 (11), 2116–2124. doi:10.1160/TH17-06-0379

Andereya, S., Streich, N., Schmidt-Rohlfing, B., Mumme, T., Müller-Rath, R., and Schneider, U. (2006). Comparison of modern marker proteins in serum and synovial fluid in patients with advanced osteoarthrosis and rheumatoid arthritis. *Rheumatol. Int.* 26 (5), 432–438. doi:10.1007/s00296-005-0006-2

Baker, K., Grainger, A., Niu, J., Clancy, M., Guermazi, A., Crema, M., et al. (2010). Relation of synovitis to knee pain using contrast-enhanced MRIs. *Ann. Rheum. Dis.* 69 (10), 1779–1789. doi:10.1136/ard.2009.121426

Berlinberg, A., Ashbeck, E. L., Roemer, F. W., Guermazi, A., Hunter, D. J., Westra, J., et al. (2019). Diagnostic performance of knee physical exam and participant-reported symptoms for MRI-detected effusion-synovitis among participants with early or late stage knee osteoarthritis: data from the Osteoarthritis Initiative. *Osteoarthr. Cartilage* 27 (1), 80–89. doi:10.1016/j.joca.2018.09.004

Bryk, M., Chwastek, J., Kostrzewa, M., Mlost, J., Pędracka, A., and Starowicz, K. (2020). Alterations in anandamide synthesis and degradation during osteoarthritis progression in an animal model. *Int. J. Mol. Sci.* 21 (19), 1–19. doi:10.3390/ijms21197381

Chaplan, S. R., Bach, F. W., Pogrel, J. W., Chung, J. M., and Yaksh, T. L. (1994). Quantitative assessment of tactile allodynia in the rat paw. *J. Neurosci. Methods* 53 (1), 55–63. doi:10.1016/0165-0270(94)90144-9

Chu, X. Q., Wang, J. J., Dou, L. D., and Zhao, G. (2015). Cartilage oligomeric matrix protein and matrix metalloproteinase-3 expression in the serum and joint fluid of a reversible osteoarthritis rabbit model. *Genet. Mol. Res.* 14 (4), 14207–14215. doi:10.4238/2015.November.13.4

Clauw, D. J., and Hassett, A. L. (2017). The role of centralised pain in osteoarthritis. *Clin. Exp. Rheumatol.* 107 (5), 79–84.

Cui, N., Hu, M., and Khalil, R. A. (2017). Biochemical and biological attributes of matrix metalloproteinases. *Prog. Mol. Biol. Transl. Sci.* 147, 1–73. doi:10.1016/bs.pmbts.2017.02.005

DeGroot, J., Bank, R. A., Tchetverikov, I., Verzijl, N., and TeKoppele, J. M. (2002). Molecular markers for osteoarthritis: the road ahead. *Curr. Opin. Rheumatol.* 14 (5), 585–589. doi:10.1097/00002281-200209000-00019

Deshpande, B. R., Katz, J. N., Solomon, D. H., Yelin, E. H., Hunter, D. J., Messier, S. P., et al. (2016). Number of persons with symptomatic knee osteoarthritis in the US: impact of race and ethnicity, age, sex, and obesity. *Arthritis Care Res.* 68 (12), 1743–1750. doi:10.1002/acr.22897

Deuis, J. R., Dvorakova, L. S., and Vetter, I. (2017). Methods used to evaluate pain behaviors in rodents. *Front. Mol. Neurosci.* 10, 284. doi:10.3389/fnmol.2017.00284

Duerr, S., Stremme, S., Soeder, S., Bau, B., and Aigner, T. (2004). MMP-2/gelatinase A is a gene product of human adult articular chondrocytes and is increased in osteoarthritic cartilage. *Clin. Exp. Rheumatol.* 22 (5), 603–608.

Fotopoulos, V. C., Tzinia, A., Tzurbakis, M., Kalfakakou, V., Levidiotou-Stefanou, S., and Georgoulis, A. (2012). Expression levels of matrix metalloproteinase (MMP)-9 and its specific inhibitor TIMP-1, in septic and aseptic arthritis of the knee. *Knee Surg. Sports Traumatol. Arthrosc.* 20 (6), 1159–1167. doi:10.1007/s00167-011-1676-9

Georgiev, T., Ivanova, M., Kopchev, A., Velikova, T., Miloshov, A., Kurteva, E., et al. (2018). Cartilage oligomeric protein, matrix metalloproteinase-3, and Coll2-1 as serum biomarkers in knee osteoarthritis: a cross-sectional study. *Rheumatol. Int.* 38 (5), 821–830. doi:10.1136/annrheumdis-2018-eular.2939

Goldring, M. B., and Otero, M. (2011). Inflammation in osteoarthritis. *Curr. Opin. Rheumatol.* 23, 471. doi:10.1097/BOR.0b013e328349c2b1

Hannocks, M. J., Zhang, X., Gerwien, H., Chashchina, A., Burmeister, M., Korpos, E., et al. (2019). The gelatinases, MMP-2 and MMP-9, as fine tuners of neuroinflammatory processes. *Matrix Biol.* 75-76, 102–113. doi:10.1016/j.matbio.2017.11.007

Havelin, J., Imbert, I., Cormier, J., Allen, J., Porreca, F., and King, T. (2016). Central sensitization and neuropathic features of ongoing pain in a rat model of advanced osteoarthritis. *J. Pain* 17 (3), 374–382. doi:10.1016/j.jpain.2015.12.001

Haywood, A. R., Hathway, G. J., and Chapman, V. (2018). Differential contributions of peripheral and central mechanisms to pain in a rodent model of osteoarthritis. *Scientific Rep.* 8 (1). doi:10.1038/s41598-018-25581-8

Higashiyama, R., Miyaki, S., Yamashita, S., Yoshitaka, T., Lindman, G., Ito, Y., et al. (2010). Correlation between MMP-13 and HDAC7 expression in human knee osteoarthritis. *Mod. Rheumatol.* 20 (1), 11–17. doi:10.1007/s10165-009-0224-7

Jung, Y. O., Do, J. H., Kang, H. J., Yoo, S. A., Yoon, C. H., Kim, H. A., et al. (2006). Correlation of sonographic severity with biochemical markers of synovium and cartilage in knee osteoarthritis patients. *Clin. Exp. Rheumatol.* 24 (3), 253–259.

Jüngel, A., Ospelt, C., Lesch, M., Thiel, M., Sunyer, T., Schorr, O., et al. (2010). Effect of the oral application of a highly selective MMP-13 inhibitor in three different animal models of rheumatoid arthritis. *Ann. Rheum. Dis.* 69 (5), 898–902. doi:10.1136/ard.2008.106021

Kim, K. S., Choi, H. M., Lee, Y. A., Choi, I. A., Lee, S. H., Hong, S. J., et al. (2011). Expression levels and association of gelatinases MMP-2 and MMP-9 and collagenases MMP-1 and MMP-13 with VEGF in synovial fluid of patients with arthritis. *Rheumatol. Int.* 31 (4), 543–547. doi:10.1007/s00296-010-1592-1

Kim, Y. H., Kwon, H.-J., and Kim, D.-S. (2012). Matrix metalloproteinase 9 (MMP-9)-dependent processing of βig-h3 protein regulates cell migration, invasion, and adhesion. *J. Biol. Chem.* 287 (46), 38957–38969. doi:10.1074/jbc.m112.357863

Koskinen, A., Vuolteenaho, K., Nieminen, R., Moilanen, T., and Moilanen, E. (2011). Leptin enhances MMP-1, MMP-3 and MMP-13 production in human

osteoarthritic cartilage and correlates with MMP-1 and MMP-3 in synovial fluid from oa patients. *Clin. Exp. Rheumatol.* 29 (1), 57–64.

Kurzepa, J. M, A., Mądro, G., Kurzepa, J., Celiński, K., Kazmierak, W., et al. (2014). Role of MMP-2 and MMP-9 and their natural inhibitors in liver fibrosis, chronic pancreatitis and non-specific inflammatory bowel diseases. *Hepatobiliary Pancreatic Dis. Int.* 13 (6), 570–579. doi:10.1016/S1499-3872(14)60261-7

Lampropoulou-Adamidou, K., Lelovas, P., Karadimas, E. V., Liakou, C., Triantafillopoulos, I. K., Dontas, I., et al. (2014). Useful animal models for the research of osteoarthritis. *Eur. J. Orthop. Surg. Traumatol.*, 24, 263. doi:10.1007/s00590-013-1205-2

Le Bleu, H. K., Kamal, F. A., Kelly, M., Ketz, J. P., Zuscik, M. J., and Elbarbary, R. A. (2017). Extraction of high-quality RNA from human articular cartilage. *Anal. Biochem.* 518, 134–138. doi:10.1016/j.ab.2016.11.018

Lee, S. Y., Lee, S. H., Na, H. S., Kwon, J. Y., Kim, G. Y., Jung, K. A., et al. (2018). The therapeutic effect of STAT3 signaling-suppressed MSC on pain and articular cartilage damage in a rat model of monosodium iodoacetate-induced osteoarthritis. *Front. Immunol.* 9, 2881. doi:10.3389/fimmu.2018.02881

Li, H., Li, L., Min, J., Yang, H., Xu, X., Yuan, Y., et al. (2012). Levels of metalloproteinase (MMP-3, MMP-9), NF-kappaB ligand (RANKL), and nitric oxide (NO) in peripheral blood of osteoarthritis (OA) patients. *Clin. Lab.* 58 (7-8), 755–762. doi:10.7754/Clin.Lab.2011.110823

Li, N.-G., Shi, Z.-H., Tang, Y.-P., Wang, Z.-J., Song, S.-L., Qian, L.-H., et al. (2011). New hope for the treatment of osteoarthritis through selective inhibition of MMP-13. *Curr. Med. Chem.* 18 (7), 977–1001. doi:10.2174/092986711794940905

Li, Z., Yuan, B., Pei, Z., Zhang, K., Ding, Z., Zhu, S., et al. (2019). Circ_0136474 and MMP-13 suppressed cell proliferation by competitive binding to miR-127-5p in osteoarthritis. *J. Cell Mol. Med.* 23 (10), 6554–6564. doi:10.1111/jcmm.14400

Lipari, L., and Gerbino, A. (2013). Expression of gelatinases (MMP-2, MMP-9) in human articular cartilage. *Int. J. Immunopathol. Pharmacol.* 26 (3), 817–823. doi:10.1177/039463201302600331

Lockwood, S. M., Bannister, K., and Dickenson, A. H. (2019). An investigation into the noradrenergic and serotonergic contributions of diffuse noxious inhibitory controls in a monoiodoacetate model of osteoarthritis. *J. Neurophysiol.* 121 (1), 96–104. doi:10.1152/jn.00613.2018

Ma, T. W., Li, Y., Wang, G. Y., Li, X. R., Jiang, R. L., Song, X. P., et al. (2017). Changes in synovial fluid biomarkers after experimental equine osteoarthritis. *J. Vet. Res.* 61 (4), 503–508. doi:10.1515/jvetres-2017-0056

Mahmoud, R. K., El-Ansary, A. K., El-Eishi, H. H., Kamal, H. M., and El-Saeed, N. H. (2005). Matrix metalloproteinases MMP-3 and MMP-1 levels in sera and synovial fluids in patients with rheumatoid arthritis and osteoarthritis. *Ital. J. Biochem.* 54 (3-4), 248–257.

Malek, N., Mrugala, M., Makuch, W., Kolosowska, N., Przewlocka, B., Binkowski, M., et al. (2015). A multi-target approach for pain treatment. *Pain* 156 (5), 890–903. doi:10.1097/j.pain.0000000000000132

Martignetti, J. A., Aqeel, A. A., Sewairi, W. A., Boumah, C. E., Kambouris, M., Mayouf, S. A., et al. (2001). Mutation of the matrix metalloproteinase 2 gene (MMP2) causes a multicentric osteolysis and arthritis syndrome. *Nat. Genet.* 28 (3), 261–265. doi:10.1038/90100

Mathiessen, A., and Conaghan, P. G. (2017). Synovitis in osteoarthritis: current understanding with therapeutic implications. *Arthritis Res. Ther.* 19 (1), 18. doi:10.1186/s13075-017-1229-9

Mehana, E.-S. E., Khafaga, A. F., and El-Blehi, S. S. (2019). The role of matrix metalloproteinases in osteoarthritis pathogenesis: an updated review. *Life Sci.* 234, 116786. doi:10.1016/j.lfs.2019.116786

Mlost, J., Kostrzewa, M., Malek, N., and Starowicz, K. (2018a). Molecular understanding of the activation of CB1 and blockade of TRPV1 receptors: implications for novel treatment strategies in osteoarthritis. *Int. J. Mol. Sci.* 19 (2), 342. doi:10.3390/ijms19020342

Mlost, J., Wąsik, A., Michaluk, J. T., Antkiewicz-Michaluk, L., and Starowicz, K. (2018b). Changes in monoaminergic neurotransmission in an animal model of osteoarthritis: the role of endocannabinoid signaling. *Front. Mol. Neurosci.* 1, 466. doi:10.3389/fnmol.2018.00466

Mlost, J., Kostrzewa, M., Borczyk, M., Bryk, M., Chwastek, J., Korostyński, M., et al. (2021). CB2 agonism controls pain and subchondral bone degeneration induced by mono-iodoacetate: implications GPCR functional bias and tolerance development. *Biomed. Pharmacother.* 136, 111283. doi:10.1016/j.biopha.2021.111283

Mugnaini, C., Kostrzewa, M., Bryk, M., Mahmoud, A. M., Brizzi, A., Lamponi, S., et al. (2020). Design, synthesis, and physicochemical and pharmacological profiling of 7-Hydroxy-5-oxopyrazolo[4,3-b]pyridine-6-carboxamide derivatives with antiosteoarthritic activity in vivo. *J. Med. Chem.* 63 (13), 7369–7391. doi:10.1021/acs.jmedchem.0c00595

Murphy, S. L., Phillips, K., Williams, D. A., and Clauw, D. J. (2012). The role of the central nervous system in osteoarthritis pain and implications for rehabilitation. *Curr. Rheumatol. Rep.* 14 (6), 576–582. doi:10.1007/s11926-012-0285-z

Neuhold, L. A., Killar, L., Zhao, W., Sung, M. L., Warner, L., Kulik, J., et al. (2001). Postnatal expression in hyaline cartilage of constitutively active human collagenase-3 (MMP-13) induces osteoarthritis in mice. *J. Clin. Invest.* 107 (1), 35–44. doi:10.1172/JCI10564

Orr, C., Vieira-Sousa, E., Boyle, D. L., Buch, M. H., Buckley, C. D., Cañete, J. D., et al. (2017). Synovial tissue research: a state-of-the-art review. *Nat. Rev. Rheumatol.* 13 (8), 463–475. doi:10.1038/nrrheum.2017.115

McInnes, K., Aktaş, E., Atay, Ç., Yilmaz, B., Arikan, M., and Güngör, Ş. (2016). Serum and knee synovial fluid matrixmetalloproteinase-13 and tumor necrosis factor-alpha levels in patients with late stage osteoarthritis. *Acta Orthopaed. Traumatol. Turcica* 50 (6), 670–673. doi:10.1016/j.aott.2015.11.003

Pajak, A., Kostrzewa, M., Malek, N., Korostynski, M., and Starowicz, K. (2017). Expression of matrix metalloproteinases and components of the endocannabinoid system in the knee joint are associated with biphasic pain progression in a rat model of osteoarthritis. *J. Pain Res.* 10, 1973–1989. doi:10.2147/jpr.s132682

Piao, S., Du, W., Wei, Y., Yang, Y., Feng, X., and Bai, L. (2020). Protectin DX attenuates IL-1β-induced inflammation via the AMPK/NF-κB pathway in chondrocytes and ameliorates osteoarthritis progression in a rat model. *Int. Immunopharmacol.* 78, 106043. doi:10.1016/j.intimp.2019.106043

Piecha, D., Weik, J., Kheil, H., Becher, G., Timmermann, A., Jaworski, A., et al. (2010). Novel selective MMP-13 inhibitors reduce collagen degradation in bovine articular and human osteoarthritis cartilage explants. *Inflamm. Res.* 59 (5), 379–389. doi:10.1007/s00011-009-0112-9

Que, Q., Guo, X., Zhan, L., Chen, S., Zhang, Z., Ni, X., et al. (2019). The GLP-1 agonist, liraglutide, ameliorates inflammation through the activation of the PKA/CREB pathway in a rat model of knee osteoarthritis. *J. Inflammation* 16 (1), 13. doi:10.1186/s12950-019-0218-y

Radenkovic, S., Konjevic, G., Jurisic, V., Karadzic, K., Nikitovic, M., and Gopcevic, K. (2014). Values of MMP-2 and MMP-9 in tumor tissue of basal-like breast cancer patients. *Cell Biochem. Biophys.* 68 (1), 143–152. doi:10.1007/s12013-013-9701-x

Radosinska, J., Barancik, M., and Vrbjar, N. (2017). Heart failure and role of circulating MMP-2 and MMP-9. *Panminerva Med.* 59 (3), 241–253. doi:10.23736/S0031-0808.17.03321-3

Roemer, F. W., Guermazi, A., Felson, D. T., Niu, J., Nevitt, M. C., Crema, M. D., et al. (2011). Presence of MRI-detected joint effusion and synovitis increases the risk of cartilage loss in knees without osteoarthritis at 30-month follow-up: the MOST study. *Ann. Rheum. Dis.* 70 (10), 1804–1809. doi:10.1136/ard.2011.150243

Rousseau, J. Ch., and Garnero, P. (2012). Biological markers in osteoarthritis. *Bone* 51 (2), 265–277. doi:10.1016/j.bone.2012.04.001

Scanzello, C. R. (2017). Role of low-grade inflammation in osteoarthritis. *Curr. Opin. Rheumatol.* 29 (1), 79–85. doi:10.1097/BOR.0000000000000353

Scanzello, C. R., and Goldring, S. R. (2012). The role of synovitis in osteoarthritis pathogenesis. *Bone* 51 (2), 249–257. doi:10.1016/j.bone.2012.02.012

Singh, A., Rajasekaran, N., Hartenstein, B., Szabowski, S., Gajda, M., Angel, P., et al. (2013). Collagenase-3 (MMP-13) deficiency protects C57BL/6 mice from antibody-induced arthritis. *Arthritis Res. Ther.* 15 (6), R222. doi:10.1186/ar4423

Sun, S., Bay-Jensen, A. C., Karsdal, M. A., Siebuhr, A. S., Zheng, Q., Maksymowych, W. P., et al. (2014). The active form of MMP-3 is a marker of synovial inflammation and cartilage turnover in inflammatory joint diseases. *BMC Musculoskelet. Disord.* 15 (1), 93. doi:10.1186/1471-2474-15-93

Thakur, M., Rahman, W., Hobbs, C., Dickenson, A. H., and Bennett, D. L. (2012). Characterisation of a peripheral neuropathic component of the rat monoiodoacetate model of osteoarthritis. *PLoS One* 7 (3), e33730. doi:10.1371/journal.pone.0033730

Torres, L., Dunlop, D. D., Peterfy, C., Guermazi, A., Prasad, P., Hayes, K. W., et al. (2006). The relationship between specific tissue lesions and pain severity in

persons with knee osteoarthritis. *Osteoarthr Cartil* 14 (10), 1033–1040. doi:10.1016/j.joca.2006.03.015

Vina, E. R., and Kwoh, C. K. (2018). Epidemiology of osteoarthritis: literature update. *Physiol. Behav.* 30 (2), 160–167. doi:10.1097/bor.0000000000000479

Visse, R., and Nagase, H. (2003). Matrix metalloproteinases and tissue inhibitors of metalloproteinases: structure, function, and biochemistry. *Circ. Res.* 92 (8), 827–839. doi:10.1161/01.RES.0000070112.80711.3D

Wang, C., Chi, Q., Xu, C., Xu, K., Zhang, Y., Liu, Y., et al. (2019). Expression of LOXs and MMP-1, 2, 3 by ACL fibroblasts and synoviocytes impact of coculture and TNF-α. *J. Knee Surg.* 32 (4), 352–360. doi:10.1055/s-0038-1641592

Wang, M., Sampson, E. R., Jin, H., Li, J., Ke, Q. H., Im, H. J., et al. (2013). MMP13 is a critical target gene during the progression of osteoarthritis. *Arthritis Res. Ther.* 15 (1), R5. doi:10.1186/ar4133

Wojdasiewicz, P., Poniatowski, Ł. A., and Szukiewicz, D. (2014). The role of inflammatory and anti-inflammatory cytokines in the pathogenesis of osteoarthritis. *Mediators Inflamm.* 2014, 1–19. doi:10.1155/2014/561459

Xue, M., McKelvey, K., Shen, K., Minhas, N., March, L., Park, S. Y., et al. (2014). Endogenous MMP-9 and not MMP-2 promotes rheumatoid synovial fibroblast survival, inflammation and cartilage degradation. *Rheumatology (Oxford)* 53 (12), 2270–2279. doi:10.1093/rheumatology/keu254

Zeng, G. Q., Chen, A. B., Li, W., Song, J. H., and Gao, C. Y. (2015). High MMP-1, MMP-2, and MMP-9 protein levels in osteoarthritis. *Genet. Mol. Res.* 14 (4), 14811–14822. doi:10.4238/2015.November.18.46

Zhou, M., Qin, S., Chu, Y., Wang, F., Chen, L., and Lu, Y. (2014). Immunolocalization of MMP-2 and MMP-9 in human rheumatoid synovium. *Int. J. Clin. Exp. Pathol.* 7 (6), 3048–3056.

Živanović, S., Rackov, L. P., Živanović, A., Jevtić, M., Nikolić, S., and Kocić, S. (2011). Cartilage oLIGOMERIC mATRIX pROTEIN - inflammation biomarker in knee osteoarthritis. *Bosnian J. Basic Med. Sci.* 11 (2), 27. doi:10.17305/bjbms.2011.2619

Conflict of Interest: The authors declare that the research was conducted in the absence of any commercial or financial relationships that could be construed as a potential conflict of interest.

frontiers in Pharmacology

ORIGINAL RESEARCH
published: 29 April 2021
doi: 10.3389/fphar.2021.673831

MMP24 Contributes to Neuropathic Pain in an FTO-Dependent Manner in the Spinal Cord Neurons

Longfei Ma[1†], Yangyuxin Huang[1†], Fengjiang Zhang[1†], Dave Schwinn Gao[1], Na Sun[1], Jinxuan Ren[1], Suyun Xia[1], Jia Li[1], Xinyi Peng[1], Lina Yu[1], Bao-Chun Jiang[2] and Min Yan[1]**

[1]Department of Anesthesiology, Second Affiliated Hospital of Zhejiang University School of Medicine, Hangzhou, China, [2]Institute of Pain Medicine and Special Environmental Medicine, Nantong University, Nantong, China

Nerve injury-induced gene expression change in the spinal cord is critical for neuropathic pain genesis. RNA N^6-methyladenosine (m^6A) modification represents an additional layer of gene regulation. We showed that spinal nerve ligation (SNL) upregulated the expression of matrix metallopeptidase 24 (MMP24) protein, but not *Mmp24* mRNA, in the spinal cord neurons. Blocking the SNL-induced upregulation of spinal MMP24 attenuated local neuron sensitization, neuropathic pain development and maintenance. Conversely, mimicking MMP24 increase promoted the spinal ERK activation and produced evoked nociceptive hypersensitivity. Methylated RNA Immunoprecipitation Sequencing (MeRIP-seq) and RNA Immunoprecipitation (RIP) assay indicated the decreased m^6A enrichment in the *Mmp24* mRNA under neuropathic pain condition. Moreover, fat-mass and obesity-associated protein (FTO) was colocalized with MMP24 in spinal neurons and shown increased binding to the *Mmp24* mRNA in the spinal cord after SNL. Overexpression or suppression of FTO correlates with promotion or inhibition of MMP24 expression in cultured spinal cord neurons. In conclusion, SNL promoted the m^6A eraser FTO binding to the *Mmp24* mRNA, which subsequently facilitated the translation of MMP24 in the spinal cord, and ultimately contributed to neuropathic pain genesis.

Keywords: neuropathic pain, matrix metallopeptidase 24, fat-mass and obesity-associated protein, N6-methyladenosine, spinal cord

OPEN ACCESS

Edited by:
Serena Boccella, University of Campania Luigi Vanvitelli, Italy

Reviewed by:
Yuan-Xiang Tao, Rutgers, The State University of New Jersey, United States
Tzer-Bin Lin, Taipei Medical University, Taiwan

****Correspondence:***
Bao-Chun Jiang
jiangbaochun@ntu.edu.cn
Min Yan
zryanmin@zju.edu.cn

[†]These authors have contributed equally to this work and share first authorship

Specialty section:
This article was submitted to Inflammation Pharmacology, a section of the journal Frontiers in Pharmacology

Received: *28 February 2021*
Accepted: *06 April 2021*
Published: *29 April 2021*

Citation:
Ma L, Huang Y, Zhang F, Gao DS, Sun N, Ren J, Xia S, Li J, Peng X, Yu L, Jiang B and Yan M (2021) MMP24 Contributes to Neuropathic Pain in an FTO-Dependent Manner in the Spinal Cord Neurons. Front. Pharmacol. 12:673831. doi: 10.3389/fphar.2021.673831

INTRODUCTION

Nerve injury-induced neuropathic pain is a refractory and debilitating disease (Mitka, 2003). Limited treatments are available for this disorder because most therapies work only symptomatically via neurotransmission blockade but ignore the underlying pain pathogenesis and its phasic progression. The development of more efficient treatment of this disease comes to a standstill due to our incomplete understanding of mechanisms underlying the neuropathic pain induction and maintenance (Ji et al., 2009). Abnormal gene expression changes in the dorsal root ganglion (DRG) and spinal cord are the crucial molecular basis for developing and maintaining neuropathic pain (Jiang et al., 2016; Pokhilko et al., 2020).

Epigenetic processes, such as DNA methylation, histone modifications, and non-coding RNAs, frequently regulate pain-related gene expression (Jiang et al., 2018; Wu et al., 2019; Lin et al., 2020). RNA methylation mediated RNA post-transcriptional modification has recently been emphasized as a significant epigenetic modification (He and He, 2021). N6-methyladenosine (m^6A) is the most prevalent and dynamic modification in mRNA with a preference for the 3′-untranslated region (3′-

UTR) and the transcription starting site (Dominissini et al., 2012; Meyer et al., 2012; Fu et al., 2014). m^6A is installed by "writer" complex composed of methyltransferase-like 14 (METTL14), methyltransferase-like 3 (METTL3) and Wilms' tumor 1-associating protein (WTAP), and removed by "eraser" demethylases fat-mass and obesity-associated protein (FTO) and AlkB homolog 5 (ALKBH5) (Dominissini et al., 2012; Zheng et al., 2013; Fu et al., 2014; Liu et al., 2015). This modification is recognized by m^6A-binding proteins (Dominissini et al., 2012; Fu et al., 2014; Liu et al., 2015) to mediate various mRNA biogenesis, such as RNA stability, translation, splicing and export (Yang et al., 2018). In particular, recent evidence revealed that neuropathic pain could be partially attributed to the methyltransferases/demethylases-induced RNA m^6A modification dysregulation of pain-associated genes in the DRG (Li et al., 2020; Albik and Tao, 2021). However, the role of spinal m^6A modification in the neuropathic pain genesis remains largely unknown.

Increasing evidence suggests that proteases such as matrix metalloproteases (MMPs), caspases, and cathepsin S play a vital role in the genesis of neuropathic pain by regulating neuroinflammation in the central nervous system (Ji et al., 2009; Hannocks et al., 2019; Jiang et al., 2020a), through the cleavage of the extracellular matrix proteins, chemokines, and cytokines (Manicone and McGuire, 2008). The MMP family includes more than 20 members. Among them, MMP2 and MMP9 are involved in the regulation of neuropathic pain during the early and late phase, respectively, through the cleavage/activation of interleukin 1 beta (IL-1β) in the extracellular matrix and subsequent phosphorylation of extracellular signal-regulated kinase 1/2 [pERK1/2, a marker for spinal neuron hyper-sensitization (Zhuang et al., 2005)] (Kawasaki et al., 2008). MMP24 is abundantly expressed throughout the nervous system (Hayashita-Kinoh et al., 2001) and could degrade several extracellular matrix components, including cell-adhesion molecule N-cadherin to promote neurite outgrowth in cultured cells (Hayashita-Kinoh et al., 2001). Mouse strain lacking in MMP24 was found absent of thermal hyperalgesia with inflammation model (Folgueras et al., 2009). However, whether MMP24 in the spinal cord participates in the development or maintenance of neuropathic pain is still elusive.

Here, we report that spinal nerve ligation (SNL) leads to a significant increase in the level of MMP24 protein, but not *Mmp24* mRNA, in the spinal cord. This increase contributes to the SNL-induced neuropathic pain induction and maintenance, possibly by the activation of ERK1/2. Mechanistically, SNL promoted FTO binding to the *Mmp24* mRNA for the erasure of m^6A enrichment and possibly accelerated the *Mmp24* mRNA translation in the spinal cord.

MATERIALS AND METHODS

Animals

Male C57BL/6J mice (6–8 weeks old for *in vivo* experiments) were purchased from SLAC Laboratory (Shanghai, CN). Rodents were hosted in a centralized location in the Second Affiliated Hospital of Zhejiang University (SAHZU), School of Medicine, with a standardized circadian cycle with 12 h of light and darkness. Mouse chow and water were provided, ad libitum. All experiments were approved by the Zhejiang Animal Care and Use Committee and the Ethics Committee of SAHZU, School of Medicine. Utmost care was taken to ensure the welfare of the rodents and kept their usage to a minimum. Behavioral experiments were undertaken with blinded investigators, with no knowledge of the viral content or other preparatory conditions.

Animal Model

L4 spinal nerve ligation (SNL) was carried out according to the methods previously described (Decosterd and Woolf, 2000; Wang and Wang, 2003; Rigaud et al., 2008). In brief, mice were anesthetized with Nembutal. The lower back was dissected until the transverse lumbar process was exposed. After the process was removed, the underneath L4 spinal nerve was ligated with a silk 6–0 thread. A slight distal location was chosen for transection around the ligation site. Subsequent layers of muscle and skin were closed. The sham groups undertook identical procedures, but without the transection or ligature of the corresponding nerve.

Behavioral Tests

Mechanical and thermal pain tests along with locomotor function assessments were performed as described in the previous studies (He et al., 2011; Zhao et al., 2013; Daskalaki et al., 2018). Each behavioral test was carried out at 1 h interval.

Paw withdrawal frequencies (PWF) were defined as a response to physical stimulation via von Frey filaments. In short, the animal was introduced to an individual Plexiglas chamber on an elevated mesh screen. Two calibrated von Frey filaments (0.07 and 0.4 g) (DanMic Global. Campbell, CA) were utilized to stimulate the hind paw for ~1 s and the hind paw was stimulated repeatedly 10 times at 5 min interval. Paw withdrawal responses were aggregated, averaged over the number of trials, and calculated in percentage, which resulted in the PWF ((number of paw withdrawals/10 trials) × 100 = % response frequency).

A Model 336 Analgesia Meter (IITC Inc. Life Science Instruments. Woodland Hills, CA) was utilized to measure paw withdrawal latencies (PWL) to the noxious application of heat. In short, the rodent was introduced to an individual Plexiglas chamber on a glass plate. The analgesic meter's light emitter beamed through a keyhole onto the hind paw's plantar surface, with the stimuli switched off upon paw withdrawal. The paw withdrawal latency was logged, defined as time passed between initiation of the stimuli to paw withdrawal. Five trials were undertaken with an interval of 5 min each. 20 s cut-off limit was defined to eliminate any tissue injury.

Locomotor function tests the righting, grasping, and placing reflexes after PWF and PWL. Righting reflex: rodent placed supine on a flat surface, the time it takes to upright itself to a normal position was recorded. Grasping reflex: rodent placed on a meshed wire, any contact or grasp of the wire was recorded.

Placing reflex: rodent placed on the edge of a surface with the hind leg in a lower position than forelimbs, while leaving hindlimbs just off contact with the edge of a platform, and recorded whether hind paws reflexively placed on the platform. Each trial was repeated at a 5 min interval five times and the scores for each reflex were recorded on the basis of counts of each normal reflex.

Intraspinal and Intrathecal Injection

The intraspinal injection was performed as described previously (Jiang et al., 2016). In short, after anesthetized with Nembutal, mice underwent hemilaminectomy at the L1-L2 vertebral segments. The intraspinal injection was carried out ipsilaterally on the left side. By using a glass micropipette, each animal received two injections (5×10^5 TU per injection, 0.8 mm from the midline, 0.5 mm apart in rostrocaudal axis, 0.5 mm deep) of lentivirus following the L3-L4 dorsal root entry zone after exposure of spinal cord. The tip of glass micropipette should reach a depth of lamina II-IV of the spinal cord. Finally, the dorsal muscle and skin were sutured layer by layer.

Intrathecal injection of siRNA (20 μM, 10 μL) was performed daily for two to three consecutive days in sham or SNL mice. Mice were held firmly in place over the pelvic girdle and between L5 and L6 vertebrae inserted a 30-gauge needle attached to a 25 μL microsyringe. A slight flick of the tail after a sudden advancement of the needle confirmed the proper insertion of the needle into the subarachnoid space (Jiang et al., 2016). TurboFect *in vivo* transfection reagent (Thermo Fisher, R0541) was used to improve delivery and prevent siRNA degradation. *Mmp24* siRNA1 (sense: 5′-GAG AUU CGU CUU CUU CAA ATT-3′, antisense: 5′-UUU GAA GAA GAC GAA UCU CTT-3′), *Mmp24* siRNA2 (sense: 5′-GGA UAU UAC ACC UAC UUC UTT-3′, antisense: 5′-AGA AGU AGG UGU AAU AUC CTT-3′), *Mmp24* siRNA3 (sense: 5′-CUA UCU UCC AAU UCA AGA ATT-3′, antisense: 5′-UUC UUG AAU UGG AAG AUA GTT-3′).

Spinal Dorsal Horn Neuron Culture and Viral Transduction

Primary spinal neuronal cultures were prepared from 1 to 2 week old C57BL/6J mice using a procedure modified from our previously described method (Jiang et al., 2016). In short, a laminectomy was conducted and the spinal cord was carefully removed after decapitation. Superficial dorsal horn was isolated and then cut into several strips. The strips were incubated at 37°C for 45 min in Hanks' balanced salt solution (HBSS, Invitrogen) containing papain (15 U/ml, Worthington Biochemical), then rinsed 3 times with HBSS, and placed in mixed Neurobasal Medium (Invitrogen) containing 5% fetal bovine serum (FBS, Invitrogen), heat-inactivated horse serum (5%, Invitrogen), B-27 (1%, Invitrogen), L-glutamax-1 (2 mM, Invitrogen), streptomycin (100 μg/ml, Invitrogen) and penicillin (100 U/ml, Invitrogen). A Fire-polished Pasteur pipette was used to dissociate fragments by gentle trituration mechanically. The resulting cell suspension was plated onto 6-well plates coated with poly-D-lysine and collagen. The cells were incubated at 37°C with 95% O_2, 5% CO_2. After the neurons were treated with cytosine arabinoside, 2–10 μL virus (titer $\geq 1 \times 10^{13}$) was added to each well. The neurons were collected 3 days after virus transduction.

TABLE 1 | Primers sequence for qRT-PCR or RIP-PCR.

Gene	Sequences	Size
Mmp24	F 5′-TGACCCCAGTGCTATCATGG-3′ R 5′-TCTCAGATGGCGAGTGGATC-3′	176 bp
Fto	F 5′-GTGAGGACGAGTCCAGCTTC-3′ R 5′-AGGTGCCTGTTGAGCACTCT-3′	225 bp
Mettl3	F 5′-AAGGAGCCGGCTAAGAAGTC-3′ R 5′-TCACTGGCTTTCATGCACTC-3′	248 bp
Mettl14	F 5′- TGAGAGTGCGGATAGCATTG-3′ R 5′-TCTCTTCCTCCTGCTGCATT-3′	200 bp
Alkbh5	F 5′-GGAACCTGTGCTTTCTCTGC-3′ R 5′-TGCTCAGGGATTTTGTTTCC-3′	176 bp
Wtap	F 5′-GCAAGAGTGCACCACTCAAA-3′ R 5′-CATTTTGGGCTTGTTCCAGT-3′	161 bp
Tuba1a	F 5′-GTGCATCTCCATCCATGTTG-3′ R 5′-GTGGGTTCCAGGTCTACGAA-3′	210 bp

Reverse Transcription (RT)-PCR

Total RNA from the cultured samples or tissue was extracted and purified using miRNeasy kit with genome DNA Eliminator Columns (QIAGEN, Germany). The SuperScript™ First-Strand Synthesis System (Invitrogen/Thermo Fisher) was then used to reverse-transcribe RNA. Each sample was run in a 20 μL reaction with 20 ng cDNA, 10 μL SsoAdvanced Universal SYBR Green Supermix (Bio-Rad Laboratories, CA) and 250 nM forward and reverse primers. *Tuba1a* was used as an internal control for normalization. Real-time PCR was performed on the Applied Biosystems QuantStudio5 system (Applied Biosystems, CA). ΔCt method ($2^{-\Delta\Delta Ct}$) was applied for mRNA levels calculation. All data were normalized to *Tuba1a*, which has been demonstrated to be stable even after peripheral nerve injury insult (Zhao et al., 2013; Wu et al., 2016). All the primers are listed in **Table 1**.

Plasmids Construction and Virus Production

The *Mmp24* and *Fto* coding sequences were synthesized by Tsingke Biological Technology (Beijing, CN), and were further inserted into pro-viral plasmids pLV-CMV-MCS-Ubi-ZSGreen and pAAV-CMV-MCS-F2A-EGFP, respectively, using the Seamless Cloning and Assembly Kit (SunBio, CN). pLV-CMV-ZSGreen or pAAV-CMV-EGFP was used as the corresponding control (SunBio, CN). Lentiviruses and adeno-associated viruses packaging were completed by the Tsingke Biological Technology (Beijing, CN) and Sunbio Technology (Shanghai, CN). The *Fto* coding region's shRNA (GenBank accession number NM_011936.2) was designed to target the sequence 5′-GTC TCG TTG AAA TCC TTT GAT-3′. A scramble shRNA was used as control (5′-TTC TCC GAA CGT GTC ACG T-3′). Both *Fto* and scrambled shRNA oligonucleotides were inserted to pAAV-CAG-EGFP-U6-shRNA and packaged into adeno-associated virus by SunBio. All the constructs were sequenced to prove sequence integrity.

Immunohistochemistry

After anesthetized with Nembutal, mice were perfused with cold PBS and 4% paraformaldehyde through the ascending aorta. Following perfusion, the L4 spinal cord segments were removed, post-fixed in the same fixative at 4°C overnight and dehydrated. Spinal cord sections (25 μm) were cut in a cryostat and processed for immunofluorescence. The sections were blocked for 1 h at room temperature in PBS containing 5% goat or donkey serum and then incubated overnight at 4°C with the following primary antibodies: mouse anti-FTO (1:100, Abcam), rabbit anti-MMP24 (1:100, Affinity), mouse anti-NeuN (1:500, Abcam), rabbit anti-NeuN (1:500, Abcam), mouse anti-GFAP (1:500, EMD Millipore), rabbit anti-GFAP (1:500, Abcam), mouse anti-IBA1 (1:200, Sigma), rabbit anti-IBA1 (1:200, Wako). After wash, the sections were then incubated with corresponding second antibodies with either Alexa FluorTM 488- or Alexa FluorTM 594-labeled (1:500, Invitrogen) at room temperature for 1 h. 4′, 6-diamidino-2-phenylindole (DAPI) (Abcam) was finally utilized for slides mounting. Leica DMI4000 fluorescence microscope was used for immunofluorescence-labeled image examination (Leica, Germany).

Western Blotting

Cytosolic and nuclear proteins were extracted from the L4 spinal cord as previous study (Zhao et al., 2017). Ice-cold lysis buffer was utilized for the tissue homogenization, which contained 10 mM Tris, 5 mM EGTA, 2 mM $MgCl_2$, 1 mM DTT, 1 mM phenylmethylsulfonyl fluoride, and 40 μM leupeptin. After centrifugation (4°C, 15 min, 1,500 g), the supernatants were gathered for cytosolic proteins and the pellets for nuclear proteins. The protein sample concentration was measured using Detergent Compatible Bradford Protein Assay Kit (Beyotime, CN). After heated at 99°C for 5 min, the samples were loaded onto an SDS-polyacrylamide gel (Genshare Biology, CN) and then electrophoretically transferred onto a polyvinylidene fluoride membrane (Millipore, Burlington, MA, United States). The membranes were blocked with 5% nonfat milk TBST for 1 h and then incubated overnight with the following antibodies: mouse anti-FTO antibody (1:1,000, Abcam), rabbit anti-METTL3 antibody (1:1,000, Abcam), rabbit anti-METTL14 antibody (1:1,000, Proteintech), rabbit anti-ALKBH5 antibody (1:1,000, Abcam), mouse anti-WTAP antibody (1:100, Santa Cruz), rabbit anti-MMP24 antibody (1:1,000, Affinity), mouse anti-histone H3 (1:3,000, Santa Cruz), mouse anti-GAPDH (1:1,000, Zhongshan Golden Bridge Biotechnology), rabbit anti-phospho-ERK1/2 (Thr202/Thy204, 1:2,000, CST), rabbit anti-ERK1/2 (1:2,000, CST). Horseradish peroxidase-conjugated anti-mouse or rabbit secondary antibody (1:5,000, Jackson ImmunoResearch) were utilized for protein detection and Clarity Western ECL Substrate (EMD Millipore) for visualization and ChemiDoc XRS + System (Bio-Rad) for exposure. NIH ImageJ software was utilized for quantification of the intensity of blots with densitometry. After each was normalized to the corresponding GAPDH or histone H3 (for nucleus proteins), the relative density values of the treated groups or different time points were determined by dividing the optical density values from these groups by the average value of the naïve/control groups.

RNA Immunoprecipitation Assay

Magna RIP Kit (EMD Millipore, Darmstadt, Germany) was used for the RNA Immunoprecipitation (RIP) assay. The spinal cord homogenates were suspended in the RIP lysis buffer containing RNase inhibitor and protease inhibitor cocktail. The RIP lysate was incubated on ice for 5 min and kept in −80°C. Use the RIP wash buffer to wash Magnetic Beads Protein A/G suspension for each IP. Magnetic Beads Protein A/G re-suspended in RIP wash buffer were incubated with Mouse anti-FTO antibody (4 μg; Santa Cruz), mouse anti-m^6A antibody (4 μg; Abcam), or normal mouse IgG for 30 min at room temperature. The Beads Protein A/G-antibody complexes were re-suspended into the RIP immunoprecipitation buffer after being washed three times with RIP wash buffer. The RIP lysate supernatants were incubated with beads-antibody complex in the RIP buffer overnight at 4°C by rotating after being thawed and centrifuged at 14,000 rpm for 10 min at 4°C. RIP wash buffer was used to wash the samples six times. After incubating the beads in the proteinase K buffer at 55°C for 30 min by shaking, the RNA was eluted and purified by phenol/chloroform extraction from the beads. The RNA enrichment was analyzed by quantitative real-time PCR. The RIP lysate supernatant was used as input. All primers are listed in **Table 1**.

Methylated RNA Immunoprecipitation Sequencing (MeRIP-Seq) and MeRIP-Seq Libraries

Following the manufacturer's procedure, Trizol reagent (Invitrogen, CA, United States) was used to extract total RNA. Bioanalyzer 2,100 and RNA 6,000 Nano LabChip Kit (Agilent, CA, United States) were utilized to analyze the total RNA quality and quantity with RIN number >7.0. To isolate Poly (A) mRNA, nearly more than 200 ug of total RNA were gathered and mixed with poly-T oligo attached magnetic beads (Invitrogen). After purification, divalent cations were applied to fragment the poly(A) mRNA fractions into 50–150 nt oligonucleotides under elevated temperature. The cleaved RNA fragments were then incubated in IP buffer (0.5% Igepal CA-630, 50 mM Tris-HCl and 750 mM NaCl) supplemented with BSA (0.5 μg/μL) for 2 h at 4°C with m^6A-specific antibody (No.202003, Synaptic Systems, Germany). The mixture was then incubated together with protein-A beads and eluted with elution buffer (6.7 mM m^6A and 1 × IP buffer). 75% ethanol was used to precipitate the eluted RNA. In conformity to a strand-specific library preparation by dUTP method, untreated input control fragments and eluted m^6A-containing fragments (IP) are converted to the final cDNA library. The average insert size for the paired-end libraries was ~100 bp. Following the vendor's recommended protocol, the paired-end 2 × 100 bp sequencing was then carried out on an Illumina Novaseq™ 6,000 platform at the LC-BIO Bio-tech Ltd. (Hangzhou, CN).

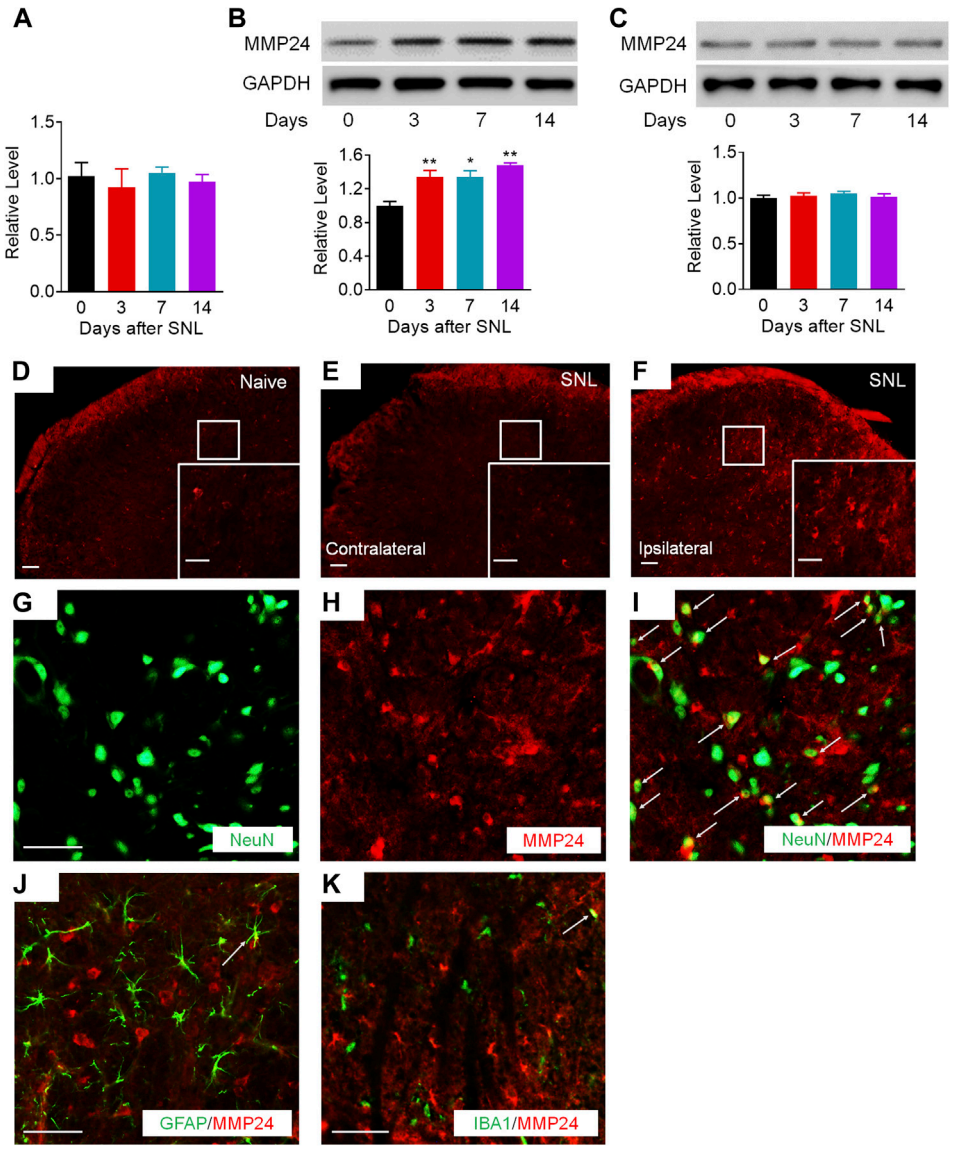

FIGURE 1 | MMP24 protein is increased in the spinal cord after SNL **(A)**. Expression of *Mmp24* mRNA after SNL. $n = 4$ mice/group/time point. **(B)**. Expression of MMP24 protein in the spinal cord after SNL surgery. $n = 3$–6 mice/time point. One-way ANOVA followed by *post hoc* Tukey test. $F_{time}(3, 8) = 29.00$. $^{*}p < 0.05$, $^{**}p < 0.01$ vs. the corresponding control group (0 day). **(C)**. Expression of MMP24 protein in the spinal cord after sham surgery. $n = 3$ mice/time point. **(D–F)**. Representative images of MMP24 immunofluorescence in the L4 dorsal horn. MMP24 immunoreactivity was low in naïve mice, but increased in the ipsilateral dorsal horn compared with the contralateral dorsal horn 7 days after SNL. Scale bar: 50 μm; 25 μm (insets). **(G–K)**. Double staining of MMP24 and markers of neuron, astrocytes, and microglia on day 14 after SNL. Scale bar: 50 μm.

Firstly, to remove the reads that contained adaptor contamination, undetermined bases and low-quality bases, in-house Perl scripts and Cutadapt (Kechin et al., 2017) were applied. By using FastQC (http://www.bioinformatics.babraham.ac.uk/projects/fastqc/), the sequence quality was further validated. To map reads, bowtie (Langmead and Salzberg, 2012) were utilized to reference genome with default parameters. Mapped reads are then provided as input for MACS2 (Zhang et al., 2008), which helps to identify m^6A peaks that can be adapted for visualization on the UCSC genome browser. *De novo* motif finding is carried out by using MEME (Bailey et al., 2009), followed by localization of the motif in respect of peak summit by in-house Perl scripts. By using ChIPseeker (Yu et al., 2015), called peaks are annotated by the intersection with gene architecture. MeRIP-seq data files were submitted to the GEO repository through the access code: GSE171004.

Statistical Analysis

The cells were suspended evenly and dispersed randomly in each well for *in vitro* trials. The animals were randomly distributed into various treatment groups for *in vivo* experiments. All of the results

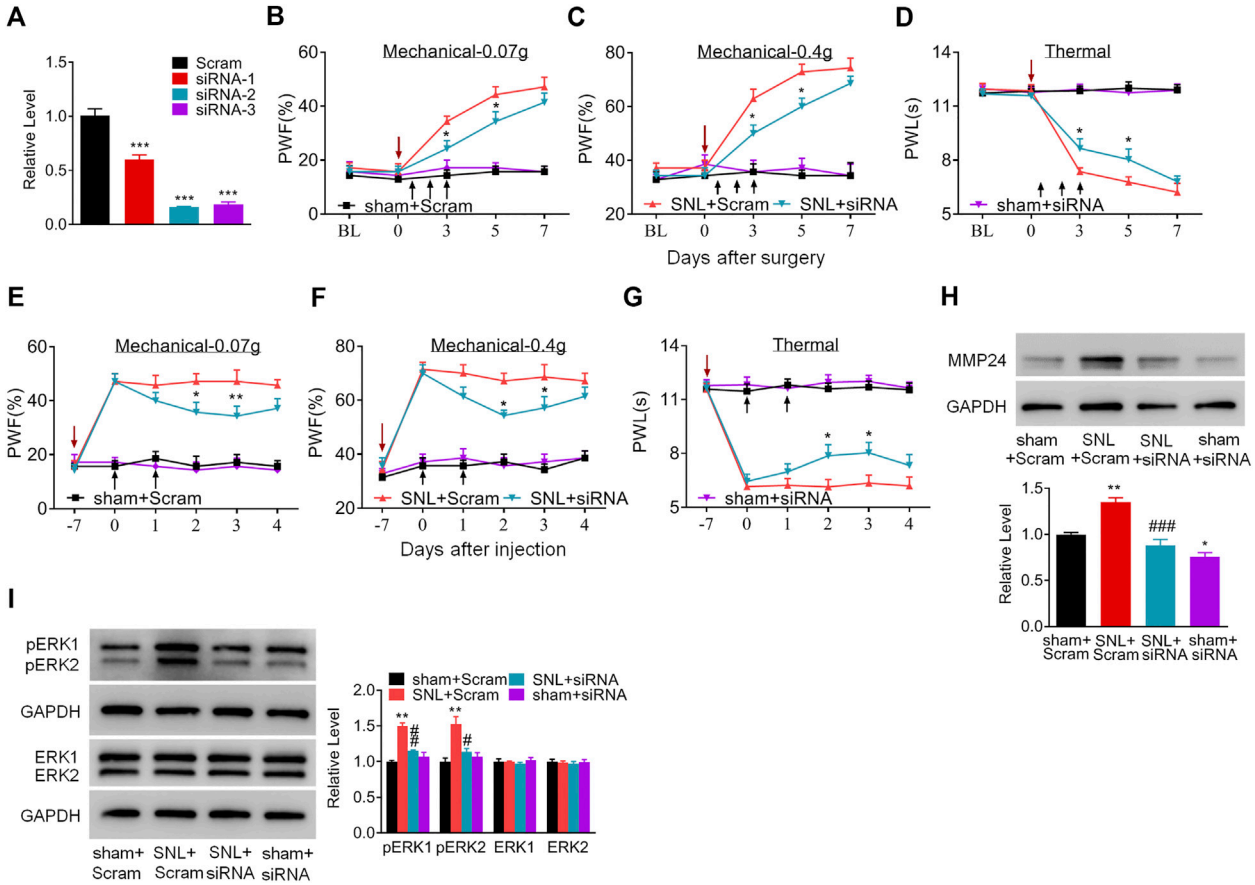

FIGURE 2 | Blocking the increased spinal MMP24 attenuates SNL-induced pain hyperalgesia **(A)**. Effect of three *Mmp24* siRNAs on the expression of *Mmp24* mRNA, among which siRNA-2 shows the best knockdown effect in the cultured spinal cord cells. $n = 3$ repeats, One-way ANOVA followed by *post hoc* Tukey test. F_{group} (3, 8) = 92.87, $^{***}p < 0.001$ vs. scrambled siRNA (Scram) group. **(B–D)**. Effect of intrathecal injection of *Mmp24* siRNA (siRNA) or control scrambled siRNA (Scram) into the sham or SNL mice on the paw withdrawal responses to mechanical **(B, C)** and heat stimuli **(D)** from day 3 to 7 after SNL as indicated. $n = 7$ mice/group. Two-way RM ANOVA followed by *post hoc* Tukey test. F_{group} (3, 90) = 48.41 for **(B)**, F_{group} (3, 90) = 58.89 for **(C)**, F_{group} (3, 90) = 120.0 for **(D)**. $^{*}p < 0.05$ vs. the SNL plus Scram group. The red arrow indicates surgery day and black arrow indicates siRNA intrathecal injection. **(E–G)**. Effect of intrathecal injection of *Mmp24* siRNA (siRNA) or control scrambled siRNA (Scram) into the sham or SNL mice on the paw withdrawal responses to mechanical **(E, F)** and heat stimuli **(G)** 7 days after SNL as indicated. $n = 7$ mice/group. Two-way RM ANOVA followed by *post hoc* Tukey test. F_{group} (3, 90) = 53.66 for **(E)**, F_{group} (3, 90) = 61.53 for **(F)**, F_{group} (3, 90) = 136.7 for **(G)**. $^{*}p < 0.05$, $^{**}p < 0.01$ vs. the SNL plus Scram group. The red arrow indicates surgery day and black arrow indicates siRNA intrathecal injection. **(H)**. MMP24 protein expression in the spinal cord of sham or SNL mice intrathecally injected with *Mmp24* siRNA (siRNA) or scrambled siRNA (Scram) on day 10 after SNL (2 days after the last siRNA injection). $n = 3$ mice/group. One-way ANOVA followed by *post hoc* Tukey test. F_{group} (3, 8) = 29.00, $^{*}p < 0.05$, $^{**}p < 0.01$ vs. sham plus Scram group. $^{\#\#\#}p < 0.001$ vs. SNL plus Scram group. **(I)**. Effect of *Mmp24* siRNA or scrambled siRNA on SNL-induced increase in the phosphorylation of ERK1/2 in the spinal cord on day 10 after SNL or sham surgery (2 days after the last siRNA injection). $n = 3$ mice/group. One-way ANOVA followed by *post hoc* Tukey test. F_{group} (3, 8) = 29.00 for pERK1, F_{group} (3, 8) = 11.72 for pERK2. $^{**}p < 0.01$ vs. the sham plus Scram group; $^{\#}p < 0.05$, $^{\#\#}p < 0.01$ vs. the SNL plus Scram group.

were specified as mean ± SEM. For the biochemical results, two-tailed, unpaired Student's *t*-test (two groups) and one-way ANOVA (> 2 groups) were utilized for the data analyses. For the behavioral results, two-way ANOVA was used for the data analyses. Pairwise comparisons between means were tested by the *post hoc* Tukey method (GraphPad Prism 8) when ANOVA showed significant differences. The detailed analyzed process utilized in each experiment was elaborated in the matching figure legends. The sample sizes were determined based on the previous reports, pilot studies in the field and power analyses (power of 0.90 at $p < 0.05$) (Ferreira et al., 2001; Zhao et al., 2013; Millard et al., 2016; Daskalaki et al., 2018; Sato et al., 2018). Significance was set at $p < 0.05$.

RESULTS

MMP24 Protein Upregulation in the Spinal Cord after SNL

We first examined whether the MMP24 enrichment was altered in the spinal cord after SNL, a preclinical animal model that mimics nerve injury-induced neuropathic pain in the clinical setting (Rigaud et al., 2008). Unilateral SNL did not alter the level of *Mmp24* mRNA in the spinal cord from day 3 to 14 post-SNL (**Figure 1A**). However, the expression of MMP24 protein was significantly increased in a time-dependent manner in the spinal cord after SNL (**Figure 1B**), but not after sham surgery

TABLE 2 | Locomotor functions.

Treatments	Functional test		
	Placing	Grasping	Righting
LV-*Gfp*	5 (0)	5 (0)	5 (0)
LV-*Mmp24*	5 (0)	5 (0)	5 (0)
Mmp24 siRNA + SNL	5 (0)	5 (0)	5 (0)
Mmp24 siRNA + sham	5 (0)	5 (0)	5 (0)
Scrambled siRNA + sham	5 (0)	5 (0)	5 (0)
Scrambled siRNA + SNL	5 (0)	5 (0)	5 (0)

Scores for placing, grasping and righting reflexes were based on counts of each normal reflex exhibited in five trials. All values are Mean (SEM). n = *6 mice/group.*

(**Figure 1C**). Immunostaining further confirmed that the MMP24 protein was dramatically increased in the ipsilateral dorsal horn, but not in the contralateral dorsal horn, on day 7 post-SNL (**Figures 1D–F**). The distribution of MMP24 in the spinal dorsal horn was also checked by double immunostaining with different cell markers. As shown in **Figures 1G–K**, MMP24 was predominantly colocalized with the neuronal-specific nuclear protein (NeuN) (**Figures 1G–I**), and rarely with the glial fibrillary acidic protein (GFAP) (**Figure 1J**), or ionized calcium-binding adaptor molecule (IBA-1) (**Figure 1K**) in the spinal dorsal horn on day 14 after SNL. The above evidence suggests that the increased MMP24 protein in the spinal dorsal horn may involve neuropathic pain.

Blocking Spinal MMP24 Increase Attenuates Neuropathic Pain Development and Maintenance

Does the increased MMP24 in the spinal cord participate in nerve injury-induced pain hypersensitivity? To this end, we first examined the effect of blocking spinal MMP24 increase on the development of SNL-induced pain hypersensitivity. As shown in **Figure 2A**, siRNA-2 displayed the best knockdown effect compared to the scrambled siRNA (Scram) in the cultured spinal cord cells. Thus, siRNA-2 (*Mmp24* siRNA) and its control scrambled siRNA were intrathecally injected into the sham or SNL mice. Intrathecal injection of *Mmp24* siRNA attenuated SNL-induced mechanical allodynia as demonstrated by a decrease in PWF to mechanical stimuli and ameliorated SNL-induced thermal hyperalgesia as indicated by the increase in PWL to heat stimulation from day 3 to 5 compared to the scrambled siRNA-treated SNL mice (**Figures 2B–D**). No changes were observed in basal mechanical and heat responses in sham mice following injection with either siRNA (**Figures 2B–D**). Moreover, we also observed the role of MMP24 in the maintenance phase of neuropathic pain through intrathecal injection of *Mmp24* siRNA or scrambled siRNA into the sham or SNL mice 7 days after SNL. Consistently, blunted mechanical allodynia and heat hyperalgesia were observed on days 9 and 10 after SNL from the *Mmp24* siRNA-treated mice compared to the scrambled siRNA-treated mice (**Figures 2E–G**). The basal pain behavior of the sham mice (**Figures 2E–G**) and the locomotor functions of the siRNA-treated mice were not affected (**Table 2**). As expected, a noticeable decrease in the amount of MMP24 protein was detected in the spinal cord from the *Mmp24* siRNA-treated mice compared with the scrambled siRNA-treated mice on day 10 after SNL (**Figure 2H**). Consistently, intrathecal injection of *Mmp24* siRNA dampened the SNL-induced spinal neuronal sensitization as indicated by abolishing the SNL-induced increase in pERK1/2 in the spinal cord (**Figure 2I**). Together, the results described above demonstrate that spinal MMP24 is necessary for SNL-induced central sensitization and pain hypersensitivities.

MMP24 Overexpression Causes Neuropathic Pain-like Symptoms

We then asked whether the increased MMP24 in the spinal cord would be sufficient to induce neuropathic pain? To this end, we performed intraspinal lentivirus (LV) injection that expressed full-length *Mmp24* (LV-*Mmp24*) into naïve mice. As shown in **Figures 3A–C**, LV-*Mmp24*, but not its control LV-*Gfp*, induced mechanical allodynia as indicated by an increase in PWF to mechanical stimulation and heat hyperalgesia as demonstrated by a decrease in PWL to heat stimulation from day 3 to 12 post-injection. The locomotor functions were not affected after viral injection (**Table 2**). Expectedly, the level of MMP24 protein in the L4 spinal cord was significantly increased 12 days after intraspinal injection with LV-*Mmp24* compared to that of LV-*Gfp* (**Figure 3D**). These behavioral observations were further supported by the following evidence of spinal dorsal horn central sensitization. The level of pERK1/2 was markedly elevated in the L4 spinal dorsal horn on day 12 after intraspinal injection with LV-*Mmp24* compared to that of LV-*Gfp* (**Figure 3E**).

m^{6}A Modification in the Spinal *Mmp24* mRNA Was Decreased under Neuropathic Pain Condition

Although *Mmp24* mRNA remained unchanged after SNL, the MMP24 protein was significantly increased in the spinal cord (**Figures 1A,B**), suggesting that the translation efficiency of spinal *Mmp24* mRNA may be elevated under neuropathic pain condition. Of note, RNA m^{6}A modification is known to play an important role in mRNA translation (He and He, 2021). To this end, we carried out methylated RNA immunoprecipitation sequencing (MeRIP-seq) assay to observe the changes of m^{6}A sites across the transcriptome in the spinal cord on day 7 after peripheral nerve injury (**Figure 4A**). Consistent with previous studies in the DRG (Li et al., 2020), m^{6}A sites change after nerve injury occurred predominantly at the 3′-UTR (55.09%) and to lesser extents at coding regions (29.61%), and 5′-UTR (15.3%) (**Figures 4B,C**). Approximately 55.6% (1,910/3,437) transcripts exhibited a loss of m^{6}A sites, 33.9% (1,165/3,437) transcripts exhibited a gain of m^{6}A sites, and 10.5% (362/3,437) transcripts exhibited both a loss and gain of m^{6}A sites compared to the sham group (**Figures 4B,C**). Notably, *Mmp24* mRNA exhibited a considerable loss of m^{6}A sites at the 3′-UTR (**Figure 4D**). We then performed RIP-PCR to validate the MeRIP-seq results. The

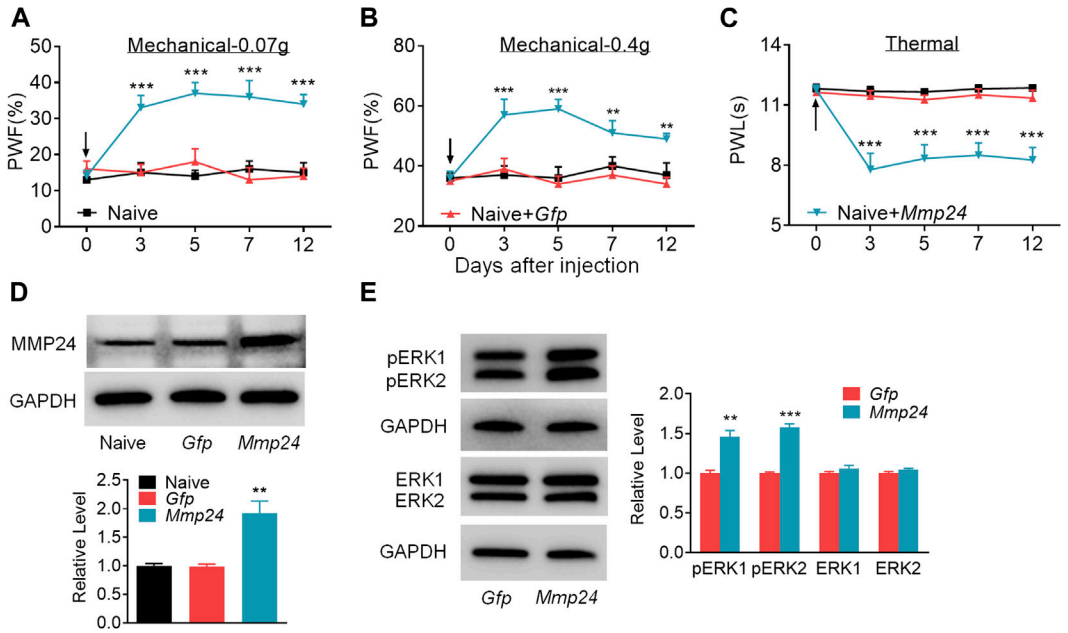

FIGURE 3 | Spinal MMP24 overexpression triggers pain hyperalgesia **(A–C)**. Effect of intraspinal injection of LV-*Mmp24* (*Mmp24*) or LV-*Gfp* (*Gfp*) into the naïve mice on the paw withdrawal responses to mechanical **(A, B)** and heat stimuli **(C)** on day 3, 5, 7, and 12 after injection. $n = 10$ mice/group. Two-way RM ANOVA followed by *post hoc* Tukey test. $F_{group}(2, 90) = 56.05$ for **(A)**, $F_{group}(2, 90) = 29.72$ for **(B)**, $F_{group}(2, 90) = 69.17$ for **(C)**. $^{**}p < 0.01$, $^{***}p < 0.001$ vs. the Naive plus *Gfp* group. Black arrow indicates intraspinal virus injection. **(D)**. MMP24 protein expression in the spinal cord of naïve mice 12 days after intraspinal injection with LV-*Mmp24* (*Mmp24*) or LV-*Gfp* (*Gfp*). $n = 3$ mice/group. One-way ANOVA followed by *post hoc* Tukey test. $F_{group}(2, 6) = 16.82$, $^{**}p < 0.01$ vs. *Gfp* group. **(E)**. pERK1/2 and ERK1/2 expression in the spinal cord of naïve mice 12 days after intraspinal injection with LV-*Mmp24* (*Mmp24*) or LV-*Gfp* (*Gfp*). $n = 3$ mice/group. $^{**}p < 0.01$, $^{***}p < 0.001$ vs. the *Gfp* group by two-tailed unpaired Student's *t*-test.

immunoprecipitation identified the m^{6}A enrichment of the *Mmp24* mRNA fragments with anti-m^{6}A in the spinal cord (**Figure 4E**). However, the activity of immunoprecipitation from the spinal cord on day 7 post-SNL was significantly decreased compared to the sham group (**Figure 4E**). In summary, we found that m^{6}A modification in the *Mmp24* mRNA was decreased in the spinal cord under neuropathic pain conditions, suggesting the role of m^{6}A modification in regulating MMP24 translation.

m^{6}A Modification-Related Genes Expression in the Spinal Cord after SNL

To determine the specific regulators responsible for the m^{6}A modification in the *Mmp24* mRNA, we first examined the expression of m^{6}A modification-related methyltransferases, including METTL3, METTL14, and WTAP, and demethylases, including FTO and ALKBH5 in the spinal cord under neuropathic pain condition. Unexpectedly, none of *Mettl3*, *Mettl14*, *Wtap*, *Fto*, and *Alkbh5* mRNAs showed an obvious change in the spinal cord from day 3 to 14 after SNL (**Figure 5A**). To further check the nucleus and cytoplasm distribution of the protein above, we extracted the nucleus protein of the spinal cord and found that none of the METTL3, METTL14, WTAP, FTO, and ALKBH5 protein exhibited a significant change from day 3 to 14 after SNL (**Figures 5B,C**). FTO was recently reported to play a vital role in neuropathic pain genesis by diminishing the m^{6}A enrichment in pain-related mRNAs in the DRG neurons (Li et al., 2020). Furthermore, FTO expression was found enriched in the spinal cord relative to that of DRG or cortex (Li et al., 2020), and higher than the other demethylase ALKBH5 in the spinal cord (**Figure 5D**), suggesting the possible role of spinal FTO in neuropathic pain genesis. Likewise, as shown in **Figures 5E–I**, FTO in the spinal dorsal horn was also expressed in the neurons but not in microglia or astrocytes. Therefore, we hypothesize that FTO may be accountable for the m^{6}A modification of *Mmp24* mRNA in the spinal neurons.

Spinal FTO Is Responsible for the Decreased m^{6}A Enrichment and Increased Translation of MMP24 after SNL in the Spinal Cord Neurons

To demonstrate the role of FTO in the regulation of MMP24, we first checked the distribution pattern of FTO and MMP24. Double immunostaining showed the colocalization of FTO and MMP24 in the spinal dorsal horn (**Figures 6A–C**). Moreover, the RIP assay further revealed that FTO could bind to the *Mmp24* mRNA from the spinal cord (**Figure 6D**), and there was a significant elevation in the binding activity from the spinal cord 7 days after SNL (**Figure 6D**). It indicates that the

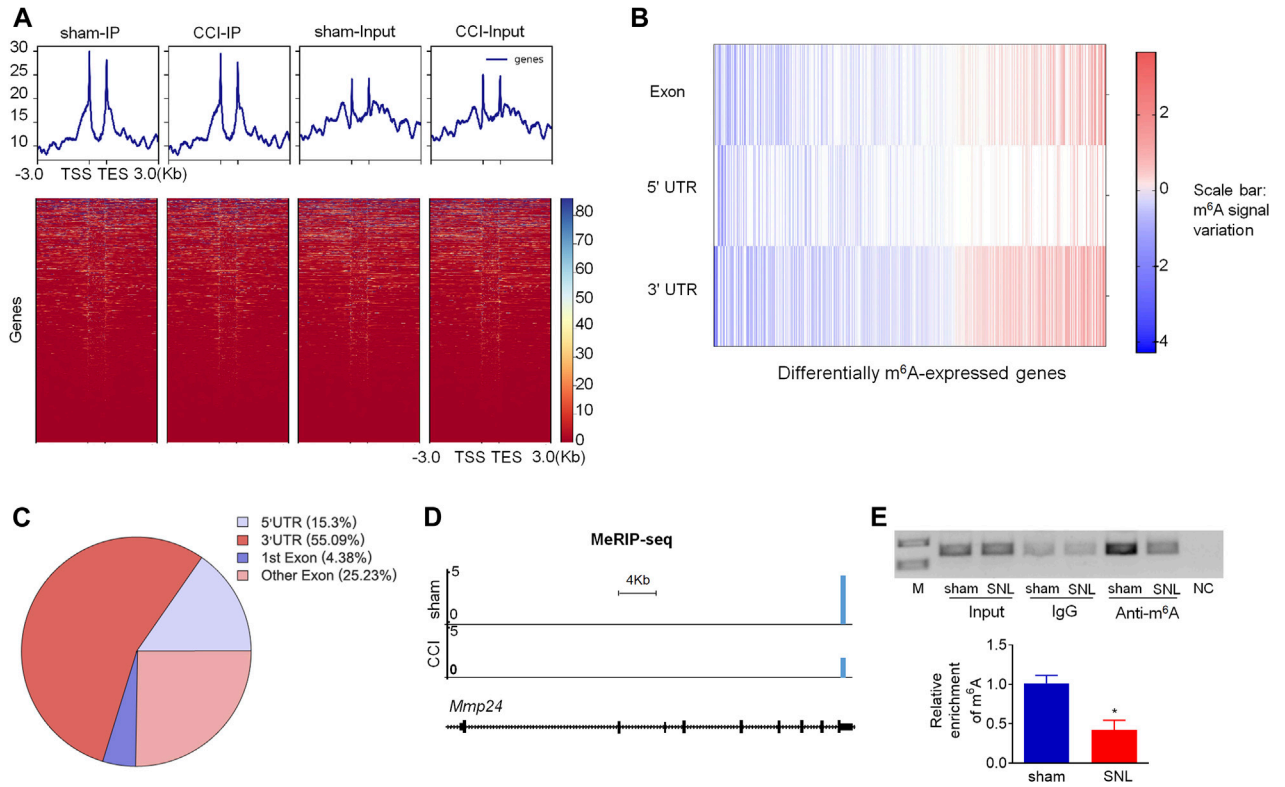

FIGURE 4 | m^{6}A modification in spinal *Mmp24* mRNA is decreased after SNL **(A)**. Heatmap of the MeRIP-seq signals from the spinal cord after chronic constriction injury (CCI) or sham surgery. Mean-normalized MeRIP-seq densities of equal bins along the gene. 3-kb region flanking the TSS or the TES are plotted. Red to blue color gradient of the heatmap represents the relative m^{6}A level. **(B–C)**. Dynamic changes **(B)** and distribution **(C)** of m^{6}A sites across transcripts from the spinal cord on day 7 after CCI or sham surgery. **(D)**. MeRIP-seq assay showed the example tracks of *Mmp24* mRNA from the spinal cord on day 7 after CCI or sham surgery. m^{6}A sites (blue) are indicated at the 3′-UTR. **(E)**. Level of *Mmp24* mRNA fragments immunoprecipitated by mouse anti-m^{6}A in the spinal cord on day 7 after SNL or sham surgery. Input: total purified fragment. $n = 4$ biological repeats (4 mice/repeat). M: ladder marker. NC: negative control (H2O). $^*p < 0.05$ vs. the sham group by two-tailed unpaired Student's *t*-test.

SNL-induced decrease in the m^{6}A enrichment in *Mmp24* mRNA may be due to the increased FTO occupation in the *Mmp24* mRNA after SNL.

We further examined the effect of FTO on the expression of MMP24 in the cultured spinal neurons. The expression of FTO was first verified 3 days after transduction with AAV5 that expressed full-length *Fto* (AAV5-*Fto*) or *Gfp* (AAV5-*Gfp*) (**Figure 6E**). A significant increase in the level of MMP24 protein was observed 3 days after transduction with AAV5-*Fto* compared to the AAV5-*Gfp*-treated group (**Figure 6E**). Interestingly, the level of *Mmp24* mRNA was not altered on day 3 after transduction with AAV5-*Fto* compared to AAV5-*Gfp* (**Figure 6F**). We further checked the effect of FTO knockdown on the expression of MMP24 in the cultured spinal neurons through the transduction of AAV5 that expressed *Fto* shRNA (AAV5-*Fto* shRNA) or control shRNA (AAV5-scrambled shRNA). The knockdown effect of FTO was confirmed 3 days after transduction of AAV5-*Fto* shRNA (**Figure 6G**). As expected, the MMP24 protein was markedly downregulated 3 days after transduction with AAV5-*Fto* shRNA compared with that of AAV5-scrambled shRNA (**Figure 6G**). However, the level of *Mmp24* mRNA was not significantly altered in AAV5-*Fto* shRNA-treated group compared to the AAV5-scrambled shRNA-treated group (**Figure 6H**), suggesting that FTO may promote the translation of *Mmp24* mRNA in the spinal neurons. We further transduced AAV5-*Fto* into cultured spinal neurons and found that FTO overexpression produced a marked loss of m^{6}A enrichment in the *Mmp24* mRNA compared to the control group (**Figure 6I**). This decrease was reversed by blocking FTO overexpression in the cultured spinal neurons co-transduced with AAV5-*Fto* shRNA (**Figure 6I**). Given the role of m^{6}A modification in mRNA translation (Jia et al., 2019; Zhang M. et al., 2020; Zhang Z. et al., 2020; Liu et al., 2020; Song et al., 2020), the evidence described above indicates that FTO likely erased the m^{6}A enrichment in *Mmp24* mRNA to promote the translation of *Mmp24* mRNA in the spinal cord neurons under neuropathic pain condition.

DISCUSSION

This study demonstrates that SNL results in an accelerated translation of *Mmp24* mRNA in the spinal cord. Increased spinal MMP24 contributes to the SNL-induced central

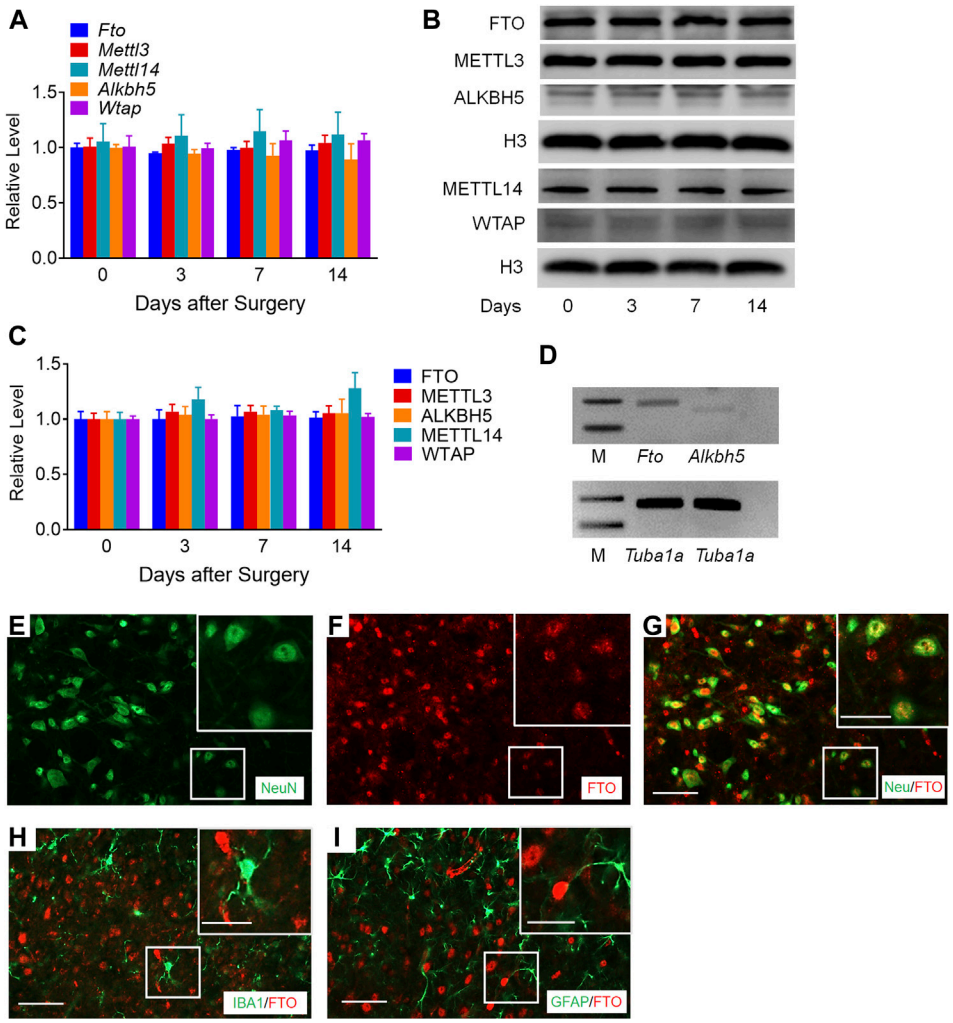

FIGURE 5 | m^{6}A-related genes expression in the spinal cord after SNL **(A)**. Expression of *Fto*, *Mettl3*, *Alkbh5*, *Mettl14*, and *Wtap* mRNAs in the spinal cord from day 3 to 14 after SNL. n = 3–5 mice/group/time point. **(B–C)**. Expression of nuclear FTO, METTL3, ALKBH5, METTL14 and WTAP proteins in the spinal cord from day 3 to 14 after SNL. *n* = 7–13 mice/group/time point. **(D)**. The relative expression of *Fto* and *Alkbh5* mRNA in the spinal cord. *n* = 3 repeats. M: ladder marker. **(E–I)**. Representative images of double staining between FTO and markers of neuron, astrocytes and microglia in the spinal dorsal horn. Scale bar: 50 μm; 25 μm (insets).

sensitization and nociceptive hyperalgesia. Mechanistically, SNL leads to an elevation of FTO occupation in the *Mmp24* mRNA. Increased occupation of FTO contributes to reducing m^{6}A enrichment in *Mmp24* mRNA in the spinal neurons after SNL, which subsequently accelerates the translation of MMP24 and eventually contributes to neuropathic pain by activating ERK (**Figure 7**).

MMP24 was explicitly detected in neurons of both the central and peripheral nervous systems (Hayashita-Kinoh et al., 2001; Sekine-Aizawa et al., 2001) and identified as a brain-specific MMP (Llano et al., 1999; Wang and Pei, 2001). The present study showed that MMP24 was mainly expressed in the spinal neurons as it was co-expressed with NeuN-labeled individual neurons. Meanwhile, our results also supported the existence of MMP24 in the spinal astrocytes and microglia after SNL even though at a low abundance. Besides, the morphologic observation of the MMP24-labeled cells proved the presence of MMP24 in the matrix of the dorsal horn, supporting the role of MMP24, as an extracellular matrix metalloproteinase, in regulating cleavage of the cell-cell adhesion molecule N-cadherin to influence the neuronal circuit formation and plasticity (Komori et al., 2004; Folgueras et al., 2009).

Previous studies showed that mice with genetically ablated MMP24 exhibited a lowered severity of mechanical allodynia after partial sciatic nerve injury or spinal cord transection (Komori et al., 2004) through the lowered degradation of chondroitin sulfate proteoglycans, which are abundant in neuronal tissues and inhibit neurite outgrowth (Dou and Levine, 1994). Deletion of *Mmp24* also relieved thermal pain after the inflammation model through increased interaction between mast cells and nociceptive neurites (Folgueras et al., 2009). Our study further demonstrated the involvement of spinal MMP24 in the different phases of neuropathic pain. Specifically, blocking the SNL-induced increase in MMP24 in the spinal cord

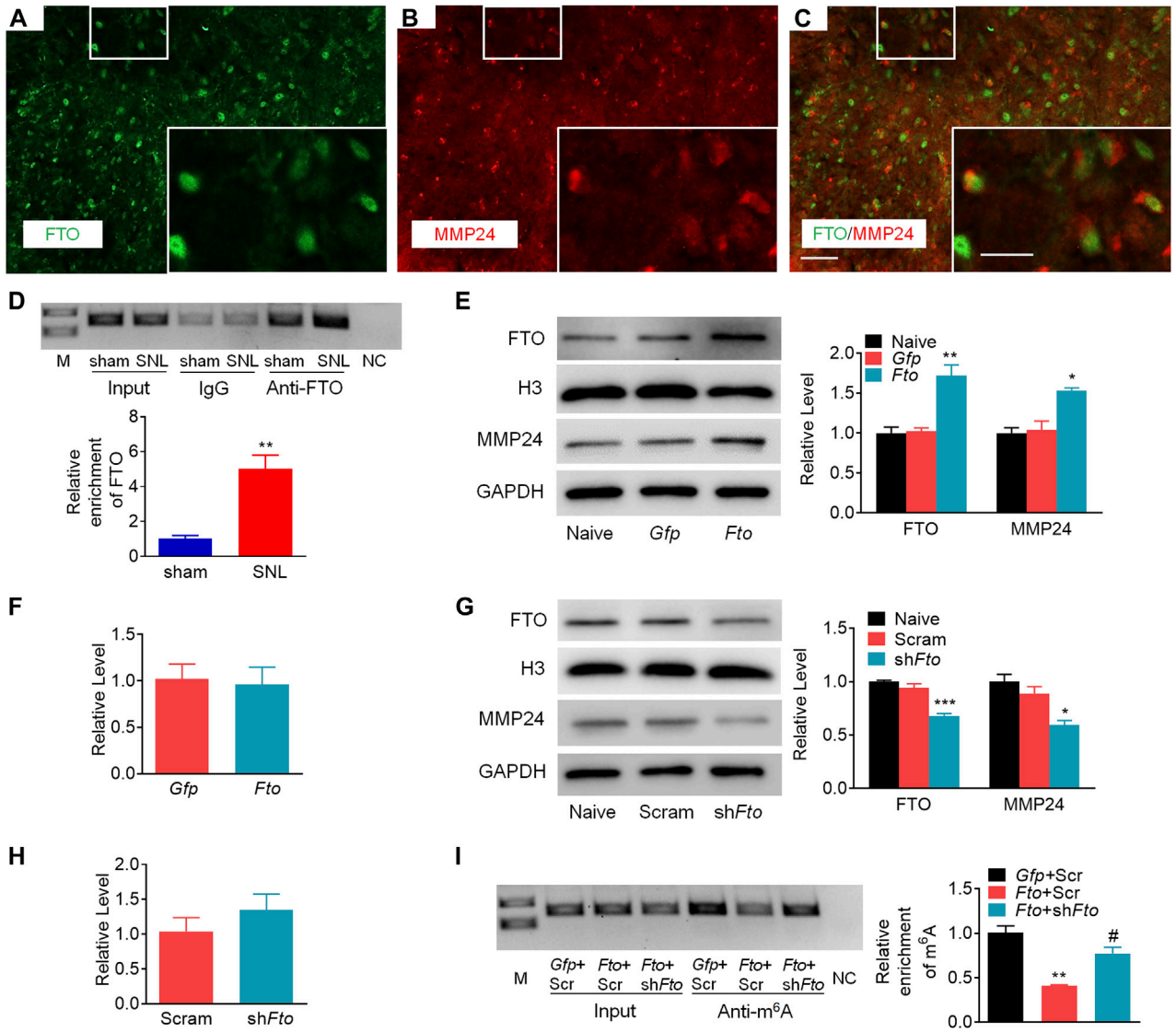

FIGURE 6 | FTO promotes the expression of MMP24 in the spinal neurons **(A–C)**. Representative images of the colocalization between FTO and MMP24 in the spinal dorsal horn. Scale bar: 50 μm; 25 μm (insets). **(D)**. Level of *Mmp24* mRNA fragments immunoprecipitated by mouse anti-FTO in the spinal cord on day 7 after SNL or sham surgery. Input: total purified fragment. n = 3 biological repeats (4 mice/repeat). M: ladder marker. NC: negative control (H2O). $^{**}p < 0.01$ vs. the sham group by two-tailed unpaired Student's t-test. **(E)**. Expression of FTO and MMP24 in the cultured spinal neurons on day 3 after transduction with AAV5-*Gfp* (*Gfp*) or AAV5-*Fto* (*Fto*). n = 3 repeats. One-way ANOVA followed by *post hoc* Tukey test. F_{group} (2, 6) = 19.98 for FTO, F_{group} (2, 6) = 14.37 for MMP24. $^{*}p < 0.05$, $^{**}p < 0.01$ vs. the *Gfp* group. **(F)**. Expression of *Mmp24* mRNA in the cultured spinal neurons on day 3 after transduction with AAV5-*Gfp* (*Gfp*) or AAV5-*Fto* (*Fto*). n = 3 repeats **(G)**. Expression of FTO and MMP24 in the cultured spinal neurons on day 3 after transduction with AAV5-*Fto* shRNA (sh*Fto*) or AAV5-scrambled shRNA (Scram). n = 3 repeats. One-way ANOVA followed by *post hoc* Tukey test. F_{group} (2, 6) = 46.71 for FTO, F_{group} (2, 6) = 12.07 for MMP24. $^{*}p < 0.05$, $^{***}p < 0.001$ vs. the Scram group. **(H)**. Expression of *Mmp24* mRNA in the cultured spinal neurons on day 3 after transduction with AAV5-*Fto* shRNA (sh*Fto*) or AAV5-scrambled shRNA (Scram). n = 3 repeats **(I)**. Enrichment of *Mmp24* mRNA fragments immunoprecipitated by anti-m^{6}A from the cultured spinal neurons transduced viruses as shown. *Gfp*: AAV5-*Gfp*; Scr: AAV5-scrambled shRNA; *Fto*: AAV5-*Fto*; sh*Fto*: AAV5-*Fto* shRNA. n = 3 biological repeats/group. One-way ANOVA followed by *post hoc* Tukey test. F_{group} (2, 6) = 24.41. $^{**}p < 0.01$ vs. the *Gfp* plus Scr group. $^{\#}p < 0.05$ vs. the *Fto* plus Scr group.

attenuates both the mechanical allodynia and heat hyperalgesia in both development and maintenance phases, accompanied by lessened activation ERK1/2. Moreover, intraspinal specific overexpression of MMP24 by LV persistently induced both the mechanical allodynia and heat hyperalgesia with the activation of ERK1/2 absence of SNL. MMP24 was reported to show the ability to proteolytically activate MMP2 (Llano et al., 1999), which could cleave pro-IL-1β to activate ERK in the spinal cord (Kawasaki et al., 2008). Furthermore, MMP24 was required for the inflammatory response to TNF-α and IL-1β in the peripheral nervous system (Folgueras et al., 2009). Thus, MMP24 is likely to activate ERK through inflammatory mediators like IL-1β and TNF-α in the spinal cord. ERK1/2 phosphorylation has been widely considered in recent years as a spinal neuron sensitization

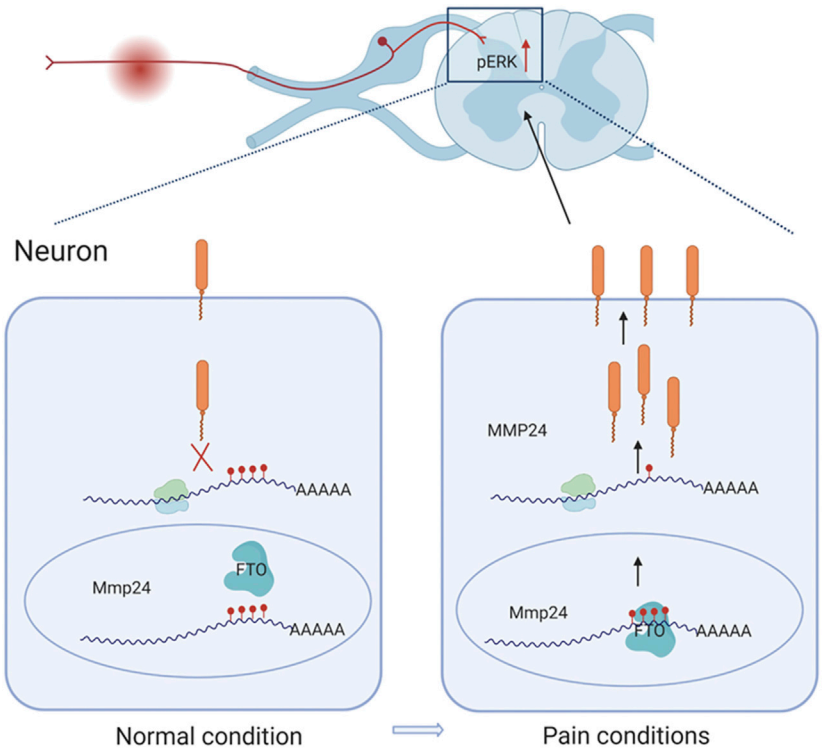

FIGURE 7 | Schematic representation of the mechanism of MMP24 participation in neuropathic pain. Black arrows depict promotion. Red arrows represent upregulation. Never injury can facilitate the binding of FTO to *Mmp24* mRNA in spinal neurocytes nuclei and subsequently lead to the reduced level of m^{6}A modification followed by the enhanced translation of its mRNA. Increased MMP24 can facilitate ERK phosphorylation in the spinal cord and induce neuropathic pain.

marker (Zhuang et al., 2005; Gu et al., 2018). Its activation could subsequently induce the expression and release of various downstream pain-related genes like *Cxcl10*, *Ccl2*, and *Ccl7*, or affect neuronal excitability of the central neurons, and eventually trigger the pain behaviors (Jiang et al., 2020a; Jiang et al., 2020b).

Mounting evidence indicates that epigenetic alterations play a critical role in neuropathic pain induction and maintenance, including histone acetylation/methylation, DNA methylation and non-coding RNAs (Penas and Navarro, 2018). Spinal coactivator-associated arginine methyltransferase 1 (CARM1) regulated histone methylation of the potassium channel promoter to participate in neuropathic pain development (Hsieh et al., 2021). Also, spinal ten-eleven translocation methylcytosine dioxygenase 1 (Tet1) decreased the DNA methylation state in metabotropic glutamate receptor subtype 5 (mGluR5) promoter to mediate spinal plasticity and pain hypersensitivity (Hsieh et al., 2017). Epigenetic modification at the transcriptional level has achieved much progress in neuropathic pain genesis these years, while the translational level epigenetic regulation is still incomplete. Interestingly, the current study demonstrates that although the level of *Mmp24* mRNA was not altered in SNL, the expression of MMP24 protein was significantly increased in the spinal cord in a time-dependent manner, suggesting the accelerated translation of spinal *Mmp24* mRNA after SNL. A previous study showed that m^{6}A enrichment in many transcripts was changed in the DRG upon peripheral nerve injury. This change contributed to increased translation during axon regeneration, revealing the critical role of m^{6}A modification in response to nerve injury (Weng et al., 2018). Our MeRIP-seq and RIP-PCR assay showed a considerable loss of m^{6}A sites in *Mmp24* mRNA in the spinal cord under neuropathic pain. It suggests that m^{6}A modification in *Mmp24* mRNA may be accountable for the accelerated translation of *Mmp24* mRNA. Indeed, we found that after SNL, the increased level of MMP24 protein (not *Mmp24* mRNA) was accompanied by a higher occupancy of FTO in the *Mmp24* mRNA and the consequently lessened enrichment of m^{6}A. Moreover, FTO overexpression erased the m^{6}A sites in the *Mmp24* mRNA and increased the level of MMP24 protein. Conversely, FTO knockdown markedly increased the m^{6}A enrichment in the *Mmp24* mRNA and reduced the expression of MMP24 protein, but not *Mmp24* mRNA, in the spinal neurons. Together, the accelerated *Mmp24* mRNA translation after SNL in the spinal cord was likely resulted from the lowered FTO-mediated m^{6}A modification in *Mmp24* mRNA.

Previous studies displayed that FTO was localized in the nucleus in neurons in the central nervous system, including the hippocampus and midbrain (Hess et al., 2013; Li et al., 2017). Functionally, FTO bound to the m^{6}A sites and reduced the m^{6}A enrichment to mediate the biogenesis of its target transcripts in the central neurons (Hess et al., 2013; Leonetti et al., 2020). Consistently, the present study revealed that FTO was co-expressed with NeuN in nuclei of the spinal neurons and colocalized with MMP24. However, the expression of spinal FTO was not altered after SNL. How the FTO preferentially binds to *Mmp24* mRNA under the neuropathic pain condition is unclear. This could be due to that the binding of FTO and *Mmp24* mRNA

in the spinal cord is regulated by nerve injury-sensitive signaling pathways (Bresson et al., 2020), such as the upregulation of mediators in promoting the interaction of FTO and *Mmp24* mRNA or downregulation of competitors in competing for the binding between FTO and *Mmp24* mRNA (Song et al., 2019; Ontiveros et al., 2020). Although demethylase FTO, as an "eraser", removed the m^6A in *Mmp24* mRNA after SNL, the specific "reader" decoding the m^6A modification in the *Mmp24* mRNA remains unknown. Previous studies found that m^6A promoted translation efficiency via the reader proteins (Roundtree et al., 2017), like YTHDF1 (Jia et al., 2019). However, recent studies from C.H. et al. found that the effect of m^6A on translation was highly heterogeneous and depended on the binding of specific RNA binding proteins (Zhang Z. et al., 2020). For example, the newly identified m^6A effector YBX3, opposite to YTHDF1 in function, mediated m^6A effect by repressing the translation of YBX3-bound m^6A transcripts (Snyder et al., 2015; Zhang Z. et al., 2020). Here, the m^6A loss-mediated promotion in *Mmp24* mRNA translation possibly depends on the effectors like YBX3, but not YTHDF1. Further investigation is warrented for its identification.

In summary, our study reveals an FTO-triggered epigenetic mechanism of MMP24 upregulation in the spinal cord after SNL. Blocking the SNL-induced increase of MMP24 in the spinal cord mitigated pain hypersensitivity both in the development and maintenance phase without altering the basal/acute responses or locomotor functions. MMP24 may be an endogenous initiator of neuropathic pain and could be a potential target for this disorder's prevention and treatment.

DATA AVAILABILITY STATEMENT

The raw data supporting the conclusions of this article will be made available by the authors, without undue reservation.

ETHICS STATEMENT

The animal study was reviewed and approved by the Zhejiang Animal Care and Use Committee and the Ethics Committee of SAHZU, School of Medicine.

AUTHOR CONTRIBUTIONS

MY, BJ, and LM conceived the project and designed the experiments. MY, FZ, and LY coordinated and supervised all experiments. LM, YH, NS, JR, DG, and XP conducted most of the molecular, biochemical, and morphological experiments. LM, YH, FZ, JL, and LY performed most of the animal surgery and behavioral experiments. LM, YH, FZ, SX, JL, and LY analyzed the data and did the statistical analysis. LM, MY, BJ, and DG wrote and revised the manuscript. All authors have read and agreed to submit this manuscript for publication.

FUNDING

This study was supported by the National Natural Science Foundation of China (NSFC 81471128, 81771197, 81771189, 82071227), Zhejiang Provincial Natural Science Foundation of China (LZ18H090001, LY18H090006), grants for Scientific Research from the Chinese Ministry of Health-Zhejiang Health Department, China (2018272998).

ACKNOWLEDGMENTS

We thank XZ, CL, and SC (the Second Affiliated Hospital of Zhejiang University) for technical support. **Figure 7** of this paper was created with the aid of BioRender.

REFERENCES

Albik, S., and Tao, Y.-X. (2021). Emerging Role of RNA m6A Modification in Chronic Pain. *Pain*, Publish Ahead of Print. doi:10.1097/j.pain.0000000000002219

Bailey, T. L., Boden, M., Buske, F. A., Frith, M., Grant, C. E., Clementi, L., et al. (2009). MEME SUITE: Tools for Motif Discovery and Searching. *Nucleic Acids Res.* 37, W202–W208. doi:10.1093/nar/gkp335

Bresson, S., Shchepachev, V., Spanos, C., Turowski, T. W., Rappsilber, J., and Tollervey, D. (2020). Stress-Induced Translation Inhibition through Rapid Displacement of Scanning Initiation Factors. *Mol. Cell* 80 (3), 470–484. doi:10.1016/j.molcel.2020.09.021

Daskalaki, M. G., Tsatsanis, C., and Kampranis, S. C. (2018). Histone Methylation and Acetylation in Macrophages as a Mechanism for Regulation of Inflammatory Responses. *J. Cell Physiol.* 233 (9), 6495–6507. doi:10.1002/jcp.26497

Decosterd, I., and Woolf, C. J. (2000). Spared Nerve Injury: an Animal Model of Persistent Peripheral Neuropathic Pain. *Pain* 87 (2), 149–158. doi:10.1016/S0304-3959(00)00276-1

Dominissini, D., Moshitch-Moshkovitz, S., Schwartz, S., Salmon-Divon, M., Ungar, L., Osenberg, S., et al. (2012). Topology of the Human and Mouse m6A RNA Methylomes Revealed by m6A-Seq. *Nature* 485 (7397), 201–206. doi:10.1038/nature11112

Dou, C., and Levine, J. (1994). Inhibition of Neurite Growth by the NG2 Chondroitin Sulfate Proteoglycan. *J. Neurosci.* 14 (12), 7616–7628. doi:10.1523/jneurosci.14-12-07616.1994

Ferreira, R., Naguibneva, I., Pritchard, L. L., Ait-Si-Ali, S., and Harel-Bellan, A. (2001). The Rb/chromatin Connection and Epigenetic Control: Opinion. *Oncogene* 20 (24), 3128–3133. doi:10.1038/sj.onc.1204337

Folgueras, A. R., Valdes-Sanchez, T., Llano, E., Menendez, L., Baamonde, A., Denlinger, B. L., et al. (2009). Metalloproteinase MT5-MMP Is an Essential Modulator of Neuro-Immune Interactions in Thermal Pain Stimulation. *Proc. Natl. Acad. Sci.* 106 (38), 16451–16456. doi:10.1073/pnas.0908507106

Fu, Y., Dominissini, D., Rechavi, G., and He, C. (2014). Gene Expression Regulation Mediated through Reversible m6A RNA Methylation. *Nat. Rev. Genet.* 15 (5), 293–306. doi:10.1038/nrg3724

Gu, P., Pan, Z., Wang, X.-M., Sun, L., Tai, L. W., and Cheung, C. W. (2018). Histone Deacetylase 5 (HDAC5) Regulates Neuropathic Pain through SRY-Related HMG-Box 10 (SOX10)-dependent Mechanism in Mice. *Pain* 159 (3), 526–539. doi:10.1097/j.pain.0000000000001125

Hannocks, M.-J., Zhang, X., Gerwien, H., Chashchina, A., Burmeister, M., Korpos, E., et al. (2019). The Gelatinases, MMP-2 and MMP-9, as Fine Tuners of Neuroinflammatory Processes. *Matrix Biol.* 75-76, 102–113. doi:10.1016/j.matbio.2017.11.007

Hayashita-Kinoh, H., Kinoh, H., Okada, A., Komori, K., Itoh, Y., Chiba, T., et al. (2001). Membrane-type 5 Matrix Metalloproteinase Is Expressed in Differentiated Neurons and Regulates Axonal Growth. *Cell Growth Differ.* 12 (11), 573–580.

He, P. C., and He, C. (2021). m(6) A RNA Methylation: from Mechanisms to Therapeutic Potential. *EMBO J.* 40 (3), e105977. doi:10.15252/embj.2020105977

He, X.-B., Yi, S.-H., Rhee, Y.-H., Kim, H., Han, Y.-M., Lee, S.-H., et al. (2011). Prolonged Membrane Depolarization Enhances Midbrain Dopamine Neuron Differentiation via Epigenetic Histone Modifications. *Stem Cells* 29 (11), 1861–1873. doi:10.1002/stem.739

Hess, M. E., Hess, S., Meyer, K. D., Verhagen, L. A. W., Koch, L., Brönneke, H. S., et al. (2013). The Fat Mass and Obesity Associated Gene (Fto) Regulates Activity of the Dopaminergic Midbrain Circuitry. *Nat. Neurosci.* 16 (8), 1042–1048. doi:10.1038/nn.3449

Hsieh, M.-C., Ho, Y.-C., Lai, C.-Y., Chou, D., Wang, H.-H., Chen, G.-D., et al. (2017). Melatonin Impedes Tet1-dependent mGluR5 Promoter Demethylation to Relieve Pain. *J. Pineal Res.* 63 (4), e12436. doi:10.1111/jpi.12436

Hsieh, M.-C., Ho, Y.-C., Lai, C.-Y., Wang, H.-H., Yang, P.-S., Cheng, J.-K., et al. (2021). Blocking the Spinal Fbxo3/CARM1/K+ Channel Epigenetic Silencing Pathway as a Strategy for Neuropathic Pain Relief. *Neurotherapeutics*. doi:10.1007/s13311-020-00977-5

Ji, R.-R., Xu, Z.-Z., Wang, X., and Lo, E. H. (2009). Matrix Metalloprotease Regulation of Neuropathic Pain. *Trends Pharmacol. Sci.* 30 (7), 336–340. doi:10.1016/j.tips.2009.04.002

Jia, R., Chai, P., Wang, S., Sun, B., Xu, Y., Yang, Y., et al. (2019). m6A Modification Suppresses Ocular Melanoma through Modulating HINT2 mRNA Translation. *Mol. Cancer* 18 (1), 161. doi:10.1186/s12943-019-1088-x

Jiang, B.-C., Cao, D.-L., Zhang, X., Zhang, Z.-J., He, L.-N., Li, C.-H., et al. (2016). CXCL13 Drives Spinal Astrocyte Activation and Neuropathic Pain via CXCR5. *J. Clin. Invest.* 126 (2), 745–761. doi:10.1172/JCI81950

Jiang, B.-C., Liu, T., and Gao, Y.-J. (2020a). Chemokines in Chronic Pain: Cellular and Molecular Mechanisms and Therapeutic Potential. *Pharmacol. Ther.* 212, 107581. doi:10.1016/j.pharmthera.2020.107581

Jiang, B.-C., Zhang, J., Wu, B., Jiang, M., Cao, H., Wu, H., et al. (2020b). G Protein-Coupled Receptor GPR151 Is Involved in Trigeminal Neuropathic Pain through the Induction of Gβγ/extracellular Signal-Regulated Kinase-Mediated Neuroinflammation in the Trigeminal Ganglion. *Pain* Publish Ahead of Print. doi:10.1097/j.pain.0000000000002156

Jiang, B.-C., Zhang, W.-W., Yang, T., Guo, C.-Y., Cao, D.-L., Zhang, Z.-J., et al. (2018). Demethylation of G-Protein-Coupled Receptor 151 Promoter Facilitates the Binding of Krüppel-like Factor 5 and Enhances Neuropathic Pain after Nerve Injury in Mice. *J. Neurosci.* 38 (49), 10535–10551. doi:10.1523/JNEUROSCI.0702-18.2018

Kawasaki, Y., Xu, Z.-Z., Wang, X., Park, J. Y., Zhuang, Z.-Y., Tan, P.-H., et al. (2008). Distinct Roles of Matrix Metalloproteases in the Early- and Late-phase Development of Neuropathic Pain. *Nat. Med.* 14 (3), 331–336. doi:10.1038/nm1723

Kechin, A., Boyarskikh, U., Kel, A., and Filipenko, M. (2017). cutPrimers: A New Tool for Accurate Cutting of Primers from Reads of Targeted Next Generation Sequencing. *J. Comput. Biol.* 24 (11), 1138–1143. doi:10.1089/cmb.2017.0096

Komori, K., Nonaka, T., Okada, A., Kinoh, H., Hayashita-Kinoh, H., Yoshida, N., et al. (2004). Absence of Mechanical Allodynia and Abeta-Fiber Sprouting after Sciatic Nerve Injury in Mice Lacking Membrane-type 5 Matrix Metalloproteinase. *FEBS Lett.* 557 (1-3), 125–128. doi:10.1016/s0014-5793(03)01458-3

Langmead, B., and Salzberg, S. L. (2012). Fast Gapped-Read Alignment with Bowtie 2. *Nat. Methods* 9 (4), 357–359. doi:10.1038/nmeth.1923

Leonetti, A. M., Chu, M. Y., Ramnaraign, F. O., Holm, S., and Walters, B. J. (2020). An Emerging Role of m6A in Memory: A Case for Translational Priming. *Int. J. Mol. Sci.* 21 (20), 7447. doi:10.3390/ijms21207447

Li, L., Zang, L., Zhang, F., Chen, J., Shen, H., Shu, L., et al. (2017). Fat Mass and Obesity-Associated (FTO) Protein Regulates Adult Neurogenesis. *Hum. Mol. Genet.* 26 (13), 2398–2411. doi:10.1093/hmg/ddx128

Li, Y., Guo, X., Sun, L., Xiao, J., Su, S., Du, S., et al. (2020). N 6 -Methyladenosine Demethylase FTO Contributes to Neuropathic Pain by Stabilizing G9a Expression in Primary Sensory Neurons. *Adv. Sci.* 7 (13), 1902402. doi:10.1002/advs.201902402

Lin, T.-B., Lai, C.-Y., Hsieh, M.-C., Ho, Y.-C., Wang, H.-H., Yang, P.-S., et al. (2020). Inhibiting MLL1-WDR5 Interaction Ameliorates Neuropathic Allodynia by Attenuating Histone H3 Lysine 4 Trimethylation-dependent Spinal mGluR5 Transcription. *Pain* 161 (9), 1995–2009. doi:10.1097/j.pain.0000000000001898

Liu, L., Wu, Y., Li, Q., Liang, J., He, Q., Zhao, L., et al. (2020). METTL3 Promotes Tumorigenesis and Metastasis through BMI1 m6A Methylation in Oral Squamous Cell Carcinoma. *Mol. Ther.* 28 (10), 2177–2190. doi:10.1016/j.ymthe.2020.06.024

Liu, N., Dai, Q., Zheng, G., He, C., Parisien, M., and Pan, T. (2015). N6-methyladenosine-dependent RNA Structural Switches Regulate RNA-Protein Interactions. *Nature* 518 (7540), 560–564. doi:10.1038/nature14234

Llano, E., Pendás, A. M., Freije, J. P., Nakano, A., Knäuper, V., Murphy, G., et al. (1999). Identification and Characterization of Human MT5-MMP, a New Membrane-Bound Activator of Progelatinase a Overexpressed in Brain Tumors. *Cancer Res.* 59 (11), 2570–2576.

Manicone, A., and McGuire, J. (2008). Matrix Metalloproteinases as Modulators of Inflammation. *Semin. Cell Dev. Biol.* 19 (1), 34–41. doi:10.1016/j.semcdb.2007.07.003

Meyer, K. D., Saletore, Y., Zumbo, P., Elemento, O., Mason, C. E., and Jaffrey, S. R. (2012). Comprehensive Analysis of mRNA Methylation Reveals Enrichment in 3′ UTRs and Near Stop Codons. *Cell* 149 (7), 1635–1646. doi:10.1016/j.cell.2012.05.003

Millard, C. J., Varma, N., Saleh, A., Morris, K., Watson, P. J., Bottrill, A. R., et al. (2016). The Structure of the Core NuRD Repression Complex Provides Insights into its Interaction with Chromatin. *Elife* 5, e13941. doi:10.7554/eLife.13941

Mitka, M. (2003). Virtual Textbook" on Pain Developed: Effort Seeks to Remedy Gap in Medical Education. *JAMA* 290 (18), 2395. doi:10.1001/jama.290.18.239510.1001/jama.290.1.27

Ontiveros, R. J., Shen, H., Stoute, J., Yanas, A., Cui, Y., Zhang, Y., et al. (2020). Coordination of mRNA and tRNA Methylations by TRMT10A. *Proc. Natl. Acad. Sci. USA* 117 (14), 7782–7791. doi:10.1073/pnas.1913448117

Penas, C., and Navarro, X. (2018). Epigenetic Modifications Associated to Neuroinflammation and Neuropathic Pain after Neural Trauma. *Front. Cell Neurosci.* 12, 158. doi:10.3389/fncel.2018.00158

Pokhilko, A., Nash, A., and Cader, M. Z. (2020). Common Transcriptional Signatures of Neuropathic Pain. *Pain* 161 (7), 1542–1554. doi:10.1097/j.pain.0000000000001847

Rigaud, M., Gemes, G., Barabas, M.-E., Chernoff, D. I., Abram, S. E., Stucky, C. L., et al. (2008). Species and Strain Differences in Rodent Sciatic Nerve Anatomy: Implications for Studies of Neuropathic Pain. *Pain* 136 (1-2), 188–201. doi:10.1016/j.pain.2008.01.016

Roundtree, I. A., Evans, M. E., Pan, T., and He, C. (2017). Dynamic RNA Modifications in Gene Expression Regulation. *Cell* 169 (7), 1187–1200. doi:10.1016/j.cell.2017.05.045

Sato, T., Chang, H.-C., Bayeva, M., Shapiro, J. S., Ramos-Alonso, L., Kouzu, H., et al. (2018). mRNA-binding Protein Tristetraprolin Is Essential for Cardiac Response to Iron Deficiency by Regulating Mitochondrial Function. *Proc. Natl. Acad. Sci. USA* 115 (27), E6291–E6300. doi:10.1073/pnas.1804701115

Sekine-Aizawa, Y., Hama, E., Watanabe, K., Tsubuki, S., Kanai-Azuma, M., Kanai, Y., et al. (2001). Matrix Metalloproteinase (MMP) System in Brain: Identification and Characterization of Brain-specific MMP Highly Expressed in Cerebellum. *Eur. J. Neurosci.* 13 (5), 935–948. doi:10.1046/j.0953-816x.2001.01462.x

Snyder, E., Soundararajan, R., Sharma, M., Dearth, A., Smith, B., and Braun, R. E. (2015). Compound Heterozygosity for Y Box Proteins Causes Sterility Due to Loss of Translational Repression. *PLoS Genet.* 11 (12), e1005690, doi:10.1371/journal.pgen.1005690

Song, P., Feng, L., Li, J., Dai, D., Zhu, L., Wang, C., et al. (2020). β-Catenin Represses miR455-3p to Stimulate m6A Modification of HSF1 mRNA and Promote its Translation in Colorectal Cancer. *Mol. Cancer* 19 (1), 129. doi:10.1186/s12943-020-01244-z

Song, T., Yang, Y., Wei, H., Xie, X., Lu, J., Zeng, Q., et al. (2019). Zfp217 Mediates m6A mRNA Methylation to Orchestrate Transcriptional and Post-transcriptional Regulation to Promote Adipogenic Differentiation. *Nucleic Acids Res.* 47 (12), 6130–6144. doi:10.1093/nar/gkz312

Wang, L. X., and Wang, Z. J. (2003). Animal and Cellular Models of Chronic Pain. *Adv. Drug Deliv. Rev.* 55 (8), 949–965. doi:10.1016/s0169-409x(03)00098-x

Wang, X., and Pei, D. (2001). Shedding of Membrane Type Matrix Metalloproteinase 5 by a Furin-type Convertase. *J. Biol. Chem.* 276 (38), 35953–35960. doi:10.1074/jbc.M103680200

Weng, Y.-L., Wang, X., An, R., Cassin, J., Vissers, C., Liu, Y., et al. (2018). Epitranscriptomic m6A Regulation of Axon Regeneration in the Adult Mammalian Nervous System. *Neuron* 97 (2), 313–325. doi:10.1016/j.neuron.2017.12.036

Wu, S., Bono, J., and Tao, Y.-X. (2019). Long Noncoding RNA (lncRNA): a Target in Neuropathic Pain. *Expert Opin. Ther. Targets* 23 (1), 15–20. doi:10.1080/14728222.2019.1550075

Wu, S., Marie Lutz, B., Miao, X., Liang, L., Mo, K., Chang, Y.-J., et al. (2016). Dorsal Root Ganglion Transcriptome Analysis Following Peripheral Nerve Injury in Mice. *Mol. Pain* 12, 174480691662904. doi:10.1177/1744806916629048

Yang, Y., Hsu, P. J., Chen, Y.-S., and Yang, Y.-G. (2018). Dynamic Transcriptomic m6A Decoration: Writers, Erasers, Readers and Functions in RNA Metabolism. *Cell Res* 28 (6), 616–624. doi:10.1038/s41422-018-0040-8

Yu, G., Wang, L.-G., and He, Q.-Y. (2015). ChIPseeker: an R/Bioconductor Package for ChIP Peak Annotation, Comparison and Visualization. *Bioinformatics* 31 (14), 2382–2383. doi:10.1093/bioinformatics/btv145

Zhang, M., Zhai, Y., Zhang, S., Dai, X., and Li, Z. (2020). Roles of N6-Methyladenosine (m6A) in Stem Cell Fate Decisions and Early Embryonic Development in Mammals. *Front. Cel Dev. Biol.* 8, 782. doi:10.3389/fcell.2020.00782

Zhang, Y., Liu, T., Meyer, C. A., Eeckhoute, J., Johnson, D. S., Bernstein, B. E., et al. (2008). Model-based Analysis of ChIP-Seq (MACS). *Genome Biol.* 9 (9), R137. doi:10.1186/gb-2008-9-9-r137

Zhang, Z., Luo, K., Zou, Z., Qiu, M., Tian, J., Sieh, L., et al. (2020). Genetic Analyses Support the Contribution of mRNA N6-Methyladenosine (m6A) Modification to Human Disease Heritability. *Nat. Genet.* 52 (9), 939–949. doi:10.1038/s41588-020-0644-z

Zhao, J.-Y., Liang, L., Gu, X., Li, Z., Wu, S., Sun, L., et al. (2017). DNA Methyltransferase DNMT3a Contributes to Neuropathic Pain by Repressing Kcna2 in Primary Afferent Neurons. *Nat. Commun.* 8, 14712. doi:10.1038/ncomms14712

Zhao, X., Tang, Z., Zhang, H., Atianjoh, F. E., Zhao, J.-Y., Liang, L., et al. (2013). A Long Noncoding RNA Contributes to Neuropathic Pain by Silencing Kcna2 in Primary Afferent Neurons. *Nat. Neurosci.* 16 (8), 1024–1031. doi:10.1038/nn.3438

Zheng, G., Dahl, J. A., Niu, Y., Fedorcsak, P., Huang, C.-M., Li, C. J., et al. (2013). ALKBH5 Is a Mammalian RNA Demethylase that Impacts RNA Metabolism and Mouse Fertility. *Mol. Cell* 49 (1), 18–29. doi:10.1016/j.molcel.2012.10.015

Zhuang, Z.-Y., Gerner, P., Woolf, C. J., and Ji, R.-R. (2005). ERK Is Sequentially Activated in Neurons, Microglia, and Astrocytes by Spinal Nerve Ligation and Contributes to Mechanical Allodynia in This Neuropathic Pain Model. *Pain* 114 (1-2), 149–159. doi:10.1016/j.pain.2004.12.022

Conflict of Interest: The authors declare that the research was conducted in the absence of any commercial or financial relationships that could be construed as a potential conflict of interest.

frontiers in Pharmacology

REVIEW
published: 12 May 2021
doi: 10.3389/fphar.2021.642820

Modulation of Pathological Pain by Epidermal Growth Factor Receptor

Jazlyn P. Borges[1,2], *Katrina Mekhail*[3,4], *Gregory D. Fairn*[3,4,5,6,7†], *Costin N. Antonescu*[3,7] *and Benjamin E. Steinberg*[1,2,8*]

[1]Neurosciences and Mental Health Program, The Hospital for Sick Children, Toronto, ON, Canada, [2]Department of Physiology, University of Toronto, Toronto, ON, Canada, [3]Keenan Research Centre for Biomedical Science, St. Michael's Hospital, Toronto, ON, Canada, [4]Department of Biochemistry, University of Toronto, Toronto, ON, Canada, [5]Department of Surgery, University of Toronto, Toronto, ON, Canada, [6]Department of Laboratory Medicine and Pathobiology, University of Toronto, Toronto, ON, Canada, [7]Department of Chemistry and Biology, Ryerson University, Toronto, ON, Canada, [8]Department of Anesthesia and Pain Medicine, The Hospital for Sick Children, Toronto, ON, Canada

Chronic pain has been widely recognized as a major public health problem that impacts multiple aspects of patient quality of life. Unfortunately, chronic pain is often resistant to conventional analgesics, which are further limited by their various side effects. New therapeutic strategies and targets are needed to better serve the millions of people suffering from this devastating disease. To this end, recent clinical and preclinical studies have implicated the epidermal growth factor receptor signaling pathway in chronic pain states. EGFR is one of four members of the ErbB family of receptor tyrosine kinases that have key roles in development and the progression of many cancers. EGFR functions by activating many intracellular signaling pathways following binding of various ligands to the receptor. Several of these signaling pathways, such as phosphatidylinositol 3-kinase, are known mediators of pain. EGFR inhibitors are known for their use as cancer therapeutics but given recent evidence in pilot clinical and preclinical investigations, may have clinical use for treating chronic pain. Here, we review the clinical and preclinical evidence implicating EGFR in pathological pain states and provide an overview of EGFR signaling highlighting how EGFR and its ligands drive pain hypersensitivity and interact with important pain pathways such as the opioid system.

Keywords: epidermai growth factor receptor, neuropathic pain, animal models, inflammation, membrane traffic, receptor tyrosine kinase

OPEN ACCESS

Edited by:
Francesco De Logu,
University of Florence, Italy

Reviewed by:
Nasiara Karim,
University of Malakand, Pakistan
Xuehai Guan,
Guangxi Medical University, China

***Correspondence:**
Benjamin E. Steinberg
benjamin.steinberg@sickkids.ca

†ORCID:
Gregory D. Fairn
orcid.org/0000-0001-6508-168X

Specialty section:
This article was submitted to Inflammation Pharmacology, a section of the journal Frontiers in Pharmacology

Received: *16 December 2020*
Accepted: *26 April 2021*
Published: *12 May 2021*

Citation:
Borges JP, Mekhail K, Fairn GD, Antonescu CN and Steinberg BE (2021) Modulation of Pathological Pain by Epidermal Growth Factor Receptor. Front. Pharmacol. 12:642820. doi: 10.3389/fphar.2021.642820

INTRODUCTION

Chronic pain is an international health priority (Kamerman et al., 2015), with a prevalence approaching 30% in North American adults (Moulin et al., 2002; Johannes et al., 2010). In addition to the physical and psychological toll chronic pain places on patients and their families, its societal and economic strain are unparalleled (Gaskin and Richard, 2012). A significant proportion of patients with chronic pain suffer from neuropathic pain (Yawn et al., 2009). Neuropathic pain is defined as pain that arises from a lesion or disease of the somatosensory nervous system (International Association for the Study of Pain, 2017). Clinically, neuropathic pain is characterized by spontaneous pain, increased response to noxious stimuli (hyperalgesia), and the perception of pain from innocuous stimuli (mechanical allodynia) (Baron, 2006). Many clinical pathologies, such as cancer, trauma, and diabetes, can result in neuropathic pain development (Kamerman et al., 2015; Bouhassira and Attal, 2019; Edwards et al., 2019). Unfortunately,

neuropathic pain is often resistant to standard analgesics, which are further limited by a variety of adverse side effects (Colloca et al., 2017; Cavalli et al., 2019). As such, a better understanding of the molecular mechanisms of pain hypersensitivity is greatly needed to identify new therapeutic targets and novel treatments for neuropathic pain patients.

Growth factors and their cognate receptors promote pain sensitization and have been identified as therapeutic targets in the treatment of neuropathic pain (Chang et al., 2016). These include nerve growth factor (NGF) (Chang et al., 2016), brain-derived neurotrophic factor (Chen et al., 2014), platelet-derived growth factor (Narita et al., 2005; Donica et al., 2014; Xu et al., 2016; Barkai et al., 2019) and insulin-like growth factor 1 (Wang et al., 2014; Forster et al., 2019). The receptors of these growth factors belong to the receptor tyrosine kinase (RTK) family. More recently another RTK, the epidermal growth factor receptor (EGFR), has been identified as a potential therapeutic target for neuropathic pain. EGFR has crucial roles in prenatal development and adult tissue homeostasis, as signaling by the active receptor controls a wide array of cellular functions including growth, proliferation, metabolism and survival (Miettinen et al., 1995; Sibilia and Wagner, 1995; Threadgill et al., 1995; Sibilia et al., 1998). Thus, aberrant signaling by EGFR drives tumorigenesis and the progression of many cancers (Sigismund et al., 2018). Various therapeutics have been designed to target EGFR in cancer treatments, including antibody therapeutics such as cetuximab, and small-molecule tyrosine kinase inhibitors such as gefitinib and erlotinib (Lemmon et al., 2014).

Here, we first review the clinical and genetic evidence implicating EGFR in pain, emphasizing neuropathic pain, which has been the primary focus of recent studies. We next provide an overview of EGFR signaling, highlighting possible mechanisms by which EGFR and its ligands may influence pain hypersensitivity and modulate inflammatory mediators of pain. We propose future studies directed at better understanding the role of the EGFR family in pain signalling in order to allow evaluation of whether EGFR-related therapeutics may be repositioned for the treatment of neuropathic pain.

Clinical Data and Genetic Links

Pain begins with the detection of noxious stimuli by specialized peripheral sensory neurons, termed nociceptors (Julius and Basbaum, 2001; Basbaum et al., 2009; Baral et al., 2019). These fibers innervate tissues and organs and have cell bodies located within the dorsal root and trigeminal ganglia. Following stimulation such as extremes in temperature, mechanical injury and injurious chemicals, nociceptors transduce electrical signals that travel to the dorsal horn of the spinal cord, where nociceptors synapse with second-order neurons that carry signals to higher central nervous system relay centres. Structural lesions or disease processes that affect signaling along these somatosensory pathways can result in neuropathic pain. The resulting somatosensory dysfunction can lead to spontaneous pain, allodynia and hypersensitivity (Scholz et al., 2019). For example, cancer can result in direct damage to the nervous system through a primary tumor or a metastatic process or can indirectly trigger chemotherapy-induced neuropathy (Bennett et al., 2019).

Current pharmacological agents used for neuropathic pain span a wide breadth of drug classes. As shown in **Figure 1A** and extensively reviewed elsewhere, these include gabapentinoids, antidepressants, namely tricyclic antidepressants (TCAs) and selective serotonin and norepinephrine reuptake inhibitors (SNRIs), topical agents (lidocaine and capsaicin), and opioids (Alper and Lewis, 2002; Rauck et al., 2009; Kremer et al., 2016; Chincholkar, 2018; Coderre, 2018; Schembri, 2019; Windsor et al., 2019; Ardeleanu et al., 2020; Kapustin et al., 2020; Gress et al., 2020; Chalil et al., 2021). Use of these and other analgesic medication classes is often limited by inadequate efficacy or side effects, necessitating the ongoing identification of novel drug targets. To that end, a variety of emerging potential therapeutic agents for neuropathic pain are being repositioned or developed for clinical trial. These include monoclonal antibodies against inflammatory mediators, cannabinoids, and inhibitors of G protein-coupled receptors and N-methyl-D-aspartate receptors (**Figure 1B**) (Karppinen et al., 2003; Stahel et al., 2016; Jung et al., 2017; Wang et al., 2017; Aiyer et al., 2018; Mapplebeck et al., 2018; Kreutzwiser and Tawfic, 2019; Alkislar et al., 2020; Haleem and Wright, 2020; Kushnarev et al., 2020; Maayah et al., 2020; Yu et al., 2020; Zhang W. et al., 2020; Matarazzo et al., 2021).

Here, we focus on EGFR as an important mediator of neuropathic pain and an emerging therapeutic target. The first clinical evidence for the involvement of EGFR in neuropathic pain was observed in cancer-induced neuropathic pain and later expanded to non-cancer patients (Kersten and Cameron, 2012; Kersten et al., 2013). In what follows, we present the clinical trial and genetic association data linking EGFR to pathological pain states, with an emphasis on human neuropathic pain.

Clinical Studies

Clinical evidence provided through case reports and clinical trials suggest that therapeutics targeting EGFR may alleviate pain in both cancer patients and non-cancer patients afflicted with neuropathic pain. Phase III clinical trials have reported that a significant proportion of patients with non-small cell lung cancer (NSCLC) experienced pain relief following treatment with erlotinib (Bezjak et al., 2006; Cappuzzo et al., 2010) in addition to significant improvements in physical functioning and quality of life (Bezjak et al., 2006). A phase III clinical trial of afatinib, a tyrosine kinase inhibitor of ErbB family proteins (EGFR, HER2, HER3 and HER4), also reported that a significant proportion of patients with advanced NSCLC experienced pain relief (Hirsh et al., 2013). However, in these studies, it remains unclear as to whether pain relief was attributable to the effects of EGFR therapy on the tumor or a direct effect of EGFR therapy on neuropathic pain signaling.

A case study by Kersten and colleagues reported that a patient with rectal cancer experienced pain relief with cetuximab treatment despite tumor progression (Kersten and Cameron, 2012). Notably, administration of 20% the patient's normal cetuximab dose did not relieve pain, suggesting cetuximab-induced pain relief was not due to placebo effect. A follow-up case series reported that four of five cancer and non-cancer

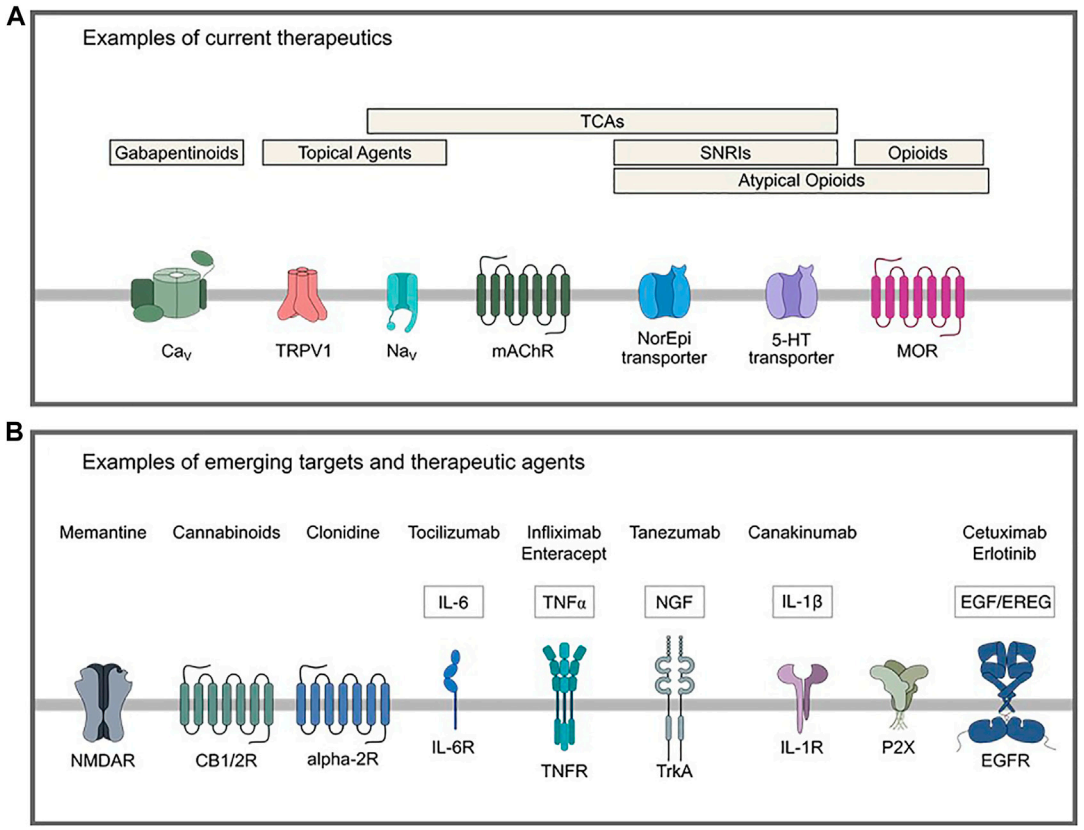

FIGURE 1 | Examples of current and emerging potential therapeutics for treatment of neuropathic pain. **(A)** Current therapeutics include gabapentinoids that act on the α2δ-1 calcium channel subunit, topical agents with targets such as TRPV1 or voltage-gated sodium channels, opioids, atypical opioids (mixed/partial agonists, some of which have actions as an SNRI or NI), TCAs that act on various distinct targets such as serotonergic, adrenergic and cholinergic systems and fast voltage-gated sodium channels, and SNRIs. **(B)** Examples of emerging potential targets and therapeutics for neuropathic pain. 5-HT: 5-hydroxytryptamine, CB1/2: cannabinoid receptor type 1/2, Ca_V: voltage-gated calcium channel, EGF: epidermal growth factor, EGFR: epidermal growth factor receptor, EREG: epiregulin, IL: interleukin, IL-6R: interleukin-6 receptor, IL-1R: interleukin-1 receptor, mAChR: muscarinic acetylcholine receptor, MOR: mu-opioid receptor, Na_V voltage-gated sodium channel, NGF: nerve growth factor, NI: norepinephrine reuptake inhibitor, SNRI: selective serotonin reuptake inhibitor, TCA: tricyclic antidepressant, TNF: tumor necrosis factor, TNFR: tumor necrosis factor receptor, TrkA: tropomyosin receptor kinase A, TRPV1: transient receptor potential cation channel subfamily V member 1.

patients with neuropathic pain, two male and two female patients, experienced a self-reported reduction in pain from 9 to 1 on a 10-point scale shortly after intravenous administration of cetuximab or panitumumab, two antibody therapies directed against EGFR (Kersten et al., 2013). Another study by Kersten and colleagues reported that cetuximab treatment provided pain relief for eighteen out of twenty patients afflicted with neuropathic pain, including cancer and non-cancer patients of both sexes (Kersten et al., 2015). In a randomized control trial, male and female neuropathic pain patients experienced the greatest average pain reduction following open-label or blinded cetuximab treatment, and the lowest average pain reduction with the blinded placebo (Kersten et al., 2019). Importantly, unlike many current treatment options for neuropathic pain, the side effects observed in patients treated with various therapeutics that target EGFR, including cetuximab and panitumumab (monoclonal antibody therapeutics) and/or erlotinib and gefitinib (tyrosine kinase inhibitors, TKI), were generally mild to moderate (Kersten et al., 2015; Kersten et al., 2019). Together, these data suggest EGFR as a potential therapeutic target for patients afflicted with neuropathic pain that in the treatment of cancer-related neuropathic pain may be at least partly distinct from the effect of EGFR therapies on the tumor itself. Understanding the mechanism by which the EGFR signaling pathway contributes to neuropathic pain is an important research priority that may lead to improved outcomes for patients with neuropathic pain.

Genetic Links

There is a growing body of genetic studies that are identifying important pathways in acute and chronic pain. One such study is the Orofacial Pain Perspective Evaluation Risk Assessment (OPPERA), which examined the environmental, biosocial, and genetic factors that may lead to painful temporomandibular disorders (Fillingim et al., 2011; Maixner et al., 2011; Slade et al., 2013). Subsequent genetic analyses of the OPPERA study cohorts revealed single nucleotide polymorphisms (SNPs) of EGFR and one of its cognate ligands, epiregulin (EREG), that may be associated with the development of chronic pain in temporomandibular disorders (Martin et al.,

2017; Verma et al., 2020). Specifically, EREG and EGFR SNPs have a high association with the development of temporomandibular disorders in European females (Martin et al., 2017), with the variants of EREG SNPs decreasing circulating EREG mRNA (Verma et al., 2020). This decrease was found to be associated with protection against chronic pain but paradoxically increases the risk of systemic hypersensitivity in acute pain (Verma et al., 2020). This clinical observation is consistent with animal studies in which antibody inhibition of circulating EREG demonstrates similarly opposing effects in acute and chronic pain (Verma et al., 2020). Collectively, these studies suggest that EGFR and EREG may have roles in the development of chronic pain but may also protect against sensitization in acute pain. However, due to the limitations of these cohorts, including small sample sizes and limited evaluation of sex as an important biological variable, additional studies are required. Future work may include broader and diverse samples for genetic analyses and sex-specific *in vivo* studies will allow validation of the possible link between EREG and chronic pain across different patient populations.

Transcriptional profiling of macrophages from synovial fluids of patients suffering from rheumatoid arthritis (RA) and pancreatic cancer, has further implicated potential roles of the EGFR signaling pathway in pain (Wangzhou et al., 2021). This was revealed by an interactome map of human DRG RNA-seq and macrophages derived from patient synovial tissue (single-cell RNA-seq). Three of the transcripts enriched in the RA macrophages include heparin-binding EGF-like growth factor (HB-EGF), EREG and decorin, a TGF-β derived proteoglycan binding peptide, that when released by the macrophage have the potential to activate EGFR in the DRG. A similar analysis using bulk RNA-seq of pancreatic cancer patients and non-cancer patients revealed that of the 41 ligands that are upregulated in cancerous tissues, four activate or modulate EGFR, including the EGFR ligand TGF-α, and modulators CEACAM1, FGF1, and TFF1 (Wangzhou et al., 2021). While these associations do not directly entail causality, mechanistic *in vivo* evidence is limited to the use of animal models. Thus, these data highlight potential interactions in human tissues–specifically, between EGFR within the DRG and ligands associated with pain-associated diseases and underscore the importance of investigating the role of EGFR in chronic pain.

EPIDERMAL GROWTH FACTOR RECEPTOR

EGFR has central roles in development and in the maintenance of homeostasis in adult tissues, including the central and peripheral nervous systems, where it exerts neurotrophic actions (Aguirre et al., 2007; Chong et al., 2008; Garcez et al., 2009; Hu et al., 2010; Sinor-Anderson and Lillien, 2011). Ligand binding and activation of EGFR occurs within the plasma membrane. Structurally, EGFR contains an extracellular region, the ligand-binding domain, transmembrane region, and intracellular region containing an intrinsic tyrosine kinase domain and a c-terminal tail that harbors many tyrosine residues that become phosphorylated upon ligand binding (Lemmon and Schlessinger, 2010). EGFR is one of four members of the ErbB family of RTKs, the others being HER2, HER3 and HER4. These family members bind different ligands (or no ligand in the case of HER2), and form various homo- or heterodimers [for review see Lemmon et al. (2014)]. EGFR may bind various ligands that are characterized into two groups based on their binding affinity: high-affinity ligands include EGF, transforming growth factor alpha (TGF-α), betacellulin and (HB-EGF); and low affinity ligands include amphiregulin, epiregulin (EREG), and epigen (Freed et al., 2017). The binding of high- or low-affinity ligands not only leads to the formation of distinct structural dimers, but generates transient or sustained signalling, respectively, and thus different cellular physiological outcomes (Freed et al., 2017).

Depending on the cellular expression of HER2, HER3, and HER4, ligand-binding to EGFR induces receptor homo- or heterodimerization, and the activation of intrinsic tyrosine kinase domains that leads to phosphorylation of the receptor's c-terminal cytosolic tail (Lemmon et al., 2014). These phosphotyrosine residues are part of motifs that allow binding of various SH2- and PTB-domain containing proteins, leading to the subsequent activation of various intracellular signaling pathways, such as phosphatidylinositol-3-kinase (PI3K)-Akt, Ras-Erk, and signal transducer and activator of transcription (STAT) proteins (Han and Lo, 2012; Sugiyama et al., 2019) (**Figure 2**). Following ligand binding at the cell surface, EGFR undergoes internalization and intracellular vesicle traffic, a phenomenon that regulates EGFR signaling in multiple ways (Vieira et al., 1996; Sigismund et al., 2008; Garay et al., 2015; Reis et al., 2015; Villaseñor et al., 2015; Pinilla-Macua et al., 2016; Chen et al., 2017; Leyton-Puig et al., 2017; Pascolutti et al., 2019; Thapa et al., 2020). The complexity of these signaling pathways is underscored by the compartmentalization of signalling intermediates of various isoforms, and membrane traffic of these proteins and the receptor–all of which have important roles in contributing to signal fidelity and specificity (Sugiyama et al., 2019).

Epidermal Growth Factor Receptor in Animal Models of Pain

Animal models of pain are important and necessary to understand fundamental mechanisms of disease and to identify new therapeutic targets (Mogil et al., 2010). Various animal models of pain have been designed to mimic distinct clinical pathologies (Gregory et al., 2013). For example, models of neuropathic pain include spared nerve injury, in which the sciatic nerve undergoes partial injury (Cichon et al., 2018), spinal nerve ligation (Chung et al., 2004), and paclitaxel-induced neuropathy (Griffiths et al., 2018). Pain perception varies among individuals and an analogous heterogeneous response to nociceptive stimuli

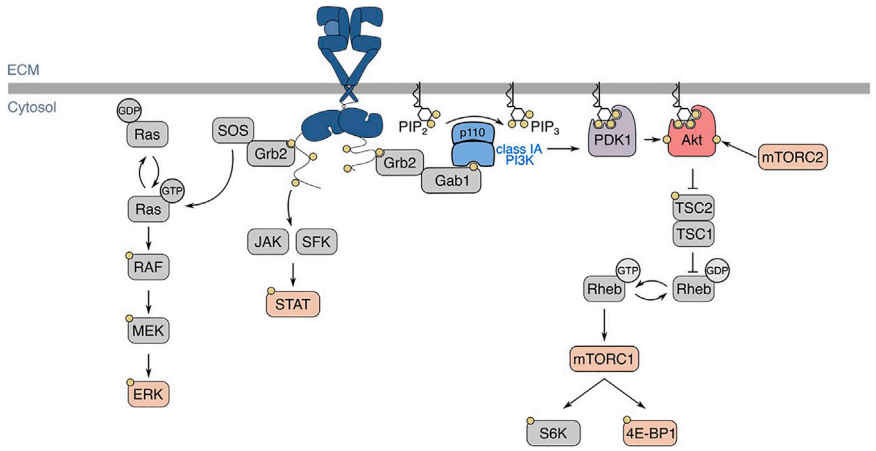

FIGURE 2 | EGFR structure, ligand-binding, and signaling pathways. In the basal state, EGFR exists in an autoinhibited conformation. Ligand-binding allows for the formation of homo- or heterodimers, which activates EGFR intrinsic tyrosine kinase domains and ensues signal transduction, shown here as an EGFR homodimer with one ligand bound. Various signalling pathways are initiated by the active EGFR, such as Ras-Erk, JAK/SFK-STAT, and PI3K-Akt. Regarding EGFR-PI3K-Akt signalling, EGFR autophosphorylation at Y1068 allows for the activation of class IA PI3K. The active PI3K subsequently phosphorylates $PI(4,5)P_2$ (PIP_2) into $PI(3,4,5)P_3$, which recruits kinases PDK1 and Akt to the plasma membrane. There, Akt is phosphorylated by PDK1 and mTORC2 at T308 and S473, respectively. EGFR: epidermal growth factor receptor, JAK: Janus kinase, SFK: Src-family kinase, STAT: signal transducer and activator of transcription, PI3K: phosphoinositide 3-kinase, PDK1: phosphoinositide-dependent kinase 1, mTORC: mechanistic target of rapamycin complex, TSC: tuberous sclerosis complex, SOS: son of sevenless, Grb2: growth factor receptor-bound protein 2, Gab1: Grb2-associated binding protein 1.

can be observed in rodents. As pain cannot be measured directly in animal models, methods that quantify nociceptive behaviours have been developed (reviewed by (Deuis et al., 2017) as a surrogate outcome.

EGFR has been shown to mediate hypersensitivity in various animal models of pain. Systemic administration of various EGFR inhibitors (AG-1478, gefitinib, lapatinib) reverses complete Freund's adjuvant (CFA)-, spared nerve injury (SNI)- and chronic constriction injury (CCI)-induced mechanical allodynia, as well as carrageenan-induced thermal hypersensitivity (Martin et al., 2017). Systemic administration of these inhibitors also reduces nociceptive behaviours in the late phase of the formalin test (Martin et al., 2017). However, a recent report has shown that gefitinib administration does not block spinal nerve ligation (SNL)-induced mechanical allodynia, though the authors suggest that the discrepancy between this and previous findings may be due to differences in SNI and SNL models of neuropathic pain (Puig et al., 2020). In the SNL model, the L5 and L6 spinal nerves are ligated whereas in the SNI model, the tibial and common peroneal nerves are ligated and sectioned 2–3 mm from the ligation, leaving the sural nerve intact (Challa, 2015). The methodology of and challenges associated with each of these models have been described previously [reviewed by (Challa, 2015)]. Intrathecal delivery of gefitinib or EGFR siRNA reverses chronic constriction of the DRG (CCD)-induced mechanical, heat, and cold hypersensitivity (Wang et al., 2019). Inhibition of EGFR with cetuximab attenuates nociceptive behaviors in a mouse model of oral cancer pain (Scheff et al., 2020). Given these data, it appears that EGFR may have roles in driving hypersensitivity across multiple pain models, though this may vary with context.

Epidermal Growth Factor Receptor Is Expressed Within the Dorsal Root Ganglion and Spinal Dorsal Horn

The dorsal horn, dorsal root ganglia, and trigeminal ganglia are important areas in pain modulation (Ji et al., 2016; Esposito et al., 2019), and multiple studies have detected EGFR expression within primary afferents and immune cells within these areas (Werner et al., 1988; Puig et al., 2020). Immunohistochemistry (IHC) staining for EGFR in primary afferents suggest a heterogeneous expression pattern within afferent nerve fibers of various diameters in human and rat DRG (Werner et al., 1988; Birecree et al., 1991; Huerta et al., 1996; Martin et al., 2017). Recent studies have demonstrated that EGFR may be broadly expressed in many different sensory fiber types as indicated by cellular colocalization of EGFR with NF200, CGRP, and IB4 in the rat DRG and spinal cord (Wang et al., 2019; Puig et al., 2020). These data imply that EGFR is expressed in myelinated, unmyelinated peptidergic, and unmyelinated non-peptidergic fibers, respectively. However, within the spinal cord, EGFR does not colocalize with neuron-specific nuclear protein (NeuN), suggesting second-order neurons may not express EGFR (Puig et al., 2020). IHC staining of other ErbB family proteins (HER2, HER3 and HER4) demonstrates that these receptors are also differentially expressed within the DRG and dorsal horn (Pearson and Carroll, 2004). Collectively, these studies establish EGFR expression in many different afferent nerve fibres.

EGFR expression has also been detected in non-neuronal cell types, namely immune and glial cells, within the DRG and dorsal horn. Microglia, the resident macrophages of the CNS, may have key roles in the establishment and maintenance of neuropathic

pain (Tsuda, 2016). Cellular colocalization of EGFR with OX42 (Puig et al., 2020) and western blotting of isolated (spinal) microglia suggest microglia within the rat spinal cord express EGFR (Qu et al., 2012). Satellite glial cells of the DRG may have roles in neuropathic pain by releasing soluble pain mediators, such as growth factors and cytokines (Wei et al., 2019). IHC of human DRGs suggests satellite and interstitial Schwann cells express EGFR (Werner et al., 1988), and colocalization of EGFR with glutamate synthase suggests satellite cells express EGFR within the rat DRG (Wang et al., 2019). Though some reports have shown that astrocyte expression of EGFR is downregulated within the postnatal rat brain (Scholze et al., 2014), other studies have shown that EGFR is expressed within astrocytes and other cell types, possibly macrophages, within the gray matter of the female rat spinal cord (Erschbamer et al., 2007; Li et al., 2014). Collectively, these studies provide evidence that EGFR is expressed both in sensory neurons as well as in immune and supportive cells relevant to pain, providing an anatomic and cellular substrate for several possible mechanisms of action of EGFR in neuropathic pain.

Epidermal Growth Factor Receptor is Upregulated Within the Dorsal Root Ganglion in Various Pain Models

EGFR mRNA increases in the ipsilateral DRG of male rats following SNL or CCD (Wang et al., 2019) as well as spinal cord injury (SCI) (Erschbamer et al., 2007; Li et al., 2014). This increase in EGFR mRNA was also observed following SCI in a subpopulation of sensory neurons within the DRG (Erschbamer et al., 2007). Contact of vertebral pulposus (NP) tissue with peripheral nerves has been used to emulate the contribution of inflammatory mediators secreted by NP tissue to pain associated with radiculopathy (Takebayashi et al., 2001; Cuellar et al., 2005; Egeland et al., 2013). Contact of NP tissue with exposed dorsal nerve roots leads to increased HER3, but not EGFR, HER2 or HER4 mRNA within the DRG (Kongstorp et al., 2019), suggesting other ErbB proteins may have roles in mediating pain. Given that HER3 and EGFR may form heterodimers, how the regulated expression of EGFR and other HER family members observed following nerve lesions may alter nociception and contribute to neuropathic pain warrants further investigation.

EGFR phosphorylation at Y1068 leads to PI3K-Akt signaling, a phenomenon that may be increased within the DRG in various models of pain, including CFA and SNI (Martin et al., 2017). EGFR is also phosphorylated at Y1068 within the ipsilateral DRG following CCD, but is not activated within the contralateral DRG or within the spinal cord (Wang et al., 2019). Thus, given the evidence published to date, EGFR phosphorylation (Y1068) may be upregulated within the DRG in inflammatory and neuropathic pain models.

Since EGFR may be activated directly by ligand-binding or indirectly through transactivation by other receptors, we next discuss EGFR ligands and their implicated roles in pain.

Direct Actions of Epidermal Growth Factor Receptor by Ligand-Binding

A key regulatory mechanism of RTK signaling involves controlling the availability of active-form ligands to the receptor. Many RTK ligands are initially synthesized as transmembrane proteins (Adrain and Freeman, 2014) and in the case of EGFR, pro-ligands are made soluble by the membrane-bound metalloprotease, ADAM-17, which proteolytically processes more than 80 substrates including cytokines, adhesion molecules and cognate ligand precursors of EGFR (Quarta et al., 2019). Multiple ADAM-17 substrates are involved in pain hypersensitivity and inflammation, and as such, recent studies have sought to elucidate the role of ADAM-17 in nociception and pain sensitization. Scheff and colleagues demonstrated that the supernatant of some oral cancer cell lines is sufficient to induce nociceptive behavior in mice, which was attenuated by EGFR inhibition, and that this supernatant contained higher levels of ADAM17 than non-nociceptive cell lines. Importantly, pathway analysis revealed enhanced PI3K-Akt and mTORC1 signaling upon treatment with nociceptive oral cancer cell supernatant (Scheff et al., 2020). Together, these data suggest a model in which cleaved targets of ADAM-17 may induce hyperalgesia through the EGFR signaling axis. However, establishing a causal link between elevated ADAM17, EGFR ligands and nociception and pain sensitization requires additional research, as some ADAM substrates may transactivate EGFR, including IL-6, which in ovarian cancer, may exhibit crosstalk with EGFR in both its membrane-bound and soluble state (Colomiere et al., 2009). However, consistent with these studies, other evidence further suggests that ADAM-17 may have roles in neuropathic pain, as levels of ADAM17 mRNA increase in the ipsilateral dorsal horn following partial sciatic nerve ligation of mice (Brifault et al., 2019). Additionally, hypomorphic ADAM-17 (ADAM-17$^{ex/ex}$) mice have elevated mechanical thresholds and impaired sensitivity to heat and cold and the DRG of ADAM-17$^{ex/ex}$ mice contain fewer β-4 positive neurons, which are canonically responsive to thermal nociceptive stimuli (Quarta et al., 2019).

Following binding of active-form ligand, the activation of EGFR allows for various signaling pathways to take place that may drive hypersensitivity. There is a wealth of information about the specific roles and actions of distinct EGFR and ErbB ligands in a variety of physiological and pathophysiological settings [reviewed by Citri and Yarden (2006), Ho et al. (2017)]. Importantly, some EGFR ligands of both high and low affinity have been implicated in mediating pain associated with various diseases such as temporomandibular disorder (Martin et al., 2017), vertebral disc herniation and degeneration and radiculopathy (Huang et al., 2017; Kongstorp et al., 2019), rheumatoid arthritis and cancer (Wangzhou et al., 2021) (summarized in **Table 1**).

Though some EGFR ligands have been specifically investigated, the contribution of others in pain signaling can only be inferred and require experimental confirmation. Thus, we focus here on EREG and EGF which have been investigated most thoroughly in this context.

TABLE 1 | Summary of EGFR ligands and their implicated actions in pain.

Ligand	Receptor(s)	Evaluated nocifensive stimuli	Mechanistic findings	Implicated human pain conditions	References
High affinity ligands					
EGF	EGFR	Mechanical	GRK2 phosphorylation; opioid receptor downregulation	Opioid tolerance	Chen et al. (2008), Puig et al. (2020)
BTC	EGFR, HER4	—	—	—	—
	EGFR, HER4	Mechanical	↑ DRG neuron intracellular Ca^{2+}	RA	Wangzhou et al. (2021)
HB-EGF					
TGFα	EGFR	—	—	Pancreatic cancer	Wangzhou et al. (2021)
Low affinity ligands					
AREG	EGFR	—	—	—	—
EREG	EGFR, HER4	Heat; capsaicin; mechanical; formalin	PI3K-Akt-mTORC1 signaling activation; ↑ spontaneous C fibre firing; ↑ capsaicin-evoked DRG neuron intracellular Ca^{2+}	RA; radiculopathy; peripheral nerve injury	Huang et al. (2017), Martin et al. (2017), Kongstorp et al. (2019), Wangzhou et al. (2021)
EPGN	EGFR	—	—	—	—

Experimental evidence for and suggested roles of EGFR ligands in pain. Evaluated nocifensive stimuli, mechanistic findings and human conditions in which ligands have been implicated to contribute to pain are indicated. EGF: epidermal growth factor, BTC: betacellulin, HB-EGF: heparin-binding epidermal growth factor-like growth factor, TGFα: transforming growth factor alpha, AREG: amphiregulin, EREG: epiregulin, EPGN: epigen. PGE2: prostaglandin E2. i. t.: intrathecal, DRG: dorsal root ganglion, RA: rheumatoid arthritis, SNI: spared nerve injury, CFA: complete Freund's adjuvant. — indicates no available data.

Epidermal Growth Factor Receptor Ligands and Their Roles in Pain

EREG, but not other EGFR ligands (EGF, amphiregulin, betacellulin, TGF-α), enhances formalin-induced nocifensive behaviors in mice with EREG administration alone being sufficient to induce heat and mechanical hypersensitivity (Martin et al., 2017). For comparison, EREG-enhanced formalin-induced nocifensive behaviours are comparable to those produced by an established pain modulator, NGF. Importantly, inhibition of the NGF receptor, TrkA, does not block EREG-induced effects, suggesting the mechanism by which EREG promotes pain occurs independently of NGF receptor activity (Martin et al., 2017).

Whether EREG is the only EGFR ligand capable of inducing mechanical hypersensitivity has been addressed recently: EGF administration alone is sufficient to induce mechanical but not thermal hypersensitivity (Puig et al., 2020). However, this effect takes repeated administration over several days to take place, while EREG-induced hypersensitivity occurs within an hour (Puig et al., 2020). Intraplantar administration of HB-EGF is sufficient to induce mechanical sensitivity in male and female mice (Wangzhou et al., 2021), which peaks 1 h after HB-EGF administration after which animals recover to an extent over the course of days.

Whether differences in ligand affinity may contribute to these potential differences remains to be determined. TGF-α may have potential roles in pancreatic cancer pain (Wangzhou et al., 2021). However, whether TGF-α administration alone is sufficient to induce hypersensitivity remains to be investigated. Thus, whether other EGFR ligands may participate in sensitization of other contexts is as of yet unclear. Different EGFR ligands may distinctly contribute to neuropathic pain by different patterns of expression and secretion, or by distinct regulation of the magnitude or duration of EGFR signaling following ligand binding. Collectively, this diversity of EGFR ligand regulation may contribute to context-dependent action of each EGFR ligand in promoting pain sensitization, though further mechanistic studies are required to fully delineate whether this is indeed the case.

Despite the complexity of EGFR ligand signaling, there has been substantial evidence to support a key role for EREG in pain signaling. Following lumbar vertebral disc herniation, EREG is released from intervertebral disks by the NP and annulus fibrosus in patients (Huang et al., 2017), or by NP cells in female rats (Kongstorp et al., 2019). Application of NP-derived EREG onto spinal dorsal nerve roots reduces evoked C-fiber responses but increases their spontaneous activity (Kongstorp et al., 2019), and thus, EREG may act as to mediate neuropathic pain through peripheral mechanisms.

As described above, recent evidence has demonstrated that inhibition of EREG reverses or enhances hypersensitivity in chronic or acute pain models, respectively (Verma et al., 2020). This suggests that EREG mitigates pain during the early stages of its development but eventually contributes to the establishment of chronic pain (Verma et al., 2020). It remains to be elucidated as to whether EREG has direct roles in the establishment of chronic pain or in the maintenance of the chronic pain state.

As both EGFR and its ligands can be expressed in various immune cells relevant to pain and nociception, EREG may have roles in inflammation-driven pain. Clinical data shows increased levels of EREG in leukocytes of patients with temporomandibular disorders (Martin et al., 2017) and RA (Wangzhou et al., 2021). Levels of circulating EREG increase following CFA and SNI (Martin et al., 2017) in rats. Thus, we next discuss EREG and its roles in inflammation in the context of pain.

Epiregulin May Modulate Pain by Altering Inflammation

The inflammatory responses involved in both injury and various diseases drive the development and maintenance of neuropathic pain by promoting mechanical allodynia, neuronal

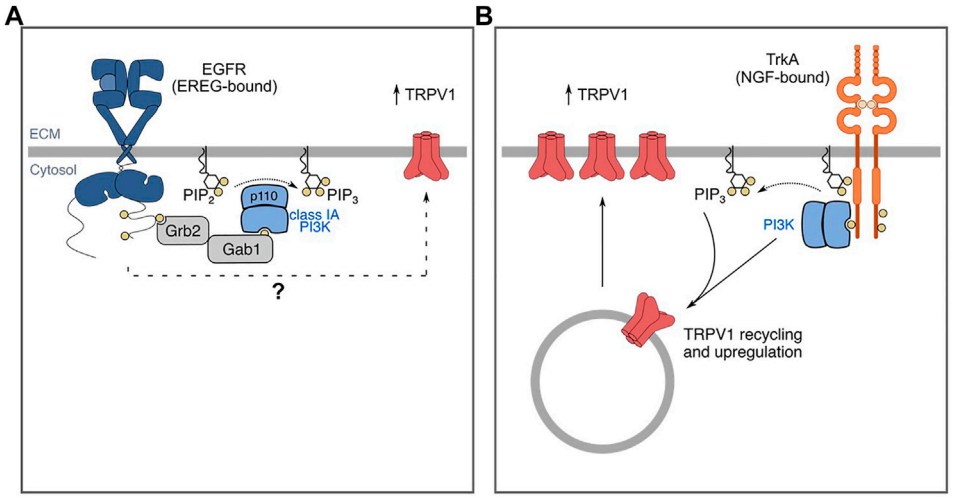

FIGURE 3 | EGF/EREG-EGFR and NGF-TrkA signaling mechanisms that contribute to pain/sensitization. **(A)** EREG-mediated sensitivity to formalin and capsaicin involves TRPV1. **(B)** Similarly, NGF mediates sensitivity to capsaicin and formalin. NGF-TrkA signalling mediates traffic of TRPV1 to the plasma membrane through a PI3K-dependent mechanism. The mechanisms by which NGF mediates sensitivity through these signaling intermediates is more well-characterized and thus, the mechanisms by which EREG-EGFR signaling promotes sensitivity warrants further investigation. The mechanisms by which other EGFR ligands mediate sensitivity are incompletely understood. Additionally, whether and how EREG-EGFR and EGF-EGFR signaling may promote sensitivity to distinct stimuli in various animal models remain to be elucidated.

hypersensitivity, and central sensitization (Baral et al., 2019). EGFR and its cognate ligands have various roles in inflammation, which may also contribute to neuropathic pain pathogenesis. Following their activation, various immune cells secrete EGFR ligands (Burgel and Nadel, 2008). Macrophages exhibit enhanced levels of EREG mRNA following LPS stimulation (Oshima et al., 2011). Primary microglia express membrane-bound EGF (Coniglio et al., 2012), and in mice, EGF expression is enhanced 4 days following spinal cord contusion injury (Greenhalgh et al., 2018).

EREG contributes to inflammation, in part, by modulating the expression of cytokines and growth factors in inflammatory diseases (Murakami et al., 2013; Harada et al., 2015). The expression of pro-inflammatory cytokines in the spinal cord, DRG, injured nerves or skin are associated with pain behaviors and the development of abnormal spontaneous activity from compressed, injured and inflamed DRG neurons (Zhang and An, 2007). Reports first demonstrated that EREG may act synergistically with cytokines to propagate the inflammatory response as the ligand itself is expressed following *in vitro* stimulation with interleukin (IL)-6 and IL-17 (Murakami et al., 2013). EREG subsequently further stimulates an increase in EREG mRNA expression as well as that of IL-6, and enhances NFκB signaling through PI3Kα, IKKα or IKKγ (Murakami et al., 2013). A follow-up study demonstrated that the serum of individuals with RA have elevated levels of several growth factors including EREG, an observation also made in rodent models of RA (Harada et al., 2015). Importantly, the study reports that only EREG levels increase during the early phase of inflammation, while other growth factors were present in the joints at later phases of inflammation (Harada et al., 2015). Additionally, *in vitro* analysis of joint synovial fluid in mice with cytokine-induced RA demonstrates that the neutralization of EREG decreases the expression of growth factors and thereby downregulates further EREG expression (Harada et al., 2015). This collectively suggests that EREG may have a key role in the development of inflammation and pain, however further studies evaluating the functional role of EREG in inflammatory processes are required.

Epiregulin-Epidermal Growth Factor Receptor Signaling Mechanisms That May Contribute to Hyperalgesia and Allodynia

Intrathecal administration of EREG triggers signaling cascades within the DRG that promote pain sensitization (Martin et al., 2017). Inhibition of PI3K or mTORC1, but not MEK1/2, blocks EREG-enhanced pain behaviors following formalin administration, suggesting EREG-enhanced hypersensitivity occurs by a PI3K- and mTORC1-dependent, MEK-independent mechanism (Martin et al., 2017). Here, we describe the signaling cascades activated by EGFR and how the resultant activation of the intermediate proteins PI3K, mTORC1 and MAPK drive peripheral and central sensitization.

Phosphatidylinositol 3-Kinase

PI3Ks are lipid kinases that catalyze the phosphorylation of the 3-position of phosphoinositol. There are three classes of PI3Ks, each generally responsible for generating a different phosphoinositide (phosphorylated derivative of phosphatidylinositol) (Jean and Kiger, 2014). The various phosphoinositides generated by PI3K act upstream of many signaling pathways. While PI3Ks are canonically known to drive cellular growth, PI3K have also been widely shown to mediate pain in various contexts. Inhibition of PI3K using

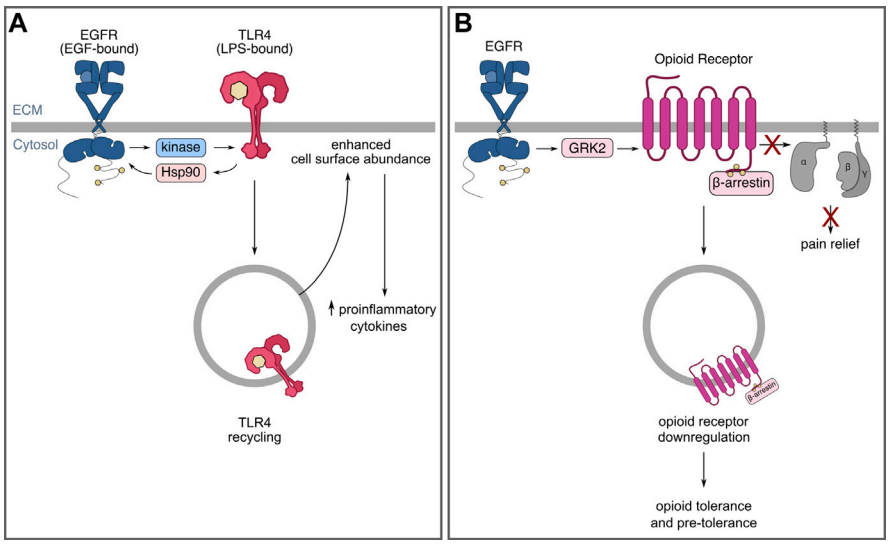

FIGURE 4 | EGFR may modulate immune responses and opioid tolerance by controlling receptor localization and receptor crosstalk. **(A)** EGFR is required for aspects of TLR4 signalling as well as TLR4 recycling and cell-surface enrichment following LPS stimulation. **(B)** EGFR and opioid receptor crosstalk leading to opioid receptor internalization and downregulation that may contribute to tolerance.

wortmannin (Xu et al., 2011; Guo et al., 2017), which may inhibit all classes of PI3K (McNamara and Degterev, 2011), or LY24002 (LY) (Liu et al., 2018), which inhibits class I and III PI3K (Gharbi et al., 2007), perturbs CCI-induced mechanical and thermal hyperalgesia in male rats. In male rodents, inhibition of PI3K using wortmannin reduces carrageenan-induced thermal and mechanical hypersensitivity, as well as late-phase formalin-induced pain behaviors (Xu et al., 2011).

PI3Ks have been shown to contribute to both the establishment and maintenance of neuropathic pain, of which class I PI3Ks have been implicated to have significant roles. However, there remains limited understanding of the importance of the different class I PI3K isoforms in pain. Specific class I PI3K isoforms, which catalyze the phosphorylation of phosphatidylinositol-4,5-bisphosphate ($PI(4,5)P_2$) into phosphatidylinositol-3,4,5-trisphosphate (PIP_3), are differentially expressed within the nervous system. The differential distribution of class I PI3K isoforms (α, β, γ, δ) within various neuron types, supportive cells and immune cells within the DRG and spinal dorsal horn has been implicated in mechanisms of pain (Leinders et al., 2014). After 4 h of intraplantar carrageenan administration, mRNA levels of PI3K α and PI3Kβ or PI3Kγ and PI3Kδ significantly increase within the DRG or spinal cord, respectively. Intrathecal pre-treatment with a PI3Kβ inhibitor blocks carrageenan-induced mechanical allodynia, while inhibitors specific to other PI3K isoforms are not capable of blocking carrageenan-induced mechanical allodynia (Leinders et al., 2014). In contrast, pre-treatment with a PI3Kγ-specific inhibitor but not inhibitors of other PI3K isoforms blocks intraplantar carrageenan-induced mechanical allodynia. Additionally, protein levels of some class I PI3K catalytic and regulatory subunits increase following CCI (Liu et al., 2018). Collectively, these data suggest that the differential distribution of class I PI3K isoforms have distinct roles in nociception. However, the roles of class I PI3K isoforms in different models of pain and in response to other nociceptive stimuli remain to be elucidated. Thus, while there is evidence of upregulation of, and a functional role for class I PI3Ks in pain, further investigation into their precise contributions to pain is warranted.

There is also some evidence that PI3K contributes specifically to EGFR-dependent pain (**Figure 3A**). PI3K inhibition by wortmannin attenuates EREG-enhanced formalin-induced nociceptive behaviors, suggesting EREG-mediated hyperalgesia occurs through a PI3K-dependent mechanism (Martin et al., 2017). However, it should be noted that PI3K is a common signaling intermediate for many receptors implicated in pain and as such, PI3K may be required by other growth factor receptors (namely RTKs) that mediate pain, such as FGFR (Zhang M. et al., 2020). Consistent with this, NGF-TrkA-mediated pain occurs through a PI3K-dependent mechanism (Bonnington and McNaughton, 2003). Hence, further mechanistic study of how PI3K may specifically mediate pain signaling downstream of EGFR in neurons and/or relevant immune cells in the context of pain will be very informative.

One protein that is affected by EREG and/or PI3K activation is the transient receptor potential cation channel subfamily V member 1 (TRPV1). TRPV1 has been widely studied for its roles in thermal hyperalgesia and responds to polymodal stimuli including noxious heat and vanilloid substances such as capsaicin (Jardín et al., 2017). Administration of EREG alone is sufficient to induce thermal hyperalgesia (Martin et al., 2017). In addition, EREG enhances capsaicin-induced nocifensive behaviors. Administration of the TRPV1 antagonist AMG 9810 blocks EREG-induced hyperalgesia in the late phase of the formalin test (Martin et al., 2017). These data suggest that one of the mechanisms by which EREG may promote sensitivity involves TRPV1. However, whether EREG enhances TRPV1 activity

through mechanisms such as transcriptional regulation, or by enhancing cell surface abundance, remain to be determined (**Figure 3A**). Similarly, NGF administration has also been reported to promote sensitization in part by inducing TRPV1 upregulation through a PI3K-dependent mechanism (**Figure 3B**) (Stein et al., 2006; Zhu and Oxford, 2007a; Stratiievska et al., 2018).

The mechanism by which NGF mediates TRPV1 upregulation has been studied in greater detail than that of EREG. In F-11 cells, a cellular model of undifferentiated sensory neurons, NGF-stimulation leads to increased cell surface TRPV1 (Stein et al., 2006; Stratiievska et al., 2018), and inhibition of PI3K with wortmannin blocks this effect (Stratiievska et al., 2018). NGF stimulation enhances plasma membrane TRPV1 with constant cytosolic TRPV1 (Pinho-Ribeiro et al., 2017). It is unclear as to whether TRPV1 may be transcriptionally upregulated or whether this enhanced traffic to the cell surface occurs with constant total TRPV1 expression, the latter of which would indicate NGF mediates TRPV1 traffic to the cell surface. In addition, patch-clamp recordings of mouse DRG neurons suggests that NGF stimulation leads to an increase in maximum current, but not the EC50 in response to capsaicin through enhanced cell-surface TRPV1 (Stein et al., 2006). Some evidence suggests that the regulation of TRPV1 and PI3K may be reciprocal.

Class I PI3K activation canonically leads to the phosphorylation and activation of Akt and although some studies suggest roles for Akt in hypersensitivity following formalin administration (Xu et al., 2011), others suggest Akt may not have a significant role as Akt phosphorylation may decrease in the late phase of the formalin test, but this observation was not statistically significant (Pezet et al., 2008). Thus, whether and how Akt may be involved in sensitization by EREG or other EGFR ligands remains poorly understood.

In F-11 cells, in addition to PI3K signaling leading to enhanced cell surface TRPV1, ectopic TRPV1 expression enhances NGF-stimulated PI3K-dependent Akt phosphorylation at T308 and S473, both of which are required for full activation of Akt (Stratiievska et al., 2018). Furthermore, NGF-enhanced capsaicin-induced nocifensive behaviors are greatly reduced in PI3K-deficient mice (p85α-null), suggesting that class I PI3K is important in driving sensitization (Zhu and Oxford, 2007a). It remains to be elucidated as to whether EREG-induced sensitization through TRPV1 requires specific PI3K subunit isoforms, and whether EGFR augments TRPV1 cell surface expression. Like EREG, NGF may be produced by immune cells such as macrophages (Shutov et al., 2016). However, the therapeutic potential of anti-NGF treatments (or TrkA inhibitors) in the treatment of pain is more established (Da Silva et al., 2019). Additionally, whether EREG-mediated signaling cascades occur in primary afferents, immune cells, or both, remains to be elucidated.

Mechanistic Target of Rapamycin Complex

The mammalian target of rapamycin (mTOR) controls cellular metabolism and many other cellular functions by incorporating diverse signals from ligand-binding to intracellular cues regarding energy and nutrient availability (Liu and Sabatini, 2020). In mammals, mTOR functions as the catalytic subunit of at least two complexes (C1 and C2) that are distinct in their composition, activation, and cellular functions, which have been reviewed elsewhere (Kim and Guan, 2019; Liu and Sabatini, 2020). Importantly, mTORC1 is activated by PI3K-Akt signaling and mediates some critical aspects of PI3K-Akt signaling (Manning and Toker, 2017).

Given the activation of mTORC1 downstream of PI3K-Akt signaling, this kinase may mediate some of the important pain signals driven by EGFR and/or PI3K. Consistent with this, mTORC1 inhibitors such as rapamycin (also known as sirolimus) and rapamycin derivatives such as temsirolimus (CCI-779) inhibit mTORC1 and have been used in clinical trials for cancer therapy (Zhou and Huang, 2010; Dreyling et al., 2016;). Administration of rapamycin (or another inhibitor of PI3K and mTORC1, PI-103) reduces nociceptive behaviors in the late phase of the formalin test (Xu et al., 2011). In male mice, local (intraplantar) or systemic (intraperitoneal) administration of temsirolimus attenuates SNI- and carrageenan-induced mechanical hypersensitivity, and SNI-induced cold hypersensitivity in the acetone test. However, local or systemic administration of temsirolimus treatment does not block SNI- or carrageenan-induced heat hypersensitivity, suggesting mTORC1 may contribute to SNI-induced mechanical and heat hypersensitivity, but not cold hypersensitivity (Obara et al., 2011).

Similarly, temsirolimus and rapamycin block EREG-mediated hypersensitivity in the formalin test (Martin et al., 2017). Hence, while some evidence for mTORC1 exists in mediating pain signaling, given that rapamycin, and potentially its derivatives, may inhibit both mTOR complexes (Zhou and Huang, 2010), the mechanism(s) by which mTOR complexes may contribute to EREG mediated pain sensitization remains to be further examined.

Mitogen-Activated Protein Kinase

The family of mitogen-activated protein kinases (MAPKs) includes three major members: extracellular regulated kinase (ERK), p38 and c-jun N-terminal Kinase (JNK). Notably, EGFR signaling activates Erk in most cell types leading to proliferation and differentiation (Dong et al., 2004; Wee and Wang, 2017). p38 and JNK are activated in a cell and tissue-context-dependent manner, in which stresses such as tissue damage can lead to the activation of p38 and JNK signaling, in which both have roles in various programmed cell death pathways (Jin et al., 2003; Zhuang et al., 2005; Cuadrado and Nebreda, 2010; Lee et al., 2020). Following peripheral nerve injury, these MAPKs are differentially expressed in astrocytes and in microglia, important cellular players in the development of neuropathic pain (Jin et al., 2003; Zhuang et al., 2005; Zhuang et al., 2006). Different MAPKs are necessary for the development of distinct phases of neuropathic pain. For instance, the phosphorylation and activation of p38 and ERK in spinal microglia is necessary to establish SNL-induced nociceptive behaviors in mice (Jin et al., 2003; Zhuang et al., 2005), whereas JNK or ERK activation in spinal astrocytes is necessary for the development and maintenance of SNL-

induced mechanical allodynia, which is blocked by inhibition of JNK (Ji et al., 2009; Zhuang et al., 2005; Zhuang et al., 2006). Nociceptive stimuli (mechanical, heat, cold) but not innocuous light touch induce ERK activation within the dorsal horn. Pre-treatment with MEK inhibitor PD 98059 blocks formalin-induced nocifensive and nociceptive behaviors in rats (Ji et al., 1999). Additionally, pre-administration of a p38 inhibitor prevents SNL-induced mechanical allodynia (Jin et al., 2003).

In terms of drug development, p38 MAPK is a novel target of cytokine-suppressive anti-inflammatory drugs due to its regulatory role in the synthesis of inflammatory intermediates (Anand et al., 2011). In the CFA model of inflammatory pain, CFA administration leads to activation of p38 and ERK1/2 in the DRG, and inhibition of p38 may reduce neuronal sensitization (Zhang et al., 2018). Additionally, chronic compression of the DRG induces mechanical allodynia that is attenuated following intrathecal injections of MAPK inhibitors in rats (Qu et al., 2016). In a clinical trial, patients with nerve trauma, radiculopathy or carpal tunnel syndrome, that were treated with dilmapimod, a p38 MAPK inhibitor, demonstrated a significant reduction in pain (Anand et al., 2011). However, larger clinical trials assessing dilmapimod use are needed for clinically meaningful effect sizes and diversity of cohorts to demonstrate the analgesic effects of inhibiting p38 MAPK (Anand et al., 2011). While these studies collectively indicate that p38 MAPK, Erk and JNK may each contribute to pain, whether and how EGFR modulation or pain requires these signals remains to be examined.

Indirect Actions of Epidermal Growth Factor Receptor Through Crosstalk With Signaling by Other Receptors

Recent evidence has shown that EGFR has non-canonical roles in regulating physiological processes such as inflammation, and pathophysiological functions in inflammatory pain and neuropathic pain. Though we have discussed how EGFR may regulate pain through direct ligand-induced activation of EGFR and canonical downstream signaling intermediates, EGFR also controls cellular processes indirectly through crosstalk with other plasma membrane receptors. Ligand-bound EGFR may induce the activation of another receptor or another receptor may transactivate EGFR. Here, we focus on two mechanisms by which EGFR regulates pain-generating processes through receptor crosstalk.

Epidermal Growth Factor Receptor Crosstalk: Toll-Like Receptor 4

Toll-like receptors (TLRs) have key roles in the activation of the innate immune system by detecting pathogen-associated molecular patterns (PAMPs) and damage-associated molecular patterns (DAMPs) associated with various microbes and cellular damage, respectively (Kawasaki and Kawai, 2014). Upon binding their respective PAMPs or DAMPs, active TLRs mediate immune responses and cytokine production (Kawasaki and Kawai, 2014). TLR activation in various cell types, including microglia, astrocytes, and sensory neurons, has been implicated in the development of persistent pain [reviewed by Lacagnina et al. (2018)]. Among the most widely studied of these is TLR4, which makes up part of the extracellular lipopolysaccharide (LPS) receptor. Lipopolysaccharides (endotoxins) are a major constituent of the gram-negative bacterial outer membrane that mediate various inflammatory signaling pathways (Mazgaeen and Gurung, 2020). In the context of pain signaling, LPS stimulation may sensitize TRPV1-positive neurons within trigeminal ganglia by sensitizing capsaicin-induced inward calcium currents and release of calcitonin gene-related peptide, a pain mediator (Diogenes et al., 2011). Furthermore, LPS may contribute to pain sensitization mediated by other triggers, as seen for example by blockage of paclitaxel-induced capsaicin sensitization in DRG and spinal dorsal horn neuron by administration of the TLR4 antagonist, LPS-RS (Li et al., 2015).

While EGF may be sufficient to induce microglial chemotaxis (Nolte et al., 1997), this may involve cross-talk with LPS and/or TLR4 signaling, as EGFR can also affect the LPS-induced chemotaxis of primary microglia. Inhibition of EGFR with AG1478 blocks LPS-induced chemotaxis of primary microglia (Qu et al., 2015). Moreover, inhibition of EGFR in primary microglia (Qu et al., 2012), and inhibition or shRNA silencing of EGFR in bone marrow-derived macrophages (BMDM) (Chattopadhyay et al., 2015), blocks LPS-induced production of proinflammatory cytokines IL-1β and TNFα *in vitro*. A similar result has been reported in bone marrow derived macrophages and RAW 264.7 cells, in which inhibition of EGFR reduces LPS-stimulated IL-1β, IL-6, IL-10 and TNFα expression (Tang et al., 2020), indicating that EGFR is essential for LPS-induced regulation of inflammation in macrophages.

While TLR4 activation may stimulate EGFR activation to elicit changes in inflammatory signaling, other studies suggest that EGFR may also act as an upstream mediator of TLR4 signaling, perhaps as part of a reciprocal activation mechanism involving EGFR and TLR4. In human mammary epithelial cells, EGF stimulation induces TLR4 phosphorylation and inhibition of EGFR with erlotinib blocks EGF-stimulated TLR4 phosphorylation, suggesting EGFR stimulation alone is sufficient to induce TLR4 activation (De et al., 2015). siRNA silencing of TLR4 does not block EGF-stimulated EGFR phosphorylation (Y1068) (De et al., 2015), suggesting that EGFR may act as an upstream mediator of TLR4 signaling. In support of this notion in an *in vivo* LPS instillation model of endotoxemia, EGFR inhibition improves animal survival in part by attenuating IL-6, TNFα and CXCL1 upregulation (De et al., 2015). Additionally, in a rat SCI model, inhibition of EGFR prevents the transcritpional upregulation of IL-1β and TNFα, further highlighting the ability of EGFR to modulate pro-inflammatory signaling (Qu et al., 2012).

The mechanisms by which EGFR may be required for TLR4 signaling have been recently investigated. Some evidence suggests that TLR4 may transactivate EGFR through protein intermediates, such as Hsp90 (Thuringer et al., 2011), while other evidence suggests that the Src family kinase, Lyn, may be required for some pathways activated by EGFR-mediated TLR4 signalling (De et al., 2015). A recent study has shown that EGFR augments TLR4 cell surface abundance in murine

bone marrow-derived macrophages by mediating TLR4 internalization and subsequent traffic that leads to TLR4 recycling (Tang et al., 2020), which may in turn enhance the magnitude or duration of TLR4 signaling. These results were not sex-dependent (Tang et al., 2020), unlike other neuroimmune mechanisms of pain (Mapplebeck et al., 2018). Collectively, these data present evidence for mechanisms by which EGFR may control signalling by receptors involved in inflammatory responses, such as TLR4, and that this regulation may be part of positive feedback linking activation of EGFR and TLR4 in select cells such as macrophages (**Figure 4A**). Future studies should be directed at investigating the functional implications of the extensive crosstalk between TLR and EGFR signaling pathways on pain sensitization and chronic neuropathic and non-neuropathic pain.

Epidermal Growth Factor Receptor Crosstalk: Opioid Receptors

Opioids continue to be a mainstay of pain management; however preclinical and clinical evidence suggests that continued use may contribute to neural changes that promote the transition from acute to chronic pain [reviewed in Kandasamy and Price (2015)]. The "hyperalgesic priming" model developed by Jon Levine and colleagues describes that following the resolution of an acute "priming" stimulus (e.g., carrageenan), a secondary stimulus (that is normally subthreshold) leads to a prolonged state of hypersensitivity (Kandasamy and Price, 2015). One such secondary stimulus is prostaglandin E2 (PGE_2), which drives sensitization of peripheral nerve terminals and is a major cause of inflammatory pain (Scholze et al., 2014). Opioids may induce the prolongation or maintenance of PGE_2-induced hyperalgesia (Araldi et al., 2015), and some evidence has shown that EGFR may be required for this process as well. DAMGO, a mu-opioid receptor agonist, prolongs PGE_2-induced hyperalgesia. Importantly, DAMGO-induced hyperalgesia prolongation is blocked by inhibition of EGFR (Araldi et al., 2018), suggesting that EGFR is required for mu-opioid receptor-mediated prolongation of PGE_2-induced hyperalgesia. This evidence demonstrates that EGFR may have roles in the mechanisms by which opioid receptors prolong states of hypersensitivity.

EGFR may also participate in driving opioid tolerance through opioid receptor downregulation (**Figure 4B**). Opioids have widely been reported to have low analgesic efficacy in patients and animal models of neuropathic pain, which may be, in part, due to their downregulation in neuropathic pain (Obara et al., 2007). Opioid receptors of mu (MOR), delta (DOR), and kappa (KOR) subtypes, are G-protein coupled receptors (GPCRs) (Allouche et al., 2014) expressed within the nervous system, including the DRG (Zhou et al., 2014; Sun et al., 2017) and dorsal horn (Ikoma et al., 2007; Zhou et al., 2014). Upon ligand-binding, the active GPCR induces not only canonical G-protein signaling, but also the activation of GPCR kinases (GRKs) that promote the association of β-arrestins to the receptor, thereby inducing receptor internalization and eventual down-regulation (Allouche et al., 2014). Accumulating evidence demonstrates that various opioid receptors are down-regulated in various animal models of neuropathic pain (Obara et al., 2007).

Crosstalk between EGFR and G-protein-coupled receptors (GPCRs), including that between EGFR and opioid receptors (Belcheva et al., 2003; Chen et al., 2008; Clayton et al., 2010; Lennon et al., 2014), has been established in various contexts and may result in EGFR-driven downregulation of opioid receptors. EGF pre-treatment promotes agonist-induced DOR and MOR internalization, and EGF stimulation alone promotes GRK2 traffic to the plasma membrane, EGFR association with GRK2, and GRK2 phosphorylation *in vitro* (Chen et al., 2008). Similarly, EGFR may attenuate G-protein signaling and lead to the downregulation of other GPCRs through GRK2 phosphorylation, such as the dopamine D2-like receptor, D_3R (Sun et al., 2018). Since opioid receptor agonists induce receptor internalization that may lead to their downregulation, it has been proposed that opioid receptor downregulation in neuropathic pain is due to the disease itself, rather than medication (agonist)-induced downregulation (Sun et al., 2017). However, as these studies indicate, EGFR-dependent modulation of opioid receptors may have a central role in pain and in opioid tolerance.

Consistent with a possible role of EGFR in modulating opioid receptor signaling, clinical case reports indicate that pharmacological inhibition of EGFR may have effects on opioid efficacy and tolerance. In the case series conducted by Kersten and colleagues, some patients were able to decrease their opioid dose significantly within days following treatment with cetuximab (Kersten et al., 2013). In addition, these patients experienced significant pain relief for the first time in months and experienced improvements in physical functioning. This notion has been supported by preclinical evidence, in which inhibition of EGFR (gefitinib) reverses morphine tolerance in rats following SNL by restoring the analgesic effect of morphine against mechanical allodynia (Puig et al., 2020). This suggests that therapeutics targeting EGFR may be repurposed to restore the analgesic effect of morphine in neuropathic pain, though this should be replicated with larger and more diverse cohorts to determine whether the generalizability of these findings. In this case, EGFR inhibitors may provide both direct analgesic effects in addition to improving the pharmacologic benefit and safety of opioids in patients with neuropathic pain.

The above is analogous to observations made in a rat CFA model, where inhibition of NGF-TrkA signaling reversed morphine tolerance (Mousa et al., 2007). In the SNL model, PDGFR inhibition similarly restores morphine analgesic effects in male rats (Donica et al., 2014) and inhibition of PDGFR-β reverses morphine tolerance, but does not eliminate the acute analgesic effect of morphine in rats (Wang et al., 2012). Administration of PDGFR agonist (PDGFR-BB) induces mechanical allodynia, which is blocked by inhibition of EGFR with gefitinib (Puig et al., 2020). However, whether PDGFR and EGFR crosstalk in driving opioid tolerance remains to be determined. Thus, while RTK signaling may drive opioid tolerance, the contribution of various RTKs such as EGFR in specific contexts warrants further investigation. Although studies by Puig et al. (EGFR) and Donica et al. (PDGFR) observed that administration of gefitinib or imatinib, respectively, do not reverse SNL-induced mechanical allodynia, treatment with these respective inhibitors restores the analgesic effect of

morphine in rats. Importantly, whether EGFR may drive opioid tolerance through peripheral or central mechanisms is incompletely understood.

CONCLUDING REMARKS

Chronic pain, particularly chronic neuropathic pain, remains a global health priority due to a paucity of effective and well tolerated therapies. Inhibitors of EGFR may exert analgesic effects in patients with neuropathic pain with minimal side effects. These empiric clinical findings are supported by various preclinical models of pain hypersensitivity. However, the use of EGFR inhibitors in neuropathic pain treatment may be cost-prohibitive, with costs per month in the thousands of dollars (Wang et al., 2013; Yang et al., 2020). Additionally, preclinical studies demonstrating roles of EGFR in pathological non-neuropathic pain are limited, and whether inhibitors of EGFR exert analgesic effects in patients with pathological, non-neuropathic pain remains to be determined. Considerable work remains in both the clinical and preclinical spheres to evaluate the benefit of repurposing EGFR inhibitors for patient care and understanding the mechanistic basis for EGFR's involvement in pain.

The mechanisms by which EGFR may mediate or contribute to the initiation and maintenance of neuropathic pain are likely diverse given the pleiotropic cellular functions of this receptor family. These may include both direct actions of the receptor by binding its cognate ligands and indirect actions through transactivation. Few studies have investigated the signaling mechanisms by which EREG may mediate sensitization, though it appears that similar to NGF-mediated sensitization, this mechanism requires PI3K. Thus, an outstanding and fundamental question surrounds whether RTKs have shared mechanisms by which they impact pain hypersensitivity or have distinct pathways. The latter is important as the differential contributions and molecular pathways may inform pharmacologic strategies with increased context specificity. Current evidence suggests that class I PI3K are the main contributors in neuropathic pain. Future work directed at delineating the specific roles of specific class I isoforms would be beneficial since there are a variety of pan- and isoform-specific inhibitors in clinical trial. Importantly, there are other pain mediators, such as STAT3 (Liu et al., 2013; Zhang et al., 2017; Hu et al., 2020), that are also activated by EGFR (Han and Lo, 2012). The extent to which these targets contribute to EGFR-mediated hypersensitivity remains to be elucidated.

Limitations of animal models of pain [reviewed by Mogil (2009)] are influenced by many factors such as methodological differences, strain and genotype, social interactions, and sex affect various aspects of pain physiology and pathophysiology (Deuis et al., 2017). Sex differences in neuroimmunology and pain perception [reviewed by Mapplebeck et al. (2016), Rosen et al. (2017)] and in the expression of EGFR, its ligands and EGFR signalling (Treister et al., 2005; Liu et al., 2016; Zhang et al., 2019) are well documented. Yet, many clinical and pre-clinical studies provide little data around sex and gender as a variable in their studies. As a result, whether sex differences exist in the mechanisms by which EGFR mediates pain, and the therapeutic implications of such differences, remains to be elucidated.

EGFR may influence pain directly or indirectly by controlling traffic of other pain-associated proteins, such as TRPV1 or TLR4 and opioid receptors, respectively. Given the importance of neuro-immune interactions in pain, the roles EGFR in these processes warrant further investigation. The reduced effectiveness of opioids and increased tolerance in patients with neuropathic pain remains problematic. As such, the preclinical evidence suggesting that EGFR inhibition may reverse morphine tolerance is exciting and requires further evaluation.

The evidence we reviewed here positions EGFR as an important player in pathological pain states and provides the impetus for the clinical and biomedical research communities to investigate EGFR as a potential therapeutic target.

AUTHOR CONTRIBUTIONS

All authors listed have made a substantial, direct, and intellectual contribution to the work and approved it for publication.

FUNDING

This work was supported by a project grant from the International Anesthesia Research Society Mentored Research Award to BS, a project grant from the Canadian Institutes of Health Research (PJT-156355) to GF, and an Ontario Early Researcher Award and CIHR New Investigator Award to CA.

ACKNOWLEDGMENTS

Figures were generated using BioRender.com and inkscape.org.

REFERENCES

Adrain, C., and Freeman, M. (2014). Regulation of Receptor Tyrosine Kinase Ligand Processing. *Cold Spring Harbor Perspect. Biol.* 6 (Issue 1), a008995. doi:10.1101/cshperspect.a008995

Aguirre, A., Dupree, J. L., Mangin, J. M., and Gallo, V. (2007). A Functional Role for EGFR Signaling in Myelination and Remyelination. *Nat. Neurosci.* 10 (8), 990–1002. doi:10.1038/nn1938

Aiyer, R., Mehta, N., Gungor, S., and Gulati, A. (2018). A Systematic Review of NMDA Receptor Antagonists for Treatment of Neuropathic Pain in Clinical Practice. *The Clin. J. Pain* 34 (5), 450–467. doi:10.1097/ajp.0000000000000547

Alkislar, I., Miller, A. R., Hohmann, A. G., Sadaka, A. H., Cai, X., Kulkarni, P., et al. (2020). Inhaled Cannabis Suppresses Chemotherapy-Induced Neuropathic Nociception by Decoupling the Raphe Nucleus: A Functional Imaging Study in Rats. *Biol. Psychiatry Cogn. Neurosci. Neuroimaging* 6, 479–489. doi:10.1016/j.bpsc.2020.11.015

Allouche, S., Noble, F., and Marie, N. (2014). Opioid Receptor Desensitization: Mechanisms and its Link to Tolerance. *Front. Pharmacol.* 5, 280. doi:10.3389/fphar.2014.00280

Alper, B. S., and Lewis, P. R. (2002). Review: Tricyclic Antidepressants, Capsaicin, Gabapentin, and Oxycodone Are Effective for Postherpetic Neuralgia. *Evidence-based Med. (English Ed.)* 7 (5), 147. doi:10.1136/ebm.7.5.147

Anand, P., Shenoy, R., Palmer, J. E., Baines, A. J., Lai, R. Y. K., Robertson, J., et al. (2011). Clinical Trial of the P38 MAP Kinase Inhibitor Dilmapimod in Neuropathic Pain Following Nerve Injury. *Eur. J. Pain* 15, 1040–1048. doi:10.1016/j.ejpain.2011.04.005

Araldi, D., Ferrari, L. F., and Levine, J. D. (2015). Repeated Mu-Opioid Exposure Induces a Novel Form of the Hyperalgesic Priming Model for Transition to Chronic Pain. *J. Neurosci.* 35 (36), 12502–12517. doi:10.1523/jneurosci.1673-15.2015

Araldi, Dionéia., Ferrari, L. F., and Levine, J. D. (2018). Role of GPCR (Mu-opioid)-receptor Tyrosine Kinase (Epidermal Growth Factor) Crosstalk in Opioid-Induced Hyperalgesic Priming (Type II). *Pain* 159, 864–875. doi:10.1097/j.pain.0000000000001155

Ardeleanu, V., Toma, A., Pafili, K., Papanas, N., Motofei, I., Diaconu, C. C., et al. (2020). Current Pharmacological Treatment of Painful Diabetic Neuropathy: A Narrative Review. *Medicina* 56 (1), 25. doi:10.3390/medicina56010025

Baral, P., Udit, S., and Chiu, I. M. (2019). Pain and Immunity: Implications for Host Defence. *Nat. Rev. Immunol.* 19, 433–447. doi:10.1038/s41577-019-0147-2

Barkai, O., Puig, S., Lev, S., Title, B., Katz, B., Eli-Berchoer, L., et al. (2019). Platelet-derived Growth Factor Activates Nociceptive Neurons by Inhibiting M-Current and Contributes to Inflammatory Pain. *Pain* 160, 1281–1296. doi:10.1097/j.pain.0000000000001523

Baron, R. (2006). Mechanisms of Disease: Neuropathic Pain-A Clinical Perspective. *Nat. Rev. Neurol.* 2, 95–106. doi:10.1038/ncpneuro0113

Basbaum, A. I., Bautista, D. M., Scherrer, G., and Julius, D. (2009). Cellular and Molecular Mechanisms of Pain. *Cell* 139 (2), 267–284. doi:10.1016/j.cell.2009.09.028

Belcheva, M. M., Tan, Y., Heaton, V. M., Clark, A. L., and Coscia, C. J. (2003). μ Opioid Transactivation and Down-Regulation of the Epidermal Growth Factor Receptor in Astrocytes: Implications for Mitogen-Activated Protein Kinase Signaling. *Mol. Pharmacol.* 64, 1391–1401. doi:10.1124/mol.64.6.1391

Bennett, M. I., Kaasa, S., Barke, A., Korwisi, B., Rief, W., and Treede, R.-D. (2019). The IASP classification of chronic pain for ICD-11: chronic cancer-related pain. *Pain* 160 (1), 38–44. doi:10.1097/j.pain.0000000000001363

Bezjak, A., Tu, D., Seymour, L., Clark, G., Trajkovic, A., Zukin, M., et al. (2006). Symptom Improvement in Lung *Cancer* Patients Treated with Erlotinib: Quality of Life Analysis of the National *Cancer* Institute of Canada Clinical Trials Group Study BR.21. *Jco* 24 (24), 3831–3837. doi:10.1200/jco.2006.05.8073

Birecree, E., King, L. E., and Nanney, L. B. (1991). Epidermal Growth Factor and its Receptor in the Developing Human Nervous System. *Dev. Brain Res.* 60 (2), 145–154. doi:10.1016/0165-3806(91)90043-i

Bonnington, J. K., and McNaughton, P. A. (2003). Signalling Pathways Involved in the Sensitisation of Mouse Nociceptive Neurones by Nerve Growth Factor. *J. Physiol.* 551, 433–446. doi:10.1113/jphysiol.2003.039990

Bouhassira, D., and Attal, N. (2019). The Multiple Challenges of Neuropathic Pain. *Neurosci. Lett.* 702, 6–10. doi:10.1016/j.neulet.2018.11.054

Brifault, C., Kwon, H., Campana, W. M., and Gonias, S. L. (2019). LRP1 Deficiency in Microglia Blocks Neuro-inflammation in the Spinal Dorsal Horn and Neuropathic Pain Processing. *Glia* 67 (6), 1210–1224. doi:10.1002/glia.23599

Burgel, P. R., and Nadel, J. A. (2008). Epidermal Growth Factor Receptor-Mediated Innate Immune Responses and Their Roles in Airway Diseases. *Eur. Respir. J.* 32, 1068–1081. doi:10.1183/09031936.00172007

Cappuzzo, F., Ciuleanu, T., Stelmakh, L., Cicenas, S., Szczésna, A., Juhász, E., et al. (2010). Erlotinib as Maintenance Treatment in Advanced Non-small-cell Lung Cancer: a Multicentre, Randomised, Placebo-Controlled Phase 3 Study. *Lancet Oncol.* 11 (6), 521–529. doi:10.1016/s1470-2045(10)70112-1

Cavalli, E., Mammana, S., Nicoletti, F., Bramanti, P., and Mazzon, E. (2019). The Neuropathic Pain: An Overview of the Current Treatment and Future Therapeutic Approaches. *Int. J. Immunopathology Pharmacol.* 33, 2058738419838383. doi:10.1177/2058738419838383

Chalil, A., Staudt, M. D., Harland, T. A., Leimer, E. M., Bhullar, R., and Argoff, C. E. (2021). A Safety Review of Approved Intrathecal Analgesics for Chronic Pain Management. *Expert Opin. Drug Saf.* 20, 439–451. doi:10.1080/14740338.2021.1889513

Challa, S. R. (2015). Surgical Animal Models of Neuropathic Pain: Pros and Cons. *Int. J. Neurosci.* 125 (3), 170–174. doi:10.3109/00207454.2014.922559

Chang, D. S., Hsu, E., Hottinger, D. G., and Cohen, S. P. (2016). Anti-nerve Growth Factor in Pain Management: Current Evidence. *J. Pain Res.* 9, 373–383. doi:10.2147/JPR.S89061

Chattopadhyay, S., Veleeparambil, M., Poddar, D., Abdulkhalek, S., Bandyopadhyay, S. K., Fensterl, V., et al. (2015). EGFR Kinase Activity Is Required for TLR4 Signaling and the Septic Shock Response. *EMBO Rep.* doi:10.15252/embr.201540337

Chen, P.-H., Bendris, N., Hsiao, Y.-J., Reis, C. R., Mettlen, M., Chen, H.-Y., et al. (2017). Crosstalk between CLCb/Dyn1-Mediated Adaptive Clathrin-Mediated Endocytosis and Epidermal Growth Factor Receptor Signaling Increases Metastasis. *Dev. Cel* 40 (3), 278–288. doi:10.1016/j.devcel.2017.01.007

Chen, W., Walwyn, W., Ennes, H. S., Kim, H., Mcroberts, J. A., and Marvizón, J. C. G. (2014). BDNF Released during Neuropathic Pain Potentiates NMDA Receptors in Primary Afferent Terminals. *Eur. J. Neurosci.* 39 (9), 1439–1454. doi:10.1111/ejn.12516

Chen, Y., Long, H., Wu, Z., Jiang, X., and Lan, M. (2008). EGF Transregulates Opioid Receptors through EGFR-Mediated GRK2 Phosphorylation and Activation. *Mol. Biol. Cel* 19, 2973–2983. doi:10.1091/mbc.E07-10-1058

Chincholkar, M. (2018). Analgesic Mechanisms of Gabapentinoids and Effects in Experimental Pain Models: a Narrative Review. *Br. J. Anaesth.* 120 (6), 1315–1334. doi:10.1016/j.bja.2018.02.066

Chong, V. Z., Webster, M. J., Rothmond, D. A., and Weickert, C. S. (2008). Specific Developmental Reductions in Subventricular Zone ErbB1 and ErbB4 mRNA in the Human Brain. *Int. J. Dev. Neurosci.* 26 (7), 791–803. doi:10.1016/j.ijdevneu.2008.06.004

Chung, J. M., Kim, H. K., and Chung, K. (2004). Segmental Spinal Nerve Ligation Model of Neuropathic Pain. *Methods Mol. Med.* 99, 35–45. doi:10.1385/1-59259-770-x:203

Cichon, J., Sun, L., and Yang, G. (2018). Spared Nerve Injury Model of Neuropathic Pain in Mice. *Bio-Protocol* 8 (6), e2777. doi:10.21769/bioprotoc.2777

Citri, A., and Yarden, Y. (2006). EGF-ERBB Signalling: towards the Systems Level. *Nat. Rev. Mol. Cel Biol* 7 (7), 505–516. doi:10.1038/nrm1962

Clayton, C. C., Bruchas, M. R., Lee, M. L., and Chavkin, C. (2010). Phosphorylation of the μ-opioid Receptor at Tyrosine 166 (Tyr3.51) in the DRY Motif Reduces Agonist Efficacy. *Mol. Pharmacol.* 77 (3), 339–347. doi:10.1124/mol.109.060558

Coderre, T. J. (2018). Topical Drug Therapeutics for Neuropathic Pain. *Expert Opin. Pharmacother.* 19 (11), 1211–1220. doi:10.1080/14656566.2018.1501026

Colloca, L., Ludman, T., Bouhassira, D., Baron, R., Dickenson, A. H., Yarnitsky, D., et al. (2017). Neuropathic Pain. *Nat. Rev. Dis. Primers*. doi:10.1038/nrdp.2017.2

Colomiere, M., Ward, A. C., Riley, C., Trenerry, M. K., Cameron-Smith, D., Findlay, J., et al. (2009). Cross Talk of Signals between EGFR and IL-6R through JAK2/STAT3 Mediate Epithelial-Mesenchymal Transition in Ovarian Carcinomas. *Br. J. Cancer* 100 (1), 134–144. doi:10.1038/sj.bjc.6604794

Coniglio, S. J., Eugenin, E., Dobrenis, K., Stanley, E. R., West, B. L., Symons, M. H., et al. (2012). Microglial Stimulation of Glioblastoma Invasion Involves Epidermal Growth Factor Receptor (EGFR) and Colony Stimulating Factor 1 Receptor (CSF-1R) Signaling. *Mol. Med.* 9 (18), 519–527. doi:10.1158/1538-7445.am2012-46

Cuadrado, A., and Nebreda, A. R. (2010). Mechanisms and Functions of P38 MAPK Signalling. *Biochem. J.* 429 (3), 403–417. doi:10.1042/bj20100323

Cuellar, J. M., Montesano, P. X., Antognini, J. F., and Carstens, E. (2005). Application of Nucleus Pulposus to L5 Dorsal Root Ganglion in Rats Enhances Nociceptive Dorsal Horn Neuronal Windup. *J. Neurophysiol.* 94 (1), 35–48. doi:10.1152/jn.00762.2004

Da Silva, J. T., Evangelista, B. G., Venega, R. A. G., Seminowicz, D. A., and Chacur, M. (2019). Anti-NGF Treatment Can Reduce Chronic Neuropathic Pain by Changing Peripheral Mediators and Brain Activity in Rats. *Behav. Pharmacol.* 30 (1), 79–88. doi:10.1097/FBP.0000000000000422

De, S., Zhou, H., DeSantis, D., Croniger, C. M., Li, X., and Stark, G. R. (2015). Erlotinib Protects against LPS-Induced Endotoxicity Because TLR4 Needs

EGFR to Signal. *Proc. Natl. Acad. Sci. United States America* 112 (31), 9680–9685. doi:10.1158/1538-7445.am2015-1944

Deuis, J. R., Dvorakova, L. S., and Vetter, I. (2017). Methods Used to Evaluate Pain Behaviors in Rodents. *Front. Mol. Neurosci.* 10, 284. doi:10.3389/fnmol.2017.00284

Diogenes, A., Ferraz, C. C. R., Akopian, A. N., Henry, M. A., and Hargreaves, K. M. (2011). LPS Sensitizes TRPV1 via Activation of TLR4 in Trigeminal Sensory Neurons. *J. Dent Res.* 90 (6), 759–764. doi:10.1177/0022034511400225

Dong, J., Ramachandiran, S., Tikoo, K., Jia, Z., Lau, S. S., and Monks, T. J. (2004). EGFR-independent Activation of P38 MAPK and EGFR-dependent Activation of ERK1/2 Are Required for ROS-Induced Renal Cell Death. *Am. J. Physiology-Renal Physiol.* 287 (5), F1049–F1058. doi:10.1152/ajprenal.00132.2004

Donica, C. L., Cui, Y., Shi, S., and Gutstein, H. B. (2014). Platelet-derived Growth Factor Receptor-β Antagonism Restores Morphine Analgesic Potency against Neuropathic Pain. *PLoS ONE* 9 (5), e97105. doi:10.1371/journal.pone.0097105

Dreyling, M., Jurczak, W., Jerkeman, M., Silva, R. S., Rusconi, C., Trneny, M., et al. (2016). Ibrutinib versus Temsirolimus in Patients with Relapsed or Refractory Mantle-Cell Lymphoma: an International, Randomised, Open-Label, Phase 3 Study. *The Lancet* 387 (10020), 770–778. doi:10.1016/s0140-6736(15)00667-4

Edwards, H. L., Mulvey, M. R., and Bennett, M. I. (2019). Cancer-Related Neuropathic Pain. *Cancers* 11 (3), 373. doi:10.3390/cancers11030373

Egeland, N. G., Moen, A., Pedersen, L. M., Brisby, H., and Gjerstad, J. (2013). Spinal Nociceptive Hyperexcitability Induced by Experimental Disc Herniation Is Associated with Enhanced Local Expression of Csf1 and FasL. *PAIN* 154 (9), 1743–1748. doi:10.1016/j.pain.2013.05.034

Erschbamer, M., Pernold, K., and Olson, L. (2007). Inhibiting Epidermal Growth Factor Receptor Improves Structural, Locomotor, Sensory, and Bladder Recovery from Experimental Spinal Cord Injury. *J. Neurosci.* 27 (24), 6428–6435. doi:10.1523/jneurosci.1037-07.2007

Esposito, M. F., Malayil, R., Hanes, M., and Deer, T. (2019). Unique Characteristics of the Dorsal Root Ganglion as a Target for Neuromodulation. *Pain Med. (Malden, Mass.)* 20 (Suppl. 1), S23–S30. doi:10.1093/pm/pnz012

Fillingim, R. B., Slade, G. D., Diatchenko, L., Dubner, R., Greenspan, J. D., Knott, C., et al. (2011). Summary of Findings from the OPPERA Baseline Case-Control Study: Implications and Future Directions. *J. pain : official J. Am. Pain Soc.* 12 (Issue 11 Suppl. l), T102. doi:10.1016/j.jpain.2011.08.009NIH Public Access

Forster, R., Sarginson, A., Velichkova, A., Hogg, C., Dorning, A., Horne, A. W., et al. (2019). Macrophage-derived Insulin-like Growth Factor-1 Is a Key Neurotrophic and Nerve-Sensitizing Factor in Pain Associated with Endometriosis. *FASEB J.* 33 (10), 11210–11222. doi:10.1096/fj.201900797R

Freed, D. M., Bessman, N. J., Kiyatkin, A., Salazar-Cavazos, E., Byrne, P. O., Moore, J. O., et al. (2017). EGFR Ligands Differentially Stabilize Receptor Dimers to Specify Signaling Kinetics. *Cell* 171 (3), 683–695.e18. doi:10.2210/pdb5wb7/pdb

Garay, C., Judge, G., Lucarelli, S., Bautista, S., Pandey, R., Singh, T., et al. (2015). Epidermal Growth Factor-Stimulated Akt Phosphorylation Requires Clathrin or ErbB2 but Not Receptor Endocytosis. *Mol. Biol. Cel* 26 (19), 3504–3519. doi:10.1091/mbc.e14-09-1412

Garcez, R. C., Teixeira, B. L., dos Santos Schmitt, S., Alvarez-Silva, M., and Trentin, A. G. (2009). Epidermal Growth Factor (EGF) Promotes the *In Vitro* Differentiation of Neural Crest Cells to Neurons and Melanocytes. *Cell Mol. Neurobiol.* 29 (8), 1087. doi:10.1007/s10571-009-9406-2

Gaskin, D. J., and Richard, P. (2012). The Economic Costs of Pain in the United States. *The J. Pain* 13 (8), 715–724. doi:10.1016/j.jpain.2012.03.009

Gharbi, S. I., Zvelebil, M. J., Shuttleworth, S. J., Hancox, T., Saghir, N., Timms, J. F., et al. (2007). Exploring the Specificity of the PI3K Family Inhibitor LY294002. *Biochem. J.* 404 (1), 15–21. doi:10.1042/bj20061489

Greenhalgh, A. D., Zarruk, J. G., Healy, L. M., Baskar Jesudasan, S. J., Jhelum, P., Salmon, C. K., et al. (2018). Peripherally Derived Macrophages Modulate Microglial Function to Reduce Inflammation after CNS Injury. *PLOS Biol.* 16 (10), e2005264. doi:10.1371/journal.pbio.2005264

Gregory, N. S., Harris, A. L., Robinson, C. R., Dougherty, P. M., Fuchs, P. N., and Sluka, K. A. (2013). An Overview of Animal Models of Pain: Disease Models and Outcome Measures. *J. Pain : Official J. Am. Pain Soc.* 14 (11), 1255–1269. doi:10.1016/j.jpain.2013.06.008

Gress, K., Charipova, K., Jung, J. W., Kaye, A. D., Paladini, A., Varrassi, G., et al. (2020). A Comprehensive Review of Partial Opioid Agonists for the Treatment of Chronic Pain. *Best Pract. Res. Clin. Anaesthesiology* 34 (3), 449–461. doi:10.1016/j.bpa.2020.06.003

Griffiths, L. A., Duggett, N. A., Pitcher, A. L., and Flatters, S. J. L. (2018). Evoked and Ongoing Pain-like Behaviours in a Rat Model of Paclitaxel-Induced Peripheral Neuropathy. *Pain Res. Management* 2018, 8217613. doi:10.1155/2018/8217613

Guo, J.-R., Wang, H., Jin, X.-J., Jia, D.-L., Zhou, X., and Tao, Q. (2017). Effect and Mechanism of Inhibition of PI3K/Akt/mTOR Signal Pathway on Chronic Neuropathic Pain and Spinal Microglia in a Rat Model of Chronic Constriction Injury. *Oncotarget* 8 (32), 52923–52934. doi:10.18632/oncotarget.17629

Haleem, R., and Wright, R. (2020). A Scoping Review on Clinical Trials of Pain Reduction with Cannabis Administration in Adults. *J. Clin. Med. Res.* 12 (6), 344–351. doi:10.14740/jocmr4210

Han, W., and Lo, H.-W. (2012). Landscape of EGFR Signaling Network in Human Cancers: Biology and Therapeutic Response in Relation to Receptor Subcellular Locations. *Cancer Lett.* 318 (2), 124–134. doi:10.1016/j.canlet.2012.01.011

Harada, M., Kamimura, D., Arima, Y., Kohsaka, H., Nakatsuji, Y., Nishida, M., et al. (2015). Temporal Expression of Growth Factors Triggered by Epiregulin Regulates Inflammation Development. *J. Immunol.* 194 (3), 1039–1046. doi:10.4049/jimmunol.1400562

Hirsh, V., Cadranel, J., Cong, X. J., Fairclough, D., Finnern, H. W., Lorence, R. M., et al. (2013). Symptom and Quality of Life Benefit of Afatinib in Advanced Non–small-cell Lung *Cancer* Patients Previously Treated with Erlotinib or Gefitinib: Results of a Randomized Phase IIb/III Trial (LUX-Lung 1). *J. Thorac. Oncol.* 8 (2), 229–237. doi:10.1097/jto.0b013e3182773fce

Ho, J., Moyes, D. L., Tavassoli, M., and Naglik, J. R. (2017). The Role of ErbB Receptors in Infection. *Trends Microbiol.* 25 (11), 942–952. doi:10.1016/j.tim.2017.04.009

Hu, Q., Zhang, L., Wen, J., Wang, S., Li, M., Feng, R., et al. (2010). The Egf Receptor-Sox2-Egf Receptor Feedback Loop Positively Regulates the Self-Renewal of Neural Precursor Cells. *STEM CELLS* 28 (2), 279–286. doi:10.1002/stem.246

Hu, Z., Deng, N., Liu, K., Zhou, N., Sun, Y., and Zeng, W. (2020). CNTF-STAT3-IL-6 *Axis* Mediates Neuroinflammatory Cascade across Schwann Cell-Neuron-Microglia. *Cel Rep.* 31 (7), 107657. doi:10.1016/j.celrep.2020.107657

Huang, B. R., Chen, T. S., Bau, D. T., Chuang, I. C., Tsai, C. F., Chang, P. C., et al. (2017). EGFR Is a Pivotal Regulator of Thrombin-Mediated Inflammation in Primary Human Nucleus Pulposus Culture. *Scientific Rep.* doi:10.1038/s41598-017-09122-3

Huerta, J. J., Diaz-Trelles, R., Naves, F. J., Llamosas, M. M., Del Valle, M. E., and Vega, J. A. (1996). Epidermal Growth Factor Receptor in Adult Human Dorsal Root Ganglia. *Anat. Embryol.* 194 (3), 253–257. doi:10.1007/bf00187136

Ikoma, M. D., Kohno, M. D., and Baba, M. D. (2007). Differential Presynaptic Effects of Opioid Agonists on Aδ- and C-Afferent Glutamatergic Transmission to the Spinal Dorsal Horn. *Anesthesiology: J. Am. Soc. Anesthesiologists* 107 (5), 807–812. doi:10.1097/01.anes.0000286985.80301.5e

International Association for the Study of Pain (2017). IASP Terminology. Pain Terms. Neuropathic Pain. Available at: https://www.iasp-pain.org/Education/Content.aspx?ItemNumber=1698#Neuropathicpain.

Jardín, I., López, J. J., Diez, R., Sánchez-Collado, J., Cantonero, C., Albarrán, L., et al. (2017). TRPs in Pain Sensation. *Front. Physiol.* 8, 392. doi:10.3389/fphys.2017.00392

Jean, S., and Kiger, A. A. (2014). Classes of Phosphoinositide 3-kinases at a Glance. *J. Cel Sci.* 127 (Pt 5), 923–928. doi:10.1242/jcs.093773

Ji, R.-R., Baba, H., Brenner, G. J., and Woolf, C. J. (1999). Nociceptive-specific Activation of ERK in Spinal Neurons Contributes to Pain Hypersensitivity. *Nat. Neurosci.* 2 (12), 1114–1119. doi:10.1038/16040

Ji, R.-R., Chamessian, A., and Zhang, Y. Q. (2016). Pain Regulation by Non-neuronal Cells and Inflammation. *Science* 354 (6312), 572–577. doi:10.1126/science.aaf8924

Ji, R. R., Xu, Z. Z., Wang, X., and Lo, E. H. (2009). Matrix Metalloprotease Regulation of Neuropathic Pain. *Trends Pharmacol. Sci.* 30 (7), 336–340. doi:10.1016/j.tips.2009.04.002

Jin, S. X., Zhuang, Z. Y., Woolf, C. J., and Ji, R. R. (2003). p38 Mitogen-Activated Protein Kinase Is Activated after a Spinal Nerve Ligation in Spinal Cord Microglia and Dorsal Root Ganglion Neurons and Contributes to the Generation of Neuropathic Pain. *J. Neurosci.* 23 (10), 4017–4022. doi:10.1523/jneurosci.23-10-04017.2003

Johannes, C. B., Le, T. K., Zhou, X., Johnston, J. A., and Dworkin, R. H. (2010). The Prevalence of Chronic Pain in United States Adults: Results of an Internet-Based Survey. *J. Pain* 11 (11), 1230–1239. doi:10.1016/j.jpain.2010.07.002

Julius, D., and Basbaum, A. I. (2001). Molecular Mechanisms of Nociception. *Nature* 413 (6852), 203–210. doi:10.1038/35093019

Jung, Y.-H., Kim, Y. O., Lin, H., Cho, J.-H., Park, J.-H., Lee, S.-D., et al. (2017). Discovery of Potent Antiallodynic Agents for Neuropathic Pain Targeting P2X3 Receptors. *ACS Chem. Neurosci.* 8 (7), 1465–1478. doi:10.1021/acschemneuro.6b00401

Kamerman, P. R., Wadley, A. L., Davis, K. D., Hietaharju, A., Jain, P., Kopf, A., et al. (2015). World Health Organization Essential Medicines Lists: where Are the Drugs to Treat Neuropathic Pain? *PAIN* 156 (5). doi:10.1097/01.j.pain.0000460356.94374.a1

Kandasamy, R., and Price, T. J. (2015). The Pharmacology of Nociceptor Priming. *Pain control*, 15–37. doi:10.1007/978-3-662-46450-2_2

Kapustin, D., Bhatia, A., McParland, A., Trivedi, A., Davidson, A., Brull, R., et al. (2020). Evaluating the Impact of Gabapentinoids on Sleep Health in Patients with Chronic Neuropathic Pain: a Systematic Review and Meta-Analysis. *Pain (Amsterdam)* 161 (3), 476–490. doi:10.1097/j.pain.0000000000001743

Karppinen, J., Korhonen, T., Malmivaara, A., Paimela, L., Kyllönen, E., Lindgren, K.-A., et al. (2003). Tumor Necrosis Factor-Alpha Monoclonal Antibody, Infliximab, Used to Manage Severe Sciatica. *Spine (Philadelphia, Pa. 1976)* 28 (8), 750–753. doi:10.1097/01.brs.0000058944.38900.ce

Kawasaki, T., and Kawai, T. (2014). Toll-Like Receptor Signaling Pathways. *Front. Immunol.* 5, 461. doi:10.3389/fimmu.2014.00461

Kersten, C., Cameron, M. G., Laird, B., and Mjåland, S. (2015). Epidermal Growth Factor Receptor-Inhibition (EGFR-I) in the Treatment of Neuropathic Pain. *Br. J. Anaesth.* 115 (5), 761–767. doi:10.1093/bja/aev326

Kersten, Christian., Cameron, M. G., Bailey, A. G., Fallon, M. T., Laird, B. J., Paterson, V., et al. (2019). Relief of Neuropathic Pain through Epidermal Growth Factor Receptor Inhibition: A Randomized Proof-Of-Concept Trial. *Pain Med. (Malden, Mass.)*. doi:10.1093/pm/pnz101

Kersten, Christian., and Cameron, M. G. (2012). Cetuximab Alleviates Neuropathic Pain Despite Tumour Progression. *BMJ Case Rep.* 20 (12), 2495–2505. doi:10.1136/bcr.12.2011.5374

Kersten, Christian., Cameron, M. G., and Mjåland, S. (2013). Epithelial Growth Factor Receptor (EGFR)-inhibition for Relief of Neuropathic Pain—A Case Series. *Scand. J. Pain* 4 (Issue 1), 3–7. doi:10.1016/j.sjpain.2012.11.011

Kim, J., and Guan, K.-L. (2019). mTOR as a Central Hub of Nutrient Signalling and Cell Growth. *Nat. Cel. Biol.* 21 (Issue 1), 63–71. doi:10.1038/s41556-018-0205-1Springer Science and Business Media LLC

Kongstorp, M., Schjølberg, T., Jacobsen, D. P., Haugen, F., and Gjerstad, J. (2019). Epiregulin Is Released from Intervertebral Disks and Induces Spontaneous Activity in Pain Pathways. *Pain Rep.* 4 (2), e718. doi:10.1097/PR9.0000000000000718

Kremer, M., Salvat, E., Muller, A., Yalcin, I., and Barrot, M. (2016). Antidepressants and Gabapentinoids in Neuropathic Pain: Mechanistic Insights. *Neuroscience* 338, 183–206. doi:10.1016/j.neuroscience.2016.06.057

Kreutzwiser, D., and Tawfic, Q. A. (2019). Expanding Role of NMDA Receptor Antagonists in the Management of Pain. *CNS Drugs* 33 (4), 347–374. doi:10.1007/s40263-019-00618-2

Kushnarev, M., Pirvulescu, I. P., Candido, K. D., and Knezevic, N. N. (2020). Neuropathic Pain: Preclinical and Early Clinical Progress with Voltage-Gated Sodium Channel Blockers. *Expert Opin. Investig. Drugs* 29 (3), 259–271. doi:10.1080/13543784.2020.1728254

Lacagnina, M. J., Watkins, L. R., and Grace, P. M. (2018). Toll-like Receptors and Their Role in Persistent Pain. *Pharmacol. Ther.* 184, 145–158. doi:10.1016/j.pharmthera.2017.10.006

Lee, S., Rauch, J., and Kolch, W. (2020). Targeting MAPK Signaling in Cancer: Mechanisms of Drug Resistance and Sensitivity. *Int. J. Mol. Sci.* 21 (3), 1–29. doi:10.3390/ijms21031102

Leinders, M., Koehrn, F. J., Bartok, B., Boyle, D. L., Shubayev, V., Kalcheva, I., et al. (2014). Differential Distribution of PI3K Isoforms in Spinal Cord and Dorsal Root Ganglia: Potential Roles in Acute Inflammatory Pain. *Pain* 155 (6), 1150–1160. doi:10.1016/j.pain.2014.03.003

Lemmon, M. A., and Schlessinger, J. (2010). Cell Signaling by Receptor Tyrosine Kinases. *Cell* 141 (7), 1117–1134. doi:10.1016/j.cell.2010.06.011Elsevier Inc

Lemmon, M. A., Schlessinger, J., and Ferguson, K. M. (2014). The EGFR Family: Not So Prototypical Receptor Tyrosine Kinases. *Cold Spring Harbor Perspect. Biol.* 6 (Issue 4), a020768. doi:10.1101/cshperspect.a020768

Lennon, F. E., Mirzapoiazova, T., Mambetsariev, B., Poroyko, V. A., Salgia, R., Moss, J., et al. (2014). The Mu Opioid Receptor Promotes Opioid and Growth Factor-Induced Proliferation, Migration and Epithelial Mesenchymal Transition (EMT) in Human Lung Cancer. *PLoS ONE* 9 (3), e91577. doi:10.1371/journal.pone.0091577

Leyton-Puig, D., Isogai, T., Argenzio, E., van den Broek, B., Klarenbeek, J., Janssen, H., et al. (2017). Flat Clathrin Lattices Are Dynamic Actin-Controlled Hubs for Clathrin-Mediated Endocytosis and Signalling of Specific Receptors. *Nat. Commun.* 8 (1), 16068. doi:10.1038/ncomms16068

Li, Y., Adamek, P., Zhang, H., Tatsui, C. E., Rhines, L. D., Mrozkova, P., et al. (2015). The *Cancer* Chemotherapeutic Paclitaxel Increases Human and Rodent Sensory Neuron Responses to TRPV1 by Activation of TLR4. *J. Neurosci.* 35 (39), 13487–13500. doi:10.1523/jneurosci.1956-15.2015

Li, Z.-W., Li, J.-J., Wang, L., Zhang, J.-P., Wu, J.-J., Mao, X.-Q., et al. (2014). Epidermal Growth Factor Receptor Inhibitor Ameliorates Excessive Astrogliosis and Improves the Regeneration Microenvironment and Functional Recovery in Adult Rats Following Spinal Cord Injury. *J. Neuroinflammation* 11 (1), 71. doi:10.1186/1742-2094-11-71

Liu, F., Jiao, Y., Jiao, Y., Garcia-Godoy, F., Gu, W., and Liu, Q. (2016). Sex Difference in EGFR Pathways in Mouse Kidney-Potential Impact on the Immune System. *BMC Genet.* 17 (1). doi:10.1186/s12863-016-0449-3

Liu, G. Y., and Sabatini, D. M. (2020). mTOR at the Nexus of Nutrition, Growth, Ageing and Disease. *Nat. Rev. Mol. Cel Biol.* 21 (4), 183–203. doi:10.1038/s41580-019-0199-y

Liu, W., Lv, Y., and Ren, F. (2018). PI3K/Akt Pathway Is Required for Spinal Central Sensitization in Neuropathic Pain. *Cell Mol. Neurobiol.* 38 (3), 747–755. doi:10.1007/s10571-017-0541-x

Liu, X., Tian, Y., Lu, N., Gin, T., Cheng, C. H. K., and Chan, M. T. V. (2013). Stat3 Inhibition Attenuates Mechanical Allodynia through Transcriptional Regulation of Chemokine Expression in Spinal Astrocytes. *PLOS ONE* 8 (10), e75804. doi:10.1371/journal.pone.0075804

Maayah, Z. H., Takahara, S., Ferdaoussi, M., and Dyck, J. R. B. (2020). The Anti-inflammatory and Analgesic Effects of Formulated Full-Spectrum Cannabis Extract in the Treatment of Neuropathic Pain Associated with Multiple Sclerosis. *Inflamm. Research : Official J. Eur. Histamine Res. Soc.* 69 (6), 549–558. doi:10.1007/s00011-020-01341-1

Maixner, W., Diatchenko, L., Dubner, R., Fillingim, R. B., Greenspan, J. D., Knott, C., et al. (2011). Orofacial Pain Prospective Evaluation and Risk Assessment Study - the OPPERA Study. *J. Pain* 12 (11 Suppl. L), T4. doi:10.1016/j.jpain.2011.08.002

Manning, B. D., and Toker, A. (2017). AKT/PKB Signaling: Navigating the Network. *Cell* 169 (3), 381–405. doi:10.1016/j.cell.2017.04.001

Mapplebeck, J. C. S., Beggs, S., and Salter, M. W. (2016). Sex Differences in Pain: a Tale of Two Immune Cells. *PAIN* 157. , 2016 Available at: https://journals.lww.com/pain/Fulltext/2016/02001/Sex_differences_in_pain__a_tale_of_two_immune.2.aspx. doi:10.1097/j.pain.0000000000000389

Mapplebeck, J. C. S., Dalgarno, R., Tu, Y., Moriarty, O., Beggs, S., Kwok, C. H. T., et al. (2018). Microglial P2X4R-Evoked Pain Hypersensitivity Is Sexually Dimorphic in Rats. *PAIN* 159 (9). Available at: https://journals.lww.com/pain/Fulltext/2018/09000/Microglial_P2X4R_evoked_pain_hypersensitivity_is.12.aspx. doi:10.1097/j.pain.0000000000001265

Martin, L. J., Smith, S. B., Khoutorsky, A., Magnussen, C. A., Samoshkin, A., Sorge, R. E., et al. (2017). Epiregulin and EGFR Interactions Are Involved in Pain Processing. *J. Clin. Invest.* 127 (9), 3353–3366. doi:10.1172/JCI87406

Matarazzo, A. P., Elisei, L. M. S., Carvalho, F. C., Bonfílio, R., Ruela, A. L. M., Galdino, G., et al. (2021). Mucoadhesive Nanostructured Lipid Carriers as a Cannabidiol Nasal Delivery System for the Treatment of Neuropathic Pain. *Eur. J. Pharm. Sci.* 159, 105698. doi:10.1016/j.ejps.2020.105698

Mazgaeen, L., and Gurung, P. (2020). Recent Advances in Lipopolysaccharide Recognition Systems. *Int. J. Mol. Sci.* 21 (2). doi:10.3390/ijms21020379

McNamara, C. R., and Degterev, A. (2011). Small-molecule Inhibitors of the PI3K Signaling Network. *Future Med. Chem.* 3 (5), 549–565. doi:10.4155/fmc.11.12

Miettinen, P. J., Berger, J. E., Meneses, J., Phung, Y., Pedersen, R. A., Werb, Z., et al. (1995). Epithelial Immaturity and Multiorgan Failure in Mice Lacking

Epidermal Growth Factor Receptor. *Nature* 376 (6538), 337–341. doi:10.1038/376337a0

Mogil, J. S. (2009). Animal Models of Pain: Progress and Challenges. *Nat. Rev. Neurosci.* 10 (4), 283–294. doi:10.1038/nrn2606

Mogil, J. S., Davis, K. D., and Derbyshire, S. W. (2010). The Necessity of Animal Models in Pain Research. *PAIN* 151 (1). Available at: https://journals.lww.com/pain/Fulltext/2010/10000/The_necessity_of_animal_models_in_pain_research.7.aspx. doi:10.1016/j.pain.2010.07.015

Moulin, D. E., Clark, A. J., Speechley, M., and Morley-Forster, P. K. (2002). Chronic Pain in Canada - Prevalence, Treatment, Impact and the Role of Opioid Analgesia. *Pain Res. Manag.* 7, 323085. doi:10.1155/2002/323085

Mousa, S. A., Cheppudira, B. P., Shaqura, M., Fischer, O., Hofmann, J., Hellweg, R., et al. (2007). Nerve Growth Factor Governs the Enhanced Ability of Opioids to Suppress Inflammatory Pain. *Brain*. doi:10.1093/brain/awl330

Murakami, M., Harada, M., Kamimura, D., Ogura, H., Okuyama, Y., Kumai, N., et al. (2013). Disease-association Analysis of an Inflammation-Related Feedback Loop. *Cel Rep.* 3 (3), 946–959. doi:10.1016/j.celrep.2013.01.028

Narita, M., Usui, A., Narita, M., Niikura, K., Nozaki, H., Khotib, J., et al. (2005). Protease-activated Receptor-1 and Platelet-Derived Growth Factor in Spinal Cord Neurons Are Implicated in Neuropathic Pain after Nerve Injury. *J. Neurosci.* 25 (43), 10000–10009. doi:10.1523/JNEUROSCI.2507-05.2005

Nolte, C., Kirchhoff, F., and Kettenmann, H. (1997). Epidermal Growth Factor Is a Motility Factor for Microglial Cells In Vitro: Evidence for EGF Receptor Expression. *Eur. J. Neurosci.* 9 (8), 1690–1698. doi:10.1111/j.1460-9568.1997.tb01526.x

Obara, I., Makuch, W., Spetea, M., Schütz, J., Schmidhammer, H., Przewlocki, R., et al. (2007). Local Peripheral Antinociceptive Effects of 14-O-Methyloxymorphone Derivatives in Inflammatory and Neuropathic Pain in the Rat. *Eur. J. Pharmacol.* 558 (1), 60–67. doi:10.1016/j.ejphar.2006.11.037

Obara, I., Tochiki, K. K., Géranton, S. M., Carr, F. B., Lumb, B. M., Liu, Q., et al. (2011). Systemic Inhibition of the Mammalian Target of Rapamycin (mTOR) Pathway Reduces Neuropathic Pain in Mice. *Pain* 152 (11), 2582–2595. doi:10.1016/j.pain.2011.07.025

Oshima, H., Popivanova, B. K., Oguma, K., Kong, D., Ishikawa, T., and Oshima, M. (2011). Activation of Epidermal Growth Factor Receptor Signaling by the Prostaglandin E2 Receptor EP4 Pathway during Gastric Tumorigenesis. *Cancer Sci.* 102 (4), 713–719. doi:10.1111/j.1349-7006.2011.01847.x

Pascolutti, R., Algisi, V., Conte, A., Raimondi, A., Pasham, M., Upadhyayula, S., et al. (2019). Molecularly Distinct Clathrin-Coated Pits Differentially Impact EGFR Fate and Signaling. *Cel Rep.* 27 (10), 3049–3061. doi:10.1016/j.celrep.2019.05.017

Pearson, R. J., and Carroll, S. L. (2004). ErbB Transmembrane Tyrosine Kinase Receptors Are Expressed by Sensory and Motor Neurons Projecting into Sciatic Nerve. *J. Histochem. Cytochem.* 52 (10), 1299–1311. doi:10.1177/002215540405201006

Pezet, S., Marchand, F., D'Mello, R., Grist, J., Clark, A. K., Malcangio, M., et al. (2008). Phosphatidylinositol 3-kinase Is a Key Mediator of Central Sensitization in Painful Inflammatory Conditions. *J. Neuroscience : Official J. Soc. Neurosci.* 28 (16), 4261–4270. doi:10.1523/jneurosci.5392-07.2008

Pinho-Ribeiro, F. A., Verri, W. A., and Chiu, I. M. (2017). Nociceptor Sensory Neuron–Immune Interactions in Pain and Inflammation. *Trends Immunol.* 38 (1), 5–19. doi:10.1016/j.it.2016.10.001

Pinilla-Macua, I., Watkins, S. C., and Sorkin, A. (2016). Endocytosis Separates EGF Receptors from Endogenous Fluorescently Labeled HRas and Diminishes Receptor Signaling to MAP Kinases in Endosomes. *Proc. Natl. Acad. Sci.* 113 (8), 2122–2127. doi:10.1073/pnas.1520301113

Puig, S., Donica, C. L., and Gutstein, H. B. (2020). EGFR Signaling Causes Morphine Tolerance and Mechanical Sensitization in Rats. *ENeuro* 7 (2). doi:10.1523/ENEURO.0460-18.2020

Qu, W.-S., Liu, J.-L., Li, C.-Y., Li, X., Xie, M.-J., Wang, W., et al. (2015). Rapidly Activated Epidermal Growth Factor Receptor Mediates Lipopolysaccharide-Triggered Migration of Microglia. *Neurochem. Int.* 90, 85–92. doi:10.1016/j.neuint.2015.07.007

Qu, W., Tian, D., Guo, Z., Fang, J., Zhang, Q., Yu, Z., et al. (2012). Inhibition of EGFR/MAPK Signaling Reduces Microglial Inflammatory Response and the Associated Secondary Damage in Rats after Spinal Cord Injury. *J. Neuroinflammation* 9 (1), 178. doi:10.1186/1742-2094-9-178

Qu, Y. J., Jia, L., Zhang, X., Wei, H., and Yue, S. W. (2016). MAPK Pathways Are Involved in Neuropathic Pain in Rats with Chronic Compression of the Dorsal Root Ganglion. *Evidence-Based Complement. Altern. Med.* 2016, 6153215. doi:10.1155/2016/6153215

Quarta, S., Mitrić, M., Kalpachidou, T., Mair, N., Schiefermeier-Mach, N., Andratsch, M., et al. (2019). Impaired Mechanical, Heat, and Cold Nociception in a Murine Model of Genetic TACE/ADAM17 Knockdown. *FASEB J.* 33 (3), 4418–4431. doi:10.1096/fj.201801901r

Rauck, R. L., Wallace, M. S., Burton, A. W., Kapural, L., and North, J. M. (2009). Intrathecal Ziconotide for Neuropathic Pain: A Review. *Pain Pract.* 9 (5), 327–337. doi:10.1111/j.1533-2500.2009.00303.x

Reis, C. R., Chen, P.-H., Srinivasan, S., Aguet, F., Mettlen, M., and Schmid, S. L. (2015). Crosstalk between Akt/GSK3β Signaling and Dynamin-1 Regulates Clathrin-Mediated Endocytosis. *EMBO J.* 34 (16), 2132–2146. doi:10.15252/embj.201591518

Rosen, S., Ham, B., and Mogil, J. S. (2017). Sex Differences in Neuroimmunity and Pain. *J. Neurosci. Res.* doi:10.1002/jnr.23831

Scheff, N. N., Ye, Y., Conley, Z., Quan, J. W., Ronald Lam, Y. V., Klares, R., et al. (2020). ADAM17-EGFR Signaling Contributes to Oral Cancer Pain. *Pain*. doi:10.1097/j.pain.0000000000001926

Schembri, E. (2019). Are Opioids Effective in Relieving Neuropathic Pain? *SN Compr. Clin. Med.* 1 (1), 30–46. doi:10.1007/s42399-018-0009-4

Scholz, J., Finnerup, N. B., Attal, N., Aziz, Q., Baron, R., Bennett, M. I., et al. (2019). The IASP Classification of Chronic Pain for ICD-11: Chronic Neuropathic Pain. *PAIN* 160 (1). Available at: https://journals.lww.com/pain/Fulltext/2019/01000/The_IASP_classification_of_chronic_pain_for.7.aspx. doi:10.1097/j.pain.0000000000001365

Scholze, A. R., Foo, L. C., Mulinyawe, S., and Barres, B. A. (2014). BMP Signaling in Astrocytes Downregulates EGFR to Modulate Survival and Maturation. *PLoS ONE* 9 (10), e110668. doi:10.1371/journal.pone.0110668

Shutov, L. P., Warwick, C. A., Shi, X., Gnanasekaran, A., Shepherd, A. J., Mohapatra, D. P., et al. (2016). The Complement System Component C5a Produces Thermal Hyperalgesia via Macrophage-To-Nociceptor Signaling that Requires NGF and TRPV1. *J. Neurosci.* 36 (18), 5055–5070. doi:10.1523/jneurosci.3249-15.2016

Sibilia, M., and Wagner, E. F. (1995). Strain-dependent Epithelial Defects in Mice Lacking the EGF Receptor. *Science* 269 (5221), 234–238. doi:10.1126/science.7618085

Sibilia, Maria., Steinbach, J. P., Stingl, L., Aguzzi, A., and Wagner, E. F. (1998). A Strain-independent Postnatal Neurodegeneration in Mice Lacking the EGF Receptor. *EMBO J.* 17 (3), 719–731. doi:10.1093/emboj/17.3.719

Sigismund, S., Argenzio, E., Tosoni, D., Cavallaro, E., Polo, S., and Di Fiore, P. P. (2008). Clathrin-Mediated Internalization Is Essential for Sustained EGFR Signaling but Dispensable for Degradation. *Dev. Cel* 15 (2), 209–219. doi:10.1016/j.devcel.2008.06.012

Sigismund, S., Avanzato, D., and Lanzetti, L. (2018). Emerging Functions of the EGFR in Cancer. *Mol. Oncol.* 12 (1), 3–20. doi:10.1002/1878-0261.12155

Sinor-Anderson, A., and Lillien, L. (2011). Akt1 Interacts with Epidermal Growth Factor Receptors and Hedgehog Signaling to Increase Stem/transit Amplifying Cells in the Embryonic Mouse Cortex. *Dev. Neurobiol.* 71 (9), 759–771. doi:10.1002/dneu.20878

Slade, G. D., Fillingim, R. B., Sanders, A. E., Bair, E., Greenspan, J. D., Ohrbach, R., et al. (2013). Summary of Findings from the OPPERA Prospective Cohort Study of Incidence of First-Onset Temporomandibular Disorder: Implications and Future Directions. *J. Pain* 14 (12 Suppl. L). doi:10.1016/j.jpain.2013.09.010

Stahel, M., Becker, M., Graf, N., and Michels, S. (2016).SYSTEMIC INTERLEUKIN 1β INHIBITION IN PROLIFERATIVE DIABETIC RETINOPATHY: A Prospective Open-Label Study Using Canakinumab. *Philadelphia. Pa. Retina.* 36, 385–391. doi:10.1097/iae.0000000000000701

Stein, A. T., Ufret-Vincenty, C. A., Hua, L., Santana, L. F., and Gordon, S. E. (2006). Phosphoinositide 3-kinase Binds to TRPV1 and Mediates NGF-Stimulated TRPV1 Trafficking to the Plasma Membrane. *J. Gen. Physiol.* 128 (5), 509–522. doi:10.1085/jgp.200609576

Stratiievska, A., Nelson, S., Senning, E. N., Lautz, J. D., Smith, S. E. P., and Gordon, S. E. (2018). Reciprocal Regulation Among TRPV1 Channels and Phosphoinositide 3-kinase in Response to Nerve Growth Factor. *ELife* 7, e38869. doi:10.7554/elife.38869

Sugiyama, M. G., Fairn, G. D., and Antonescu, C. N. (2019). Akt-ing up Just about Everywhere: Compartment-specific Akt Activation and Function in Receptor Tyrosine Kinase Signaling. *Front. Cel Dev. Biol.* 7, 70. doi:10.3389/fcell.2019.00070

Sun, L., Zhao, J.-Y., Gu, X., Liang, L., Wu, S., Mo, K., et al. (2017). Nerve Injury–Induced Epigenetic Silencing of Opioid Receptors Controlled by DNMT3a in Primary Afferent Neurons. *PAIN* 158 (6). doi:10.1097/j.pain.0000000000000894

Sun, N., Zhang, X., Guo, S., Le, H. T., Zhang, X., and Kim, K.-M. (2018). Molecular Mechanisms Involved in Epidermal Growth Factor Receptor-Mediated Inhibition of Dopamine D3 Receptor Signaling. *Biochim. Biophys. Acta (Bba) - Mol. Cel Res.* 1865 (9), 1187–1200. doi:10.1016/j.bbamcr.2018.06.001

Takebayashi, T., Cavanaugh, J. M., Cüneyt Özaktay, A., Kallakuri, S., and Chen, C. (2001). Effect of Nucleus Pulposus on the Neural Activity of Dorsal Root Ganglion. *Spine* 26 (8). Available at: https://journals.lww.com/spinejournal/Fulltext/2001/04150/Effect_of_Nucleus_Pulposus_on_the_Neural_Activity.18.aspx. doi:10.1097/00007632-200104150-00018

Tang, J., Zhou, B., Scott, M. J., Chen, L., Lai, D., Fan, E. K., et al. (2020). EGFR Signaling Augments TLR4 Cell Surface Expression and Function in Macrophages via Regulation of Rab5a Activation. *Protein&Cell* 11 (2), 144–149. doi:10.1007/s13238-019-00668-8

Thapa, N., Chen, M., Horn, H. T., Choi, S., Wen, T., and Anderson, R. A. (2020). Phosphatidylinositol 3-kinase Signalling Is Spatially Organized at Endosomal Compartments by Microtubule-Associated Protein 4. *Nat. Cel Biol.* 22 (11), 1357–1370. doi:10.1038/s41556-020-00596-4

Threadgill, D. W., Dlugosz, A. A., Hansen, L. A., Tennenbaum, T., Lichti, U., Yee, D., et al. (1995). Targeted Disruption of Mouse EGF Receptor: Effect of Genetic Background on Mutant Phenotype. *Science* 269 (5221), 230–234. doi:10.1126/science.7618084

Thuringer, D., Hammann, A., Benikhlef, N., Fourmaux, E., Bouchot, A., Wettstein, G., et al. (2011). Transactivation of the Epidermal Growth Factor Receptor by Heat Shock Protein 90 via Toll-like Receptor 4 Contributes to the Migration of Glioblastoma Cells. *J. Biol. Chem.* 286 (5), 3418–3428. doi:10.1074/jbc.M110.154823

Treister, N. S., Richards, S. M., Lombardi, M. J., Rowley, P., Jensen, R. V., and Sullivan, D. A. (2005). Sex-related Differences in Gene Expression in Salivary Glands of BALB/c Mice. *J. Dental Res.* 84 (2), 160–165. doi:10.1177/154405910508400210

Tsuda, M. (2016). Microglia in the Spinal Cord and Neuropathic Pain. *J. Diabetes Invest.* 7 (1), 17–26. doi:10.1111/jdi.12379

Verma, V., Khoury, S., Parisien, M., Cho, C., Maixner, W., Martin, L. J., et al. (2020). The Dichotomous Role of Epiregulin in Pain. *Pain* 161 (5), 1052–1064. doi:10.1097/j.pain.0000000000001792

Vieira, A. V., Lamaze, C., and Schmid, S. L. (1996). Control of EGF Receptor Signaling by Clathrin-Mediated Endocytosis. *Science* 274 (5295), 2086–2089. doi:10.1126/science.274.5295.2086American Society for the Advancement of Science

Villaseñor, R., Nonaka, H., Del Conte-Zerial, P., Kalaidzidis, Y., and Zerial, M. (2015). Regulation of EGFR Signal Transduction by Analogue-To-Digital Conversion in Endosomes. *ELife* 4, e06156. doi:10.7554/elife.06156

Wang, H., Qin, J., Gong, S., Feng, B., Zhang, Y., and Tao, J. (2014). Insulin-Like Growth Factor-1 Receptor-Mediated Inhibition of A-type K+ Current Induces Sensory Neuronal Hyperexcitability through the Phosphatidylinositol 3-Kinase and Extracellular Signal-Regulated Kinase 1/2 Pathways, Independently of Akt. *Endocrinology* 155 (1), 168–179. doi:10.1210/en.2013-1559

Wang, Shuo., Liu, S., Xu, L., Zhu, X., Liu, W., Tian, L., et al. (2019). The Upregulation of EGFR in the Dorsal Root Ganglion Contributes to Chronic Compression of Dorsal Root Ganglions-Induced Neuropathic Pain in Rats. *Mol. Pain* 15, 1744806919857297. doi:10.1177/1744806919857297

Wang, Siying., Peng, L., Li, J., Zeng, X., Ouyang, L., Tan, C., et al. (2013). A Trial-Based Cost-Effectiveness Analysis of Erlotinib Alone versus Platinum-Based Doublet Chemotherapy as First-Line Therapy for Eastern Asian Nonsquamous Non-small-cell Lung *Cancer*. *PLoS ONE* 8 (3), e55917. doi:10.1371/journal.pone.0055917

Wang, Y.-J., Zuo, Z.-X., Wu, C., Liu, L., Feng, Z.-H., and Li, X.-Y. (2017). Cingulate Alpha-2A Adrenoceptors Mediate the Effects of Clonidine on Spontaneous Pain Induced by Peripheral Nerve Injury. Available at: https://www.frontiersin.org/article/10.3389/fnmol.2017.00289.Frontiers in Molecular Neuroscience. 10289doi:10.3389/fnmol.2017.00289

Wang, Y., Barker, K., Shi, S., Diaz, M., Mo, B., and Gutstein, H. B. (2012). Blockade of PDGFR-β Activation Eliminates Morphine Analgesic Tolerance. *Nat. Med.* 18 (3), 385–387. doi:10.1038/nm.2633

Wangzhou, A., Paige, C., Neerukonda, S. V., Naik, D. K., Kume, M., David, E. T., et al. (2021). A Ligand-Receptor Interactome Platform for Discovery of Pain Mechanisms and Therapeutic Targets. *Sci. Signaling* 14 (674), eabe1648. doi:10.1126/scisignal.abe1648

Wee, P., and Wang, Z. (2017). Epidermal Growth Factor Receptor Cell Proliferation Signaling Pathways. *Cancers* 9 (5), 1–45. doi:10.3390/cancers9050052

Wei, Z., Fei, Y., Su, W., and Chen, G. (2019). Emerging Role of Schwann Cells in Neuropathic Pain: Receptors, Glial Mediators and Myelination. *Front. Cell Neurosci.* 13, 116. doi:10.3389/fncel.2019.00116

Werner, M. H., Nanney, L. B., Stoscheck, C. M., and King, L. E. (1988). Localization of Immunoreactive Epidermal Growth Factor Receptors in Human Nervous System. *J. Histochem. Cytochem.* 36 (1), 81–86. doi:10.1177/36.1.3275713

Windsor, R. B., Tham, S. W., Adams, T. L., and Anderson, A. (2019). The Use of Opioids for Treatment of Pediatric Neuropathic Pain: A Literature Review. *Clin. J. Pain* 35 (6), 509–514. Available at: https://journals.lww.com/clinicalpain/Fulltext/2019/06000/The_Use_of_Opioids_for_Treatment_of_Pediatric.9.aspx. doi:10.1097/ajp.0000000000000712

Xu, Q., Fitzsimmons, B., Steinauer, J., O'Neill, A., Newton, A. C., Hua, X. Y., et al. (2011). Spinal Phosphinositide 3-Kinase-Akt-Mammalian Target of Rapamycin Signaling Cascades in Inflammation-Induced Hyperalgesia. *J. Neurosci.* 31 (6), 2113–2124. doi:10.1523/JNEUROSCI.2139-10.2011

Xu, Y., Liu, J., He, M., Liu, R., Belegu, V., Dai, P., et al. (2016). Mechanisms of PDGF siRNA-Mediated Inhibition of Bone Cancer Pain in the Spinal Cord. *Scientific Rep.* doi:10.1038/srep27512

Yang, S. C., Lai, W. W., Hsu, J. C., Su, W. C., and Wang, J. Der. (2020). Comparative Effectiveness and Costeffectiveness of Three First-Line EGFR-Tyrosine Kinase Inhibitors: Analysis of Real-World Data in a Tertiary Hospital in Taiwan. *PLoS ONE* 15 (4), 1–13. doi:10.1371/journal.pone.0231413

Yawn, B. P., Wollan, P. C., Weingarten, T. N., Watson, J. C., Hooten, W. M., and Melton, L. J., III (2009). The Prevalence of Neuropathic Pain: Clinical Evaluation Compared with Screening Tools in a Community Population. *Pain Med.* 10 (3), 586–593. doi:10.1111/j.1526-4637.2009.00588.x

Yu, Y., Lu, S.-T., Sun, J.-P., and Zhou, W. (2020). Safety of Low-Dose Tanezumab in the Treatment of Hip or Knee Osteoarthritis: A Systemic Review and Meta-Analysis of Randomized Phase III Clinical Trials. *Pain Med.* 22 (3), 585–595. doi:10.37766/inplasy2020.6.0096

Zhang, J.-M., and An, J. (2007). Cytokines, Inflammation and Pain. *Int. Anesthesiology Clin.* 45 (2), 27. doi:10.1097/aia.0b013e318034194e

Zhang, M., Jin, F., Zhu, Y., and Qi, F. (2020). Peripheral FGFR1 Regulates Myofascial Pain in Rats via the PI3K/AKT Pathway. *Neuroscience* 436, 1–10. doi:10.1016/j.neuroscience.2020.04.002

Zhang, M. Z., Sasaki, K., Li, Y., Li, Z., Pan, Y., Jin, G. N., et al. (2019). The Role of the EGF Receptor in Sex Differences in Kidney Injury. *J. Am. Soc. Nephrol.* 30 (9), 1659–1673. doi:10.1681/ASN.2018121244

Zhang, T., Zhang, N., Zhang, R., Zhao, W., Chen, Y., Wang, Z., et al. (2018). Preemptive Intrathecal Administration of Endomorphins Relieves Inflammatory Pain in Male Mice via Inhibition of P38 MAPK Signaling and Regulation of Inflammatory Cytokines. *J. Neuroinflammation* 15 (1), 320. doi:10.1186/s12974-018-1358-3

Zhang, W., Zhu, Z., and Liu, Z. (2020). The Role and Pharmacological Properties of the P2X7 Receptor in Neuropathic Pain. *Brain Res. Bull.* 155, 19–28. doi:10.1016/j.brainresbull.2019.11.006

Zhang, X.-S., Li, X., Luo, H.-J., Huang, Z.-X., Liu, C.-C., Wan, Q., et al. (2017). Activation of the RAGE/STAT3 Pathway in the Dorsal Root Ganglion Contributes to the Persistent Pain Hypersensitivity Induced by Lumbar Disc Herniation. *Pain Physician* 20 (5), 419–427.

Zhou, H., and Huang, S. (2010). The Complexes of Mammalian Target of Rapamycin. *Curr. Protein Pept. Sci.* 11 (6), 409–424. doi:10.2174/138920310791824093

Zhou, X.-L., Yu, L.-N., Wang, Y., Tang, L.-H., Peng, Y.-N., Cao, J.-L., et al. (2014). Increased Methylation of the MOR Gene Proximal Promoter in Primary Sensory Neurons Plays a Crucial Role in the Decreased Analgesic Effect of

Opioids in Neuropathic Pain. *Mol. Pain* 10 (1), 51. doi:10.1186/1744-8069-10-51

Zhu, W., and Oxford, G. S. (2007a). Phosphoinositide-3-kinase and Mitogen Activated Protein Kinase Signaling Pathways Mediate Acute NGF Sensitization of TRPV1. *Mol. Cell Neurosci.* 34 (4), 689–700. doi:10.1016/j.mcn.2007.01.005

Zhuang, Z. Y., Gerner, P., Woolf, C. J., and Ji, R. R. (2005). ERK Is Sequentially Activated in Neurons, Microglia, and Astrocytes by Spinal Nerve Ligation and Contributes to Mechanical Allodynia in This Neuropathic Pain Model. *Pain* 114 (1–2), 149–159. doi:10.1016/j.pain.2004.12.022

Zhuang, Z. Y., Wen, Y. R., Zhang, D. R., Borsello, T., Bonny, C., Strichartz, G. R., et al. (2006). A Peptide C-Jun N-Terminal Kinase (JNK) Inhibitor Blocks Mechanical Allodynia after Spinal Nerve Ligation: Respective Roles of JNK Activation in Primary Sensory Neurons and Spinal Astrocytes for Neuropathic Pain Development and Maintenance. *J. Neurosci.* 26 (13), 3551–3560. doi:10.1523/jneurosci.5290-05.2006

Conflict of Interest: The authors declare that the research was conducted in the absence of any commercial or financial relationships that could be construed as a potential conflict of interest.

frontiers in Pharmacology

ORIGINAL RESEARCH
published: 25 May 2021
doi: 10.3389/fphar.2021.668337

Optogenetic Manipulations of Amygdala Neurons Modulate Spinal Nociceptive Processing and Behavior Under Normal Conditions and in an Arthritis Pain Model

Mariacristina Mazzitelli[1], *Kendall Marshall*[1], *Andrew Pham*[1], *Guangchen Ji*[1,2] and *Volker Neugebauer*[1,2,3]*

[1]Department of Pharmacology and Neuroscience, School of Medicine, Texas Tech University Health Sciences Center, Lubbock, TX, United States, [2]Center of Excellence for Translational Neuroscience and Therapeutics, Texas Tech University Health Sciences Center, Lubbock, TX, United States, [3]Garrison Institute on Aging, Texas Tech University Health Sciences Center, Lubbock, TX, United States

OPEN ACCESS

Edited by:
Serena Boccella,
University of Campania Luigi Vanvitelli, Italy

Reviewed by:
Vijay K Samineni,
Washington University in St. Louis, United States
Eugene Dimitrov,
Rosalind Franklin University of Medicine and Science, United States
Benedict Kolber,
The University of Texas at Dallas, United States

***Correspondence:**
Volker Neugebauer
volker.neugebauer@ttuhsc.edu

Specialty section:
This article was submitted to Inflammation Pharmacology, a section of the journal Frontiers in Pharmacology

Received: 16 February 2021
Accepted: 15 April 2021
Published: 25 May 2021

Citation:
Mazzitelli M, Marshall K, Pham A, Ji G and Neugebauer V (2021) Optogenetic Manipulations of Amygdala Neurons Modulate Spinal Nociceptive Processing and Behavior Under Normal Conditions and in an Arthritis Pain Model.
Front. Pharmacol. 12:668337.
doi: 10.3389/fphar.2021.668337

The amygdala is an important neural substrate for the emotional–affective dimension of pain and modulation of pain. The central nucleus (CeA) serves major amygdala output functions and receives nociceptive and affected–related information from the spino-parabrachial and lateral–basolateral amygdala (LA–BLA) networks. The CeA is a major site of extra–hypothalamic expression of corticotropin releasing factor (CRF, also known as corticotropin releasing hormone, CRH), and amygdala CRF neurons form widespread projections to target regions involved in behavioral and descending pain modulation. Here we explored the effects of modulating amygdala neurons on nociceptive processing in the spinal cord and on pain-like behaviors, using optogenetic activation or silencing of BLA to CeA projections and CeA–CRF neurons under normal conditions and in an acute pain model. Extracellular single unit recordings were made from spinal dorsal horn wide dynamic range (WDR) neurons, which respond more strongly to noxious than innocuous mechanical stimuli, in normal and arthritic adult rats (5–6 h postinduction of a kaolin/carrageenan–monoarthritis in the left knee). For optogenetic activation or silencing of CRF neurons, a Cre–inducible viral vector (DIO–AAV) encoding channelrhodopsin 2 (ChR2) or enhanced Natronomonas pharaonis halorhodopsin ($eNpHR_{3.0}$) was injected stereotaxically into the right CeA of transgenic Crh–Cre rats. For optogenetic activation or silencing of BLA axon terminals in the CeA, a viral vector (AAV) encoding ChR2 or $eNpHR_{3.0}$ under the control of the CaMKII promoter was injected stereotaxically into the right BLA of Sprague–Dawley rats. For wireless optical stimulation of ChR2 or $eNpHR_{3.0}$ expressing CeA–CRF neurons or BLA–CeA axon terminals, an LED optic fiber was stereotaxically implanted into the right CeA. Optical activation of CeA–CRF neurons or of BLA axon terminals in the CeA increased the evoked responses of spinal WDR neurons and induced pain-like behaviors (hypersensitivity and vocalizations) under normal condition. Conversely, optical silencing of CeA–CRF neurons or of BLA axon terminals in the CeA decreased the evoked responses of spinal WDR neurons and

vocalizations, but not hypersensitivity, in the arthritis pain model. These findings suggest that the amygdala can drive the activity of spinal cord neurons and pain-like behaviors under normal conditions and in a pain model.

Keywords: amygdala, spinal dorsal horn, pain modulation, optogenetics, electrophysiology, corticotropin releasing hormone, corticotropin releasing factor

HIGHLIGHTS

- Optical activation of BLA axon terminals in CeA or of CeA–CRF neurons increased the evoked activity of spinal dorsal horn neurons and induced nocifensive and emotional responses under normal conditions, mimicking the pain state.
- Optical silencing of BLA axons in CeA or of CeA–CRF neurons in an arthritis pain model decreased the enhanced activity of spinal dorsal horn neurons and reduced emotional responses, but not the hypersensitivity.
- The data provide direct evidence for the modulation of pain-like behaviors and spinal neuronal activity by BLA–CeA signaling and CeA–CRF neurons on under normal conditions and in an arthritis pain model.

INTRODUCTION

Pain is a complex medical condition resulting from the mutual interaction of multiple components, such as sensory, cognitive and emotional–affective. The amygdala, a limbic brain structure, plays a critical role in the affective aspects of behavior and in pain modulation (Veinante et al., 2013; Vachon-Presseau et al., 2016a; Kato et al., 2018; Neugebauer, 2020). The amygdala consists of distinct nuclei, including the central nucleus (CeA), the basolateral complex (BLA), and interposed between them the intercalated cell clusters (ITC). The CeA serves major amygdala output functions and receives purely nociceptive information from the spinal cord via the parabrachial (PB) area of the brainstem and highly integrated multimodal inputs from the thalamus and cortex via the BLA complex (Veinante et al., 2013; Kato et al., 2018; Thompson and Neugebauer, 2019; Neugebauer, 2020). The amygdala processes information from different brain regions and connects to ascending and descending pain modulatory systems and other areas of the central nervous system (CNS) involved in behaviors and cognitive and emotional functions (DeBerry et al., 2015).

The BLA is composed of glutamatergic pyramidal neurons that project to the CeA as well as to several cortical regions, including the medial prefrontal cortex (mPFC) and anterior cingulate cortex (ACC) (Neugebauer et al., 2009; Toyoda et al., 2011; Veinante et al., 2013; Janak and Tye, 2015; Neugebauer, 2020). Through associative processing, emotional-affective significance is conferred to polymodal sensory inputs from the thalamus and cortex that are transmitted to the CeA for further processing. The BLA–CeA circuit has been implicated in the generation and modulation of pain-like behaviors (Thompson and Neugebauer, 2017; Corder et al., 2019; Neugebauer, 2020). The CeA is mainly composed by GABAergic neurons and many co-express neuropeptides such as somatostatin (SOM), protein kinase C delta (PKCδ), dynorphin and corticotropin releasing factor (CRF). Interestingly, expression of those neuropeptides signifies distinct neuronal CeA subpopulations that may serve different functions in anxiety, fear and pain (Haubensak et al., 2010; Li et al., 2013; McCullough et al., 2018; Wilson et al., 2019; Neugebauer et al., 2020). Importantly, the CeA contains the highest density of extra–hypothalamic CRF neurons, which project to different areas of the CNS important for regulating behaviors and pain (Pomrenze et al., 2015). CRF cell bodies are found mostly in the lateral division (CeL) of the CeA and their projections target several nuclei of the hypothalamus, the bed nucleus of the stria terminalis and different areas of the brainstem, including periaqueductal gray (PAG) and PB (Pomrenze et al., 2015; De Guglielmo et al., 2019). CeA–CRF neurons have been linked to the pain modulatory effects of kappa opioid receptors (Ji and Neugebauer, 2020; Hein et al., 2021).

Here we test the hypothesis that selective activation of BLA–CeA terminals or CeA–CRF neurons has facilitatory effects under normal condition and selective silencing of these elements has beneficial inhibitory effects in a pain state. To address our hypothesis, we combined optogenetic strategies with electrophysiological and behavioral assays. Optogenetics utilize genetically–modified light–sensitive channels (opsins) to target specific neuronal populations, allowing the control of neuronal activity with light (Deisseroth, 2015).

RESULTS

This study investigated the contribution of optical manipulation of BLA axon terminals in the CeA and of CeA–CRF neurons on the neuronal activity of spinal dorsal horn neurons and pain–like behaviors under normal conditions and in an arthritis pain model (*Arthritis pain model*). To do so, viral vectors coding light–sensitive channels were injected into BLA or CeA, and an optical fiber delivering light of appropriate length was implanted 4 weeks after surgery and 2 days before testing (**Figure 1A**). For optical manipulation of BLA axon terminals in the CeA, we stereotaxically injected adeno–associated viral vector encoding channelrhodopsin 2 (ChR2) or enhanced Natronomonas pharaonis halorhodopsin ($eNpHR_{3.0}$) fused to yellow fluorescent protein (YFP) under the control of CaMKII promoter into the BLA of SD rats (**Figure 1B**). For control experiments, only YFP was expressed in the BLA. For optical manipulation of CRF neurons in the CeA, we stereotaxically injected a Cre–inducible (DIO) adeno–associated viral vector encoding

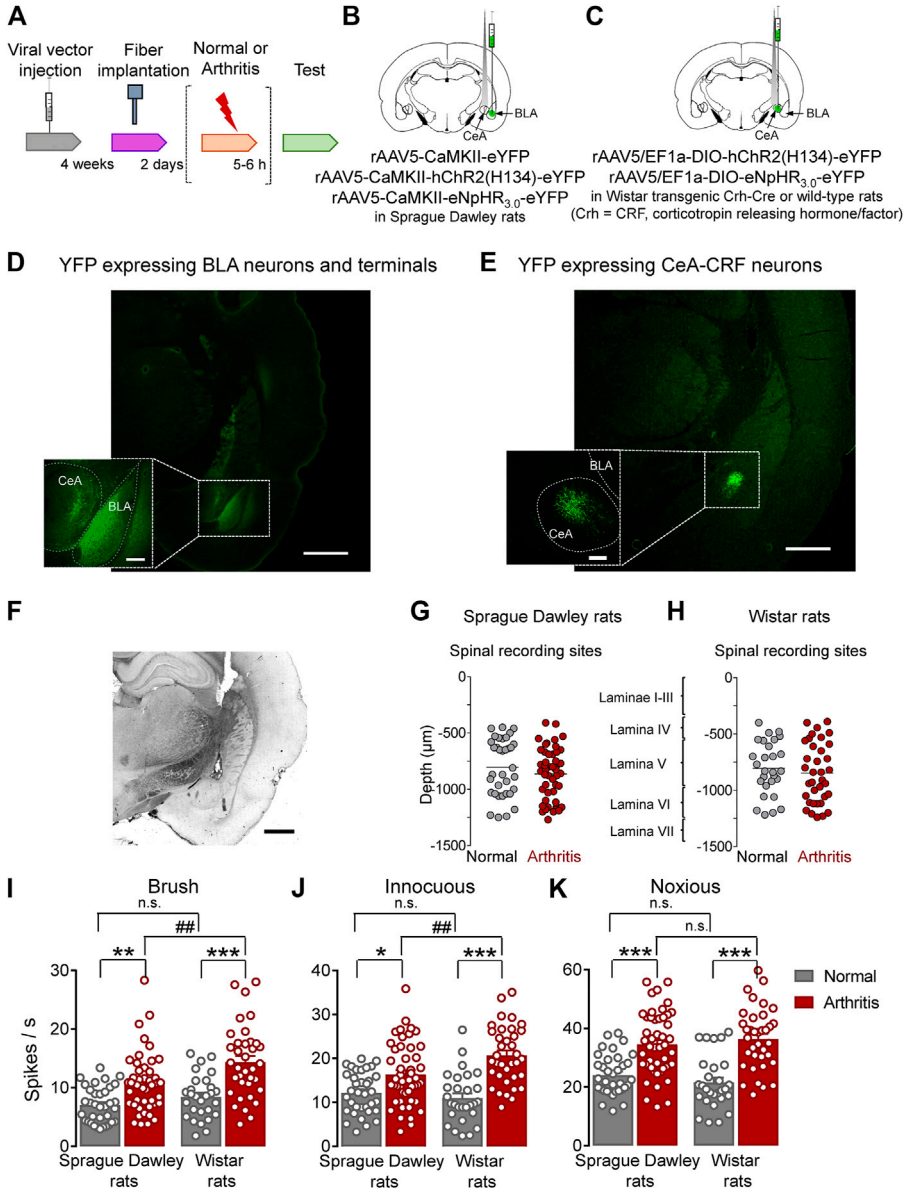

FIGURE 1 | Overview of experimental strategy and arthritis pain-related changes in spinal dorsal horn neurons. **(A)** Experimental design. **(B)** Schematic illustration of viral vector injection into the BLA to express light–sensitive channels under the control of CaMKII in BLA–CeA axon terminals, and application of light into CeA. **(C)** Schematic illustration of the injection of the Cre-inducible viral vector into the CeA to express light–sensitive channels in CRF neurons, and application of light into CeA. **(D)** Representative image of viral vector–mediated YFP expression in BLA and YFP expressing BLA axon terminals in CeA (green, eYFP). Scale bars, 1000 µm (lower magnification image), 200 µm (higher magnification image). **(E)** Representative image of viral vector-mediated YFP expression in CeA–CRF neurons (green, eYFP). Scale bars, 1000 µm (lower magnification image), 200 µm (higher magnification image). **(F)** LED fiber track into the CeA. Scale bar 1000 µm **(G)** Depths of recording electrode tips from the dorsal surface of the spinal cord of Sprague Dawley rats. **(H)** Depths of recording electrodes in the spinal cord of Wistar rats. Also shown is the estimated correlation with dorsal horn laminae. **(I–K)** Spinal neuronal activity evoked by brushing the skin **(I)** and innocuous **(J)** and noxious **(K)** compression of the left knee joint was increased in arthritic SD and arthritic Wistar rats compared to normal naïve rats. In normal naïve rats, no significant difference was found in evoked responses between SD and Wistar strains. In the arthritis pain model, neuronal activity evoked by innocuous **(I, J)**, but not noxious **(K)**, stimulation of the arthritic knee was significantly higher in arthritic Wistar rats than arthritic SD rats. Bar histograms show means ± SEM. SD: Normal, $n = 35$ in 13 rats; Arthritis, $n = 48$ in 18 rats; Wistar: Normal, $n = 28$ in 12 rats; Arthritis, $n = 36$ in 14 rats. *, **, ***$p < 0.05$, 0.01, 0.001 compared to normal; $p < 0.01$ compared to SD; one–way ANOVA with Bonferroni posthoc tests.

ChR2 or enhanced $eNpHR_{3.0}$ fused to YFP into the CeA of transgenic Crh–Cre rats (Crh = CRF, corticotropin releasing hormone/factor) (**Figure 1C**). For control experiments, a viral vector was injected into the CeA of wild type rats. Histological verification confirmed selective eYFP expression in BLA or CeA (**Figures 1D,E**). An LED fiber was stereotaxically inserted into the CeA to deliver blue (473 nm) light for activation or yellow (590 nm) light for inhibition (**Figure 1F**).

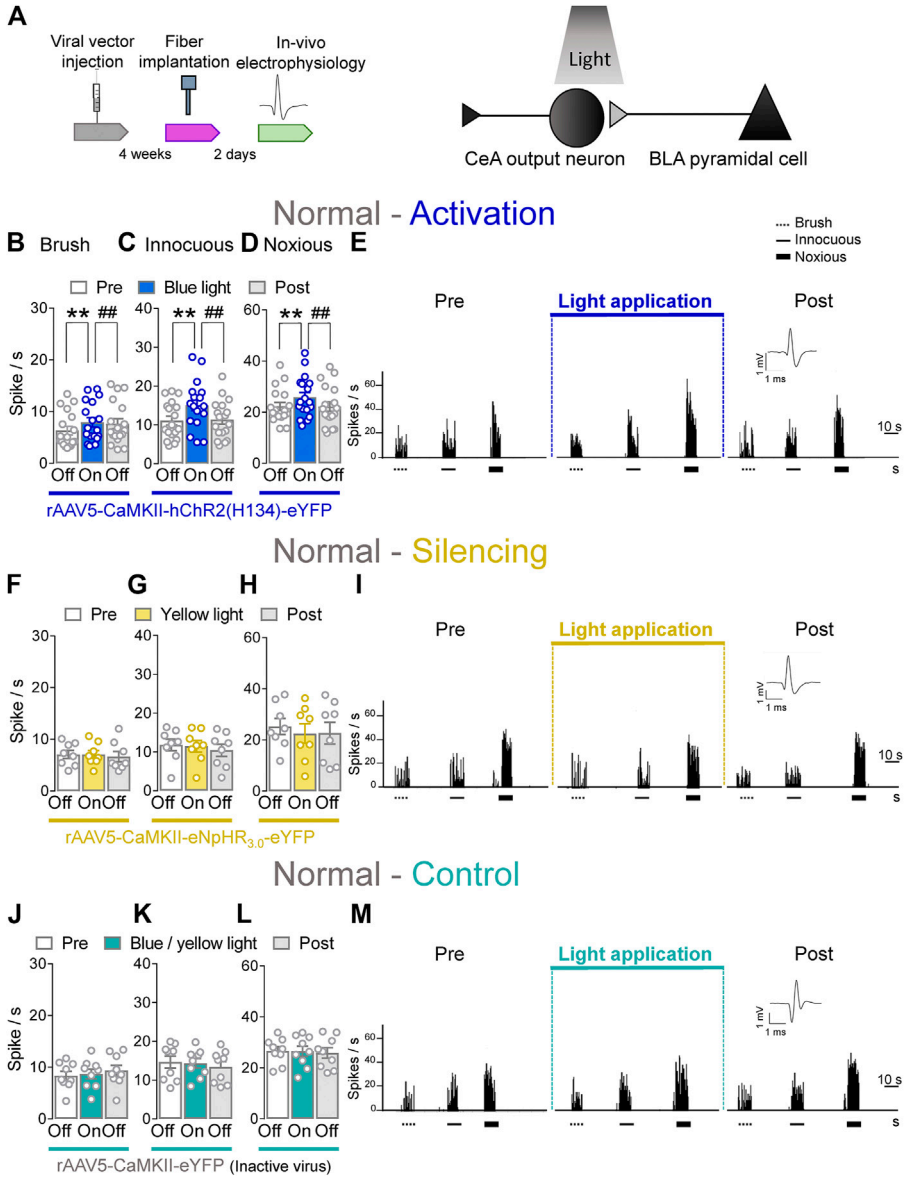

FIGURE 2 | Optogenetic activation of BLA axon terminals in the CeA under normal condition increases evoked activity of spinal cord neurons. **(A)** Experimental design. Neuronal WDR activity ($n = 18$) evoked by brushing the skin **(B)** and innocuous **(C)** and noxious **(D)** compression of the left knee joint was significantly enhanced by optical activation of ChR2 on the BLA–CeA terminals with blue (473 nm) light ("On", 20 Hz, 5 mW, 5–10 min) compared to no light ("Off") values in normal naive rats. **(E)** Peristimulus time histograms (500 ms bin size) show recordings of an individual WDR neuron before, during and after blue (473 nm) light application (20 Hz, 5 mW, 5–10 min) in a normal naïve rat. Bar histograms show means ± SEM. **, $^{\#\#}p < 0.01$, repeated measures one-way ANOVA with Bonferroni posthoc tests **(F–H)** Same display as **(B–D)** but for BLA–CeA terminal inhibition with yellow (590 nm) light ("On") to activate eNpHR$_{3.0}$ ($n = 8$). **(I)** Same display as **(E)** but for BLA–CeA terminal silencing. **(J–L)** Same display as **(B–D)** but in YFP–expressing control rats with either blue (473 nm, $n = 4$) or yellow (590 nm, $n = 5$) light ("On") application ($n = 9$). **(M)** Same display as **(E)** but in a YFP–expressing control rat.

Extracellular single unit recordings from WDR neurons in the deep dorsal horn (lamina IV–VI; mostly lamina V) of the lumbar enlargement (L2–L4, **Figures 1G,H**) showed significantly increased responses to innocuous brushing the skin (I) and to innocuous (J) and to noxious (K) compression of the arthritic (left) knee with a calibrated forceps (10 s, *In vivo spinal cord electrophysiology*) in arthritic compared to normal naïve SD rats (Normal, $n = 35$ neurons in 13 rats; Arthritis, $n = 48$ in 18 rats; **Figure 1I**, $p < 0.01$, $F_{(3, 143)} = 16.53$; **Figure 1J**, $p < 0.05$, $F_{(3, 143)} = 16.75$; **Figure 1K**, $p < 0.001$, $F_{(3, 143)} = 20.88$; one-way ANOVA with Bonferroni posthoc tests) and in arthritic compared to normal naïve Wistar rats (Normal, $n = 28$ neurons in 12 rats; Arthritis, $n = 36$ in 14 rats; **Figure 1I**, $p < 0.001$; **Figure 1J**, $p < 0.001$; **Figure 1K**, $p < 0.001$; for F values see above, one–way ANOVA with Bonferroni posthoc tests). The responses to the three outcome measures were not significantly different between

SD and Wistar strains under normal conditions ($p > 0.05$, one–way ANOVA with Bonferroni posthoc tests). While qualitatively similar increases in the arthritis pain model were found for SD and Wistar rats, the spinal neuronal activity evoked by innocuous brushing the skin and innocuous, but not noxious, compression of the arthritic knee was significantly higher in arthritic Wistar than arthritic SD rats (**Figure 1I**, $p < 0.01$; **Figure 1J**, $p < 0.0$; **Figure 1K**, $p > 0.05$; for F values see above, one–way ANOVA with Bonferroni posthoc tests).

Facilitatory Effects of Optical Activation of BLA–CeA Terminals on Spinal Nociceptive Activity in Naïve Rats

To determine the contribution of BLA–CeA terminals on spinal dorsal horn neurons, extracellular single unit recordings of WDR neurons in the deep layers of the spinal dorsal horn (L2–L4) were performed 4 weeks after rAAV5–CaMKII–(opsin)–eYFP or rAAV5–CaMKII–eYFP (control) injections into the BLA in normal rats. Optical stimulation of ChR2 or $eNpHR_{3.0}$ was achieved by the stereotaxic implantation of an LED optical fiber for blue (473 nm) or yellow (590 nm) light into the CeA 2 days before testing (**Figure 2A**, *Optogenetic strategy* and *In vivo spinal cord electrophysiology*). Activation of ChR2 at the BLA–CeA terminals by blue (473 nm) light ("On", 5–10 min, 20 Hz, 5 mW) significantly increased the activity of WDR neurons evoked by brief (10 s) innocuous brush ($p < 0.01$, $F_{(2, 34)} = 12.1$) and innocuous ($p < 0.01$, $F_{(2, 34)} = 11.89$) and noxious compression ($p < 0.01$, $F_{(2, 34)} = 7.153$; repeated measures one–way ANOVA with Bonferroni posthoc tests, $n = 18$) of the left knee joint with a calibrated forceps (*In vivo spinal cord electrophysiology*) compared to no light exposure ("Off") in normal rats (**Figures 2B–E**). The effects of optical activation were reversible (**Figures 2B–E**).

Conversely, optogenetic silencing of $eNpHR_{3.0}$ expressing BLA–CeA terminals by yellow (590 nm) light ("On", 5–10 min, 20 Hz, 5 mW) application had no significant effects on the responses of WDR neurons to brief (10 s) brushing the skin ($p > 0.05$, $F_{(2, 14)} = 0.5215$) and innocuous ($p > 0.05$, $F_{(2, 14)} = 1.64$) and noxious compression ($p > 0.05$, $F_{(2, 14)} = 0.9986$, repeated measures one–way ANOVA with Bonferroni posthoc tests, $n = 8$) of the left knee joint compared to no light application ("Off") in normal rats (**Figures 2F–I**). In YFP–control rats, the application of blue (473 nm) or yellow (590 nm) light ("On", 5–10 min, 20 Hz, 5 mW) into the CeA did not affect the evoked responses of spinal WDR neurons ($p > 0.05$; **Figure 2J**, $F_{(2, 16)} = 1.982$; **Figure 2K**, $F_{(2, 16)} = 1.757$; **Figure 2L**, $F_{(2, 16)} = 0.1571$; repeated measures one–way ANOVA with Bonferroni posthoc tests, $n = 9$) compared to no light exposure ("Off") in normal rats (**Figures 2J–M**). Data for blue ($n = 4$) and yellow ($n = 5$) light exposure in control rats were combined because no difference was observed. Optical manipulations in the amygdala did not induce any non-evoked (by peripheral stimuli) activity in spinal neurons. The data suggest that activation of BLA–CeA inputs has facilitatory effects on spinal nociceptive processing under normal condition.

Whole–cell patch clamp experiments (*Patch–clamp electrophysiology in amygdala slices*) were performed to validate our optogenetics approach (**Supplementary Figure S1**). Application of continuous or pulsed (20 Hz) blue light for 5 s at the BLA–CeA terminals expressing ChR2 (**Supplementary Figure S1A**) induced firing activity of a CeA neuron in the laterocapsular division (CeLC) in an amygdala–containing slice obtained from a normal rat. No difference was detected between continuous and pulsed light exposure on the CeLC neuronal activity, validating our experimental approach using pulsed light exposure in the CeA in the *in vivo* studies. Yellow light was applied as control (**Supplementary Figures S1B, C**).

Inhibitory Effects of Optical Silencing of BLA–CeA Terminals on Spinal Nociceptive Activity in Arthritic Rats

Next, we investigated the contribution of optical manipulations of the BLA–CeA terminals to spinal nociceptive processing in the arthritis pain model (**Figure 3A**). The evoked responses of dorsal horn WDR neurons were enhanced in arthritic rats (5–6 h post induction) compared to normal conditions (**Figures 1I–K**). In the arthritis condition, activation of BLA–CeA terminals by blue (473 nm) light ("On", 5–10 min, 20 Hz, 5 mW) delivered through an optical fiber stereotaxically implanted into the CeA (*Optogenetic strategy*) had no significant effect on the responses of WDR neurons to brief (10 s) brushing the skin ($p > 0.05$, $F_{(2, 26)} = 1.642$) and innocuous ($p > 0.05$, $F_{(2, 26)} = 1.36$) and noxious compression ($F_{(2, 26)} = 0.2889$, repeated measures one–way ANOVA with Bonferroni posthoc tests, $n = 14$) of the left knee joint with a calibrated forceps (*In vivo spinal cord electrophysiology*) compared to no light exposure ("Off", **Figures 3B–E**).

In contrast, optogenetic silencing of BLA terminals in the CeA by yellow (590 nm) light ("On", 5–10 min, 20 Hz, 5 mW) application into the CeA, had significant inhibitory effects on the activity of WDR neurons evoked by brush ($p < 0.01$, $F_{(2, 38)} = 20.94$) and innocuous ($p < 0.01$, $F_{(2, 38)} = 10.54$) and noxious ($p < 0.01$, $F_{(2, 38)} = 18.53$, repeated measures one–way ANOVA with Bonferroni posthoc tests, $n = 20$) stimulation of the left (arthritic) knee joint compared to no light exposure ("Off") in arthritic rats (**Figures 3F–I**). The effects of optical inhibition were reversible (**Figures 3F–I**). In YFP–control rats, application of blue (473 nm) or yellow (590 nm) light ("On", 5–10 min, 20 Hz, 5 mW) delivered by an optical fiber in the CeA (*Optogenetic strategy*) did not affect the evoked responses of WDR neurons by brief (10 s) mechanical stimulation ($p > 0.05$; **Figures 3J,** $F_{(2, 26)} = 0.3145$; **Figures 3K,** $F_{(2, 26)} = 3.092$; **Figures 3L,** $F_{(2, 26)} = 0.382$; repeated measures one–way ANOVA with Bonferroni posthoc tests, $n = 14$) of the knee joint compared to no light application ("Off") in arthritic rats (**Figures 3J–M**). Data for blue ($n = 7$) and yellow ($n = 7$) light exposure were combined because no difference was detected. These results suggest inhibitory effects of silencing BLA–CeA terminals on spinal nociceptive processing in an arthritis pain model.

Brain slice physiology showed that application of continued or pulsed (20 Hz) yellow light for 5 s to the BLA–CeA terminals

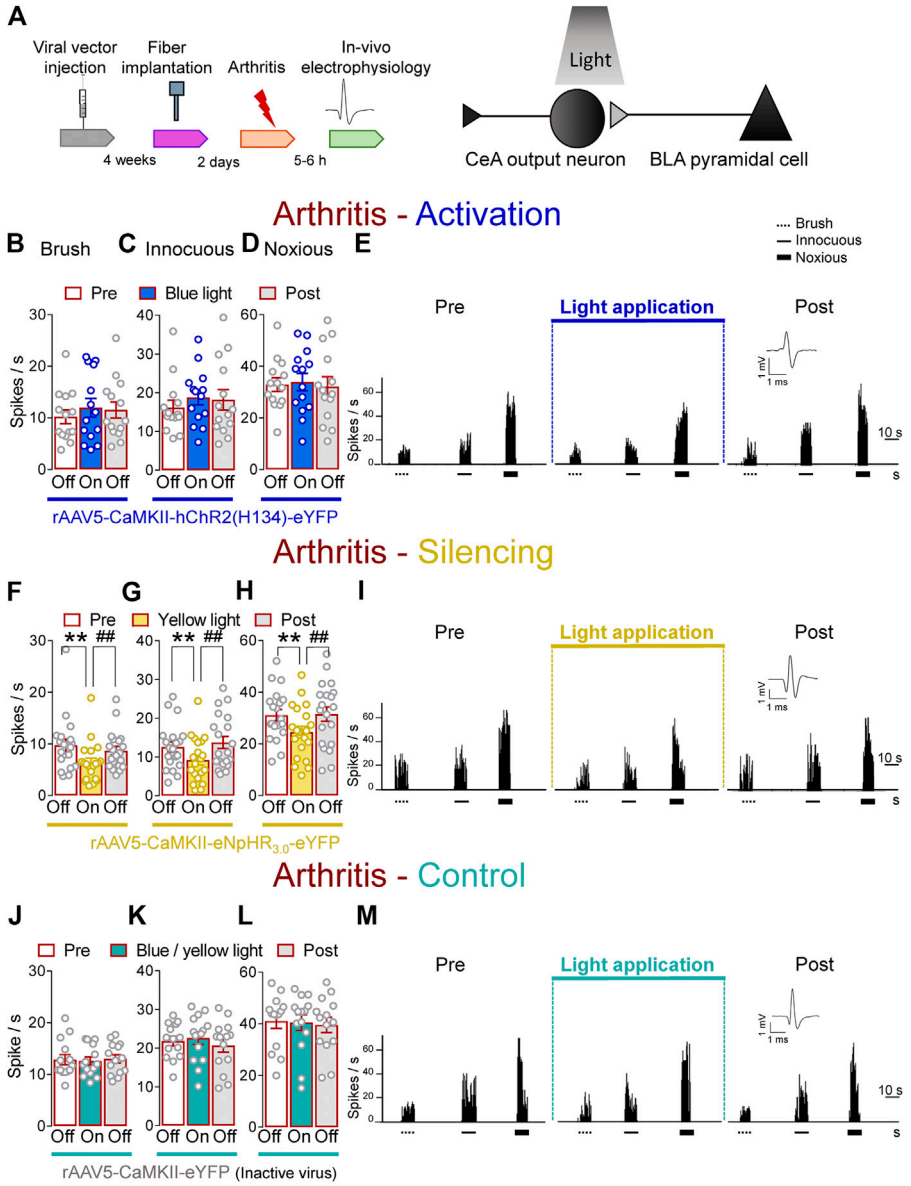

FIGURE 3 | Optogenetic silencing of BLA axon terminals in the CeA in the arthritis pain model reduces the increased activity of spinal cord neurons. **(A)** Experimental design. Responses of WDR neurons (n = 14) to brushing the skin **(B)** and innocuous **(C)** and noxious **(D)** compression of the left knee joint were not significantly affected by the optical activation of ChR2 expressed on BLA–CeA terminals with blue (473 nm) light ("On", 20 Hz, 5 mW, 5–10 min) compared to no light ("Off") values in arthritic rats. **(E)** Peristimulus time histograms (500 ms bin size) show recordings of a single WDR neuron before, during and after blue (473 nm) light application (20 Hz, 5 mW, 5–10 min) in an arthritic rat. Bar histograms show means ± SEM . **(F–H)** Same display as **(B–D)** but for BLA–CeA terminal inhibition with yellow (590 nm) light ("On") to activate $eNpHR_{3.0}$ (n = 8). **(I)** Same display as **(E)** but for BLA–CeA terminal silencing (n = 20). **, $^{\#\#}p < 0.01$, repeated measures one–way ANOVA with Bonferroni posthoc tests. **(J–L)** Same display as **(B–D)** but in YFP–expressing control rats with blue (473 nm, n = 7) or yellow (590 nm, n = 7) light ("On") application (n = 14). **(M)** Same display as **(E)** but in a YFP–expressing control rat.

expressing $eNpHR_{3.0}$ inhibited action potential firing of CeLC neuron in a brain slice from an arthritic rat. No difference was detected between the effects of continuous and pulsed light exposure on CeLC neuronal activity, supporting our experimental approach using pulsed light in the *in vivo* studies. Blue light was applied as control (**Supplementary Figures S1D, E**).

Facilitatory Effects of Optical Activation of CeA–CRF Neurons on Spinal Nociceptive Activity in Naïve Rats

CeA–CRF neurons are involved in behavioral modulation, pain and fear (Pomrenze et al., 2015; Neugebauer et al., 2020). Therefore, we aimed to explore the involvement of CeA–CRF neurons on the activity of spinal neurons using optogenetics in

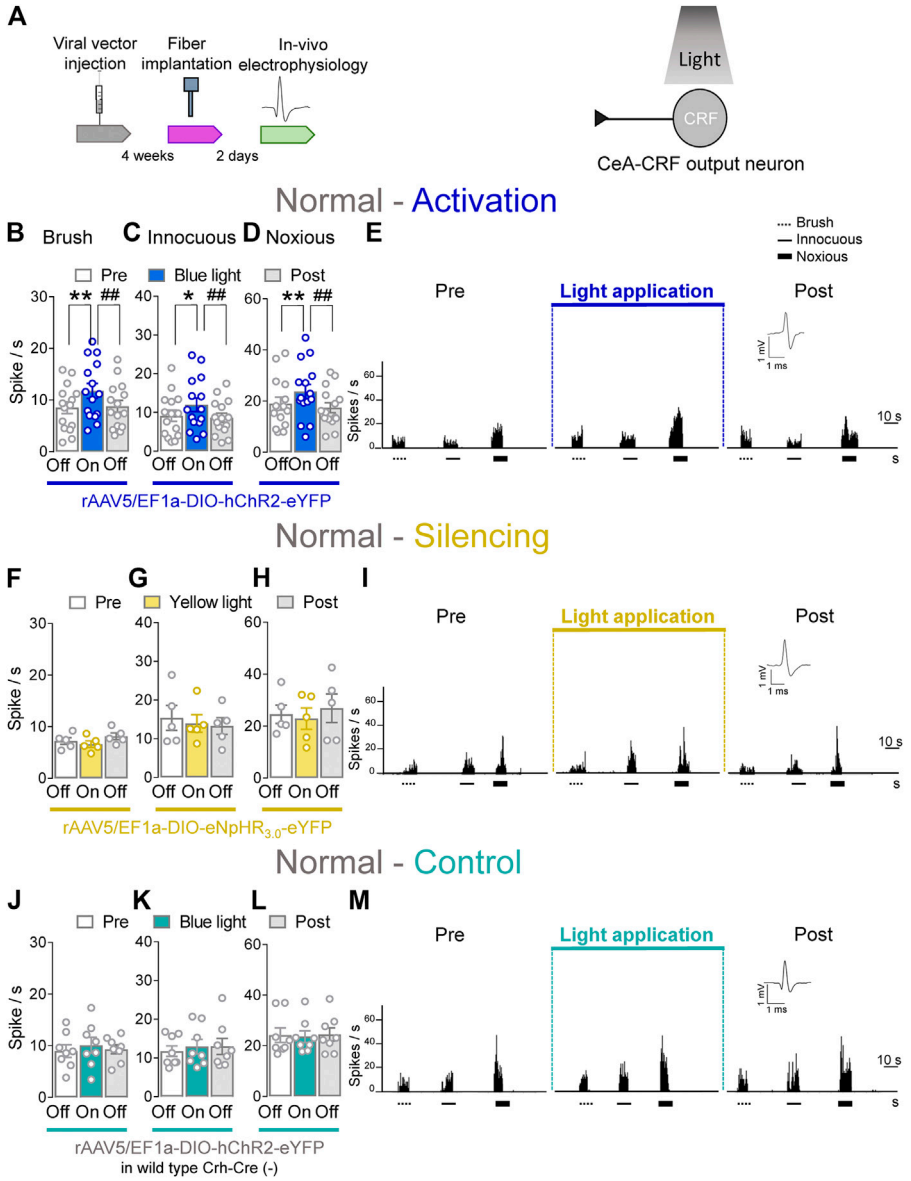

FIGURE 4 | Optogenetic activation of CeA-CRF neurons under normal conditions increases evoked activity of spinal cord neurons. **(A)** Experimental design. Responses of WDR neurons (n = 15) to brushing the skin **(B)** and innocuous **(C)** and noxious **(D)** compression of the left knee joint were significantly enhanced by optical activation of ChR2 expressing CeA–CRF neurons with blue (473 nm) light ("On", 20 Hz, 5 mW, 5–10 min) compared to no light ("Off") values in normal naive rats. **(E)** Peristimulus time histograms (500 ms bin size) show recordings of an individual WDR neuron recorded before, during and after blue (473 nm) light application (20 Hz, 5 mW, 5–10 min) in a normal naïve rat. Bar histograms show means ± SEM. *, $p < 0.05$, **, $^{\#\#}p < 0.01$, repeated measures one–way ANOVA with Bonferroni posthoc tests. **(F–H)** Same display as **(B–D)** but for silencing of $eNpHR_{3.0}$ expressing CeA–CRF neurons with yellow (590 nm) light ("On") exposure (n = 5). (I) Same display as **(E)** but for CeA–CRF neuron silencing. **(J–L)** Same display as **(B–D)** but in wild type control rats with blue (473 nm) light ("On") application (n = 8). **(M)** Same display as **(E)** but in a wild type control rat.

transgenic Crh–Cre rats. Extracellular single unit recording from WDR neurons in the deep dorsal horn (L2–L4) were performed 4 weeks after rAAV5–DIO–(opsin)–eYFP injections into the CeA in normal rats to express ChR2 or $eNpHR_{3.0}$ in CeA–CRF neurons. An LED optical fiber delivering blue (473 nm) or yellow (590 nm) light was stereotaxically implanted into the CeA 2 days before testing to stimulate ChR2 or eNpHR3.0 (**Figure 4A**, *Optogenetic strategy* and *In vivo spinal cord electrophysiology*). Activation of CeA–CRF neurons by blue (473 nm) light ("On", 5–10 min, 20 Hz, 5 mW) significantly increased the activity of WDR neurons evoked by brief (10 s) innocuous brush ($p < 0.01$, $F_{(2, 28)} = 13.44$) and innocuous ($p < 0.05$, $F_{(2, 28)} = 7.622$) and noxious mechanical stimulation ($p < 0.01$, $F_{(2, 28)} = 10.04$; repeated measures one–way ANOVA with Bonferroni posthoc tests, n = 15) of the left knee joint with a calibrated forceps (*In vivo spinal cord electrophysiology*)

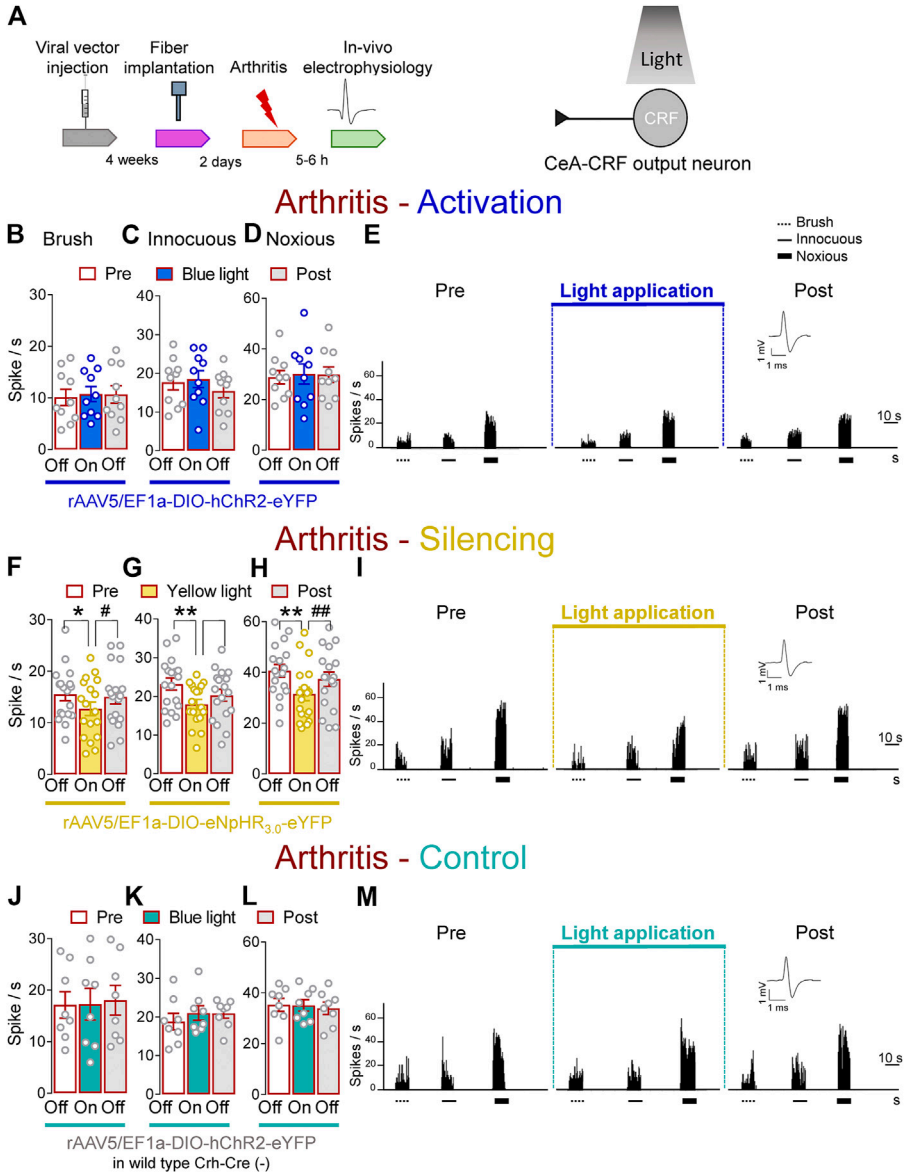

FIGURE 5 | Optogenetic silencing of CeA-CRF neurons in the arthritis pain model reduces the increased activity of spinal cord neurons. **(A)** Experimental design. Responses of WDR neurons (n = 10) to brushing the skin **(B)** and innocuous **(C)** and noxious **(D)** compression of the left knee joint were not significantly affected by optical activation of ChR2 expressing CeA–CRF neurons with blue (473 nm) light ("On", 20 Hz, 5 mW, 5–10 min) compared to no light ("Off") values in arthritic rats. **(E)** Peristimulus time histograms (500 ms bin size) of a single WDR neuron recorded before, during and after blue (473 nm) light application (20 Hz, 5 mW, 5–10 min) in an arthritic rat. Bar histograms show means ± SEM. **(F–H)** Same display as **(B–D)** but for silencing of $eNpHR_{3.0}$ expressing CeA–CRF neurons with yellow (590 nm) light ("On"). **(I)** Same display as **(E)** but for CeA–CRF neuron silencing (n = 18). *, **$p < 0.05$, 0.01 compared to no light ("Off") values; $p < 0.05$, 0.01 compared to light ("On") values, repeated measures one–way ANOVA with Bonferroni posthoc tests. **(J–L)** Same display as **(B–D)** but in wild type control rats with blue (473 nm) light ("On") application (n = 8). **(M)** Same display as **(E)** but in a wild type control rat.

compared to no light application ("Off") under normal condition (**Figures 4B–E**). The effects of optical activation were reversible (**Figures 4B–E**).

Conversely, optical silencing of CeA–CRF neurons by yellow (590 nm) light application ("On", 5–10 min, 20 Hz, 5 mW) had no significant effects on the activity of WDR neurons evoked by brief (10 s) brushing the skin ($p > 0.05$, $F_{(2,\ 8)} = 3.796$) and innocuous ($p > 0.05$, $F_{(2,\ 8)} = 0.36150$) and noxious ($p > 0.05$, $F_{(2,\ 8)} = 1.467$; repeated measures one–way ANOVA with Bonferroni posthoc tests, n = 5) stimulation of the left knee joint compared to no light exposure ("Off") in normal naive rats (**Figures 4F–I**). In normal wild type rats (control), the application of blue (473 nm) light ("On", 5–10 min, 20 Hz, 5 mW) did not significantly change the responses of WDR neurons to mechanical stimulation of the knee joint ($p > 0.05$; **Figure 4J**, $F_{(2,\ 14)} = 0.7263$; **Figure 4K**, $F_{(2,\ 14)} = 0.9692$; **Figure 4L**, $F_{(2,\ 14)} =$

0.09817; repeated measures one–way ANOVA with Bonferroni posthoc tests, n = 8) compared to no light exposure ("Off"; **Figures 4J–M**). The data suggest that activation of CeA–CRF neurons has facilitatory effects on spinal cord neuronal activity under normal conditions.

Whole–cell patch clamp recordings (*Patch–clamp electrophysiology in amygdala slices* and **Supplementary Figures S2A–C**) were made of CeA–CRF neurons identified by their YFP expression (De Guglielmo et al., 2019). Application of continuous or pulsed (20 Hz) blue light for 5 s induced action potential firing of a CRF neuron in an amygdala slice from a normal rat. No difference was detected between continuous and pulsed light effects on CeA–CRF activity, supporting our experimental approach using pulsed light in the *in vivo* studies. Yellow light was applied as control (**Supplementary Figures S2B,C**).

Inhibitory Effects of Optical Silencing of CeA–CRF Neurons on Spinal Nociceptive Activity in Arthritic Rats

Next, we determined the effects of optical manipulations of CeA–CRF neurons on spinal nociceptive processing in the arthritis pain model (**Figure 5A**). The responses of spinal WDR neurons were enhanced in arthritic rats (5–6 h post induction) compared to normal conditions (**Figures 1I–K**). In the arthritis pain model, activation of CeA–CRF neurons by blue (473 nm) light ("On", 5–10 min, 20 Hz, 5 mW) through an optical fiber in the CeA (*Optogenetic strategy*) had no significant effects on the responses of WDR neurons to brief (10 s) brushing the skin ($p > 0.05$, $F_{(2,\ 18)} = 0.4702$) and to innocuous ($p > 0.05$, $F_{(2,\ 18)} = 3.283$) and to noxious compression ($p > 0.05$, $F_{(2,\ 18)} = 0.3161$, repeated measures one–way ANOVA with Bonferroni posthoc tests, n = 10) of the left (arthritic) knee joint with a calibrated forceps (*In vivo spinal cord electrophysiology*) compared to no light exposure ("Off", **Figures 5B–E**).

In contrast, optogenetic silencing of CeA–CRF neurons by yellow (590 nm) light ("On", 5–10 min, 20 Hz, 5 mW) application into the CeA significantly inhibited the activity of WDR neurons evoked by brush ($p < 0.05$, $F_{(2,\ 34)} = 5.383$) and innocuous ($p < 0.01$, $F_{(2,\ 34)} = 8.554$) and noxious ($p < 0.01$, $F_{(2,\ 34)} = 15.08$, repeated measures one–way ANOVA with Bonferroni posthoc tests, n = 18) stimulation of the left knee joint compared to no light exposure ("Off") in arthritic rats (**Figures 5F–I**). The effects of optical inhibition were reversible (**Figures 5F–I**). In normal wild type rats (control), the application of blue (473 nm) light ("On", 5–10 min, 20 Hz, 5 mW) did not change the responses of WDR neurons to brief (10 s) mechanical stimulation ($p > 0.05$; **Figure 5J**, $F_{(2,\ 14)} = 0.206$; **Figure 5K**, $F_{(2,\ 14)} = 1.025$; **Figure 5L**, $F_{(2,\ 14)} = 0.1829$, noxious; repeated measures one–way ANOVA with Bonferroni posthoc tests, n = 8) compared to no light application ("Off") in arthritic rats (**Figures 5J–M**). The results suggest inhibitory effects of silencing CeA–CRF neurons on spinal nociceptive processing in an arthritis pain model.

As a validation of the optogenetic approach, application of continuous or pulsed (20 Hz) yellow light for 5 s inhibited action potential firing in a CRF neuron (*Facilitatory effects of optical activation of CeA–CRF neurons on spinal nociceptive activity*) in an amygdala slice from an arthritic rat (*Patch–clamp electrophysiology in amygdala slices* and **Supplementary Figures S2D,E**). No difference was detected between the effects of continuous and pulsed light exposure on CRF neuronal activity, supporting our experimental approach using pulsed light in the CeA in the *in vivo* studies. Blue light was applied as control (**Supplementary Figures S2D,E**).

Effects of Optical Manipulation of Amygdala Activity on Pain–like Behaviors

We evaluated the behavioral consequences of optogenetic manipulations of BLA–CeA terminals or CeA–CRF neurons (**Figure 6**, *Pain–related behaviors*) in normal and arthritic rats. Optogenetic activation of ChR2 expressing BLA–CeA terminals with blue (473 nm) light ("On", 5–10 min, 20 Hz, 5 mW) significantly increased audible and ultrasonic vocalizations in response to brief (10 s) noxious compression of the left knee joint with a calibrated forceps (*Pain–related behaviors*) compared to no light ("Off") in normal naïve rats (**Figure 6A**, $p < 0.01$, $t = 3.533$; **Figure 6B**, $p < 0.05$, $t = 2.862$; n = 13, paired t-test). Similarly, withdrawal thresholds of nocifensive reflexes evoked by mechanical compression of the knee joint (*Pain–related behaviors*) were significantly decreased by optical activation of BLA–CeA terminals in normal naïve rats (**Figure 6C**, $p < 0.05$, $t = 3.913$, $n = 5$, paired t-test). In the arthritis pain model, optogenetic silencing of $eNpHR_{3.0}$ expressing BLA–CeA terminals with yellow (593 nm) light ("On", 5–10 min, 20 Hz, 5 mW) had significant inhibitory effects on audible and ultrasonic vocalizations evoked by noxious compression of the left (arthritic) knee joint (**Figure 6D**, $p < 0.01$, $t = 4.415$; **Figure 6E**, $p < 0.005$, $t = 4.89$; n = 11, paired t-test compared to no light ("Off")). Surprisingly, mechanical withdrawal thresholds were not affected by optical silencing of the BLA–CeA terminals in arthritic rats (**Figure 6F**, $p > 0.05$, $t = 1.881$, n = 6, paired t-test).

Activation of ChR2 expressing CeA–CRF neurons by the application of blue (473 nm) light ("On", 5–10 min, 20 Hz, 5 mW) significantly increased audible and ultrasonic vocalizations evoked by brief (10 s) noxious stimulation of the left knee joint with a calibrated forceps (*Pain–related behaviors*) compared to no light ("Off") in normal naïve transgenic rats ($p < 0.05$; **Figure 6G**, $t = 3.271$; **Figure 6H**, $t = 2.378$; n = 8, paired t-test). Optical activation of CeA–CRF neurons significantly decreased withdrawal thresholds of nocifensive reflexes evoked by mechanical compression of the knee joint (*Pain–related behaviors*) in normal naïve transgenic rats (**Figure 6I**, $p < 0.05$, $t = 3.994$, n = 5, paired t-test). In arthritic transgenic rats, optical silencing of $eNpHR_{3.0}$ expressing CeA–CRF neurons with yellow (593 nm) light ("On", 5–10 min, 20 Hz, 5 mW) significantly reduced audible and ultrasonic vocalizations evoked by noxious compression (*Pain–related behaviors*) of the left (arthritic) knee joint compared to no light ("Off"; **Figure 6J**, $p < 0.005$, $t = 7.888$; **Figure 6K**, $p < 0.01$, $t =$

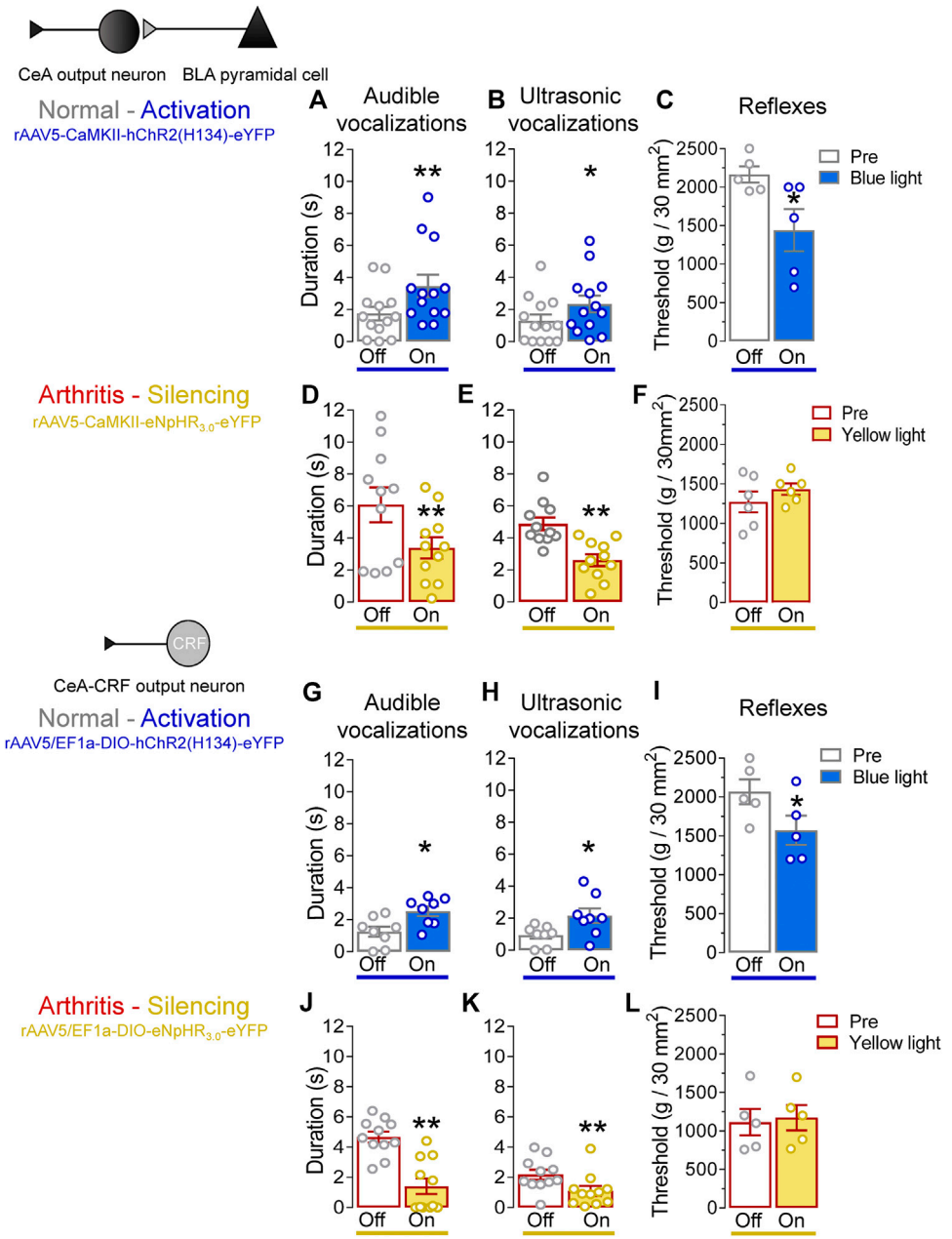

FIGURE 6 | Effects of optogenetic amygdala manipulations on pain-related behaviors in normal and arthritis conditions. **(A)** Audible and **(B)** ultrasonic vocalizations evoked by noxious compression of the knee joint with a calibrated forceps were significantly increased by the activation of ChR2 on BLA–CeA terminals with blue (473 nm) light application ("On", 20 Hz, 5 mW, 5–10 min) into the CeA compared to no light ("Off") values in normal naïve rats (n = 13). **(C)** Mechanical withdrawal thresholds were significantly reduced by blue light (473 nm) exposure in normal naïve rats (n = 5), indicating hypersensitivity. **(D–F)** Same display as **(A–C)** but for silencing of eNpHR$_{3.0}$ expressing BLA–CeA terminals with yellow light (590 nm) in arthritic rats (audible and ultrasonic vocalizations, n = 11; reflexes, n = 6). **(G–I)** Same display as **(A–C)** but for activation of ChR2 expressing CeA–CRF neurons in normal naïve transgenic rats (audible and ultrasonic vocalizations, n = 8; reflexes, n = 5). **(J–L)** Same display as **(A–C)** but for silencing of eNpHR$_{3.0}$ expressing CeA–CRF neurons with yellow light (590 nm) in arthritic transgenic rats (audible and ultrasonic vocalizations, n = 11; reflexes, n = 5). *, **p < 0.05, 0.01 compared to no light ("Off") values, paired t–test.

4.518; n = 11, paired t-test). Just like optical silencing of BLA-CeA terminals, silencing of CeA-CRF neurons had no significant effect on mechanical withdrawal thresholds (*Pain–related behaviors*) in arthritic transgenic rats (**Figure 6L**, t = 1.729, n = 5, paired t-test).

DISCUSSION

Preclinical (Neugebauer et al., 2009; Apkarian et al., 2013; Thompson and Neugebauer, 2017; Neugebauer, 2020) and clinical (Kulkarni et al., 2007; Liu et al., 2010; Simons et al.,

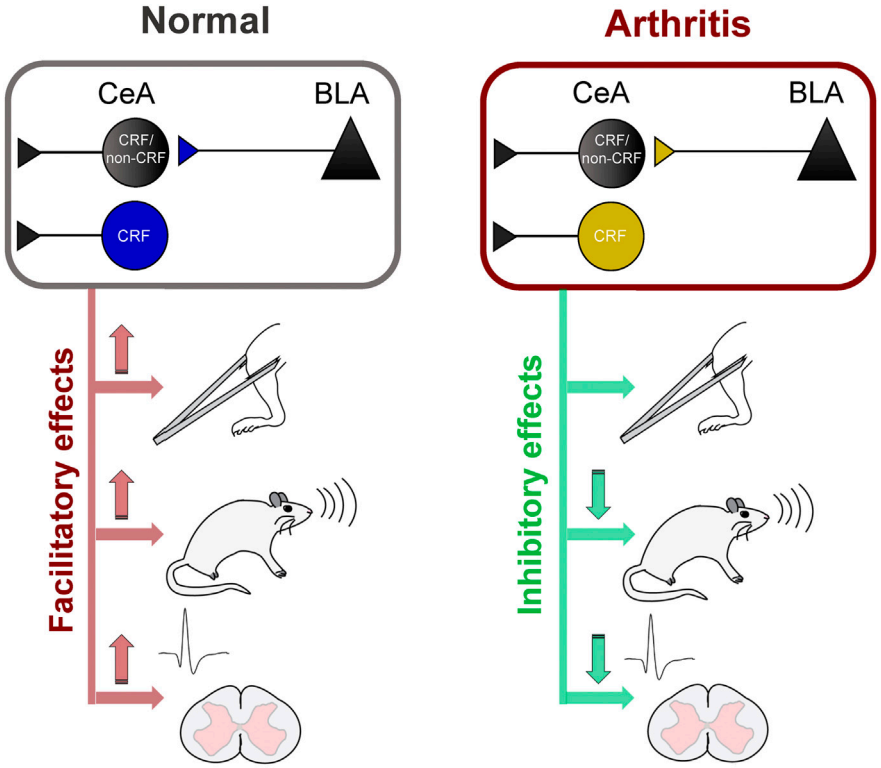

FIGURE 7 | Diagram summarizing key results (Left) Activation of BLA–CeA terminals or CeA–CRF neurons has facilitatory effects on spinal nociceptive processing, vocalizations and mechanical withdrawal thresholds under normal conditions (Right) Silencing of BLA–CeA terminals or CeA–CRF neurons has inhibitory effects on spinal nociceptive processing and vocalizations, but not on withdrawal reflexes, in an arthritis pain model.

2014) studies have linked the amygdala to averse-affective aspects of pain and pain modulation. The role of individual cell types and interactions with spinal nociceptive processing as part of the descending control system remain to be determined. Evidence from preclinical research showed changes in the amygdala neurocircuitry in pain state. For instance, *in vivo* recordings revealed increased background activity and evoked responses of CeA and BLA neurons to mechanical peripheral stimuli in acute (arthritis) and neuropathic (spinal nerve ligation, SNL) pain models (Neugebauer and Li, 2003; Ji et al., 2009; Ji and Neugebauer, 2009; Ji et al., 2017; Kim et al., 2017). Mechanistic analyses in brain slice physiology experiments detected increased excitatory transmission at the PB–CeA and BLA–CeA synapses and impaired inhibitory control resulting in CeA hyperactivity in pain conditions (Neugebauer et al., 2003; Han et al., 2005; Ikeda et al., 2007; Fu and Neugebauer, 2008; Ren and Neugebauer, 2010; Kiritoshi and Neugebauer, 2018; Miyazawa et al., 2018; Wilson et al., 2019). Interestingly, amygdala pain mechanisms exhibit hemispheric lateralization with the right amygdala showing pain-related synaptic plasticity and activity changes that are involved in pain facilitatory amygdala functions (Carrasquillo and Gereau, 2008; Ji and Neugebauer, 2009; Goncalves and Dickenson, 2012; Simons et al., 2014; Miyazawa et al., 2018; Nation et al., 2018; Allen et al., 2021). Therefore, our focus on the right hemisphere in this project is justified although it will be important for future studies to perform similar manipulations in the left amygdala to determine any differences.

Pharmacological interventions that increase amygdala output have been shown to evoke pain behaviors in the absence of injury, whereas strategies that decrease amygdala output generally inhibit pain behaviors (reviewed in Neugebauer, 2020). However, there is also evidence for pain inhibitory amygdala functions (Wilson et al., 2019). A cell–type specific analysis is needed for the better understanding of amygdala pain mechanisms, and the optogenetic strategy employed here is an important step in that direction. The involvement of individual cell–types (PKCδ, SOM, CRF; see *Introduction*) in pain–related amygdala neuroplasticity has not been fully explored and is currently an area of extensive research (Wilson et al., 2019; Li and Sheets, 2020; Adke et al., 2021). Here we show that optogenetic activation of CRF neurons or of BLA input to the CeA generates nocifensive emotional responses (vocalizations) and mechanical hypersensitivity under normal conditions in the absence of tissue injury or pathology, whereas silencing of CRF neurons or of BLA input to CeA inhibits vocalizations in an arthritis pain model.

CRF output neurons in the CeA are known to project to hypothalamic nuclei, the basal forebrain and several brainstem areas involved in behaviors and pain modulation such as the periaqueductal gray (PAG), locus coeruleus (LC) and PB (Pomrenze et al., 2015; Neugebauer et al., 2020) regions.

Several lines of research show that CRF projecting neurons in the CeA promote averse–affective behaviors (Fendt et al., 1997; Mccall et al., 2015; Pomrenze et al., 2015; Pomrenze et al., 2019) and that the CRF system in the amygdala is endogenously activated in pain conditions and is critically involved in amygdala pain mechanisms (Mcnally and Akil, 2002; Ji et al., 2007; Ji and Neugebauer, 2007; Fu and Neugebauer, 2008; Ji and Neugebauer, 2020; Hein et al., 2021). The BLA–CeA network is known to convey highly integrated polymodal information from thalamus and cortex and encodes averse-affective aspects of pain (Veinante et al., 2013; Corder et al., 2019; Thompson and Neugebauer, 2019; Neugebauer, 2020). The BLA neurons project to the CeA directly through excitatory synapses or indirectly via the intercalated cells (ITC) that mediate feed–forward inhibition of amygdala output from CeA neurons. ITC inhibitory tone is also driven by excitatory cortical synapses from the medial prefrontal cortex (Cheriyan et al., 2016; Kiritoshi and Neugebauer, 2018; Thompson and Neugebauer, 2019). Failure of cortical inhibitory control allows pain–related dysfunctions of this neurocircuitry resulting in increased excitatory transmission and hyperactivity of the CeA and is thought to correlate with the emotional–affective dimension of pain and pain-associated cortical deficits (Ji et al., 2010; Bushnell et al., 2013; Ren et al., 2013; Vachon-Presseau et al., 2016b; Kiritoshi and Neugebauer, 2018).

This study advances knowledge about pain-related amygdala functions by providing direct evidence for pain–facilitating effects of BLA–CeA transmission and CeA–CRF activation under normal conditions and their contribution to spinal nociceptive processing and behaviors in a pain condition (**Figure 7**). Sadler et al. (2017) demonstrated that optogenetic (ChR2) activation of right CeA neurons induced mechanical allodynia and increased visceromotor responses to noxious bladder distension in naïve rats, suggesting pronociceptive effects of the right amygdala to drive pain–like behaviors. Our results show that optical (ChR2) activation of glutamatergic (CaMKII) BLA–CeA terminals and of CRF–CeA neurons in the right hemisphere increases evoked responses of spinal dorsal horn WDR neurons (**Figures 2**, **4**) and induces or increases vocalizations and mechanical sensitivity (**Figure 6**) under normal conditions, suggesting a critical role of these elements in so-called functional pain conditions in the absence of tissue injury or pathology. This study also showed that optical ($eNpHR_{3.0}$) silencing of BLA–CeA terminals and CeA–CRF neurons decreased the increased activity of spinal WDR neurons (**Figures 3**, **5**) and vocalizations (**Figure 3**) in the arthritis pain model, suggesting a significant contribution of amygdala activity to pain–related neuronal changes at the spinal cord level and to emotional pain-like behaviors. Optogenetic stimulation of $eNpHR_{3.0}$ has been used before to silence CRF neurons in the amygdala (De Guglielmo et al., 2019; Ji and Neugebauer, 2020). The fact that optogenetic manipulations of the BLA–CeA and CeA–CRF elements had similar effects may suggest that excitatory BLA input to CeA targets CRF neurons or that both engage similar CeA circuits.

A surprising finding was that optical silencing of BLA–CeA and CeA–CRF neurons in the arthritis pain model did not affect mechanical hypersensitivity whereas optical activation did generate hypersensitivity. Previous studies showed that chemogenetic inhibition of PKCδ or SOM amygdala neurons had differential effects on mechanical sensitivity in a neuropathic model (1–2 weeks after induction), suggesting that they may play different, perhaps time-dependent, roles than CRF neurons (Wilson et al., 2019). Continued (15 days), but not acute, bilateral chemogenetic inhibition of CeA–CRF neurons increased the mechanical threshold in a neuropathic pain model at the 2–weeks time point, and ipsi- but not contra-lateral (to nerve injury) ablation of CeA neurons projecting to locus coeruleus also increased mechanical threshold 2 weeks after induction of neuropathic pain (Andreoli et al., 2017; Wilson et al., 2019). We interpret our data to suggest that activation of these amygdala elements has the potential to modulate not only affective but also sensory pain–like behaviors (reflexes). However, in the arthritis pain condition, these amygdala elements may not be the only or main contributors, and other cell types, synapses or pathways would need to be silenced to inhibit mechanical hypersensitivity. Still, optogenetic silencing of BLA–CeA terminals and CeA–CRF neurons inhibited the responses of spinal WDR neurons in the pain condition but not the mechanical reflex thresholds. The tests for the evaluation of the mechanical sensitivity engage a reflex arc in the spinal cord that mediates fast responses to an external stimulus (Burke et al., 1979; Brown and Fyffe, 1981). The reflexes do not necessarily require integrative brain processing, although the sensory inputs ascend in the spinal cord to reach CNS regions and spinal reflexes are modulated and under the control of supraspinal systems. It is possible that the spinal WDR neurons recorded here in the deep dorsal horn are not, or not critically, involved in the spinally mediated nocifensive reflexes even though they are targeted by projections from brainstem regions of the descending pain modulatory system recruited by higher brain regions, including the amygdala (Bingel and Tracey, 2008; Ossipov, 2012; Bushnell et al., 2013; Chen and Heinricher, 2019; Neugebauer, 2020). Perhaps neurons other than those modulated by the amygdala are more important for spinal nocifensive reflexes, and the spinal neurons modulated by the amygdala serve to convey information to the brain rather than drive motor responses, at least in pain conditions and in the arthritis model studied here. We did not determine if the spinal neurons recorded here are projection neurons. This potential shortcoming of our study remains to be addressed.

Some other caveats need to be considered. In this study two strains of rats were used to address our hypothesis. SD rats were used previously in our lab and we elected this strain for the optogenetic manipulation of the BLA–CeA synapse for consistency. Transgenic Wistar rats allowed the optogenetic modulation of CRF neurons in the CeA considering that the Cre technology was available only on the Wistar background rats at the beginning of this project (Pomrenze et al., 2015). The effects of optogenetic BLA–CeA or CeA–CRF modulations were similar arguing against significant differences in amygdala circuitry in these strains. Previous studies from our group (Ji and

Neugebauer, 2020; Hein et al., 2021) and others (De Guglielmo et al., 2019) successfully used the pulsed optical protocol to manipulate the activity of specific pathways. Patch-clamp analysis validated the optogenetic protocol parameters used in the *in vivo* studies (**Supplementary Figures S1, S2**). In control experiments for optogenetic manipulation of the BLA–CeA synapse, we injected CaMKII–eYFP control vector (not coding opsins) into the BLA of SD rats in combination with either blue (473 nm) or yellow (590 nm) light illumination, which had no effects on spinal cord neuronal activity and behaviors. We used wild type rats injected with hChR2–eYFP expressing viral vector into the CeA in combination with blue (473 nm) light to control for optogenetic manipulation of CeA–CRF neurons in Crh–Cre transgenic rats. We decided not to test the effects of $eNpHR_{3.0}$–eYFP expressing viral vector injected into the CeA in combination with yellow (590 nm) light in wild type rats on the WDR responses and behaviors, because we did not expect any electrophysiological and behavioral significant changes. The critical contribution of PB inputs to the CeA has been explored previously, but the selective optical modulation of PB axon terminals onto CRF and non–CRF neurons in the CeA was not addressed in this study but needs to be explored to advance our knowledge about cell- and synapse-specific roles of the PB–CeA circuitry in amygdala pain–mechanisms.

In conclusion, this study provides strong evidence for pain–facilitating effects of BLA–CeA transmission and CeA–CRF neurons on spinal nociceptive processing and pain–like behaviors under normal conditions and their critical involvement in behavioral changes and spinal nociceptive processing in an arthritis pain model (**Figure 7**). The data also suggest that interventions controlling amygdala activity and output may represent a desirable strategy for pain management.

MATERIALS AND METHODS

Animals

Male Sprague–Dawley (SD) and hemizygous transgenic and wild type Crh–Cre rats (Crh = CRF, corticotropin releasing hormone/factor) on Wistar background (Pomrenze et al., 2015; De Guglielmo et al., 2019; Pomrenze et al., 2019) (initial breeding pairs kindly provided by Dr Robert Messing, UT Austin), 250–350 g at time of testing, were housed in a temperature–controlled room under a 12 h day/night cycle with unrestricted access to food and water. Experimental procedures were approved by the Institutional Animal Care and Use Committee (IACUC; protocol #14006) at Texas Tech University Health Sciences Center and conform to the guidelines of the International Association for the Study of Pain (IASP) and National Institutes of Health (NIH). Rats were randomly assigned to the different experimental groups. Experiments were performed in a blinded fashion as much as possible so that the investigators were blinded to viral vector injections, but not pain model, and different investigators performed the behavioral tests and analyses whereas electrophysiological experiments and analyses were done by the same experimenter for technical reasons.

Experimental Protocol

Extracellular single–unit recordings of dorsal horn WDR neurons (*In vivo spinal cord electrophysiology*) or behavioral tests (*Pain–related behaviors*) were done before, during and after light application into the amygdala in naïve and arthritic rats (5–6 h after the induction, *Arthritis pain model*). For optogenetic activation or silencing of presumed glutamatergic BLA axon terminals in the CeA (*Optogenetic strategy*), a viral vector (AAV) encoding ChR2 or $eNpHR_{3.0}$ under the control of the CaMKII promoter was injected stereotaxically into the right BLA of SD rats. For optogenetic activation or silencing of CRF neurons, a Cre–inducible viral vector (DIO–AAV) encoding ChR2 or $eNpHR_{3.0}$ was injected into the CeA of transgenic Wistar rats. Viral vector injections were performed four weeks before the experiments to allow the expression of the light–sensitive channels. For wireless optical stimulation of ChR2 or $eNpHR_{3.0}$ expressing CRF–CeA neurons or BLA–CeA axon terminals, an LED optic fiber was inserted into the CeA two days before the experiment. The effects of optogenetic stimulation on behavioral and electrophysiological outcome measures were assessed during 5–10 min of pulsed light application into the amygdala (CeA).

Arthritis Pain Model

The well–established monoarthritis pain model that mimics the acute phase of the human osteoarthritis condition was induced in the left knee as described in detail previously (Neugebauer et al., 2007). Rats were briefly anesthetized with isoflurane (2–3%; precision vaporizer, Harvard Apparatus) for the separate injections of kaolin (4% in sterile saline, 100 µL) and carrageenan (2% in sterile saline, 100 µL) into the joint cavity (K/C arthritis model) followed by repetitive flexions and extensions of the leg for 5 min after each injection. This well–established paradigm produces an aseptic use–dependent mono–arthritis with damage to the cartilage, and localized inflammation in only one knee joint. K/C arthritis develops rapidly within hours and persists for more than a week, and it is associated with pain behaviors and neural activity changes in the peripheral and central nervous system. As a control group we used naïve rats undergoing similar handling but without intraarticular injections, because data from our previous studies found no differences between naïve and sham (saline injection or needle insertion) rats, justifying the use of naïve rats as an appropriate control for the K/C pain model, which is well established in our laboratories (Neugebauer et al., 2003; Gregoire and Neugebauer, 2013; Kiritoshi and Neugebauer, 2015; Mazzitelli and Neugebauer, 2019).

Optogenetic Strategy

For optical activation or silencing of presumed glutamatergic BLA axon terminals, a viral vector (rAAV5–CaMKII–hChR2(H134R)–eYFP or rAAV5–CaMKII–$eNpHR_{3.0}$–eYFP) (1µL, 10^{12} units/100 µL) was injected into the BLA using a 5 µL Hamilton syringe (33 gauge) to express ChR2 or $eNpHR_{3.0}$ in BLA terminals of SD rats. For control experiments, rAAV5–CaMKII–eYFP was used. The coordinates for the injections into BLA were as follows: 2.3 mm caudal to bregma, 4.5–4.8 mm lateral to midline, and 8.0–8.5 mm deep. For optical

activation or silencing of CRF neurons, a viral vector (rAAV5/EF1a–DIO–hChR2–eYFP or rAAV5/EF1a–DIO–eNpHR$_{3.0}$–eYFP; 1 µL, 10^{12} units/100 µL) was injected into the CeA using a 5 µL Hamilton syringe to express ChR2 or eNpHR$_{3.0}$ in CRF neurons of transgenic Wistar rats. For control experiments, viral vectors were injected in wild type rats. The coordinates for the injections into CeA were as follows: 2.5 mm caudal to bregma, 4.0–4.3 mm lateral to midline, and 7.3–7.6 mm deep. After injection, we waited 10 min for the virus to diffuse into the tissue before retracting the injection needle. All viral vectors were purchased from the vector core facility at the University of North Carolina, Chapel Hill, NC, aliquoted upon arrival, stored at −80°C and thawed before use. To activate light sensitive molecules with blue (473 nm) or yellow (590 nm) light, we used a head-mounted wireless system delivering LED light pulses (20 Hz, 5 mW, 5–10 min; Teleopto, Amuza, San Diego, CA, United States) through an optical fiber (200 µm diameter) stereotaxically implanted into the CeA two days before testing, using a small drill hole made in the anesthetized rat (isoflurane, 2–3%, precision vaporizer). Implanted fibers were held in place with dental acrylic as previously described (Thompson et al., 2015; Kiritoshi et al., 2016; Kim et al., 2017; Mazzitelli and Neugebauer, 2019; Ji and Neugebauer, 2020). Prior to surgery, function of each optic fiber was tested. The optical stimulation started 5 min before the evaluation of the electrophysiological and behavioral responses and continued during testing period (5–10 min). Each test stimulus (*In vivo spinal cord electrophysiology* and *In vivo spinal cord electrophysiology*) was applied only once.

In vivo Spinal Cord Electrophysiology

Extracellular single-unit recordings were made from spinal (L2–L4) wide dynamic range (WDR) neurons, which are known to respond more strongly to stimuli of noxious than innocuous intensities (D'mello and Dickenson, 2008; Willis and Coggeshall, 2012) as described previously (Pernia-Andrade et al., 2009; Di Cesare Mannelli et al., 2015; Mazzitelli and Neugebauer, 2019; Ji and Neugebauer, 2020). To characterize neurons and for test stimuli, we used touch applied with a painter's brush to the skin around the knee (10 s, 1 stroke per second) and innocuous (500 g/30 mm^2) and noxious (1500 g/30 mm^2) compression of the knee for 10 s with a calibrated forceps equipped with a force transducer whose output was displayed in grams on an LED screen. On the day of the experiment, the rat was anesthetized with isoflurane (2–3%, precision vaporizer). The spinal segments L2–L4 were exposed by laminectomy. The animal was then secured in a stereotaxic frame (David Kopf Instruments), supported by clamps attached to the vertebral processes on both sides, and the dura was carefully removed. The exposed area of the spinal cord was first framed by agar and then filled with mineral oil. Body temperature was maintained at 37°C by using a temperature–controlled blanket system. A glass insulated carbon filament electrode (4–6 MΩ) was inserted perpendicularly to the spinal cord surface using a microdrive (David Kopf Instruments) to record the activity of dorsal horn neurons. Anesthesia was maintained with isoflurane (2%, precision vaporizer) throughout the experiment. The recorded signals were amplified, band–pass filtered (300 Hz–3 kHz), and processed by a data acquisition interface (CED 1401 Plus). Spike2 software (version 4; CED) was used for spike sorting, data storage, and analysis of single–unit activity. Spike (action potential) size and configuration were monitored continuously. After a neuron was identified, a template was created for the spikes of each individual neuron during an initial recording period of 5 min, capturing the waveform within set limits of variability for parameters such as amplitude, duration, and rise time using Spike2 software. Subsequent spikes of the neuron were matched to that template (spike sorting), and only spikes within the set limits of variability were counted as signals of that particular neuron. Only neurons were included in the study whose spike configuration matched the preset template and could be clearly discriminated from background noise throughout the experiment. Only neurons were included that were identified within a depth of 1200 µm from the dorsal surface of the spinal cord, had a receptive field on the ipsilateral knee and responded more strongly to noxious (1500 g/30 mm^2) than innocuous (500 g/30 mm^2) compression of the knee or brushing the skin. Mechanical test stimuli were applied to the left knee joint for 10 s, and the interval between stimuli was 30 s. Neuronal activity was measured as spikes/s. Measurements were repeated about every 5 min before, during (5–10 min), and after light application into the CeA. Neuronal activity was then analyzed off-line. Net evoked activity was calculated by subtracting any ongoing activity preceding the mechanical stimulus from the total activity during stimulation.

Pain–Related Behaviors

Vocalizations were measured before, during and after light application into CeA (*Experimental protocol* and *In vivo spinal cord electrophysiology*). Duration of vocalizations in the audible (20 Hz–16 kHz, supraspinally organized nocifensive responses) and ultrasonic (25 ± 4 kHz, limbic–driven negative emotional–affective signals) ranges (Brudzynski, 2007) were measured in naïve and arthritic rats, 5–6 h after the induction as in our previous studies (*Arthritis pain model*) (Neugebauer et al., 2007; Thompson et al., 2015; Kiritoshi et al., 2016; Mazzitelli and Neugebauer, 2019). Rats were briefly anesthetized with isoflurane (2–3%, precision vaporizer) and placed in a custom designed recording chamber (U.S. Patent 7,213,538) to ensure a fixed distance from the sound detectors. A microphone connected to a preamplifier was used to record audible vocalizations, and a bat detector connected to a filter and amplifier (UltraVox four–channel system; Noldus Information Technology) measured ultrasonic vocalizations. After recovery from the brief anesthesia, vocalizations were evoked by brief (10 s) noxious (1500 g/30 mm^2) stimuli applied to the left (normal or arthritic) knee joint using a calibrated forceps (*In vivo spinal cord electrophysiology*). Vocalizations were recorded for 1 min and analyzed using Ultravox 2.0 software (Noldus Information Technology).

Hindlimb withdrawal thresholds were evaluated as described previously (Neugebauer et al., 2007). A calibrated forceps with force transducer (*In vivo spinal cord electrophysiology*) was used to compress the left knee joint with continuously increasing intensity until a withdrawal reflex was evoked. The average value from 2-3 trials was used to calculate the withdrawal

threshold, which was defined as the force required for evoking a reflex response.

Patch–Clamp Electrophysiology in Amygdala Slices

Brain slices containing the right amygdala were obtained from normal and arthritic SD rats and Crh-Cre Wistar rats as previously described (Kiritoshi and Neugebauer, 2015; Kiritoshi et al., 2016; Kiritoshi and Neugebauer, 2018; Hein et al., 2021). Brains were quickly removed and immersed in an oxygenated ice–cold sucrose–based physiological solution containing (in mM): 87 NaCl, 75 sucrose, 25 glucose, 5 KCl, 21 $MgCl_2$, 0.5 $CaCl_2$ and 1.25 NaH_2PO_4). Coronal brain slices (400 μm) were obtained using a Vibratome (Series 1000 Plus, The Vibratome Co., St. Louis, MO) and incubated in oxygenated artificial cerebrospinal fluid (ACSF, in mM: 117 NaCl, 4.7 KCl, 1.2 NaH_2PO_4, 2.5 $CaCl_2$, 1.2 $MgCl_2$, 25 $NaHCO_3$ and 11 glucose) at room temperature (21°C) for at least 1 h before patch recordings. A single brain slice was transferred to the recording chamber and submerged in ACSF (31 ± 1°C) superfusing the slice at ~2 ml/ min. Only one or two brain slices per animal were used.

To determine the effects of optical activation or silencing of BLA axon terminals in the CeA, whole–cell patch–clamp recordings were performed from visually identified neurons in the laterocapsular (CeLC) division using infrared (IR) DIC videomicroscopy. To determine the effects of optical activation of CeA–CRF neurons, whole–cell patch-clamp recordings were made from visually identified CRF neurons in the CeL, using DIC–IR videomicroscopy and fluorescence illumination (BX51, Olympus, Waltham, MA). YFP–expressing neurons were visualized using an LED illumination system (X–Cite Xylis) and an ET–EYFP filter set (49,003, excitation: 500 ± 20 nm, ET500/20x; emission: 535 ± 30 nm, ET535/35m; Chroma Technology Corp, Bellows Falls, VT). Recording electrodes (tip resistance 5–8 MΩ) were made from borosilicate glass and filled with intracellular solution containing (in mM): 122 K–gluconate, 5 NaCl, 0.3 $CaCl_2$, 2 $MgCl_2$, 1 EGTA, 10 HEPES, 5 Na_2–ATP, and 0.4 Na_3–GTP; pH was adjusted to 7.2–7.3 with KOH and osmolarity to 280 mOsm/ kg with sucrose. On the day of recording, 0.2% biocytin was added to the intracellular solution. Data acquisition and analysis were done using a dual 4–pole Bessel filter (Warner Instr, Hamden, CT), low–noize Digidata 1322 interface (Axon Instr, Molecular Devices, Sunnyvale, CA, United States), Axoclamp–2B amplifier (Axon Instr, Molecular Devices, Sunnyvale, CA, United States), and pClamp9 software (Axon Instr.). Headstage voltage was monitored continuously on an oscilloscope to ensure precise performance of the amplifier. If series resistance (monitored with pClamp9 software) changed more than 10%, the neuron was discarded. To characterize the electroresponsive properties of recorded neurons, depolarizing current pulses (500 ms, 25 pA step) were applied.

For neuronal activation or inhibition, a continuous light (5 ms, 5–10 mW) or a train of pulses (5 ms, 20 Hz, 5–10 mW) of blue (470 nm) or yellow (585 nm) light, delivered for 5 s onto the slice through the 40x objective of the microscope (Olympus). In one set of experiments, blue light was used to activate ChR2 expressing BLA axon terminals or CRF neurons to evoke neuronal activity, and yellow light served as control. In a different set of experiments, yellow light was used to silence $eNpHR_{3.0}$ expressing BLA fiber terminals and CRF expressing neurons, whereas blue light served as control. In this group of experiments the recorded cell was manually depolarized to induce firing (Pomrenze et al., 2015). CeA neurons are not spontaneously active at their normal resting potential in current clamp. Therefore, manual depolarization through current injection until firing threshold was reached was necessary for the induction of neuronal firing.

Histology

Verification of spinal recording and optical stimulation sites in the amygdala. At the end of each experiment, the recording site in spinal dorsal horn was marked with an electrical current (500 μA, 5 s) through the recording electrode, and spinal lumbar enlargements were removed and submerged in 4% paraformaldehyde at 4°C overnight. Brain tissues containing the optical fiber tract were also removed and placed in paraformaldehyde. Tissues were then stored in 30% sucrose before they were frozen–sectioned at 30 μm. Viral vector expression (**Figures 1D,E**) and locations of the tips of the optical fibers (**Figure 5**) were examined using bright–field or confocal microscopy. Lesion/ recording sites were identified by macroscopic inspection, correlated with the depth of recording indicated on the micromanipulator, and then plotted on a graph showing the depth of the electrode tip from the dorsal surface of the spinal cord (**Figures 1G,H**).

Verification of recorded amygdala neurons. To confirm the location and to visualize the recorded neurons, the recorded slices were fixed in 4% paraformaldehyde in 0.1 M phosphate buffer (PB) for 12–24 h at 4°C. Slices were then washed in phosphate buffed saline (PBS) (3 × 10 min), permeabilized in PBS containing 0.3% Triton X–100 for 60 min, and incubated with fluorescently–conjugated streptavidin (1:1000, Streptavidin, Alexa Fluor 405 conjugate, Life Technologies) for 12–24 h at 4°C. Finally, the slices were washed in PBS (3 × 10 min), mounted on slides with Vectashield mounting medium (Vector Laboratories), and imaged under a confocal microscope (FV3000, Olympus, Center Valley, PA).

Data and Statistical Analysis

All averaged values are presented as means ± SEM. GraphPad Prism 7.0 software (Graph–Pad Software, San Diego, CA) was used for all statistical analyses. Statistical significance was accepted at the level $p < 0.05$. One–way ANOVA (repeated measures where appropriate) with Bonferroni post hoc tests were used for multiple comparisons, and paired *t*–tests were

used for comparison of two sets of data that had Gaussian distribution and similar variance as indicated.

DATA AVAILABILITY STATEMENT

The original contributions presented in the study are included in the article/**Supplementary Material**, further inquiries can be directed to the corresponding authors.

ETHICS STATEMENT

The animal study was reviewed and approved by the Institutional Animal Care and Use Committee (IACUC; protocol #14006) at Texas Tech University Health Sciences Center.

AUTHOR CONTRIBUTIONS

MM, KM, AP and GJ carried out experiments and analyzed data. MM created figures and provided a first draft of the manuscript. VN conceived the study, developed the experimental design, supervised data analysis and presentation, and finalized the manuscript.

FUNDING

Work in the authors laboratory is supported by National Institute of Health (NIH) grants R01 NS118731, R01 NS109255, R01 NS106902, and R01 NS038261 and USDA grant 2021-67017-34026.

ACKNOWLEDGMENTS

We thank Robert Messing, University of Texas at Austin, TX, for kindly providing the initial Crh-Cre transgenic rat breeding pairs.

SUPPLEMENTARY MATERIAL

The Supplementary Material for this article can be found online at: https://www.frontiersin.org/articles/10.3389/fphar.2021.668337/full#supplementary-material

FIGURE S1 | Brain slice physiology validation of optogenetic strategy for BLA–CeA modulation. **(A)** Image of a biocytin labeled (recorded) neuron (light blue) in the CeLC, viral vector–mediated YFP expression in BLA, and YFP–expressing BLA axon terminals in CeA (green, eYFP). Recordings of a CeLC neuron **(B)** in current clamp show depolarization and induction of neuronal firing when continuous or pulsed (20 Hz) blue light (5–10 mW, 5 s) was applied **(C)** to activate ChR2–YFP expressing BLA terminals in an amygdala slice from a normal rat. Neuron was manually depolarized to –44 mV. Yellow light served as control. Scale bar 200 µm. **(D, E)** Recordings of another CeLC neuron. Same display as in (B, C) but with yellow light application to eNpHR3.0 expressing BLA terminals in an amygdala slice obtained from an arthritic rat. Blue light served as control. Neuron was manually depolarized to –43 mV to generate action potential firing.

FIGURE S2 | Brain slice physiology validation of optogenetic strategy for CeA-CRF modulation. **(A)** Image of a biocytin labeled (recorded) CeA–CRF neuron (light blue) co–expressing YFP and viral vector–mediated YFP expression in CeA–CRF neurons (green, eYFP). Recordings of a YFP–expressing neuron in a brain slice from a transgenic Crh–Cre rat **(B)** in current clamp show depolarization and induction of neuronal firing when continuous or pulsed (20 Hz) blue light (5–10 mW, 5 s) was applied **(C)** to activate ChR2 expressing CeA–CRF neurons (slice obtained from a normal rat). Neuron was manually depolarized to –53 mV. Yellow light served as control. Scale bar 100 µm. **(D, E)** Recordings of another CeA–CRF neuron. Same display as in (B, C) but with yellow light application to eNpHR3.0 expressing CeA–CRF neurons in an amygdala slice obtained from an arthritic rat. Blue light served as control. Neuron was manually depolarized to generate action potential firing.

REFERENCES

Adke, A. P., Khan, A., Ahn, H. S., Becker, J. J., Wilson, T. D., Valdivia, S., et al. (2021). Cell-Type Specificity of Neuronal Excitability and Morphology in the Central Amygdala. *eNeuro* 8. doi:10.1523/eneuro.0402-20.2020

Allen, H. N., Bobnar, H. J., and Kolber, B. J. (2021). Left and Right Hemispheric Lateralization of the Amygdala in Pain. *Prog. Neurobiol.* 196, 101891. doi:10.1016/j.pneurobio.2020.101891

Andreoli, M., Marketkar, T., and Dimitrov, E. (2017). Contribution of Amygdala CRF Neurons to Chronic Pain. *Exp. Neurol.* 298, 1–12. doi:10.1016/j.expneurol.2017.08.010

Apkarian, A. V., Neugebauer, V., Koob, G., Edwards, S., Levine, J. D., Ferrari, L., et al. (2013). Neural Mechanisms of Pain and Alcohol Dependence. *Pharmacol. Biochem. Behav.* 112, 34–41. doi:10.1016/j.pbb.2013.09.008

Bingel, U., and Tracey, I. (2008). Imaging CNS Modulation of Pain in Humans. *Physiology* 23, 371–380. doi:10.1152/physiol.00024.2008

Brown, A. G., and Fyffe, R. E. (1981). Direct Observations on the Contacts Made between Ia Afferent Fibres and Alpha-Motoneurones in the Cat's Lumbosacral Spinal Cord. *J. Physiol.* 313, 121–140. doi:10.1113/jphysiol.1981.sp013654

Brudzynski, S. M. (2007). Ultrasonic Calls of Rats as Indicator Variables of Negative or Positive States: Acetylcholine-Dopamine Interaction and Acoustic Coding. *Behav. Brain Res.* 182, 261–273. doi:10.1016/j.bbr.2007.03.004

Burke, R. E., Walmsley, B., and Hodgson, J. A. (1979). HRP Anatomy of Group Ia Afferent Contacts on Alpha Motoneuroness. *Brain Res.* 160, 347–352. doi:10.1016/0006-8993(79)90430-x

Bushnell, M. C., Čeko, M., and Low, L. A. (2013). Cognitive and Emotional Control of Pain and its Disruption in Chronic Pain. *Nat. Rev. Neurosci.* 14, 502–511. doi:10.1038/nrn3516

Carrasquillo, Y., and Gereau, R. W. T. (2008). Hemispheric Lateralization of a Molecular Signal for Pain Modulation in the Amygdala. *Mol. Pain* 4, 24. doi:10.1186/1744-8069-4-24

Chen, Q., and Heinricher, M. M. (2019). Descending Control Mechanisms and Chronic Pain. *Curr. Rheumatol. Rep.* 21, 13. doi:10.1007/s11926-019-0813-1

Cheriyan, J., Kaushik, M. K., Ferreira, A. N., and Sheets, P. L. (2016). Specific Targeting of the Basolateral Amygdala to Projectionally Defined Pyramidal Neurons in Prelimbic and Infralimbic Cortex. *eNeuro* 3. doi:10.1523/eneuro.0002-16.2016

Corder, G., Ahanonu, B., Grewe, B. F., Wang, D., Schnitzer, M. J., and Scherrer, G. (2019). An Amygdalar Neural Ensemble that Encodes the Unpleasantness of Pain. *Science* 363, 276–281. doi:10.1126/science.aap8586

D'mello, R., and Dickenson, A. H. (2008). Spinal Cord Mechanisms of Pain. *Br. J. Anaesth.* 101, 8–16. doi:10.1093/bja/aen088

De Guglielmo, G., Kallupi, M., Pomrenze, M. B., Crawford, E., Simpson, S., Schweitzer, P., et al. (2019). Inactivation of a CRF-dependent Amygdalofugal Pathway Reverses Addiction-like Behaviors in Alcohol-dependent Rats. *Nat. Commun.* 10, 1238. doi:10.1038/s41467-019-09183-0

DeBerry, J. J., Robbins, M. T., and Ness, T. J. (2015). The Amygdala Central Nucleus Is Required for Acute Stress-Induced Bladder Hyperalgesia in a Rat Visceral Pain Model. *Brain Res.* 1606, 77–85. doi:10.1016/j.brainres.2015.01.008

Deisseroth, K. (2015). Optogenetics: 10 Years of Microbial Opsins in Neuroscience. *Nat. Neurosci.* 18, 1213–1225. doi:10.1038/nn.4091

Di Cesare Mannelli, L., Pacini, A., Corti, F., Boccella, S., Luongo, L., Esposito, E., et al. (2015). Antineuropathic Profile of N-Palmitoylethanolamine in a Rat Model of Oxaliplatin-Induced Neurotoxicity. *PLoS One* 10, e0128080. doi:10.1371/journal.pone.0128080

Fendt, M., Koch, M., and Schnitzler, H.-U. (1997). Corticotropin-releasing Factor in the Caudal Pontine Reticular Nucleus Mediates the Expression of Fear-

Potentiated Startle in the Rat. *Eur. J. Neurosci.* 9, 299–305. doi:10.1111/j.1460-9568.1997.tb01400.x

Fu, Y., and Neugebauer, V. (2008). Differential Mechanisms of CRF1 and CRF2 Receptor Functions in the Amygdala in Pain-Related Synaptic Facilitation and Behavior. *J. Neurosci.* 28, 3861–3876. doi:10.1523/jneurosci.0227-08.2008

Gonçalves, L., and Dickenson, A. H. (2012). Asymmetric Time-dependent Activation of Right Central Amygdala Neurones in Rats with Peripheral Neuropathy and Pregabalin Modulation. *Eur. J. Neurosci.* 36, 3204–3213. doi:10.1111/j.1460-9568.2012.08235.x

Gregoire, S., and Neugebauer, V. (2013). 5-HT2CR Blockade in the Amygdala Conveys Analgesic Efficacy to SSRIs in a Rat Model of Arthritis Pain. *Mol. Pain* 9, 41. doi:10.1186/1744-8069-9-41

Han, J. S., Li, W., and Neugebauer, V. (2005). Critical Role of Calcitonin Gene-Related Peptide 1 Receptors in the Amygdala in Synaptic Plasticity and Pain Behavior. *J. Neurosci.* 25, 10717–10728. doi:10.1523/jneurosci.4112-05.2005

Haubensak, W., Kunwar, P. S., Cai, H., Ciocchi, S., Wall, N. R., Ponnusamy, R., et al. (2010). Genetic Dissection of an Amygdala Microcircuit that Gates Conditioned Fear. *Nature* 468, 270–276. doi:10.1038/nature09553

Hein, M., Ji, G., Tidwell, D., D'souza, P., Kiritoshi, T., Yakhnitsa, V., et al. (2021). Kappa Opioid Receptor Activation in the Amygdala Disinhibits CRF Neurons to Generate Pain-like Behaviors. *Neuropharmacology* 185, 108456. doi:10.1016/j.neuropharm.2021.108456

Ikeda, R., Takahashi, Y., Inoue, K., and Kato, F. (2007). NMDA Receptor-independent Synaptic Plasticity in the Central Amygdala in the Rat Model of Neuropathic Pain. *Pain* 127, 161–172. doi:10.1016/j.pain.2006.09.003

Janak, P. H., and Tye, K. M. (2015). From Circuits to Behaviour in the Amygdala. *Nature* 517, 284–292. doi:10.1038/nature14188

Ji, G., Fu, Y., Ruppert, K. A., and Neugebauer, V. (2007). Pain-related Anxiety-like Behavior Requires CRF1 Receptors in the Amygdala. *Mol. Pain* 3, 13. doi:10.1186/1744-8069-3-13

Ji, G., Horvath, C., and Neugebauer, V. (2009). NR2B Receptor Blockade Inhibits Pain-Related Sensitization of Amygdala Neurons. *Mol. Pain* 5, 21. doi:10.1186/1744-8069-5-21

Ji, G., and Neugebauer, V. (2007). Differential Effects of CRF1 and CRF2 Receptor Antagonists on Pain-Related Sensitization of Neurons in the Central Nucleus of the Amygdala. *J. Neurophysiol.* 97, 3893–3904. doi:10.1152/jn.00135.2007

Ji, G., and Neugebauer, V. (2009). Hemispheric Lateralization of Pain Processing by Amygdala Neurons. *J. Neurophysiol.* 102, 2253–2264. doi:10.1152/jn.00166.2009

Ji, G., and Neugebauer, V. (2020). Kappa Opioid Receptors in the Central Amygdala Modulate Spinal Nociceptive Processing through an Action on Amygdala CRF Neurons. *Mol. Brain* 13, 128. doi:10.1186/s13041-020-00669-3

Ji, G., Sun, H., Fu, Y., Li, Z., Pais-Vieira, M., Galhardo, V., et al. (2010). Cognitive Impairment in Pain through Amygdala-Driven Prefrontal Cortical Deactivation. *J. Neurosci.* 30, 5451–5464. doi:10.1523/jneurosci.0225-10.2010

Ji, G., Zhang, W., Mahimainathan, L., Narasimhan, M., Kiritoshi, T., Fan, X., et al. (2017). 5-HT2C Receptor Knockdown in the Amygdala Inhibits Neuropathic-Pain-Related Plasticity and Behaviors. *J. Neurosci.* 37, 1378–1393. doi:10.1523/jneurosci.2468-16.2016

Kato, F., Sugimura, Y. K., and Takahashi, Y. (2018). Pain-Associated Neural Plasticity in the Parabrachial to Central Amygdala Circuit : Pain Changes the Brain, and the Brain Changes the Pain. *Adv. Exp. Med. Biol.* 1099, 157–166. doi:10.1007/978-981-13-1756-9_14

Kim, H., Thompson, J., Ji, G., Ganapathy, V., and Neugebauer, V. (2017). Monomethyl Fumarate Inhibits Pain Behaviors and Amygdala Activity in a Rat Arthritis Model. *Pain* 158, 2376–2385. doi:10.1097/j.pain.0000000000001042

Kiritoshi, T., Ji, G., and Neugebauer, V. (2016). Rescue of Impaired mGluR5-Driven Endocannabinoid Signaling Restores Prefrontal Cortical Output to Inhibit Pain in Arthritic Rats. *J. Neurosci.* 36, 837–850. doi:10.1523/jneurosci.4047-15.2016

Kiritoshi, T., and Neugebauer, V. (2015). Group II mGluRs Modulate Baseline and Arthritis Pain-Related Synaptic Transmission in the Rat Medial Prefrontal Cortex. *Neuropharmacology* 95, 388–394. doi:10.1016/j.neuropharm.2015.04.003

Kiritoshi, T., and Neugebauer, V. (2018). Pathway-Specific Alterations of Cortico-Amygdala Transmission in an Arthritis Pain Model. *ACS Chem. Neurosci.* 9, 2252–2261. doi:10.1021/acschemneuro.8b00022

Kulkarni, B., Bentley, D. E., Elliott, R., Julyan, P. J., Boger, E., Watson, A., et al. (2007). Arthritic Pain Is Processed in Brain Areas Concerned with Emotions and Fear. *Arthritis Rheum.* 56, 1345–1354. doi:10.1002/art.22460

Li, H., Penzo, M. A., Taniguchi, H., Kopec, C. D., Huang, Z. J., and Li, B. (2013). Experience-dependent Modification of a Central Amygdala Fear Circuit. *Nat. Neurosci.* 16, 332–339. doi:10.1038/nn.3322

Li, J.-N., and Sheets, P. L. (2020). Spared Nerve Injury Differentially Alters Parabrachial Monosynaptic Excitatory Inputs to Molecularly Specific Neurons in Distinct Subregions of the Central Amygdala. *Pain* 161, 166–176. doi:10.1097/j.pain.0000000000001691

Liu, C. C., Ohara, S., Franaszczuk, P., Zagzoog, N., Gallagher, M., and Lenz, F. A. (2010). Painful Stimuli Evoke Potentials Recorded from the Medial Temporal Lobe in Humans. *Neuroscience* 165, 1402–1411. doi:10.1016/j.neuroscience.2009.11.026

Mazzitelli, M., and Neugebauer, V. (2019). Amygdala Group II mGluRs Mediate the Inhibitory Effects of Systemic Group II mGluR Activation on Behavior and Spinal Neurons in a Rat Model of Arthritis Pain. *Neuropharmacology* 158, 107706. doi:10.1016/j.neuropharm.2019.107706

Mccall, J. G., Al-Hasani, R., Siuda, E. R., Hong, D. Y., Norris, A. J., Ford, C. P., et al. (2015). CRH Engagement of the Locus Coeruleus Noradrenergic System Mediates Stress-Induced Anxiety. *Neuron* 87, 605–620. doi:10.1016/j.neuron.2015.07.002

McCullough, K. M., Morrison, F. G., Hartmann, J., Carlezon, W. A., Jr., and Ressler, K. J. (2018). Quantified Coexpression Analysis of Central Amygdala Subpopulations. *eNeuro* 5, 10-18. doi:10.1523/eneuro.0010-18.2018

Mcnally, G. P., and Akil, H. (2002). Role of Corticotropin-Releasing Hormone in the Amygdala and Bed Nucleus of the Stria Terminalis in the Behavioral, Pain Modulatory, and Endocrine Consequences of Opiate Withdrawal. *Neuroscience* 112, 605–617. doi:10.1016/s0306-4522(02)00105-7

Miyazawa, Y., Takahashi, Y., Watabe, A. M., and Kato, F. (2018). Predominant Synaptic Potentiation and Activation in the Right Central Amygdala Are Independent of Bilateral Parabrachial Activation in the Hemilateral Trigeminal Inflammatory Pain Model of Rats. *Mol. Pain* 14, 1744806918807102. doi:10.1177/1744806918807102

Nation, K. M., De Felice, M., Hernandez, P. I., Dodick, D. W., Neugebauer, V., Navratilova, E., et al. (2018). Lateralized Kappa Opioid Receptor Signaling from the Amygdala Central Nucleus Promotes Stress-Induced Functional Pain. *Pain* 159, 919–928. doi:10.1097/j.pain.0000000000001167

Neugebauer, V. (2020). Amygdala Physiology in Pain. *Handbook Behav. Neurosci.* 26, 101–113. doi:10.1016/b978-0-12-815134-1.00004-0

Neugebauer, V., Galhardo, V., Maione, S., and Mackey, S. C. (2009). Forebrain Pain Mechanisms. *Brain Res. Rev.* 60, 226–242. doi:10.1016/j.brainresrev.2008.12.014

Neugebauer, V., Han, J. S., Adwanikar, H., Fu, Y., and Ji, G. (2007). Techniques for Assessing Knee Joint Pain in Arthritis. *Mol. Pain* 3, 8. doi:10.1186/1744-8069-3-8

Neugebauer, V., Li, W., Bird, G. C., Bhave, G., and Gereau, R. W. (2003). Synaptic Plasticity in the Amygdala in a Model of Arthritic Pain: Differential Roles of Metabotropic Glutamate Receptors 1 and 5. *J. Neurosci.* 23, 52–63. doi:10.1523/jneurosci.23-01-00052.2003

Neugebauer, V., and Li, W. (2003). Differential Sensitization of Amygdala Neurons to Afferent Inputs in a Model of Arthritic Pain. *J. Neurophysiol.* 89, 716–727. doi:10.1152/jn.00799.2002

Neugebauer, V., Mazzitelli, M., Cragg, B., Ji, G., Navratilova, E., and Porreca, F. (2020). Amygdala, Neuropeptides, and Chronic Pain-Related Affective Behaviors. *Neuropharmacology* 170, 108052. doi:10.1016/j.neuropharm.2020.108052

Ossipov, M. H. (2012). The Perception and Endogenous Modulation of Pain. *Scientifica (Cairo)* 2012, 561761. doi:10.6064/2012/561761

Pernia-Andrade, A. J., Kato, A., Witschi, R., Nyilas, R., Katona, I., Freund, T. F., et al. (2009). Spinal Endocannabinoids and CB1 Receptors Mediate C-Fiber-Induced Heterosynaptic Pain Sensitization. *Science* 325, 760–764. doi:10.1126/science.1171870

Pomrenze, M. B., Giovanetti, S. M., Maiya, R., Gordon, A. G., Kreeger, L. J., and Messing, R. O. (2019). Dissecting the Roles of GABA and Neuropeptides from

Rat Central Amygdala CRF Neurons in Anxiety and Fear Learning. *Cell Rep* 29, 13e14–21. doi:10.1016/j.celrep.2019.08.083

Pomrenze, M. B., Millan, E. Z., Hopf, F. W., Keiflin, R., Maiya, R., Blasio, A., et al. (2015). A Transgenic Rat for Investigating the Anatomy and Function of Corticotrophin Releasing Factor Circuits. *Front. Neurosci.* 9, 487. doi:10.3389/fnins.2015.00487

Ren, W., Kiritoshi, T., Grégoire, S., Ji, G., Guerrini, R., Calo, G., et al. (2013). Neuropeptide S: a Novel Regulator of Pain-Related Amygdala Plasticity and Behaviors. *J. Neurophysiol.* 110, 1765–1781. doi:10.1152/jn.00874.2012

Ren, W., and Neugebauer, V. (2010). Pain-related Increase of Excitatory Transmission and Decrease of Inhibitory Transmission in the Central Nucleus of the Amygdala Are Mediated by mGluR1. *Mol. Pain* 6, 93. doi:10.1186/1744-8069-6-93

Sadler, K. E., Mcquaid, N. A., Cox, A. C., Behun, M. N., Trouten, A. M., and Kolber, B. J. (2017). Divergent Functions of the Left and Right Central Amygdala in Visceral Nociception. *Pain* 158, 747–759. doi:10.1097/j.pain.0000000000000830

Simons, L. E., Moulton, E. A., Linnman, C., Carpino, E., Becerra, L., and Borsook, D. (2014). The Human Amygdala and Pain: Evidence from Neuroimaging. *Hum. Brain Mapp.* 35, 527–538. doi:10.1002/hbm.22199

Thompson, J. M., Ji, G., and Neugebauer, V. (2015). Small-conductance Calcium-Activated Potassium (SK) Channels in the Amygdala Mediate Pain-Inhibiting Effects of Clinically Available Riluzole in a Rat Model of Arthritis Pain. *Mol. Pain* 11, 51. doi:10.1186/s12990-015-0055-9

Thompson, J. M., and Neugebauer, V. (2017). Amygdala Plasticity and Pain. *Pain Res. Manag.* 2017, 8296501. doi:10.1155/2017/8296501

Thompson, J. M., and Neugebauer, V. (2019). Cortico-limbic Pain Mechanisms. *Neurosci. Lett.* 702, 15–23. doi:10.1016/j.neulet.2018.11.037

Toyoda, H., Li, X. Y., Wu, L. J., Zhao, M. G., Descalzi, G., Chen, T., et al. (2011). Interplay of Amygdala and Cingulate Plasticity in Emotional Fear. *Neural Plast.* 2011, 813749. doi:10.1155/2011/813749

Vachon-Presseau, E., Centeno, M. V., Ren, W., Berger, S. E., Tétreault, P., Ghantous, M., et al. (2016a). The Emotional Brain as a Predictor and Amplifier of Chronic Pain. *J. Dent Res.* 95, 605–612. doi:10.1177/0022034516638027

Vachon-Presseau, E., Tétreault, P., Petre, B., Huang, L., Berger, S. E., Torbey, S., et al. (2016b). Corticolimbic Anatomical Characteristics Predetermine Risk for Chronic Pain. *Brain* 139, 1958–1970. doi:10.1093/brain/aww100

Veinante, P., Yalcin, I., and Barrot, M. (2013). The Amygdala between Sensation and Affect: a Role in Pain. *J. Mol. Psychiatry* 1, 9. doi:10.1186/2049-9256-1-9

Willis, W. D., Jr, and Coggeshall, R. E. (2012). *Sensory Mechanisms of the Spinal Cord: Volume 1 Primary Afferent Neurons and the Spinal Dorsal Horn*(Berlin: Springer).

Wilson, T. D., Valdivia, S., Khan, A., Ahn, H.-S., Adke, A. P., Martinez Gonzalez, S., et al. (2019). Dual and Opposing Functions of the Central Amygdala in the Modulation of Pain. *Cel. Rep.* 29, 332–346. doi:10.1016/j.celrep.2019.09.011

Conflict of Interest: The authors declare that the research was conducted in the absence of any commercial or financial relationships that could be construed as a potential conflict of interest.

The handling editor declared a past co-authorship with one of the authors MM.

frontiers in Pharmacology

ORIGINAL RESEARCH
published: 27 September 2021
doi: 10.3389/fphar.2021.697912

β2-and β3-Adrenergic Receptors Contribute to Cancer-Evoked Pain in a Mouse Model of Osteosarcoma *via* Modulation of Neural Macrophages

Gennaro Bruno[1,2†], Francesco De Logu[1†], Daniel Souza Monteiro de Araujo[1†], Angela Subbiani[1,2], Federica Lunardi[3], Sofia Rettori[1], Romina Nassini[1], Claudio Favre[2†] and Maura Calvani[2†]*

[1]Department of Health Sciences, Clinical Pharmacology Unit, University of Florence, Florence, Italy, [2]Division of Pediatric Oncology/Hematology, Meyer University Children's Hospital, Florence, Italy, [3]Department of Clinical and Experimental Medicine, University of Pisa, Pisa, Italy

OPEN ACCESS

Edited by:
Pallavi R. Devchand,
University of Calgary, Canada

Reviewed by:
Paola Bagnoli,
University of Pisa, Italy
Kyle L. Flannigan,
University of Calgary, Canada

***Correspondence:**
Romina Nassini
romina.nassini@unifi.it

[†]These authors have contributed equally to this work

Specialty section:
This article was submitted to Inflammation Pharmacology, a section of the journal Frontiers in Pharmacology

Received: 20 April 2021
Accepted: 15 September 2021
Published: 27 September 2021

Citation:
Bruno G, De Logu F, Souza Monteiro de Araujo D, Subbiani A, Lunardi F, Rettori S, Nassini R, Favre C and Calvani M (2021) β2-and β3-Adrenergic Receptors Contribute to Cancer-Evoked Pain in a Mouse Model of Osteosarcoma via Modulation of Neural Macrophages. Front. Pharmacol. 12:697912. doi: 10.3389/fphar.2021.697912

The mechanisms involved in the development and maintenance of cancer pain remain largely unidentified. Recently, it has been reported that β-adrenergic receptors (β-ARs), mainly β2-and β3-ARs, contribute to tumor proliferation and progression and may favor cancer-associated pain and neuroinflammation. However, the mechanism underlying β-ARs in cancer pain is still unknown. Here, we investigated the role of β1-, β2-and β3-ARs in a mouse model of cancer pain generated by the para-tibial injection of K7M2 osteosarcoma cells. Results showed a rapid tumor growth in the soft tissue associated with the development of mechanical allodynia in the hind paw ipsilateral to the injected site. In addition to reduce tumor growth, both propranolol and SR59230A, β1-/β2-and β3-AR antagonists, respectively, attenuated mechanical allodynia, the number of macrophages and an oxidative stress by-product accumulated in the ipsilateral tibial nerve. The selective β1-AR antagonist atenolol was able to slightly reduce the tumor growth but showed no effect in reducing the development of mechanical allodynia. Results suggest that the development of the mechanical allodynia in K7M2 osteosarcoma-bearing mice is mediated by oxidative stress associated with the recruitment of neural macrophages, and that antagonism of β2-and β3-ARs contribute not solely to the reduction of tumor growth, but also in cancer pain. Thus, the targeting of the β2-and β3-ARs signaling may be a promising therapeutic strategy against both tumor progression and the development of cancer-evoke pain in osteosarcoma.

Keywords: β-adrenergic receptors, cancer pain, osteosarcoma, neuroinflammation, macrophages

INTRODUCTION

Pain is one of the most common invalidating symptoms of cancer, affecting approximately 70% of cancer patients worldwide every year (van den Beuken-van Everdingen et al., 2007). Despite the significant advances in understanding, early detection, and treatment of cancer, progress in the knowledge of pain related to cancer and improvement in the use of analgesics have been limited. Causes of cancer pain are multifactorial and complex and are likely connected with an array of tumor- and host-related factors (Lam and Schmidt, 2010). Numerous receptors and their activators

have been studied for a better understanding of the cancer pain mechanisms. These comprise the transient receptor potential (TRP) channels, including the vanilloid 1 (TRPV1) and ankyrin 1 (TRPA1) subtypes which are involved in bone (Ghilardi et al., 2005), and melanoma (Antoniazzi et al., 2019; De Logu et al., 2021) cancer pain models, respectively. The contribution of the acid-sensing ion channels (ASICs) has been reported in an osteolysis-induced bone cancer pain (Nagae et al., 2007) and the protease-activator receptor 2 (PAR2) in peripheral neurons is the target of serine proteases and tryptase released from cancer cells to promote the prolonged mechanical allodynia in mouse cancer nociceptive models (Lam and Schmidt, 2010).

β-ARs are G protein coupled receptors constituted of seven transmembrane domains (Hein and Kobilka, 1995; Hein, 2006), which mediate catecholamine-induced activation of adenylate cyclase. Three β-AR subtypes have been identified, the β1-, β2- and β3-ARs, which are mostly known for their role in the regulation of cardiovascular, airway, uterine, and other peripheral functions (Hein, 2006). β-ARs have also been implicated in functions of the central nervous system, including the regulation of sympathetic tone, as well as different disorders, including those associated with learning and memory, mood and food intake (Hein and Kobilka, 1995; Hein, 2006). Given their expression in peripheral nervous systems (Hein, 2006), emerging evidence also suggests a contribution of β-ARs in modulating different chronic pain conditions (Yalcin et al., 2010; Bunevicius et al., 2013; Zhang et al., 2018). β-ARs seem to be involved in pain processes mainly through activation of immunoregulatory cells, including T-cells (Laukova et al., 2012; Slota et al., 2015), mast cells (Chi et al., 2004), and macrophages (Chiarella et al., 2014; Kim et al., 2014) with associated increases in pro-inflammatory cytokines and nociceptors sensitization (Binshtok et al., 2008; Czeschik et al., 2008). Expression of β2-ARs within the nociceptive system suggested their potential implication in nociception and pain (Nicholson et al., 2005; Kanno et al., 2010; Hartung et al., 2014; Ciszek et al., 2016; Zhang et al., 2018), and human genetic studies also confirmed the contribution of β2-ARs to chronic pain disorders (Diatchenko et al., 2006). However, the recruitment of β2-ARs in the participation to pro- or antinociceptive mechanisms might depend on the considered stimulus since analgesic actions were observed with an agonist in a visceral pain model (Bentley and Starr, 1986) and with an antagonist in inflammatory pain models (Parada et al., 2003; Nackley et al., 2007). Conversely, either the stimulation or inhibition of the β1-AR subtype did not directly participate to the antinociceptive mechanisms in models of neuropathic pain (Yalcin et al., 2009a; Yalcin et al., 2009b). Instead, the β3-AR subtype has been primarily associated with metabolic regulation both in physiological and pathological conditions (Schena and Caplan, 2019).

Neuropathic pain resulting from nerve injury may be attributable to an excessive immune response leading to the development of neuroinflammation in the peripheral (Trevisan et al., 2016; De Logu et al., 2017) or central nervous system (Tsuda et al., 2003). Neuroinflammation is an established cause of neuropathic pain in the sciatic nerve ligation mouse model (De Logu et al., 2017), in the reperfusion ischemia mouse model (De Logu et al., 2020a), and in the trigeminal nerve ligation mouse model (Trevisan et al., 2016). Moreover, inflammatory processes are involved in different pathologies, including cancer. It is widely recognized that the immune system interacts with the sensory nervous system contributing to maintenance of chronic pain (De Logu et al., 2017; De Logu et al., 2020a).

In model of sciatic nerve injury in rat, noradrenergic perivascular axons germinate in the dorsal root ganglia (DRG) to form unusual structures around axotomized sensory neurons of large diameter able to mediate pain signaling (McLachlan et al., 1993). In addition, increased mRNA levels of β2-AR in ipsilateral DRGs after sciatic nerve injury has been observed (Maruo et al., 2006). Moreover, the neuropathy produced by the axotomy of DRG neurons was relieved by manipulation of adrenergic receptors (ARs) (Chung and Chung, 2002), and noradrenaline, by the β3-AR stimulation, has been reported to mediate the release of adenosine-triphosphate (ATP) from DRG neurons, thus causing mechanical allodynia in rat model of peripheral nerve injury (Kanno et al., 2010). Immune cells respond by activation of ARs, primarily the β2-ARs, which regulate a variety of functions ranging from cellular migration to cytokine secretion (Wieduwild et al., 2020). However, little is known about the involvement of β-ARs in cancer evoked-pain.

Here, we investigated whether β1-, β2-and β3-ARs contribute to pain in a mouse model of osteosarcoma generated by the para-tibial injection of K7M2 cells, using different β-ARs blockers. Although the selectivity of the most of β-ARs blockers is questionable, based on previously reported data (Dal Monte et al., 2013; Calvani et al., 2019) we used atenolol, propranolol and SR59230A as blockers to modulate β1-, β2-and β3-ARs downstream effects, respectively. We observed that pharmacological antagonism of β2-and β3-ARs, reduced tumor growth and the ensuing mechanical allodynia caused by K7M2 osteosarcoma cells inoculation. Tumor growth was associated with an increase in the number of $F4/80^+$ cells inside the tibial nerve that was attenuated by β2-and β3-ARs antagonism. These results corroborate the role of neuroinflammation in cancer pain and introduce the role of β-ARs as crucial players in the development and maintenance of chronic pain and in the modulation of neuroinflammation.

MATERIALS AND METHODS

Tumor Syngeneic Model

BALB/c mice (male, 4 weeks old, Envigo RMS) were used. Mice were housed in a temperature- and humidity-controlled vivarium (12 h dark/light cycle, free access to food and water). Behavioral experiments were done in a quiet, temperature-controlled (20–22°C) room between 9 am and 5 pm and were performed by an operator blinded to the drug treatment. Animals were anesthetized with a mixture of ketamine and xylazine (90 mg/kg and 3 mg/kg, respectively, i.p.) and euthanized with inhaled CO_2 plus 10–50% O_2.

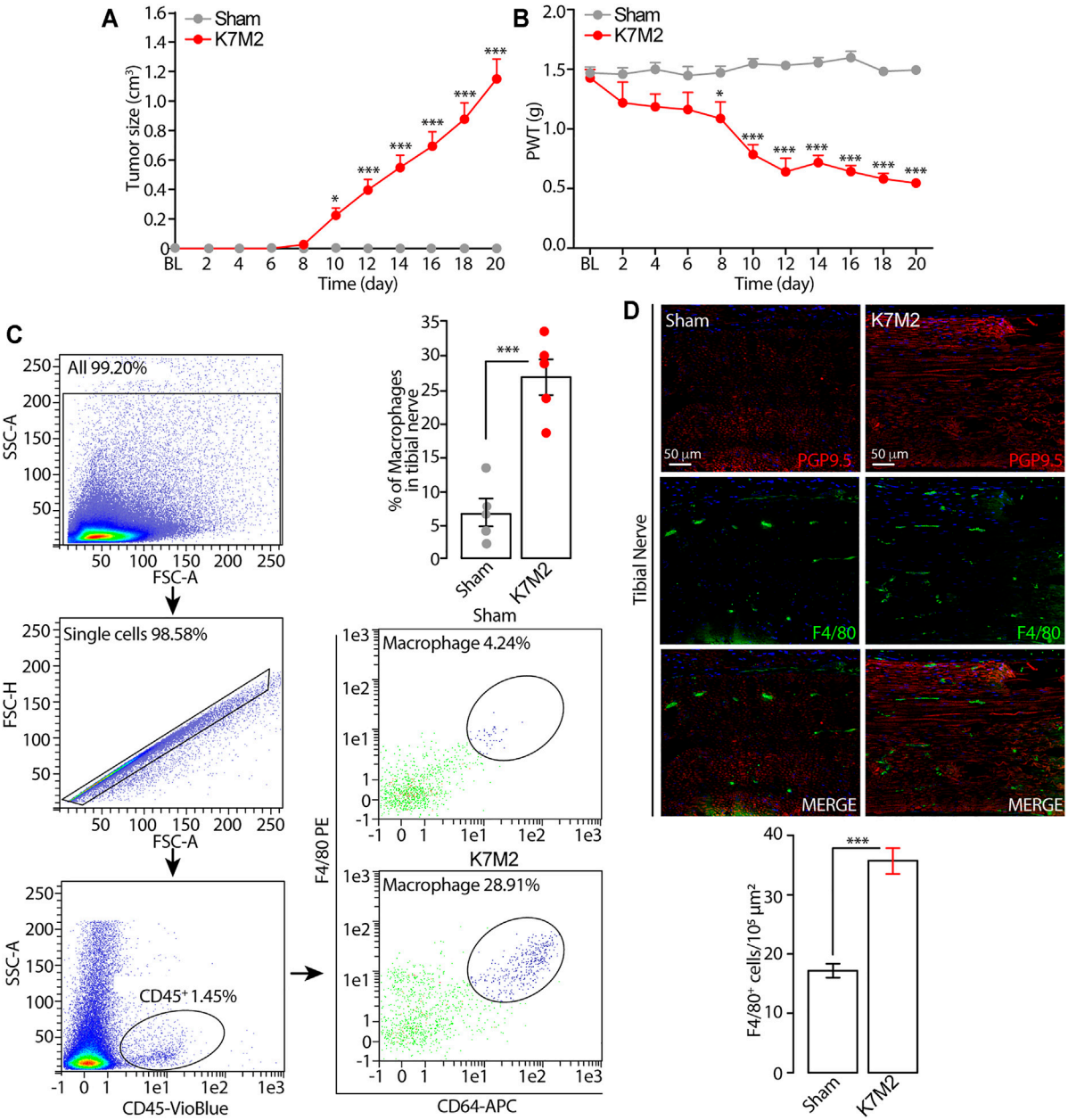

FIGURE 1 | Tumor growth and mechanical allodynia induced by K7M2 osteosarcoma cells in BALB/c mice **(A** and **B)** Time dependent increase in tumor size and mechanical allodynia after para-tibial K7M2 osteosarcoma cell inoculation or sham in BALB/c mice **(C)** Representative gating strategy of flow cytometry analysis and relative quantification of F4/80$^+$/CD64$^+$ monocytes/macrophages in tibial nerve, and **(D)** typical images and pooled data of F4/80$^+$ cells in the ipsilateral tibial nerve (stained with the neural marker PGP9.5) after para-tibial K7M2 osteosarcoma cell inoculation or sham in BALB/c mice. BL, baseline. PWT, paw withdrawal threshold. N = 6 mice. *$p < 0.05$, ***$p < 0.001$ K7M2 vs Sham. Data are presented as mean ± SEM, data points overlaid (C, D). Two-way ANOVA and Bonferroni post hoc test (A, B), unpaired student t-test (C, D).

Osteosarcoma K7M2 (CRL-2836, American Type Culture Collection, ATCC) murine cells were grown in Dulbecco′s Modified Eagle′s Medium (DMEM) supplemented with 10% fetal bovine serum (FBS), penicillin/streptomycin solution (1x) and glutamine (2 mM) at 37°C, 5% CO_2 atmosphere, and 21% O_2.

For cells inoculation, 50 µl of K7M2 (7×10^5) cells were suspended in phosphate buffer saline (PBS) and injected para-tibial. Control groups (sham) were injected with 50 µl of PBS. K7M2 cell lines are isogenic with the BALB/c mouse strain. Tumor growth rate was evaluated by measuring tumor mass with a caliber, and tumor mass volume calculated as volume = [(length x width)2/2]. Mice were sacrificed at day 20 after K7M2 cells inoculation or sham. SR59230A (Tocris Bioscence), propranolol (Merck Life Science) and atenolol (Merck Life Science) (10 mg/kg

i.p.) or vehicle (NaCl 0.9%) were administered twice a day (every 8 h) starting from day 10 after K7M2 cells inoculation, when a palpable tumor was present, or sham. Phenyl-alpha-tert-butyl nitrone (PBN, 100 mg/kg, i.p.) or vehicle (4% dimethyl sulfoxide, DMSO, 4% tween 80 in 0.9% NaCl) was given at day 14 after K7M2 cells inoculation.

Mechanical Allodynia

The measurement of mechanical paw withdrawal threshold (PWT) was carried out using von Frey filaments of increasing stiffness (0.02–2 g) applied to the plantar surface of the mouse hindpaw, according to the up-and-down paradigm (Chaplan et al., 1994). The 50% mechanical paw-withdrawal threshold (g) response was then calculated from the resulting scores.

Tibial Nerve Dissociation and Flow Cytometry Analysis

Tibial nerves were dissected from euthanized mice and mechanically dissociated to obtain a single cell suspension. Briefly, nerves were dissociated in a solution containing HEPES (25 mM), Hanks' Balanced Salt solution (HBSS, 1x), FBS 10% and dnase (10 μM) by using the gentleMACS Octo Dissociator (Miltenyi Biotec). Cells were then stained with anti-CD45-VioBlue conjugated antibody (130-110-664, Miltenyi Biotec), anti-F4/80-PE conjugated antibody (130-116-449, Miltenyi Biotec), and anti-CD64-APC conjugated antibody (130-126-950, Miltenyi Biotec). After staining, cells were subjected to flow cytometry by using a Miltenyi Biotec MACSQuant Analyzer 10. Results were analyzed by using FlowlogicTM Software. Gating strategy is reported in **Figure 1A**.

Immunofluorescence

The tumor and tibial nerve were dissected from anesthetized and transcardially perfused with PBS, followed by 4% paraformaldehyde, mice. The tibial nerve and the hindlimb were postfixed for 24 h, and cryoprotected in sucrose 30%. Immunofluorescence staining was performed according to standard procedures. Briefly, after the antibody retrieval with citrate buffer pH 6, tissue sections (10 μm) were incubated with the following primary antibodies: F4/80 [1: 50, MA516624, rat monoclonal (Cl:A3-1), RRID:AB_2538120 Thermo Fisher Scientific], PGP9.5 (1:250, ab108986, rabbit monoclonal, RRID:AB_ 10891773 Abcam), β1 receptor (1:400, ab3442, rabbit polyclonal, RRID:AB_ 10890808 Abcam), β2 receptor (1:100, ab182136, rabbit monoclonal, RRID:AB_ 2747383 Abcam), β3 receptor (1:100, ab94506, rabbit monoclonal, RRID:AB_ 10863818 Abcam) diluted in block solution (5% normal goat serum and normal donkey serum, in PBS and triton-x100, PBST) 1 h at room temperature. Sections were then incubated for 2 h in the dark with the fluorescent secondary antibody polyclonal, Alexa Fluor® 488 (1:600, Thermo Fisher Scientific) or Alexa Fluor® 594 (1:600, Thermo Fisher Scientific). Sections were coverslipped using a water-based mounting medium with 4′6′-diamidino-2-phenylindole (DAPI, Abcam). The analysis of negative controls (non-immune serum) was simultaneously performed to exclude the presence of non-specific immunofluorescent staining, cross-immunostaining, or fluorescence bleed-through. For histological evaluation, sections were stained with hematoxylin/eosin and based on the morphology, the boundaries of the nerve trunk corresponding to the epineurium were identified and reported in adjacent immunofluorescence images with dashed lines. The number of $F4/80^+$ cells was counted in 10^4 μm^2 boxes in the tibial nerve trunk.

H_2O_2 Assay

H_2O_2 level was assessed by using the Amplex Red® assay (Thermo Fisher Scientific). Tibial nerve tissue was rapidly removed and placed into modified Krebs/HEPES buffer [composition in mmol/l: 99.01 NaCl, 4.69 KCl, 2.50 $CaCl_2$, 1.20 $MgSO_4$, 1.03 KH_2PO_4, 25.0 $NaHCO_3$, 20.0 Na-HEPES, and 5.6 glucose (pH 7.4)]. Samples were minced and incubated with Amplex red (100 μM) and HRP (1 U/ml) (1 h, 37°C) in modified Krebs/HEPES buffer protected from light. Fluorescence excitation and emission were at 540 and 590 nm, respectively. H_2O_2 production was calculated using H_2O_2 standard and expressed as μmol/l of mg of dry tissue.

RAW 264.7 cells were seeded in 96-well plates (30.000 cells/well) and grown in phenol red-free Roswell Park Memorial Institute (RPMI). The cultured medium was replaced with Krebs-Ringer phosphate (KRP, composition in mM: 2 $CaCl_2$; 5.4 KCl; 0.4 $MgSO_4$; 135 NaCl; 10 D-glucose; 10 HEPES [pH 7.4]) added with SR59230A, propranolol, atenolol (all, 100 nM) or vehicle (0.01% DMSO in KRP) for 20 min at room temperature. Cells were activated by the addition of phorbol-myristate-acetate (PMA, 16 μM), along with Amplex Red (50 μM) and HRP (1 U/ml) at a total volume of 100 μl. Signal was detected 60 min after exposure to the stimuli, at 560 nm H_2O_2 release was calculated using H_2O_2 standards and expressed as nmol/1 (Idelman et al., 2015).

Statistical Analysis

The group size of n = 6 animals for behavioral experiments was determined by sample size estimation using G*Power (v3.1) (Faul et al., 2007) to detect size effect in a post-hoc test with type 1 and 2 error rates of 5 and 20%, respectively. Mice were allocated to vehicle or treatment groups using a randomization procedure (http://www.randomizer.org/). Investigators were blinded to the treatments, which were revealed only after data collection. No animals were excluded from experiments.

Results are expressed as mean ± standard error of the mean (SEM). For multiple comparisons, a one-way analysis of variance (ANOVA) followed by the post-hoc Bonferroni's test or Dunnett's test was used. Two groups were compared using Student's t-test. For behavioral experiments with repeated measures, the two-way mixed model ANOVA followed by the post-hoc Bonferroni's test was used. Statistical analyses were performed on raw data using Graph Pad Prism 8 (GraphPad Software Inc.). p values less than 0.05 ($p < 0.05$) were considered significant. Statistical tests used and the sample size for each analysis are listed in the figure legends.

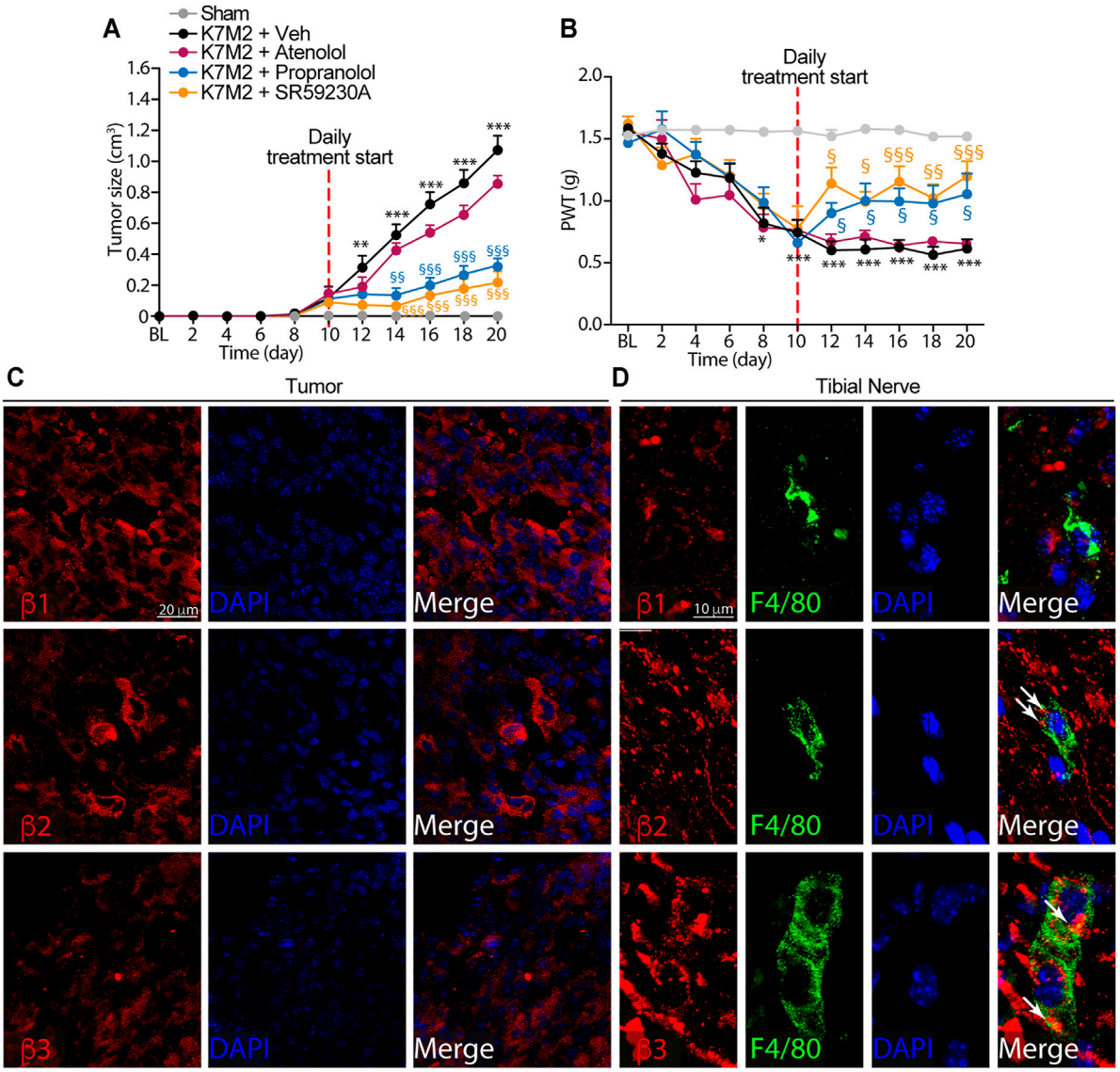

FIGURE 2 | β2-and β3-, but not β1-ARs antagonism reduce K7M2 osteosarcoma growth and mechanical allodynia in BALB/c mice **(A)** Time dependent increase in tumor size and **(B)** mechanical allodynia after para-tibial K7M2 osteosarcoma cell inoculation or sham in BALB/c mice treated (daily, starting from day 10) with atenolol (10 mg/kg, i.p.), propranolol (10 mg/kg, i.p.), SR59230A (10 mg/kg, i.p.), or vehicle (Veh) (C and D) Representative immunofluorescence images of β1-, β2-and β3-ARs expression in **(C)** tumor cells and **(D)** macrophages (F4/80$^+$ cells) in tibial nerve, 20 days after para-tibial inoculation of K7M2 osteosarcoma cells. BL, baseline. PWT, paw withdrawal threshold. N = 6 mice. $^{**}p < 0.01$, $^{***}p < 0.001$ vs Sham; $^{§}p < 0.05$, $^{§§}p < 0.01$, $^{§§§}p < 0.001$ vs K7M2 + Veh. Data are presented as mean ± SEM. Two-way ANOVA and Bonferroni post hoc test.

RESULTS

Para-Tibial K7M2 Osteosarcoma Cell Inoculation Induces Mechanical Allodynia and Recruits Macrophages in Tibial Nerve

Para-tibial inoculation of K7M2 osteosarcoma cells into the hindlimb of BALB/c mice induced a time-dependent (0–20 days) increase in hindlimb thickness, mainly due to tumor growth (**Figure 1A**). Tumor growth was associated with a parallel increase in mechanical allodynia (**Figure 1B**) and in the number of F4/80$^+$/CD64$^+$ monocytes/macrophages inside the tibial nerve trunk ipsilateral to the inoculated hindlimb, as shown by flow cytometric analysis and immunofluorescence staining (**Figures 1C, D**). Control (sham) mice did not develop either the increase in the hindlimb volume or mechanical allodynia or in the number of monocytes/macrophages inside the tibial nerve ipsilateral to the injected hindlimb (**Figures 1A–D**). These data show a time-dependent association between the tumor mass growth and the development of the mechanical allodynia and for the first time that the tumor growth in K7M2 osteosarcoma-

bearing mice is associated with an increased neuroinflammation in the tibial nerve, revealed by the increased number of macrophages ($F4/80^+/CD64^+$ cells).

β-ARs Antagonism Reduces Osteosarcoma Tumor Growth and Mechanical Allodynia

To investigate a possible role of β-ARs in the modulation of tumor growth and mechanical allodynia induced by para-tibial inoculation of K7M2 osteosarcoma cells, 10 days after K7M2 osteosarcoma cells inoculation, when allodynia was already present, mice were treated with the β1-AR antagonist atenolol, the β1-/β2-AR antagonist propranolol, the β3-AR antagonist SR59230A, or vehicle. As already reported in other cancer mouse models (Calvani et al., 2019; Bruno et al., 2020; Calvani et al., 2020), the treatment with β2-and β3-AR antagonists induced a significant reduction in tumor size (**Figure 2A**), thus confirming a pivotal role of β2-and β3-ARs in tumor growth. Conversely, the treatment with atenolol induced a slight, but not significant, reduction in the tumor size, denoting a minor role of the β1-AR subtype in controlling tumor growth (**Figure 2A**). Surprisingly, K7M2 osteosarcoma-bearing mice treated with propranolol and SR59230A, but not with atenolol exhibited a marked reduction in the mechanical allodynia (**Figure 2B**).

To investigate the role played by the β-ARs in tumor and in macrophages accumulating in the neural space, we first evaluated the expression of the three β-AR subtypes in tumor cells and in macrophages located in the tibial nerve. Immunofluorescence staining showed the expression of all three β-AR subtypes in the tumor cells (**Figure 2C**). Macrophages only expressed β2-and β3- but not β1-AR (**Figure 2D**).

Overall, these data showed that while β-ARs blockade, mainly β2-and β3-ARs and to a lesser extent β1-AR, is able to significantly influence the osteosarcoma tumor growth, the targeting of β2-and β3-ARs, but not of β1-AR, mitigated the established mechanical allodynia resulting from osteosarcoma tumor growth.

β2-and β3-ARs Antagonism on Neural Macrophages Modulates Neuroinflammation Responsible of Mechanical Allodynia

We previously observed that the development of mechanical allodynia in several neuropathic pain models (De Logu et al., 2017; De Logu et al., 2020a; De Logu et al., 2020b; De Logu et al., 2021) was associated with the increase in monocytes/macrophages inside the sciatic nerve ipsilateral to the injury. Thus, based on results showing the efficacy of β-AR antagonism to reduce the mechanical allodynia (**Figure 2B**), we then investigated whether the number of macrophages recruited in tibial nerve of osteosarcoma-bearing mice, could be modulated by β-AR antagonists administration.

We observed that the repeated treatment with the β1/2- and β3-AR antagonists (propranolol and SR59230A), but not with the β1-AR antagonist (atenolol), showed a significant reduction in the number of macrophages in tibial nerve compared to vehicle-treated mice (**Figures 3A, B**).

It has been known that the increase in macrophages number evokes an increase in oxidative stress at the tissue level, leading to the development of pain (De Logu et al., 2017; De Logu et al., 2020a; De Logu et al., 2020b; De Logu et al., 2021). Accordingly, in the tibial nerve of K7M2 osteosarcoma-bearing mice, we observed an increase in H_2O_2 levels compared to sham mice (**Figure 3C**), and the repeated treatment with propranolol and SR59230A, but not with atenolol, significantly reduced the increase in H_2O_2 levels in tibial nerve (**Figure 3C**). Given the absence of the β1-AR expression in macrophages, we speculated that the analgesic effect observed in K7M2 osteosarcoma-bearing mice following the repeated treatment with propranolol and SR59230A, was mainly due to a modulation of neuroinflammation (H_2O_2 release) dependent on β2-and β3-ARs blockade on tibial macrophages. To corroborate our hypothesis, we stimulated a murine macrophage cell line (RAW 264.7) with the pro-oxidant agent phorbol 12-myristate 13-acetate (PMA) alone or in combination with the different β-AR antagonists. Results showed that PMA induced a release of H_2O_2 from RAW 264.7 macrophages which was reduced in the presence of β2-and β3-AR but not with β1-AR antagonists (**Figure 3D**).

To finally confirm that the increase in H_2O_2 level was associated to mechanical allodynia in our model, K7M2 osteosarcoma-bearing mice were treated with the antioxidant PBN, at day 14 after cells inoculation, when mechanical allodynia was already established. Data showed that a single injection of PBN was able to transiently revert mechanical allodynia (**Figure 3E**).

Overall, our data suggest that macrophages accumulating in tibial nerve of K7M2 osteosarcoma-bearing mice induce the development of mechanical allodynia by releasing oxidative stress, and that this process is finely regulated by β2-and β3- but not by β1-ARs modulation.

DISCUSSION

Cancer-induced pain represents a high-priority complication related to tumor growth, not only in primary bone cancer, but also in bone cancer metastasis. Despite the growing interest in the research of new treatments for cancer pain, opioids remain the leading therapeutic option, which, however, shows marked limitations. Poor understanding of molecular mechanisms implicated in the development and maintenance of cancer-induced pain limits the identification of novel therapeutic targets for this condition. Previous studies highlighted the role of β-ARs modulation in models of various neuropathic pain (Kanno et al., 2010; Fávaro-Moreira et al., 2012; Zhang et al., 2018). However, the mechanism by which these receptors promote the development and maintenance of pain is poorly understood. Our data show that β-ARs, mainly β2-and β3-ARs sustain both tumor growth and cancer pain in a syngeneic osteosarcoma murine model. Indeed, the systemic treatment with the β1-AR antagonist atenolol did not affect

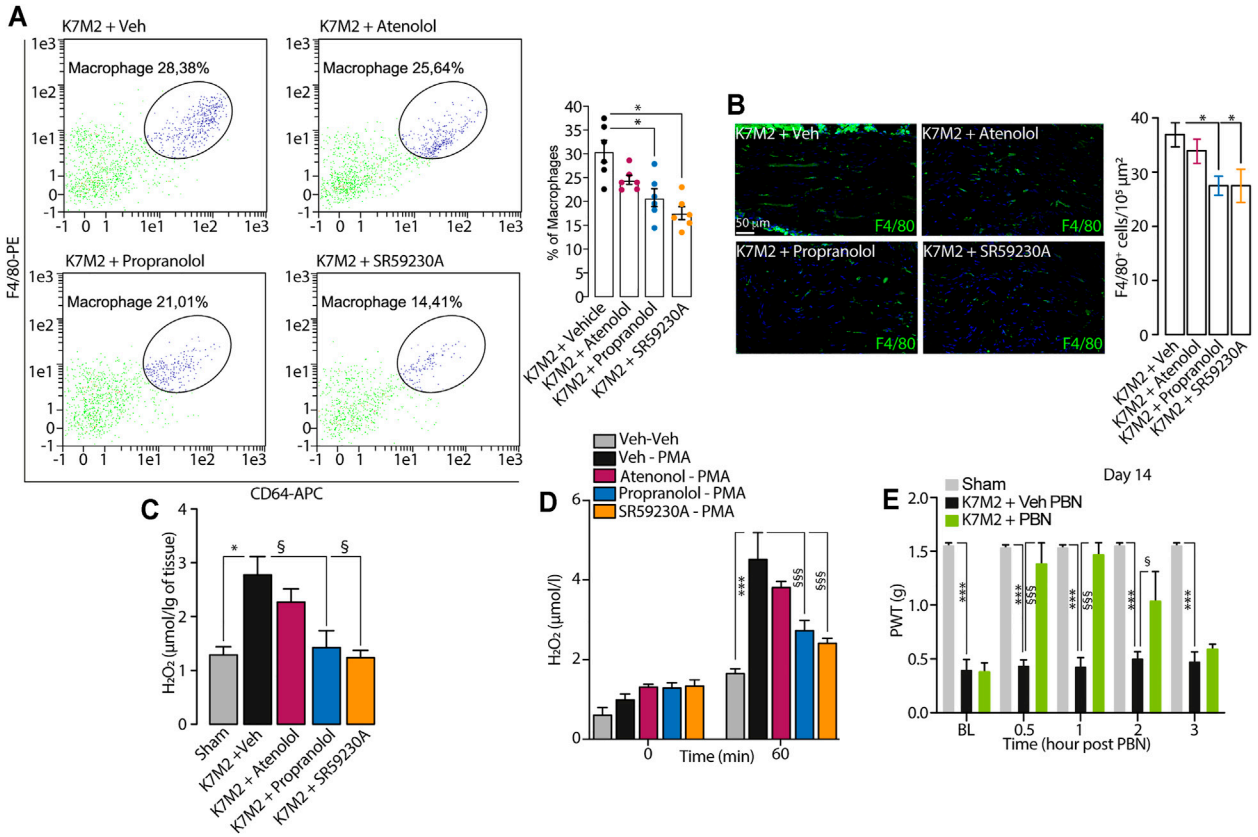

FIGURE 3 | β2-and β3-AR antagonists reduce neuroinflammation in tibial nerve of K7M2 osteosarcoma-bearing mice **(A)** Representative flow cytometry analysis and relative quantification of F4/80$^+$/CD64$^+$ macrophages **(B)** typical immunofluorescence images and pooled data of F4/80$^+$ cells and **(C)** H_2O_2 content in the tibial nerve after para-tibial K7M2 osteosarcoma cell inoculation or sham in BALB/c mice treated (daily, starting from day 10) with atenolol (10 mg/kg, i.p.) propranolol (10 mg/kg, i.p.), SR59230A (10 mg/kg, i.p.) or vehicle (Veh) **(D)** H_2O_2 level in RAW 264.7 stimulated with PMA (16 μM) in presence of SR59230A, propranolol, atenolol (all, 100 nM) or Veh (n = 3 independent experiments) **(E)** Mechanical allodynia at day 14 after para-tibial K7M2 osteosarcoma cell inoculation or sham in BALB/c mice treated with PBN (100 mg/kg, i.p.) or Veh. BL, baseline. PWT, paw withdrawal threshold. N = 6 mice. *$p < 0.05$, ***$p < 0.001$ vs Sham, Veh-Veh; $^{§}p < 0.05$, $^{§§§}p < 0.001$ vs K7M2 + Veh, Veh-PMA, K7M2 + Veh PBN. Data are presented as mean ± SEM. One-way (A–C) or two-way (D–E) ANOVA and Bonferroni post hoc test.

osteosarcoma tumor growth, while the β1/2- and β3-ARs antagonists, propranolol and SR59230A respectively, reduced osteosarcoma tumor growth and were also able to modulate the mechanical allodynia developed with the tumor growth. As these receptors are expressed both on tumor cells and inflammatory cells, including macrophages, administration of β-ARs antagonists is able to target both of these pathological processes.

First, we showed that the osteosarcoma-bearing mice developed a sustained mechanical allodynia, starting from day 10 after K7M2 osteosarcoma cells inoculation, that was absent in sham mice. Then, based on previous data that showed the pivotal role of peripheral nerve macrophages in the development of pain in mouse models of neuropathic and cancer pain (De Logu et al., 2017; De Logu et al., 2020a; De Logu et al., 2021), we wondered whether also in this cancer model, macrophages in the peripheral (tibial) nerve, which runs ipsilateral to the tumor, played a role in the development and maintenance of mechanical allodynia. Data showed that the number of neural macrophages in the tibial nerve of osteosarcoma-bearing mice were clearly increased compared to sham mice.

To test the involvement of the β-ARs in the maintenance of cancer-related pain in osteosarcoma-bearing mice, we treated the mice (daily) with the β1-AR antagonist atenolol, the β1/2-AR antagonist propranolol and the β3-AR antagonist SR59230A. Results showed that atenolol treatment had no effect in reducing mechanical allodynia, while propranolol and SR59230A treatment significantly reduced the mechanical allodynia. Moreover, propranolol and SR59230A were also able to reduce the tumor growth, confirming the crucial role of the β2-and β3-AR subtypes in sustaining pro-tumoral signaling in agreement with previous data obtained in other mouse models of cancer (Lamkin et al., 2012; Magnon et al., 2013; Calvani et al., 2019; Bruno et al., 2020; Calvani et al., 2020).

Since the development of mechanical allodynia was associated with an increase in neural macrophages and that β-ARs antagonism was able to reduce osteosarcoma-induced pain, we wondered if there was a correlation between β-ARs activity and the modulation of neuroinflammation. Surprisingly, β2-and β3-ARs antagonists were able to significantly reduce the number of macrophages in the tibial nerve compared to

vehicle treated mice. According to previously reported data showing that peripheral β2-and β3-ARs drive functional pain *via* increased activation of immune cells which promote neuroinflammation and neuropathic pain (Kanno et al., 2010; Zhang et al., 2018), and in the light of our previous data (De Logu et al., 2017; De Logu et al., 2020a; De Logu et al., 2021), our results suggested that the reduction in mechanical allodynia observed in propranolol- and SR59230A-treated mice was partially due to the reduced inflammatory cells (macrophages) in tibial nerve associated with the decreased tumor size following drug treatment. Furthermore, the evaluation of β-ARs expression in osteosarcoma tumor and in neural (tibial nerve) macrophages, showed that while all the three β-ARs were expressed in the tumor, only the β2-and β3-AR subtypes were expressed on neural macrophages. These results, together with data showing that both β1/2-AR and β3-AR but not β1-AR antagonism was able to affect cancer-evoked mechanical allodynia, supported the hypothesis that β2-and β3-AR signaling on neural macrophages sustained the mechanical allodynia developed in osteosarcoma-bearing mice.

To corroborate this hypothesis, we focused our attention to the increase in the oxidative stress as biological process correlated to the macrophages activity in the tibial nerves, and responsible for the nociceptor activation and the ensuing pain condition (De Logu et al., 2017). We observed that, in tibial nerves of osteosarcoma-bearing mice, the amount of H_2O_2, a reactive oxygen species (ROS) known to be responsible of nociception activation in several pain model (Antoniazzi et al., 2019; Brusco et al., 2020; De Logu et al., 2021), resulted increased compared to sham mice, and that treatment with propranolol and SR59230A, but not with atenolol, abrogated this effect *in vivo*. Accordingly, ROS (H_2O_2) production in murine macrophages was reverted by the treatment with propranolol and SR59230A, but not with atenolol. Finally, we reported that the treatment with an antioxidant transiently abrogated the established mechanical allodynia *in vivo*, thus confirming a leading role of oxidative burst in maintaining pain condition.

To date, there are no clinical studies aiming at investigating whether the use of β-AR antagonists could be effective in counteract cancer-pain in humans. However, a phase 2 study (NCT01222091) aimed at exploring whether propranolol treatment improved thermal and mechanical hypersensitivity after administration of an opioid (remifentanil), showed that concomitant infusion of propranolol with remifentanil prevented the remifentanil-induced post infusion hyperalgesia (Chu et al., 2012). These data highlight the great significance of investigating the role of the β-adrenergic system as pharmacological target for preventing different type of pain.

Overall, our data suggest a role for the β-ARs signaling, mainly through β2-and β3-ARs, in sustaining both tumor growth and cancer-induced pain in a syngeneic osteosarcoma murine model and identify macrophages recruited in the peripheral nerve and oxidative stress generation, as cellular and molecular mediators for the development of such pain. Furthermore, our study highlights the ability of β-ARs antagonists in modulating both tumor growth and the induction of cancer-evoked pain, giving to these receptors unique features as promising therapeutic targets for cancer therapy and associated pain.

DATA AVAILABILITY STATEMENT

The raw data supporting the conclusions of this article will be made available by the authors, without undue reservation.

ETHICS STATEMENT

The animal study was reviewed and approved by University of Florence research permit n° 936/2017-PR.

AUTHOR CONTRIBUTIONS

GB, FL, RN, MC, CF conceived and supervised the project, interpreted the results and finalized the manuscript. GB, FL, DA, RN contributed to experimental designs, performed experiments, interpreted the results, generated figures and wrote the manuscript. GB, DA, AS, FL performed experiments, interpreted the results. All authors discussed the results and revision of the manuscript and approved the manuscript.

FUNDING

The research leading to these results has received funding from AIRC under IG 2020-ID. 24503 project–P.I. RN.

REFERENCES

Antoniazzi, C. T. D., Nassini, R., Rigo, F. K., Milioli, A. M., Bellinaso, F., Camponogara, C., et al. (2019). Transient Receptor Potential Ankyrin 1 (TRPA1) Plays a Critical Role in a Mouse Model of Cancer Pain. *Int. J. Cancer* 144, 355–365. doi:10.1002/ijc.31911

Bentley, G. A., and Starr, J. (1986). The Antinociceptive Action of Some Beta-Adrenoceptor Agonists in Mice. *Br. J. Pharmacol.* 88, 515–521. doi:10.1111/j.1476-5381.1986.tb10231.x

Binshtok, A. M., Wang, H., Zimmermann, K., Amaya, F., Vardeh, D., Shi, L., et al. (2008). Nociceptors Are Interleukin-1beta Sensors. *J. Neurosci.* 28, 14062–14073. doi:10.1523/JNEUROSCI.3795-08.2008

Bruno, G., Cencetti, F., Pini, A., Tondo, A., Cuzzubbo, D., Fontani, F., et al. (2020). β3-Adrenoreceptor Blockade Reduces Tumor Growth and Increases Neuronal Differentiation in Neuroblastoma via SK2/S1P2 Modulation. *Oncogene* 39, 368–384. doi:10.1038/s41388-019-0993-1

Brusco, I., Li Puma, S., Chiepe, K. B., da Silva Brum, E., de David Antoniazzi, C. T., de Almeida, A. S., et al. (2020). Dacarbazine Alone or Associated with Melanoma-Bearing Cancer Pain Model Induces Painful Hypersensitivity by TRPA1 Activation in Mice. *Int. J. Cancer* 146, 2797–2809. doi:10.1002/ijc.32648

Bunevicius, A., Hinderliter, A., Klatzkin, R., Patel, A., Arizmendi, C., and Girdler, S. S. (2013). Beta-Adrenergic Receptor Mechanisms and Pain Sensitivity in Women with Menstrually Related Mood Disorders. *J. Pain* 14, 1349–1360. doi:10.1016/j.jpain.2013.05.014

Calvani, M., Bruno, G., Dabraio, A., Subbiani, A., Bianchini, F., Fontani, F., et al. (2020). β3-Adrenoreceptor Blockade Induces Stem Cells Differentiation in Melanoma Microenvironment. *Int. J. Mol. Sci.* 21, 1420. doi:10.3390/ijms21041420

Calvani, M., Bruno, G., Dal Monte, M., Nassini, R., Fontani, F., Casini, A., et al. (2019). β3 -Adrenoceptor as a Potential Immuno-Suppressor Agent in Melanoma. *Br. J. Pharmacol.* 176, 2509–2524. doi:10.1111/bph.14660

Chaplan, S. R., Bach, F. W., Pogrel, J. W., Chung, J. M., and Yaksh, T. L. (1994). Quantitative Assessment of Tactile Allodynia in the Rat Paw. *J. Neurosci. Methods* 53, 55–63. doi:10.1016/0165-0270(94)90144-9

Chi, D. S., Fitzgerald, S. M., Pitts, S., Cantor, K., King, E., Lee, S. A., et al. (2004). MAPK-Dependent Regulation of IL-1- and Beta-Adrenoreceptor-Induced Inflammatory Cytokine Production from Mast Cells: Implications for the Stress Response. *BMC Immunol.* 5, 22. doi:10.1186/1471-2172-5-22

Chiarella, S. E., Soberanes, S., Urich, D., Morales-Nebreda, L., Nigdelioglu, R., Green, D., et al. (2014). β_2-Adrenergic Agonists Augment Air Pollution-Induced IL-6 Release and Thrombosis. *J. Clin. Invest.* 124, 2935–2946. doi:10.1172/JCI75157

Chu, L. F., Cun, T., Ngai, L. K., Kim, J. E., Zamora, A. K., Young, C. A., et al. (2012). Modulation of Remifentanil-Induced Postinfusion Hyperalgesia by the β-Blocker Propranolol in Humans. *Pain* 153, 974–981. doi:10.1016/j.pain.2012.01.014

Chung, J. M., and Chung, K. (2002). Importance of Hyperexcitability of DRG Neurons in Neuropathic Pain. *Pain Pract.* 2, 87–97. doi:10.1046/j.1533-2500.2002.02011.x

Ciszek, B. P., O'Buckley, S. C., and Nackley, A. G. (2016). Persistent Catechol-O-Methyltransferase-Dependent Pain Is Initiated by Peripheral β-Adrenergic Receptors. *Anesthesiology* 124, 1122–1135. doi:10.1097/ALN.0000000000001070

Czeschik, J. C., Hagenacker, T., Schäfers, M., and Büsselberg, D. (2008). TNF-Alpha Differentially Modulates Ion Channels of Nociceptive Neurons. *Neurosci. Lett.* 434, 293–298. doi:10.1016/j.neulet.2008.01.070

Dal Monte, M., Casini, G., Filippi, L., Nicchia, G. P., Svelto, M., and Bagnoli, P. (2013). Functional Involvement of β3-Adrenergic Receptors in Melanoma Growth and Vascularization. *J. Mol. Med. (Berl)* 91, 1407–1419. doi:10.1007/s00109-013-1073-6

De Logu, F., De Prá, S. D., de David Antoniazzi, C. T., Kudsi, S. Q., Ferro, P. R., Landini, L., et al. (2020). Macrophages and Schwann Cell TRPA1 Mediate Chronic Allodynia in a Mouse Model of Complex Regional Pain Syndrome Type I. *Brain Behav. Immun.* 88, 535–546. doi:10.1016/j.bbi.2020.04.037

De Logu, F., Nassini, R., Materazzi, S., Carvalho Gonçalves, M., Nosi, D., Rossi Degl'Innocenti, D., et al. (2017). Schwann Cell TRPA1 Mediates Neuroinflammation that Sustains Macrophage-dependent Neuropathic Pain in Mice. *Nat. Commun.* 8, 1887. doi:10.1038/s41467-017-01739-2

De Logu, F., Trevisan, G., Marone, I. M., Coppi, E., Padilha Dalenogare, D., Titiz, M., et al. (2020). Oxidative Stress Mediates Thalidomide-Induced Pain by Targeting Peripheral TRPA1 and central TRPV4. *BMC Biol.* 18, 197. doi:10.1186/s12915-020-00935-9

De Logu, F., Marini, M., Landini, L., Souza Monteiro de Araujo, D., Bartalucci, N., Trevisan, G., et al. (2021). Peripheral Nerve Resident Macrophages and Schwann Cells Mediate Cancer-Induced Pain. *Cancer Res.* 81 (12), 3387–3401. doi:10.1158/0008-5472.can-20-3326

Diatchenko, L., Anderson, A. D., Slade, G. D., Fillingim, R. B., Shabalina, S. A., Higgins, T. J., et al. (2006). Three Major Haplotypes of the Beta2 Adrenergic Receptor Define Psychological Profile, Blood Pressure, and the Risk for Development of a Common Musculoskeletal Pain Disorder. *Am. J. Med. Genet. B Neuropsychiatr. Genet.* 141b, 449–462. doi:10.1002/ajmg.b.30324

Faul, F., Erdfelder, E., Lang, A. G., and Buchner, A. (2007). G*Power 3: A Flexible Statistical Power Analysis Program for the Social, Behavioral, and Biomedical Sciences. *Behav. Res. Methods* 39, 175–191. doi:10.3758/bf03193146

Fávaro-Moreira, N. C., Parada, C. A., and Tambeli, C. H. (2012). Blockade of β_1-, β_2- and β_3-Adrenoceptors in the Temporomandibular Joint Induces Antinociception Especially in Female Rats. *Eur. J. Pain* 16, 1302–1310. doi:10.1002/j.1532-2149.2012.00132.x

Ghilardi, J. R., Röhrich, H., Lindsay, T. H., Sevcik, M. A., Schwei, M. J., Kubota, K., et al. (2005). Selective Blockade of the Capsaicin Receptor TRPV1 Attenuates Bone Cancer Pain. *J. Neurosci.* 25, 3126–3131. doi:10.1523/JNEUROSCI.3815-04.2005

Hartung, J. E., Ciszek, B. P., and Nackley, A. G. (2014). β2- and β3-Adrenergic Receptors Drive COMT-Dependent Pain by Increasing Production of Nitric Oxide and Cytokines. *Pain* 155, 1346–1355. doi:10.1016/j.pain.2014.04.011

Hein, L. (2006). Adrenoceptors and Signal Transduction in Neurons. *Cell Tissue Res.* 326, 541–551. doi:10.1007/s00441-006-0285-2

Hein, L., and Kobilka, B. K. (1995). Adrenergic Receptor Signal Transduction and Regulation. *Neuropharmacology* 34, 357–366. doi:10.1016/0028-3908(95)00018-2

Idelman, G., Smith, D. L. H., and Zucker, S. D. (2015). Bilirubin Inhibits the Up-Regulation of Inducible Nitric Oxide Synthase by Scavenging Reactive Oxygen Species Generated by the Toll-Like Receptor 4-Dependent Activation of NADPH Oxidase. *Redox Biol.* 5, 398–408. doi:10.1016/j.redox.2015.06.008

Kanno, T., Yaguchi, T., and Nishizaki, T. (2010). Noradrenaline Stimulates ATP Release from DRG Neurons by Targeting Beta(3) Adrenoceptors as a Factor of Neuropathic Pain. *J. Cel Physiol.* 224, 345–351. doi:10.1002/jcp.22114

Kim, M. H., Gorouhi, F., Ramirez, S., Granick, J. L., Byrne, B. A., Soulika, A. M., et al. (2014). Catecholamine Stress Alters Neutrophil Trafficking and Impairs Wound Healing by β2-Adrenergic Receptor-Mediated Upregulation of IL-6. *J. Invest. Dermatol.* 134, 809–817. doi:10.1038/jid.2013.415

Lam, D. K., and Schmidt, B. L. (2010). Serine Proteases and Protease-Activated Receptor 2-Dependent Allodynia: A Novel Cancer Pain Pathway. *Pain* 149, 263–272. doi:10.1016/j.pain.2010.02.010

Lamkin, D. M., Sloan, E. K., Patel, A. J., Chiang, B. S., Pimentel, M. A., Ma, J. C., et al. (2012). Chronic Stress Enhances Progression of Acute Lymphoblastic Leukemia via β-Adrenergic Signaling. *Brain Behav. Immun.* 26, 635–641. doi:10.1016/j.bbi.2012.01.013

Laukova, M., Vargovic, P., Csaderova, L., Chovanova, L., Vlcek, M., Imrich, R., et al. (2012). Acute Stress Differently Modulates β1, β2 and β3 Adrenoceptors in T Cells, but Not in B Cells, from the Rat Spleen. *Neuroimmunomodulation* 19, 69–78. doi:10.1159/000329002

Magnon, C., Hall, S. J., Lin, J., Xue, X., Gerber, L., Freedland, S. J., et al. (2013). Autonomic Nerve Development Contributes to Prostate Cancer Progression. *Science* 341, 1236361. doi:10.1126/science.1236361

Maruo, K., Yamamoto, H., Yamamoto, S., Nagata, T., Fujikawa, H., Kanno, T., et al. (2006). Modulation of P2X Receptors via Adrenergic Pathways in Rat Dorsal Root Ganglion Neurons after Sciatic Nerve Injury. *Pain* 120, 106–112. doi:10.1016/j.pain.2005.10.016

McLachlan, E. M., Jänig, W., Devor, M., and Michaelis, M. (1993). Peripheral Nerve Injury Triggers Noradrenergic Sprouting within Dorsal Root Ganglia. *Nature* 363, 543–546. doi:10.1038/363543a0

Nackley, A. G., Tan, K. S., Fecho, K., Flood, P., Diatchenko, L., and Maixner, W. (2007). Catechol-O-Methyltransferase Inhibition Increases Pain Sensitivity through Activation of Both Beta2- and Beta3-Adrenergic Receptors. *Pain* 128, 199–208. doi:10.1016/j.pain.2006.09.022

Nagae, M., Hiraga, T., and Yoneda, T. (2007). Acidic Microenvironment Created by Osteoclasts Causes Bone Pain Associated with Tumor Colonization. *J. Bone Miner Metab.* 25, 99–104. doi:10.1007/s00774-006-0734-8

Nicholson, R., Dixon, A. K., Spanswick, D., and Lee, K. (2005). Noradrenergic Receptor mRNA Expression in Adult Rat Superficial Dorsal Horn and Dorsal Root Ganglion Neurons. *Neurosci. Lett.* 380, 316–321. doi:10.1016/j.neulet.2005.01.079

Parada, C. A., Yeh, J. J., Joseph, E. K., and Levine, J. D. (2003). Tumor Necrosis Factor Receptor Type-1 in Sensory Neurons Contributes to Induction of Chronic Enhancement of Inflammatory Hyperalgesia in Rat. *Eur. J. Neurosci.* 17, 1847–1852. doi:10.1046/j.1460-9568.2003.02626.x

Schena, G., and Caplan, M. J. (2019). Everything You Always Wanted to Know about β3-AR * (* but Were Afraid to Ask). *Cells* 8, 357. doi:10.3390/cells8040357

Slota, C., Shi, A., Chen, G., Bevans, M., and Weng, N. P. (2015). Norepinephrine Preferentially Modulates Memory CD8 T Cell Function Inducing Inflammatory Cytokine Production and Reducing Proliferation in Response to Activation. *Brain Behav. Immun.* 46, 168–179. doi:10.1016/j.bbi.2015.01.015

Trevisan, G., Benemei, S., Materazzi, S., De Logu, F., De Siena, G., Fusi, C., et al. (2016). TRPA1 Mediates Trigeminal Neuropathic Pain in Mice Downstream of Monocytes/Macrophages and Oxidative Stress. *Brain* 139, 1361–1377. doi:10.1093/brain/aww038

Tsuda, M., Shigemoto-Mogami, Y., Koizumi, S., Mizokoshi, A., Kohsaka, S., Salter, M. W., et al. (2003). P2X4 Receptors Induced in Spinal Microglia Gate Tactile Allodynia after Nerve Injury. *Nature* 424, 778–783. doi:10.1038/nature01786

van den Beuken-van Everdingen, M. H., de Rijke, J. M., Kessels, A. G., Schouten, H. C., van Kleef, M., and Patijn, J. (2007). Prevalence of Pain in Patients with Cancer: A Systematic Review of the Past 40 Years. *Ann. Oncol.* 18, 1437–1449. doi:10.1093/annonc/mdm056

Wieduwild, E., Girard-Madoux, M. J., Quatrini, L., Laprie, C., Chasson, L., Rossignol, R., et al. (2020). β2-Adrenergic Signals Downregulate the Innate Immune Response and Reduce Host Resistance to Viral Infection. *J. Exp. Med.* 217, e20190554. doi:10.1084/jem.20190554

Yalcin, I., Choucair-Jaafar, N., Benbouzid, M., Tessier, L. H., Muller, A., Hein, L., et al. (2009). Beta(2)-Adrenoceptors Are Critical for Antidepressant Treatment of Neuropathic Pain. *Ann. Neurol.* 65, 218–225. doi:10.1002/ana.21542

Yalcin, I., Tessier, L. H., Petit-Demoulière, N., Doridot, S., Hein, L., Freund-Mercier, M. J., et al. (2009). Beta2-Adrenoceptors Are Essential for Desipramine, Venlafaxine or Reboxetine Action in Neuropathic Pain. *Neurobiol. Dis.* 33, 386–394. doi:10.1016/j.nbd.2008.11.003

Yalcin, I., Tessier, L. H., Petit-Demoulière, N., Waltisperger, E., Hein, L., Freund-Mercier, M. J., et al. (2010). Chronic Treatment with Agonists of Beta(2)-Adrenergic Receptors in Neuropathic Pain. *Exp. Neurol.* 221, 115–121. doi:10.1016/j.expneurol.2009.10.008

Zhang, X., Hartung, J. E., Bortsov, A. V., Kim, S., O'Buckley, S. C., Kozlowski, J., et al. (2018). Sustained Stimulation of β2- and β3-Adrenergic Receptors Leads to Persistent Functional Pain and Neuroinflammation. *Brain Behav. Immun.* 73, 520–532. doi:10.1016/j.bbi.2018.06.017

Conflict of Interest: The authors declare that the research was conducted in the absence of any commercial or financial relationships that could be construed as a potential conflict of interest.

The reviewer PB declared a shared affiliation with one of the authors, FL, to the handling editor at time of review.

Publisher's Note: All claims expressed in this article are solely those of the authors and do not necessarily represent those of their affiliated organizations, or those of the publisher, the editors and the reviewers. Any product that may be evaluated in this article, or claim that may be made by its manufacturer, is not guaranteed or endorsed by the publisher.

Advantages of publishing in Frontiers

OPEN ACCESS
Articles are free to read for greatest visibility and readership

FAST PUBLICATION
Around 90 days from submission to decision

HIGH QUALITY PEER-REVIEW
Rigorous, collaborative, and constructive peer-review

TRANSPARENT PEER-REVIEW
Editors and reviewers acknowledged by name on published articles

Frontiers
Avenue du Tribunal-Fédéral 34
1005 Lausanne | Switzerland

Visit us: www.frontiersin.org
Contact us: frontiersin.org/about/contact

REPRODUCIBILITY OF RESEARCH
Support open data and methods to enhance research reproducibility

DIGITAL PUBLISHING
Articles designed for optimal readership across devices

FOLLOW US
@frontiersin

IMPACT METRICS
Advanced article metrics track visibility across digital media

EXTENSIVE PROMOTION
Marketing and promotion of impactful research

LOOP RESEARCH NETWORK
Our network increases your article's readership